UNCLASSIFIED

AD NUMBER

AD841847

LIMITATION CHANGES

TO:

Approved for public release; distribution is unlimited.

FROM:

Distribution authorized to U.S. Gov't. agencies and their contractors; Critical Technology; SEP 1968. Other requests shall be referred to Air Force Materiel Laboratory, MAAE, Wright-Patterson AFB, OH 45433. This document contains export-controlled technical data.

AUTHORITY

afml, usaf ltr, 12 jan 1972

THIS PAGE IS UNCLASSIFIED

AD841847

AFML-TR-68-163
Volume 1

TENSILE PROPERTIES AND FRACTURE TOUGHNESS OF 6A1-4V TITANIUM

C. E. Hartbower
W. G. Reuter
P. P. Crimmins

TECHNICAL REPORT AFML-TR-68-163, Volume 1
September 1968

DDC
OCT 29 1968

This document is subject to special export controls and each transmittal to foreign governments or foreign nationals may be made only with prior approval of the Air Force Materials Laboratory (MAAE), Wright-Patterson Air Force Base, Ohio 45433

Air Force Materials Laboratory
Air Force Systems Command
Wright-Patterson Air Force Base, Ohio

390

NOTICES

When Government drawings, specifications, or other data are used for any purpose other than in connection with a definitely related Government procurement operation, the United States Government thereby incurs no responsibility nor any obligation whatsoever; and the fact that the Government may have formulated, furnished, or in any way supplied the said drawings, specifications, or other data, is not to be regarded by implication or otherwise as in any manner licensing the holder or any other person or corporation, or conveying any rights or permission to manufacture, use, or sell any patented invention that may in any way be related thereto.

This document is subject to special export controls and each transmittal to foreign governments or foreign nationals may be made only with prior approval of the Air Force Materials Laboratory (MAAE), Wright-Patterson Air Force Base, Ohio 45433.

Information in this report is embargoed under the Department of State ITIAR. This report may be released to foreign governments by departments or agencies of the U.S. Government subject to approval of Air Force Materials Laboratory, Materials Support Division or higher authority within the Air Force. Private individuals or firms require a Department of State Export license.



Copies of this report should not be returned unless return is required by security considerations, contractual obligations, or notice on a specific document.

Report AFML-TR-68-163, Volume 1

TENSILE PROPERTIES AND FRACTURE TOUGHNESS OF 6Al-4V TITANIUM

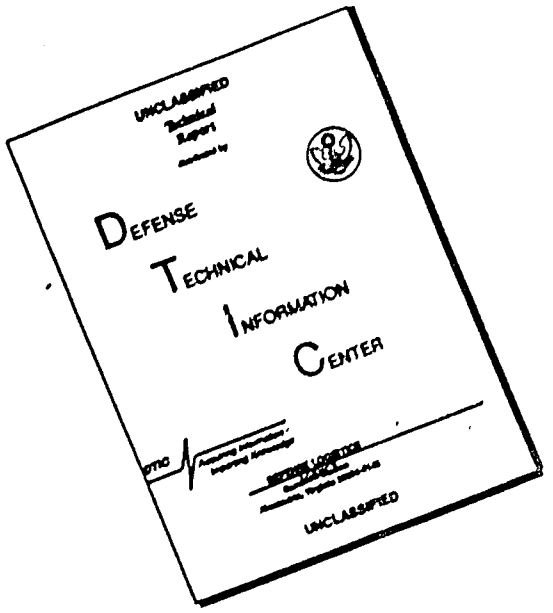
C. E. Hartbower
W. G. Reuter
P. P. Crimmins

Aerojet-General Corporation
Sacramento, California 95813

This document is subject to special export controls and each transmittal to foreign governments or foreign nationals may be made only with prior approval of the Air Force Materials Laboratory (MAAE), Wright-Patterson Air Force Base, Ohio 45433

Period Covered: February 1967 through April 1968

DISCLAIMER NOTICE



THIS DOCUMENT IS BEST QUALITY AVAILABLE. THE COPY FURNISHED TO DTIC CONTAINED A SIGNIFICANT NUMBER OF PAGES WHICH DO NOT REPRODUCE LEGIBLY.

FOREWORD

This report was prepared by Aerojet-General Corporation, Sacramento, California, under USAF Contract F33615-67-C-1358. The contract was initiated under Project No. 7381, a Materials Applications, Task No. 738106, "Materials Information Development", and administered under the direction of the Air Force Materials Laboratory, Wright-Patterson Air Force Base, Ohio, with Mr. S. O. Davis and Mr. A. W. Gunderson (MAAE) as Project Engineers.

The study program at the Aerojet-General Corporation was performed under the management of P. P. Crimmins, Manager of Structural Metals Research and Development, Materials Advanced Technology Department, with Messrs. C. E. Hartbower and W. G. Reuter as Principal Investigators.

The authors gratefully acknowledge the many helpful comments and suggestions made by S. O. Davis and A. W. Gunderson of the Air Force Materials Laboratory during the conduct of this program. Also, the authors gratefully acknowledge the many helpful comments and suggestions made by Harry Benenson of Aerojet-General Corporation in connection with the statistical analysis of the data, and the significant contributions of Leo Albertin in plane-strain fracture-toughness testing.

This report covers the period February 1967 to April 1968. The report was submitted by the authors in June 1968.

This technical report has been reviewed and approved.

D. A. SHINN
Chief, Aeronautical Systems Support Branch
Materials Support Division
Air Force Materials Laboratory

ABSTRACT

Phase I of a MIL-HDBK data collection has been completed to provide room- and elevated-temperature-tensile and fracture-toughness data on 6Al-4V titanium at a 0.2% offset yield strength of approximately 160 ksi. The material was from second-stage Minuteman rocket-motor cases. The elevated-temperature tensile data were for temperatures up to 330°F. The fracture-toughness data include plane-strain K_{Ic} from part-through-crack (PTC) tensile tests of 109 forgings, plane-stress K_c from fatigue-precracked center-notch (CW) tensile tests of 18 forgings, and precrack Charpy slow-bend and impact tests of specimens cut from the fractured CN-tensile specimens. The latter 18 forgings were from nine hydroburst chambers, four of which were premature proof-test failures and five were deliberately hydroburst in the Minuteman development program.

The uniaxial tensile-data means were determined for each temperature and plots of percent-of-room temperature tensile-properties versus temperature were constructed for input to MIL-HDBK-5. For room-temperature, the A-basis values of ultimate strength, yield strength, and percent elongation were 166.3 ksi, 153.0 ksi, and 10.2%, respectively; the B-basis values were 168.8 ksi and 156.4 ksi, respectively. The PTC-tensile K_{Ic} data were examined for the variation in fracture toughness attributable to between-forging, between-heat, and between-test-laboratory variability, first on the basis of engineering plots of data from individual laboratories, forgings, billets, and heats, and then by statistical-analysis techniques. Based on the engineering plots, tests of multiple forgings from a single heat of titanium and multiple forgings from a single billet of titanium revealed differences in K_{Ic} from forging to forging when the surface precrack was deep (approximately 50% of specimen thickness) but little or no difference in K_{Ic} with a shallow crack (approximately 25% of specimen thickness). Comparisons between laboratories revealed differences between test results in some forgings but not all. Based on statistical analysis, a significant difference was indicated between K_{Ic} values at the two crack depths investigated. However, statistically, there was not a significant difference between forgings or between heats with shallow cracks, whereas, with deeper cracks there was a significant difference between heats but not a significant difference between forgings. When the data from the shallow cracks were pooled and plotted on probability paper, the population mean was 39.1 ksi-in.$^{\frac{1}{2}}$ with a standard deviation of 1.6 ksi-in.$^{\frac{1}{2}}$. Based on all of the 540 tests, treated as a non-normal distribution, the A-basis value was 30.6 and the B-basis value was 35.2 ksi-in.$^{\frac{1}{2}}$.

The CN-tensile K_{Ic} values ranged from 31.2 to 74.6 ksi-in.$^{\frac{1}{2}}$; thus, the K_{Ic} values in some forgings were appreciably higher than any values measured in the PTC-tensile tests of 109 forgings tested with a different crack orientation. Precrack Charpy slow-bend W/A values were found to provide a good estimate of the CN-tensile K_{Ic} values through the relationship $K_{Ic} = 0.17(W/A)_{PCSB} + 16.2$ ksi-in.$^{\frac{1}{2}}$ where $(W/A)_{PCSB}$ is the precrack Charpy slow-bend value in in.-lb/in.^{2}. The CN-tensile K_c data based on the onset of crack instability as determined by an acoustical technique ranged from 71 to 137 ksi-in.$^{\frac{1}{2}}$ for the 18 forgings tested. Precrack Charpy impact W/A values were found to provide a good estimate of the CN-tensile K_c values through the relationship $K_c = 0.10(W/A)_{PCI} + 6.7$ ksi-in.$^{\frac{1}{2}}$.

THIS ABSTRACT IS SUBJECT TO SPECIAL EXPORT CONTROLS AND EACH TRANSMITTAL TO FOREIGN GOVERNMENTS OR FOREIGN NATIONALS MAY BE MADE ONLY WITH PRIOR APPROVAL OF THE AIR FORCE MATERIALS LABORATORY (MAAE), WRIGHT-PATTERSON AIR FORCE BASE, OHIO 45433.

TABLE OF CONTENTS

		Page
I.	INTRODUCTION	1
II.	MATERIAL	3
	A. Room- and Elevated-Temperature Tensile and PTC Tensile Data	3
	B. Center-Notch Tensile and Precrack Charpy Data	3
III.	TEST PROCEDURE	5
	A. Uniaxial Tensile Tests	5
	1. Room-Temperature	5
	2. Elevated Temperature	5
	B. Part-Through-Crack Tensile Tests	5
	C. Center-Notch Tensile Tests	10
	D. Precrack Charpty Tests	10
IV.	DISCUSSION OF RESULTS	13
	A. Uniaxial Tensile Data	13
	1. Room Temperature	13
	2. Elevated Temperature	15
	B. Part-Through-Crack Tensile K_{Ic} Data	17
	C. Center-Notch Tensile Data	30
	1. Plane Strain K_{Ic} Data	30
	2. Plane Stress K_c Data	37
	D. Precrack Charpy Data	41
	1. Slow Bend	41
	2. Impact	46
	E. Correlation with Full-Scale Chamber Performance	51
V.	Appendices	59
	A. Uniaxial-Tensile Test	59
	B. Part-Through-Crack Tensile Test	76
	C. Center-Notch Tensile Test	174
	D. Precrack Charpy Test	198
	E. Statistical Analysis	262

LIST OF TABLES

Table		Page
I	Forging Code, Heat, Chemistry and Beta Transus	4
II	Forgings for Elevated Temperature Tensile Testing	7
III	Suggested Input to MIL-HDBK-5	16
IV	Number of Observations for t-Test of Difference Between Two Means	31
V	Summary of CN-Tensile Plane-Strain K_{Ic} Data and Precrack Charpy Slow-Bend W/A Data	33
VI	Summary of CN-Tensile Plane-Stress K_c Data and Precrack Charpy Impact W/A Data	39

ILLUSTRATIONS

Figure		Page
1	Round 0.252-in.-dia Tensile	6
2	Part-Through-Crack Tensile Specimen	8
3	Center-Notch Tensile Specimen	11
4	Room Temperature Tensile Results Versus Probability	14
5	Ultimate Tensile Strength at Elevated Temperature Versus Probability	18
6 (a&b)	Yield Strength at Elevated Temperature Versus Probability	19
7	Percent Elongation at Elevated Temperature Versus Probability	20
8	Effect of Temperature on Ultimate Tensile Strength (F_{tu}) of Solution Treated and Aged Ti-6Al-4V Alloy	21
9	Effect of Temperature on Yield Strength (F_{ty}) of Solution Treated and Aged Ti-6Al-4V Alloy	22
10	Effect of Temperature on Percent Elongation of Solution Treated and Aged Ti-6Al-4V Alloy	23
11	K_{Ic} Versus Probability for a/Q ∿ 0.02	25
12	K_{Ic} Versus Probability for a/Q ∿ 0.04	27
13	K_{Ic} Versus F_G/F_{ty} for a/Q ∿ 0.02	28
14	K_{Ic} Versus F_G/F_{ty} for a/Q ∿ 0.04	29
15	Relationship Between K_{Ic} Values Based on AO-PD and AO-PP	36
16	Relationship Between K_{Ic} and Yield Strength Together with the Scatter Band for K_{Ic} from 109 Forgings as Determined by PTC-Tensile Tests	38
17	Relationship Between K_c Values Based on AC-PC and AM-PM	42
18	Relationship Between K_c and Yield Strength Together with the Scatter Band for K_{Ic} from 109 Forgings as Determined by PTC-Tensile Test	43
19	Relationship Between K_{Ic} and K_c	44
20	Typical COD-Load X-Y Plot for Fwd and Aft Cylinders of Chamber R26	45
21	Graphical Solution for K_{Ic} Based on Precrack Charpy Slow Bend	47

Illustrations (cont.)

Figure		Page
22	Relationship Between K_{Ic} and Precrack Charpy Slow Bend	48
23	Graphical Solution for K_c Based on Precrack Charpy Impact	49
24	Relationship Between K_c and Precrack Charpy Impact	50
25	Anisotropy in the Cylindrical Forging	52
26	Fracture in Chamber R-30	53
27	Bar Graph Summary of Precrack Charpy and Center-Notch Tensile Test Results	54
28	Relationship Between Precrack Charpy W/A (in.-lb/in.^{2}) and CN-Tensile Critical Stress Intensity (ksi-in.$^{1/2}$)	55

I.

INTRODUCTION

The overall objective of this study is to provide fracture toughness data on 6Al-4V titanium for inclusion in MIL-HDBK-5, Metallic Materials and Elements for Flight Vehicle Structures. The 6Al-4V titanium alloy used in the data collection is production-lot material from solid-propellant rocket-motor cases, heat treated to an ultimate strength range of 165 to 180 ksi.

The data collection is being conducted in two phases. The objective of Phase 1, reported herein, was to compile (1) room- and elevated-temperature uniaxial-tensile-test data, (2) plane-strain fracture-toughness data from part-through-crack (PTC) tensile tests, (3) plane-stress and plane-strain fracture-toughness data from through-crack center-notch (CN) tensile tests, and (4) precrack Charpy slow-bend and impact W/A values for material cut from the broken CN-tensile tests. The uniaxial-tensile and the PTC-tensile tests were taken from trim stock cut from 52-in.-dia cylindrical forgings; approximately 100 forgings were tested for the uniaxial-tensile and PTC-tensile data. The CN-tensile tests were cut from nine hydroburst chambers; four of the chambers were premature proof-test failures and five were deliberately hydroburst tested in the Minuteman development program. The deliberately hydroburst chambers met all design criteria.

Additionally, it was the objective of Phase I to examine the part-through-crack tensile plane-strain fracture-toughness (K_{Ic}) data to determine the variation in K_{Ic} attributable to between-forging, between-heat, and between-test-laboratory variability. Also, the data were to be examined to determine the variation in K_{Ic} attributable to crack and specimen dimensions. These factors were examined first on the basis of engineering plots of the K_{Ic} data and then by statistical analysis.

Statistical analysis, based on methods of variance analysis and partitioning into component parts, was to be used to establish (1) the number of test observations necessary to determine differences in K_{Ic} at a given confidence level and (2) the K_{Ic} value above which at least 99% A-Basis and 90% B-Basis of the population values is expected to fall, with a confidence of 95%.

The test results obtained with the CN-tensile and the precrack Charpy slow-bend and impact tests were to be examined for correlation between the CN-tensile K_{Ic} and K_c data and the precrack Charpy slow-bend and impact data.

Phase 2 of the data collection will be to correlate laboratory test results with full-scale Minuteman chamber performance. The materials for the second phase will be obtained from 15 full-scale hydroburst Minuteman chambers,

including eight of the chambers from Phase 1. Ten of the 15 chambers will be premature proof-test failures and five successfully hydroburst chambers. Testing domes, adapters, and cylinders from the 10 chambers will provide data on 69 forgings, involving three different forging practices. The crack toughness measurements will be made by precrack Charpy impact tests, oriented to fracture in the chamber-axial direction, and cut from 0.1-in. and 0.19-in. wall sections on both sides of each girth weld (parent-metal tests only). Selected forgings in each chamber will be tested at -40, RT, 200 and 320°F. Particular attention will be directed to the material in the immediate vicinity of the fracture origin.

II.

MATERIAL

The 6Al-4V titanium used in the second-stage Minuteman is solution-treated and aged to 155 ksi minimum yield strength with ultimate tensile strength in the range of 165 to 180 ksi. The material is in the form of (1) trim stock 0.6 in. thick cut from as-forged chamber barrel sections for the purpose of qualification testing and (2) forged-and-machined components generally ranging in thickness from 0.10 to 0.20 in.

A. ROOM- AND ELEVATED-TEMPERATURE TENSILE AND PTC TENSILE DATA

The test material for Phase 1 of the data collection was supplied in the form of trim stock, i.e., arc segments (nominally of 80° arc length x 0.6 in. thick x 3/4 in. wide) cut from 52-in.-dia cylinders forged by Cameron Ironworks, Inc., Houston, Texas. The test material was solution treated while still an integral part of the forged cylinders. The material was aged after being separated from the parent forging, but processed with the forging during its aging treatment. Solution treatment was carried out 60°F below the beta transus, water quenched, and aged in the range of 900 to 1050°F. The aging temperature for each forging was selected on the basis of laboratory heat treatment of tensile blanks taken from the trim stock cut from each forging; with few exceptions, the aging was done at 1000°F for 8 hr. Thus, the qualification room-temperature tensile data, the elevated tensile test data, and the PTC fracture-toughness data were all obtained from trim stock.

The room-temperature tensile data are from approximately 100 forgings involving over 50 heats of 6Al-4V titanium; the elevated temperature tensile data are from approximately 50 forgings involving over 25 heats of 6Al-4V titanium; and the PTC tensile tests are from 109 forgings involving over 50 heats of 6Al-4V titanium. Chemistry of the forgings is listed in Table I, together with the forging identification and heat numbers. Details of Cameron Ironwork's forging practice are contained in Appendix B.

B. CENTER-NOTCH-TENSILE AND PRECRACK-CHARPY DATA

The CN-tensile and precrack-Charpy data were for material taken from 44-in.- and 52-in.-dia cylindrical forgings of failed and successfully hydrobrust second-stage Minuteman chambers. One of the chambers, SN 2192109, contained forgings that had been tested previously by the PTC-tensile specimen (forgings 69B and 77B, as reported in Appendix B). The 3- x 12-in. CN-tensile specimens were cut from the cylindrical forgings with the 12-in. length in the chamber axial direction, i.e., the crack propagation was in the chamber hoop direction. This specimen orientation involved the least curvature in the test piece (52-in.-dia radius of curvature in the 3-in. direction). Test specimens oriented for crack propagation in the axial direction would have required straightening, which, in turn, would probably have altered the properties of the test material.

TABLE I

FORGING CODE, HEAT, CHEMISTRY AND BETA TRANSUS

Titanium Heat Code	Number	Forging	Chemistry Al	V	Fe	O_2	C	N_2	H_2	Beta Transus (°F)
1642	13272	1,4	6.60	4.35	0.12	0.12	0.040	0.022	0.0023	1825-50
1643		9	6.20	4.00	0.13	0.15	0.040	0.015	0.0026	1825
1644	13282	5,6,7	6.50	4.10	0.13	0.14	0.030	0.019	0.0033	1825-50
1967		14	6.30	4.12	0.08	0.18	0.025	0.007	0.0016	1830
1968	2796	13	6.20	4.14	0.11	0.17	0.022	0.007	0.0017	1830
2018	2833	17	6.17	4.25	0.09	0.19	0.019	0.005	0.0016	1830
2043		19	6.38	4.31	0.18	0.16	0.023	0.008	0.0016	1835
2045		21	6.20	4.17	0.16	0.19	0.020	0.004	0.0016	1835
2046		22	6.20	4.03	0.16	0.18	0.029	0.005	0.0016	1835
2047	2826	23	6.40	4.25	0.15	0.18	0.028	0.008	0.0016	1835
2073	2839	26	6.13	4.27	0.17	0.17	0.022	0.006	0.0017	1835
2074	2842	27	6.13	4.16	0.17	0.15	0.026	0.011	0.0019	1835
2100	2847	29	6.38	4.32	0.17	0.18	0.029	0.009	0.0016	1830
2102		30	6.30	4.34	0.18	0.17	0.025	0.005	0.0016	1835
2148	2893	31A,B	6.23	4.27	0.15	0.16	0.019	0.007	0.0017	1835
2150	2892	33A,B	6.31	4.41	0.15	0.18	0.021	0.006	0.0023	1835
2169	2896	43A,B	6.35	4.31	0.16	0.18	0.024	0.005	0.0019	1835
2201	5172	45A	6.30	4.10	0.15	0.13	0.022	0.015	0.005	1820-35
2202	2906	36A,B	6.30	4.38	0.17	0.17	0.025	0.008	0.0030	1835
2203	2905	37A,B	6.41	4.28	0.16	0.17	0.022	0.009	0.0030	1835
2204	2904	44B	6.38	4.24	0.15	0.17	0.025	0.010	0.0016	1835
2205	2888	39A	6.26	4.17	0.14	0.18	0.021	0.008	0.0017	1835
2274	2924	42B,42C	6.31	4.33	0.17	0.18	0.026	0.008	0.0016	1835
2395	2890	50A,B	6.27	4.42	0.18	0.17	0.026	0.010	0.0017	1830
2397		52B	6.44	4.31	0.16	0.20	0.029	0.012	0.0029	1830
2398	2592	53B,54A,B	6.28	4.27	0.14	0.18	0.025	0.010	0.0016	1830
2423		55A,B	6.37	4.42	0.17	0.18	0.021	0.011	0.0024	1830
2479	2966	56A,B,60B	6.28	4.36	0.18	0.17	0.021	0.011	0.0019	1830
2480	2968	57A,B,58B	6.43	4.35	0.18	0.20	0.028	0.010	0.0017	1830
2481	2481	59A	6.45	4.37	0.17	0.20	0.027	0.011	0.0024	1830
2528	2993	61A,B,62A,B	6.32	4.38	0.17	0.18	0.022	0.007	0.0019	1830
2529	2992	63A,B	6.30	4.25	0.18	0.17	0.029	0.008	0.0016	1830
2531	2969	65A	6.33	4.28	0.19	0.18	0.026	0.015	0.0018	1830
2532	2971	66B	6.43	4.40	0.18	0.18	0.023	0.013	0.0022	1830
2554	2995	69A,B	6.31	4.41	0.15	0.17	0.021	0.011	0.0016	1830
2555	2997	70A,B,71A	6.45	4.47	0.16	0.19	0.026	0.009	0.0014	1830
2576	3010	73A,B,74A,B	6.27	4.37	0.16	0.17	0.021	0.008	0.0033	1825
2577	3006	75A,80A,B	6.48	4.39	0.17	0.18	0.026	0.008	0.0035	1825
2578	2999	76A,77A,B	6.42	4.48	0.15	0.19	0.027	0.007	0.0015	1825
2579	3009	78A,79A,B	6.18	4.30	0.17	0.19	0.030	0.009	0.0039	1825
2634	3012	81A	6.30	4.34	0.18	0.17	0.023	0.011	0.0055	1825
2635	3017	82A	6.40	4.26	0.17	0.17	0.027	0.006	0.0029	1825
2636	3021	83A,84B	6.39	3.90	0.15	0.18	0.024	0.009	0.0024	1825
2696	D5911	86A,87A,B	6.40	4.20	0.12	0.19	0.025	0.012	0.004	1830±5
2697	D5938	90A,B,91A,B,92A	6.20	4.10	0.14	0.18	0.023	0.012	0.005	1825
2700	3032	93A,B	6.22	4.32	0.18	0.17	0.026	0.008	0.0024	1825
2701	3033	94B	6.29	4.11	0.17	0.19	0.022	0.009	0.0023	1825
2714	3057	96A,B,98A	6.32	4.32	0.17	0.18	0.021	0.006	0.0019	1825
2715	3054	97A,B	6.28	4.44	0.17	0.17	0.022	0.006	0.0025	1825
2779	D5937	100A,B,101A 102A,B	6.30	4.10	0.14	0.16	0.025	0.012	0.0040	1830±5
2803	35D-6112	104A,B,105A,B 107A,B	6.40	4.10	0.13	0.16	0.023	0.009	0.0050	1830±5
2846	35D-6111	108A,B,109B 110B,111B	6.20	3.90	0.14	0.18	0.023	0.012	0.0050	1835±5
2847	39D-6113	112A,B	6.40	4.20	0.18	0.16	0.025	0.011	0.0050	1830±5

III.

TEST PROCEDURE

A. UNIAXIAL TENSILE TESTS

1. Room Temperature

The room-temperature tensile data were compiled from Minuteman summary inspection documentation. The specimen was a 0.252-in.-dia round tensile bar, as shown in Figure 1. The tests were conducted in accordance with Federal Test Method 151-R3.

2. Elevated Temperature

The elevated-temperature tensile tests were conducted from 150 to 330°F. Nine to twelve specimens (Figure 1) were machined from the trim stock of each forging, with three or four specimens tested at each temperature. Table II lists the forgings tested; details of the test procedure are appended (Appendix A).

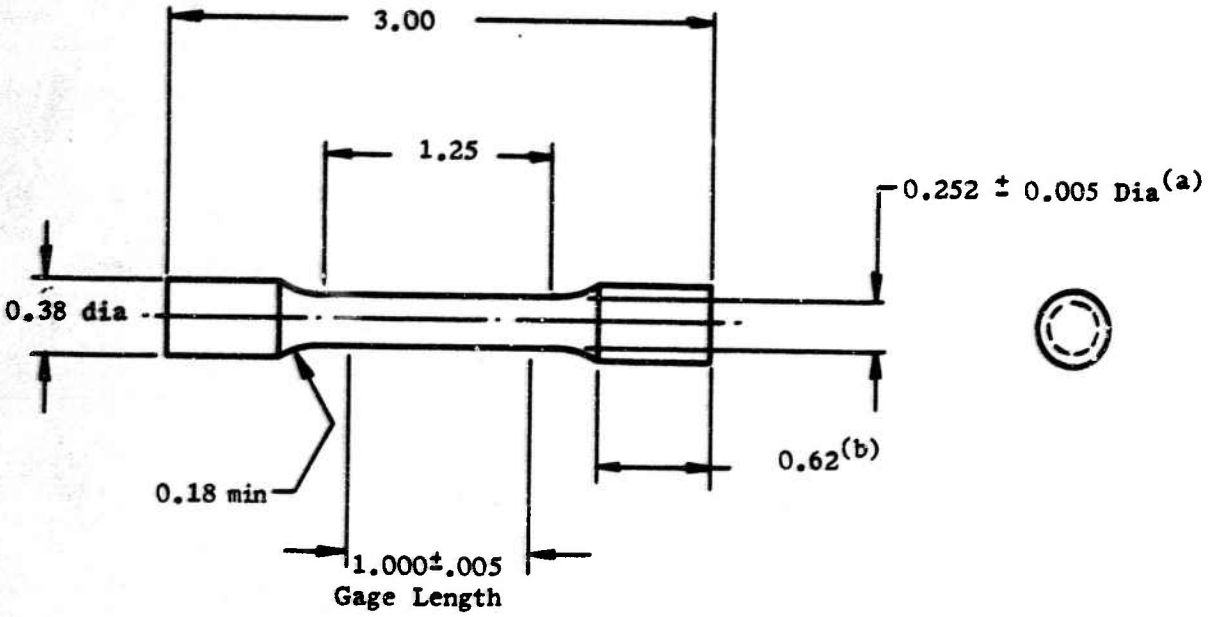
B. PART-THROUGH-CRACK TENSILE TESTS

The part-through-crack (PTC) or surface-cracked specimen was originally developed for the purpose of simulating flaws of a type frequently encountered in service. Surface-crack specimens sometimes are used to obtain direct information on the effects of realistic flaws in terms of fracture strength versus crack depth or area. The test is also used to obtain plane-strain fracture-toughness data (K_{Ic}).

The conventional expression for the stress-intensity factor for this specimen is an approximate solution derived by Irwin[1] for a semi-elliptical surface crack in an infinite solid. Another approximate solution is provided by Paris and Sih.[2] These solutions, as discussed in Appendix B, were used in a computer program for obtaining K_{Ic} data from 708 PTC-tensile tests of 109 forgings. The details of test procedure are contained in Appendix B. The test specimen (Figure 2) was nominally 0.125 in. thick x 3/4 in. wide, with two semi-elliptical flaw sizes tested, viz., 0.002 sq in. ($a/2c = 0.40$) and 0.010 sq in. ($a/2c = 0.28$) where a is the crack depth and $2c$ is the crack length.

---

(1) George Irwin, Journal of Applied Mechanics, Vol. 84E, No. 4, Dec 1962.
(2) P. C. Paris and G. C. Sih, "Stress Analysis of Cracks," ASTM STP-381, p. 30, June 1964.



(a) Diameter of the reduced section may be smaller at center than at ends. Difference shall not exceed 1 percent of diameter at center.

(b) Ends may be of any shape to fit the holders of the testing machine in such a manner that the load is axial.

Figure 1. Round 0.252-in.-dia Tensile

TABLE II

FORGINGS FOR ELEVATED TEMPERATURE TENSILE TESTING

Forged Component		Forged Component		Forged Component	
Serial No.	Heat No.	Serial No.	Heat No.	Serial No.	Heat No.
1	--	74A	3010	97A	3054
9	--	74B	3010	97B	3054
19	--	76A	2999	98A	3057
26	2839	77A	2999	101A	D5937
30	--	77B	2999	102A	D5937
37A	2905	78A	3009	104A	D6112
42C	2924	79B	3009	104B	D6112
43B	2896	80A	3006	105A	D6112
45A	5172	80B	3006	107A	D6112
54B	2952	82A	3017	107B	D6112
55B	--	87A	D5911	108A	D6111
56A	2966	90A	D5938	108B	D6111
57A	2968	90B	D5938	109B	D6111
60B	2966	91A	D5938	111B	D6111
61B	2993	91B	D5938	112A	D6113
62A	2993	92A	D5938		
65A	2969	92B	3032		
73A	3010	93B	3032		
73B	3010	96B	3057		

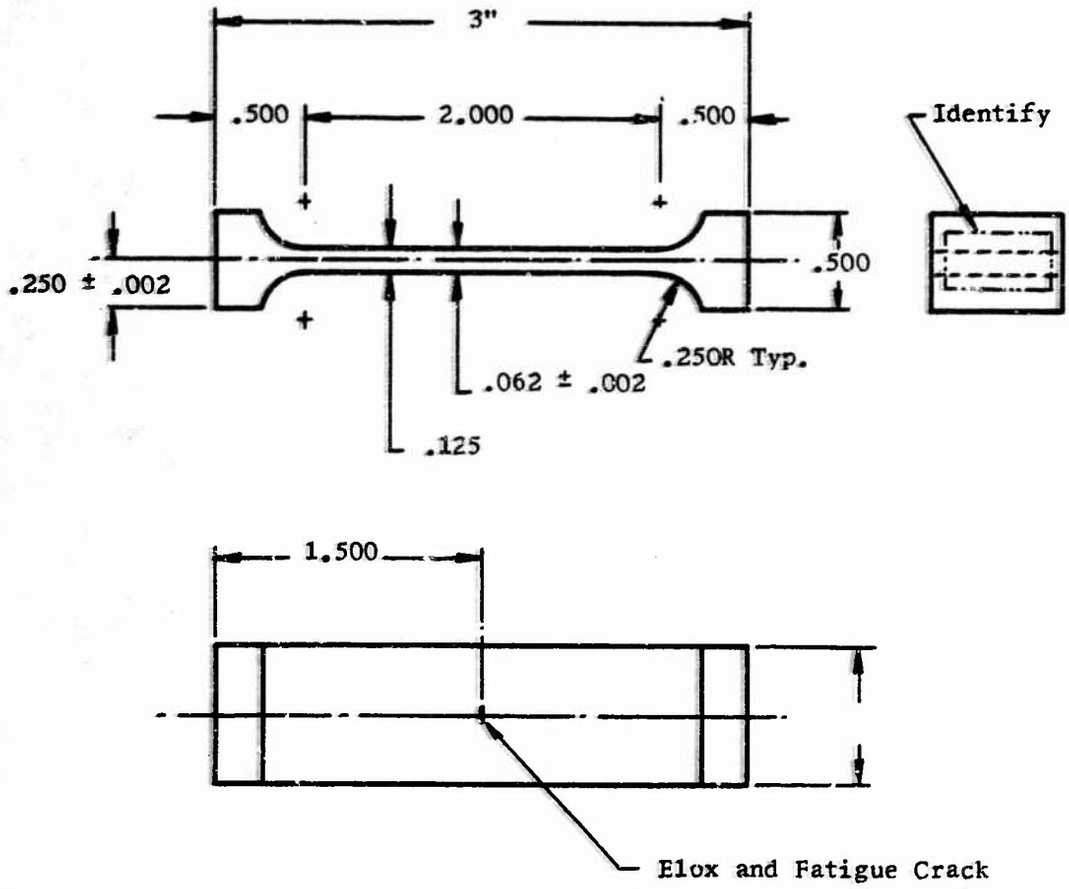


Figure 2. Part-Through-Crack Tensile Specimen

Information of the premature proof-test failures and the hydrotest behavior of the various chambers from which the CN-tensile data were taken is contained in Appendix C. In summary, the proof-test failure histories were as follows:

Chamber	Failure Pressure or Stress	No. of Cycles	Failure Location	Origin of Failure
R26	96 ksi	1	Fwd cyl near weld	Surface crack
2191456	457 psig	1	Fwd weld	Interacting porosity
673078	590 psig	11	Center near weld	Surface crack
R369	380 psig	1	Aft cyl near weld	Surface crack

Thus, with the exception of Chamber SN 2191456, the premature proof-test failures originated from part-through surface cracks (always in the ID surface) adjacent to the weld. Cracking in Chamber SN 673078 was in the weld heat-affected zone; in R26 and R369, it was in the increased-thickness chamber wall adjacent to the girth welds, but outside the darkly etched heat-affected zone.

C. CENTER-NOTCH TENSILE TESTS

The center-notch fracture-toughness testing was done with 3- x 12-in. panels containing an electric-discharge-machined slot, extended and sharpened by fatigue cycling. The test-specimen design is shown in Figure 3. The specimens were cut from 44- and 52-in.-dia barrel sections with the length of the test specimen in the axial direction of the chamber. The 52-in.-dia curvature was left in the test pieces. The specimens were tested in a pin-and-clevis loading fixture at 10,000 psi/min loading speed using a Baldwin-Weidermann 60,000-lb tensile machine. The tests were conducted in air at room temperature (70°F). The components from the chambers hydroburst at 212 and 320°F were tested at the respective hydrotest temperature as well as at room temperature.

Each center-notch tensile test was instrumented with two crack-opening-displacement (COD) gages and an accelerometer. The critical stress intensity factor (K_{Ic}) corresponding to plane-strain instability was calculated in four ways, viz., (1) based on the initial fatigue-crack length and the load corresponding to the deviation from linearity in the COD-versus-load plot, (2) based on the crack length (COD gage) and load corresponding to the deviation from linearity, (3) based on the initial fatigue-crack length and the load corresponding to pop-in as determined from stress-wave emission, and (4) based on the crack length (COD gage) and load corresponding to pop-in.

Plane stress instability was calculated in three ways, viz., (1) based on the crack length (from the COD gage) and load corresponding to the inflection in the stress-wave count-rate curve; (2) based on the crack length (COD gage) and maximum load as seen on the X-Y recording of the COD-gage output, and (3) based on the crack length as measured in the fracture surface and maximum load. Further details on the test method and calculations are contained in Appendix C.

D. PRECRACK CHARPY TESTS

In recent years, the precrack Charpy impact test has been used as a screening test in a number of research and development programs, including extensive use in the Aerojet 260-in.-dia solid-propellant rocket motor case development[3,4] and in the Boeing-North-American supersonic transport development program.[5] In common with other fracture toughness test specimens, the precracked Charpy suffers from limitations because of the small size of the specimen. However, the capacity of this specimen to measure high values of fracture toughness is much greater than its small size would indicate. The reason is that yielding of the net section, which occurs in tough materials, has comparatively little effect on the total energy absorbed in fracturing a Charpy specimen.

The merits and limitations of the precrack Charpy specimen for measuring fracture toughness are discussed in Appendix D, together with data that show the precrack Charpy test to be at least qualitative, in many materials semi-quantitative, and in some material conditions a quantitative measure of fracture toughness for high-strength sheet materials.

Assuming the precrack Charpy impact value to provide an approximation of G_c, the stress-intensity factor can be estimated from the precrack Charpy impact W/A value, based on the relationship

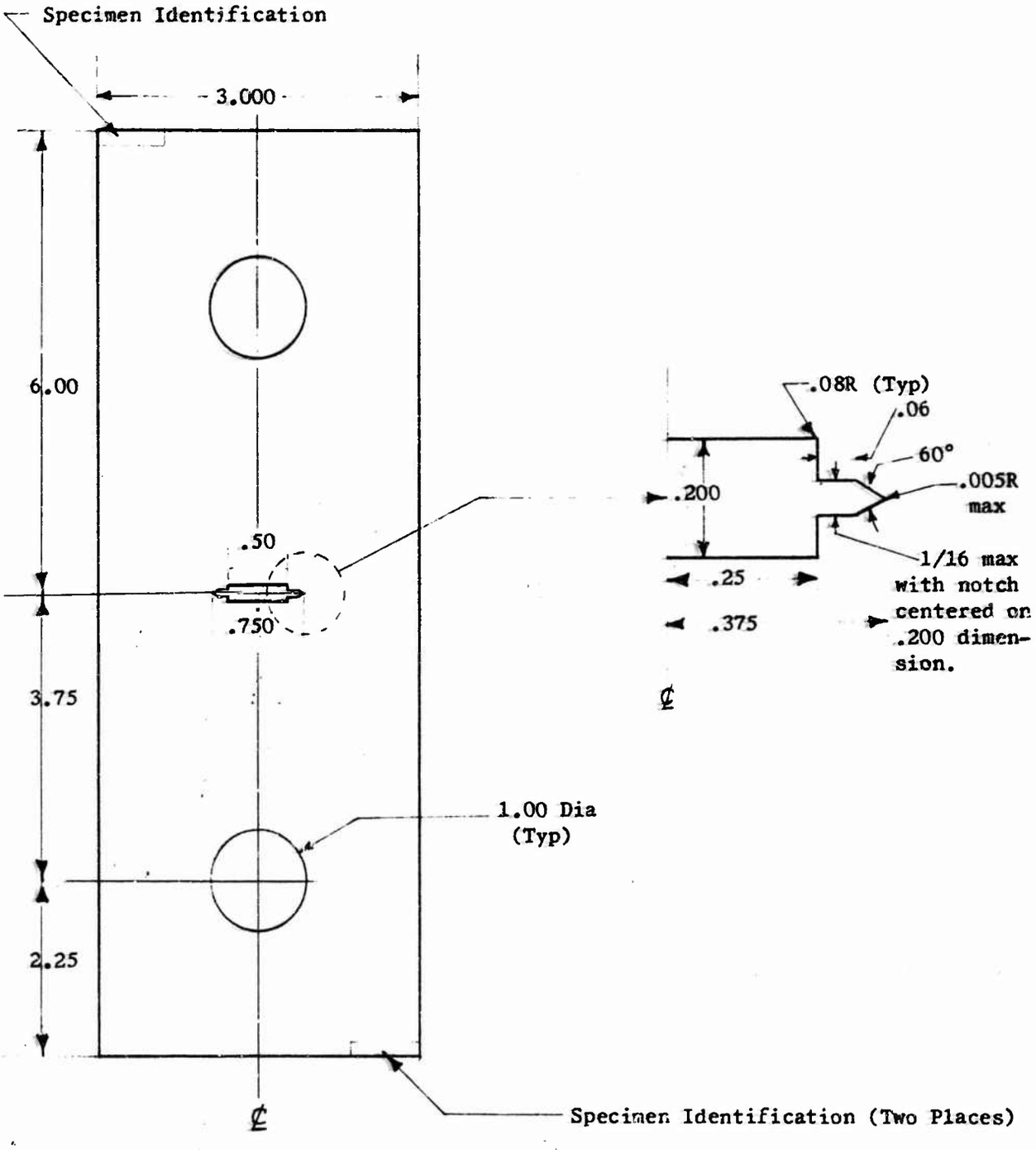
$$K_c^2 = E\, G_c$$

$$K_c = \left[E\, (W/A)_{pci} \right]^{1/2}$$

(3) L. Albertin, et al., Evaluation of High Nickel Steel for Application in Large Booster Motor Fabrication, Final Report ML-TDR-64-115 on Contract AF 33(657)-8740, April 1964.

(4) 260-In.-Dia Motor Feasibility Demonstration Program, Final Report NASA CR 72126 on Contract NAS3-6284, Vol. V, Appendix B: Material and Process Evaluation Program (240 pages) and Appendix C: Material Characterization Reports (324 pages) 8 April 1966.

(5) Thick Section Fracture Toughness, Final Report ML-TDR-64-236, Oct 1964 on Contract AF 33(657)-11461 by Boeing and North-American in a joint venture.



Note: Pin holes and center notch both must be located on specimen centerline ± .005.

Figure 3. Center-Notch Tensile Specimen

and assuming the precrack Charpy slow-bend value to provide an approximation of the plane-strain fracture toughness, the critical stress-intensity factor K_{Ic} can be estimated from the precrack Charpy slow-bend W/A value based on the relationship

$$(1-\mu^2)K_{Ic}^2 = E\,G_{Ic}$$

$$K_{Ic} = \left[E\,(W/A)_{pcsb}/(1-\mu^2)\right]^{1/2}$$

where μ is Poisson's ratio and E is Young's modulus.

IV.

DISCUSSION OF RESULTS

A. UNIAXIAL TENSILE DATA

1. Room Temperature Tests

Three tensile specimens oriented in the circumferential direction were cut and machined to provide triplicate specimens for each forging. The heat code, heat number, chemistry, and beta transus are listed in Table I for each forging. The heat numbers referred to in the statistical analysis portion are actually the heat code numbers, since not all the heat numbers are available.

The specimens were tested at a strain rate of 0.005 in./in./min, with the following data recorded for each test:

a. Specimen diameter
b. Maximum load
c. Load at 0.2% offset
d. Percent elongation for a 4D gage length

The room temperature tensile data were statistically analyzed as follows:

a. Using the analysis-of-variance technique (ANOVA), the test variation, forging-to-forging variation, and heat-to-heat variations were evaluated.

b. The yield strength at 0.2% offset and ultimate tensile strength, above which at least 99%, A-Basis, and 90%, B-Basis, of the population value is expected to fall with a confidence of 95%, were determined in accordance with MIL-HDBK-5, paragraph 1.3.10 and 1.4.1.

A step-by-step description of the methods used in the analysis-of-variance technique is presented in Appendix E.

For the ultimate tensile strength, yield strength at 0.2% offset, and percent elongation (4D), the measured value of each point was plotted versus cumulative percent on probability paper (Figure 4). As can be seen in Figure 4, the ultimate tensile strength and percent elongation exhibit a near normal distribution, but the yield strength exhibits a non-normal distribution. Treating the yield strength data as a non-normal distribution, the A- and B-basis values are 156 ksi and 158 ksi, respectively. These values are somewhat high because the material specification called out a minimum yield strength of 155 ksi; therefore, any value less than 155 ksi would not have been included in the data analyzed. To compensate for the truncated distribution, a best line was estimated and it was assumed that the data exhibited a normal distribution, as indicated by the straight line. The data are summarized as follows:

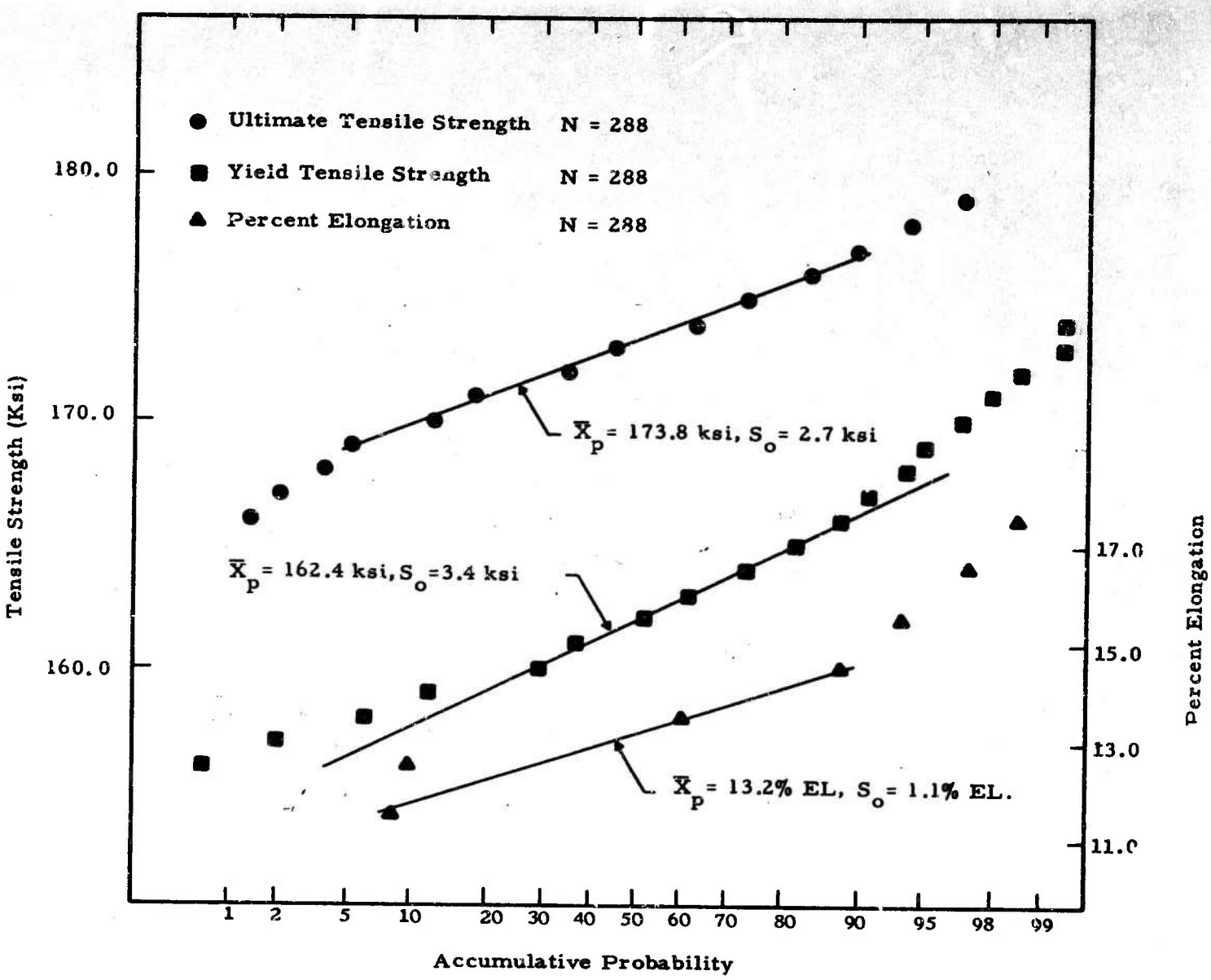


Figure 4. Room Temperature Tensile Results vs Probability

	N	S_e^2	S_F^2	S_H^2	S_o^2	$\bar{X}_P$
Ultimate Tensile Strength, ksi	288	3.13	2.77	6.96	7.29	173.8
Yield Strength at 0.2% Offset, ksi	288	4.13	3.59	8.87	11.56	162.4
Percent Elongation (4D)	288	0.6	0.5	0.6	1.1	13.2

For input to MIL-HDBK-5, the data were treated as having a normal distribution, and the results are as follows:

A-Basis, use $\bar{X} - S_o k_A$, where $k_A = 2.77$ for $n = 288$

Ultimate Tensile Strength	173.8 - 2.7(2.77) = 166.3 ksi
Yield Strength at 0.2% Offset	162.4 - 3.4(2.77) = 153.0 ksi
Percent Elongation (4D)	13.2 - 1.1(2.77) = 10.2% Elongation

B-Basis, use $\bar{X} - S_o k_B$, where $k_B = 1.77$ for $n = 288$

Ultimate Tensile Strength	173.8 - 2.7(1.77) = 168.8 ksi
Yield Strength at 0.2% Offset	162.4 - 3.4(1.77) = 156.4 ksi
Percent Elongation (4D)	13.2 - 1.1(1.77) = 11.3% Elongation

See Table III for input of above results into MIL-HDBK-5 format. The format used was suggested in Reference 6.

2. Elevated Temperature Tests

Three or four specimens oriented in the circumferential direction were tested from each forging, as listed in Table II. The specimens were tested at a strain rate of 0.005 ± 0.002 in./in./min, and the following data recorded for each test:

a. Test temperature
b. Maximum load
c. Load at 0.2% offset
d. Specimen diameter
e. Percent elongation for a 4D gage length

For input to MIL-HDBK-5, the individual property is shown as a percent of its tabulated room temperature value as either mean curves or curves that are not more than 5% above minimum boundary of all original data points on dimensional plots, whichever is lower (MIL-HDBK-5, paragraph 1.4.1.3).

(6) D. P. Moon and W. S. Hyler, MIL-HDBK-5, "Guidelines for the Presentation of Data," Air Force Materials Laboratory Technical Report AFML-TR-66-386, February 1967.

TABLE III

SUGGESTED INPUT TO MIL-HDBK-5

Table . Design Mechanical Properties of Ti-6Al-4V Extrusion

Alloy	(a)	
Form	Extrusion	
Condition	Solution Treated and Aged	
Thickness	up to 0.50 inch	
Basis	A	B
Mechanical Properties:(b)		
F_{tu}(c) ksi	166.3	168.8
F_{ty}(c) ksi	153.0	156.4
e, percent in 4D	10.2	
K_{Ic}(d) ksi-in.$^{\frac{1}{2}}$	30.6	35.2

(a) In accordance with Aerojet-General Specification AGC-34007A, the Chemistry Requirements are as follows:

	Percent		Percent
Aluminum	5.50 - 6.75	Carbon	0.10 max
Vanadium	3.50 - 4.50	Nitrogen	0.05 max
Iron	0.30 max	Hydrogen	0.0125 max
Oxygen	0.12 - 0.20	Other Elem.	0.40 max
		Titanium	Balance

(b) All values are for specimens oriented in the hoop direction of the extrusion.
(c) Heat treated as 0.5-in.-thick cylindrical extrusion, then machined to 1/4-in.-dia tensile specimens centered at mid-thickness.
(d) Same as (c), only machined to 0.125-in.-thick flat specimen, centered at mid-thickness in the extrusion wall.

For the ultimate tensile strength, yield strength at 0.2% offset and percent elongation (4D), the measured value of each point was plotted versus cumulative percent on probability paper (see Figures 5, 6, and 7). From these figures, it is apparent that the data for most of the temperatures tested exhibited a near normal distribution, between 10 and 90 percent. Since the means and minimum values were all that was required to construct the curves for suggested input to MIL-HDBK-5, it was not necessary that the data exhibit a normal distribution. The mean values for each temperature were calculated and they agreed almost exactly with the values from Figures 5, 6, and 7. The means were taken for each test temperature and Figures 8, 9, and 10 were constructed for input to MIL-HDBK-5. For detailed information concerning the construction of these figures, see Appendix E.

B. PART-THROUGH-CRACK TENSILE K_{Ic} DATA

A complete tabulation of data (computer printout) from the part-through-crack tensile tests is contained in Appendix B, together with various plots and discussion. Since the prime objective of this study is a MIL-HDBK-5 data collection, only a summary of the findings is deemed appropriate at this point in the text.

1. Engineering Analysis of Test Results

To determine the variation in K_{Ic} attributable to between-forging, between-heat, and between-laboratory variability, both an engineering evaluation (plots of K_{Ic} data versus crack and specimen dimensions) and statistical analysis were employed. The following discussion of results is based on the engineering and metallurgical observations.

Selected forgings were analyzed for the effect of specimen size (width and thickness) on the plane-strain fracture toughness (K_{Ic}) measurement. Based on a more or less constant K_{Ic} when plotted as a function of crack and specimen dimensions, it was concluded that the test specimen was adequate for testing Minuteman-chemistry 6Al-4V titanium at approximately 160 ksi yield strength.

The effect of tensile-strength variations on the K_{Ic} values was determined for the 109-forging sample; increasing yield strength in the range of 157 to 168 ksi and increasing ultimate tensile strength in the range of 167 to 178 ksi produced a slight downward trend in K_{Ic} in the overall plot of data from 109 forgings. Detailed analysis was complicated by forging-to-forging differences in K_{Ic}. Furthermore, comparison of results from the three laboratories, where forgings were tested in more than one laboratory, revealed small but significant differences between the test results in some forgings, but not all.

Data from multiple forgings from a single heat of titanium, and multiple forgings from a single billet of titanium revealed significant differences in K_{Ic} values from forging to forging when the precracks approached mid-thickness of the original forging. Forging differences for a given heat of titanium and for a given billet of titanium suggest that the differences in K_{Ic} values with deep cracks are metallurgical rather than a deficiency in the linear-elastic equations used to calculate the K_{Ic} values.

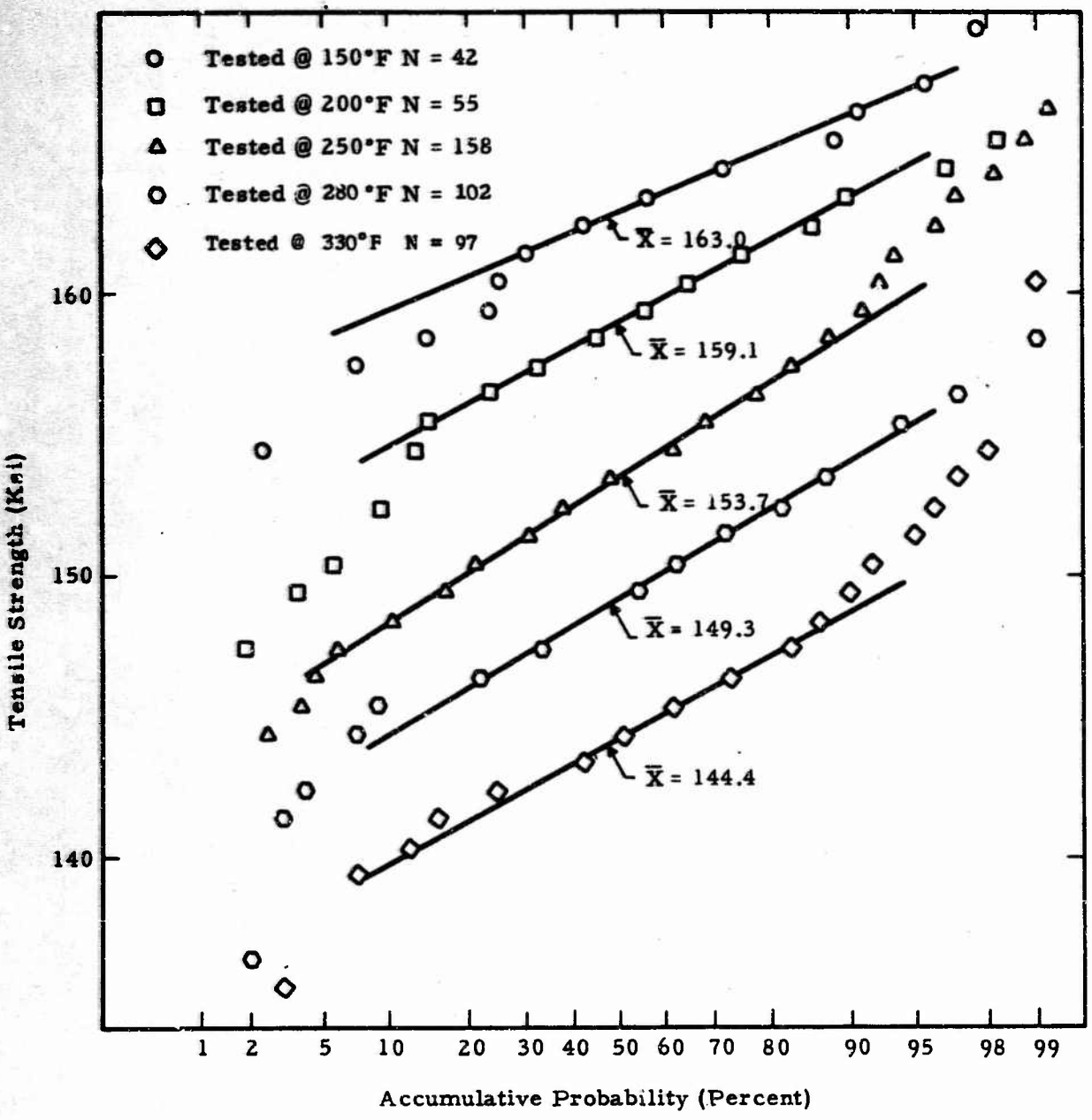


Figure 5. Ultimate Tensile Strength at Elevated Temperature vs Probability

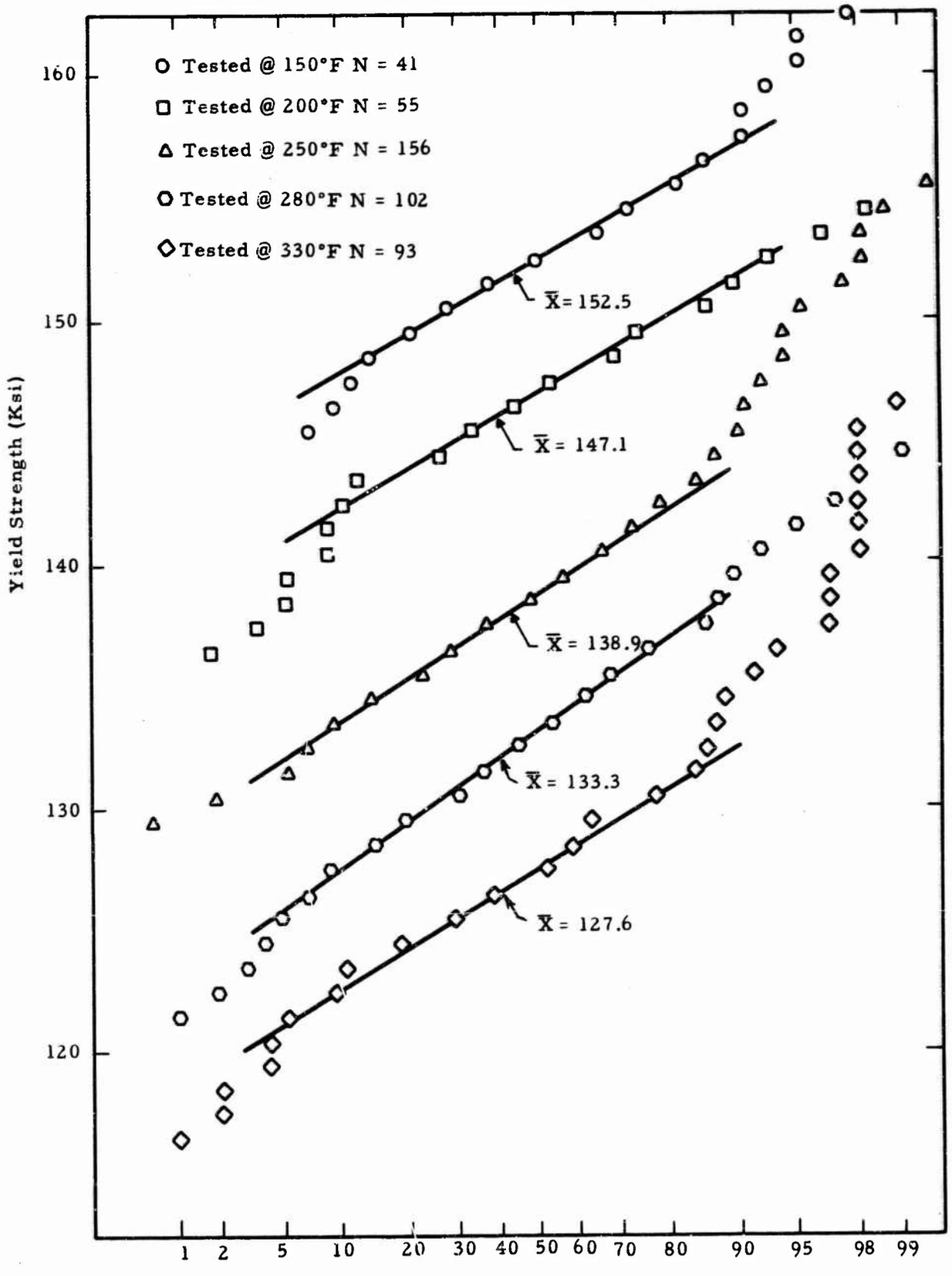


Figure 6 Yield Strength Elevated Temperature Versus Probability

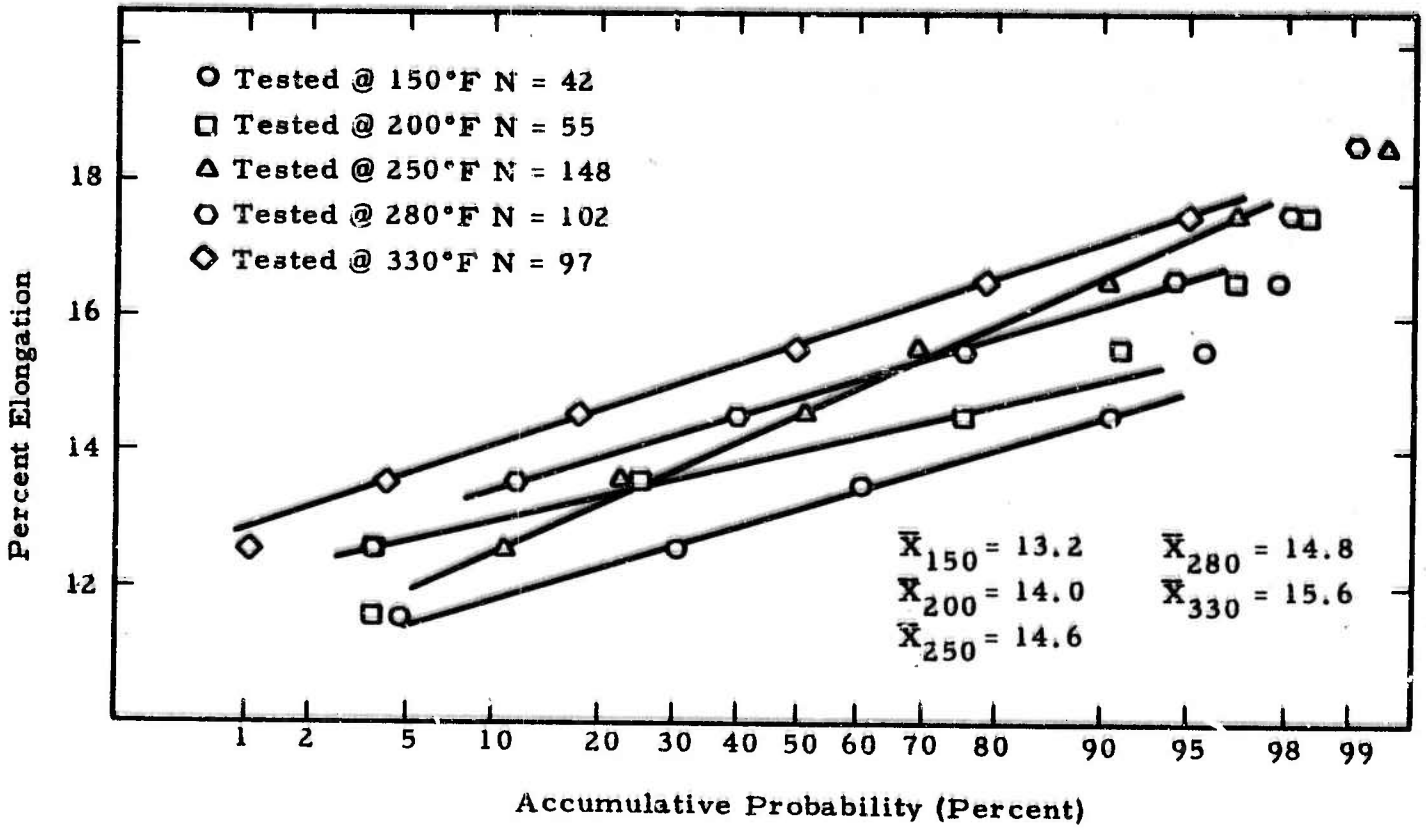


Figure 7. Percent Elongation at Elevated Temperature vs Probability

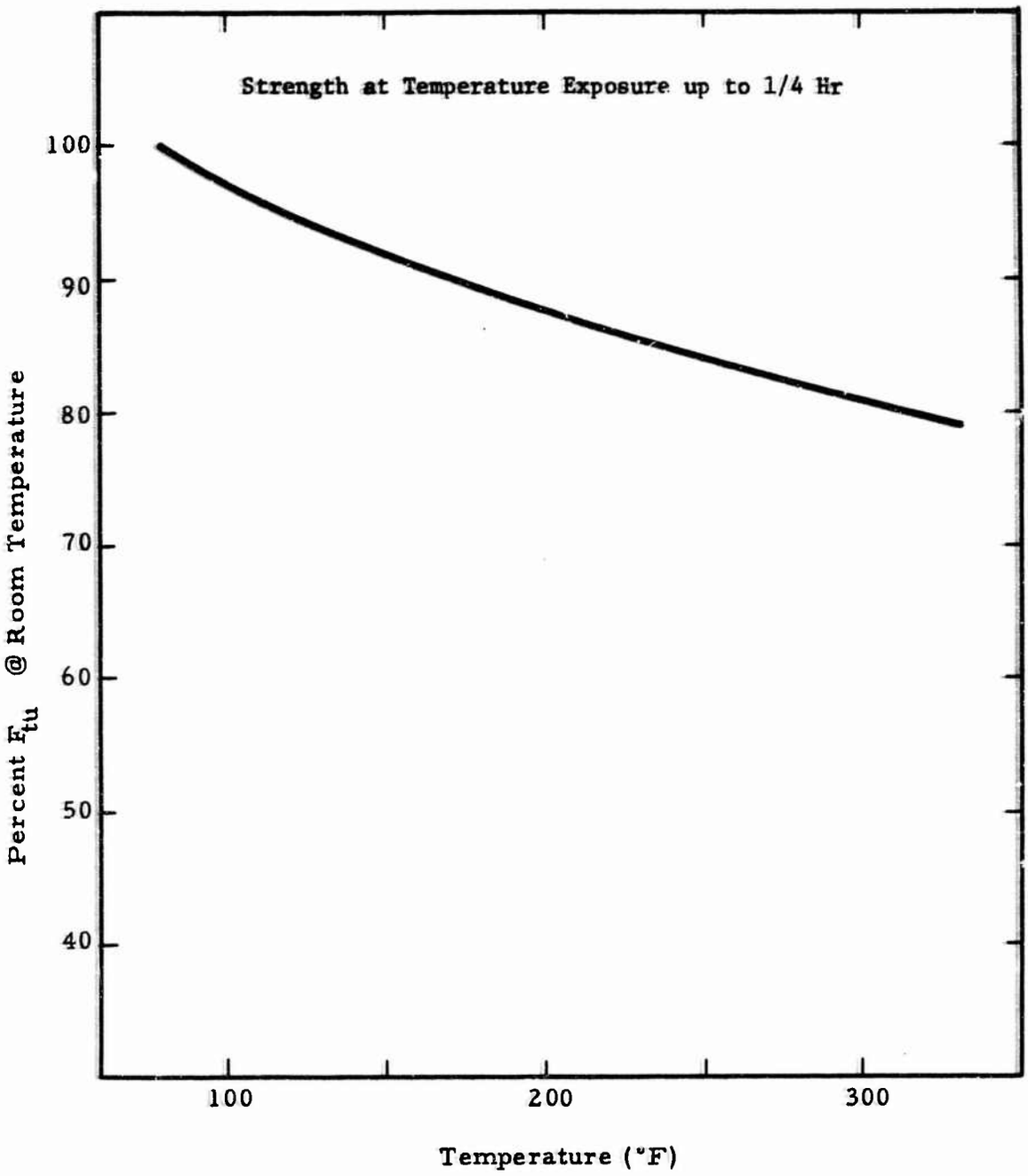


Figure 8. Effect of Temperature on Ultimate Tensile Strength (F_{tu}) of Solution Treated and Aged Ti-6Al-4V Alloy

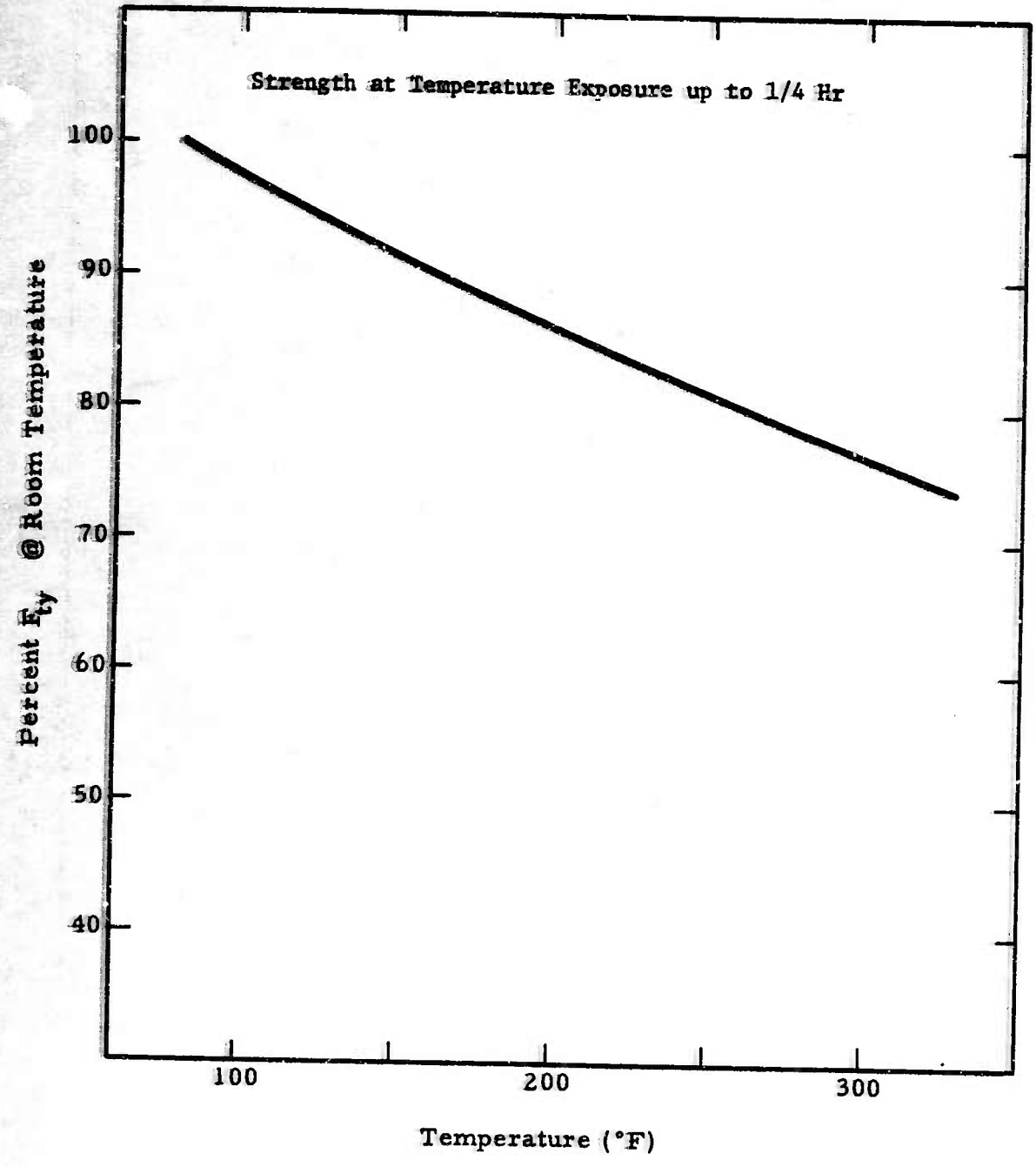


Figure 9. Effect of Temperature on Yield Strength (F_{ty}) of Solution Treated and Aged Ti-6Al-4V Alloy

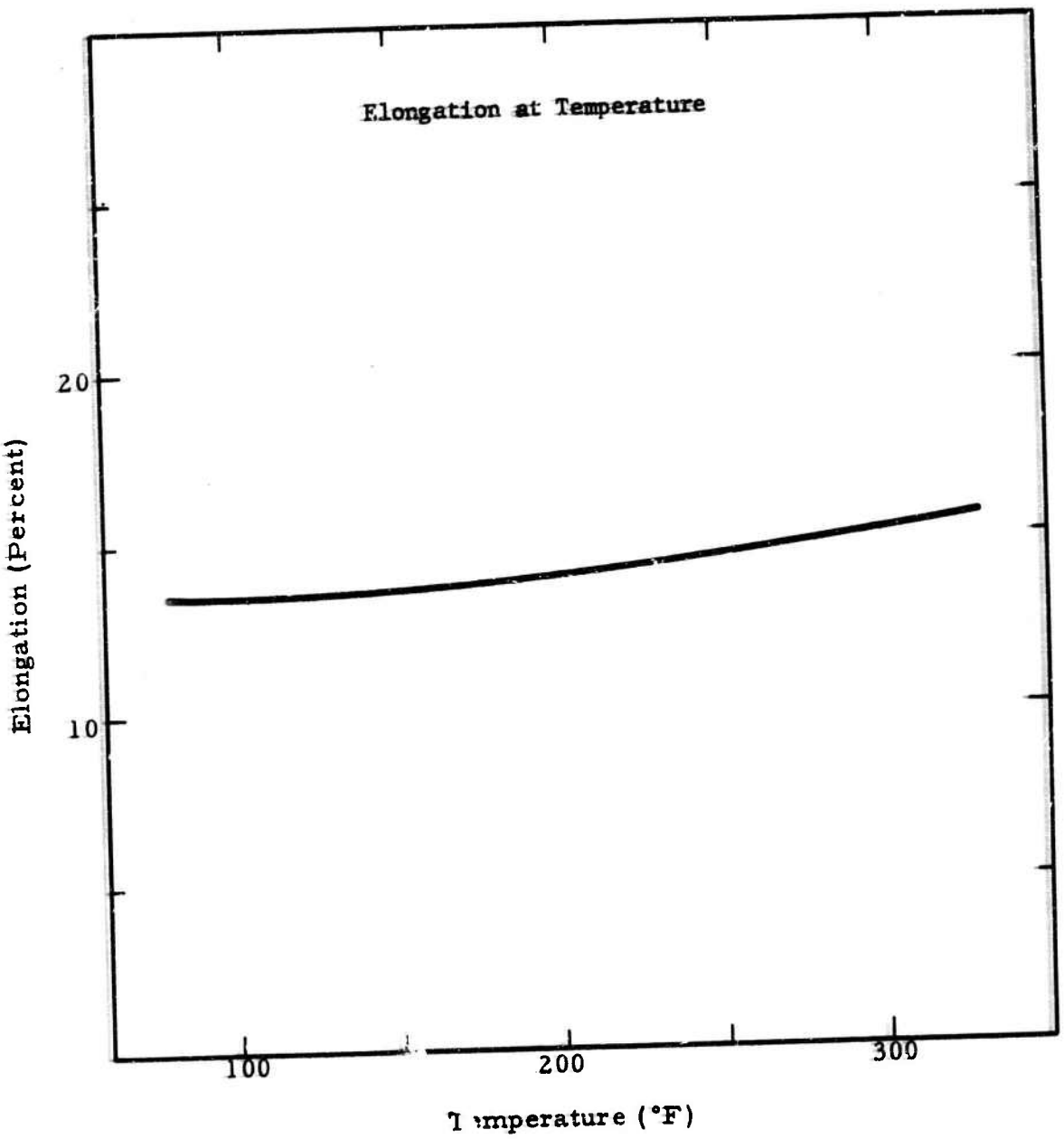


Figure 10. Effect of Temperature on Percent Elongation of Solution Treated and Aged Ti-6Al-4V Alloy

2. Statistical Analysis

The PTC data were statistically analyzed to determine the following: (1) the test variation, forging-to-forging variation, heat-to-heat variation, and laboratory-to-laboratory variation, based on analysis-of-variance technique (ANOVA); (2) the differences in K_{Ic} that can be detected for the different crack areas; (3) the number of test observations necessary to determine given differences in K_{Ic} at a given confidence level; and (4) the toughness value above which at least 99%, A-Basis, and 90%, B-Basis, of the population values are expected to fall, with a confidence of 95% (MIL-HDBK-5, paragraph 1.3.10 and 1.4.1).

A detailed description of the methods used in the analysis of variance technique is presented in Appendix E. The data for each test laboratory was analyzed separately, and for all laboratories the data for $a/Q \sim 0.02$ was separated from that of $a/Q \sim 0.04$.

a. Variation in K_{Ic} for a Crack Depth (a/Q) of Approximately 0.02 in.

The probability plot for each of the test laboratories is shown on Figure 11. As seen in Figure 11, the K_{Ic} data for each laboratory falls on a straight line, indicating that the data has a near-normal distribution.

The analysis of the K_{Ic} data was carried out separately for each laboratory and the statistical calculations for each are found in Appendix E. The results of this analysis for each laboratory are summarized in the following table:

		ksi^2-in.				
Test Laboratory	N	S_e^2 (error)	S_F^2 (forging)	S_H^2 (heat)	S_L^2 (laboratory)	$\bar{X}_L$ (ksi-in.$^{1/2}$)
Sacramento	127	1.64	0.61	1.54	2.89	38.3
Downey	68	0.91	0.87	2.17	2.25	40.1
Lycoming	89	0.81	0.63	0.38	1.44	39.9

It was determined that statistically, at the 0.05 level of significance, there was a significant difference between Sacramento data and the Downey and Lycoming data. It is possible that the significant difference may be attributed to the fact that Sacramento tested more forgings and twice as many heats as either Downey or Lycoming, and that the actual population may be broader than indicated by either Downey or Lycoming data. Included in the evaluation program were several forgings tested at two

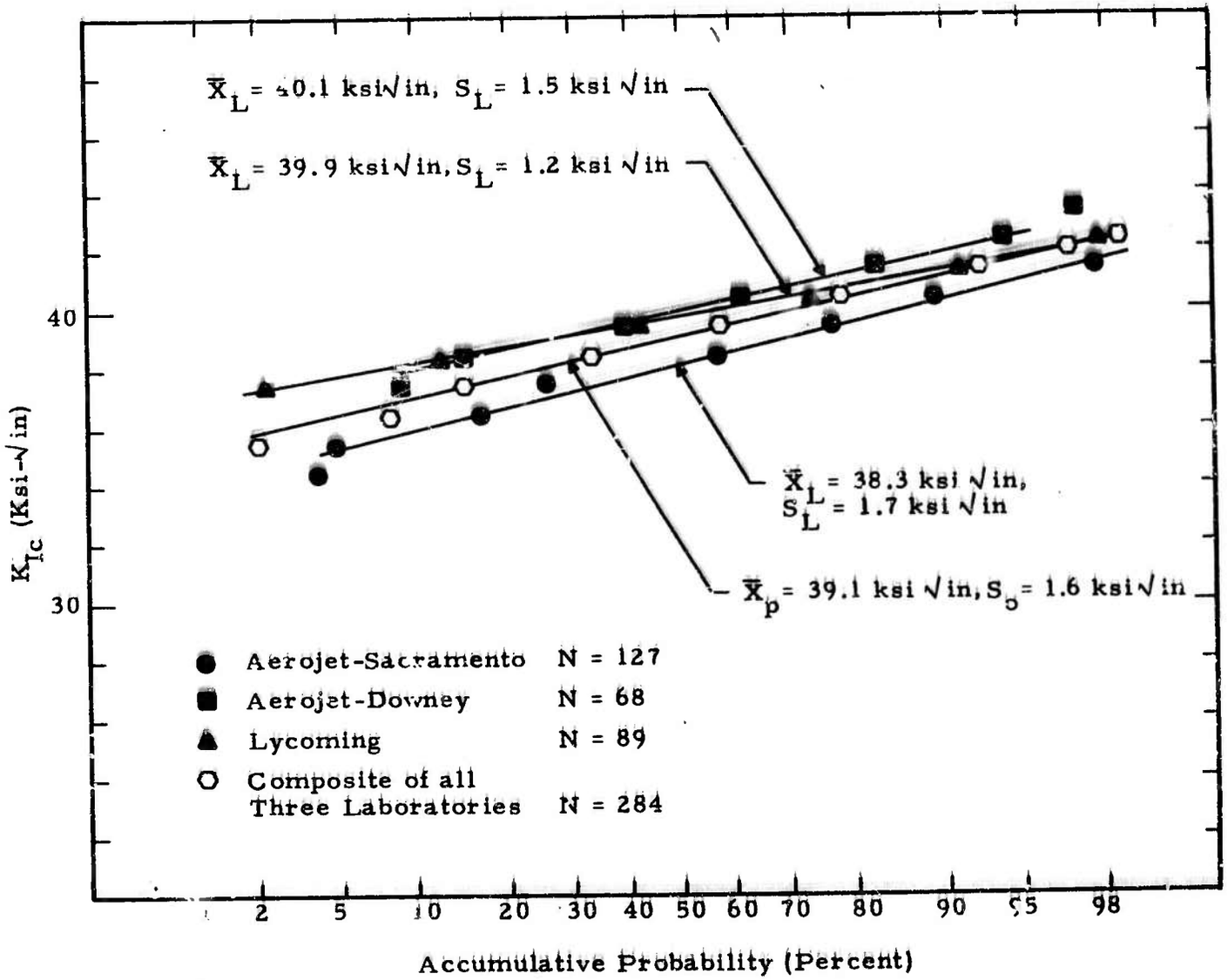


Figure 11. K_{Ic} vs Probability for a/Q ~ 0.02

laboratories; Sacramento, however, was involved in all duplicate testing. The results from the duplicate specimens were tested statistically to determine if they were equal. Of the seven sets of duplicate specimens tested, only one set indicated that the means were not equal. With this in mind, it was decided to pool the values. By pooling all of the data and plotting on probability paper (Figure 11), it was possible to obtain $\bar{X}_p$ and S_o; these are not exact values but, practically, they give a reasonable representation of the population tested at any laboratory. The best estimate of the population mean ($\bar{X}_p$) and the standard deviation (S_o) from Figure 11 is $\bar{X}_p$ = 39.1 ksi-in.$^{1/2}$ and S_o = 1.6 ksi-in.$^{1/2}$

b. Variation in K_{Ic} for a Crack Depth (a/Q) of Approximately 0.04 in.

The data for each of the test laboratories are plotted in Figure 12. As can be seen in Figure 12, Aerojet-Sacramento and Aerojet-Downey data do not exhibit a normal distribution, although Lycoming does exhibit a near-normal distribution. The analysis of the data was carried out separately for each laboratory and the statistical calculations are found in Appendix E. The results for each laboratory are summarized on the following table:

		ksi^2-in.	
Test Laboratory	N	S_e^2 (error)	S_F^2 (forging)
Sacramento	96	6.37	1.98
Downey	74	2.79	2.09
Lycoming	86	3.24	2.77

The balance of the results were not calculated because, for each laboratory, when tested for equality of heat averages, the ANOVA test indicated the data were not homogeneous. The ANOVA test results agreed with the normality plots; therefore, the K_{Ic} data were not statistically analyzed.

c. Difference in K_{Ic} That Can Be Detected for the Different Crack Areas

The data were analyzed for a/Q $\sim$ 0.02 and a/Q $\sim$ 0.04 to determine the effect of crack depth-to-thickness ratio (a/B), crack-area-to-cross-sectioned-area ratio (Ca/BW), and gross-stress-to-yield-stress ratio (F_G/F_{ty}) on K_{Ic}. There was no apparent relationship between K_{Ic} and Ca/BW or a/B, but there was a definite relationship between K_{Ic} and F_G/F_{ty}; this is shown in Figures 13 and 14. For further details of the correlation between K_{Ic} and a/B, Ca/BW, and F_G/F_{ty}, see Appendix E.

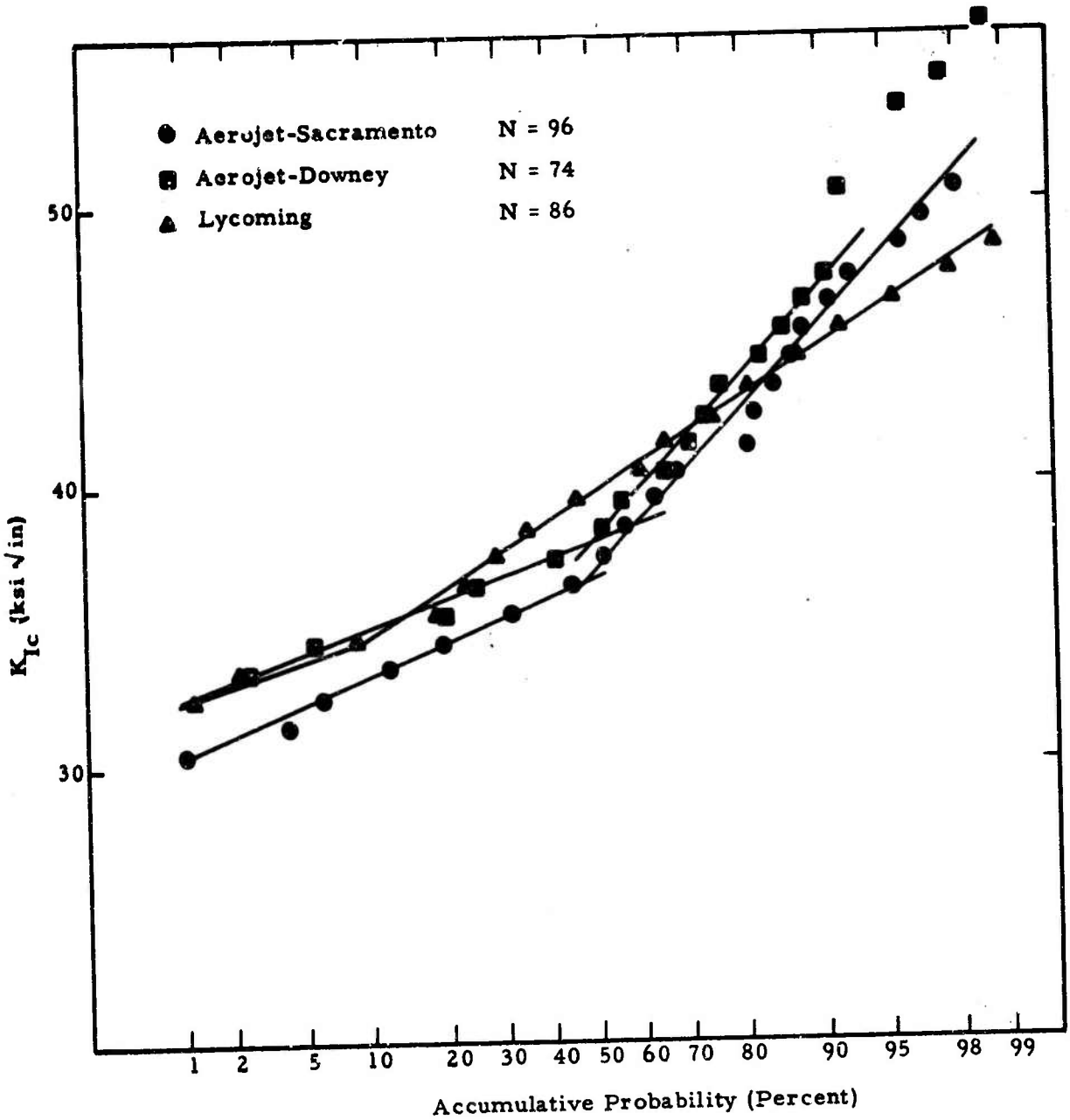


Figure 12. K_{Ic} vs Probability for a/Q ~ 0.04

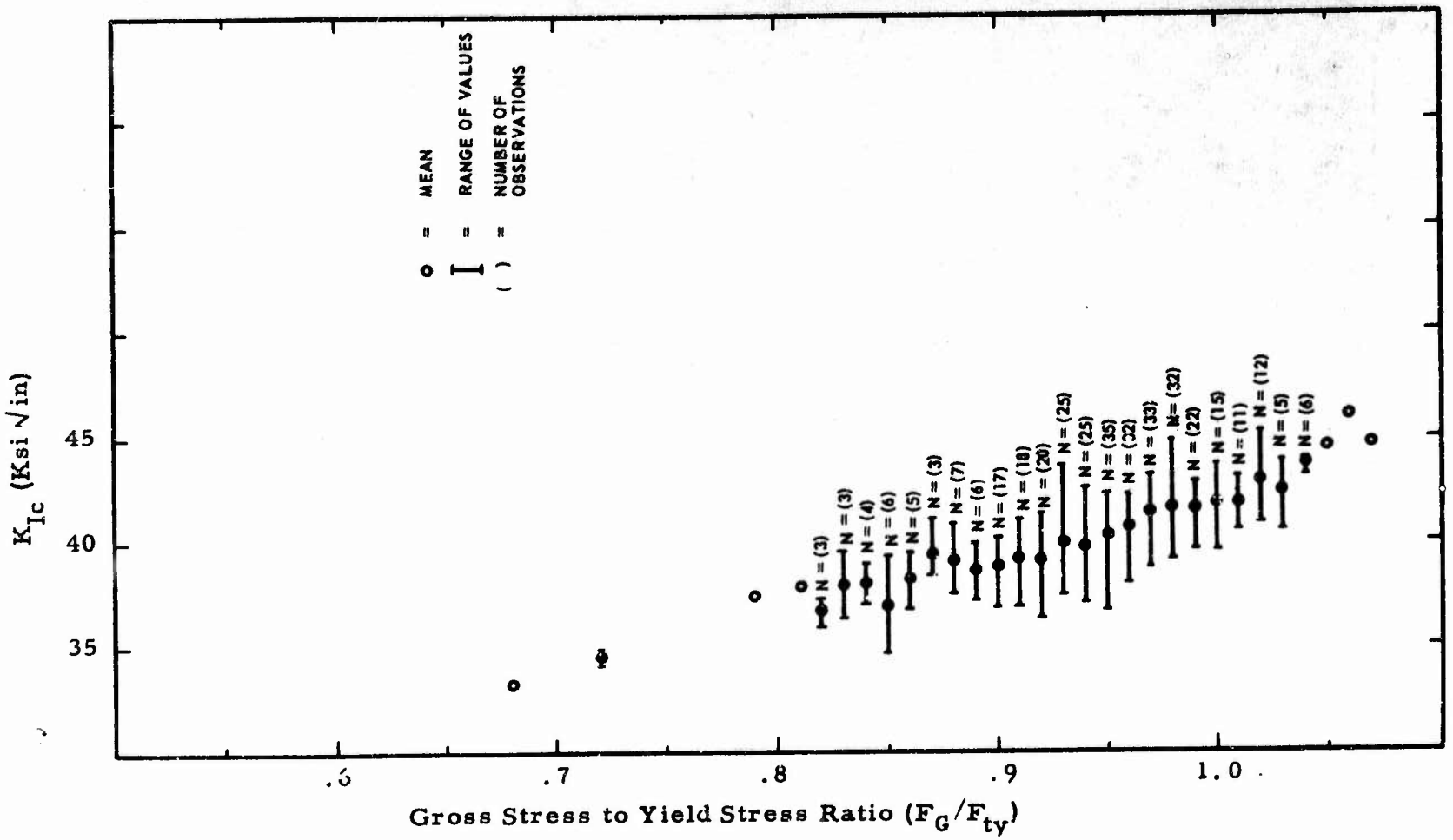


Figure 13. K_{Ic} vs F_G/F_{ty} for a/Q ~ 0.02

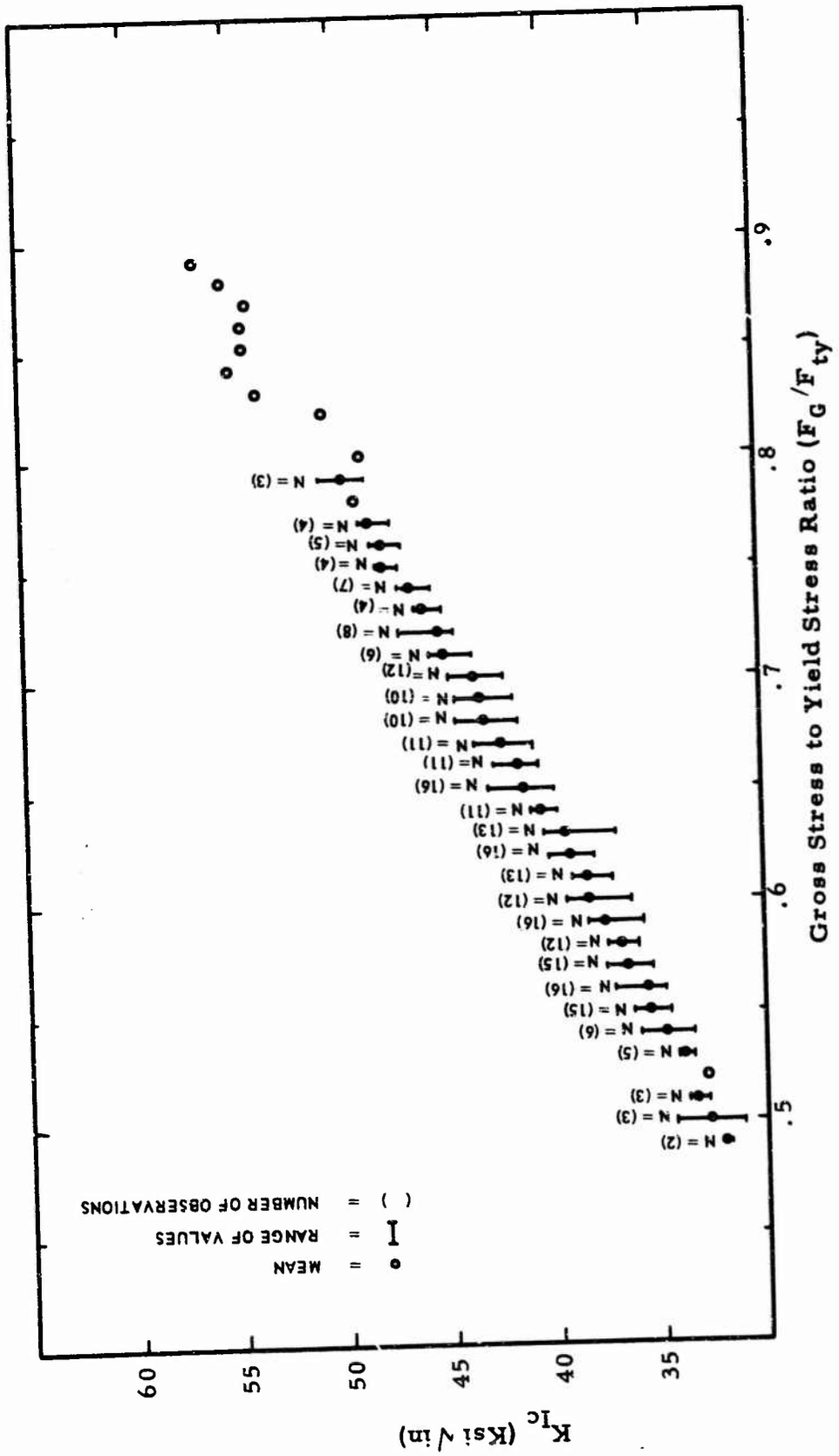


Figure 14. K_{Ic} vs F_G/F_{ty} for a/Q ~ 0.04

d. The Number of Test Observations Necessary to Determine Given Differences in K_{Ic} at a Given Confidence Level

The number of test observations necessary to determine a given difference in K_{Ic} at a given confidence level may be obtained from Table IV.(7) In order to use Table IV, substitute S = 1.6 ksi-in.$^{1/2}$ for σ and a given difference $|X_1-X_2|$ for δ, the number of required observations may then be determined by using the proper columns corresponding to the desired α and β error.

e. Data for MIL-HDBK-5

Statistically, there is a significant difference between K_{Ic} values collected for a/Q $\sim$ 0.02 and a/Q $\sim$ 0.04. From a practical standpoint, for input to MIL-HDBK-5, all of the data will be utilized and treated as a non-normal distribution.

All of the observations were listed in sequence with the smallest value as Number 1. Using a table (Rank, r, of Observations for an Unknown Distribution Having the Probability and Confidence of A and B Values)(8) and the fact that there were 540 specimens used in this test, the number of the specimens corresponding to the A-Basis is Number 2 and for B-Basis, Number 43. The values corresponding to the A-Basis and B-Basis are 30.6 ksi-in. and 35.2 ksi-in., respectively. The input of K_{Ic} data to MIL-HDBK-5 is found in Table III.

C. CENTER-NOTCH TENSILE DATA

1. Plane-Strain K_{Ic} Data

A total of 18 cylindrical forgings from nine Minuteman rocket motor cases were tested at room temperature. Two of the deliberately hydroburst chambers also were tested at elevated temperature to simulate in-flight aerodynamic heating. One of the chambers which failed in a girth weld was tested with CN tensiles centered on each of the three girth welds.

The data from these tests are tabulated as computer prinouts in Appendix C. A summary of the plane-strain K_{Ic} data is presented in Table V. The K_{Ic} value based on the initial fatigue-cracked center-notch half length (AO) and the load corresponding to deviation from linearity in the COD chart (PD) are presented as minimum K_{Ic} values. Note that the room-temperature values based on deviation from linearity in COD (AO-PD) were low, the average values ranging from 24.6 to 43.4 ksi-in.$^{1/2}$ for the 18 forgings tested; note, also, that the elevated-temperature tests produced little if any increase with

(7) G.E.P. Box, L. R. Connor, W. R. Cousins, O. L. Davies, F. R. Harmsworth, G. P. Silltto, The Design and Analysis of Industrial Experiments, O. L. Davies, ditor, Hafner Publishing Co., N.Y., 1956
(8) D. P. Moon and W. S. Hyler, ibid.

TABLE IV

NUMBER OF OBSERVATIONS FOR t-TEST OF DIFFERENCE BETWEEN TWO MEANS

The entries in this table show the number of observations needed in a t-test of the significance of the difference between two means in order to control the probabilities of the errors of the first and second kinds at α and β, respectively.

		Level of t-Test																				
		0.01					0.02					0.05					0.1					
Single-sided test		α = 0.005					α = 0.01					α = 0.025					α = 0.05					
Double-sided test		α = 0.01					α = 0.02					α = 0.05					α = 0.1					
	β	0.01	0.05	0.1	0.2	0.5	0.01	0.05	0.1	0.2	0.5	0.01	0.05	0.1	0.2	0.5	0.01	0.05	0.1	0.2	0.5	
	0.05																					0.05
	0.10																					0.10
	0.15																					0.15
	0.20																				137	0.20
	0.25															124					88	0.25
	0.30										123					87					61	0.30
	0.35					110					90					64				102	45	0.35
	0.40					85					70				100	50			108	78	35	0.40
	0.45				118	68				101	55			105	79	39		108	86	62	28	0.45
	0.50				96	55			106	82	45		106	86	64	32		88	70	51	23	0.50
	0.55			101	79	46		106	88	68	38		87	71	53	27	112	73	58	42	19	0.55
	0.60		101	85	67	39		90	74	58	32	104	74	60	45	23	89	61	49	36	16	0.60
Value of	0.65		87	73	57	34	104	77	64	49	27	88	63	51	39	20	76	52	42	30	14	0.65
$D = \frac{\delta}{\sigma}$	0.70	100	75	63	50	29	90	66	55	43	24	76	55	44	34	17	66	45	36	26	12	0.70
	0.75	88	66	55	44	26	79	58	48	38	21	67	48	39	29	15	57	40	32	23	11	0.75
	0.80	77	58	49	39	23	70	51	43	33	19	59	42	34	26	14	50	35	28	21	10	0.80
	0.85	69	51	43	35	21	62	46	38	30	17	52	37	31	23	12	45	31	25	18	9	0.85
	0.90	62	46	39	31	19	55	41	34	27	15	47	34	27	21	11	40	28	22	16	8	0.90
	0.95	55	42	35	28	17	50	37	31	24	14	42	30	25	19	10	36	25	20	15	7	0.95
	1.00	50	38	32	26	15	45	33	28	22	13	38	27	23	17	9	33	23	18	14	7	1.00
	1.1	42	32	27	22	13	38	28	23	19	11	32	23	19	14	8	27	19	15	12	6	1.1
	1.2	36	27	23	18	11	32	24	20	16	9	27	20	16	12	7	23	16	13	10	5	1.2
	1.3	31	23	20	16	10	28	21	17	14	8	23	17	14	11	6	20	14	11	9	5	1.3
	1.4	27	20	17	14	9	24	18	15	12	8	20	15	12	10	6	17	12	10	8	4	1.4
	1.5	24	18	15	13	8	21	16	14	11	7	18	13	11	9	5	15	11	9	7	4	1.5

TABLE IV (cont.)

	Level of t-Test																				
	0.01					0.02					0.05					0.1					
Single-sided test	$\alpha = 0.005$					$\alpha = 0.01$					$\alpha = 0.025$					$\alpha = 0.05$					
Double-sided test	$\alpha = 0.01$					$\alpha = 0.02$					$\alpha = 0.05$					$\alpha = 0.1$					
β	0.01	0.05	0.1	0.2	0.5	0.01	0.05	0.1	0.2	0.5	0.01	0.05	0.1	0.2	0.5	0.01	0.05	0.1	0.2	0.5	
1.6	21	16	14	11	7	19	14	12	10	6	16	12	10	8	5	14	10	8	6	4	1.6
1.7	19	15	13	10	7	17	13	11	9	6	14	11	9	7	4	12	9	7	6	3	1.7
1.8	17	13	11	10	6	15	12	10	8	5	13	10	8	6	4	11	8	7	5		1.8
1.9	16	12	11	9	6	14	11	9	8	5	12	9	7	6	4	10	7	6	5		1.9
2.0	14	11	10	8	6	13	10	9	7	5	11	8	7	6	4	9	7	6	4		2.0
Value of $D = \frac{\delta}{\sigma}$ 2.1	13	10	9	8	5	12	9	8	7	5	10	8	6	5	3	8	6	5	4		2.1
2.2	12	10	8	7	5	11	9	7	6	4	9	7	6	5		8	6	5	4		2.2
2.3	11	9	8	7	5	10	8	7	6	4	9	7	6	5		7	5	5	4		2.3
2.4	11	9	8	6	5	10	8	7	6	4	8	6	5	4		7	5	4	4		2.4
2.5	10	8	7	6	4	9	7	6	5	4	8	6	5	4		6	5	4	3		2.5
3.0	8	6	6	5	4	7	6	5	4	3	6	5	4	4		5	4	3			3.0
3.5	6	5	5	4	3	6	5	4	4		5	4	4	3		4	3				3.5
4.0	6	5	4	4		5	4	4	3		4	4	3			4					4.0

TABLE V

SUMMARY OF CENTER-NOTCH TENSILE PLANE-STRAIN K_{Ic} DATA
AND PRECRACK CHARPY SLOW-BEND W/A DATA

Chamber	Cylinder Yield, ksi	CN-Tensile K_{Ic} AO-PD*	CN-Tensile K_{Ic} AO-PP*	Slow Bend W/A (in.-lb/in.^{2})	Slow Bend W/A (ksi-in.$^{1/2}$)
R26	Fwd	27.6 - 33.1	43.8 - 52.6	173 - 238	
	165.0	Ave(2) 30.3	Ave(2) 48.2	Ave(6) 194	59
	Aft	35.9 - 51.5	70.4 - 80.5	344 - 436	
	165.0	Ave(3) 43.4	Ave(3) 74.6	Ave(6) 377	82
2191456	Fwd	27.2 - 29.6	39.6 - 43.0	119 - 132	
	159.4	Ave(3) 29.0	Ave(3) 41.2	Ave(6) 122	47
	Aft	36.4 - 44.4	55.1 - 72.8	276 - 311	
	162.0	Ave(3) 39.5	Ave(2) 63.9	Ave(6) 286	72
673078	Fwd	26.7 - 36.4	39.5 - 55.1	177 - 247	
	169.5	Ave(3) 32.9	Ave(3) 47.4	Ave(6) 209	61
	Aft	29.5 - 44.7	40.7 - 47.0	163 - 216	
	164.4	Ave(3) 36.5	Ave(2) 43.8	Ave(6) 184	58
R369	Fwd	29.4 - 31.4	25.2 - 49.6	129 - 142	
	161.7	Ave(3) 30.3	Ave(3) 40.1	Ave(6) 138	50
	Aft	30.0 - 38.1	58.7 - 61.5	229 - 256	
	166.7	Ave(3) 34.9	Ave(3) 60.0	Ave(6) 240	66
673095	Fwd	29.1 - 40.2	47.4 - 48.8	149 - 194	
	161.3	Ave(3) 34.9	Ave(3) 48.0	Ave(6) 175	56
	Aft	31.5 - 32.2	30.6 - 31.9	65 - 124	
	172.0	Ave(2) 31.8	Ave(2) 31.2	Ave(6) 95	42
673147	Fwd	35.6 - 40.0	35.2 - 48.2	136 - 161	
	168.2	Ave(3) 38.3	Ave(2) 41.7	Ave(6) 148	52
	Aft	24.7 - 33.5	37.6 - 48.0	113 - 137	
	168.6	Ave(3) 30.5	Ave(2) 42.8	Ave(6) 126	48

*AO is the fatigue cracked center-notch half length, PD is the load at deviation from linearity in the COD plot, and PP is the load at stress-wave pop-in.

TABLE V (cont.)

Chamber	Cylinder Yield, ksi	CN-Tensile K_{Ic} AO-PD*	CN-Tensile K_{Ic} AO-PP*	Slow Bend W/A (in.-lb/in.^{2})	Slow Bend W/A (ksi-in.$^{1/2}$)
674514	Fwd	23.9 - 32.4	28.5 - 36.6	113 - 136	
	166.8	Ave(2) 28.1	Ave(2) 32.5	Ave(6) 123	47
	Aft	27.6 - 29.2	(one test)	87 - 96	
	164.5	Ave(2) 28.4	32.0	Ave(6) 91	41
673122	Fwd	30.3 - 39.1	50.5 - 55.8	145 - 191	
	155.8	Ave(3) 36.2	Ave(3) 52.5	Ave(6) 172	56
	+320°F	28.6 - 42.5	78.0 - 81.7	1054 - 1299	
		Ave(3) 35.0	Ave(3) 80.0	Ave(6) 1204	--
	Aft	25.6 - 41.8	47.2 - 50.0	194 - 368	
	161.4	Ave(3) 35.0	Ave(3) 48.6	Ave(6) 261	69
	+320°F	32.7 - 52.4	93.9 - 100.5	1167 - 1482	
		Ave(3) 40.9	Ave(3) 96.6	Ave(6) 1292	--
2192109	Fwd	28.4 - 35.8	42.9 - 49.2	124 - 150	
	(69B) 163.0	Ave(3) 32.2	Ave(3) 46.9	Ave(6) 135	49
	+212°F	23.4 - 30.2	(one test)	570 - 651	
		Ave(2) 26.8	54.5	Ave(6) 612	--
	Aft	19.3 - 29.9	27.4 - 40.9	119 - 143	
	(77B) 163.0	Ave(2) 24.6	Ave(2) 34.1	Ave(6) 129	48
	+212°F	24.6 - 36.7	36.7 - 63.7	526 - 563	
		Ave(2) 30.6	Ave(2) 50.2	Ave(5) 541	--

*AO is the fatigue cracked center-notch half length, PD is the load at deviation from linearity in the COD plot, and PP is the load at stress-wave pop-in.

the average values for the two forgings tested at +320°F (35.0 and 40.9 ksi-in.$^{1/2}$) falling within the range of room-temperature test results. Figure 15 shows that with one exception, K_{Ic} values based on deviation from linearity gave conservative values as compared with K_{Ic} values based on the initial fatigue-cracked center-notch half length (AO) and the load corresponding to pop-in (PP) as determined from stress-wave emission. This plot suggests that the lower the plane-strain fracture toughness, the closer the pop-in to the deviation in linearity.

The K_{Ic} based on pop-in is taken to be the significant value of plane-strain fracture toughness, with the room-temperature averages ranging from 31.2 to 74.6 ksi-in.$^{1/2}$ for the 18 forgings tested. The elevated-temperature data were generally significantly higher than the room-temperature data; the +212°F tests gave averages of over 50 ksi-in.$^{1/2}$ and the +320°F tests, up to 96.6 ksi-in.$^{1/2}$

A comparison between the K_{Ic} data obtained with the PTC tensile and the CN-tensile specimens is appropriate at this point. Only one of the chambers, SN 2192109, contained forgings that had been previously tested with the PTC-tensile specimen.

The forward cylinder in chamber SN 2192109 was forging 69B and the aft cylinder 77B; K_{Ic} data on these forgings as determined from the PTC-tensile test are contained in Appendix B. Forging 69B was tested with the PTC-tensile by both Aerojet-Downey and Aerojet-Sacramento. The test results as compared with the CN-tensile are summarized as follows:

PART-THROUGH-CRACK TENSILE DATA		CENTER-NOTCH TENSILE DATA	
		Linearity	Pop-in
Sacramento	Downey	(AO-PD)	(AO-PP)
30.4 - 41.8	33.7 - 38.7	28.4 - 35.8	42.9 - 49.2
Avg(6) 35.8	Avg(6) 36.1	Avg(3) 32.2	Avg(3) 46.9

Forging 77B was tested with PTC tensile by Aerojet-Downey; the test results as compared with the CN-tensile are summarized as follows:

	CN-TENSILE DATA	
	Linearity	Pop-in
PTC-TENSILE DATA	(AO-PD)	(AO-PP)
35.3 - 39.4	19.3 - 29.9	27.4 - 40.9
Avg(6) 37.6	Avg(2) 24.6	Avg(2) 34.1

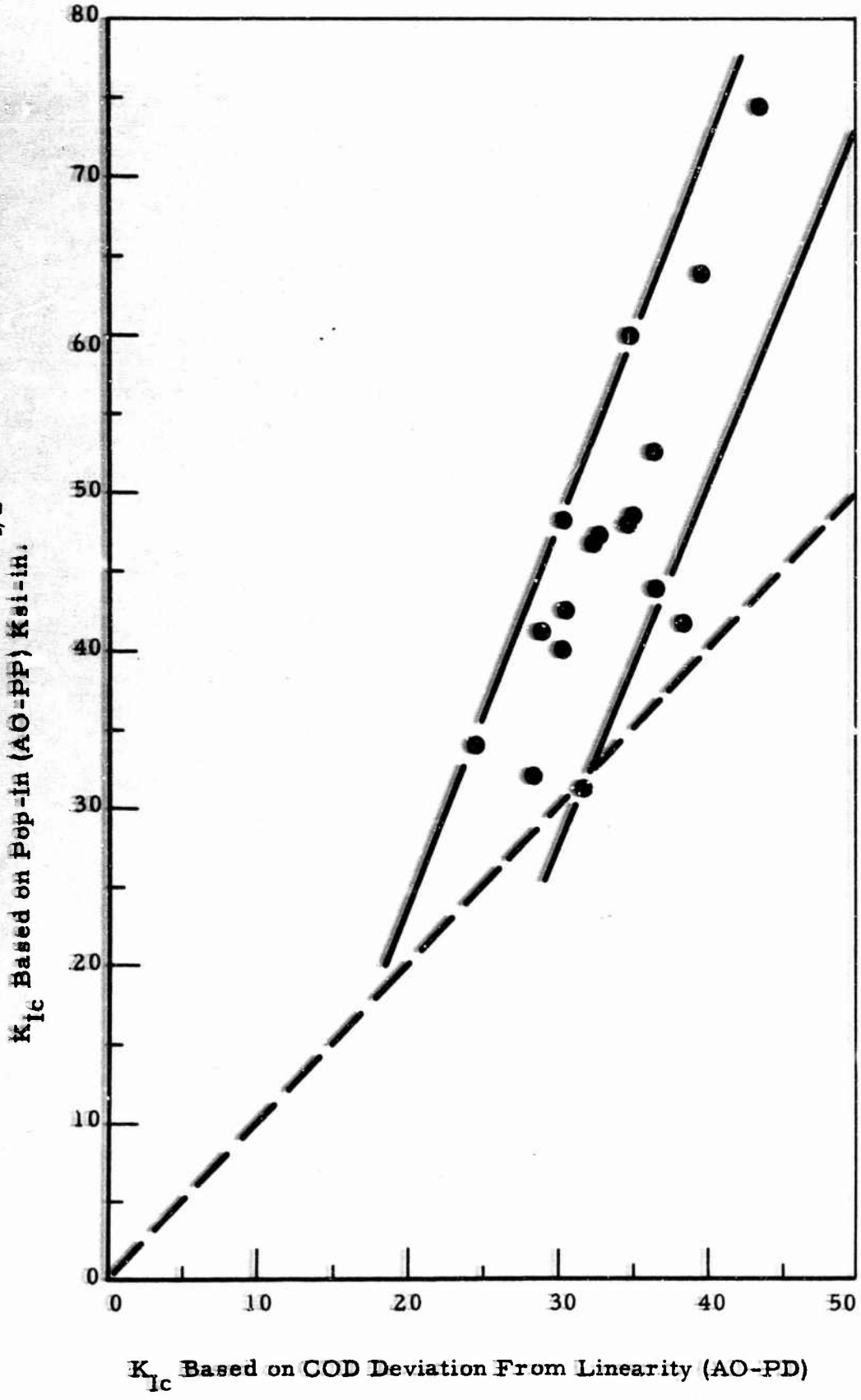


Figure 15. Relationship Between K_{Ic} Values Based on AO-PD and AO-PP

The plot of K_{Ic} data as obtained from 708 PTC-tensile tests of 109 forgings versus yield strength yielded a scatter band as shown in Figure 16. Superimposed are the K_{Ic} data obtained from the CN-tensile tests. Note that of the 18 forgings tested with the CN-tensile specimen, 1 of the K_{Ic} values based on pop-in fell in or were close to the scatter band, and 5 of the values were significantly above the scatter band. The CN-tensile K_{Ic} values based on deviation from linearity, on the other hand, tended to be conservative with 10 points falling on the scatter band and 8 of the K_{Ic} values below the band.

Allison, in a study of the premature failure of Minuteman chamber R26, conducted PTC-tensile tests of the forward cylinder near the fracture origin as well as of two locations in the aft cylinder. The K_{Ic} values calculated from their test results[9] (average of three tests) indicated a K_{Ic} value of 47 ksi-in.$^{1/2}$. This compares very well with the CN-tensile result (48.2 ksi-in.$^{1/2}$) obtained in this study. The Allison PTC-tensile test results from two locations in the aft cylinder indicated K_{Ic} values of 45 and 52 ksi-in.$^{1/2}$ (averages of two tests), as compared with 74.6 ksi-in.$^{1/2}$ from the CN-tensile tests of this investigation. This suggests that the high K_{Ic} values of 70.4 and 80.5 ksi-in.$^{1/2}$ as obtained from duplicate CN-tensile tests may be valid measurements for the particular location tested in the aft barrel.

The PTC-tensile data previously obtained in the failure analysis of chambers 673078 and 673147 agreed very well with the K_{Ic} values calculated from pop-in (AO-PP) in the CN-tensile test results.

	MINUTEMAN CHAMBER 673078		MINUTEMAN CHAMBER 673147	
	CN-Tensile	PTC-Tensile	CN-Tensile	PTC-Tensile
Fwd Cylinder	39.5 – 55.1	44.0 – 49.0	35.2 – 48.2	31 – 41
	Avg(3) 47.4	Avg(6) 46.3	Avg(2) 41.7	Avg(6) 40
Aft Cylinder	40.7 – 47.0	39.3 – 43.2	37.6 – 48.0	37 – 48
	Avg(2) 43.8	Avg(5) 40.9	Avg(2) 42.8	Avg(6) 41

2. Plane-Stress K_c Data

The plane-stress fracture-toughness K_c data from 18 cylindrical forgings are tabulated as computer printouts in Appendix C. A summary of the K_c data is presented in Table VI. The values of K_c are those obtained by (1) the conventional method with crack length (AM) and load (PM) corresponding to maximum in the crack-opening-displacement versus load plot, and (2) the stress-wave detection system with crack length (AC) and load (PC) based on

(9) V. L. Helmann, Final Report for Minuteman Second-Stage Titanium Case Improvement Program Allison Engineering Department Report No. 3590, 15 Oct 1963.

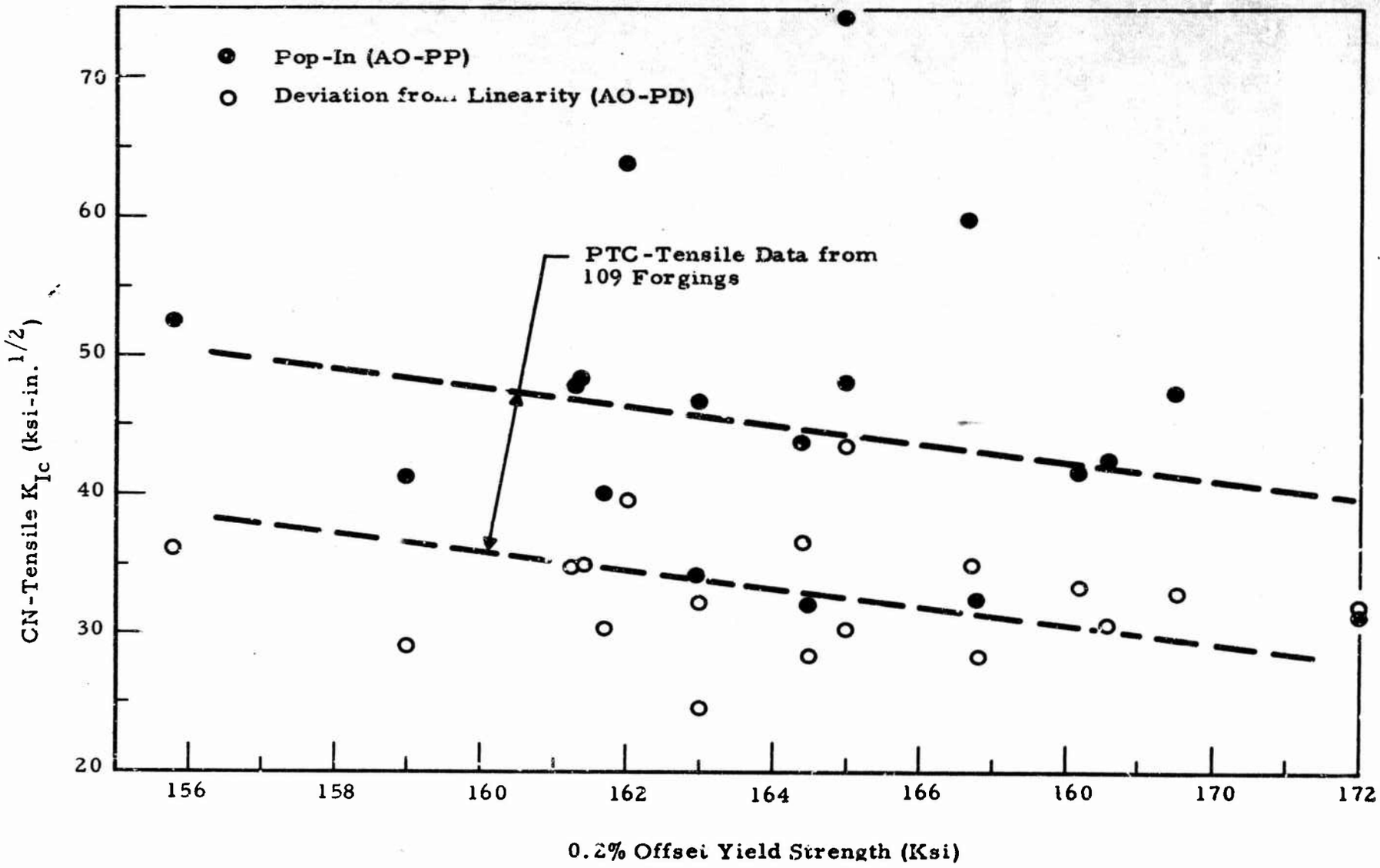


Figure 16. Relationship Between K_{Ic} and Yield Strength Together with the Scatter Band for K_{Ic} from 109 Forgings as Determined by PTC-Tensile Tests

TABLE VI

SUMMARY OF CENTER-NOTCH TENSILE PLANE-STRESS K_c DATA

AND PRECRACK CHARPY IMPACT W/A DATA

Chamber	Cylinder	CN-Tensile K_c AC-PC *	CN-Tensile K_c AM-PM *	Impact W/A (in.-lb/in.^{2})	Impact W/A ($\frac{1}{2}$) (ksi-in.$^{\frac{1}{2}}$)
R26	Fwd	61.1 - 63.8 Ave(2) 62.4	65.4 - 71.4 Ave(2) 68.4	471 - 582 Ave(6) 538	94
	Aft	97.2 - 103.6 Ave(2) 100.4	100.0 - 110.0 Ave(3) 104.0	792 - 1033 Ave(12) 905	121
2191456	Fwd	46.9 - 53.8 Ave(3) 50.6	56.3 - 61.5 Ave(3) 59.4	386 - 498 Ave(6) 443	85
	Aft	81.6 - 88.3 Ave(3) 85.9	93.6 - 102.5 Ave(3) 98.6	868 - 1032 Ave(6) 953	124
673078	Fwd	58.3 - 66.5 Ave(3) 63.6	65.5 - 75.9 Ave(3) 72.2	569 - 672 Ave(6) 628	102
	Aft	67.0 - 80.0 Ave(3) 72.0	76.5 - 86.1 Ave(3) 80.1	611 - 702 Ave(6) 652	103
R369	Fwd	56.2 - 57.0 Ave(3) 56.7	59.8 - 66.4 Ave(3) 63.2	379 - 422 Ave(6) 400	81
	Aft	76.2 - 94.3 Ave(3) 83.5	87.0 - 100.1 Ave(3) 91.6	666 - 702 Ave(6) 685	106
673095	Fwd	62.7 - 68.5 Ave(3) 66.3	65.3 - 75.9 Ave(3) 70.1	621 - 712 Ave(6) 650	103
	Aft	44.1 - 44.8 Ave(2) 44.4	44.7 - 46.6 Ave(2) 45.6	303 - 346 Ave(6) 331	74
673147	Fwd	53.7 - 67.0 Ave(3) 59.4	60.1 - 76.0 Ave(3) 67.2	475 - 534 Ave(6) 509	91
	Aft	52.5 - 53.2 Ave(2) 52.9	54.5 - 62.8 Ave(3) 58.4	408 - 510 Ave(6) 458	87
674514	Fwd	42.2 - 42.4 Ave(2) 42.3	51.8 - 52.0 Ave(2) 51.9	340 - 402 Ave(6) 379	79
	Aft	35.7 - 37.7 Ave(2) 36.7	43.0 - 43.8 Ave(2) 43.4	274 - 330 Ave(6) 308	71

Table VI (cont.)

Chamber	Cylinder	CN-Tensile K_c AC-PC*	CN-Tensile K_c AM-PM*	Impact W/A (in.-lb/in.^{2})	Impact W/A (ksi-in.$^{1/2}$)
673122	Fwd	59.8 - 75.0 Ave(3) 65.5	64.4 - 77.6 Ave(3) 70.2	547 - 654 Ave(6) 592	98
	+320°F	(one test) 128.0	154.3 - 170.7 Ave(3) 163.2	1108 - 1187 Ave(3) 1144	137
	Aft	59.7 64.6 Ave(3) 61.9	66.0 - 67.9 Ave(3) 67.2	604 - 797 Ave(6) 681	105
	+320°F	137.4 - 158.7 Ave(3) 148.0	158.0 - 187.8 Ave(3) 169.1	979 - 1108 Ave(3) 1030	130
2192109	Fwd	53.0 - 62.0 Ave(2) 58.2	62.3 - 69.3 Ave(3) 66.5	459 - 518 Ave(6) 489	89
	+212°F	(one test) 105.6	110.8 - 127.9 Ave(2) 119.3	677 - 692 Ave(3) 683	106
	Aft	43.7 - 53.3 Ave(2) 48.5	52.5 - 56.1 Ave(2) 54.3	472 - 528 Ave(6) 498	90
	+212°F	108.0 - 120.5 Ave(2) 114.2	122.2 - 145.8 Ave(2) 134.0	666 - 687 Ave(3) 679	105

*Crack Length (AM) and Load (PM) corresponding to maximum COD vs Load plot. Crack length (AC) and Load (PC) based on inflection in Stress-Wave-Count rate vs Load plot.

the inflection in the stress-wave-count rate versus load plot. Note that the K_c values based on stress-wave count rate are either the same or lower than the K_c values based on maximum load (Figure 17).

Figure 18 is the plot of K_c values as obtained from the 18 forgings versus yield strength. It is apparent that there is much greater variation in forging-to-forging K_c values than in K_{Ic} values. Note that the plane-stress fracture-toughness (K_c) of some of the forgings is little higher than the K_{Ic} values obtained from PTC-tensile tests of 109 forgings.

Figure 19 provides a comparison between plane-stress and plane-strain fracture toughness values based on stress-wave emission for the 18 forgings tested by CN-tensile. If a line is faired through the data, the following expression of the form $y = mx + b$ is indicated:

$$K_c = 1.5\ K_{Ic} - 7.5$$

Note from Table VI that there was sometimes a marked difference in toughness between cylindrical forgings of a given chamber. Such differences are typified by the COD signals as displayed in the X-Y plot for the forward and aft barrels of chamber R26 (Figure 20). Note, also, that the low-toughness component in premature-burst chambers R26 and SN 2191456 was the fracture-origin component. Chamber SN 673078, with approximately equal toughness in the two barrel components, withstood several proof-test cycles before bursting. Chamber R369 was an exception, with higher toughness in the fracture-origin barrel; however, this chamber contained a very large crack which resulted in premature failure at only 0.6 of the 627 psig proof pressure.

D. PRECRACK CHARPY DATA

The precrack Charpy specimens were cut from the broken halves of the 3- x 12-in. CN-tensile specimens. Six axial specimens (crack-propagation in the hoop direction, duplicating that in the CN-tensile specimens) and three hoop specimens were cut from each half of the CN-tensile specimens. The Charpy specimens, like the CN tensile, were tested in full chamber-wall thickness (nominally 0.10 in.). The Charpys were divided into two lots, one for impact testing at Aerojet-Sacramento and one for slow-bend testing at the Air Force Materials Laboratory (Allan W. Gunderson, Project Engineer). The slow-bend tests were all axial-oriented specimens.

1. Slow-Bend Test Data

The data from these tests are tabulated in Appendix D. A summary of the precrack Charpy slow-bend (PCSB) test results are presented in Table V, together with the CN-tensile K_{Ic} data. The data, as recorded

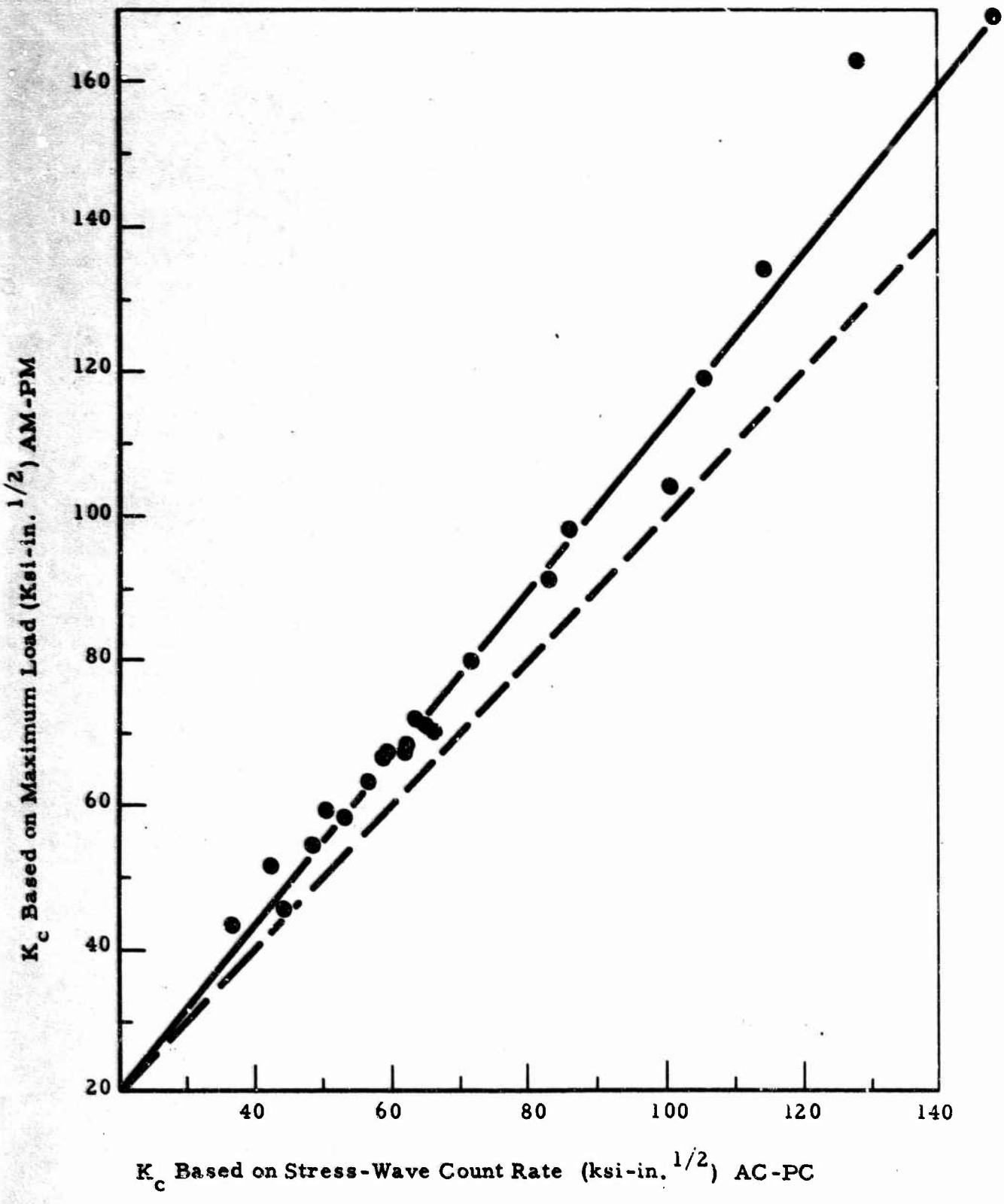


Figure 17. Relationship Between K_c Values Based on AC-PC and AM-PM

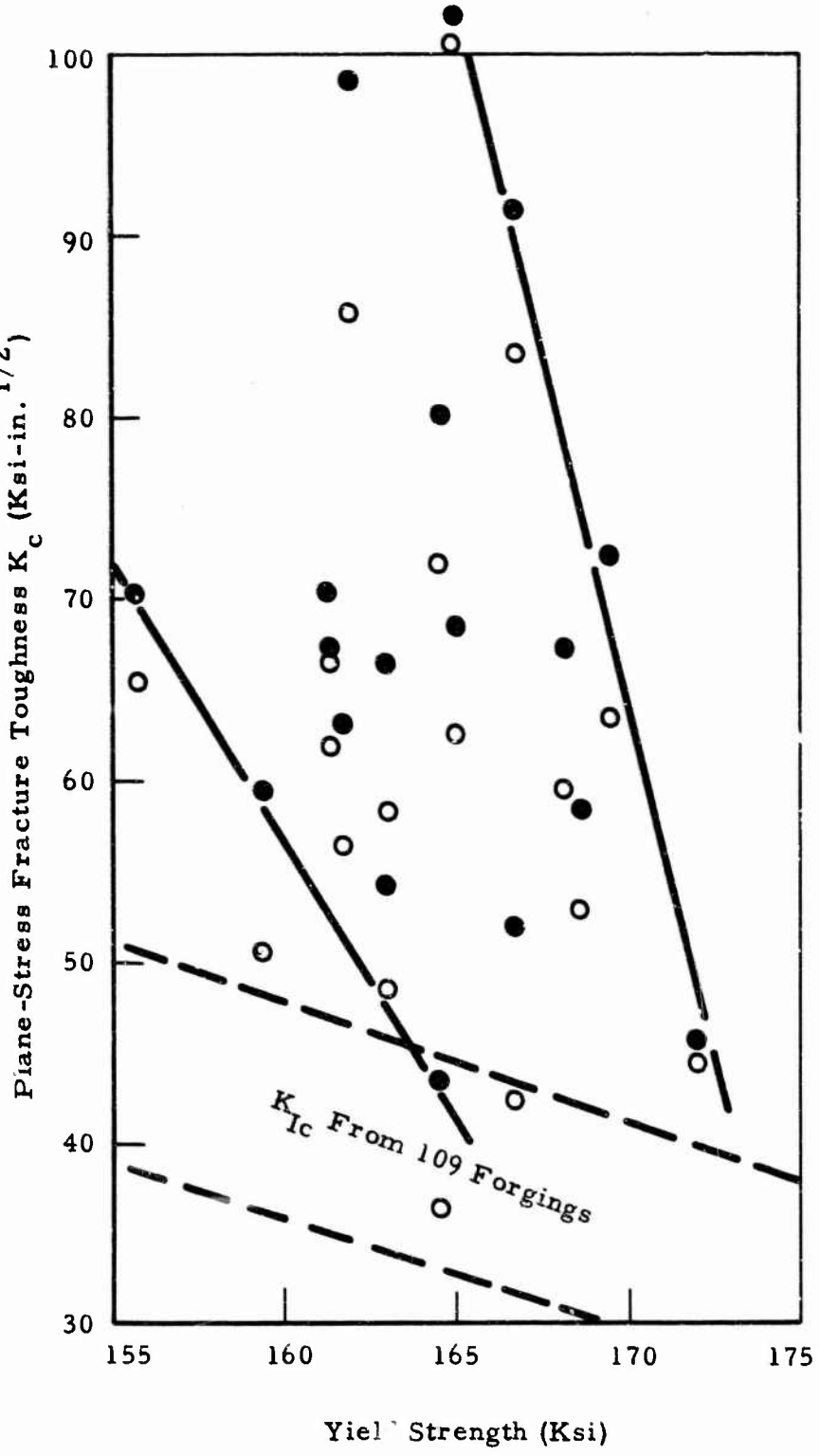


Figure 18. Relationship Between K_c and Yield Strength Together with the Scatter Band for K_{Ic} from 109 Forgings as Determined by PTC-Tensile Test

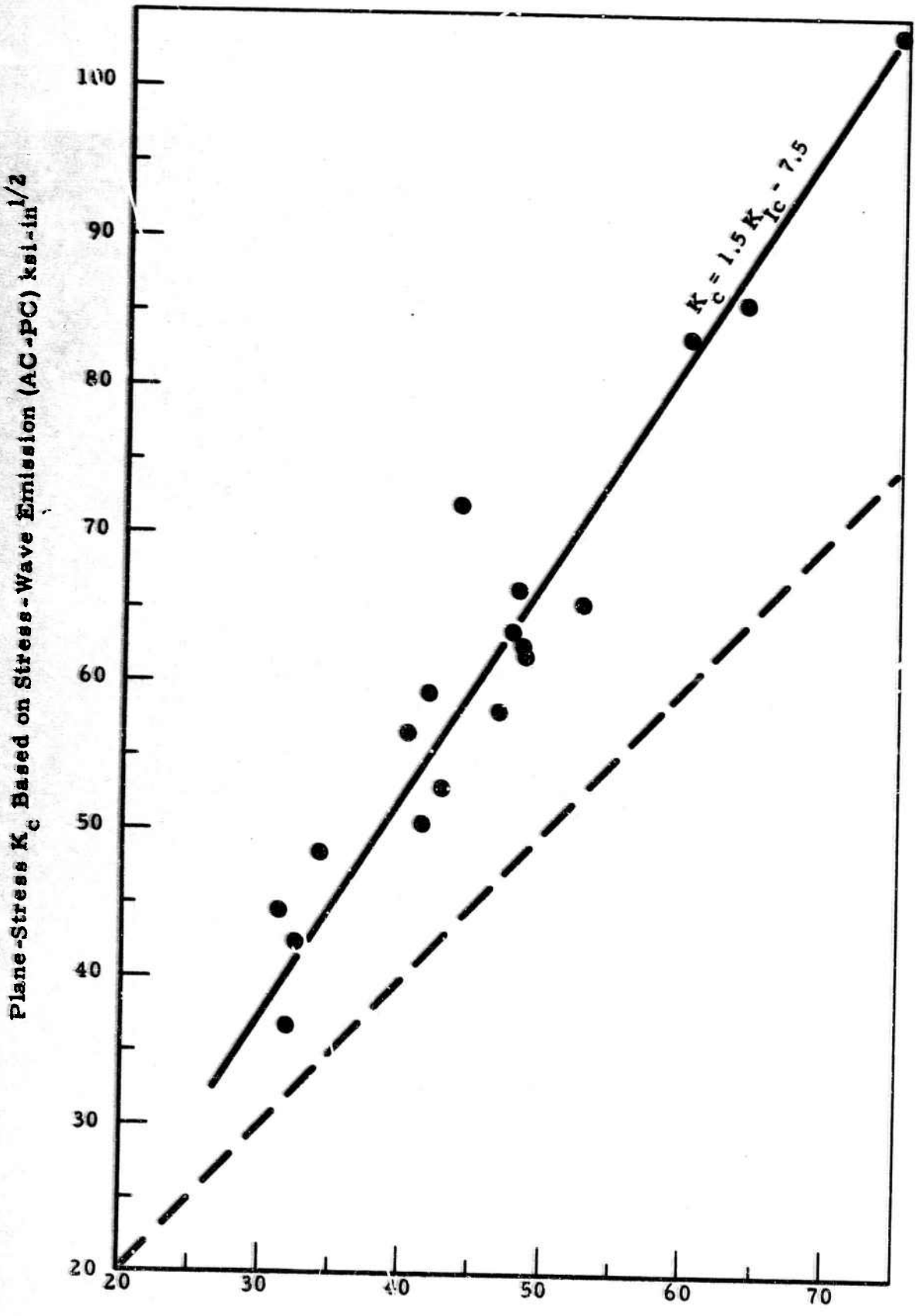


Figure 19. Relationship Between K_{Ic} and K_c

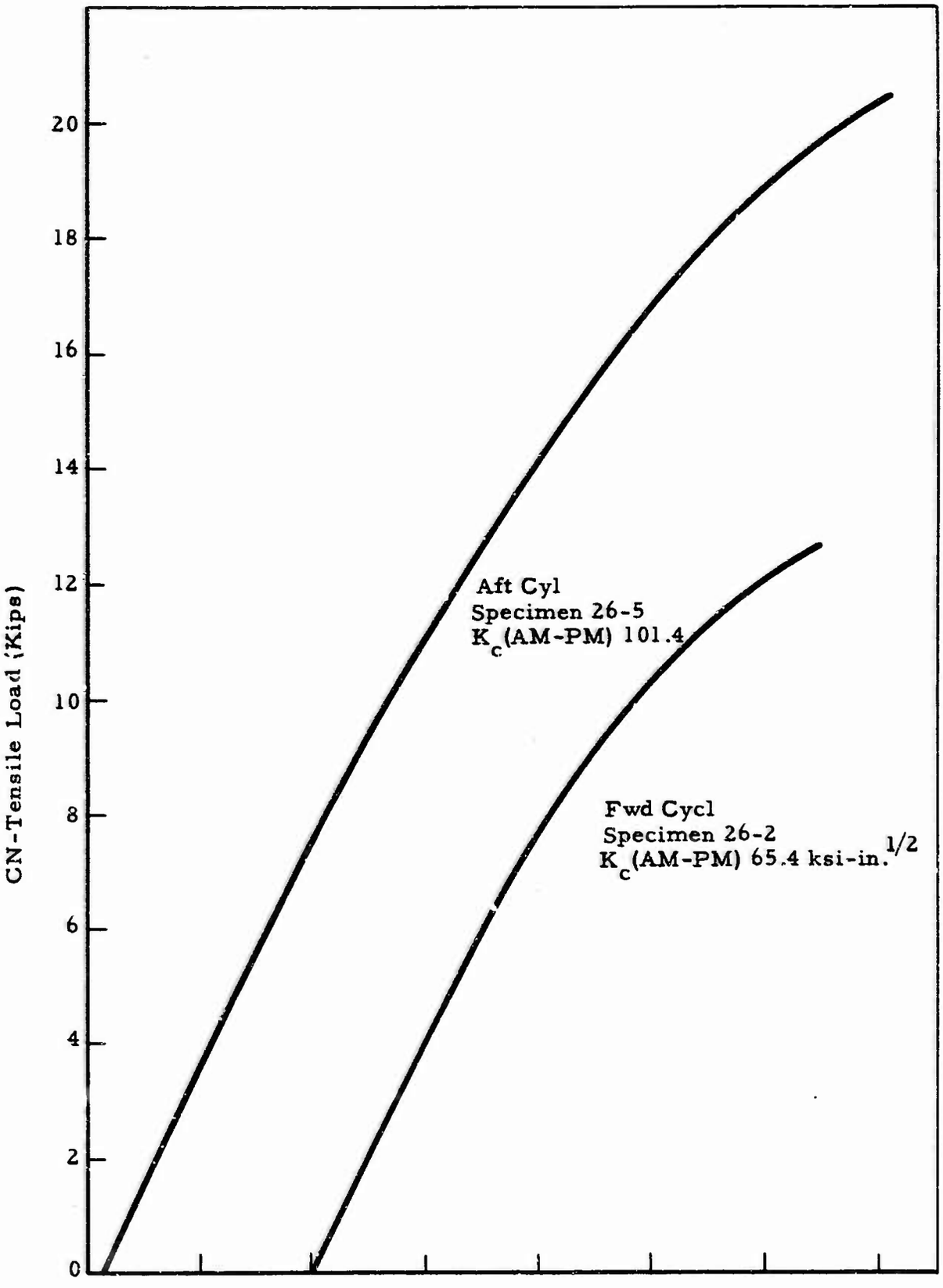


Figure 20. Typical COD-Load X-Y Plot for Fwd and Aft Cylinders of Chamber R26

from a ManLabs Slow-Bend Tester, are in inch-pounds and, therefore, the data are presented as W/A values (in.-lb/in.^{2}) as well as converted to K_c values (ksi-in.$^{1/2}$). The conversion from W/A to K_c was done graphically from Figure 21, based on the relationship

$$K_{Ic}^2 (1 - \mu^2) = E (W/A)$$

A plot of PCSB versus CN-tensile K_{Ic} values is shown in Figure 22. Note that the PCSB data consistently fell above the 1:1 correlation line. A faired line through the data points indicates an expression of the form y = mx + b, viz.,

$$PCSB = K_{Ic} + 10$$

to provide a good approximation. Thus, on an average, the PCSB test results are approximately 10 ksi-in.$^{1/2}$ higher than the K_{Ic} values as determined from the CN-tensile test. It should be noted, however, that this relationship does not exist at elevated temperature. At 320°F, the PCSB test result is as high as, and sometimes higher than, the PCI value. Thus, it appears that the possible combination of "isothermal" deformation and time-dependent embrittlement at room-temperature is no longer effective in 6Al-4V titanium at elevated temperature. Hydrogen is a possible mechanism because it is most embrittling at room temperature and ineffective (because it diffuses too rapidly) at elevated temperature.

2. Impact Test Data

The precrack Charpy impact (PCI) test results for axial specimens (crack propagation in the hoop direction, duplicating that in the CN tensile) are summarized in Table VI, together with the CN-tensile K_c data.* The PCI data are presented both in W/A units (in.-lb/in.^{2}) and converted to K_c (ksi-in.$^{1/2}$). The conversion from W/A to K_c was done graphically from Figure 23, based on the relationship

$$K_c^2 = E (W/A)$$

where E is Young's modulus for 6Al-4V titanium (16.4×10^6).

A plot of PCI versus CN-tensile K_c values is presented in Figure 24. Note that the PCI data consistently fell above the 1:1 correlation line. A faired curve through the data points indicates an expression of the form y = mx + b, viz.,

$$PCI = K_c + 25$$

*A complete tabulation of the precrack Charpy data is contained in Appendix D.

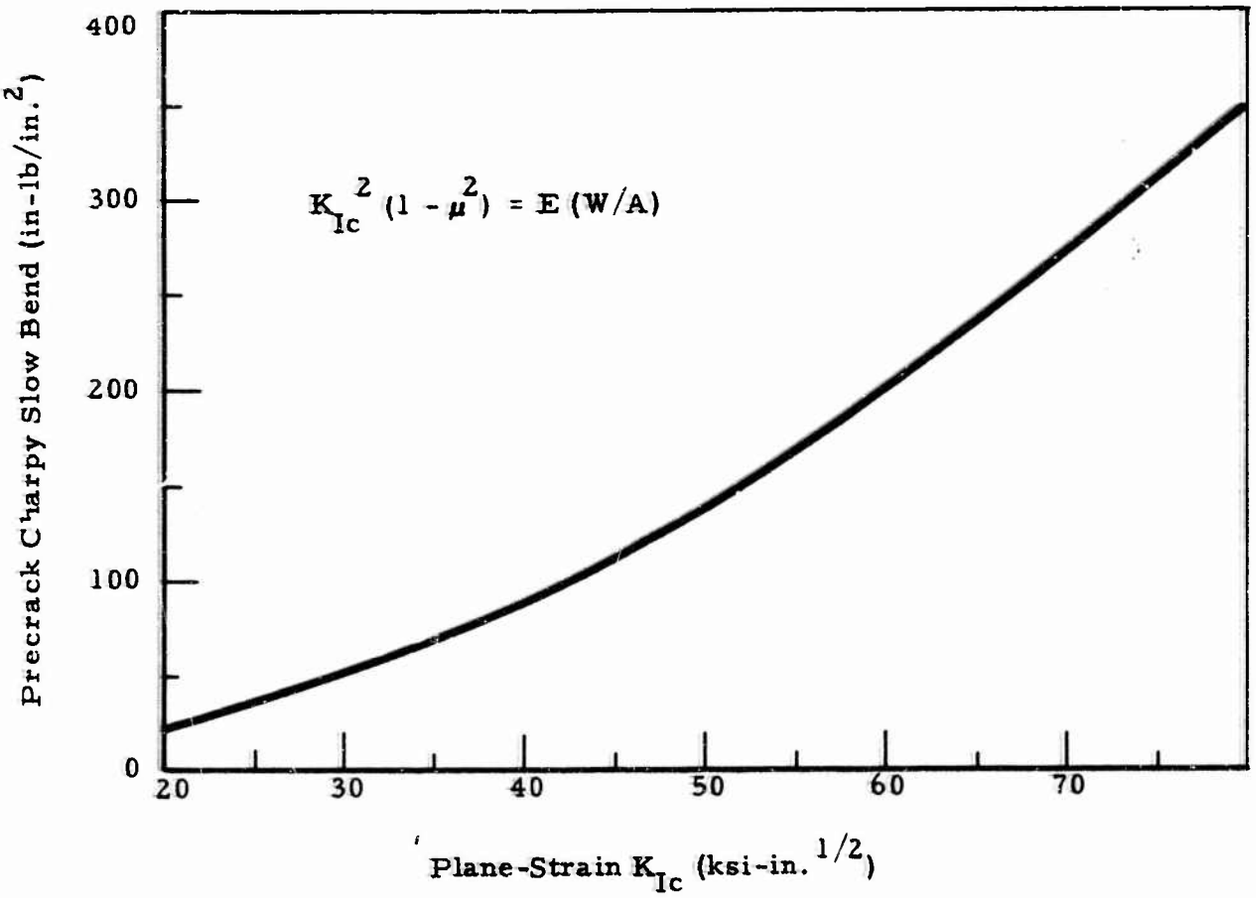


Figure 21. Graphical Solution for K_{Ic} Based on Precrack Charpy Slow Bend

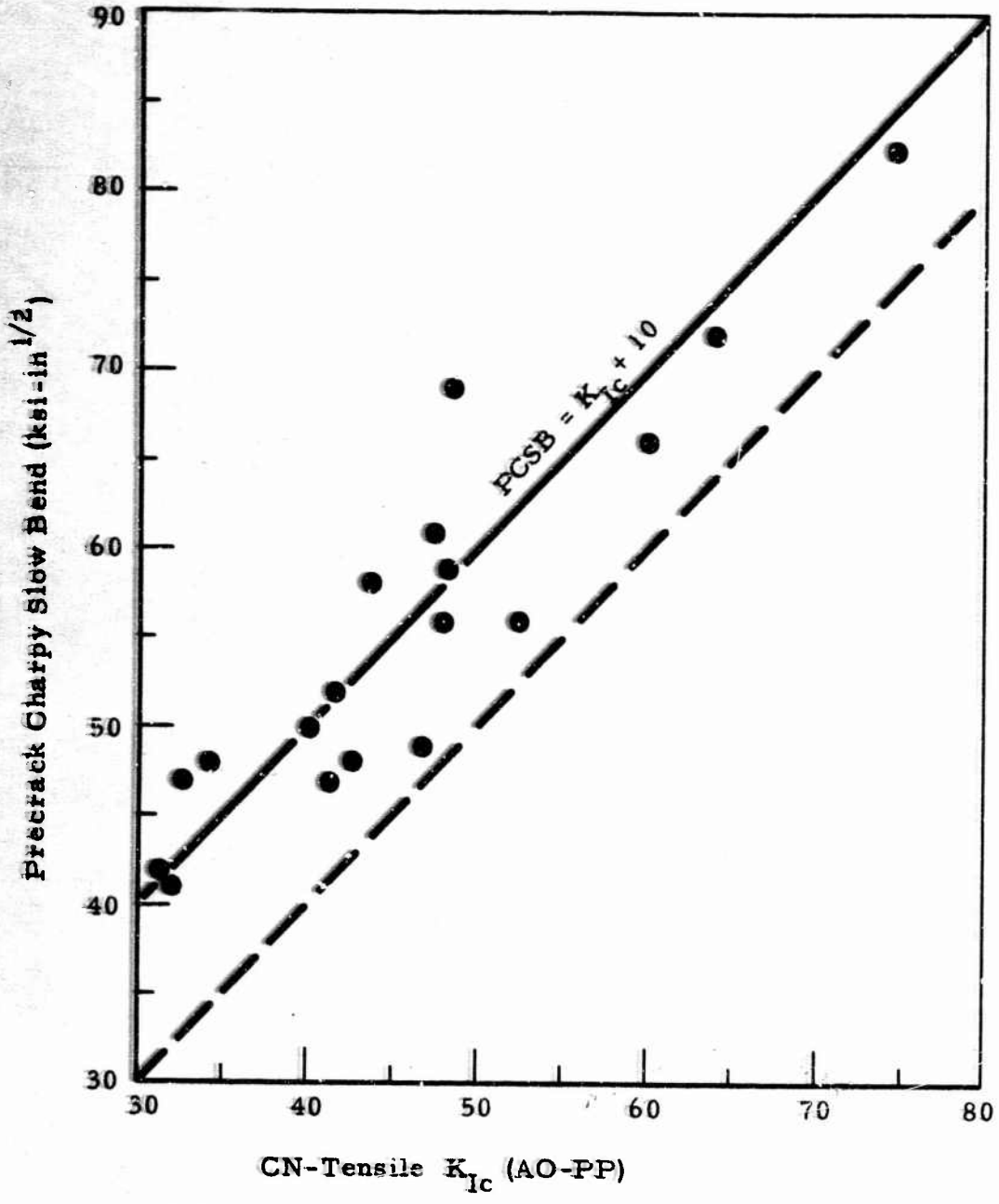


Figure 22. Relationship Between K_{Ic} and Precrack Charpy Slow Bend

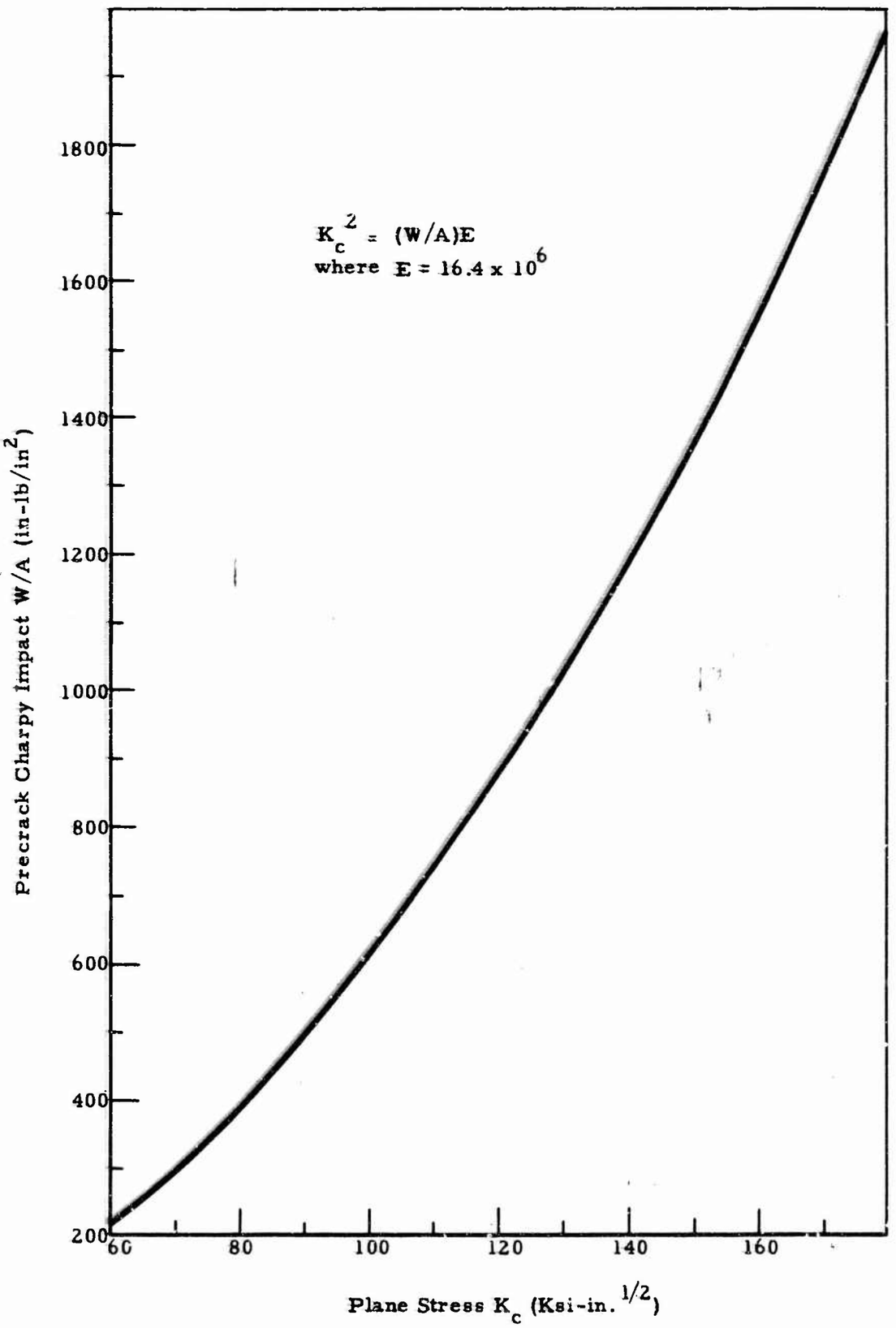


Figure 23. Graphical Solution for K_c Based on Precrack Charpy Impact

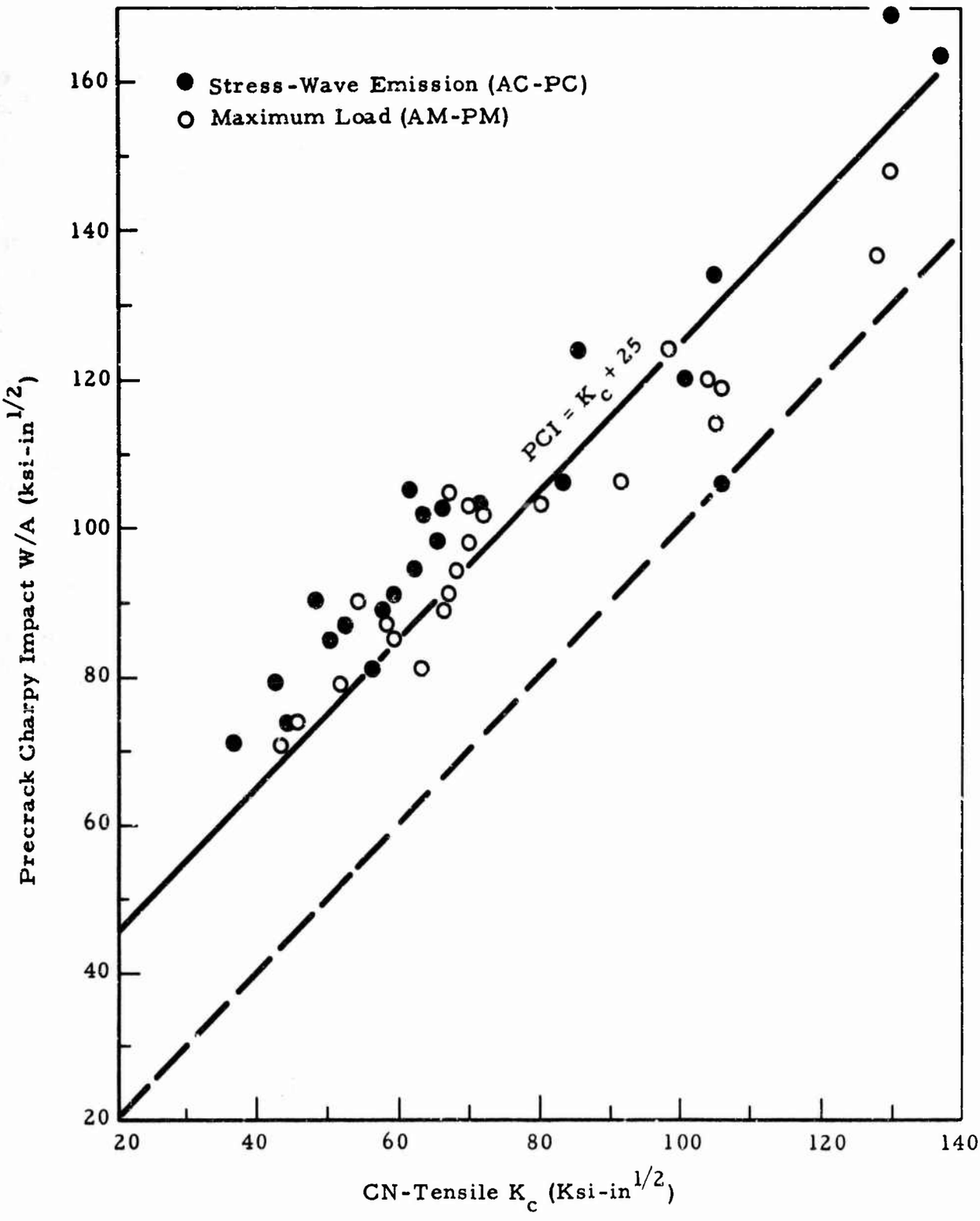


Figure 24. Relationship Between K_c and Precrack Charpy Impact

to provide a good approximation; thus, on an average, the PCI test results are approximately 25 ksi-in.$^{1/2}$ higher than the K_c values as determined from the CN-tensile test. Note that the elevated-temperature PCI data generally fell within the same scatter band as the room-temperature test results.

Figure 25 is a plot of PCI data for the two crack-propagation directions. The large scatter of approximately $\pm$ 100 in.-lb/in.^{2} requires further investigation. Fracture in most chambers occurs axially because of the 2:1 principal stress in the hoop direction; however, in some chambers, secondary crack propagation occurs in the hoop direction (as in Figure 26).

Figure 27 shows in bar-graph form, the consistently higher test result obtained in PCI as compared with PCSB, and also the differences in plane-stress and plane-strain fracture toughness from forging-to-forging in the various chambers tested. Note, that with minor exceptions, when there were significant differences in K_{Ic} and K_c values between forgings of a given chamber, there were similar differences in PCSB and PCI values.

Figure 28 is a plot of the same data as presented in Figures 22 and 24, except the precrack Charpy W/A values are plotted in in.-lb/in.^{2} units. The data were treated by method of least squares to determine the equation of the line that gave the best fit. Assuming a normal distribution and that the calculated standard deviations were true values, the limits were determined for 95 percent reliability.

Plane-Strain K_{Ic} Estimate from Precrack Charpy Slow Bend

$$K_{Ic} = 0.17 \text{ PCSB} + 16.2$$

Plane-Stress K_c Estimate from Precrack Charpy Impact

$$K_c = 0.10 \text{ PCI} + 6.7 \text{ (based on AC-PC from SWE)}$$

$$K_c = 0.10 \text{ PCI} + 12.2 \text{ (based on AM-PM at maximum load)}$$

E. CORRELATION WITH FULL-SCALE CHAMBER PERFORMANCE

The objective of Phase 2 of the data collection will be to correlate laboratory test results with full-scale Minuteman chamber performance. The materials for the second phase will be obtained from 15 full-scale hydroburst Minuteman chambers, including 8 of the chambers from phase one. Ten of the 15 chambers will be premature proof-test failure and five successfully hydroburst chambers. Testing domes, adaptors, and cylinders from the 15 chambers will provide data on 69 forgings, involving three different forging practices. The crack toughness measurements will be made by precrack Charpy impact tests, oriented to fracture in the chamber-axial direction, and cut from 0.1-in. and 0.19-in. wall sections on both sides of each girth weld

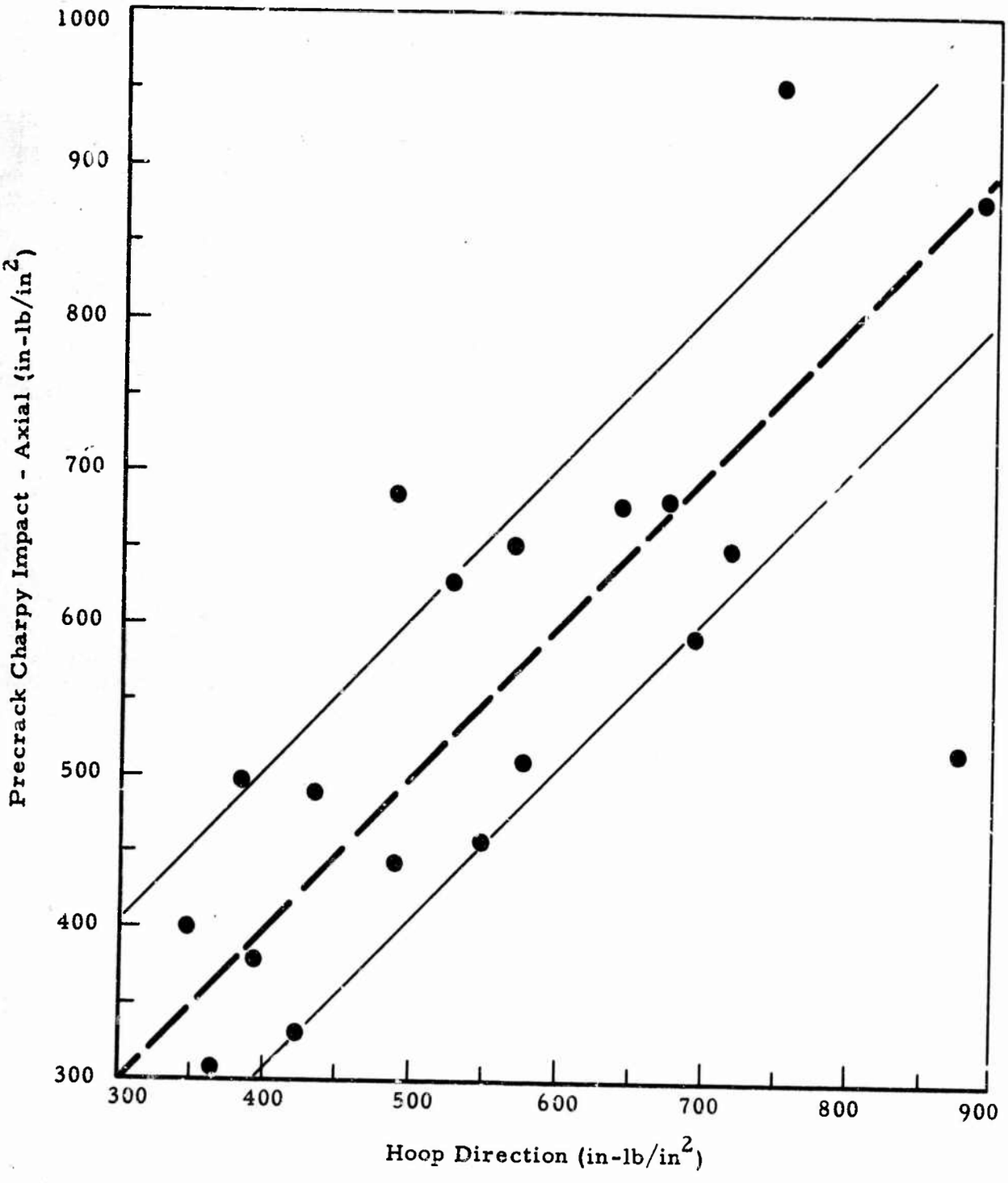


Figure 25. Anisotropy in the Cylindrical Forging

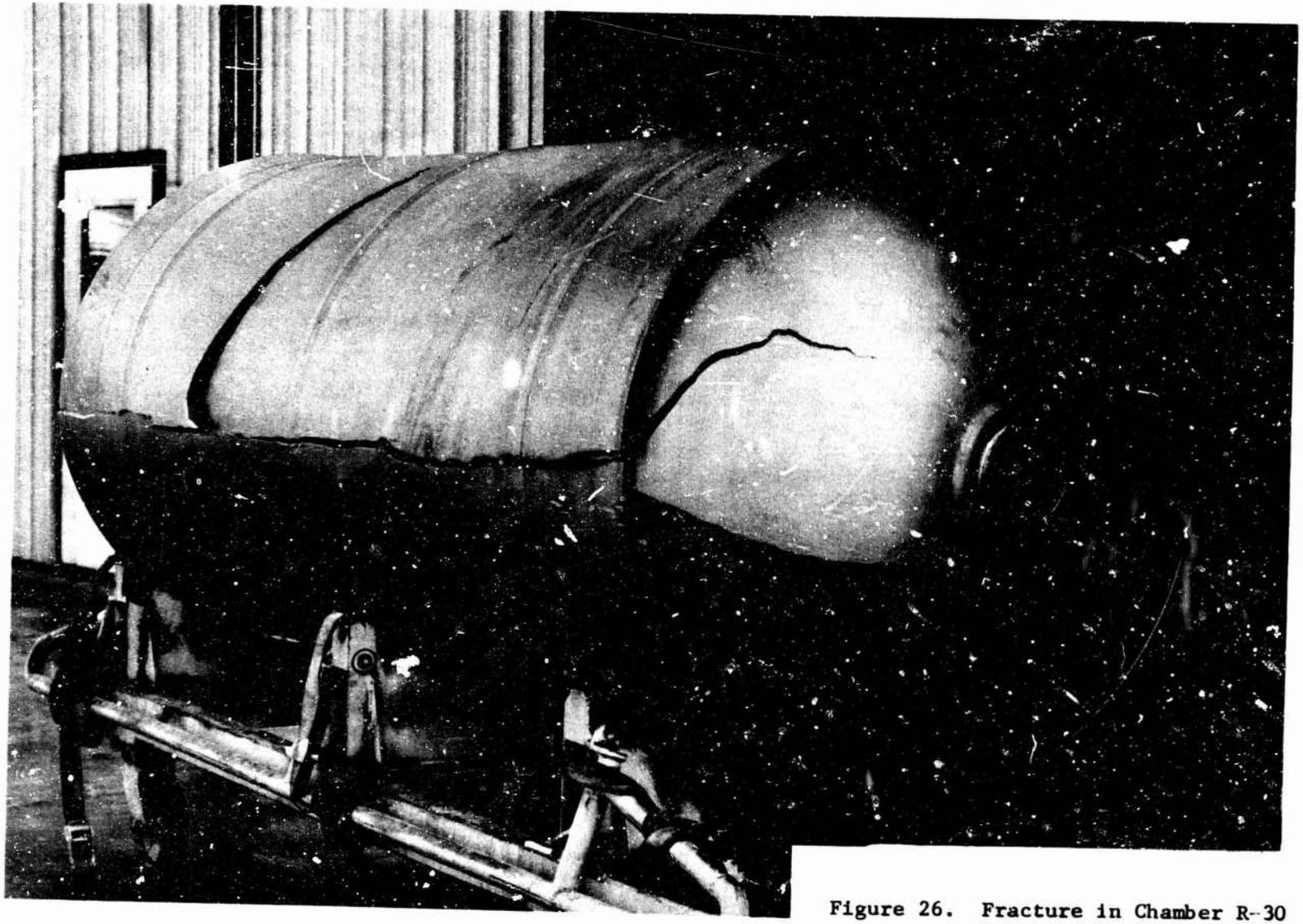


Figure 26. Fracture in Chamber R-30

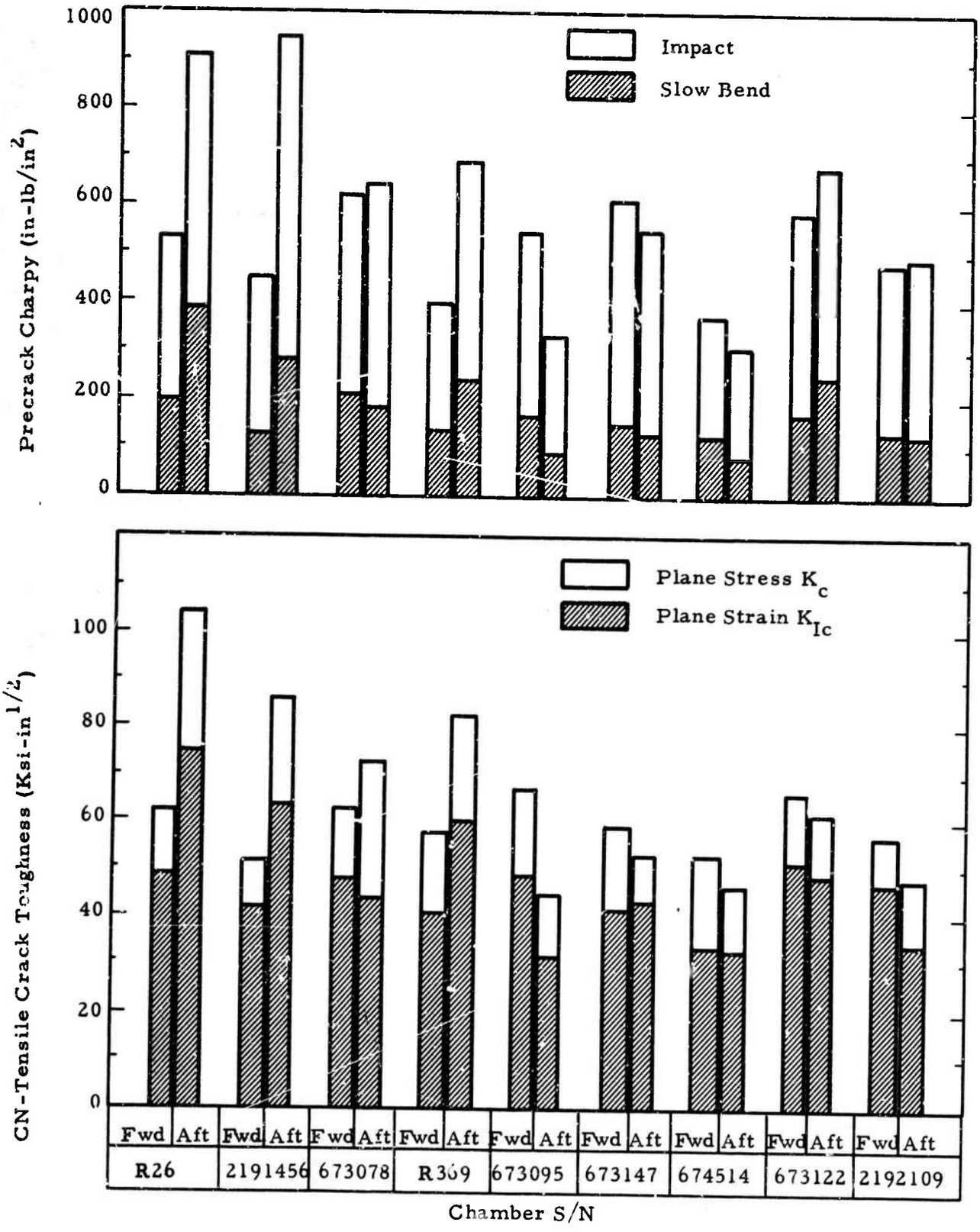


Figure 27. Bar Graph Summary of Precrack Charpy and Center-Notch Tensile Test Results

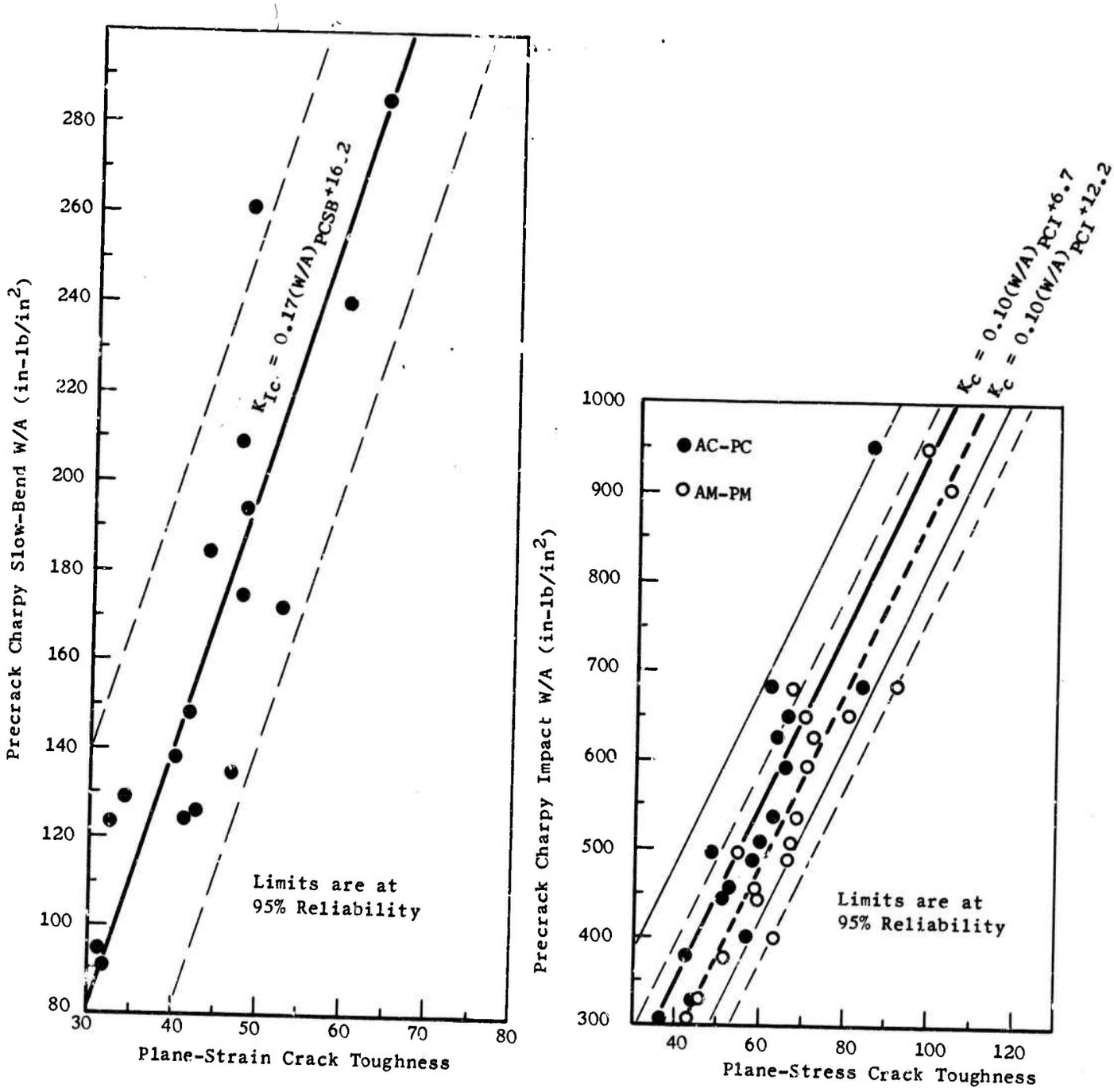


Figure 28. Relationship Between Precrack Charpy W/A (in.-lb/in.^{2}) and CN-Tensile Critical Stress Intensity (ksi-in.$^{1/2}$)

(parent-metal tests only). Selected forgings in each chamber will be tested at -40, RT, 200 and 320°F. Particular attention will be directed to the material in the immediate vicinity of the fracture origin.

No attempt was made in Phase 1 to correlate laboratory test results with full-scale Minuteman chamber performance for the following reasons: (1) anisotropy in the extruded cylinder material precluded correlation between axially oriented CN-tensile test data (fracture propagating in the hoop direction) and chamber performance (fracture propagating in the axial direction); (2) the CN-tensile specimen can only be cut in the axial direction because of the complication of curvature in the hoop direction; and (3) reliable axial-crack-propagation CN-tensile data cannot be obtained in the increased-thickness chamber wall adjacent to the girth welds where fracture usually initiates in premature proof-test failures. Another possible complication to correlation between the CN-tensile test result and full-scale chamber performance is variable crack toughness from end to end of a given forging; the extrusion process may be attended by a difference in temperature from start to finish of the extrusion process, which, in turn, could be attended by a variation in the crack toughness from end to end of the extrusion.

From the above discussion of the limitations on CN-tensile specimens cut from burst rocket-motor chambers, it may be seen that the usefulness of the precrack Charpy test as a quantitative measure of plane-stress fracture toughness is a necessary condition if full-scale chamber performance is to be evaluated. The precrack Charpy specimen is small enough that it can be cut from the increased-thickness chamber wall adjacent to the girth welds (in the parent metal outside the weld heat-affected zone) where the fracture usually initiates in premature proof-test failures. Moreover, because of the small size of the Charpy test piece, it can be cut with its length in the hoop direction to test crack toughness in the axial direction. The 44- and 52-in.-dia curvature in the 2-in. length of the precrack Charpy should have little or no effect on the measured W/A value; whereas, curvature in the 12-in. length of the CN-tensile would introduce a large bending stress with its corresponding gradient of stress through the thickness.

F. SUMMARY - PHASE I

Phase 1 of a MIL-HDBK-5 data collection has been completed to provide room-temperature and elevated-temperature-tensile data and fracture-toughness data on 6Al-4V titanium at a 0.2% offset yield strength of approximately 150 ksi. The material tested was production-lot forgings from 44- and 52-in.-dia second-stage Minuteman rocket-motor cases. The elevated-temperature tensile data were for temperatures up to 330°F. The fracture-toughness data include plane-strain K_{Ic} from part-through-crack (PTC) tensile tests of 109 forgings, plane-stress K_c from fatigue-precracked center-notch (CN) tensile tests of 18 forgings, and precrack Charpy slow-bend and impact tests of specimens cut from the fractured CN-tensile specimens. The CN-tensile and, therefore, the precrack Charpy specimens were cut from nine hydroburst Minuteman

chambers, four of which were premature proof-test failures and five were deliberately hydroburst in the Minuteman development program.

The uniaxial room- and elevated-temperature tensile data were plotted versus cumulative percent on probability paper; the plots showed a near-normal distribution. For the room-temperature data, the mean and standard deviations were taken from the plot and used to calculate the A- and B-basis values for MIL-HDBK-5. The A-basis values of ultimate tensile strength, 0.2% offset yield strength and percent elongation in 1-in. were 166.3, 153.0 ksi, and 10.2%, respectively; the B-basis values were 168.8 and 156.4 ksi, respectively. For the elevated-temperature tensile data, the means were taken for each temperature and plots of percent-of-room-temperature tensile properties versus temperature were constructed for input to MIL-HDBK-5.

The PTC-tensile K_{Ic} data were examined for the variation in fracture toughness attributable to between-forging, between-heat, and between-test-laboratory variability. The variability in K_{Ic} was examined first on the basis of engineering plots of data from individual laboratories, forgings, billets, and heats, and then by statistical-analysis techniques.

Based on the engineering plots, tests of multiple forgings from a single heat of titanium and multiple forgings from a single billet of titanium revealed differences in K_{Ic} from forging to forging when the surface precrack was deep (approximately 50% of specimen thickness). Comparisons where forgings were tested in more than one laboratory revealed differences between test results in some forgings but not all. Based on statistical analysis of the PTC-tensile data, a significant difference was indicated between K_{Ic} values obtained from the two crack depths investigated. However, statistically, there was not a significant difference between forgings or between heats with shallow cracks; whereas, with deeper cracks, there was a significant difference between heats but not a significant difference between forgings. When the data from the shallow cracks were pooled and plotted on probability paper, the population mean was estimated to be 39.1 ksi-in.$^{1/2}$ with a standard deviation of 1.6 ksi-in.$^{1/2}$ Based on all of the 540 tests, treated as a non-normal distribution, the A-basis K_{Ic} value was 30.6 ksi-in.$^{1/2}$ and the B-basis K_{Ic} value was 35.2 ksi-in.$^{1/2}$

The K_{Ic} values based on pop-in in the CN-tensile tests gave average values of K_{Ic} ranging from 31.2 to 74.6 ksi-in.$^{1/2}$ for the 18 forgings tested. Thus, the K_{Ic} values in some forgings were appreciably higher than any values measured in the PTC-tensile tests of 109 forgings. However, it should be noted that orientation of the CN-tensile specimen was such that the crack propagated in the chamber hoop direction; i.e., at 90° to the direction of crack propagation in the PTC-tensile tests. This observation, together with the fact that the PTC-tensile specimens always were taken from the ends of the cylindrical forgings, whereas the CN-tensile tests were randomly located in the forgings, precludes any conclusion regarding the correlation of K_{Ic} values as obtained from the CN- and PTC-tensile tests. A comparison of precrack Charpy slow bend

W/A values were found to provide a good estimate of the CN-tensile K_{Ic} values through the relationship:

$$K_{Ic} = 0.17\ (W/A)_{PCSB} + 16.2\ \text{ksi-in.}^{1/2}$$

where $(W/A)_{PCSB}$ is the precrack Charpy slow-bend value in in.-lb/in.^{2}. The precrack Charpy specimens were cut from the broken CN-tensile specimens, with the crack-propagation direction the same in both tests.

The plane-stress K_c fracture toughness data were based on both maximum load and the onset of crack instability as determined by the acoustical (stress-wave analysis) technique. The CN-tensile tests gave average values of K_c ranging from 71 to 137 ksi-in.$^{1/2}$ for the 18 forgings tested. The precrack Charpy impact W/A values were found to provide a good estimate of the CN-tensile K_c values through the relationship.

$$K_c = 0.10\ (W/A)_{PCI} - 6.7\ \text{ksi - in.}^{1/2}$$

where $(W/A)_{PCI}$ is the precrack Charpy impact value in in.-lb/in.^{2}. No attempt was made to correlate the laboratory test results obtained in Phase 1 with full-scale Minuteman chamber performance because (1) anisotropy in the forgings precluded correlation between CN-tensile specimens oriented for fracture in the hoop direction and chamber performance with fracture in the axial direction; and (2) reliable axial-crack-propagation CN-tensile data cannot be obtained in the increased-thickness chamber wall adjacent to the girth welds where fracture usually initiated in premature proof-test failures. Such correlations will be investigated in Phase 2 of this contract which is currently underway.

Phase 2, which is to be published as Volume 2 of this report, will seek correlation between laboratory test results with full-scale Minuteman chamber performance. The materials for the second phase will be obtained from 15 full-scale hydroburst Minuteman chambers, including eight of the chambers from Phase 1. Ten of the 15 chambers will be premature proof-test failures and five successfully hydroburst chambers. Testing domes, adaptors, and cylinders from the 15 chambers will provide data on 69 forgings, involving three different forging practices. The crack toughness measurements will be made by precrack Charpy impact tests, oriented to fracture in the chamber-axial direction, and cut from 0.1-in. and 0.19-in. wall sections on both sides of each girth weld (parent-metal tests only). Selected forgings in each chamber will be tested at -40, RT, 200 and 320°F. Particular attention will be directed to the material in the immediate vicinity of the fracture origin in the chambers under test.

APPENDIX A

UNIAXIAL-TENSILE-TEST DATA AND PROCEDURES

Appendix A

TABLE OF CONTENTS

	Page
Table I Elevated-Temperature Tensile-Test Data	61
Table II Room-Temperature Tensile-Test Data	66
Test Plan Elevated-Temperature Tensile-Test Procedure	74

Appendix A

TABLE I

ELEVATED-TEMPERATURE TENSILE-TEST DATA

Forging No.	Ultimate Tensile Strength, ksi	Yield Strength, ksi	Percent Elong. (1"Gage)	Forging No.	Tensile Strength, ksi	Yield Strength, ksi	Percent Elong. (1"Gage)
TESTED AT 150°F							
30	154.9	145.3	13.4	80A	165.9	156.3	13.0
	158.2	146.8	15.0		163.3	159.3	14.2
	157.5	145.9	13.1		166.2	154.4	14.0
42C	167.6	157.8	14.4	80B	165.6	156.1	13.5
	164.3	153.0	11.8		165.4	155.7	13.6
	169.2	160.4	13.5		165.6	155.3	12.8
54B	164.0	153.4	14.5	82A	164.4	155.2	13.5
	165.8	155.8	12.8		160.9	151.5	13.9
	159.8	150.0	12.5		162.1	152.4	13.6
	162.6	151.5	12.5	100B	164.8	153.0	12.7
61B	167.4	157.6	13.8		164.0	152.4	13.4
	162.5	150.1	15.0		164.9	153.1	12.9
	161.8	151.1	14.3		163.1	150.1	12.2
	163.6	152.5	14.9	111B	158.0	147.7	12.5
73B	163.7	154.2	14.1		163.8	153.9	13.1
	163.1	152.3	16.2		157.0	145.2	14.1
	162.6	152.9	14.3		159.0	148.5	12.8
	162.9	153.0	13.9	112A	159.4	149.5	14.5
77B	165.1	-	13.0		161.1	151.3	14.2
	164.3	153.0	12.3		158.7	149.0	14.1
	165.9	154.8	11.8		159.8	149.1	14.9
TESTED AT 200°F							
30	150.1	138.5	14.2	77B	159.8	146.2	13.3
	149.1	136.3	15.4		162.8	150.8	13.0
	147.7	137.2	14.4		161.6	148.8	11.8
	152.1	140.2	14.9	78A	162.6	150.2	11.5
42C	161.6	149.1	14.1		162.3	150.0	14.3
	164.6	153.0	14.5		163.2	150.5	14.0
	162.2	151.3	15.3	80A	163.2	152.1	13.7
54B	156.3	144.1	16.8		160.8	148.7	13.1
	161.9	149.1	15.2		162.2	148.9	14.1
	161.9	150.1	14.7	80B	159.6	148.4	13.4
	156.0	144.6	15.0		161.9	150.0	13.1
60B	164.9	154.0	14.0		159.8	148.7	14.1
	164.0	153.5	15.3	82A	158.7	148.6	13.6
	164.4	152.7	14.2		158.4	146.3	17.5
	160.5	149.1	15.0		156.6	145.5	14.0
61B	155.0	142.4	15.8		157.2	145.6	16.0
	159.9	146.6	14.9	108B	159.7	147.0	13.6
	158.5	146.0	16.2		158.0	144.2	14.8
	158.5	146.2	14.5		157.2	144.7	14.2
					158.5	145.1	14.2

Appendix A

TABLE I (cont.)

Forging No.	Ultimate Tensile Strength, ksi	Yield Strength, ksi	Percent Elong. (1"Gage)	Forging No.	Ultimate Tensile Strength, ksi	Yield Strength, ksi	Percent Elong. (1"Gage)
73B	161.3	150.9	13.9	111B	154.6	144.3	13.9
	156.8	144.4	14.9		157.5	144.3	14.1
	159.7	147.9	13.5		152.3	140.2	15.3
	162.4	151.0	14.8		156.0	144.3	14.0
74A	160.2	148.0	15.3	112A	154.2	143.1	13.4
	165.0	147.9	14.0		157.1	145.1	14.8
	160.3	148.2	14.0		158.3	147.9	14.0
	160.2	148.3	14.9		157.5	146.5	14.4
TESTED AT 250°F (FIRST TEST SERIES)							
9	145.6	131.8	15.1	91B	156.8	142.6	14.7
	144.1	131.0	15.6		154.9	141.0	14.9
	144.7	131.3	15.6		154.8	142.5	14.9
	146.3	131.5	15.6	92A	149.9	133.9	13.7
43B	152.8	138.5	14.3		154.1	135.8	16.5
	154.7	140.0	15.0		151.5	137.2	13.7
	155.1	138.9	13.5	93A	159.0	135.0	12.3
45A	153.4	138.9	15.0		152.7	135.1	13.4
	153.1	138.5	15.0		149.8	130.9	13.5
	153.9	138.8	14.1		149.4	133.4	14.8
60B	156.8	142.5	-	93B	148.7	132.4	13.9
	162.6	148.9	-		151.2	137.3	12.0
62A	154.1	142.0	15.9		153.6	139.5	14.9
	152.2	138.3	14.9	96B	164.2	151.9	12.0
	153.1	139.3	14.9		162.8	151.6	12.3
65A	155.5	138.2	14.5		163.7	152.0	12.3
	151.8	136.9	15.3	97A	152.4	138.6	12.2
	155.3	140.5	15.3		151.9	136.7	14.3
	151.5	136.8	16.7		159.1	143.8	12.9
74A	157.2	144.3	-		154.0	139.3	12.1
	157.7	142.1	-	97B	162.3	148.5	13.6
	156.0	141.1	-		166.0	155.5	12.2
	158.2	142.5	-		164.0	151.5	12.4
74B	147.7	137.5	14.3	98A	155.4	139.0	12.0
	152.7	139.3	15.2		151.3	135.9	12.7
	156.8	140.3	14.4		154.9	139.1	12.2
76A	153.7	139.8	15.2	101A	159.5	144.7	14.5
	149.0	135.4	16.0		157.7	138.0	13.0
	152.9	138.7	15.5		154.5	-	14.8
77A	162.4	150.0	12.4		157.8	143.9	13.9
	158.2	145.1	15.3	102A	150.4	137.4	14.3
	165.3	154.0	13.4		152.6	135.9	14.5
78A	158.1	143.8	-		149.5	134.0	14.7
	159.4	145.5	-	104A	151.5	135.6	14.4
	159.1	143.5	-		149.3	134.9	14.4
	157.4	142.8	-		150.8	136.5	13.5
77B	161.2	147.9	14.9	104B	152.1	137.3	14.6
	161.5	150.0	14.6		151.7	137.5	14.9
	156.3	143.3	15.2		151.5	135.8	13.6
					148.0	132.8,	13.8
					150.9	134.8	16.3

TABLE I (cont.)

Forging No.	Ultimate Tensile Strength, ksi	Yield Strength, ksi	Percent Elong. (1"Gage)	Forging No.	Ultimate Tensile Strength, ksi	Yield Strength, ksi	Percent Elong. (1"Gage)
87A	154.2	138.0	14.2	105A	157.7	141.0	15.3
	149.2	134.0	13.2		153.9	136.8	14.0
	151.2	137.3	15.2		153.9	134.9	15.2
	156.0	143.7	13.2	107A	150.6	135.2	14.7
90A	155.1	140.5	13.4		150.9	135.2	17.0
	156.7	140.8	12.9		149.9	133.9	14.9
	155.3	140.0	13.6	107B	148.7	131.7	14.3
90B	155.3	140.1	14.5		152.5	137.8	14.5
	156.8	140.1	16.3		145.8	130.2	14.7
	153.6	137.7	15.1		151.0	135.9	14.7
91A	156.6	-	14.0	108A	160.0	148.5	14.7
	157.1	141.7	14.0		153.8	139.9	14.9
	154.9	134.2	8.4		157.9	145.5	14.0
TESTED AT 250°F (SECOND TEST SERIES)							
30	143.6	129.3	16.9	78A	153.8	139.2	17.2
	144.9	131.1	16.9		154.6	140.5	18.6
42C	154.0	140.3	15.9		152.7	138.3	16.8
	158.4	145.7	15.7		156.0	142.2	16.8
	154.2	141.9	16.1	80A	152.9	139.9	17.2
54B	153.3	139.1	16.7		158.0	143.4	16.5
	148.9	137.0	16.5		158.0	144.1	16.4
	156.4	143.0	16.4	80B	155.4	140.5	17.2
	149.6	136.6	18.2		155.3	141.0	16.1
60B	160.0	147.0	16.8		156.0	141.8	16.0
	159.1	146.4	15.7	82A	151.1	137.0	17.0
	158.5	146.0	15.6		153.6	140.0	16.0
61B	151.9	135.4	18.3		153.9	138.6	17.0
	156.6	143.0	16.0	108B	154.8	139.4	16.0
	152.2	137.6	16.4		155.6	139.0	16.0
	152.5	138.2	16.0		156.4	140.3	16.0
73B	155.1	142.9	16.7		154.4	138.0	16.0
	150.4	136.9	17.0	111B	153.5	137.8	16.0
	150.1	135.0	16.6		148.9	133.9	17.0
	154.4	141.5	15.2		148.9	133.2	17.0
74A	153.8	138.6	14.7		154.4	140.0	16.5
	155.8	144.3	15.3	112A	151.5	136.5	15.2
	154.0	143.5	16.1		149.1	136.2	16.2
	154.4	141.3	14.3		147.1	134.0	17.3
77B	157.0	141.1	15.9		148.3	135.0	18.4
	154.4	139.5	14.8				
	154.5	138.8	14.5				
TESTED AT 280°F							
9	141.2	125.3	17.1	93A	148.7	131.0	14.7
	142.0	126.3	18.5		146.8	126.1	14.7
	136.6	122.1	16.5		146.6	128.3	15.6
	136.6	121.6	17.5		147.6	124.8	15.5

Appendix A

TABLE I (cont.)

Forging No.	Ultimate Tensile Strength, ksi	Yield Strength, ksi	Percent Elong. (1"Gage)
43B	154.0	123.2	14.1
	153.3	137.1	16.2
45A	150.8	134.6	14.8
	149.1	133.2	13.5
	152.0	137.2	14.6
62A	152.7	137.8	16.9
	153.6	140.0	16.8
	155.4	129.0	16.8
65A	150.3	133.8	15.0
	151.3	136.5	15.9
	150.3	135.5	14.5
	152.0	136.6	15.5
74B	152.4	136.6	16.1
	152.0	137.0	14.4
	149.0	134.4	16.0
	151.0	133.9	14.5
76A	152.3	138.4	14.5
	150.1	135.3	15.1
	149.7	135.7	15.1
	149.4	134.7	15.8
77A	156.6	140.5	14.9
	153.1	142.1	14.5
	156.9	141.3	15.1
79B	155.0	139.4	16.3
	155.0	141.0	16.4
	155.2	140.8	15.9
	154.4	139.0	14.5
87A	149.4	133.9	14.5
	147.8	132.8	14.3
	152.0	137.1	14.3
	145.7	130.3	13.9
90A	149.0	131.9	14.0
	149.3	132.8	13.9
	149.6	132.9	15.9
90B	153.1	137.3	15.8
	152.3	136.9	14.8
	151.9	135.5	16.1
91A	146.2	132.0	15.8
	147.7	131.1	15.6
	147.7	131.9	15.3
91B	150.6	135.6	15.6
	149.1	134.6	14.9
	151.2	136.3	14.8
92A	151.2	136.0	16.0
	147.6	131.4	15.4
	148.4	133.1	16.4
	148.0	132.4	16.0
93B	153.4	136.5	14.8
	147.6	131.9	14.0
	146.0	130.8	15.0
	150.7	136.8	12.7
96B	157.0	144.8	17.6
	154.1	141.2	13.8
	152.5	138.2	13.4
97A	147.4	130.6	14.0
	148.1	130.6	12.5
	147.5	130.2	12.2
	148.5	130.0	15.3
97B	156.0	141.3	14.5
	153.2	137.7	15.7
	158.0	143.2	15.1
98A	146.8	130.4	13.5
	147.2	132.0	14.2
	151.0	134.6	13.9
101A	150.7	137.8	12.9
	146.6	130.6	14.8
	147.0	130.8	15.7
	146.4	129.4	15.0
102A	146.7	127.4	16.7
	146.3	131.0	16.1
	144.8	128.3	16.3
	145.1	128.0	13.3
104A	149.7	133.3	14.2
	144.4	128.2	14.4
	148.0	132.0	15.8
104B	152.4	133.3	15.0
	148.9	130.0	15.4
	147.5	128.2	16.0
	150.6	135.1	15.2
105A	144.7	127.1	16.0
	146.7	129.0	16.8
	151.1	133.1	17.0
107A	147.4	129.9	15.8
	150.7	134.4	15.1
	149.8	132.9	15.1
	151.0	134.4	15.1
107B	146.1	128.4	15.0
	149.8	133.6	15.5
	146.0	129.3	15.4
	149.1	132.5	15.0
108A	146.8	137.4	14.5
	151.5	137.4	15.5
	151.0	135.9	15.1
	149.9	134.4	16.5

TABLE I (cont.)

Forging No.	Ultimate Tensile Strength, ksi	Yield Strength, ksi	Percent Elong. (1"Gage)	Forging No.	Ultimate Tensile Strength, ksi	Yield Strength, ksi	Percent Elong. (1"Gage)
TESTED AT 330°F							
9	135.8	119.1	17.5	93A	142.9	125.3	14.4
	133.0	116.5	17.4		143.4	126.1	15.6
	140.2	123.4	17.5		146.1	127.8	15.0
	134.2	117.0	17.5		146.0	129.4	14.6
43B	149.7	132.5	15.4	93B	139.9	122.9	15.3
	149.8	-	15.8		144.3	127.9	14.3
	141.2	-	15.7		140.3	119.9	14.2
45A	148.3	130.4	16.3	96B	152.2	140.1	14.7
	146.7	131.4	15.6		150.7	137.0	13.0
	148.2	131.5	15.7		151.6	137.9	12.0
62A	147.0	131.0	17.7	97A	145.4	128.5	15.3
	145.9	131.1	18.5		146.3	127.3	15.0
	149.3	134.6	17.8		147.5	131.0	14.2
65A	146.1	128.8	16.2		148.1	133.0	13.7
	143.3	125.7	16.0	97B	150.7	136.1	15.4
	144.3	127.7	17.7		151.9	136.6	16.5
	143.9	127.3	16.8		153.7	135.5	15.5
74B	146.5	130.3	16.4	98A	144.1	126.9	15.4
	145.8	130.9	17.9		142.1	124.2	15.2
	144.4	129.5	16.6		140.6	122.0	14.1
76A	143.2	127.8	17.4	101A	145.4	128.8	16.2
	146.1	130.9	16.3		141.4	125.0	15.9
	146.6	130.5	16.5		140.6	122.8	15.8
77A	154.3	137.6	15.2		144.0	127.7	14.4
	160.0	146.1	13.0	102A	139.3	122.7	16.0
	151.0	135.6	14.4		146.9	126.0	15.3
79B	147.4	130.4	15.1		141.7	125.3	14.4
	147.1	130.7	16.5		139.3	121.6	16.1
	147.4	128.9	17.0	104A	145.1	132.0	16.7
87A	140.6	124.2	16.0		146.2	130.0	15.5
	146.7	130.1	15.9		143.5	127.3	16.4
	147.1	130.6	15.8	104B	144.0	127.6	16.0
	142.1	124.2	14.2		142.3	124.6	16.1
90A	143.6	124.9	15.8		144.8	135.5	16.0
	147.3	127.9	14.7		147.0	130.2	15.7
	148.3	131.2	14.6	105A	144.1	129.6	16.5
90B	147.8	130.0	16.0		144.3	127.7	16.8
	143.4	125.8	16.5		142.3	126.9	18.5
	143.0	125.9	15.3	107A	142.6	126.4	17.4
91A	145.8	127.8	16.0		143.4	126.6	17.1
	145.7	128.4	15.9		142.0	124.4	17.3
	142.8	124.9	16.8	107B	145.0	-	17.7
91B	143.2	126.6	15.2		142.0	125.4	18.0
	143.2	126.1	15.7		143.7	125.5	15.7
	143.8	125.6	15.7		139.9	125.1	17.8
92A	143.2	130.4	18.0	108A	145.3	-	16.5
	145.2	129.4	16.9		143.1	126.7	15.8
	143.4	127.6	17.0		146.1	130.2	17.4
	143.4	128.3	16.6				

TABLE II

ROOM-TEMPERATURE TENSILE-TEST DATA

Forging SN		0.2% Offset Y.S. (ksi)	Ultimate Strength (ksi)	Elong. (%)	Forging SN		0.2% Offset Y.S. (ksi)	Ultimate Strength (ksi)	Elong. (%)
4		164	174	14	17		165	177	13
		165	176	14			166	175	13
		158	179	13			168	179	13
	Av	162.3	176.3	14		Av	166.3	177	13
5		165	166	16	21		162	173	14
		160	172	14			166	175	13
		157	170	14			166	177	13
	Av	160.7	169.3	14.7		Av	164.7	175	13.3
6		157	166	14	22		163	174	13
		157	168	16			164	175	11
		158	167	16			164	176	13
	Av	157.3	167	15.3		Av	163.7	175	12.3
7		161	170	16	23		160	172	16
		162	170	14			164	174	14
		162	172	14			164	175	14
	Av	161.7	170.7	14.7		Av	162.7	173.7	14.7
9		160	169	14	26		157	170	14
		156	168	14			160	171	14
		157	168	14			160	172	13
	Av	157.7	168.3	14		Av	159	171	13.7
13		160	171	16	27		164	175	14
		162	171	16			169	180	14
		162	172	16			166	175	13
	Av	161.3	171.3	16		Av	166.3	176.7	13.7
14		158	166	13	29		166	176	11
		162	172	14			165	174	13
		162	170	14			163	173	13
	Av	160.7	169.3	13.7		Av	164.7	174.3	12.3

TABLE II (cont.)

Forging SN		0.2% Offset Y.S. (ksi)	Ultimate Strength (ksi)	Elong. (%)
30		164	176	13
		163	174	13
		166	176	13
	Av	164.3	175.3	13
31A		165	174	13
		168	179	13
		169	177	11
	Av	167.3	176.7	12.3
31B		165	176	13
		172	178	13
		166	176	14
	Av	167.7	176.7	13.3
33A		156	166	13
		159	169	13
		160	170	13
	Av	158.3	168.3	13
33B		158	168	13
		158	170	9
		159	167	14
	Av	158.3	168.3	12
36A		169	179	13
		168	178	13
		166	176	11
	Av	167.7	177.7	12.3
36B		165	175	13
		167	177	13
		165	174	14
	Av	165.7	175.3	13.3
37A		166	180	13
		165	176	14
		160	173	13
	Av	163.7	176.3	13.3
37B		160	170	13
		159	168	13
		162	170	13
	Av	160.3	169.3	13
39A		160	171	13
		160	170	13
		164	174	13
	Av	161.3	171.7	13
42B		167	175	15
		168	177	15
		168	177	15
	Av	167.7	176.3	15
42C		160	172	14
		160	173	14
		160	171	14
	Av	160	172	14
43A		175	180	14
		164	172	15
		173	180	14
	Av	170.7	177.3	14.3
43B		164	173	16
		165	174	17
		165	174	18
	Av	164.7	173.7	17
44B		160	172	18
		158	169	18
		160	172	18
	Av	159.3	171	18

TABLE II (cont.)

Forging SN		0.2% Offset Y.S. (ksi)	Ultimate Strength (ksi)	Elong. (%)	Forging SN		0.2% Offset Y.S. (ksi)	Ultimate Strength (ksi)	Elong. (%)
45A		161	172	14	55A		158	173	13
		160	172	14			158	172	13
		162	173	14			160	173	14
	Av	161	172.3	14		Av	158.7	172.7	13.3
50A		162	172	11	55B		159	170	14
		162	172	13			160	172	14
		160	170	14			159	170	14
	Av	161.3	171.3	12.6			159.3	170.7	14
50B		164	174	13	56A		160	174	13
		165	174	13			164	176	13
		160	171	11			165	179	13
	Av	163	173	12.3		Av	163	176	13
52B		166	173	16.5	56B		164	174	14
		169	177	13			164	176	14
		165	172	15			167	178	14
	Av	166.7	174	14.8		Av	165	176	14
53B		161	177	14	57A		158	166	13
		161	177	13			158	170	13
		162	178	14			157	171	13
	Av	161.3	177.3	13.6		Av	157.7	169	13
54A		162	172	13	57B		160	168	14
		160	174	13			157	170	13
		166	175	13			164	173	14
	Av	162.7	173.7	13		Av	160.3	170.3	13.7
54B		165	177	13	58B		163	177	14
		163	174	13			166	178	14
		168	179	13			170	179	13
	Av	165.3	176.7	13		Av	166.3	178	13.7

TABLE II (cont.)

Forging SN		0.2% Offset Y.S. (ksi)	Ultimate Strength (ksi)	Elong. (%)
59A		166	178	13
		164	177	13
		168	179	13
	Av	166	178	13
60B		170	176	16
		170	178	16
		159	167	16
	Av	166.3	173.7	16
61A		161	172	14
		167	178	14
		166	176	15
	Av	164.7	175.3	14.3
61B		160	172	13
		160	172	11
		162	174	13
	Av	160.7	172.7	12.3
62A		167	176	15
		165	172	12
		171	179	15
	Av	167.7	175.7	14
62B		165	172	14
		165	170	14
		163	171	16
	Av	164.3	171	14.8
63A		164	170	15
		167	172	17
		167	175	17
	Av	166	172.3	16.3
63B		162	172	13
		161	172	9
		159	170	13
	Av	160.7	171.3	11.7
65A		163	174	13
		160	170	14
		164	174	13
	Av	162.3	172.7	13.3
66B		165	175	15
		166	176	15
		172	180	15
	Av	167.7	177	15
69A		164	174	13
		162	175	13
		164	175	13
	Av	163.3	174.7	13
69B		164	176	13
		162	175	11
		162	175	13
	Av	162.7	175.3	12.3
70A		159	172	14
		159	172	13
		159	172	14
	Av	159	172	13.7
70B		165	175	13
		163	171	12.5
		162	172	12.5
	Av	163.3	172.7	12.7

TABLE II (cont.)

Forging SN		0.2% Offset Y.S. (ksi)	Ultimate Strength (ksi)	Elong. (%)	Forging SN		0.2% Offset Y.S. (ksi)	Ultimate Strength (ksi)	Elong. (%)
71A		164	176	13	77A		165	176	15
		163	176	13			162	174	15
		160	174	13			165	176	15
	Av	162.3	175.3	13		Av	164	175.3	15
73A		158	173	13	77B		161	174	11
		160	174	14			165	176	13
		158	174	13			164	178	13
	Av	158.7	173.7	13.3		Av	163.3	176	12.3
73B		171	180	14	78A		173	180	12
		168	175	13			168	175	13
		166	175	13			170	180	13
	Av	168.3	176.7	13.3		Av	170.3	178.3	12.7
74A		163	174	13	79A		163	174	13
		164	174	13			164	174	13
		166	174	13			164	173	11
	Av	164.3	174	13		Av	163.7	173.7	12.3
74B		166	174	14	79B		161	172	13
		164	174	14			161	172	13
		165	173	14			160	172	13
	Av	165	173.7	14		Av	160.7	172	13
75A		164	177	14	80A		164	175	9
		164	177	13			163	174	13
		166	176	14			164	176	13
	Av	164.7	176.7	13.7		Av	163.7	175	11.7
76A		162	173	13	80B		160	174	13
		160	170	13			161	174	11
		162	172	13			160	173	11
	Av	161.3	171.7	13		Av	160.3	173.7	12.3

TABLE II (cont.)

Forging SN		0.2% Offset Y.S. (ksi)	Ultimate Strength (ksi)	Elong. (%)
81A		162	175	13
		165	178	13
		164	177	14
	Av	163.7	176.7	13.3
82A		160	173	11
		160	173	13
		163	175	13
	Av	161	173.7	12.3
83A		163	173	14
		163	173	14
		163	175	14
	Av	163	173.7	14
84B		158	166	15
		159	169	14
		159	166	14
	Av	158.7	167	14.3
86A		162	176	14
		165	178	14
		162	176	11
	Av	163	176.7	13
87A		160	171	14
		159	171	14
		160	172	13
	Av	159.7	171.3	13.7
87B		162	174	13
		161	173	13
		164	178	13
	Av	162.3	175	13
90A		158	171	13
		159	172	14
		158	172	14
	Av	158.3	171.7	13.7
90B		161	174	13
		161	174	13
		161	174	14
	Av	161	174	13.3
91A		162	174	13
		163	175	13
		163	176	14
	Av	162.7	175	13.3
91B		162	172	14
		160	172	13
		163	173	13
	Av	161.7	172.3	13.3
92A		167	177	13
		163	172	14
		166	176	15
	Av	165.3	175	14
93A		163	174	13
		164	176	13
		160	172	11
	Av	162.3	174	12.3
93B		160	172	14
		163	173	13
		161	172	14
	Av	161.3	172.3	13.7

TABLE II (cont.)

Forging SN		0.2% Offset Y.S. (ksi)	Ultimate Strength (ksi)	Elong. (%)
94B		162	172	13
		158	170	14
		159	172	14
	Av	161.7	171.3	13.7
96A		162	173	13
		158	170	13
		159	170	14
	Av	159.7	171	13.3
96B		165	175	13
		170	180	12.5
		166	175	13
	Av	167	176.7	12.7
97A		164	176	13
		163	175	13
		162	174	11
	Av	163	175	12.7
97B		162	174	11
		165	178	11
		164	177	13
	Av	163.7	176.3	11.7
98A		164	176	11
		160	173	13
		160	174	13
	Av	161.3	174.3	12.3
100A		161	174	13
		160	173	13
		161	173	13
	Av	160.7	173.3	13
100B		163	173	13
		165	174	15
		171	179	13
	Av	166.3	175.3	13.7
101A		162	174	13
		164	176	13
		162	174	13
	Av	162.7	174.7	13
102A		159	170	13
		160	172	13
		159	172	13
	Av	159.3	171.3	13
102B		163	177	13
		163	176	11
		162	174	13
	Av	162.7	175.7	12.3
104A		161	173	11
		162	174	11
		162	172	13
	Av	161.7	173	11.7
104B		162	173	13
		161	172	14
		161	174	13
	Av	161.3	173	13.3
105A		164	176	13
		162	174	13
		160	173	14
	Av	162	174.3	13.3

TABLE II (cont.)

Forging SN		0.2% Offset Y.S. (ksi)	Ultimate Strength (ksi)	Elong. (%)
105B		162	175	14
		160	173	14
		162	174	13
	Av	161.3	174	13.7
107A		158	170	13
		160	171	14
		160	172	14
	Av	159.3	171	13.7
107B		158	170	13
		161	171	13
		159	170	13
	Av	159.3	170.3	13
108A		163	174	13
		163	175	13
		162	174	13
	Av	162.7	174.3	13
108B		160	171	14
		162	174	13
		162	174	11
	Av	161.3	173	12.7
109B		160	172	13
		163	174	13
		160	172	13
	Av	161	172.7	13
110B		160	172	14
		162	173	13
		160	172	14
	Av	160.7	172.3	13.7
111B		160	171	13
		160	171	13
		161	170	13
	Av	161.3	170.7	13
112A		162	174	13
		160	172	13
		162	174	13
	Av	161.3	173.3	13
112B		163	175	14
		162	175	13
		163	176	13
	Av	163	175.3	13.3

Appendix A

ELEVATED-TEMPERATURE TENSILE TEST PROCEDURE

Operation	Description
0	Material: 6Al-4V Titanium Condition: Heat treated to 155 ksi minimum yield strength Configuration: Round tensile specimens 0.250-in. diameter Number of Test Specimens: 561
1.0	Elevated Temperature Testing: Reference: ASTM Designation E151-61T. The testing procedure shall comply with this testing practice.
2.0	General Description of Test: The specimens listed in operation 0 were tested at 150°F, 200°F, and 250°F. Rings providing 12 specimens were divided into three lots of four (4) specimens each; one lot was tested at 150°F, one at 200°F, and one at 250°F. Rings providing less than 12 specimens were divided generally into three lots of three (3) specimens each; one lot was tested at 150°F, one at 200°F, and one at 250°F; however, with rings providing eleven specimens, four (4) specimens were tested at 200°F and at 250°F and with rings providing ten specimens, four (4) specimens were tested at 200°F.
3.0	Method of Heating: Radiant heating was used.*
4.0	Conditions of Heating Gage Length: Heat gage length to the indicated nominal test temperatures within 60 seconds.
5.0	Holding Time: Holding time shall be 60 seconds before applying the load.
6.0	Temperature Control: Variation from the specified nominal test temperature was ±5°F; variation along the gage length was +5°F-10°F. Overshoot did not exceed 10°F.

* Since radiant heating was used, the thermocouple junction was shielded from direct radiation.

Operation	Description
7.0	**Temperature Measurement:**
	Thermocouples not larger than 28 gage were used for measuring temperature. Thermocouples were attached by capacitance welding. To determine the uniformity of temperature over the gage length, three thermocouples were used, one at mid-gage length and one at each end of the gage section.
8.0	**Strain Measurement:**
	A constant strain rate of 0.005 ± 0.002 in. per in. per minute was used during application of the load to approximately 0.6 percent strain offset from the straight portion of the load strain curve by using strain-pacing equipment.
9.0	**Recording of Test Results:**
	The test results include the following:
	9.1 Test temperature, heating rate, strain rate, and holding time at test temperature. 9.2 The 0.2 percent offset yield strength. 9.3 Tensile strength. 9.4 Elongation over gage length. 9.5 Stress-strain curves.

APPENDIX B

FRACTURE TOUGHNESS OF TITANIUM 6A1-4V
SECOND-STAGE MINUTEMAN ROCKET
MOTOR CASE MATERIAL

Appendix B

TABLE OF CONTENTS

		Page
I.	Introduction	81
II.	Technical Discussion	82
	A. Material	82
	B. Specimen Machining	83
	C. Specimen Testing	86
	D. Data Analysis	87
	E. Discussion of Results	92
	1. Size and Shape of Starter Flaw	92
	2. Stress Intensity as a Fracture Toughness Criteria	92
	a. K_{Ic} as a Function of Material Strength	92
	b. K_{Ic} as a Function of Specimen and Flaw Size	92
	c. Variation in Toughness from Forging to Forging	112
	d. Variation in Test Results from Laboratory to Laboratory	114
III.	Addendum	124
	B-1 Computer Print-Out of PTC-Tensile Test Data (K_{Ic} Based on Irwin's Equation)	124
	B-2 Computer Program Details	155
	B-3 Effect of Heat Tinting on Plastically Deformed Metal	166

Appendix B

LIST OF TABLES

Table		Page
I	Identification of Forging Serial Numbers to be Tested by Each Laboratory	84
II	Effect of Specimen Width and Thickness in PTC Tensile Tests, 6Al-4V Titanium Forging 53B, 161 ksi Yield	102

Appendix B

ILLUSTRATIONS

Figure		Page
1	Part-Through-Crack Tensile Specimen	85
2	Part-Through Tensile Test Grips	88
3	Flaw Shape Parameter for Surface Cracks	90
4	Relationship Between Flaw Shape and Crack Area	92
5	Typical Surface Cracks in 6Al-4V Titanium Fracture Testing	94
6	Relationship Between Ultimate Tensile Strength and Plane-Strain Fracture Toughness (K_{Ic}) in 109 6Al-4V Titanium Forgings	95
7	Relationship Between 0.2% Offset Yield Strength and Plane-Strain Fracture Toughness (K_{Ic}) in 109 6Al-4V Titanium Forgings	96
8	Effect of Craft Depth on the Relationship Between Yield Strength and K_{Ic}	97
9	Effect of Crack Depth on the Plane-Strain Fracture Toughness Measurement in Ti-6Al-4V (after Hoeppner)	99
10	Effect of Crack Depth-to-Thickness Ratio on the Plane-Strain Fracture Toughness Measurement in Ti-6Al-4V (after Hoeppner)	100
11	Effect of Crack Depth on the K_{Ic} Value and on the Net-Stress-to-Yield Ratio in MINUTEMAN Forging 53B	101
12a	Effect of Crack Depth on the K_{Ic} Value in Ti-6Al-4V Forging 63A	104
12b	Effect of Fracture Stress and Crack Area on the K_{Ic} Value in Ti-6Al-4V Forging 63A	105
13a	Effect of Crack Depth on the K_{Ic} Value in Forging 63B	106
13b	Effect of Fracture Stress and Crack Area on the K_{Ic} Value in Forging 63B	107
14a	Effect of Crack Depth on the K_{Ic} Value in Forging 66B	108
14b	Effect of Fracture Stress and Crack Area on the K_{Ic} Value in Forging 66B	109

Appendix B

ILLUSTRATIONS (cont.)

Figure		Page
15a	Effect of Crack Depth on the K_{Ic} Value in Forging 69A	110
15b	Effect of Fracture Stress and Crack Area on the K_{Ic} Value in Forging 69A	111
16	Effect of Crack Depth on the K_{Ic} Value for Forgings from Single Heats of Ti-6Al-4V (Forging Billets 90-92 Tested by Aerojet-Downey and 100-102 Tested by Lycoming)	113
17	Effect of Crack Depth on the K_{Ic} Value for Forgings from Single Heats of Ti-6Al-4V (Forging Billets 73-74 Tested by Aerojet-Downey and 108-111 Tested by Lycoming)	115
18	Variation in K_{Ic} Value from Lab to Lab in Forging 69B	116
19	Variation in K_{Ic} Value from Lab to Lab in Forging 70A	117
20	Variation in K_{Ic} Value from Lab to Lab in Forging 70B	118
21	Variation in K_{Ic} Value from Lab to Lab in Forging 71A	119
22	Effect of Crack Depth on the K_{Ic} Value in Billet 69 as Tested by Three Laboratories	121
23	Variation in K_{Ic} Value from Forging to Forging in Billet 70 as Tested by Aerojet-Downey	122
24	Variation in K_{Ic} Value from Forging to Forging in Billet 70 as Tested by Aerojet-Sacramento	123

Appendix B

I. INTRODUCTION

The investigation described in this appendix was made under Contract AF 04(694)-308 to determine the effect of surface flaws on the room-temperature behavior of 6Al-4V titanium-alloy forgings employed in second-stage MINUTEMAN solid-propellant rocket-motor case assemblies (Ref 1). It was this investigation that provided the plane-strain (K_{Ic}) fracture-toughness values for the Mil-Hdbk-5 data collection under Contract F 33615-67-C-1358.

The design and test procedure for the part-through-crack tensile specimen employed under Contract AF 04(694)-308 were specified by Space Technology Laboratories (STL), Inc., on the basis of previous studies (Ref 2), which indicated that such tests may be used as an accept-reject criterion for rocket chamber components. Two crack sizes were specified by STL; viz., a crack area of 0.010 sq. in. and a crack area at which the notch strength is equal to the 0.2% offset yield strength of the material.

The overall program consisted of testing 708 part-through-crack tensile specimens from 109 different forgings. The MINUTEMAN case fabrications (Aerojet-General Downey Plant and Lycoming) each conducted 180 tests of 30 forgings, and the Aerojet-General Sacramento Plant conducted 348 tests of 58 forgings. Five forgings were tested at each of two laboratories so that the test results between laboratories could be correlated. Data analysis in accordance with the STL procedures was performed by the respective laboratories, and finally, the test results obtained at the three laboratories were analyzed by the Aerojet-General Sacramento Plant on the basis of the concepts of linear-elastic fracture mechanics. The results of the latter analysis are presented in this appendix. Statistical analysis of the data for purposes of Mil-Hdbk-5 presentation and to determine the variation in K_{Ic} attributable to between-forging, between-heat and between-test-laboratory variability are presented in Appendix E.

(1) P. P. Crimmins and C. E. Hartbower, Fracture Toughness of Titanium 6Al-4V Second-Stage MINUTEMAN Pocket Motor Case Material, Aerojet-General Corp. Final Report 655MF on Contract AF 04(694)-308, 28 April 1965.

(2) P. N. Randall and R. P. Felgar, "Part-Through-Crack Test-Relation to Solid Propellant Rocket Cases", J. of Basic Engineering (Transactions Am. Society Mechanical Engrs.), Dec., 1964, pp 685-692.

II. TECHNICAL DISCUSSION

A. MATERIAL

The test material for this data collection was supplied in the form of arc segments (nominally of 80°-arc length x 0.6-in. thick x 3/4-in. wide) cut from 52-in. dia 6Al-4V titanium cylinders forged by Cameron Iron Works, Inc., Houston, Texas. The test material was heat treated while still an integral part of the extruded cylinders in accordance with Aerojet-General Corp. Specification AGC 34007B. The chemical and mechanical properties requirements are shown below; fracture-toughness properties are not specified.

		Check-Analysis Requirement	
Material	Percent	Under	Over
Aluminum	5.50 to 6.75	0.40	0.40
Vanadium	3.50 to 4.50	0.15	0.15
Iron	0.30 max	--	0.15
Oxygen	0.12 to 0.20	--	--
Carbon	0.10 max	--	0.04
Nitrogen	0.05 max	--	0.02
Hydrogen	0.0125 max	--	0.002
Other Elements-Total	0.40 max	--	
Titanium	Remainder	--	--

0.2% Offset Yield Strength: 155,000 psi min

Ultimate Strength: 165,000 to 180,000 psi max

Elongation (over a 4D Gage Length): 8% min

The above mechanical properties are attained by means of the forging and heat-treating procedures specified in Specification AGC 34007B. Specifically, it is required that the beta-transus temperature not be exceeded during the finish-forging operation, which will involve enough work to eliminate evidence of a Widmanstatten structure. The forging history of a typical ingot is as follows:

After casting, the ingot was conditioned by cold grinding. The ingot was then forged, starting at a temperature above the beta transus, to produce a billet approximately 22-in. dia.

The billets were then examined ultrasonically in the titanium-producer's plant, chemically analyzed and the beta-transus temperature determined.

Appendix B

The billets received by Cameron Iron Works were in the form of a 22-in. octagonal billet. Although some aspects of the forging practice used by Cameron are considered proprietary information (these aspects, therefore, are treated in general terms), the procedure was as follows: The 22-in. billet was first pressed into a 6-in. high pancake. In the next operation, a 38-in. dia hole was extruded from the center of the pancake. Subsequently, the extruded preform was subjected to surface conditioning, facing and machining to the proper radii. The preform was then ring-rolled in a Wagner ring-roller to approximately 52-in. diameter. In the next operation, the ring was surface-conditioned, faced, and a lubricant applied to the surface in the form of wire. The final extrusion was made on a 20,000-ton press in approximately 40 sec, as a back extrusion (the male die moves and the female die remains stationary). The final forging temperature was 35° to 50°F below the beta-transus.

After rough machining, the part was solution-treated (maximum temperature 60°F below the beta-transus) and water quenched (4-sec quench delay time). The aging treatment for the individual forgings was performed at a temperature between 900 and 1050°F for 8 hours. The aging temperature for each forging was selected on the basis of laboratory heat treatment of tensile blanks obtained from trim stock cut from each forging. During the aging operation, the cylinders were fixtured to obtain a specified condition of roundness.

The ring segments solution-treated and aged as an integral part of the forging were also the source of the component qualification tensile tests required for each forging. The results of the circumferentially oriented tensile tests performed to qualify each forging are presented in Table I (see Appendix A - Table I). As indicated by these data, all the forgings met the mechanical-property requirements of Specification AGC 34007B (155 ksi minimum yield and 180 ksi maximum ultimate tensile strength).

B. SPECIMEN MACHINING

The procedures outlined below are those employed by the Aerojet-Sacramento Plant in preparation of the part-through-crack (PTC) tensile specimen; the procedures employed at Aerojet-Downey and Lycoming differed only in minor details.

The PTC tensile specimen used in this program is shown in Figure 1. This configuration was produced by a shaper and a conventional high-speed-steel tool bit, although it was necessary to use a carbide tool before the actual shaping operation in order to remove a hard oxide-surface-layer formed in forging and solution treating the titanium. The 0.250-in. radius at the ends of the gage section was also produced on the shaper with a high-speed-steel tool bit. Six specimens of each forging were cut and machined in this manner to provide three specimens for testing each of the two crack sizes. To

Appendix B

TABLE I

IDENTIFICATION OF FORGING SERIAL NUMBERS
TESTED BY EACH LABORATORY

I. AEROJET-SACRAMENTO

4	30	44B	58B
5	31A	45A	59A
6	31B	50A	60B
7	33A	50B	61A
9	33B	52B	61B
13	36A	53B	62A
14	36B	54A	62B
17	37A	54B	63A
21	37B	55A	65A
22	39A	55B	66B
23	42B	56A	69A
26	42C	56B	69B
27	43A	57A	70A
29	43B	57B	70B
			71A

II. AEROJET-DOWNEY

69B(a)	75A	80B	87B
70A(a)	76A	81A	90A
70B(a)	77A	82A	90B
71A(a)	77B	83A	91A
73A	78A	84B	91B
73B	79A	86A	92A
74A	79B	87A	93A
74B	80A		

III. LYCOMING

63A(b)	96B	102B	108A
63B(b)	97A	104A	108B
66B(b)	97B	104B	109B
69A(b)	100A	105A	110B
84B	100B	105B	111B
93B	101A	107A	112A
94B	102A	107B	112B
96A			

(a) Also tested at Aerojet-Sacramento.
(b) Also tested at Aerojet-Sacramento.

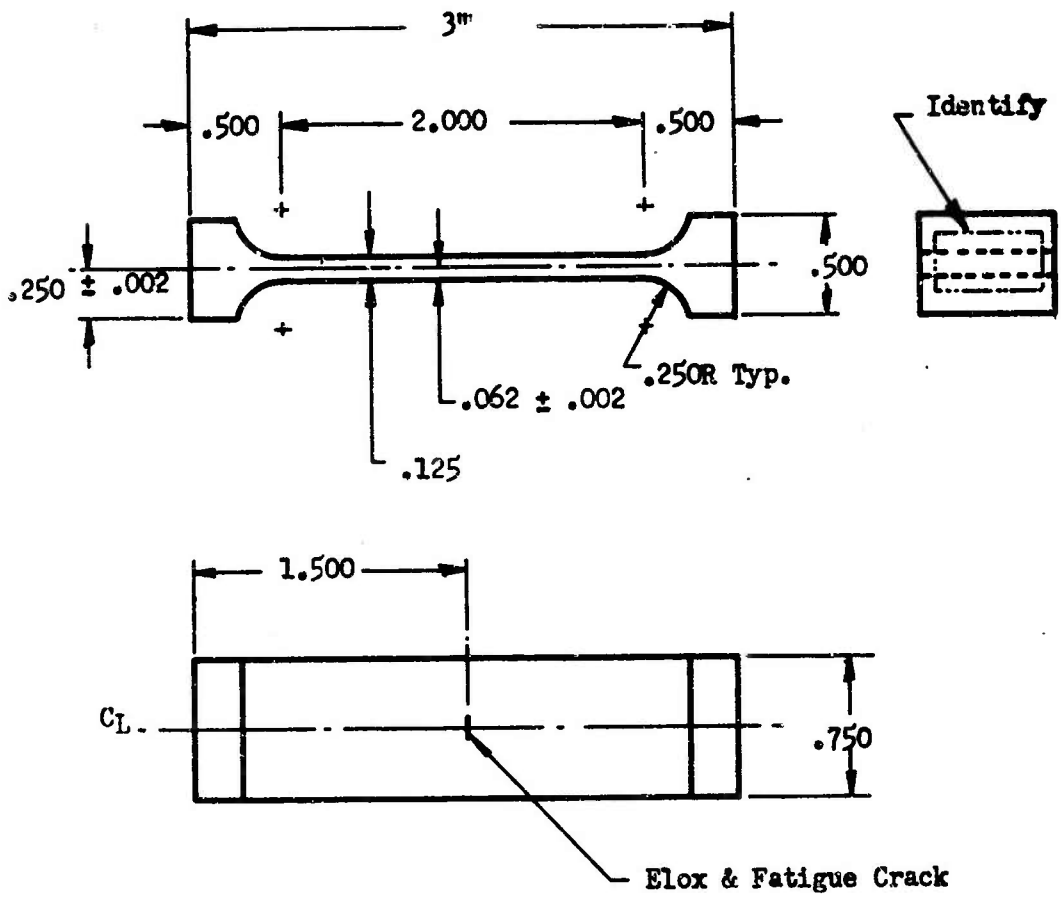


Figure 1. Part-Through-Crack Tensile Specimen

identify the inside diameter of the forged surface, the specimens were steel stamped on both ends so that the top of the identifying number pointed to the inside diameter surface. The original identification number was maintained during all machining operations.

The PTC was placed on the inside diameter surface of each specimen by a 60-amp electric discharge machine made by the Elox Corporation of Michigan. A 0.025-in. dia tungsten rod, ground to a chisel-like tip, was used as an electrode. The surface defect produced in this manner was approximately 0.028-in. long and 0.010-in. deep. The electrical discharge machining was done in oil at the following machine settings:

Current Control	Voltage Control	Down Feed	Frequency Setting	Current	Adjustment Switches
10	3	0.04	3	None	Low-fine

Because of the relatively small current used (approximately one-tenth of one amp), surface defects were machined in 50 to 70 specimens before it was necessary to resharpen the electrode.

C. SPECIMEN TESTING

1. Allocation of Test Rings

A total of 118 test rings were supplied for the evaluation. The rings tested by each of the three laboratories (Aerojet-Sacramento, Aerojet-Downey and Lycoming) are shown in Table I. As indicated in this table, duplicate tests were performed by the two Aerojet laboratories using test rings 69B, 70A, 70B, 71A, and 84B. Duplicate tests were performed by Aerojet-Sacramento and Lycoming, using test rings 63A, 63B, 66B, 69A and 84B.

2. Fatigue Cracking

Six circumferentially oriented specimens were obtained from each forging and fatigue precracked on the surface corresponding to the inner diameter of the forging. Three specimens were cracked to a length of 0.080-in., which is comparable to a nominal crack area of 0.002-sq.in.; and three specimens were cracked to a length of 0.200-in., comparable to a nominal crack area of 0.010-sq.in.

The fatigue-cracking procedure described below was used at Aerojet-Sacramento. The major difference between the techniques used in the three laboratories was that Aerojet-Downey and Lycoming used an arc burn produced by a small spot welder to produce the crack starter; an electrical discharge machine was used at Sacramento. Also, the six specimens at Lycoming were cracked simultaneously; both of the Aerojet laboratories cracked the specimens individually.

Appendix B

At Aerojet-Sacramento, fatigue cracks were formed from the starter defects by tension-tension bending fatigue on a converted Burke milling machine. The specimen was loaded as a cantilever beam. Preliminary experimentation with the fatigue cracking apparatus established the optimum fatigue stress and speed. This experimentation indicated that best control of the crack length and orientation could be obtained at 385 rpm, a 6.5-in. moment arm and an eccentric deflection of 0.75 in. The maximum fatigue stress for these conditions was approximately 50,000 psi. Under these conditions, fatigue cracks of the desired lengths were produced within 5 to 10 minutes. The extension of the fatigue crack was measured at intervals with an eyepiece with a reticle spread of 0.005 in. per division and a magnification of 2X. To facilitate reading the crack length, the fatigue cycling was interrupted and measurements made with the crack in the open position (at maximum deflection of the beam). After fatigue cracking, the STL contract procedure specified heat staining at 800°F for 1 hr; the heat staining was to facilitate measurement of the fatigue crack after testing. An evaluation of the possible effect of the heat staining on the mechanical properties of the plastic enclave at the top of the fatigue crack is discussed in Addendum B-3.

3. Tensile Testing

The specimens at Aerojet-Sacramento were tested using a Tinus Olson testing machine with specially designed grips (Figure 2). All specimens were tested at a strain rate of 0.005 in./in./min. The data recorded for each test were: (1) specimen width (W) and thickness (B), (2) maximum load (P max), (3) crack length (2c), and (4) crack depth (a). The crack dimensions were measured with a toolmaker's microscope to the nearest 0.0001-in. In many instances, the crack was found to be longer below the surface than on the surface. In all cases, the length was taken along the major axis of the ellipse. The procedures employed by Aerojet-Downey[3] and Lycoming[4] were not significantly different from those employed at Aerojet-Sacramento.

D. DATA ANALYSIS

1. Fracture Mechanics

The PTC tensile test has been used by a number of investigators because the surface crack simulates a defect-type commonly observed as a source of structural failure. The PTC tensile test provides a measure of the plane-strain fracture toughness (K_{Ic}).

The plane-strain value of fracture toughness is generally considered a more fundamental unit of fracture toughness than the plane-stress value, because within certain limits of crack size, it is independent of specimen dimensions. Furthermore, plane-strain fracture toughness is concerned with the most dangerous type of flaw; viz., a flaw which initiates catastrophic fracture before growing through the thickness. With such a flaw, both initial growth and instability are controlled by the plane-strain fracture toughness,

(3) D.F. DeSante and E. Jarasunas, Part-Through-Crack Test-Relation to MINUTEMAN Ti-6Al-4V Rocket Cases, Final Report 7513-76(01)FP, Dec 18, 1964.

(4) Private Communication.

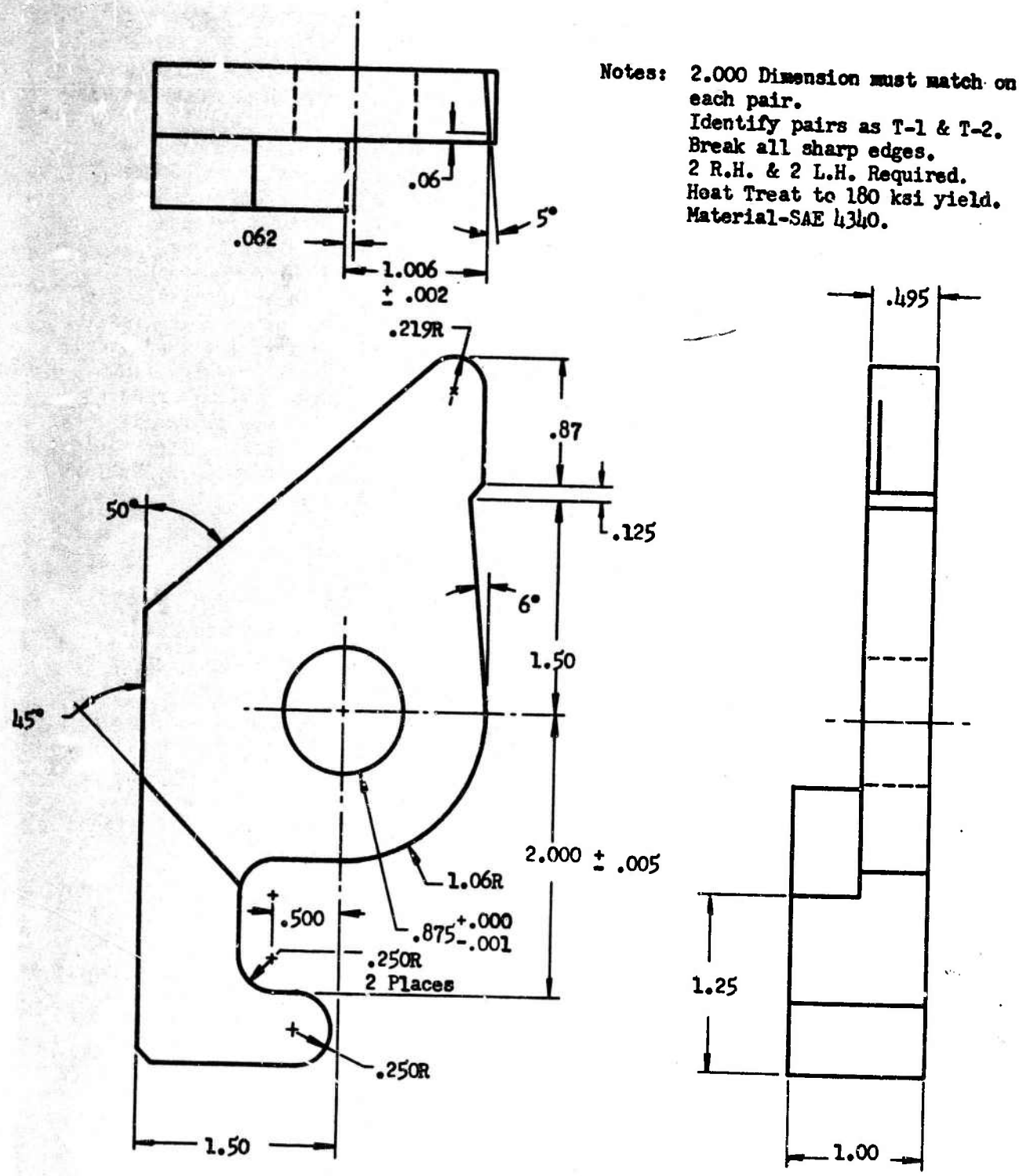


Figure 2. Part-Through Tensile Test Grips

Appendix B

K_{Ic}. A critical flaw under plane-strain conditions is most dangerous because of its relatively small size and no warning of failure due to leakage.

The expression for calculating the plane-strain fracture toughness value is:

$$K_{Ic} = F(1.21\ \pi\ a)^{1/2}/\phi$$

where F = gross stress and ϕ is the commonly tabulated elliptic integral

$$Q = \int_0^{\pi/2} (1 - k^2 \sin^2\theta)^{1/2}\ d\theta$$

where $k = 1-(a/c)^2$, and c and a are one half the major and minor axes of an ellipse. With a plastic-zone correlation, the equation becomes

$$K_{Ic} = F(1.21\ \pi\ a)^{1/2}/\ [\phi^2 - 0.212\ (F/F_{ty})^2\ ]^{1/2}$$

If the elliptic integral function and plastic-zone correlation are represented by Q

$$K_{Ic} = \frac{1.21\ \pi\ aF^2}{Q}^{1/2} \qquad (1)$$

Figure 3 is a plot of the flaw shape parameter Q as a function of flaw depth-to-length ratios (a/2c) for various fracture stress levels.

At the time the data in this report were collected, the criteria that were under consideration for valid K_{Ic} measurements were as follows:

a. gross failure stress was not to exceed the yield strength,

b. for Irwin's solution[5], the crack depth was not to exceed 50 percent of the specimen thickness,

c. crack area was not to exceed 10 percent of the specimen cross section.

Paris and Sih (Ref 6) have an approximate solution for a semi-elliptical surface crack.

---

(5) G.R. Irwin, "Crack Extension Force for a Part-Through-Crack in a Plate," J. of Applied Mechanics, Vol. 84E No. 4, Dec. 1962.
(6) "Stress Analysis of Cracks", ASTM STP 381, p. 51, equation (64).

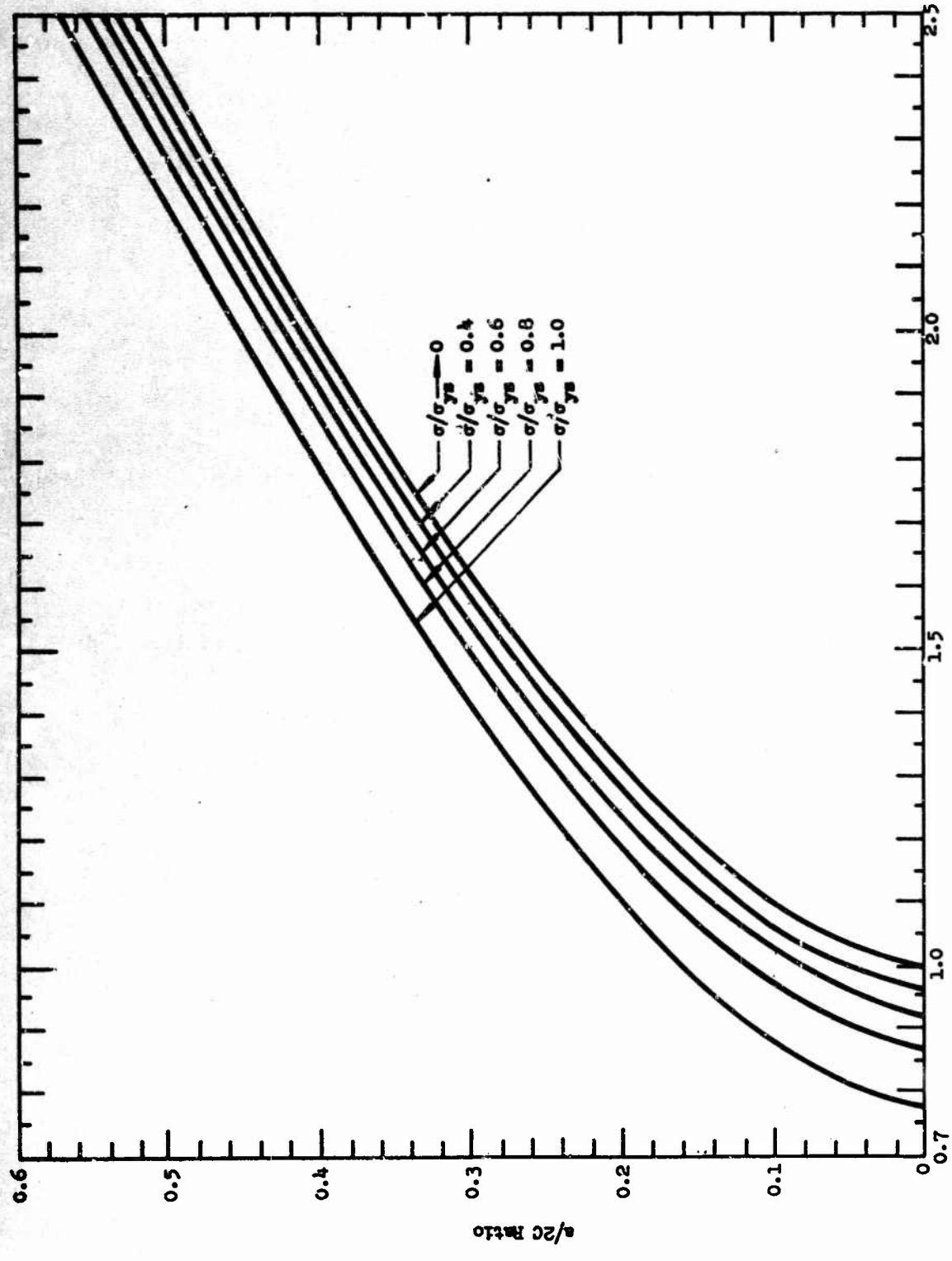


Figure 3. Flaw Shape Parameter for Surface Cracks

$$K_{Ic} = 1 + 0.12\left(1 - \frac{a}{c}\right)\frac{F\,(\pi a)^{1/2}}{\phi}\,\frac{2B}{\pi a}\tan\left(\frac{\pi a}{2B}\right)^{1/2} \qquad (2)$$

This is the stress intensity at the end of the semi-minor axis, a. Paris and Sih estimate the accuracy of the above equation to be within about ± 5 percent for a/2c from 0.5 to 0.05 and a/B from zero to 0.5. For a/2c up to about 0.1 and a/B up to about 0.75, the accuracy is still probably better than ± 10 percent.

The following comparison by W.F. Payne[7] between the solution by Irwin (without plastic-zone correction) and that of Paris and Sih, shows Irwin's solution to give a low value for crack depths exceeding a/B = 0.5.

COMPARISON OF IRWIN AND PARIS SOLUTIONS

Flaw Shape	Crack Depth	$\frac{K_{Ic}\ (\text{Irwin})}{K_{Ic}\ (\text{Paris})}$
a/2c = 0.5	0.74	1.10
	0.207	1.08
	0.410	1.02
	0.592	0.92
a/2c = 0.05	0.074	0.99
	0.207	0.97
	0.410	0.92
	0.592	0.82

In using the solution of Paris and Sih, if the crack-tip plastic-zone subtends a major portion (say half) of the distance between the crack front and the back of the test specimen, the use of elastic analyses is doubtful. In this connection, it should be recalled that the crack-tip plastic-zone extends much further ahead of the crack as it approaches the back surface than it does near midthickness; the free-surface effect extends into the thickness of the specimen for a distance which is proportional to $(K_{Ic}/F_{ty})^2$. Thus, when the thickness and/or the crack depth is less than some critical value that is proportional to $(K_{Ic}/F_{ty})^2$, the constraint-relieving influence of the free surfaces will result in fictitious K_{Ic} measurements. Based on these observations, Brown and Srawley[8] have suggested another criterion for valid K_{Ic} measurements, viz., that the crack depth should exceed 2.5 $(K_{Ic}/F_{ty})^2$ inches, where F_{ty} is the 0.2 percent offset yield strength. For a K_{Ic} of 40 ksi-in.$^{1/2}$ and a yield strength of 160 ksi

$$2.5\,(K_{Ic}/F_{ty})^2 = 0.156 \text{ in.}$$

(7) W.F. Payne, "Workshop on Fracture Mechanics," Denver, Colorado, 16 August 1964.

(8) W.F. Brown, Jr., and J.E. Srawley, "Plane-Strain Crack Toughness Testing High Strength Metallic Materials," ASTM STP No. 410, Dec. 1966.

The crack depths used in this data collection were seldom more than 1/3 of this value. The variation in K_{Ic} value as a function of specimen dimensions is discussed in the ensuing paragraphs.

E. DISCUSSION OF RESULTS

The following sections of the appendix discuss the variation in K_{Ic} attributable to between-forging, between-heat and between-test-laboratory variability as well as the variation in K_{Ic} attributable to crack and specimen dimensions. These considerations are evaluated here on the basis of engineering plots of the K_{Ic} data and then in Appendix E on the basis of statistical analysis.

The PTC-tensile fracture toughness data are presented for all 109 forgings as a computer-printout at the end of this appendix (Table I).

1. Size and Shape of Starter Flaw

Figure 4 is a plot of the ratio of fatigue-crack depth (a_o) to fatigue-crack length (2c) versus the fatigue-crack area. The data are from the replicate tests made at Sacramento, Downey, and Lycoming. Note that the crack shape was variable and that increasing crack area was attended by a decrease in the crack depth-to-length ratio. This effect is also illustrated in Figure 5, which shows typical fatigue-crack configurations obtained at Sacramento. The small cracks tended to be more nearly semicircular (a/2c-0.4 at 0.002-sq.-in. crack area), whereas the larger cracks tended to have a smaller depth-to-length ratio (2/2c-0.28 at 0.10-sq.-in. crack area). The data in Figure 4 also indicate that the flaw shapes produced by the three laboratories were similar, although there was a greater variation in the size and shape of the starter flaws at Aerojet-Sacramento.

2. Stress-Intensity Factor as a Fracture-Toughness Criterion

a. K_{Ic} as a Function of Material Strength

Figure 6 is a plot of stress-intensity factor (K_{Ic}) versus ultimate tensile strength for all three laboratories. The K_{Ic} values plotted are average values based on 6 tests without regard for crack-size limits.

Figure 7 is a plot of stress-intensity factor (K_{Ic}) versus 0.2% offset yield strength for average K_{Ic} values without regard for crack-size limits. When shallow and deep-crack test data were separated, a marked difference in scatter was noted (Figure 8). The average K_{Ic} values for shallow cracks involved appreciably less scatter than those for deep cracks. The data plotted in Figure 8 excluded all tests which violated the specified crack-size limits.

b. K_{Ic} as a Function of Specimen and Flaw Size

In a recent study by Battelle Memorial Institute (Ref 9) of flaw growth characteristics of 6Al-4V titanium sheet, a surface-crack tensile specimen was used. The material was supplied by Grumman Aircraft Engineering Corp. from the Apollo program in the form of sheet nominally 0.020, 0.040, and 0.060-in. thick. In the solution-treated and aged

(9) D.W. Hoeppner, D.E. Pettit, C.E. Feddersen, and W.S. Hyler, "Determination of Flaw Growth Characteristics of Ti-6Al-4V Sheet in the Solution-Treated and Aged Condition," NASA CR-65811, 1 Jan. 1968.

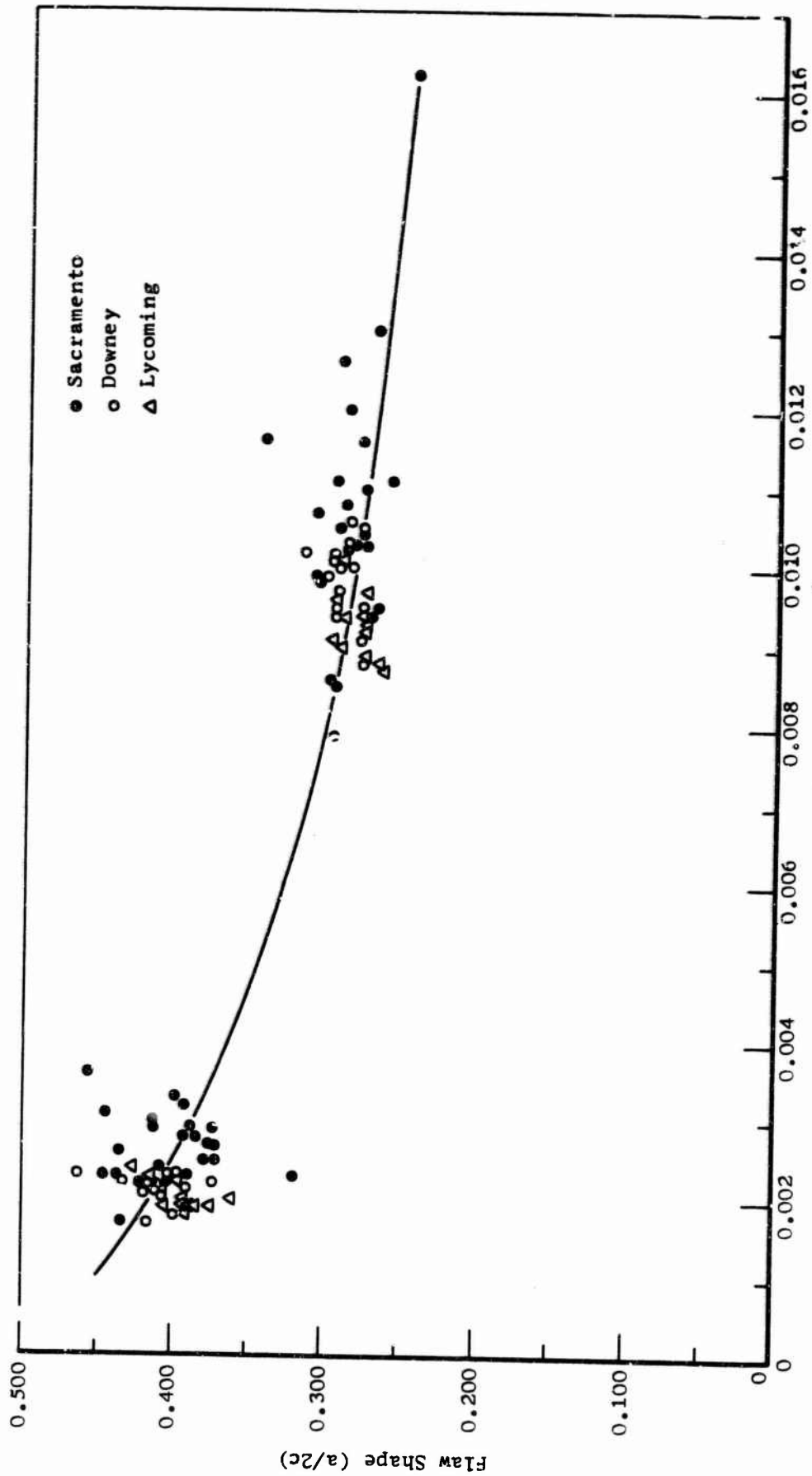


Figure 4. Relationship Between Flaw Shape and Crack Area

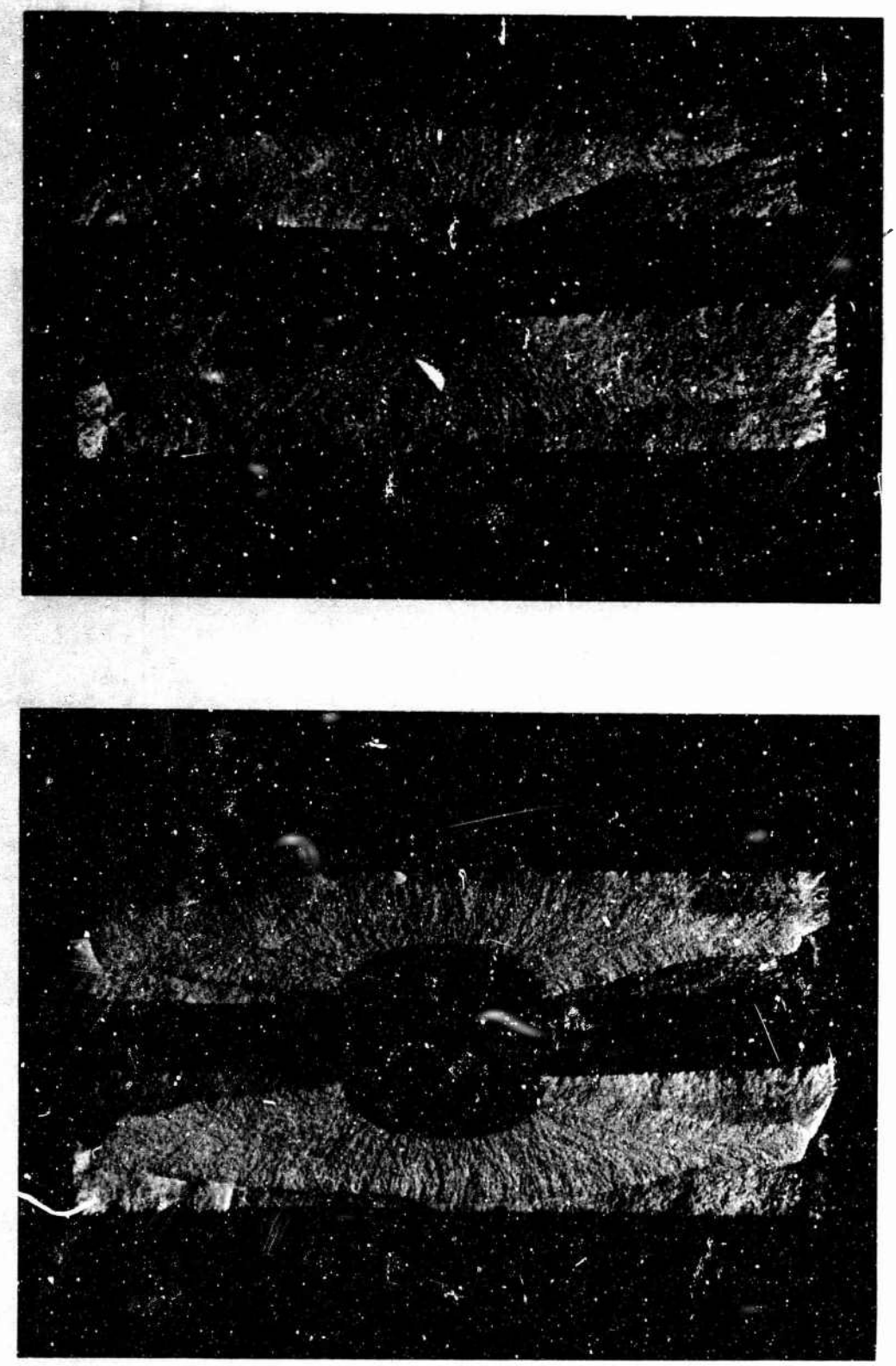


Figure 5. Typical Surface Cracks in 6Al-4V Titanium Fracture Testing

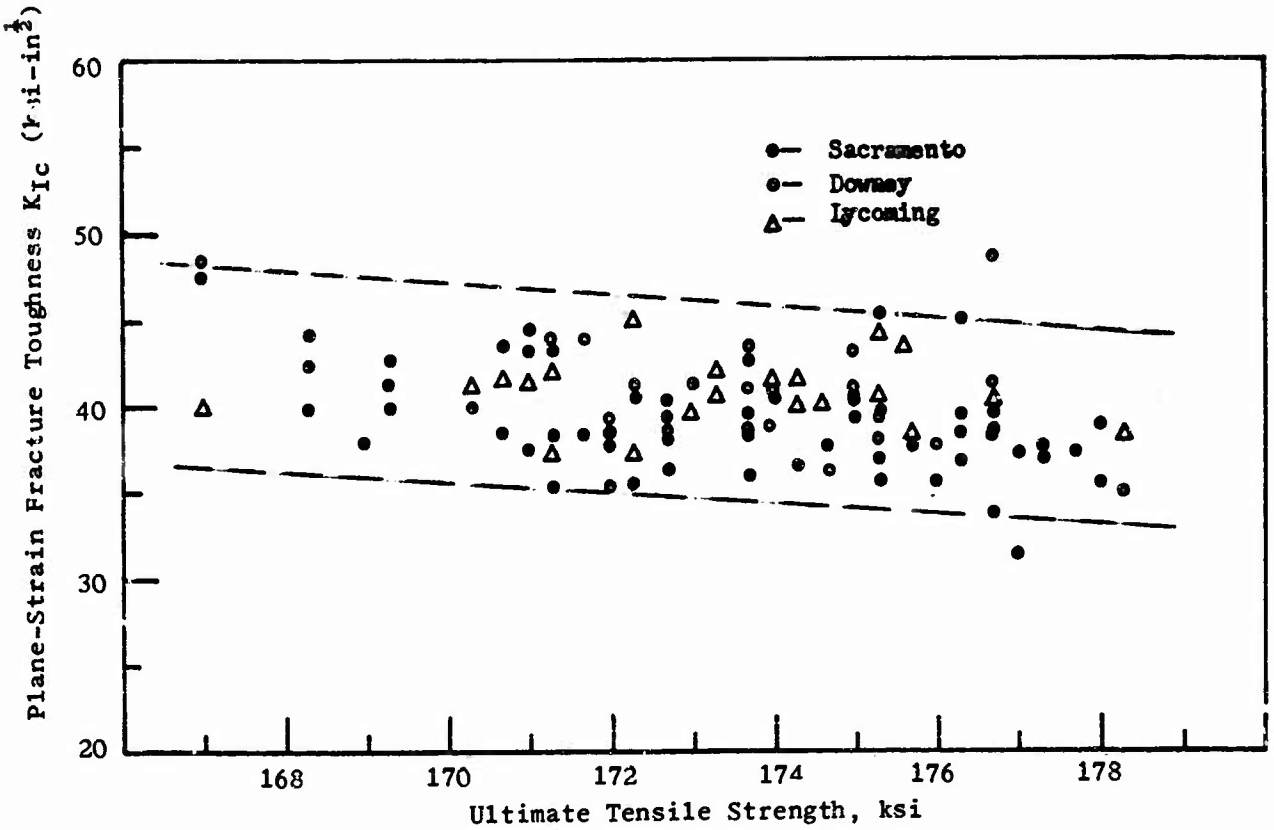


Figure 6. Relationship Between Ultimate Tensile Strength and Plane-Strain Fracture Toughness (K_{Ic}) in 109 6Al-4V Titanium Forgings

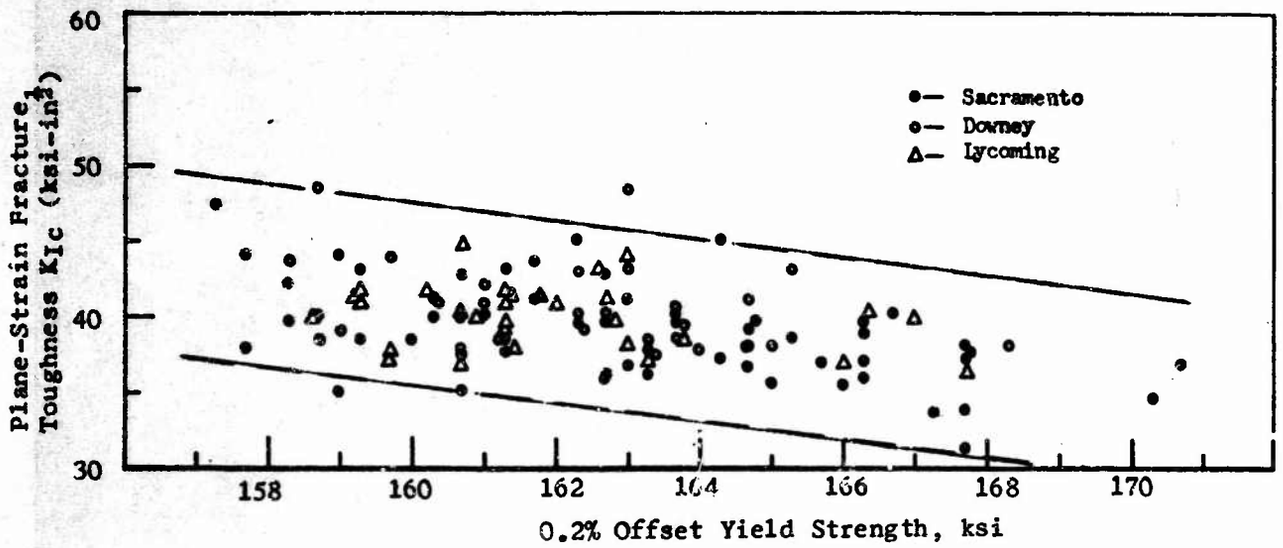


Figure 7. Relationship Between 0.2% Offset Yield Strength and Plane-Strain Fracture Toughness (K_{Ic}) in 109 6Al-4V Titanium Forgings

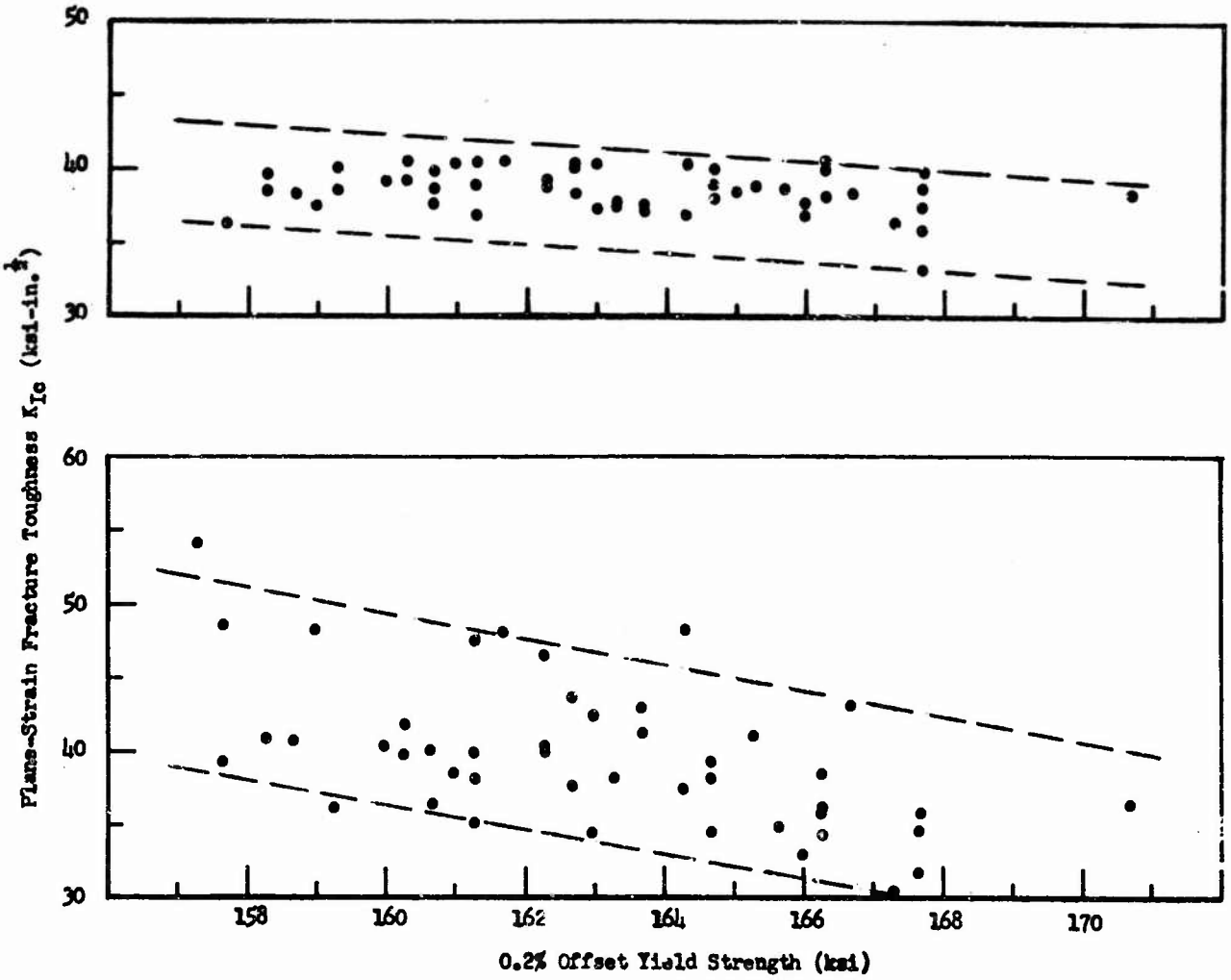


Figure 8. Effect of Craft Depth on the Relationship Between Yield Strength and K_{Ic}

condition, the sheet had the following mechanical properties (averages of three or more tests):

Gage, in.	Yield, ksi	Ultimate, ksi
0.020	162	171
0.040	162	170
0.060	160	168

The test specimen was 3-in. wide, with surface-crack depths of a/B = 0.25, 0.50, and 0.75. The flaw shapes were varied from a/2c = 0.5 to 0.1. Figures 9 and 10 were plotted from a computer-derived tabulation of data (Table 9 of Ref 7). From Figure 9, a plot of crack depth versus apparent K_{Ic} value, it is noteworthy that with the 3-in.-wide PTC-tensile specimen, all the data for a given crack shape fell on a common curve irrespective of specimen thickness and irrespective of crack depth-to-thickness ratio. Note that the apparent K_{Ic} values were strongly dependent upon crack depth, with a constant value of 40-45-ksi-in.$^{1/2}$ indicated at a crack depth of approximately 0.045 in. Obviously Irwin's criterion of a $\leq$ 0.5 B was violated in some of the tests, and Brown and Srawley's criterion of 2.5 $(K_{Ic}/F_{ty})^2$ for crack and specimen dimensions was overly conservative in these tests.

$$1.0\ (K_{Ic}/F_{ty})^2 = 0.078 \text{ in.}$$

From Figure 10, a plot of a/B versus apparent K_{Ic}, it will be seen that the 20 mil sheet was too thin to obtain a valid K_{Ic} value in this material; whereas, both 40 and 60 mil sheet permitted valid measurement with deep cracks.

In PTC-tensile testing MINUTEMAN titanium, forging 53B was selected for evaluating the effect of crack and specimen dimensions. Figure 11 shows the effect of crack depth on both the K_{Ic} value and the ratio of net-stress-to-yield strength in forging 53B. The open circles are data from specimens nominally 0.125-in. thick and 3/4-in. wide; the solid points are from specimens 1-in. wide, with thickness ranging from 0.125 to 0.200 in. The data for Figure 11 were taken from Table II.

All data taken at Aerojet-Downey were from 1-in. wide test specimens; Lycoming and Aerojet-Sacramento used 3/4-in. wide test pieces. Most of the available trim stock was not sufficiently wide to permit greater than a 3/4-in. width of test piece.

Note that the values of K_{Ic} appeared to be relatively unaffected in the range of thicknesses and crack depths investigated, in spite of high net-stress-to-yield strength ratios with small cracks.

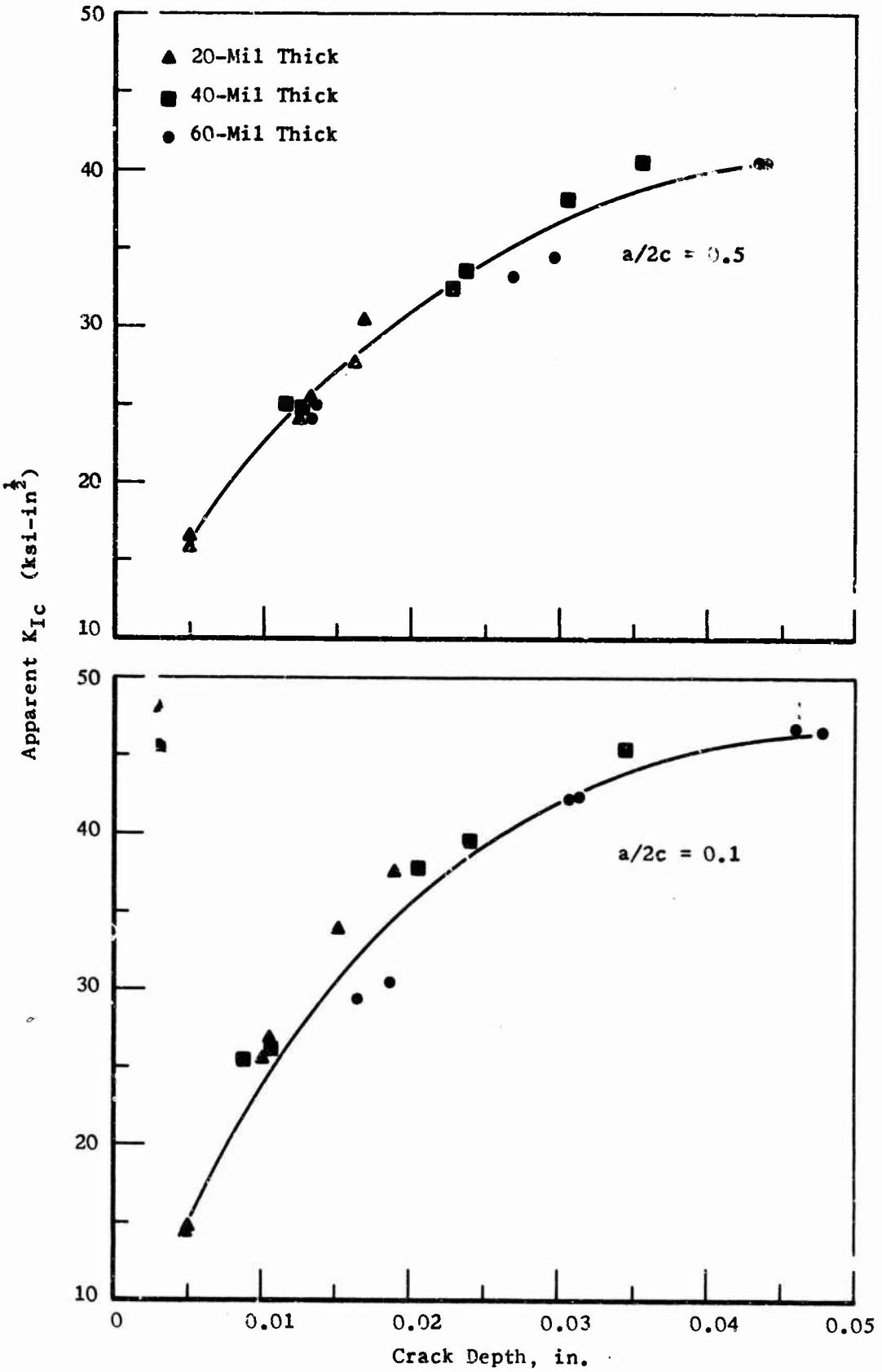


Figure 9. Effect of Crack Depth on the Plane-Strain Fracture Toughness Measurement in Ti-6Al-4V (after Hoeppner)

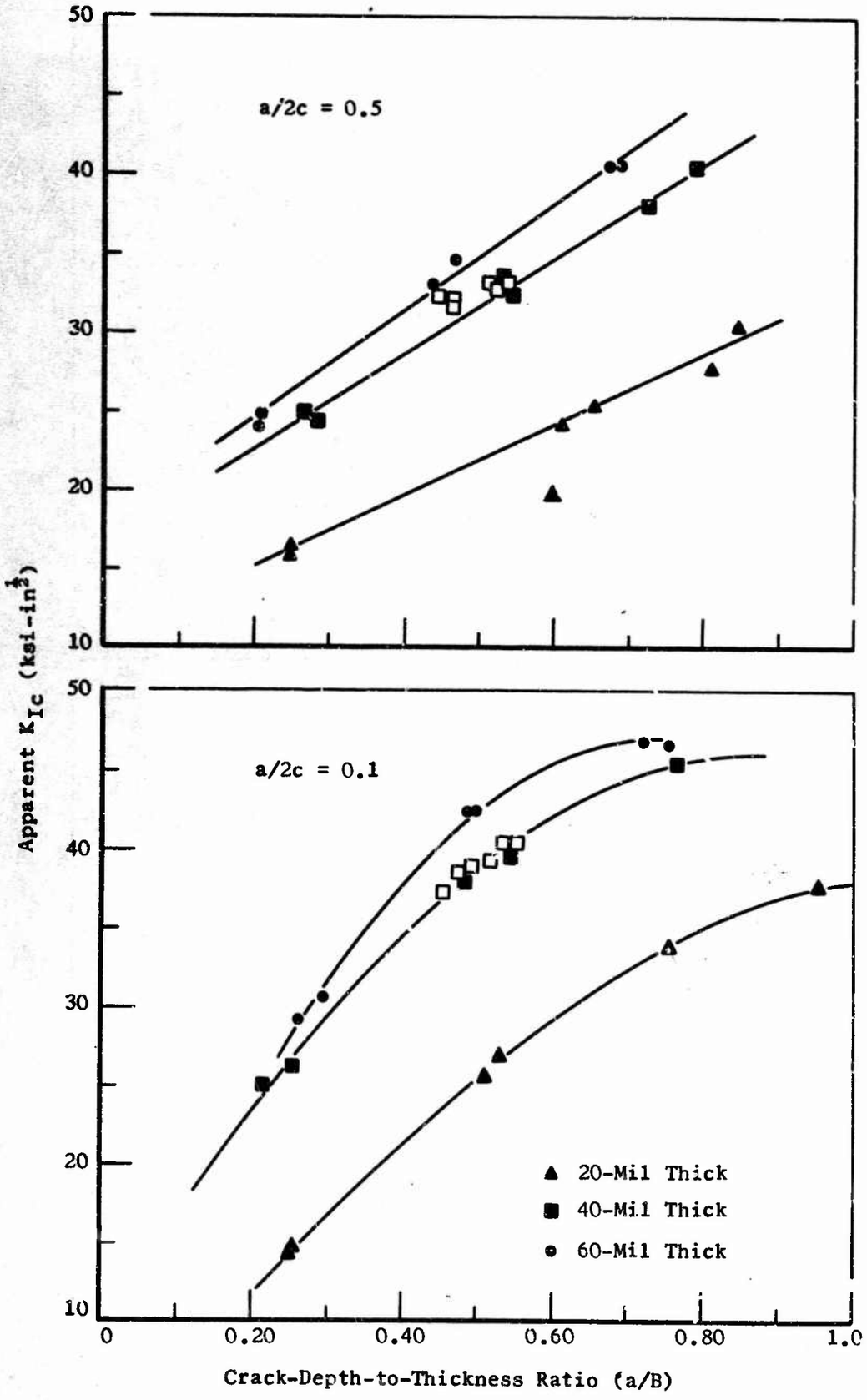


Figure 10. Effect of Crack Depth-to-Thickness Ratio on the Plane-Strain Fracture Toughness Measurement in Ti-6Al-4V (after Hoeppner)

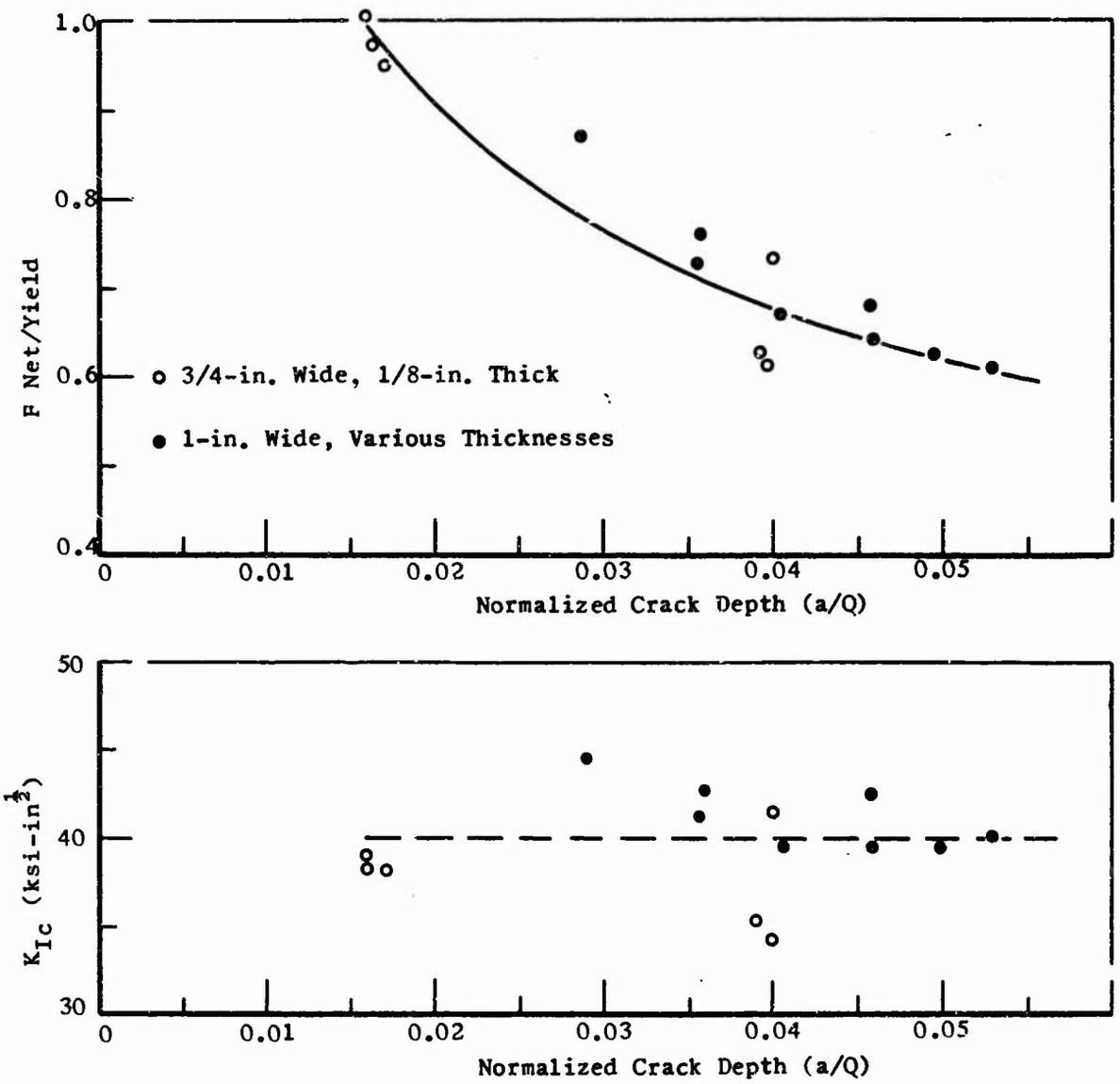


Figure 11. Effect of Crack Depth on the K_{Ic} Value and on the Net-Stress-to-Yield Ratio in MINUTEMAN Forging 53B

TABLE II

EFFECT OF SPECIMEN WIDTH AND THICKNESS IN PTC TENSILE TESTS, 6Al-4V TITANIUM FORGING 53B, 161 ksi YIELD

Width W (in.)	Thick. B (in.)	Load P-max (kips)	Stress FG (ksi)	Part-Through-Crack: Depth AO (in.)	Part-Through-Crack: Length 2C (in.)	Part-Through-Crack: Net Stress (ksi)	Part-Through-Crack: Shape a/2c	Part-Through-Crack: Norm. a/Q	Test Limits: Stress FG/FTY	Test Limits: Depth a/B	Plane-Strain K_{Ic} (ksi-in$^{\frac{1}{2}}$)
0.751	0.134	15.5	154.1	0.0314	0.0735	156.9	0.427	0.016	0.96	0.234	38.3
0.749	0.131	14.7	150.1	0.0294	0.0780	152.9	0.377	0.017	0.93	0.224	38.1
0.748	0.118	14.0	158.7	0.0274	0.0719	161.9	0.381	0.016	0.99	0.232	39.0
0.750	0.125	10.0	106.1	0.0577	0.2123	118.3	0.272	0.040	0.66	0.462	41.4
0.749	0.131	9.0	91.3	0.0599	0.2064	101.3	0.290	0.039	0.57	0.457	35.3
0.755	0.122	8.1	87.9	0.0610	0.2083	98.6	0.293	0.040	0.55	0.500	34.1
1.000	0.128	14.82	115.8	0.0492	0.1927	123.0	0.255	0.036	0.72	0.384	42.8
0.999	0.128	17.25	134.9	0.0426	0.1411	140.1	0.301	0.029	0.84	0.333	44.5
1.000	0.153	16.90	110.5	0.0599	0.1801	116.9	0.332	0.036	0.69	0.391	41.1
0.997	0.149	14.02	94.4	0.0653	0.2521	103.4	0.259	0.046	0.59	0.438	39.5
0.999	0.150	15.08	100.6	0.0622	0.2098	108.0	0.296	0.041	0.62	0.415	39.5
1.001	0.201	20.60	102.4	0.0764	0.2282	109.9	0.335	0.046	0.64	0.380	42.7
1.001	0.205	18.32	89.3	0.0815	0.2782	97.8	0.293	0.053	0.55	0.398	40.1
1.000	0.201	18.25	90.9	0.0809	0.2523	98.7	0.320	0.050	0.56	0.402	39.4

Appendix B

Figures 12-15 are plots of plane-strain fracture toughness K_{Ic} versus (1) normalized depth of crack (a/Q), (2) ratio of crack depth to specimen thickness (a/B), (3) ratio of gross fracture stress to yield strength at 0.2% offset (F_G/F_{ty}), and (4) ratio of crack area to specimen gross cross-section area (CA/BW). Also, the plotted data include K_{Ic} values calculated from two different equations; viz., Irwin's equation (1) with plastic zone correction and, Paris' equation (2) without plastic zone correction.

The size of crack used in PTC tensile testing is an important consideration, because with cracks that are too small, the gross stress may exceed the yield strength of the material; if this occurs, the calculated values of stress intensity factor are erroneous, since general yielding precludes the use of equations based on linear-elastic theory. Irwin has suggested the limits for equation (1) as $a/B \leq 0.5$ and $F/F_{ty} \leq 1.0$. Paris' equation, on the other hand, is not restricted to $a/B < 0.5$. An added requirement has been suggested; viz., that the crack area be limited to 10 percent of the specimen cross-section; i.e., $CA/BW \leq 0.10$.

In addition to testing the constancy of K_{Ic} as a function of crack size and fracture stress, Figures 12-15 show the reproducibility of the calculated K_{Ic} value from laboratory to laboratory (the rings represented in Figures 12-15 were those tested by both Aerojet-Sacramento and Lycoming; viz., 63A, 63B, 66B, and 69A).

From Figure 12a (forging 63A), note that the K_{Ic} values as calculated from Irwin's equation decreased slightly with increasing crack depth, even though some of the larger cracks were within specified limits. Paris' equation, on the other hand, gave essentially constant K_{Ic} values over the range of crack depths investigated.

In Figure 12b, the K_{Ic} values increased somewhat as the gross fracture stress approached the yield strength (i.e., as the crack area decreased); conversely, the K_{Ic} values, as calculated from Irwin, decreased slightly with increasing crack area. With Paris' equation, the K_{Ic} values were constant over the range of crack areas investigated. It should be noted that Paris' expression has not been corrected for plastic zone and, therefore, would be expected to indicate a somewhat lower value of K_{Ic} than Irwin's expression.

Ring 63B (Figure 13) showed essentially the same behavior as ring 63A.

Ring 66B (Figure 14) was different in that the K_{Ic} values obtained at Lycoming appeared to be somewhat higher than those obtained at Aerojet-Sacramento. Otherwise, the trends were the same as observed for rings 63A and 63B. Note that the K_{Ic} values calculated from Paris' expression were constant for crack areas well beyond the limits of $a/B = 0.5$ and $CA/BW = 0.1$.

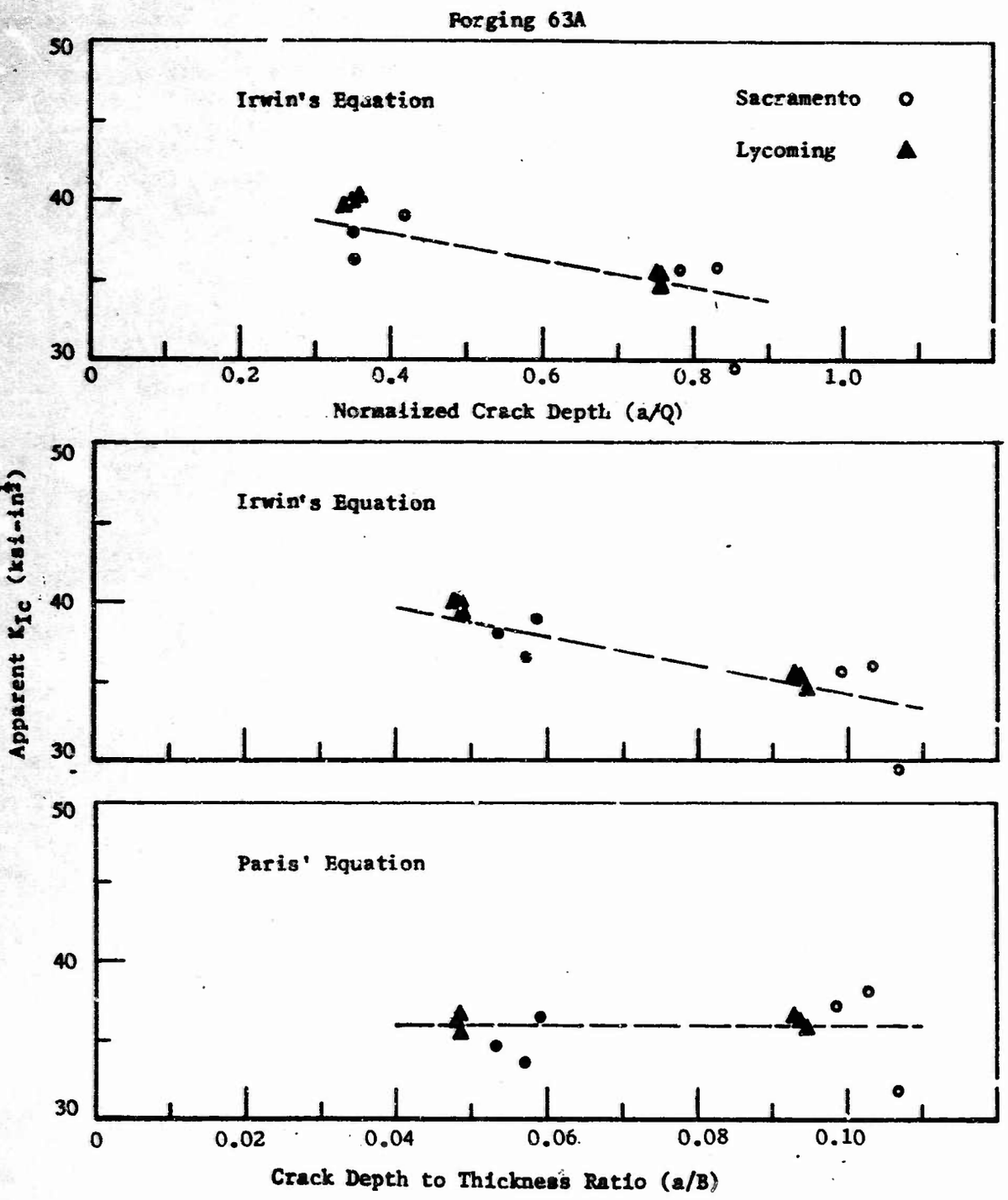


Figure 12a. Effect of Crack Depth on the K_{Ic} Value in Ti-6Al-4V Forging 63A

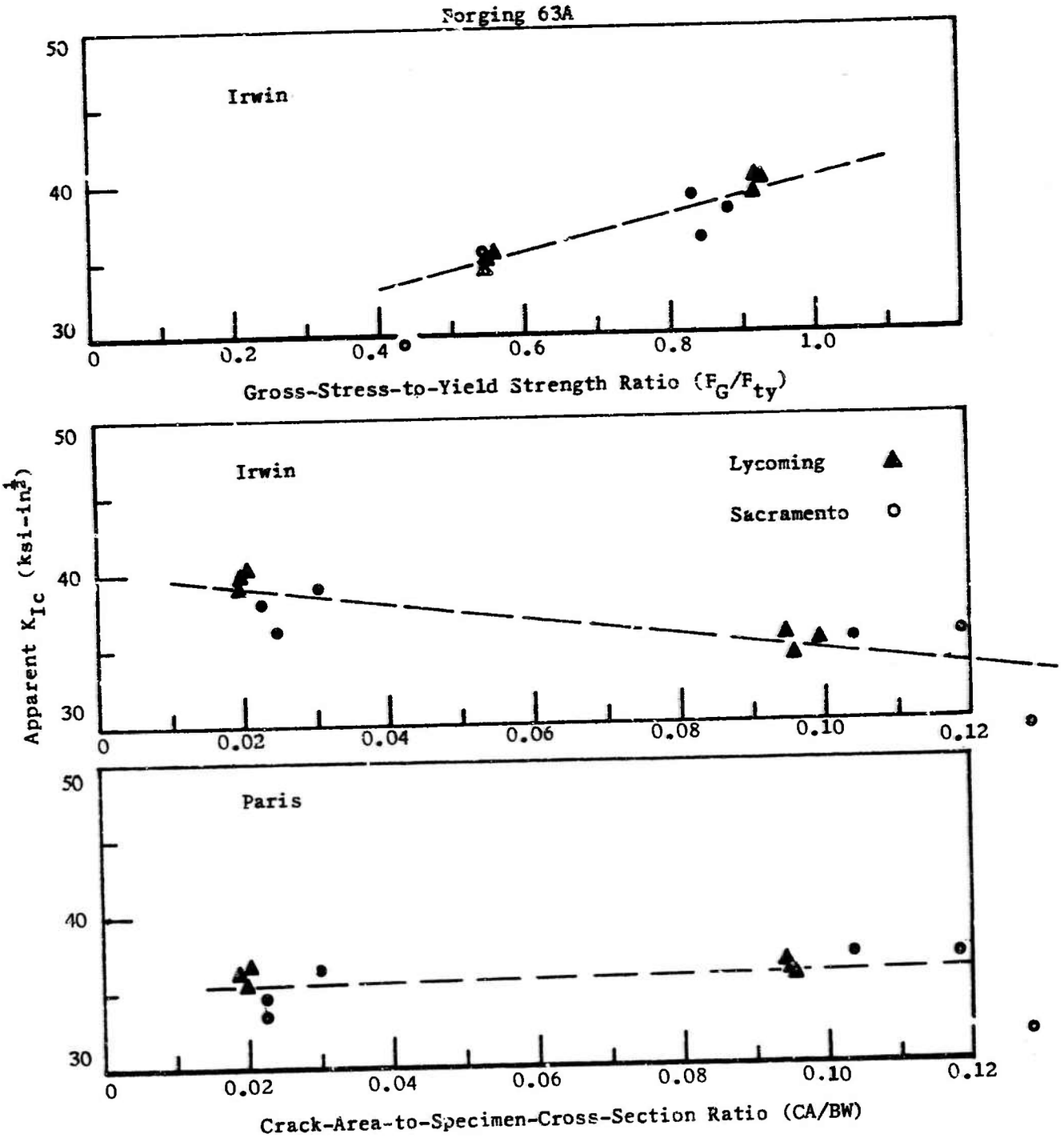


Figure 12b. Effect of Fracture Stress and Crack Area on the K_{Ic} Value in Ti-6Al-4V Forging 63A

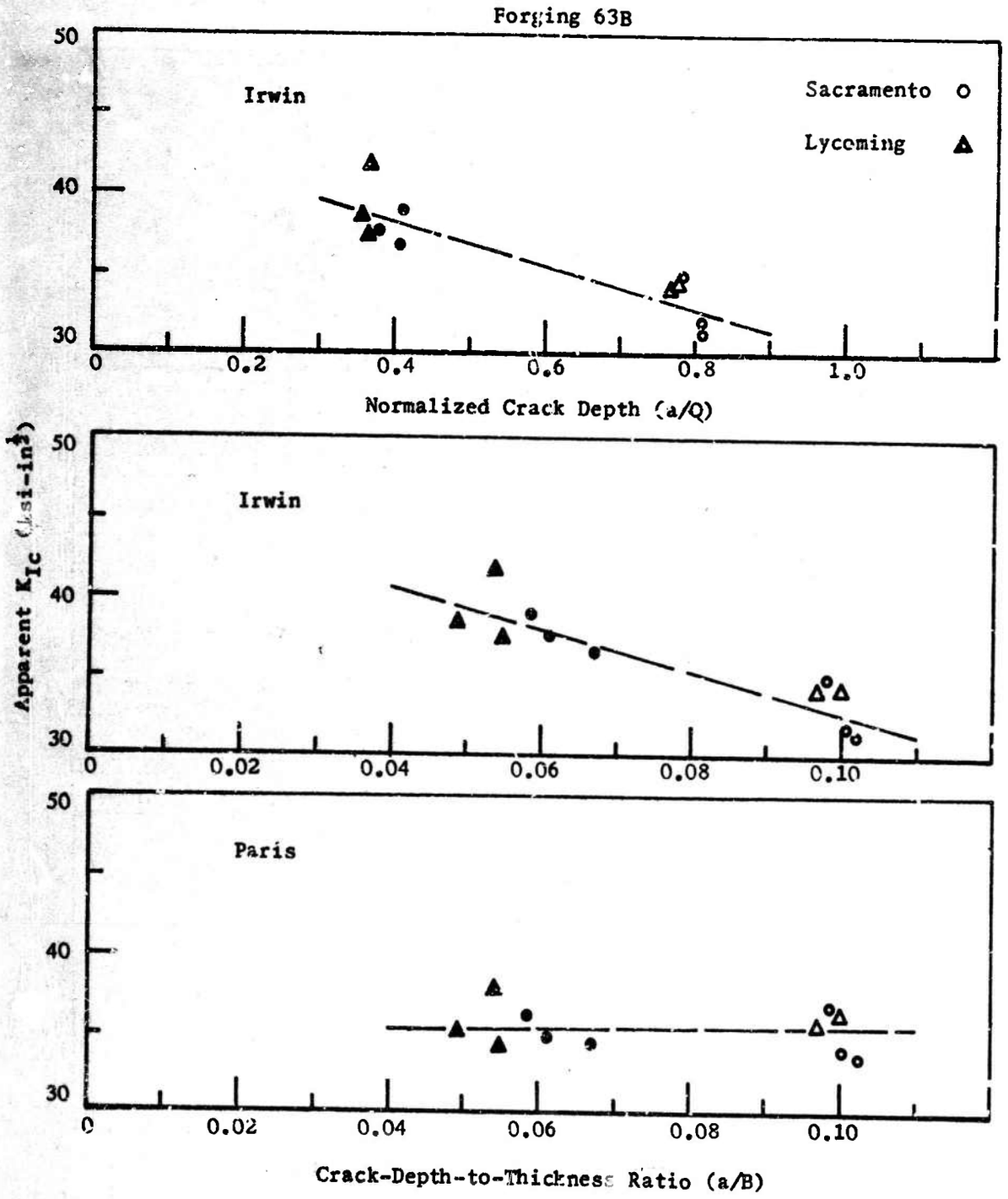


Figure 13a. Effect of Crack Depth on the K_{Ic} Value in Forging 63B

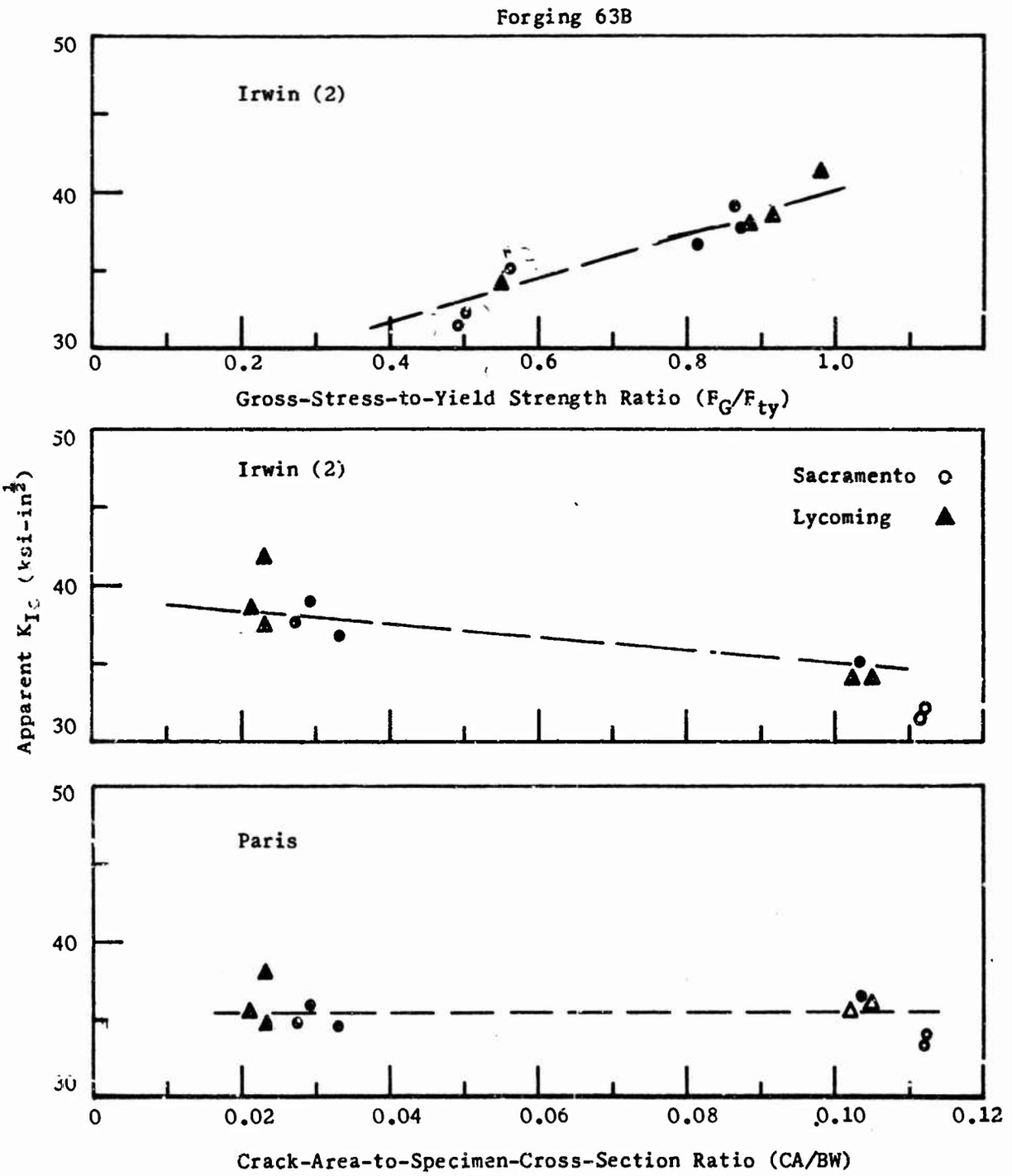


Figure 13b. Effect of Fracture Stress and Crack Area on the K_{Ic} Value in Forging 63B

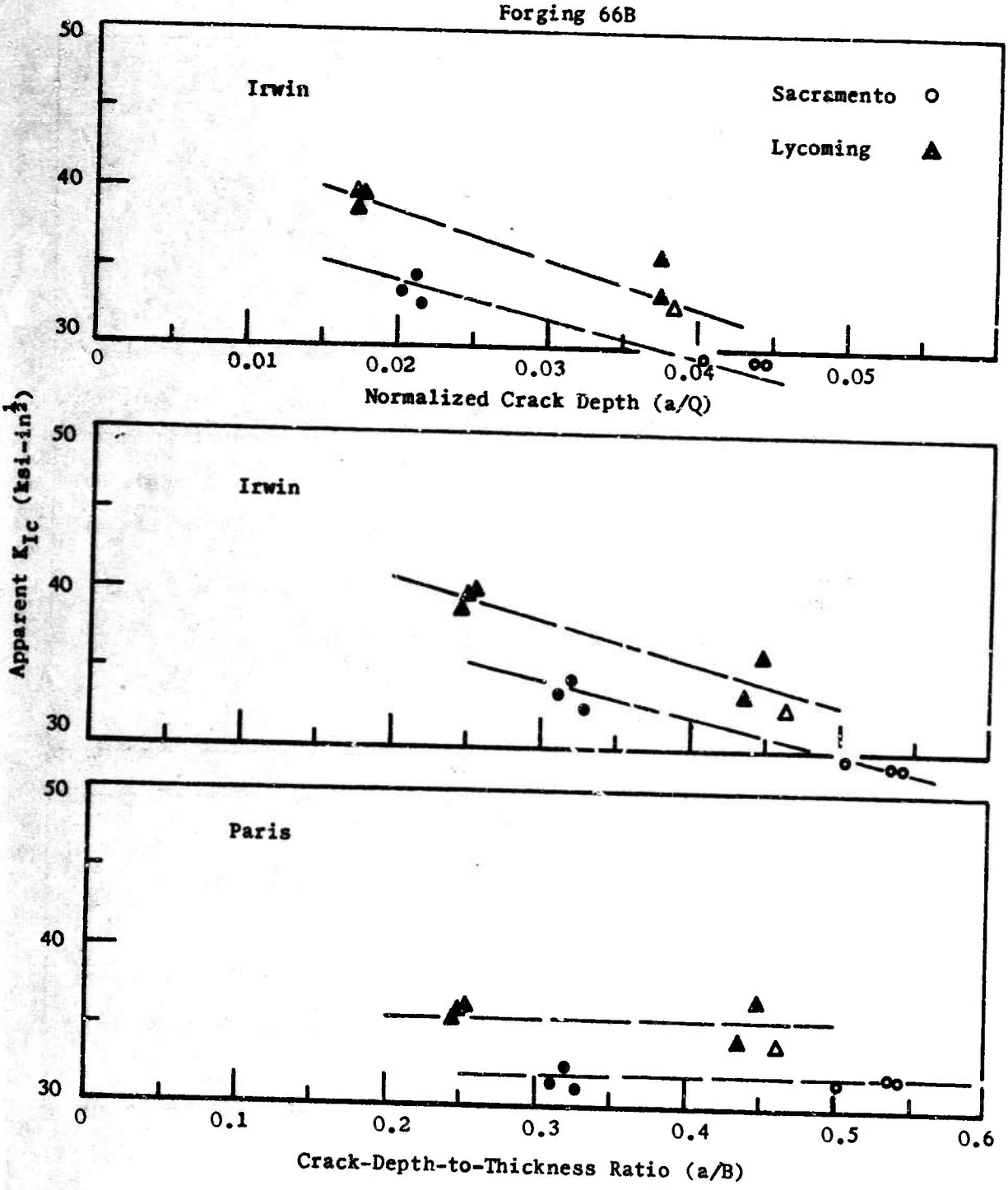


Figure 14a. Effect of Crack Depth on the K_{Ic} Value in Forging 66B

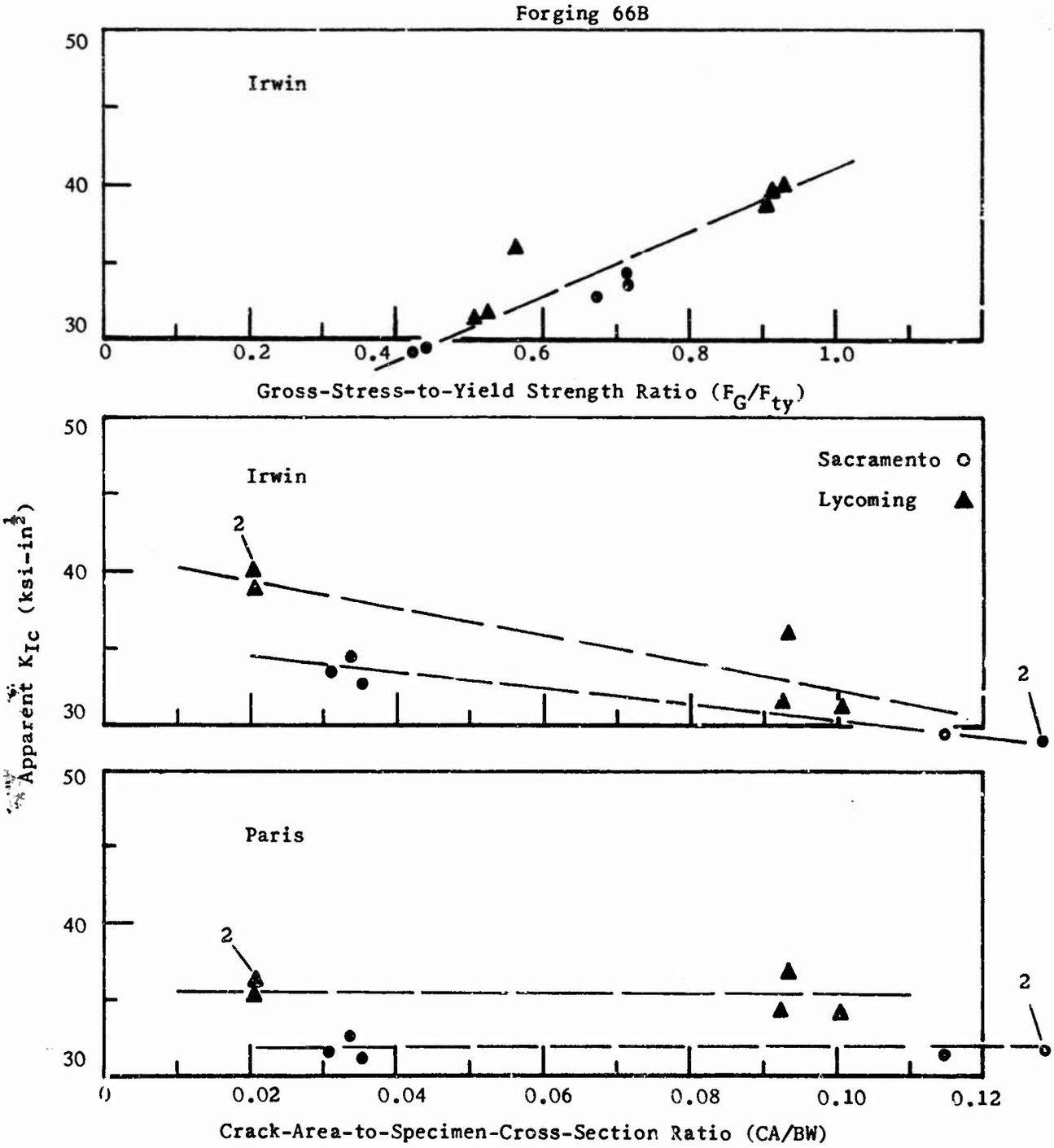


Figure 145. Effect of Fracture Stress and Crack Area on the K_{Ic} Value in Forging 66B

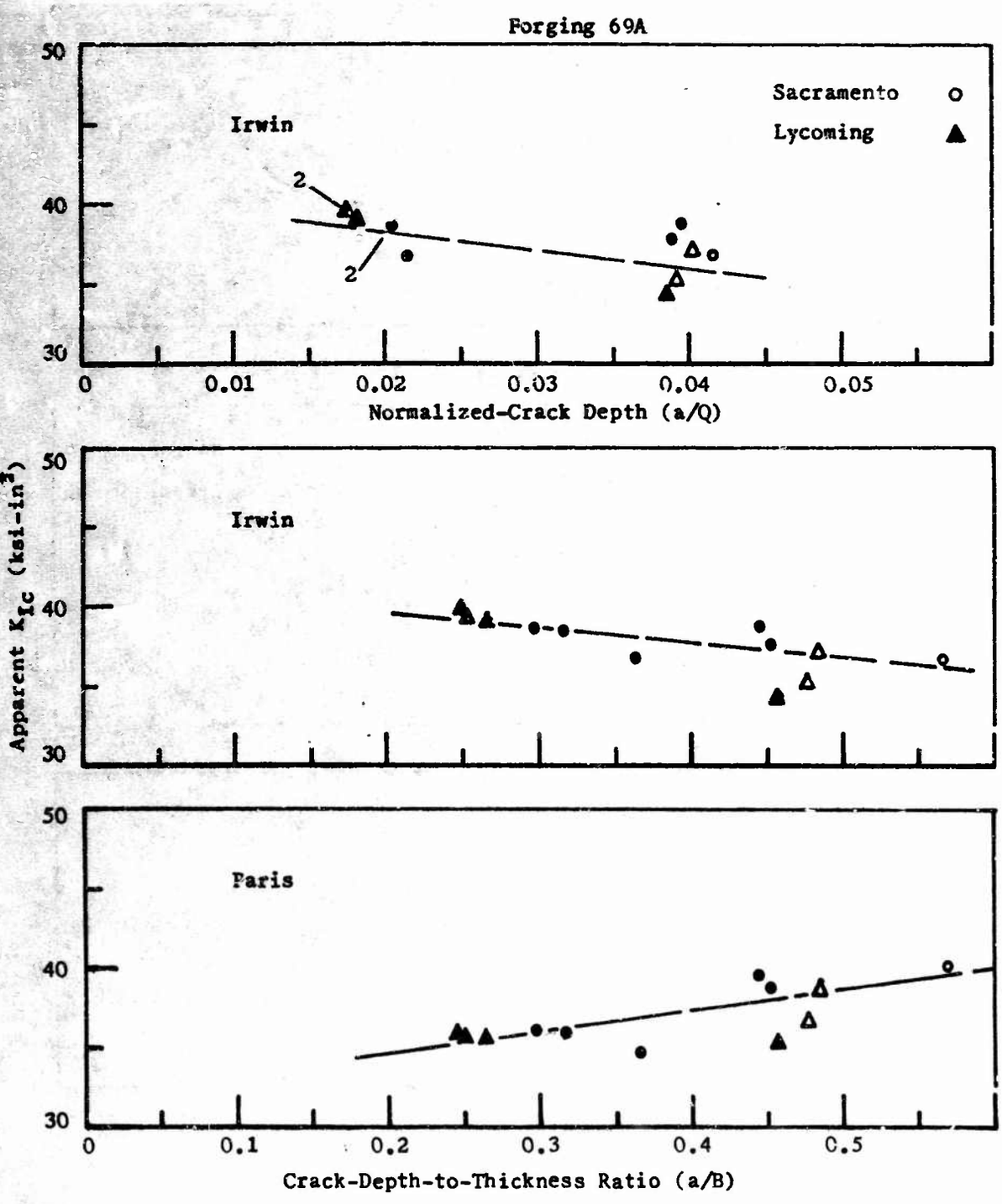


Figure 15a. Effect of Crack Depth on the K_{Ic} Value in Forging 69A

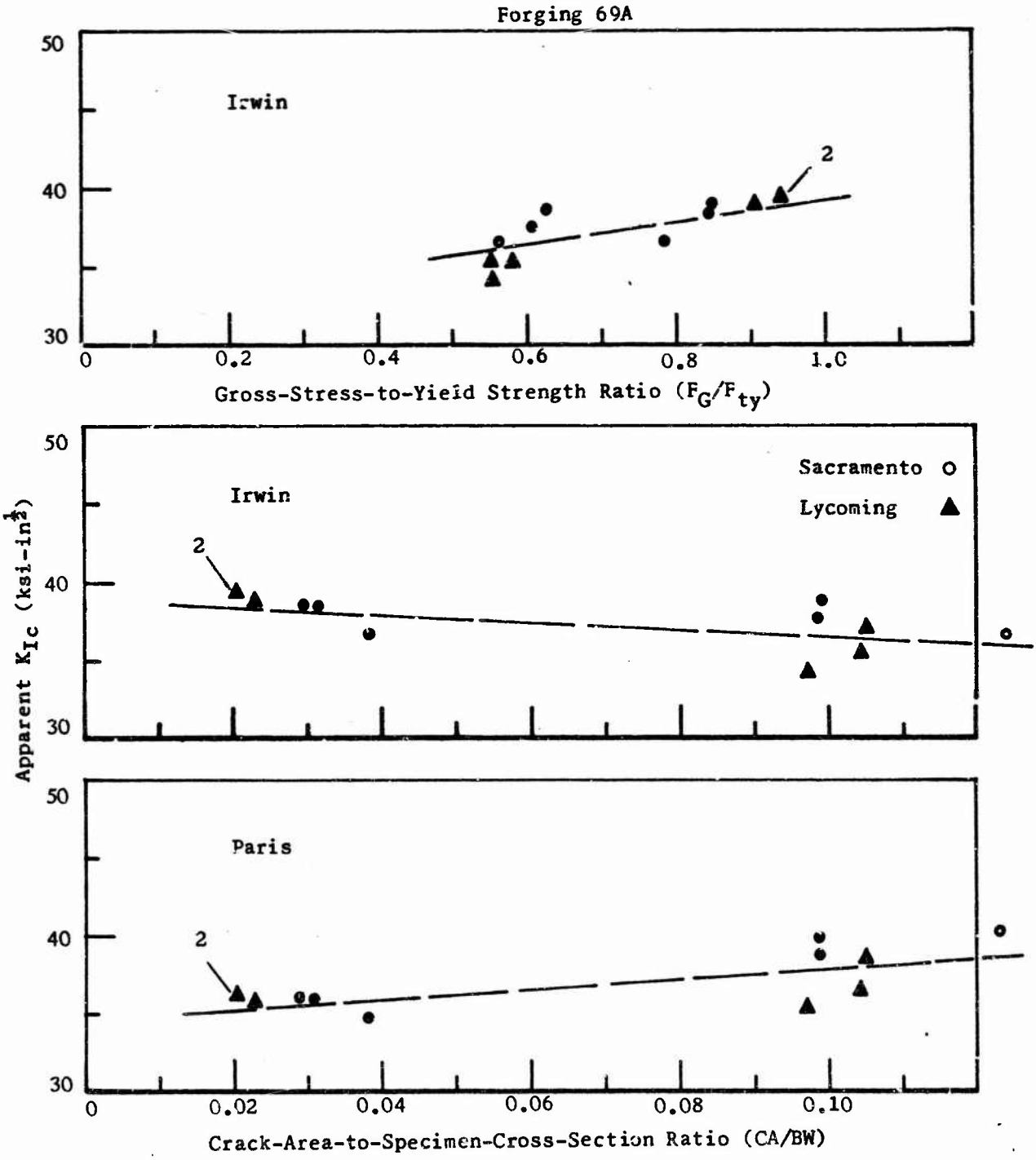


Figure 15b. Effect of Fracture Stress and Crack Area on the K_{Ic} Value in Forging 69A

In summary, from these data it is concluded that (1) the specimen dimensions used in testing MINUTEMAN 6 Al-4V titanium were adequate to give valid K_{Ic} values; (2) the crack-dimension limitations with Irwin's equation are more restrictive than with Paris' equation, with the larger cracks producing somewhat lower values of K_{Ic} than the smaller cracks tested; (3) the variability in K_{Ic} from laboratory to laboratory was not consistent - in some forgings there was an appreciable difference but in other forgings there was not. Statistical analysis of the effect of crack and specimen dimensions is discussed in Appendix E.

c. Variation in Toughness from Forging-to-Forging

From titanium producer's melt numbers, it was noted that in some instances, multiple forgings were supplied from a single heat of titanium. Furthermore, from Inspection Documentation (SID), with few exceptions, the forging heat treatment consisted of solution treating at 1750°F for 1 hour, followed by aging at 1000°F for 8 hours. Thus, comparison of toughness data from forgings with a common heat number and with a common heat treatment permitted observations with regard to the variability from forging-to-forging.

Consider, for example, TMCA heats D5937 and D5938; five forgings were produced from each heat (D5937: 100B, 101A, 102A, and 102B; and D5938: 90A, 90B, 91A, 91B, and 92A). The following table summarizes the tensile properties and fracture toughness data for each heat:

Heat No.	0.2% Offset Yield F_{ty} (ksi)	Ultimate F_{ty} (ksi)	Fracture Toughness K_{Ic} (ksi-in.$^{1/2}$)
D5937	159-171 Av (15) 162	170-179 Av (15) 174	37.5-45.9 Av (26) 40.9
D5938	158-167 Av (15) 161	171-176 Av (15) 174	35.9-47.3 Av (20) 42.0

The forgings from Heat D5937 were tested at Lycoming and those from D5938, at Aerojet-Downey. Note that the average tensile values (15 tests) for the two heats were almost identical. Likewise, the average K_{Ic} values for the two heats were nearly the same.

Figure 16 shows the effect of crack depth on K_{Ic} for forgings from single heats, viz., D5937 and D5938. From Figure 16, Heat D5937, note that the scatter in K_{Ic} was associated with deep cracks. This indicates that some processing condition such as quench rate may be affecting the homogeneity of the titanium forging near midthickness. It is interesting that the average value of K_{Ic} as obtained from the deeper cracks is not significantly different from that for the shallow cracks with Irwin's equation. For some unknown reason, Paris' equation (without plastic-zone

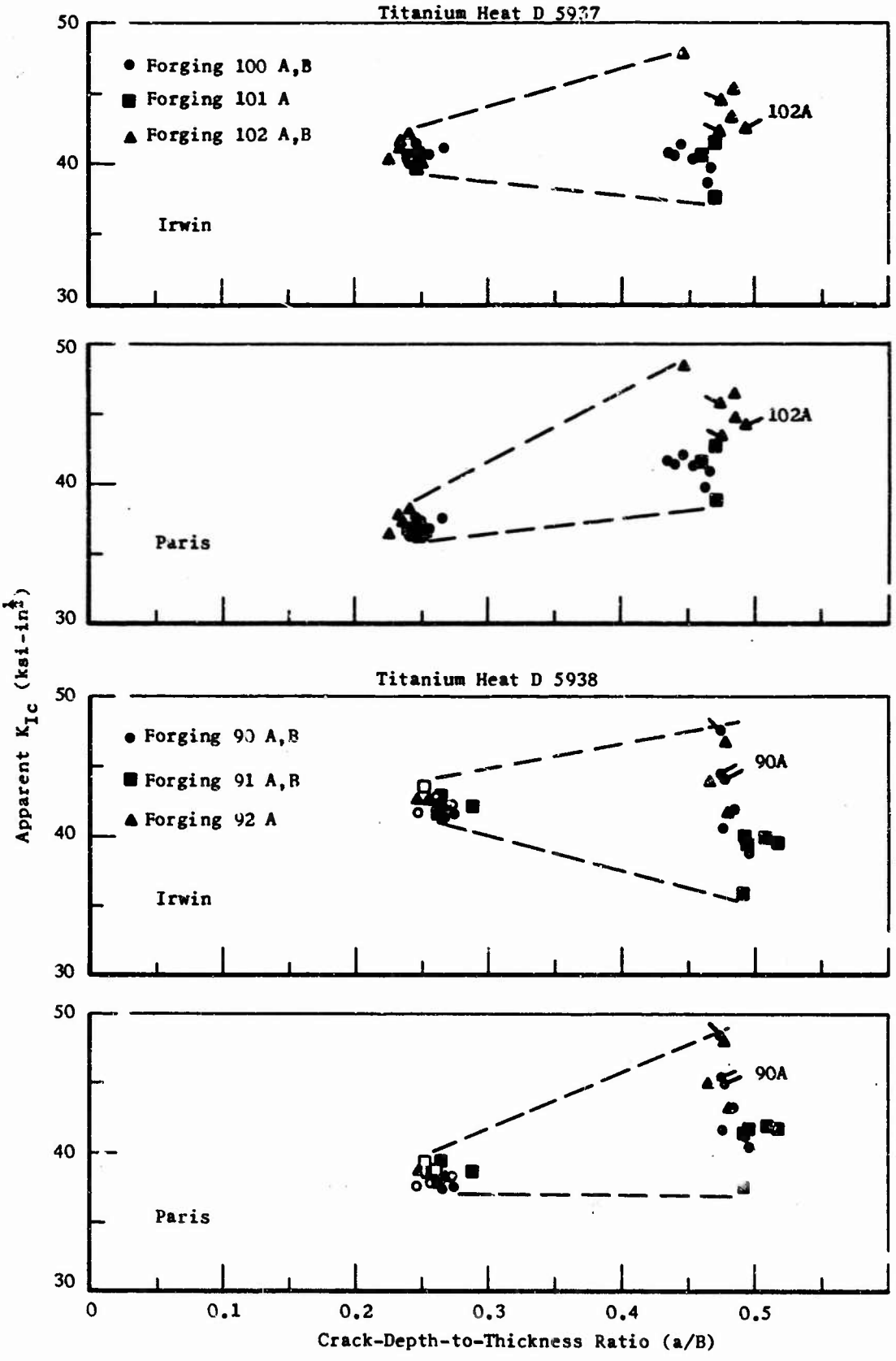


Figure 16. Effect of Crack Depth on the K_{Ic} Value for Forgings from Single Heats of Ti-6Al-4V (Forging Billets 90-92 Tested by Aerojet-Downey and 100-102 Tested by Lycoming)

correction) gave somewhat higher K_{Ic} values than Irwin's in the deeper-crack condition. The K_{Ic} values obtained from shallow cracks, on the other hand, had less than 4 ksi-in.$^{1/2}$ scatter with either equation.

The K_{Ic} values from Heat D5938, forgings 90A, 90B, 81A, 91B, and 92A, were also remarkably constant for shallow-crack tests, with less than 4 ksi-in.$^{1/2}$ scatter in 14 tests. However, with cracks approaching midthickness, as in Heat D5937, the K_{Ic} values were more widely scattered (approximately 12 ksi-in.$^{1/2}$).

Forgings from Heats D6111 and D3010 (Figure 17) showed essentially the same trends as Heats D5937 and D5938.

Since the data discussed in connection with Figures 16 and 17 are for forgings from single heats of titanium, the differences from forging to forging can be attributed to differences in forging practice. When forgings are from a single billet, they are designated A and B with the same numerical prefix, e.g., 100A and 100B. Thus, in Figure 16, the data plotted as solid circles are from a single billet from which two forgings were produced. Thus any differences between A and B forgings of a given serial number can be attributed only to the forging practice used in reducing the billet to a cylinder. It is significant to note in this connection that the scatter associated with the deep-crack tests is reduced in some cases if the billets are separated; e.g., in Figure 16, compare the data plotted as circles and triangles. Thus, the possibility remains that at approximately midthickness of the forging wall, the material is less homogeneous; i.e., a crack front at approximately midthickness produces more scatter in the calculated K_{Ic} values than a crack closer to the surface. The fact that this behavior varied from forging to forging suggests a metallurgical effect rather than a limitation with regard to fracture-mechanics analysis.

The most noteworthy observation from Figures 16 and 17 is that there was little difference between forgings when the material was tested with shallow cracks; but with deep cracks at or approaching midthickness, there were marked differences between forgings of a given heat. Thus, forging-to-forging differences accounted for the large scatter in K_{Ic} values observed for the deeper cracks. Both figures showed the same trends.

d. Variation in Test Results from Laboratory to Laboratory

Figure 14 indicated that there may be a difference in test results from lab to lab in some forgings; whereas, Figures 12, 13, and 15 did not show any significant difference. Figures 18 through 21 verify that there are differences from lab to lab, but not in all forgings.

In addition to the indications of lab-to-lab differences, these figures also verify that there is a difference in K_{Ic} values between

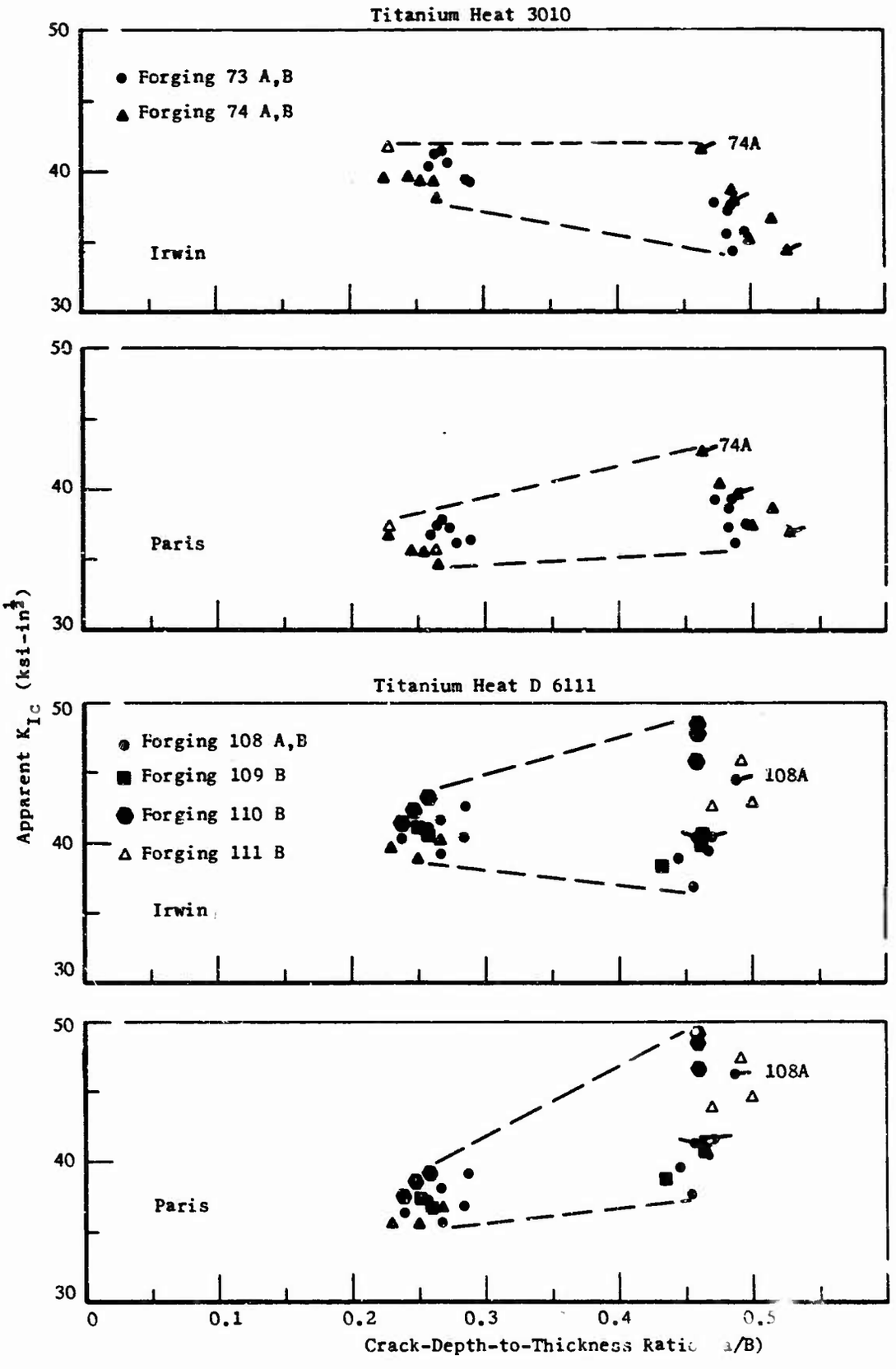


Figure 17. Effect of Crack Depth on the K_{Ic} Value for Forgings from Single Heats of Ti-6Al-4V (Forging Billets 73-74 Tested by Aerojet-Downey and 108-111 Tested by Lycoming)

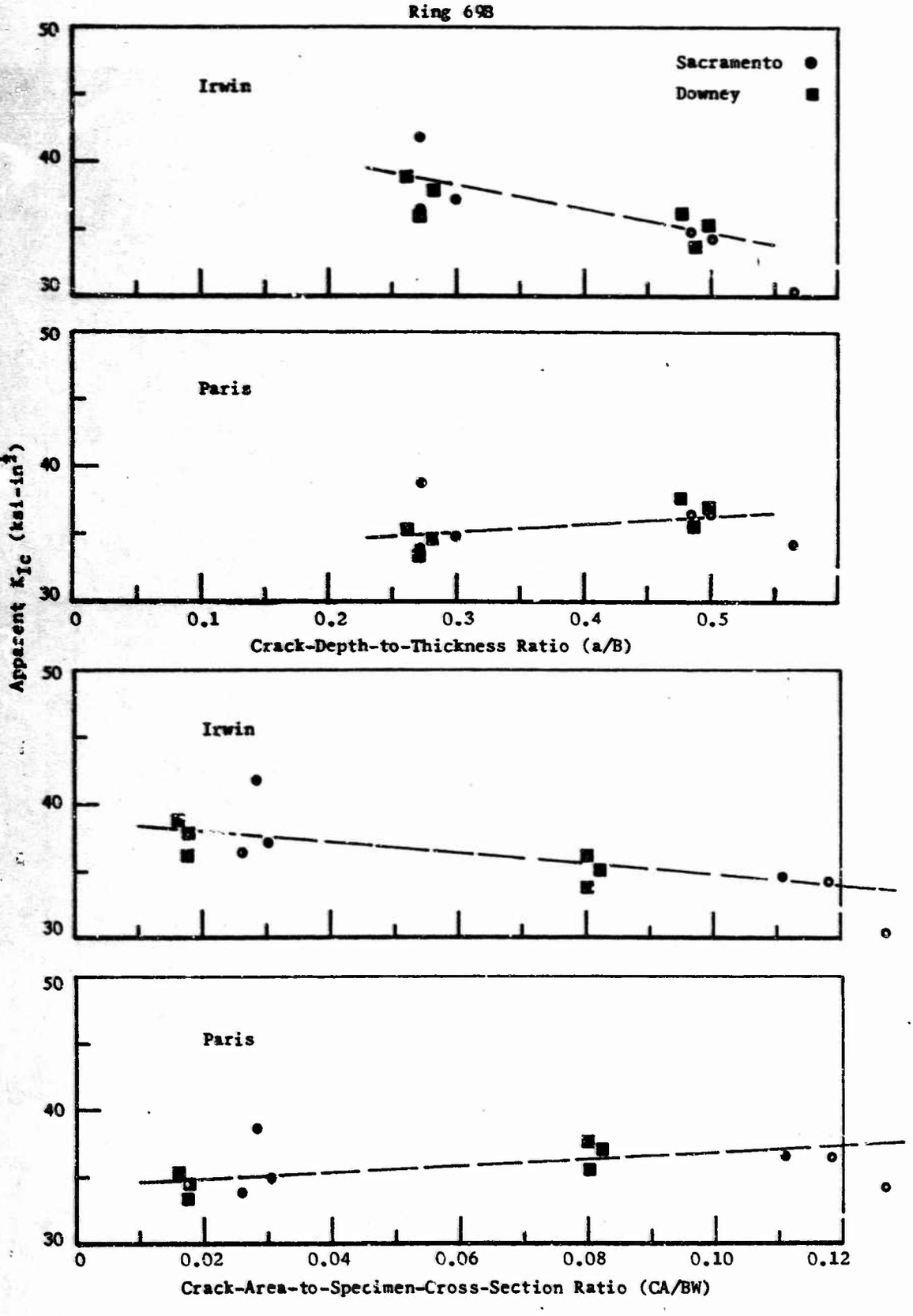


Figure 18. Variation in K_{Ic} Value from Lab to Lab in Forging 69B

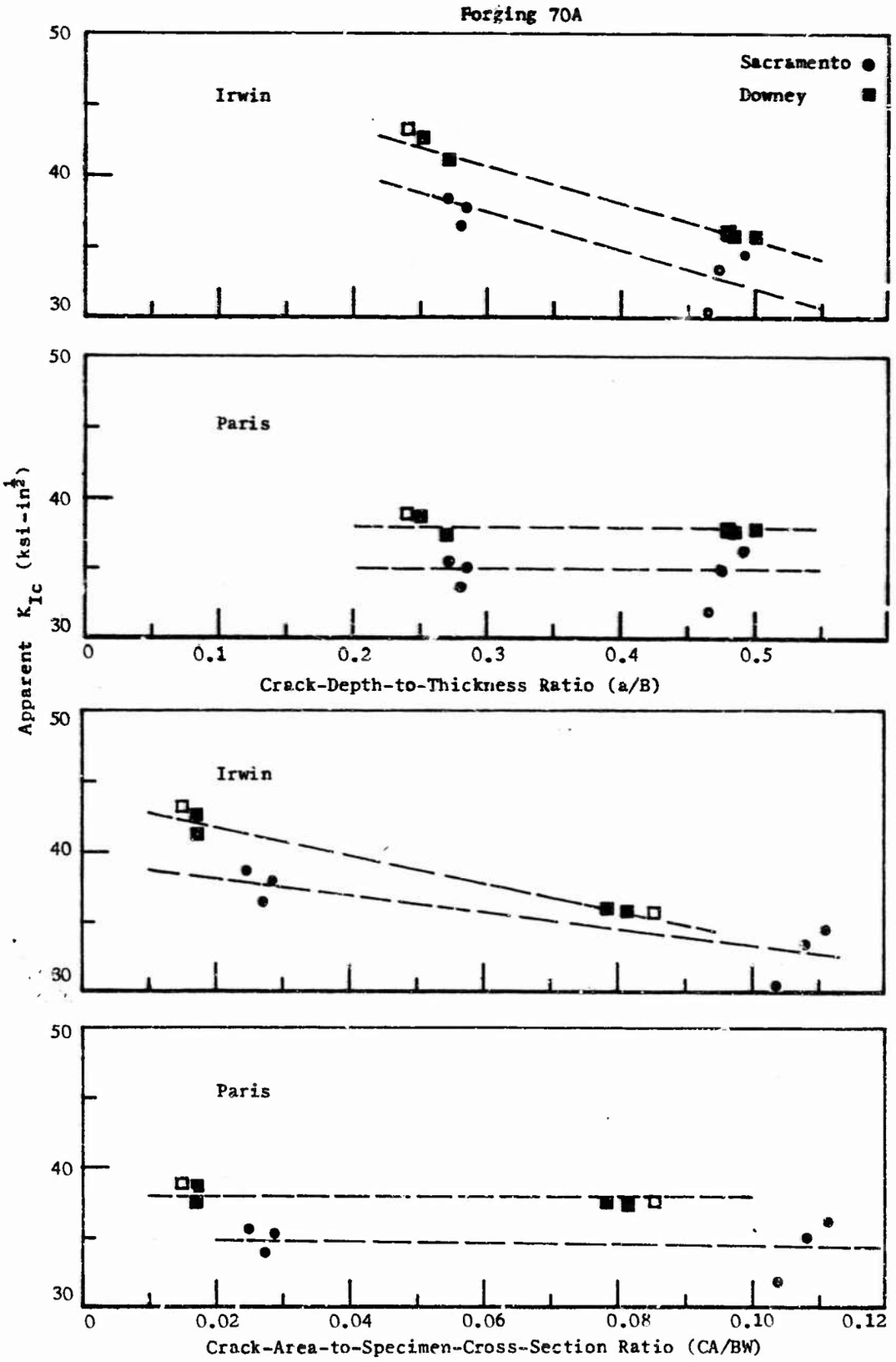


Figure 19. Variation in K_{Ic} Value from Lab to Lab in Forging 70A

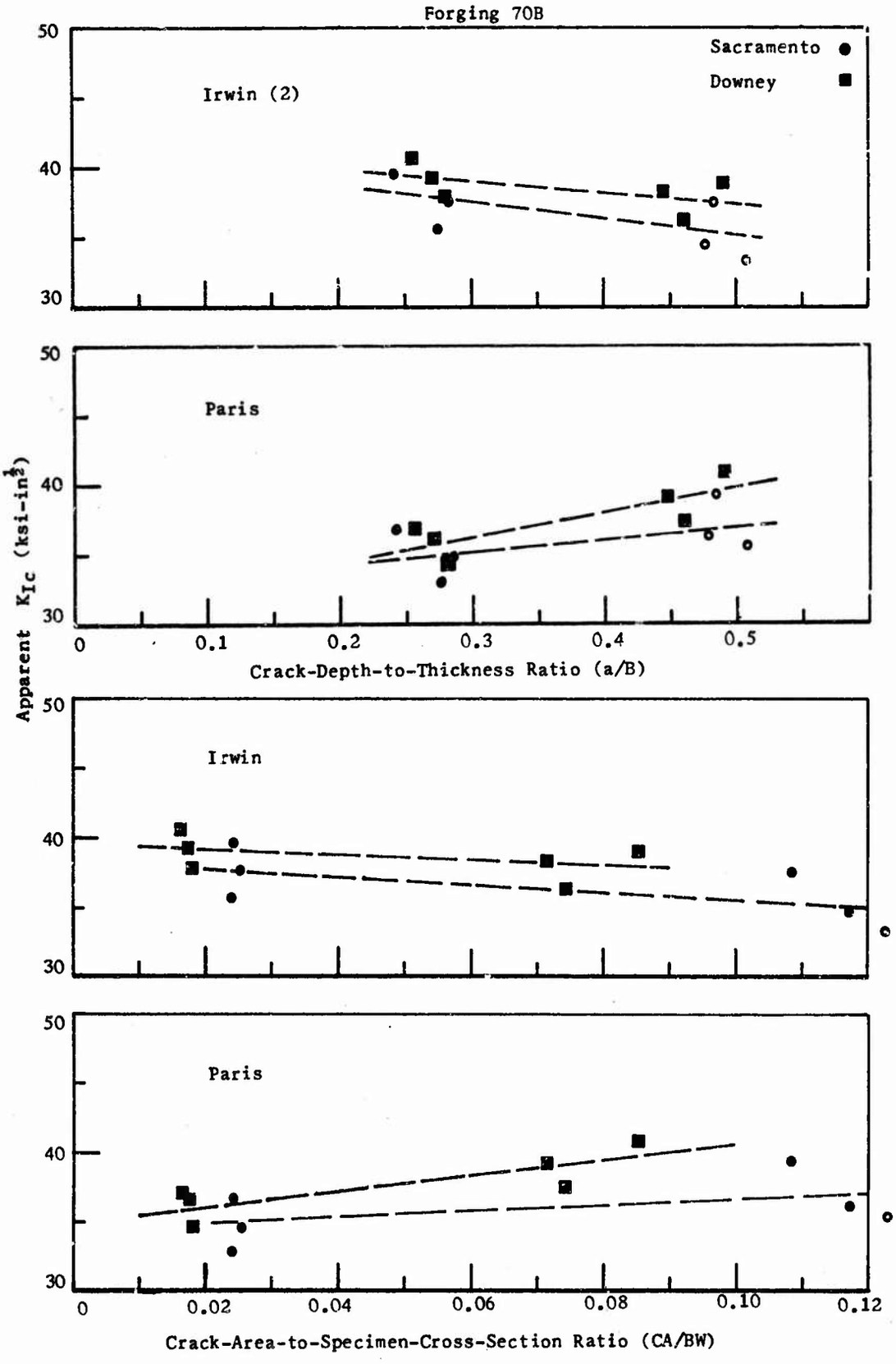


Figure 20. Variation in K_{Ic} Value from Lab to Lab in Forging 70B

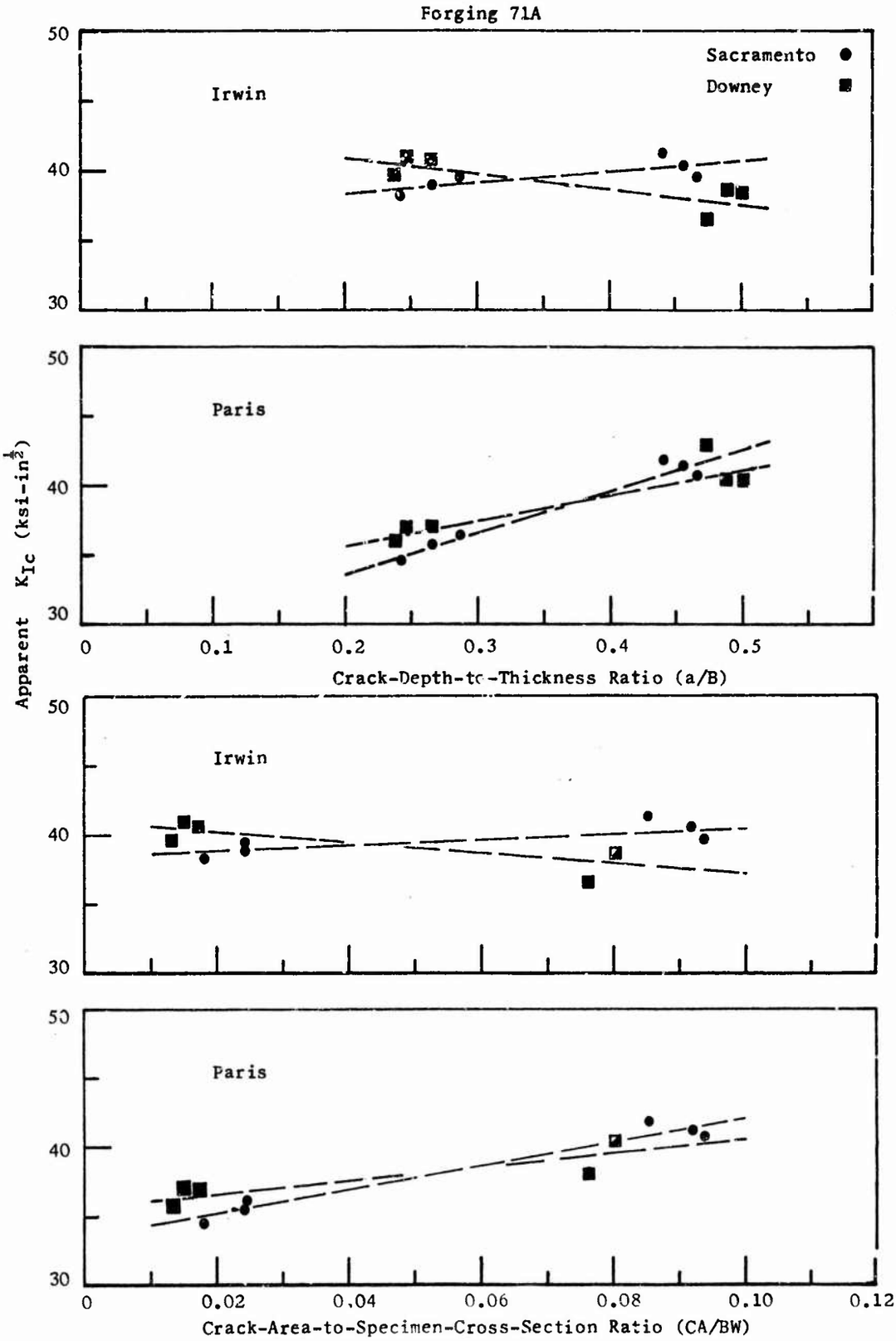


Figure 21. Variation in K_{Ic} Value from Lab to Lab in Forging 71A

Irwin's equation and Paris' equation. The fact that Paris' equation tends to give constant or rising K_{Ic} values for increasing crack depth is also verified. The fact that for some forgings with deep cracks Paris' equation without plastic-zone correction gives higher values of K_{Ic} than Irwin's is also confirmed.

In evaluating forging-to-forging differences, it was noted that there was little or no difference between labs in testing forgings 69A and 69B (Figures 15 and 18). If the data from all three labs are plotted together for billet 69, Figure 22 is the result; note that the scatter band is approximately the same for both large and small cracks in these two forgings.

Figures 19 and 20 indicate a lab-to-lab difference in testing forgings 70A and 70B. When the data from the two forgings (from a single billet) are plotted together as tested by a given laboratory, Figures 23 and 24 are the result. Note that in these forgings, like forgings 69A and 69B, the scatter band is approximately the same for both large and small cracks. Note also that the data from a given forging tends to fall on a common curve, with both labs showing forging 70A on the low side of the scatter band with deeper cracks. A superposition of Figures 23 and 24 indicate the K_{Ic} measurements at Aerojet-Downey to be slightly higher than those measured at Aerojet-Sacramento; this is consistent with the results indicated in Figures 19 and 20.

In summay, regarding the variability in K_{Ic} as a function of heat-to-heat, forging-to-forging and laboratory-to-laboratory differences, it is concluded from the engineering plots as contained in Figures 16 thru 24 that metallurgical effects are the predominating influence on the K_{Ic} values with heat-to-heat and forging-to-forging variability overshadowing differences resulting from the choice of fracture-mechanics expression used in calculating the K_{Ic} value. Moreover, comparisons between forgings from a given billet and, therefore, with a common melt and forging history up to and including breakdown of the ingot, showed significant differences between cylinders produced by a single forging practice. This confirms Harmsworth's(10) observations regarding forging-to-forging variability; viz.,

> "Although quality control is relatively well established for the most commonly used structural materials, some variation does exist in the properties of materials actually accepted for use. This variability can be sufficient to cause unexpected failure. Often this variability may be due to a lack of uniformity in processing techniques throughout the industry.....(there may also be).....variation in properties among forgings produced under the same conditions."

(10) C.L. Harmsworth, "Design Criteria and Test Techniques", AFML-TR-65-29, pp 831-838.

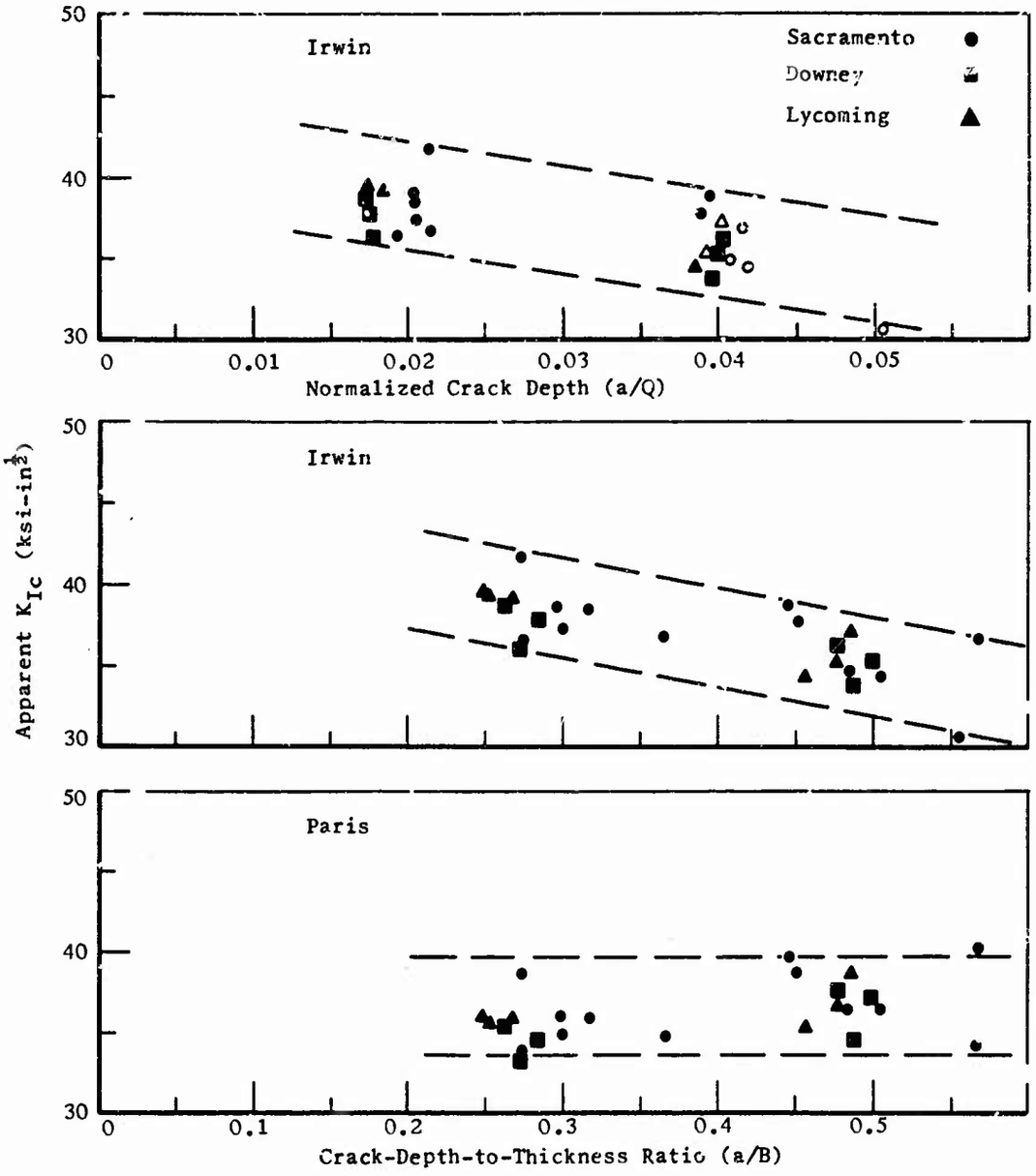


Figure 22. Effect of Crack Depth on the K_{Ic} Value in Billet 69 as Tested by Three Laboratories

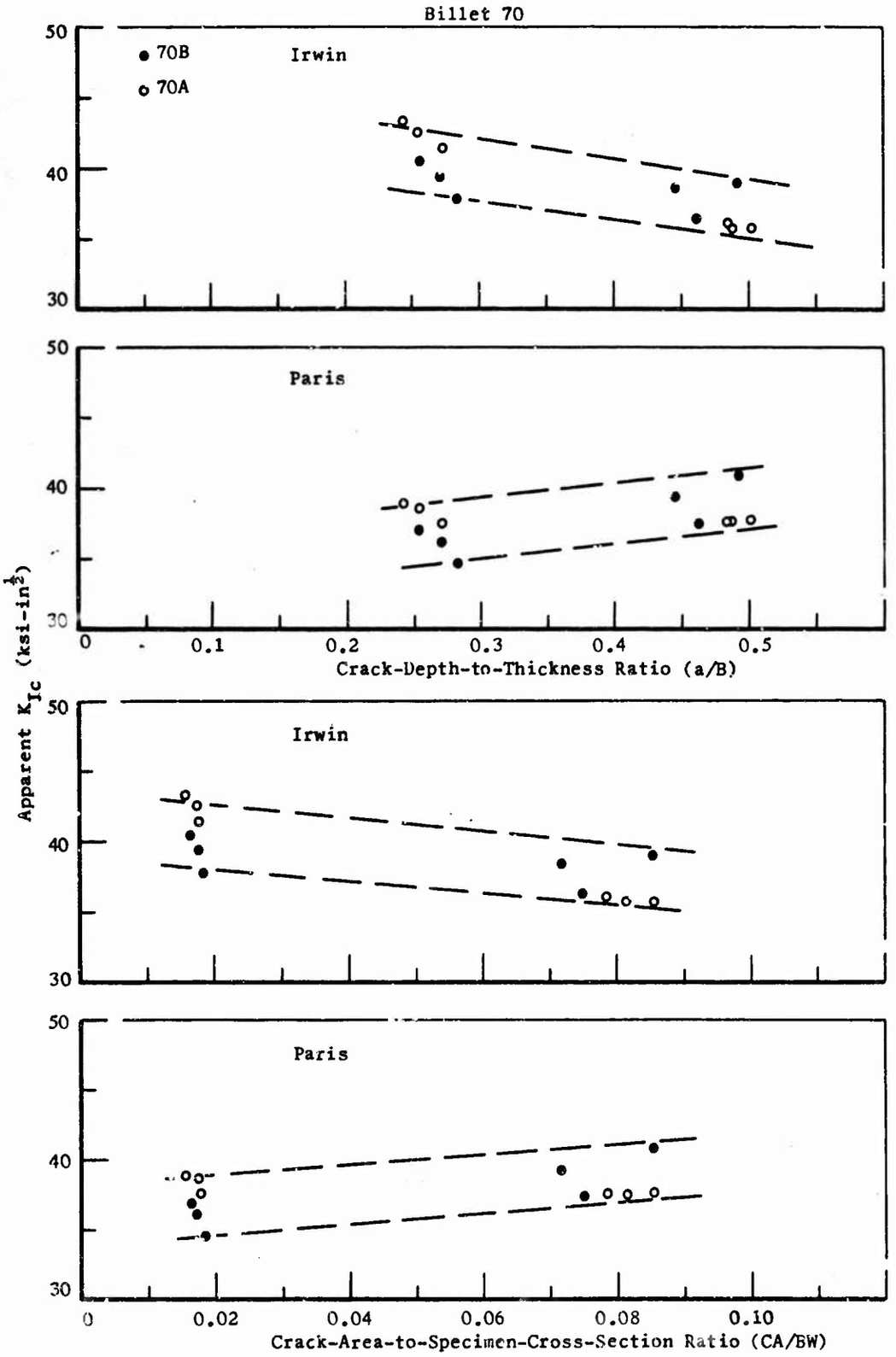


Figure 23. Variation in K_{Ic} Value from Forging to Forging in Billet 70 as Tested by Aerojet-Downey

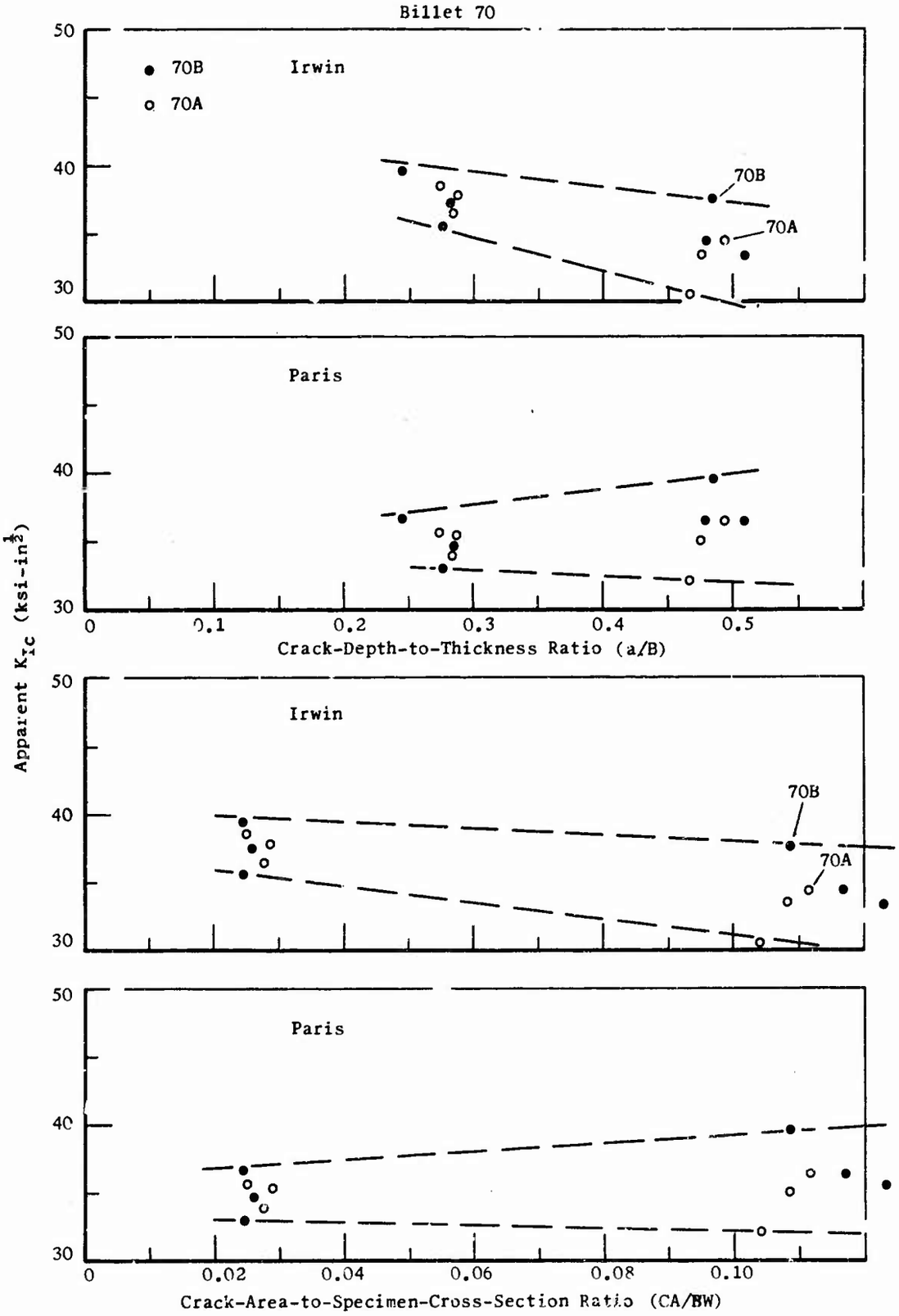


Figure 24. Variation in K_{Ic} Value from Forging to Forging in Billet 70 as Tested by Aerojet-Sacramento

ADDENDUM B-1

COMPUTER PRINTOUT OF PTC-TENSILE-TEST DATA
(K_{Ic} Based on Irwin's Equation)

PART-THROUGH-CRACK TENSILE DATA FOR MINUTEMAN 6AL-4V TITANIUM EXTRUDED CYLINDERS

FORGING SPECIMEN NUMBER	YIELD STRESS FTY (KSI)	ULT. STRESS FTU (KSI)	WIDTH W (IN.)	THICK-NESS B (IN.)	LOAD P-MAX (KIPS)	GROSS STRESS FG (KSI)	CRACK AREA CA (SQ.IN)	NET STRESS FN (KSI)	CRACK DEPTH AO (IN.)	CRACK LENGTH 2C (IN.)	CRACK SHAPE AO/2C	NORM. DEPTH AO/B	AO/B	FG/FTY	CA/BW	PLANE STRAIN KIC	
4-1	162.0	176.3	0.750	0.122	15.5	169.3	0.0020	173.0	0.0331	0.0763	0.43	0.017	0.271	1.04	0.02	43.3	*
4-2	162.0	176.3	0.750	0.121	15.7	173.4	0.0019	177.0	0.0315	0.0751	0.42	0.017	0.260	1.07	0.02	44.1	*
4-3	162.0	176.3	0.750	0.123	15.6	168.9	0.0018	172.3	0.0307	0.0765	0.40	0.017	0.250	1.04	0.02	43.2	*
4-4	162.0	176.3	0.750	0.120	10.5	116.3	0.0086	128.6	0.0562	0.1952	0.29	0.038	0.468	0.72	0.10	44.2	
4-5	162.0	176.3	0.752	0.122	11.3	123.6	0.0091	137.1	0.0589	0.1964	0.30	0.039	0.483	0.76	0.10	47.6	
4-6	162.0	176.3	0.747	0.120	11.2	124.9	0.0088	138.5	0.0564	0.1979	0.28	0.039	0.470	0.77	0.10	48.0	
5-1	161.0	169.3	0.752	0.115	12.6	146.0	0.0023	149.9	0.0340	0.0851	0.40	0.019	0.296	0.91	0.03	38.7	
5-2	161.0	169.3	0.751	0.112	13.8	164.2	0.0018	167.9	0.0300	0.0782	0.38	0.017	0.268	1.02	0.02	42.2	*
5-3	161.0	169.3	0.753	0.115	13.2	152.7	0.0019	156.0	0.0304	0.0775	0.39	0.017	0.264	0.95	0.02	38.8	
5-4	161.0	169.3	0.746	0.124	10.0	108.2	0.0116	123.7	0.0625	0.2365	0.26	0.044	0.504	0.67	0.13	44.3	*
5-5	161.0	169.3	0.753	0.116	9.9	113.7	0.0095	127.5	0.0587	0.2052	0.29	0.048	0.506	0.71	0.11	44.2	*
5-6	161.0	169.3	0.751	0.114	10.7	125.3	0.0089	140.0	0.0560	0.2034	0.28	0.039	0.491	0.78	0.10	48.6	*
6-1	157.0	167.0	0.748	0.129	15.7	162.2	0.0016	165.0	0.0291	0.0711	0.41	0.016	0.226	1.03	0.02	39.9	*
6-2	157.0	167.0	0.750	0.122	14.7	160.8	0.0017	168.8	0.0287	0.0740	0.39	0.017	0.235	1.02	0.02	40.3	*
6-3	157.0	167.0	0.748	0.131	15.7	160.7	0.0019	163.9	0.0317	0.0749	0.42	0.017	0.242	1.02	0.02	40.6	*
6-4	157.0	167.0	0.749	0.128	13.3	138.7	0.0095	154.0	0.0606	0.1992	0.30	0.041	0.473	0.88	0.10	54.8	
6-5	157.0	167.0	0.749	0.130	13.3	136.3	0.0094	150.8	0.0599	0.1990	0.30	0.041	0.461	0.87	0.10	53.6	
6-6	157.0	167.0	0.748	0.130	13.2	135.7	0.0109	152.9	0.0641	0.2162	0.30	0.044	0.493	0.86	0.11	55.5	*
7-1	162.0	170.7	0.749	0.122	14.7	160.4	0.0019	163.8	0.0306	0.0776	0.39	0.017	0.251	0.99	0.02	41.0	
7-2	162.0	170.7	0.746	0.122	14.0	153.4	0.0021	156.9	0.0314	0.0834	0.38	0.018	0.257	0.95	0.02	40.4	
7-3	162.0	170.7	0.746	0.122	14.5	160.0	0.0017	163.1	0.0285	0.0754	0.38	0.017	0.234	0.99	0.02	40.2	
7-4	162.0	170.7	0.748	0.122	10.5	114.9	0.0095	128.3	0.0583	0.2085	0.28	0.048	0.478	0.71	0.10	44.9	*
7-5	162.0	170.7	0.752	0.125	11.8	125.5	0.0086	138.4	0.0572	0.1952	0.29	0.039	0.458	0.77	0.09	48.1	
7-6	162.0	170.7	0.751	0.123	10.9	118.2	0.0103	133.0	0.0602	0.2186	0.28	0.042	0.489	0.73	0.11	47.2	*

* INDICATES PLANE STRAIN FRACTURE TOUGHNESS VALUES (KSI-IN.1/2) OBTAINED FROM TESTS WHICH EXCEEDED ONE OR MORE OF THE FOLLOWING LIMITS. FG/FTY=1.0, AO/B=0.5, AND/OR CA/BW=0.1

PART-THROUGH-CRACK TENSILE DATA FOR MINUTEMAN 6AL-4V TITANIUM EXTRUDED CYLINDERS

FORGING SPECIMEN NUMBER	YIELD STRESS FTY (KSI)	ULT. STRESS FTU (KSI)	WIDTH W (IN.)	THICK-NESS B (IN.)	LOAD P-MAX (KIPS)	GROSS STRESS FG (KSI)	CRACK AREA CA (SQ.IN)	NET STRESS FN (KSI)	CRACK DEPTH AO (IN.)	CRACK LENGTH 2C (IN.)	CRACK SHAPE AO/2C	NORM. DEPTH AO/B	AO/B	FG/FTY	CA/BW	PLANE STRAIN KIC
9-1	158.0	168.3	0.749	0.131	15.7	159.8	0.0016	162.5	0.0281	0.0744	0.38	0.017	0.215	1.01	0.02	40.0 *
9-2	158.0	168.3	0.751	0.116	13.9	159.6	0.0017	162.8	0.0294	0.0755	0.39	0.017	0.253	1.01	0.02	40.3 *
9-3	158.0	168.3	0.750	0.125	15.2	162.1	0.0016	165.0	0.0276	0.0742	0.37	0.016	0.221	1.03	0.02	40.6 *
9-4	158.0	168.3	0.750	0.119	10.7	119.9	0.0092	133.7	0.0582	0.2014	0.29	0.040	0.489	0.76	0.10	46.5 *
9-5	158.0	168.3	0.750	0.123	11.2	121.3	0.0090	134.4	0.0560	0.2049	0.27	0.040	0.455	0.77	0.10	47.0
9-6	158.0	168.3	0.749	0.119	11.5	129.6	0.0088	143.8	0.0566	0.1980	0.29	0.039	0.476	0.82	0.10	50.1
13-1	161.0	171.3	0.750	0.124	14.8	159.3	0.0017	162.3	0.0284	0.0778	0.37	0.017	0.229	0.99	0.02	40.6
13-2	161.0	171.3	0.750	0.123	14.9	161.1	0.0021	164.8	0.0318	0.0825	0.39	0.018	0.259	1.00	0.02	42.5 *
13-6	161.0	171.3	0.752	0.123	15.1	163.1	0.0018	166.4	0.0288	0.0809	0.36	0.018	0.234	1.01	0.02	42.5 *
13-3	161.0	171.3	0.749	0.131	9.7	99.3	0.0105	111.1	0.0647	0.2059	0.31	0.040	0.494	0.62	0.11	38.9 *
13-4	161.0	171.3	0.750	0.132	11.5	118.8	0.0100	132.1	0.0625	0.2023	0.31	0.041	0.477	0.74	0.10	46.6 *
13-5	161.0	171.3	0.749	0.131	11.9	121.5	0.0098	135.0	0.0614	0.2028	0.30	0.040	0.469	0.75	0.10	47.7
14-1	161.0	169.3	0.748	0.128	14.7	154.0	0.0020	157.2	0.0337	0.0741	0.45	0.016	0.263	0.96	0.02	38.4
14-2	161.0	169.3	0.748	0.119	13.6	152.8	0.0021	156.5	0.0332	0.0815	0.41	0.018	0.279	0.95	0.02	39.9
14-3	161.0	169.3	0.746	0.128	15.3	159.7	0.0019	163.0	0.0311	0.0793	0.39	0.018	0.243	0.99	0.02	41.3
14-4	161.0	169.3	0.750	0.123	9.1	98.8	0.0096	110.3	0.0592	0.2075	0.29	0.039	0.481	0.61	0.10	38.3 *
14-5	161.0	169.3	0.749	0.120	8.8	97.9	0.0086	108.3	0.0555	0.1975	0.28	0.037	0.463	0.61	0.10	36.9
14-6	161.0	169.3	0.753	0.121	10.9	119.5	0.0085	131.9	0.0555	0.1957	0.28	0.038	0.459	0.74	0.09	45.5
17-1	166.0	177.0	0.753	0.121	14.5	158.9	0.0016	161.7	0.0286	0.0703	0.41	0.015	0.236	0.96	0.02	38.6
17-2	166.0	177.0	0.752	0.121	13.7	150.0	0.0019	153.1	0.0312	0.0760	0.41	0.017	0.258	0.90	0.02	37.7
17-3	166.0	177.0	0.756	0.129	15.7	161.4	0.0012	163.4	0.0207	0.0743	0.28	0.015	0.160	0.97	0.01	38.9
17-4	166.0	177.0	0.749	0.119	8.7	97.0	0.0085	107.3	0.0555	0.1951	0.28	0.037	0.466	0.58	0.10	36.3
17-5	166.0	177.0	0.750	0.129	8.8	91.4	0.0087	100.5	0.0563	0.1978	0.28	0.037	0.436	0.55	0.09	34.4
17-6	166.0	177.0	0.750	0.122	9.2	100.8	0.0083	110.9	0.0553	0.1911	0.29	0.037	0.453	0.61	0.09	37.6

* INDICATES PLANE STRAIN FRACTURE TOUGHNESS VALUES (KSI-IN.1/2) OBTAINED FROM TESTS WHICH EXCEEDED ONE OR MORE OF THE FOLLOWING LIMITS. FG/FTY=1.0, AO/B=0.5, AND/OR CA/BW=0.1

PART-THROUGH-CRACK TENSILE DATA FOR MINUTEMAN 6AL-4V TITANIUM EXTRUDED CYLINDERS

FORGING SPECIMEN NUMBER	YIELD STRESS FTY (KSI)	ULT. STRESS FTU (KSI)	WIDTH W (IN.)	THICK-NESS B (IN.)	LOAD P-MAX (KIPS)	GROSS STRESS FG (KSI)	CRACK AREA CA (SQ.IN)	NET STRESS FN (KSI)	CRACK DEPTH AO (IN.)	CRACK LENGTH 2C (IN.)	CRACK SHAPE AO/2C	NORM. DEPTH AO/B	AO/B	FG/FTY	CA/BW	PLANE STRAIN KIC	
21-1	165.0	175.0	0.752	0.120	14.3	159.0	0.0018	162.2	0.0294	0.0760	0.39	0.017	0.245	0.96	0.02	40.1	
21-2	165.0	175.0	0.747	0.130	15.6	160.2	0.0017	163.2	0.0287	0.0774	0.37	0.017	0.221	0.97	0.02	40.7	
21-3	165.0	175.0	0.752	0.120	14.2	157.9	0.0017	160.9	0.0287	0.0762	0.38	0.017	0.239	0.96	0.02	39.7	
21-4	165.0	175.0	0.750	0.133	10.2	102.3	0.0096	113.2	0.0392	0.2067	0.29	0.039	0.445	0.62	0.10	39.6	
21-5	165.0	175.0	0.750	0.129	9.2	95.1	0.0099	106.0	0.0401	0.2095	0.29	0.040	0.466	0.58	0.10	37.0	*
21-6	165.0	175.0	0.750	0.126	9.7	103.0	0.0089	113.7	0.0387	0.2087	0.28	0.038	0.450	0.62	0.09	39.2	
22-1	164.0	175.0	0.751	0.134	13.5	134.4	0.0024	137.7	0.0364	0.0842	0.43	0.028	0.272	0.82	0.02	35.3	
22-2	164.0	175.0	0.748	0.131	15.3	156.2	0.0017	158.9	0.0295	0.0718	0.41	0.016	0.225	0.95	0.02	36.3	
22-3	164.0	175.0	0.741	0.118	13.4	152.6	0.0013	156.1	0.0308	0.0755	0.41	0.017	0.261	0.93	0.02	38.3	
22-4	164.0	175.0	0.750	0.128	10.7	110.9	0.0098	123.6	0.0605	0.2065	0.29	0.040	0.473	0.68	0.10	43.3	*
22-5	164.0	175.0	0.750	0.125	10.7	113.9	0.0088	125.7	0.0549	0.2049	0.27	0.039	0.439	0.69	0.09	43.6	
22-6	164.0	175.0	0.748	0.130	10.7	110.4	0.0093	122.1	0.0593	0.1991	0.30	0.039	0.456	0.67	0.10	42.5	
23-1	163.0	173.7	0.746	0.131	15.7	160.1	0.0018	163.2	0.0320	0.0730	0.44	0.016	0.244	0.98	0.02	39.8	
23-2	163.0	173.7	0.751	0.117	14.2	161.9	0.0015	164.7	0.0260	0.0728	0.36	0.016	0.222	0.99	0.02	39.9	
23-3	163.0	173.7	0.750	0.120	14.4	159.7	0.0018	162.9	0.0291	0.0789	0.37	0.017	0.243	0.98	0.02	41.0	
23-4	163.0	173.7	0.749	0.118	10.1	114.2	0.0088	126.8	0.0561	0.2083	0.26	0.038	0.475	0.70	0.10	43.7	
23-5	163.0	173.7	0.751	0.120	10.6	117.5	0.0097	131.7	0.0592	0.2087	0.28	0.040	0.493	0.72	0.11	46.1	*
23-6	163.0	173.7	0.750	0.119	10.7	119.6	0.0094	133.6	0.0596	0.2081	0.30	0.040	0.501	0.73	0.10	46.3	*
26-1	159.0	171.0	0.749	0.125	15.4	164.7	0.0020	168.4	0.0321	0.0811	0.40	0.018	0.257	1.04	0.02	43.3	*
26-2	159.0	171.0	0.752	0.126	15.3	160.9	0.0022	164.8	0.0356	0.0800	0.45	0.018	0.283	1.01	0.02	42.0	*
26-3	159.0	171.0	0.748	0.124	15.2	164.1	0.0020	167.7	0.0315	0.0817	0.39	0.018	0.254	1.03	0.02	43.2	*
26-4	159.0	171.0	0.749	0.117	11.1	127.1	0.0083	140.3	0.0546	0.1926	0.28	0.038	0.467	0.80	0.09	48.3	
26-5	159.0	171.0	0.748	0.130	11.1	113.9	0.0154	135.4	0.0924	0.2120	0.44	0.045	0.711	0.72	0.16	47.1	*
26-6	159.0	171.0	0.749	0.113	9.5	107.4	0.0098	120.8	0.0579	0.2165	0.27	0.041	0.491	0.68	0.11	42.2	*

* INDICATES PLANE STRAIN FRACTURE TOUGHNESS VALUES (KSI-IN.1/2) OBTAINED FROM TESTS WHICH EXCEEDED ONE OR MORE OF THE FOLLOWING LIMITS. FG/FTY=1.0, AO/B=0.5, AND/OR CA/BW=0.1

PART-THROUGH-CRACK TENSILE DATA FOR MINUSCRAN 6AL-4V TITANIUM EXTRUDED CYLINDERS

FORGING SPECIMEN NUMBER	YIELD STRESS FTY (KSI)	ULT. STRESS FTU (KSI)	WIDTH W (IN.)	THICK-NESS B (IN.)	LOAD P-MAX (KIPS)	GROSS STRESS FG (KSI)	CRACK AREA CA (SQ.IN)	NET STRESS FN (KSI)	CRACK DEPTH AO (IN.)	CRACK LENGTH 2C (IN.)	CRACK SHAPE AO/2C	NORM. DEPTH AO/B	AO/B	FG/FTY	CA/BW	PLANE STRAIN KIC
27-1	166.0	176.7	0.748	0.126	15.0	159.4	0.0018	162.5	0.0291	0.0794	0.37	0.017	0.231	0.96	0.02	40.9
27-2	166.0	176.7	0.750	0.122	14.7	161.1	0.0018	164.4	0.0309	0.0752	0.41	0.017	0.253	0.97	0.02	40.5
27-3	166.0	176.7	0.749	0.121	14.6	160.7	0.0018	163.9	0.0287	0.0787	0.36	0.017	0.237	0.97	0.02	41.1
27-4	166.0	176.7	0.757	0.127	9.0	93.7	0.0096	104.1	0.0597	0.2049	0.29	0.039	0.470	0.56	0.10	36.1
27-5	166.0	176.7	0.751	0.119	8.7	97.3	0.0083	107.3	0.0519	0.2036	0.25	0.037	0.436	0.59	0.09	36.4
27-6	166.0	176.7	0.751	0.122	10.5	114.6	0.0084	126.2	0.0536	0.2005	0.27	0.038	0.439	0.69	0.09	43.4
29-2	165.0	174.3	0.752	0.130	15.0	153.1	0.0018	155.9	0.0303	0.0751	0.40	0.016	0.233	0.93	0.02	38.3
29-3	165.0	174.3	0.752	0.130	15.3	156.0	0.0020	159.2	0.0324	0.0780	0.42	0.017	0.249	0.95	0.02	39.9
29-4	165.0	174.3	0.750	0.129	8.5	87.3	0.0093	96.7	0.0597	0.1990	0.30	0.038	0.463	0.53	0.10	33.2
29-5	165.0	174.3	0.751	0.120	8.5	94.3	0.0089	104.7	0.0559	0.2027	0.28	0.038	0.466	0.57	0.10	35.8
29-6	165.0	174.3	0.750	0.122	8.7	95.3	0.0093	106.3	0.0588	0.2049	0.29	0.039	0.482	0.58	0.10	36.6 *
30-1	164.0	175.3	0.751	0.121	14.9	163.6	0.0018	167.0	0.0304	0.0773	0.39	0.017	0.251	1.00	0.02	41.8
30-2	164.0	175.3	0.748	0.126	14.9	158.5	0.0019	161.7	0.0311	0.0757	0.41	0.017	0.247	0.97	0.02	40.0
30-3	164.0	175.3	0.749	0.129	15.3	158.2	0.0017	161.2	0.0300	0.0740	0.41	0.016	0.233	0.96	0.02	39.4
30-4	164.0	175.3	0.748	0.119	11.5	129.2	0.0087	143.2	0.0557	0.1995	0.28	0.039	0.468	0.79	0.10	49.8
30-5	164.0	175.3	0.749	0.119	12.1	135.9	0.0097	152.4	0.0626	0.1971	0.32	0.041	0.526	0.83	0.11	53.3 *
30-6	164.0	175.3	0.749	0.125	11.3	120.9	0.0092	134.1	0.0594	0.1977	0.30	0.039	0.475	0.74	0.10	46.7
31-A-2	167.0	176.7	0.749	0.123	14.2	154.0	0.0015	156.4	0.0267	0.0693	0.39	0.015	0.217	0.92	0.02	36.9
31-A-5	167.0	176.7	0.748	0.122	13.8	151.4	0.0016	154.1	0.0285	0.0693	0.41	0.015	0.234	0.91	0.02	36.3
31-A-6	167.0	176.7	0.749	0.122	13.7	150.3	0.0014	152.6	0.0236	0.0770	0.31	0.016	0.193	0.90	0.02	37.0
31-A-1	167.0	176.7	0.747	0.121	6.7	74.7	0.0086	82.6	0.0570	0.1930	0.30	0.036	0.471	0.45	0.10	27.7
31-A-3	167.0	176.7	0.749	0.122	8.2	89.5	0.0067	98.9	0.0558	0.1978	0.28	0.037	0.457	0.54	0.09	33.6
31-A-4	167.0	176.7	0.752	0.132	8.2	82.5	0.0098	91.5	0.0606	0.2056	0.29	0.039	0.459	0.49	0.10	31.7

* INDICATES PLANE STRAIN FRACTURE TOUGHNESS VALUES (KSI-IN.1/2) OBTAINED FROM TESTS WHICH EXCEEDED ONE OR MORE OF THE FOLLOWING LIMITS. FG/FTY=1.0, AO/B=0.5, AND/OR CA/BW=0.1

PART-THROUGH-CRACK TENSILE DATA FOR MINUTEMAN 6AL-4V TITANIUM EXTRUDED CYLINDERS

FORGING SPECIMEN NUMBER	YIELD STRESS FTY (KSI)	ULT. STRESS FTU (KSI)	WIDTH W (IN.)	THICK -NESS B (IN.)	LOAD P-MAX (KIPS)	GROSS STRESS FG (KSI)	CRACK AREA CA (SQ.IN)	NET STRESS FN (KSI)	CRACK DEPTH AO (IN.)	CRACK LENGTH 2C (IN.)	CRACK SHAPE AO/2C	NORM. DEPTH AO/B	AO/B	FG/FTY	CA/BW	PLANE STRAIN KIC
31-B-1	168.0	176.7	0.749	0.126	13.5	142.9	0.0015	145.3	0.0277	0.0690	0.40	0.015	0.220	0.85	0.02	34.0
31-B-2	168.0	176.7	0.748	0.130	13.9	143.2	0.0020	146.2	0.0324	0.0774	0.42	0.017	0.249	0.85	0.02	36.1
31-B-3	168.0	176.7	0.749	0.129	14.8	153.4	0.0018	156.4	0.0312	0.0746	0.42	0.016	0.242	0.91	0.02	38.2
31-B-4	168.0	176.7	0.743	0.131	7.8	79.9	0.0104	89.5	0.0616	0.2159	0.29	0.040	0.470	0.48	0.11	31.3 *
31-B-5	168.0	176.7	0.748	0.119	7.8	87.2	0.0083	96.2	0.0539	0.1965	0.27	0.036	0.453	0.52	0.09	32.4
31-B-6	168.0	176.7	0.752	0.118	7.5	84.7	0.0080	93.2	0.0507	0.2014	0.25	0.036	0.430	0.50	0.09	31.2
33-A-1	158.0	168.3	0.749	0.128	15.1	157.8	0.0016	160.4	0.0281	0.0720	0.39	0.016	0.220	1.00	0.02	38.9
33-A-2	158.0	168.3	0.749	0.128	14.3	148.9	0.0021	152.3	0.0340	0.0791	0.43	0.017	0.266	0.94	0.02	38.3
33-A-3	158.0	168.3	0.747	0.121	14.3	157.7	0.0016	160.4	0.0278	0.0721	0.39	0.016	0.230	1.00	0.02	38.9
33-A-4	158.0	168.3	0.749	0.126	10.3	109.7	0.0088	120.9	0.0582	0.1924	0.30	0.038	0.462	0.69	0.09	41.6
33-A-5	158.0	168.3	0.751	0.118	9.7	110.0	0.0086	121.9	0.0558	0.1973	0.28	0.038	0.473	0.70	0.10	41.8
33-A-6	158.0	168.3	0.750	0.129	10.0	103.2	0.0091	113.9	0.0591	0.1965	0.30	0.038	0.458	0.65	0.09	39.4
33-B-1	158.0	168.3	0.750	0.130	15.3	157.3	0.0016	160.0	0.0278	0.0751	0.37	0.017	0.214	1.00	0.02	39.5
33-B-2	158.0	168.3	0.749	0.125	14.3	152.8	0.0019	156.1	0.0321	0.0765	0.42	0.017	0.257	0.97	0.02	38.8
33-B-3	158.0	168.3	0.750	0.119	13.8	154.6	0.0019	158.0	0.0288	0.0845	0.34	0.018	0.242	0.98	0.02	40.8
33-B-4	158.0	168.3	0.744	0.130	10.4	107.4	0.0100	119.8	0.0623	0.2042	0.31	0.040	0.479	0.68	0.10	42.0 *
33-B-5	158.0	168.3	0.748	0.114	10.7	125.1	0.0087	139.4	0.0552	0.2010	0.27	0.039	0.484	0.79	0.10	48.2 *
33-B-6	158.0	168.3	0.750	0.121	10.5	115.2	0.0093	128.3	0.0591	0.2006	0.29	0.039	0.488	0.73	0.10	44.6 *
36-A-1	168.0	177.7	0.749	0.119	14.1	158.2	0.0017	161.2	0.0296	0.0725	0.41	0.016	0.249	0.94	0.02	38.9
36-A-2	168.0	177.7	0.752	0.122	14.0	152.3	0.0020	155.6	0.0307	0.0823	0.37	0.018	0.252	0.91	0.02	39.6
36-A-3	168.0	177.7	0.749	0.119	13.2	148.3	0.0017	151.2	0.0263	0.0815	0.32	0.017	0.221	0.88	0.02	37.7
36-A-4	168.0	177.7	0.748	0.126	8.3	88.2	0.0105	99.2	0.0569	0.2339	0.24	0.041	0.452	0.52	0.11	34.8 *
36-A-5	168.0	177.7	0.750	0.116	8.6	99.0	0.0086	109.9	0.0546	0.2017	0.27	0.037	0.471	0.59	0.10	37.3
36-A-6	168.0	177.7	0.750	0.125	8.6	92.0	0.0086	101.3	0.0558	0.1963	0.28	0.037	0.446	0.55	0.09	34.4

* INDICATES PLANE STRAIN FRACTURE TOUGHNESS VALUES (KSI-IN.1/2) OBTAINED FROM TESTS WHICH EXCEEDED ONE OR MORE OF THE FOLLOWING LIMITS. FG/FTY=1.0, AO/B=0.5, AND/OR CA/BW=0.1

PART-THROUGH-CRACK TENSILE DATA FOR MINUTEMAN 6AL-4V TITANIUM EXTRUDED CYLINDERS

FORGING SPECIMEN NUMBER	YIELD STRESS FTY (KSI)	ULT. STRESS FTU (KSI)	WIDTH W (IN.)	THICK-NESS B (IN.)	LOAD P-MAX (KIPS)	GROSS STRESS FG (KSI)	CRACK AREA CA (SQ.IN)	NET STRESS FN (KSI)	CRACK DEPTH AO (IN.)	CRACK LENGTH 2C (IN.)	CRACK SHAPE AO/2C	NORM. DEPTH AO/B	AO/B	FG/FTY	CA/BW	PLANE STRAIN KIC
36-B-1	166.0	175.3	0.752	0.120	13.9	154.0	0.0019	157.3	0.0315	0.0766	0.41	0.017	0.262	0.93	0.02	38.9
36-B-2	166.0	175.3	0.748	0.126	14.0	149.1	0.0019	152.1	0.0303	0.0796	0.38	0.017	0.240	0.90	0.02	38.1
36-B-3	166.0	175.3	0.749	0.129	14.8	153.3	0.0020	156.5	0.0311	0.0802	0.39	0.017	0.241	0.92	0.02	39.5
36-B-4	166.0	175.3	0.749	0.119	8.0	90.1	0.0089	100.1	0.0562	0.2025	0.28	0.038	0.472	0.54	0.10	34.1 *
36-B-5	166.0	175.3	0.749	0.119	8.5	95.1	0.0093	106.3	0.0585	0.2032	0.29	0.039	0.492	0.57	0.10	36.4 *
36-B-6	166.0	175.3	0.749	0.125	8.6	91.9	0.0093	101.9	0.0600	0.1964	0.31	0.038	0.480	0.55	0.10	34.9
37-A-1	164.0	176.3	0.751	0.122	13.7	149.2	0.0019	152.4	0.0314	0.0784	0.40	0.017	0.257	0.91	0.02	38.0
37-A-2	164.0	176.3	0.748	0.126	14.6	155.1	0.0017	158.0	0.0309	0.0715	0.43	0.016	0.245	0.95	0.02	38.0
37-A-4	164.0	176.3	0.745	0.126	14.6	155.7	0.0014	158.1	0.0273	0.0676	0.40	0.015	0.217	0.95	0.02	37.0
37-A-3	164.0	176.3	0.748	0.128	9.7	101.8	0.0096	113.1	0.0614	0.1982	0.31	0.039	0.480	0.62	0.10	39.1
37-A-5	164.0	176.3	0.749	0.130	10.2	104.7	0.0091	115.5	0.0582	0.1995	0.29	0.038	0.448	0.64	0.09	40.0
37-A-6	164.0	176.3	0.747	0.129	11.3	117.1	0.0090	129.1	0.0587	0.1943	0.30	0.038	0.455	0.71	0.09	44.7
37-B-1	160.0	169.3	0.749	0.132	15.4	155.3	0.0020	158.5	0.0338	0.0757	0.45	0.017	0.256	0.97	0.02	39.2
37-B-2	160.0	169.3	0.749	0.115	13.5	156.2	0.0022	160.2	0.0323	0.0865	0.37	0.019	0.281	0.98	0.03	42.0
37-B-3	160.0	169.3	0.751	0.121	14.2	155.9	0.0020	159.4	0.0316	0.0791	0.40	0.017	0.261	0.97	0.02	40.2
37-B-4	160.0	169.3	0.746	0.126	10.0	106.3	0.0097	118.4	0.0597	0.2059	0.29	0.040	0.474	0.66	0.10	41.3 *
37-B-5	160.0	169.3	0.751	0.122	10.3	112.2	0.0096	125.4	0.0606	0.2026	0.30	0.040	0.497	0.70	0.11	43.7 *
37-B-6	160.0	169.3	0.745	0.130	10.4	107.7	0.0096	119.6	0.0603	0.2037	0.30	0.040	0.464	0.67	0.10	41.8
39-A-1	161.0	171.7	0.753	0.128	13.2	136.7	0.0020	139.7	0.0331	0.0786	0.42	0.017	0.259	0.85	0.02	34.8
39-A-2	161.0	171.7	0.748	0.126	13.5	142.9	0.0020	146.1	0.0325	0.0800	0.41	0.017	0.258	0.89	0.02	36.7
39-A-3	161.0	171.7	0.752	0.127	14.9	156.3	0.0017	159.2	0.0285	0.0758	0.38	0.017	0.224	0.97	0.02	39.3
39-A-4	161.0	171.7	0.754	0.128	9.6	99.7	0.0091	110.0	0.0583	0.1982	0.29	0.038	0.455	0.62	0.09	38.0
39-A-5	161.0	171.7	0.751	0.123	11.0	118.6	0.0086	130.8	0.0559	0.1955	0.29	0.038	0.454	0.74	0.09	45.2
39-A-6	161.0	171.7	0.753	0.122	9.0	97.9	0.0086	108.0	0.0555	0.1975	0.28	0.037	0.455	0.61	0.09	36.9

* INDICATES PLANE STRAIN FRACTURE TOUGHNESS VALUES (KSI-IN.1/2) OBTAINED FROM TESTS WHICH EXCEEDED ONE OR MORE OF THE FOLLOWING LIMITS. FG/FTY=1.0, AO/B=0.5, AND/OR CA/BW=0.1

PART-THROUGH-CRACK TENSILE DATA FOR MINUTEMAN 6AL-4V TITANIUM EXTRUDED CYLINDER

FORGING SPECIMEN NUMBER	YIELD STRESS FTY (KSI)	ULT. STRESS FTU (KSI)	WIDTH W (IN.)	THICK-NESS B (IN.)	LOAD P-MAX (KIPS)	GROSS STRESS FG (KSI)	CRACK AREA CA (SQ.IN)	NET STRESS FN (KSI)	CRACK DEPTH AO (IN.)	CRACK LENGTH 2C (IN.)	CRACK SHAPE AO/2C	NORM. DEPTH AO/B	AO/B	FG/FTY	CA/BW	PLANE STRAIN KIC	
42-B-1	168.0	176.3	0.749	0.121	14.0	155.0	0.0021	158.6	0.0343	0.0765	0.45	0.017	0.283	0.92	0.02	39.2	
42-B-2	168.0	176.3	0.750	0.119	14.0	156.9	0.0019	160.3	0.0316	0.0765	0.41	0.017	0.266	0.93	0.02	39.6	
42-B-3	168.0	176.3	0.750	0.117	13.7	155.6	0.0022	159.6	0.0332	0.0846	0.39	0.018	0.284	0.93	0.03	41.2	
42-B-4	168.0	176.3	0.749	0.120	8.7	97.1	0.0092	108.1	0.0580	0.2011	0.29	0.038	0.483	0.58	0.10	37.0	*
42-B-5	168.0	176.3	0.749	0.129	9.0	92.9	0.0096	103.2	0.0606	0.2021	0.30	0.039	0.470	0.55	0.10	35.7	
42-B-6	168.0	176.3	0.749	0.129	9.3	96.5	0.0097	107.2	0.0603	0.2046	0.29	0.039	0.467	0.57	0.10	37.2	*
42-C-3	160.0	172.0	0.754	0.124	14.3	152.4	0.0018	155.4	0.0302	0.0766	0.39	0.017	0.244	0.95	0.02	38.5	
42-C-4	160.0	172.0	0.749	0.120	14.3	158.5	0.0019	162.0	0.0313	0.0779	0.40	0.017	0.261	0.99	0.02	40.6	
42-C-5	160.0	172.0	0.749	0.120	13.7	152.4	0.0018	155.6	0.0310	0.0751	0.41	0.017	0.258	0.95	0.02	38.2	
42-C-6	160.0	172.0	0.749	0.119	14.0	157.1	0.0017	160.2	0.0297	0.0750	0.40	0.017	0.250	0.98	0.02	39.4	
42-C-1	160.0	172.0	0.752	0.127	10.2	106.5	0.0086	117.0	0.0547	0.2005	0.27	0.038	0.431	0.67	0.09	40.4	
42-C-2	160.0	172.0	0.749	0.127	7.9	82.6	0.0123	94.9	0.0652	0.2405	0.27	0.044	0.513	0.52	0.13	33.9	*
43-A-1	171.0	177.3	0.751	0.129	15.0	154.8	0.0019	157.9	0.0321	0.0757	0.42	0.017	0.249	0.91	0.02	38.8	
43-A-2	171.0	177.3	0.749	0.124	14.1	152.2	0.0019	155.4	0.0309	0.0780	0.40	0.017	0.249	0.89	0.02	38.6	
43-A-3	171.0	177.3	0.749	0.119	14.0	156.8	0.0017	159.9	0.0306	0.0722	0.42	0.016	0.257	0.92	0.02	38.4	
43-A-4	171.0	177.3	0.752	0.125	8.2	86.9	0.0096	96.8	0.0602	0.2032	0.30	0.039	0.482	0.51	0.10	33.3	*
43-A-5	171.0	177.3	0.751	0.122	8.7	95.3	0.0091	105.8	0.0582	0.2000	0.29	0.038	0.477	0.56	0.10	36.2	
43-A-6	171.0	177.3	0.751	0.130	9.3	95.3	0.0096	105.7	0.0596	0.2058	0.29	0.039	0.458	0.56	0.10	36.7	
43-B-1	165.0	173.7	0.747	0.130	15.0	154.5	0.0019	157.5	0.0317	0.0755	0.42	0.017	0.244	0.94	0.02	38.8	
43-B-2	165.0	173.7	0.749	0.120	14.4	160.0	0.0015	162.7	0.0274	0.0690	0.40	0.015	0.228	0.97	0.02	38.5	
43-B-3	165.0	173.7	0.751	0.121	14.0	154.2	0.0016	157.0	0.0294	0.0697	0.42	0.015	0.243	0.93	0.02	37.2	
43-B-4	165.0	173.7	0.750	0.121	9.4	103.5	0.0093	115.3	0.0580	0.2035	0.29	0.039	0.479	0.63	0.10	39.8	*
43-B-5	165.0	173.7	0.750	0.124	8.8	94.9	0.0088	104.9	0.0577	0.1951	0.30	0.037	0.465	0.58	0.10	35.8	
43-B-6	165.0	173.7	0.749	0.118	9.4	106.1	0.0080	116.7	0.0542	0.1885	0.29	0.036	0.459	0.64	0.09	39.3	

* INDICATES PLANE STRAIN FRACTURE TOUGHNESS VALUES (KSI-IN.1/2) OBTAINED FROM TESTS WHICH EXCEEDED ONE OR MORE OF THE FOLLOWING LIMITS. FG/FTY=1 0. AO/B=0.5, AND/OR CA/BW=0.1

PART-THROUGH-CRACK TENSILE DATA FOR MINUTEMAN 6AL-4V TITANIUM EXTRUDED CYLINDERS

FORGING SPECIMEN NUMBER	YIELD STRESS FTY (KSI)	ULT. STRESS FTU (KSI)	WIDTH W (IN.)	THICK-NESS B (IN.)	LOAD P-MAX (KIPS)	GROSS STRESS FG (KSI)	CRACK AREA CA (SQ.IN)	NET STRESS FN (KSI)	CRACK DEPTH AO (IN.)	CRACK LENGTH 2C (IN.)	CRACK SHAPE AO/2C	NORM. DEPTH AO/B	AO/B	FG/FTY	CA/BW	PLANE STRAIN KIC	
44-B-1	159.0	171.0	0.750	0.127	13.4	140.9	0.0025	144.8	0.0365	0.0887	0.41	0.019	0.287	0.89	0.03	38.2	
44-B-2	159.0	171.0	0.752	0.126	13.2	139.8	0.0029	144.0	0.0388	0.0965	0.40	0.021	0.308	0.88	0.03	39.3	
44-B-3	159.0	171.0	0.746	0.124	13.1	141.6	0.0025	145.6	0.0355	0.0898	0.40	0.019	0.286	0.89	0.03	38.5	
44-B-4	159.0	171.0	0.749	0.125	11.0	117.5	0.0118	134.4	0.0668	0.2251	0.30	0.044	0.534	0.74	0.13	48.3	*
44-B-5	159.0	171.0	0.750	0.125	11.1	118.9	0.0101	133.3	0.0638	0.2020	0.32	0.041	0.510	0.75	0.11	46.8	*
44-B-6	159.0	171.0	0.750	0.125	11.2	119.0	0.0103	133.7	0.0632	0.2075	0.30	0.041	0.506	0.75	0.11	47.2	*
45-A-2	161.0	172.3	0.748	0.122	14.5	158.9	0.0020	162.5	0.0314	0.0811	0.39	0.018	0.257	0.99	0.02	41.5	
45-A-3	161.0	172.3	0.749	0.118	13.9	157.2	0.0018	160.4	0.0292	0.0776	0.38	0.017	0.247	0.98	0.02	40.0	
45-A-6	161.0	172.3	0.751	0.122	14.4	157.7	0.0018	160.8	0.0287	0.0780	0.37	0.017	0.235	0.98	0.02	40.2	
45-A-1	161.0	172.3	0.752	0.122	10.0	108.7	0.0092	120.8	0.0586	0.1995	0.29	0.039	0.480	0.67	0.10	41.7	*
45-A-4	161.0	172.3	0.750	0.119	9.1	101.7	0.0088	112.8	0.0571	0.1955	0.29	0.036	0.480	0.63	0.10	38.5	
45-A-5	161.0	172.3	0.749	0.118	9.3	105.8	0.0089	117.6	0.0575	0.1960	0.29	0.038	0.487	0.66	0.10	40.2	*
50-A-1	161.0	171.3	0.750	0.129	14.5	149.7	0.0020	152.9	0.0323	0.0805	0.40	0.018	0.250	0.93	0.02	38.8	
50-A-2	161.0	171.3	0.757	0.128	14.5	150.1	0.0023	153.8	0.0350	0.0850	0.41	0.019	0.273	0.93	0.02	40.0	
50-A-3	161.0	171.3	0.751	0.130	14.7	151.0	0.0021	154.3	0.0342	0.0783	0.44	0.017	0.263	0.94	0.02	38.6	
50-A-4	161.0	171.3	0.746	0.118	8.3	93.7	0.0091	104.5	0.0582	0.1990	0.29	0.038	0.493	0.58	0.10	35.6	*
50-A-5	161.0	171.3	0.751	0.127	9.5	99.7	0.0092	110.3	0.0580	0.2017	0.29	0.039	0.457	0.62	0.10	38.2	
50-A-6	161.0	171.3	0.751	0.128	9.6	100.1	0.0104	112.2	0.0639	0.2068	0.31	0.040	0.499	0.62	0.11	39.3	*
50-B-1	163.0	173.0	0.749	0.127	14.7	155.1	0.0024	159.1	0.0355	0.0864	0.41	0.019	0.280	0.95	0.03	41.7	
50-B-2	163.0	173.0	0.750	0.132	14.7	149.0	0.0022	152.4	0.0363	0.0784	0.46	0.017	0.275	0.91	0.02	38.1	
50-B-3	163.0	173.0	0.750	0.123	14.7	159.3	0.0020	162.9	0.0316	0.0808	0.39	0.018	0.257	0.98	0.02	41.5	
50-B-4	163.0	173.0	0.749	0.130	10.1	103.7	0.0104	116.2	0.0613	0.2170	0.28	0.041	0.472	0.64	0.11	41.1	*
50-B-5	163.0	173.0	0.749	0.130	11.1	114.0	0.0096	126.5	0.0613	0.1999	0.31	0.040	0.472	0.70	0.10	44.2	
50-B-6	163.0	173.0	0.749	0.131	10.3	105.0	0.0096	116.3	0.0600	0.2031	0.30	0.039	0.458	0.64	0.10	40.6	

* INDICATES PLANE STRAIN FRACTURE TOUGHNESS VALUES (KSI-IN.1/2) OBTAINED FROM TESTS WHICH EXCEEDED ONE OR MORE OF THE FOLLOWING LIMITS. FG/FTY=1.0, AO/B=0.5, AND/OR CA/BW=0.1

PART-THROUGH-CRACK TENSILE DATA FOR MINUTEMAN 6AL-4V TITANIUM EXTRUDED CYLINDERS

FORGING SPECIMEN NUMBER	YIELD STRESS FTY (KSI)	ULT. STRESS FTU (KSI)	WIDTH W (IN.)	THICK-NESS B (IN.)	LOAD P-MAX (KIPS)	GROSS STRESS FG (KSI)	CRACK AREA CA (SQ.IN)	NET STRESS FN (KSI)	CRACK DEPTH AO (IN.)	CRACK LENGTH 2C (IN.)	CRACK SHAPE AO/2C	NORM. DEPTH AO/B	AO/B	FG/FTY	CA/BW	PLANE STRAIN KIC	
52-B-1	167.0	174.0	0.752	0.127	14.7	154.3	0.0015	156.7	0.0291	0.0640	0.45	0.014	0.229	0.92	0.02	35.7	
52-B-2	167.0	174.0	0.754	0.130	15.8	161.7	0.0018	164.8	0.0319	0.0737	0.43	0.016	0.245	0.97	0.02	40.3	
52-B-5	167.0	174.0	0.749	0.120	14.3	159.4	0.0017	162.5	0.0296	0.0735	0.40	0.016	0.247	0.95	0.02	39.5	
52-B-3	167.0	174.0	0.753	0.131	10.9	110.4	0.0092	121.7	0.0600	0.1950	0.31	0.038	0.458	0.66	0.07	42.2	
52-B-6	167.0	174.0	0.752	0.130	11.2	114.3	0.0093	126.3	0.0593	0.2006	0.30	0.039	0.456	0.68	0.10	44.1	
53-B-1	161.0	177.3	0.751	0.134	15.5	154.1	0.0018	156.9	0.0314	0.0735	0.43	0.016	0.234	0.96	0.02	38.3	
53-B-2	161.0	177.3	0.749	0.131	14.7	150.1	0.0018	152.9	0.0294	0.0780	0.38	0.017	0.224	0.93	0.02	38.1	
53-B-3	161.0	177.3	0.748	0.118	14.0	158.7	0.0015	161.6	0.0274	0.0719	0.38	0.016	0.232	0.99	0.02	39.0	
53-B-4	161.0	177.3	0.750	0.125	10.0	106.1	0.0096	118.3	0.0577	0.2123	0.27	0.040	0.462	0.66	0.10	41.4	
53-B-5	161.0	177.3	0.749	0.131	9.0	91.3	0.0097	101.3	0.0599	0.2064	0.29	0.039	0.457	0.57	0.10	35.3	
53-B-6	161.0	177.3	0.755	0.122	8.1	87.9	0.0100	98.6	0.0610	0.2083	0.29	0.040	0.500	0.55	0.11	34.1	*
54-A-1	163.0	173.7	0.751	0.125	15.0	159.5	0.0019	162.8	0.0307	0.0792	0.39	0.017	0.246	0.98	0.02	41.1	
54-A-2	163.0	173.7	0.751	0.129	15.0	155.3	0.0020	158.6	0.0339	0.0743	0.46	0.016	0.263	0.95	0.02	38.8	
54-A-3	163.0	173.7	0.748	0.120	14.2	158.5	0.0020	162.2	0.0312	0.0827	0.38	0.018	0.260	0.97	0.02	41.7	
54-A-4	163.0	173.7	0.754	0.121	9.1	100.2	0.0067	110.7	0.0570	0.1944	0.29	0.037	0.471	0.61	0.10	37.8	
54-A-5	163.0	173.7	0.752	0.124	9.6	102.5	0.0095	114.2	0.0604	0.2003	0.30	0.039	0.487	0.63	0.10	39.5	*
54-A-6	163.0	173.7	0.750	0.118	8.8	99.0	0.0103	112.0	0.0589	0.2219	0.27	0.041	0.499	0.61	0.12	39.1	*
54-B-1	165.0	176.7	0.748	0.124	14.2	153.2	0.0020	156.6	0.0323	0.0788	0.41	0.017	0.260	0.93	0.02	39.3	
54-B-2	165.0	176.7	0.751	0.122	13.5	147.8	0.0023	151.6	0.0342	0.0860	0.40	0.019	0.280	0.90	0.03	39.4	
54-B-3	165.0	176.7	0.750	0.127	14.5	152.5	0.0019	155.6	0.0314	0.0761	0.41	0.017	0.247	0.92	0.02	38.4	
54-B-4	165.0	176.7	0.750	0.122	9.9	108.3	0.0088	119.8	0.0566	0.1986	0.28	0.038	0.464	0.66	0.10	41.2	
54-B-5	165.0	176.7	0.750	0.126	9.0	95.8	0.0095	106.4	0.0594	0.2027	0.29	0.039	0.471	0.58	0.10	36.7	*
54-B-6	165.0	176.7	0.746	0.129	9.2	95.1	0.0097	105.7	0.0616	0.1995	0.31	0.039	0.478	0.58	0.10	36.5	*

* INDICATES PLANE STRAIN FRACTURE TOUGHNESS VALUES (KSI-IN.1/2) OBTAINED FROM TESTS WHICH EXCEEDED ONE OR MORE OF THE FOLLOWING LIMITS. FG/FTY=1.0, AO/B=0.5, AND/OR CA/BW=0.1

PART-THROUGH-CRACK TENSILE DATA FOR MINUTEMAN 6AL-4V TITANIUM EXTRUDED CYLINDERS

FORGING SPECIMEN NUMBER	YIELD STRESS FTY (KSI)	ULT. STRESS FTU (KSI)	WIDTH W (IN.)	THICK-NESS B (IN.)	LOAD P-MAX (KIPS)	GROSS STRESS FG (KSI)	CRACK AREA CA (SQ.IN)	NET STRESS FN (KSI)	CRACK DEPTH AO (IN.)	CRACK LENGTH 2C (IN.)	CRACK SHAPE AO/2C	NORM. DEPTH AO/B	AO/B	FG/FTY	CA/BW	PLANE STRAIN KIC	
55-A-2	159.0	172.7	0.749	0.131	14.9	152.1	0.0019	155.1	0.0320	0.0750	0.43	0.017	0.244	0.96	0.02	38.2	
55-A-3	159.0	172.7	0.750	0.119	13.9	155.9	0.0017	159.7	0.0272	0.0731	0.40	0.016	0.245	0.98	0.02	38.6	
55-A-1	159.0	172.7	0.749	0.130	10.1	104.0	0.0096	115.4	0.0615	0.1990	0.31	0.039	0.473	0.65	0.10	40.1	
55-A-4	159.0	172.7	0.751	0.117	9.8	111.3	0.0089	123.8	0.0566	0.2001	0.28	0.039	0.484	0.70	0.10	42.6	*
55-A-5	159.0	172.7	0.751	0.125	10.7	114.2	0.0093	126.7	0.0585	0.2014	0.29	0.039	0.468	0.72	0.10	44.2	
55-A-6	159.0	172.7	0.752	0.129	9.6	98.5	0.0094	109.3	0.0603	0.1982	0.30	0.039	0.467	0.62	0.10	37.7	
55-B-1	159.0	170.7	0.749	0.119	14.0	156.8	0.0019	160.3	0.0313	0.0791	0.40	0.018	0.263	0.99	0.02	40.5	
55-B-3	159.0	170.7	0.749	0.128	14.5	154.2	0.0020	159.4	0.0314	0.0791	0.40	0.017	0.245	0.97	0.02	39.7	
55-B-4	159.0	170.7	0.750	0.129	15.3	158.4	0.0020	163.6	0.0330	0.0772	0.43	0.017	0.256	1.00	0.02	40.5	
55-B-2	159.0	170.7	0.752	0.131	9.2	93.6	0.0095	103.7	0.0586	0.2067	0.28	0.039	0.447	0.59	0.10	36.1	
55-B-5	159.0	170.7	0.750	0.123	9.0	98.1	0.0094	109.2	0.0596	0.2005	0.30	0.039	0.485	0.62	0.10	37.6	*
55-B-6	159.0	170.7	0.750	0.122	8.9	96.8	0.0094	107.8	0.0590	0.2026	0.29	0.039	0.484	0.61	0.10	37.2	*
56-A-1	163.0	176.0	0.752	0.121	13.2	145.2	0.0018	148.2	0.0306	0.0763	0.40	0.017	0.253	0.89	0.02	36.4	
56-A-2	163.0	176.0	0.752	0.126	14.1	148.4	0.0018	151.3	0.0301	0.0778	0.39	0.017	0.239	0.91	0.02	37.4	
56-A-5	163.0	176.0	0.749	0.121	13.3	147.2	0.0020	150.6	0.0308	0.0828	0.37	0.018	0.255	0.90	0.02	38.4	
56-A-3	163.0	176.0	0.751	0.130	8.8	89.9	0.0097	99.7	0.0614	0.2013	0.31	0.039	0.472	0.55	0.10	34.5	
56-A-4	163.0	176.0	0.751	0.126	8.6	88.8	0.0097	98.9	0.0595	0.2070	0.29	0.039	0.472	0.54	0.10	34.2	*
56-A-6	163.0	176.0	0.752	0.122	9.6	104.9	0.0093	116.8	0.0581	0.2043	0.28	0.039	0.476	0.64	0.10	40.4	*
56-B-1	165.0	176.0	0.752	0.123	14.1	152.9	0.0018	154.6	0.0283	0.0716	0.40	0.016	0.230	0.92	0.02	36.9	
56-B-5	165.0	176.0	0.756	0.120	14.4	159.0	0.0017	162.0	0.0296	0.0715	0.41	0.017	0.247	0.96	0.02	39.0	
56-B-6	165.0	176.0	0.749	0.121	14.3	157.8	0.0018	160.9	0.0295	0.0764	0.39	0.017	0.244	0.96	0.02	39.8	
56-B-2	165.0	176.0	0.750	0.126	9.0	94.7	0.0098	105.7	0.0609	0.2052	0.30	0.039	0.483	0.57	0.10	36.6	*
56-B-3	165.0	176.0	0.752	0.123	7.3	78.7	0.0098	88.0	0.0600	0.2073	0.29	0.039	0.486	0.48	0.11	30.2	*
56-B-4	165.0	176.0	0.749	0.121	7.7	84.5	0.0093	94.2	0.0575	0.2067	0.28	0.038	0.475	0.51	0.10	32.3	*

* INDICATES PLANE STRAIN FRACTURE TOUGHNESS VALUES (KSI-IN.1/2) OBTAINED FROM TESTS WHICH EXCEEDED ONE OR MORE OF THE FOLLOWING LIMITS. FG/FTY=1.0, AO/B=0.5, AND/OR CA/BW=0.1

PART-THROUGH-CRACK TENSILE DATA FOR MINUTEMAN 6AL-4V TITANIUM EXTRUDED CYLINDERS

FORGING SPECIMEN NUMBER	YIELD STRESS FTY (KSI)	ULT. STRESS FTU (KSI)	WIDTH W (IN.)	THICK -NESS B (IN.)	LOAD P-MAX (KIPS)	GROSS STRESS FG (KSI)	CRACK AREA CA (SQ.IN)	NET STRESS FN (KSI)	CRACK DEPTH AO (IN.)	CRACK LENGTH 2C (IN.)	CRACK SHAPE AO/2C	NORM. DEPTH AO/B	AO/B	FG/FTY	CA/BW	PLANE STRAIN KIC	
57-A-1	158.0	169.0	0.751	0.124	13.6	146.5	0.0019	149.5	0.0316	0.0756	0.42	0.017	0.255	0.93	0.02	36.8	
57-A-2	158.0	169.0	0.752	0.126	15.1	159.3	0.0014	161.7	0.0277	0.0656	0.42	0.015	0.220	1.01	0.02	37.6	*
57-A-3	158.0	169.0	0.751	0.117	13.2	150.4	0.0015	153.1	0.0283	0.0690	0.41	0.015	0.242	0.95	0.02	36.2	
57-A-4	158.0	169.0	0.750	0.125	9.4	99.9	0.0101	112.0	0.0603	0.2127	0.28	0.041	0.482	0.63	0.11	39.2	*
57-A-5	158.0	169.0	0.750	0.127	9.0	94.0	0.0090	103.8	0.0571	0.2004	0.28	0.038	0.450	0.59	0.09	35.7	
57-A-6	158.0	169.0	0.752	0.128	10.7	111.0	0.0091	122.6	0.0570	0.2043	0.28	0.039	0.445	0.70	0.10	42.8	
57-B-1	160.0	170.3	0.749	0.129	14.6	150.8	0.0020	154.0	0.0331	0.0768	0.43	0.017	0.257	0.94	0.02	38.2	
57-B-2	160.0	170.3	0.749	0.128	15.4	160.6	0.0020	164.0	0.0324	0.0781	0.41	0.017	0.253	1.00	0.02	41.3	*
57-B-3	160.0	170.3	0.750	0.127	14.7	154.6	0.0020	158.0	0.0312	0.0836	0.37	0.018	0.246	0.97	0.02	40.8	
57-B-4	160.0	170.3	0.748	0.120	8.7	97.5	0.0087	107.9	0.0573	0.1933	0.30	0.037	0.478	0.61	0.10	36.7	
57-B-5	160.0	170.3	0.751	0.119	10.0	112.2	0.0079	123.0	0.0528	0.1902	0.28	0.036	0.444	0.70	0.09	41.7	
57-B-6	160.0	170.3	0.749	0.120	9.8	109.0	0.0087	120.7	0.0585	0.1887	0.31	0.037	0.487	0.68	0.10	41.1	
58-B-1	166.0	178.0	0.750	0.127	14.9	156.0	0.0018	159.0	0.0295	0.0763	0.39	0.017	0.232	0.94	0.02	39.3	
58-B-3	166.0	178.0	0.747	0.120	14.2	158.4	0.0016	161.3	0.0265	0.0759	0.35	0.016	0.221	0.95	0.02	39.6	
58-B-5	166.0	178.0	0.753	0.131	15.5	157.4	0.0022	161.3	0.0341	0.0830	0.41	0.018	0.260	0.95	0.02	41.6	
58-B-2	166.0	178.0	0.745	0.121	10.0	110.7	0.0080	121.5	0.0515	0.1974	0.26	0.037	0.426	0.67	0.09	41.3	
58-B-4	166.0	178.0	0.751	0.125	9.2	97.7	0.0094	108.6	0.0580	0.2065	0.28	0.039	0.464	0.59	0.10	37.6	*
58-B-6	166.0	178.0	0.751	0.124	8.7	94.0	0.0096	104.8	0.0584	0.2103	0.28	0.039	0.471	0.57	0.10	36.3	*
59-A-1	166.0	178.0	0.750	0.127	14.3	150.1	0.0016	152.7	0.0277	0.0746	0.37	0.016	0.218	0.90	0.02	37.1	
59-A-2	166.0	178.0	0.752	0.130	14.7	150.4	0.0018	153.2	0.0308	0.0752	0.41	0.016	0.237	0.91	0.02	37.5	
59-A-3	166.0	178.0	0.752	0.126	13.3	140.9	0.0021	144.1	0.0325	0.0821	0.40	0.018	0.258	0.85	0.02	36.5	
59-A-4	166.0	178.0	0.752	0.130	9.0	91.6	0.0101	102.1	0.0617	0.2076	0.30	0.040	0.475	0.55	0.10	35.6	*
59-A-5	166.0	178.0	0.752	0.128	7.9	82.1	0.0094	91.0	0.0593	0.2029	0.29	0.038	0.463	0.49	0.10	31.3	
59-A-6	166.0	178.0	0.749	0.122	8.5	93.0	0.0089	103.1	0.0576	0.1973	0.29	0.038	0.472	0.56	0.10	35.1	

* INDICATES PLANE STRAIN FRACTURE TOUGHNESS VALUES (KSI-IN.1/2) OBTAINED FROM TESTS WHICH EXCEEDED ONE OR MORE OF THE FOLLOWING LIMITS. FG/FTY=1.0, AO/B=0.5, AND/OR CA/BW=0.1

PART-THROUGH-CRACK TENSILE DATA FOR MINUTEMAN 6AL-4V TITANIUM EXTRUDED CYLINDERS

FORGING SPECIMEN NUMBER	YIELD STRESS FTY (KSI)	ULT. STRESS FTU (KSI)	WIDTH W (IN.)	THICK-NESS B (IN.)	LOAD P-MAX (KIPS)	GROSS STRESS FG (KSI)	CRACK AREA CA (SQ.IN)	NET STRESS FN (KSI)	CRACK DEPTH AO (IN.)	CRACK LENGTH 2C (IN.)	CRACK SHAPE AO/2C	NORM. DEPTH AO/Q	AO/B	FG/FTY	CA/BW	PLANE STRAIN KIC	
60-B-1	166.0	173.7	0.750	0.121	13.5	148.8	0.0017	151.7	0.0310	0.0715	0.43	0.016	0.256	0.90	0.02	36.2	
60-B-2	166.0	173.7	0.748	0.118	12.9	146.2	0.0019	149.3	0.0307	0.0773	0.40	0.017	0.260	0.88	0.02	36.9	
60-B-3	166.0	173.7	0.743	0.123	14.7	161.4	0.0018	164.7	0.0287	0.0816	0.35	0.018	0.233	0.97	0.02	41.9	
60-B-4	166.0	173.7	0.749	0.118	8.2	92.2	0.0084	101.8	0.0549	0.1938	0.28	0.036	0.465	0.56	0.09	34.3	
60-B-5	166.0	173.7	0.749	0.123	8.1	87.7	0.0095	97.8	0.0579	0.2096	0.28	0.039	0.471	0.53	0.10	33.7	*
60-B-6	166.0	173.7	0.745	0.118	7.7	87.6	0.0088	97.4	0.0562	0.2005	0.28	0.037	0.476	0.53	0.10	33.0	*
61-A-1	164.0	175.3	0.751	0.122	13.8	150.5	0.0021	154.0	0.0321	0.0840	0.38	0.018	0.263	0.92	0.02	39.6	
61-A-2	164.0	175.3	0.750	0.119	13.7	153.5	0.0018	156.7	0.0318	0.0740	0.43	0.016	0.267	0.94	0.02	38.2	
61-A-5	164.0	175.3	0.751	0.130	15.5	158.6	0.0019	161.7	0.0316	0.0772	0.41	0.017	0.243	0.97	0.02	40.4	
61-A-3	164.0	175.3	0.751	0.130	10.0	101.9	0.0104	114.0	0.0643	0.2055	0.31	0.040	0.495	0.62	0.11	39.9	*
61-A-4	164.0	175.3	0.749	0.121	10.3	114.2	0.0096	127.7	0.0601	0.2036	0.30	0.040	0.497	0.70	0.11	44.4	*
61-A-6	164.0	175.3	0.746	0.117	8.3	95.4	0.0092	106.6	0.0571	0.2055	0.28	0.039	0.488	0.58	0.11	36.5	*
61-B-1	161.0	172.7	0.750	0.130	15.4	158.2	0.0019	161.3	0.0310	0.0788	0.39	0.017	0.238	0.98	0.02	40.7	
61-B-2	161.0	172.7	0.750	0.123	14.5	157.2	0.0017	160.2	0.0299	0.0743	0.40	0.016	0.243	0.98	0.02	39.3	
61-B-3	161.0	172.7	0.748	0.124	14.6	157.6	0.0019	160.8	0.0309	0.0768	0.40	0.017	0.249	0.98	0.02	40.1	
61-B-4	161.0	172.7	0.752	0.129	9.4	96.8	0.0095	107.4	0.0599	0.2027	0.30	0.039	0.464	0.60	0.10	37.3	
61-B-5	161.0	172.7	0.748	0.118	8.5	96.4	0.0083	106.4	0.0547	0.1921	0.28	0.036	0.464	0.60	0.09	35.9	
61-B-6	161.0	172.7	0.751	0.127	8.5	89.6	0.0098	99.9	0.0607	0.2060	0.29	0.039	0.478	0.56	0.10	34.6	*
62-A-1	168.0	175.7	0.753	0.133	15.6	159.4	0.0016	162.0	0.0287	0.0707	0.41	0.016	0.221	0.95	0.02	38.7	
62-A-2	168.0	175.7	0.752	0.131	15.1	153.4	0.0016	156.0	0.0309	0.0674	0.46	0.015	0.236	0.91	0.02	36.3	
62-A-4	168.0	175.7	0.751	0.121	14.1	154.9	0.0016	157.6	0.0276	0.0732	0.38	0.016	0.228	0.92	0.02	38.1	
62-A-3	168.0	175.7	0.752	0.128	8.8	91.7	0.0092	101.4	0.0598	0.1959	0.31	0.038	0.467	0.55	0.10	34.7	
62-A-5	168.0	175.7	0.751	0.128	9.0	93.1	0.0098	103.6	0.0610	0.2041	0.30	0.039	0.477	0.55	0.10	35.9	*
62-A-6	168.0	175.7	0.749	0.120	10.1	112.3	0.0092	125.0	0.0569	0.2051	0.28	0.039	0.474	0.67	0.10	43.2	*

* INDICATES PLANE STRAIN FRACTURE TOUGHNESS VALUES (KSI-IN.1/2) OBTAINED FROM TESTS WHICH EXCEEDED ONE OR MORE OF THE FOLLOWING LIMITS. FG/FTY=1.0, AO/B=0.5, AND/OR CA/BW=0.1

PART-THROUGH-CRACK TENSILE DATA FOR MINUTEMAN 6AL-4V TITANIUM EXTRUDED CYLINDERS

FORGING SPECIMEN NUMBER	YIELD STRESS FTY (KSI)	ULT. STRESS FTU (KSI)	WIDTH W (IN.)	THICK-NESS B (IN.)	LOAD P-MAX (KIPS)	GROSS STRESS FG (KSI)	CRACK AREA CA (SQ.IN)	NET STRESS FN (KSI)	CRACK DEPTH AO (IN.)	CRACK LENGTH 2C (IN.)	CRACK SHAPE AO/2C	NORM. DEPTH AO/B	AO/B	FG/FTY	CA/BW	PLANE STRAIN KIC	
62-B-2	164.0	171.0	0.751	0.130	14.4	147.2	0.0016	149.8	0.0286	0.0734	0.39	0.016	0.220	0.90	0.02	36.2	
62-B-3	164.0	171.0	0.750	0.130	14.7	151.2	0.0016	153.8	0.0287	0.0731	0.39	0.016	0.221	0.92	0.02	37.2	
62-B-4	164.0	171.0	0.751	0.125	14.5	154.5	0.0018	157.6	0.0320	0.0735	0.44	0.016	0.256	0.94	0.02	38.3	
62-B-1	164.0	171.0	0.748	0.126	8.4	88.9	0.0083	97.4	0.0541	0.1945	0.28	0.036	0.429	0.54	0.09	33.0	
62-B-5	164.0	171.0	0.756	0.126	9.7	101.5	0.0091	112.3	0.0592	0.1963	0.30	0.038	0.470	0.62	0.10	38.6	
62-B-6	164.0	171.0	0.750	0.125	10.0	106.7	0.0092	118.4	0.0592	0.1985	0.30	0.039	0.474	0.65	0.10	40.9	
L63A-2	166.0	172.3	0.765	0.125	14.8	155.0	0.0019	158.1	0.0300	0.0800	0.37	0.017	0.240	0.93	0.02	39.9	
L63A-5	166.0	172.3	0.765	0.123	14.5	153.7	0.0020	156.9	0.0300	0.0830	0.36	0.018	0.243	0.93	0.02	40.1	
L63A-6	166.0	172.3	0.764	0.125	14.6	153.0	0.0019	156.1	0.0306	0.0786	0.39	0.017	0.245	0.92	0.02	39.0	
L63A-1	166.0	172.3	0.765	0.125	8.7	90.8	0.0091	100.4	0.0588	0.1980	0.30	0.038	0.472	0.55	0.10	34.4	
L63A-3	166.0	172.3	0.766	0.124	8.9	93.7	0.0090	103.5	0.0576	0.1980	0.29	0.038	0.465	0.56	0.09	35.4	
L63A-4	166.0	172.3	0.765	0.126	8.9	92.4	0.0091	102.2	0.0588	0.1980	0.30	0.038	0.469	0.56	0.10	35.1	
S63A-1	166.0	172.3	0.751	0.128	14.1	146.4	0.0022	149.8	0.0343	0.0814	0.42	0.018	0.268	0.88	0.02	38.0	
S63A-2	166.0	172.3	0.750	0.125	13.0	138.1	0.0029	142.5	0.0368	0.0987	0.37	0.021	0.294	0.83	0.03	39.0	
S63A-3	166.0	172.3	0.751	0.127	13.4	140.2	0.0023	143.8	0.0364	0.0817	0.45	0.018	0.287	0.84	0.02	36.4	
S63A-4	166.0	172.3	0.749	0.124	6.7	72.7	0.0120	83.5	0.0662	0.2308	0.29	0.043	0.534	0.44	0.13	29.3	*
S63A-5	166.0	172.3	0.751	0.126	8.7	92.5	0.0099	103.2	0.0622	0.2017	0.31	0.039	0.494	0.56	0.10	35.6	*
S63A-6	166.0	172.3	0.748	0.125	8.4	89.8	0.0111	101.9	0.0645	0.2190	0.29	0.042	0.516	0.54	0.12	35.8	*
L63B-1	161.0	171.3	0.762	0.127	13.8	142.2	0.0023	145.6	0.0348	0.0840	0.41	0.018	0.274	0.88	0.02	37.5	
L63B-4	161.0	171.3	0.762	0.122	14.7	157.9	0.0022	161.7	0.0330	0.0830	0.40	0.018	0.270	0.98	0.02	41.7	
L63B-5	161.0	171.3	0.761	0.122	13.7	147.6	0.0020	150.7	0.0300	0.0830	0.36	0.016	0.246	0.92	0.02	38.5	
L63B-2	161.0	171.3	0.762	0.121	8.2	88.9	0.0094	99.1	0.0588	0.2040	0.29	0.039	0.486	0.55	0.10	34.1	*
L63B-3	161.0	171.3	0.762	0.120	8.2	89.3	0.0096	99.8	0.0600	0.2040	0.29	0.039	0.500	0.55	0.11	34.3	*

* INDICATES PLANE STRAIN FRACTURE TOUGHNESS VALUES (KSI-IN.1/2) OBTAINED FROM TESTS WHICH EXCEEDED ONE OR MORE OF THE FOLLOWING LIMITS. FG/FTY=1.0, AO/B=0.5, AND/OR CA/BW=0.1

PART-THROUGH-CRACK TENSILE DATA FOR MINUTEMAN 6AL-4V TITANIUM EXTRUDED CYLINDERS

FORGING SPECIMEN NUMBER	YIELD STRESS FTY (KSI)	ULT. STRESS FTU (KSI)	WIDTH W (IN.)	THICK-NESS B (IN.)	LOAD P-MAX (KIPS)	GROSS STRESS FG (KSI)	CRACK AREA CA (SQ.IN)	NET STRESS FN (KSI)	CRACK DEPTH AO (IN.)	CRACK LENGTH 2C (IN.)	CRACK SHAPE AO/2C	NORM. DEPTH AO/B	AO/B	FG/FTY	CA/BW	PLANE STRAIN KIC	
S63B-1	161.0	171.3	0.752	0.125	13.2	140.4	0.0026	144.4	0.0380	0.0875	0.43	0.019	0.304	0.87	0.03	37.8	
S63B-2	161.0	171.3	0.749	0.125	12.3	131.6	0.0031	136.2	0.0421	0.0948	0.44	0.020	0.337	0.82	0.03	36.7	
S63B-3	161.0	171.3	0.748	0.126	13.1	138.7	0.0028	143.0	0.0370	0.0965	0.38	0.021	0.294	0.86	0.03	38.9	
S63B-4	161.0	171.3	0.752	0.127	7.6	80.1	0.0107	90.2	0.0648	0.2101	0.31	0.040	0.510	0.50	0.11	31.4	*
S63B-5	161.0	171.3	0.750	0.125	7.7	81.7	0.0105	92.1	0.0627	0.2142	0.29	0.040	0.502	0.51	0.11	32.0	*
S63B-6	161.0	171.3	0.752	0.126	8.6	90.8	0.0098	101.3	0.0618	0.2029	0.30	0.039	0.490	0.56	0.10	35.0	*
S65A-1	163.0	172.7	0.747	0.123	12.6	137.1	0.0026	141.1	0.0362	0.0913	0.40	0.020	0.294	0.84	0.03	37.4	
S65A-2	163.0	172.7	0.750	0.126	13.6	143.9	0.0028	148.3	0.0370	0.0956	0.39	0.021	0.294	0.88	0.03	40.3	
S65A-3	163.0	172.7	0.749	0.126	13.4	141.7	0.0030	146.3	0.0376	0.1000	0.38	0.021	0.298	0.87	0.03	40.5	
S65A-4	163.0	172.7	0.749	0.126	9.7	103.3	0.0094	114.8	0.0584	0.2051	0.28	0.039	0.463	0.63	0.10	39.8	
S65A-5	163.0	172.7	0.749	0.124	10.0	107.9	0.0096	120.7	0.0604	0.2074	0.29	0.040	0.487	0.66	0.11	42.1	*
S65A-6	163.0	172.7	0.753	0.126	8.7	92.2	0.0107	103.9	0.0623	0.2182	0.29	0.041	0.494	0.57	0.11	36.5	*
L66B-1	168.0	177.0	0.762	0.125	14.8	156.5	0.0019	159.8	0.0316	0.0780	0.41	0.017	0.254	0.93	0.02	39.9	
L66B-5	168.0	177.0	0.753	0.125	14.2	151.6	0.0019	154.7	0.0306	0.0794	0.39	0.017	0.246	0.90	0.02	38.8	
L66B-6	168.0	177.0	0.764	0.125	14.7	153.7	0.0020	156.9	0.0312	0.0798	0.39	0.017	0.250	0.91	0.02	39.5	
L66B-2	168.0	177.0	0.763	0.124	9.0	94.7	0.0089	104.5	0.0557	0.2025	0.28	0.038	0.449	0.56	0.09	35.8	
L66B-3	168.0	177.0	0.762	0.124	8.4	88.5	0.0087	97.5	0.0541	0.2056	0.26	0.037	0.436	0.53	0.09	33.5	
L66B-4	168.0	177.0	0.751	0.125	8.0	85.3	0.0094	94.9	0.0578	0.2078	0.28	0.039	0.462	0.51	0.10	32.6	*
S66B-1	168.0	177.0	0.750	0.124	11.2	120.7	0.0032	125.0	0.0397	0.1015	0.39	0.021	0.320	0.72	0.03	34.3	
S66B-2	168.0	177.0	0.750	0.125	10.7	113.9	0.0033	118.1	0.0412	0.1035	0.40	0.022	0.330	0.68	0.04	32.6	
S66B-3	168.0	177.0	0.749	0.127	11.5	120.9	0.0030	124.8	0.0395	0.0958	0.41	0.020	0.311	0.72	0.03	33.5	
S66B-4	168.0	177.0	0.749	0.124	6.6	70.8	0.0130	82.3	0.0666	0.2484	0.27	0.045	0.537	0.42	0.14	29.2	*
S66B-5	168.0	177.0	0.757	0.125	6.8	71.6	0.0126	82.5	0.0684	0.2352	0.29	0.044	0.543	0.43	0.13	29.2	*
S66B-6	168.0	177.0	0.750	0.125	7.0	74.9	0.0108	84.6	0.0629	0.2178	0.29	0.041	0.503	0.45	0.11	29.4	*

* INDICATES PLANE STRAIN FRACTURE TOUGHNESS VALUES (KSI-IN.1/2) OBTAINED FROM TESTS WHICH EXCEEDED ONE OR MORE OF THE FOLLOWING LIMITS. FG/FTY=1.0, AO/B=0.5, AND/OR CA/BW=0.1

PART-THROUGH-CRACK TENSILE DATA FOR MINUTEMAN 6AL-4V TITANIUM EXTRUDED CYLINDERS

FORGING SPECIMEN NUMBER	YIELD STRESS FTY (KSI)	ULT. STRESS FTU (KSI)	WIDTH W (IN.)	THICK -NESS B (IN.)	LOAD P-MAX (KIPS)	GROSS STRESS FG (KSI)	CRACK AREA CA (SQ.IN)	NET STRESS FN (KSI)	CRACK DEPTH AO (IN.)	CRACK LENGTH 2C (IN.)	CRACK SHAPE AO/2C	NORM. DEPTH AO/B	AO/B	FG/FTY	CA/BW	PLANE STRAIN KIC
L69A-1	163.0	174.7	0.763	0.125	14.6	153.5	0.0019	156.7	0.0310	0.0792	0.39	0.017	0.249	0.94	0.02	39.4
L69A-2	163.0	174.7	0.764	0.125	14.1	147.7	0.0022	151.2	0.0334	0.0840	0.40	0.018	0.267	0.91	0.02	38.9
L69A-6	163.0	174.7	0.764	0.123	14.4	153.0	0.0019	156.2	0.0310	0.0792	0.39	0.017	0.251	0.94	0.02	39.3
L69A-3	163.0	174.7	0.764	0.122	8.5	90.7	0.0097	101.3	0.0583	0.2120	0.27	0.039	0.478	0.56	0.10	35.1 *
L69A-4	163.0	174.7	0.764	0.126	9.1	94.9	0.0101	106.1	0.0610	0.2109	0.29	0.040	0.484	0.58	0.10	37.1 *
L69A-5	163.0	174.7	0.763	0.125	8.6	89.8	0.0093	99.4	0.0572	0.2067	0.28	0.038	0.458	0.55	0.10	34.3
S69A-1	163.0	174.7	0.750	0.123	12.7	137.7	0.0029	142.2	0.0392	0.0951	0.41	0.021	0.319	0.84	0.03	38.4
S69A-2	163.0	174.7	0.751	0.126	13.1	138.4	0.0028	142.7	0.0376	0.0956	0.39	0.021	0.298	0.85	0.03	38.7
S69A-3	163.0	174.7	0.750	0.125	12.0	128.5	0.0036	133.7	0.0458	0.1003	0.46	0.022	0.366	0.79	0.04	36.8
S69A-4	163.0	174.7	0.751	0.126	9.3	98.0	0.0094	108.8	0.0569	0.2093	0.27	0.039	0.452	0.60	0.10	37.7
S69A-5	163.0	174.7	0.749	0.125	8.7	92.4	0.0116	105.5	0.0712	0.2082	0.34	0.042	0.570	0.57	0.12	36.7 *
S69A-6	163.0	174.7	0.747	0.127	9.5	100.1	0.0095	111.2	0.0566	0.2126	0.27	0.039	0.446	0.61	0.10	38.7
D69B-1	162.7	175.3	0.995	0.133	18.4	150.8	0.0020	153.3	0.0320	0.0790	0.41	0.017	0.261	0.93	0.02	38.7
D69B-3	162.7	175.3	0.997	0.131	19.1	146.5	0.0023	149.2	0.0370	0.0800	0.46	0.017	0.283	0.90	0.02	37.8
D69B-5	162.7	175.3	0.996	0.125	17.4	139.5	0.0022	142.0	0.0340	0.0820	0.41	0.018	0.272	0.86	0.02	36.2
D69B-2	162.7	175.3	0.996	0.125	10.8	86.9	0.0100	94.6	0.0610	0.2090	0.29	0.040	0.489	0.53	0.08	33.7
D69B-4	162.7	175.3	0.997	0.124	11.1	90.0	0.0102	98.1	0.0620	0.2090	0.30	0.040	0.499	0.55	0.08	35.1
D69B-6	162.7	175.3	0.995	0.127	11.7	92.2	0.0102	100.2	0.0610	0.2130	0.29	0.040	0.478	0.57	0.08	36.1
S69B-1	163.0	175.3	0.750	0.125	12.5	133.6	0.0025	137.2	0.0342	0.0921	0.37	0.020	0.274	0.82	0.03	36.4
S69B-2	163.0	175.3	0.749	0.126	12.5	132.5	0.0029	136.7	0.0379	0.0976	0.39	0.021	0.301	0.81	0.03	37.2
S69B-3	163.0	175.3	0.749	0.126	13.9	147.0	0.0027	151.4	0.0345	0.0999	0.35	0.021	0.274	0.90	0.03	41.8
S69B-4	163.0	175.3	0.749	0.124	8.0	86.1	0.0110	97.7	0.0622	0.2248	0.28	0.042	0.502	0.53	0.12	34.3 *
S69B-5	163.0	175.3	0.750	0.125	8.3	88.3	0.0104	99.3	0.0607	0.2183	0.28	0.041	0.486	0.54	0.11	34.7 *
S69B-6	163.0	175.3	0.719	0.125	6.2	69.5	0.0162	84.8	0.0708	0.2912	0.24	0.050	0.566	0.43	0.18	30.4 *

* INDICATES PLANE STRAIN FRACTURE TOUGHNESS VALUES (KSI-IN.1/2) OBTAINED FROM TESTS WHICH EXCEEDED ONE OR MORE OF THE FOLLOWING LIMITS. FG/FTY=1.0, AO/B=0.5, AND/OR CA/BW=0.1

PART-THROUGH-CRACK TENSILE DATA FOR MINUTEMAN 6AL-4V TITANIUM EXTRUDED CYLINDERS

FORGING SPECIMEN NUMBER	YIELD STRESS FTY (KSI)	ULT. STRESS FTU (KSI)	WIDTH W (IN.)	THICK-NESS B (IN.)	LOAD P-MAX (KIPS)	GROSS STRESS FG (KSI)	CRACK AREA CA (SQ.IN)	NET STRESS FN (KSI)	CRACK DEPTH AO (IN.)	CRACK LENGTH 2C (IN.)	CRACK SHAPE AO/2C	NORM. DEPTH AO/B	AO/B	FG/FTY	CA/BW	PLANE STRAIN KIC
D70A-1	159.0	172.0	0.997	0.126	19.9	158.6	0.0022	161.3	0.0320	0.0860	0.37	0.019	0.254	1.00	0.02	42.6
D70A-3	159.0	172.0	0.996	0.128	21.0	165.4	0.0019	168.0	0.0310	0.0800	0.39	0.018	0.243	1.04	0.02	43.2 *
D70A-5	159.0	172.0	0.997	0.125	19.7	157.4	0.0022	160.2	0.0340	0.0810	0.42	0.018	0.271	0.99	0.02	41.2
D70A-2	159.0	172.0	0.996	0.124	11.2	90.6	0.0106	99.0	0.0620	0.2170	0.29	0.041	0.500	0.57	0.09	35.8 *
D70A-4	159.0	172.0	0.995	0.123	11.3	91.9	0.0100	100.1	0.0600	0.2120	0.28	0.040	0.488	0.58	0.08	35.8
D70A-6	159.0	172.0	0.994	0.124	11.5	93.3	0.0097	101.2	0.0600	0.2050	0.29	0.039	0.484	0.59	0.08	36.0
S70A-1	159.0	172.0	0.750	0.124	12.4	133.1	0.0025	136.8	0.0350	0.0925	0.38	0.020	0.282	0.84	0.03	36.4
S70A-2	159.0	172.0	0.748	0.124	12.6	135.8	0.0027	139.9	0.0355	0.0958	0.37	0.020	0.286	0.85	0.03	37.9
S70A-3	159.0	172.0	0.750	0.125	13.5	143.7	0.0023	147.4	0.0341	0.0875	0.39	0.019	0.273	0.90	0.02	38.6
S70A-4	159.0	172.0	0.752	0.122	7.3	79.6	0.0095	88.8	0.0570	0.2131	0.27	0.039	0.467	0.50	0.10	30.6 *
S70A-5	159.0	172.0	0.749	0.123	8.1	87.9	0.0103	98.9	0.0608	0.2150	0.28	0.040	0.494	0.55	0.11	34.4 *
S70A-6	159.0	172.0	0.752	0.126	8.1	85.5	0.0103	95.9	0.0600	0.2178	0.28	0.040	0.476	0.54	0.11	33.5 *
D70B-1	163.3	172.7	0.994	0.125	19.3	155.2	0.0021	157.9	0.0320	0.0820	0.39	0.018	0.256	0.95	0.02	40.6
D70B-3	163.3	172.7	0.995	0.124	18.0	145.9	0.0022	148.6	0.0350	0.0810	0.43	0.018	0.282	0.89	0.02	37.8
D70B-5	163.3	172.7	0.996	0.122	18.2	150.6	0.0021	153.3	0.0330	0.0820	0.40	0.018	0.271	0.92	0.02	39.3
D70B-2	163.3	172.7	0.995	0.125	12.5	100.8	0.0089	108.6	0.0560	0.2030	0.28	0.038	0.448	0.62	0.07	38.4
D70B-4	163.3	172.7	0.995	0.124	11.7	95.0	0.0092	102.6	0.0570	0.2050	0.28	0.038	0.461	0.58	0.07	36.3
D70B-6	163.3	172.7	0.995	0.124	12.1	98.4	0.0105	107.6	0.0610	0.2200	0.28	0.041	0.492	0.60	0.09	39.0
S70B-1	164.0	172.7	0.749	0.124	12.7	136.7	0.0022	140.1	0.0343	0.0833	0.41	0.018	0.277	0.83	0.02	35.7
S70B-2	164.0	172.7	0.751	0.126	13.6	143.7	0.0023	147.4	0.0308	0.0965	0.32	0.020	0.244	0.88	0.02	39.7
S70B-3	164.0	172.7	0.751	0.124	13.1	140.9	0.0024	144.7	0.0354	0.0867	0.41	0.019	0.285	0.86	0.03	37.6
S70B-4	164.0	172.7	0.749	0.126	9.1	96.2	0.0102	107.9	0.0611	0.2135	0.29	0.040	0.485	0.59	0.11	37.7 *
S70B-5	164.0	172.7	0.749	0.126	8.2	86.4	0.0111	97.8	0.0604	0.2335	0.26	0.042	0.479	0.53	0.12	34.5 *
S70B-6	164.0	172.7	0.749	0.126	7.8	82.6	0.0116	94.3	0.0642	0.2307	0.28	0.043	0.510	0.50	0.12	33.3 *

* INDICATES PLANE STRAIN FRACTURE TOUGHNESS VALUES (KSI-IN.1/2) OBTAINED FROM TESTS WHICH EXCEEDED ONE OR MORE OF THE FOLLOWING LIMITS. FG/FTY=1.0, AO/B=0.5, AND/OR CA/BW=0.1

PART-THROUGH-CRACK TENSILE DATA FOR MINUTEMAN 6AL-4V TITANIUM EXTRUDED CYLINDERS

FORGING SPECIMEN NUMBER	YIELD STRESS FTY (KSI)	ULT. STRESS FTU (KSI)	WIDTH W (IN.)	THICK-NESS B (IN.)	LOAD P-MAX (KIPS)	GROSS STRESS FG (KSI)	CRACK AREA CA (SQ.IN)	NET STRESS FN (KSI)	CRACK DEPTH AO (IN.)	CRACK LENGTH 2C (IN.)	CRACK SHAPE AO/2C	NORM. DEPTH AO/B	AO/B	FG/FTY	CA/BW	PLANE STRAIN KIC
D71A-1	162.3	175.3	0.995	0.126	20.0	159.6	0.0019	162.0	0.0310	0.0780	0.40	0.017	0.246	0.98	0.02	40.9
D71A-4	162.3	175.3	0.995	0.127	19.7	155.5	0.0022	158.2	0.0340	0.0810	0.42	0.018	0.267	0.96	0.02	40.5
D71A-5	162.3	175.3	0.996	0.126	20.1	160.4	0.0017	162.6	0.0300	0.0720	0.42	0.016	0.238	0.99	0.01	39.6
D71A-2	162.3	175.3	0.995	0.126	11.9	94.8	0.0096	102.7	0.0600	0.2040	0.29	0.039	0.475	0.58	0.08	36.5
D71A-3	162.3	175.3	0.995	0.128	12.6	99.1	0.0102	107.8	0.0640	0.2030	0.32	0.040	0.501	0.61	0.08	38.6 *
D71A-6	162.3	175.3	0.995	0.127	12.5	99.3	0.0101	108.0	0.0620	0.2080	0.30	0.040	0.489	0.61	0.08	38.8
S71A-2	162.0	175.3	0.750	0.126	14.8	156.6	0.0017	159.5	0.0307	0.0708	0.43	0.016	0.244	0.97	0.02	38.2
S71A-4	162.0	175.3	0.748	0.124	14.0	150.4	0.0023	154.2	0.0357	0.0820	0.44	0.018	0.288	0.93	0.02	39.4
S71A-5	162.0	175.3	0.750	0.126	14.0	148.1	0.0022	151.7	0.0335	0.0831	0.40	0.018	0.266	0.91	0.02	38.9
S71A-1	162.0	175.3	0.749	0.124	10.0	107.1	0.0085	118.0	0.0566	0.1923	0.29	0.037	0.456	0.66	0.09	40.3
S71A-3	162.0	175.3	0.750	0.123	10.3	111.7	0.0079	122.1	0.0543	0.1847	0.29	0.036	0.441	0.69	0.09	41.3
S71A-6	162.0	175.3	0.749	0.122	9.6	105.1	0.0086	115.9	0.0571	0.1913	0.30	0.037	0.468	0.65	0.09	39.5
73-A-1	158.7	173.7	0.996	0.126	19.2	152.7	0.0023	155.6	0.0340	0.0880	0.39	0.019	0.270	0.96	0.02	41.4
73-A-3	158.7	173.7	0.995	0.125	19.5	157.0	0.0021	159.8	0.0330	0.0820	0.40	0.018	0.265	0.99	0.02	41.3
73-A-5	158.7	173.7	0.996	0.124	17.7	143.0	0.0026	146.0	0.0360	0.0910	0.40	0.020	0.290	0.90	0.02	39.2
73-A-2	158.7	173.7	0.995	0.127	12.2	96.8	0.0100	105.1	0.0600	0.2120	0.28	0.040	0.474	0.61	0.08	37.8
73-A-4	158.7	173.7	0.995	0.121	10.8	89.1	0.0097	96.9	0.0590	0.2090	0.28	0.039	0.486	0.56	0.08	34.4
73-A-6	158.7	173.7	0.995	0.126	12.0	96.1	0.0101	104.5	0.0610	0.2100	0.29	0.040	0.486	0.61	0.08	37.5
73-B-1	168.3	176.7	0.995	0.128	19.5	153.1	0.0023	156.0	0.0350	0.0840	0.42	0.018	0.274	0.91	0.02	40.5
73-B-3	168.3	176.7	0.995	0.127	19.6	155.3	0.0021	158.0	0.0330	0.0810	0.41	0.018	0.261	0.92	0.02	40.3
73-B-5	168.3	176.7	0.996	0.126	18.9	151.1	0.0023	153.9	0.0350	0.0820	0.43	0.018	0.279	0.90	0.02	39.4
73-B-2	168.3	176.7	0.995	0.125	11.4	91.4	0.0102	99.6	0.0620	0.2100	0.30	0.040	0.496	0.54	0.08	35.6
73-B-4	168.3	176.7	0.996	0.126	12.1	96.2	0.0097	104.2	0.0610	0.2030	0.30	0.039	0.483	0.57	0.08	37.1
73-B-6	168.3	176.7	0.995	0.125	11.4	91.7	0.0099	99.6	0.0600	0.2100	0.29	0.040	0.482	0.54	0.08	35.5

* INDICATES PLANE STRAIN FRACTURE TOUGHNESS VALUES (KSI-IN.1/2) OBTAINED FROM TESTS WHICH EXCEEDED ONE OR MORE OF THE FOLLOWING LIMITS. FG/FTY=1.0, AO/B=0.5, AND/OR CA/BW=0.1

PART-THROUGH-CRACK TENSILE DATA FOR MINUTEMAN 6AL-4V TITANIUM EXTRUDED CYLINDERS

FORGING SPECIMEN NUMBER	YIELD STRESS FTY (KSI)	ULT. STRESS FTU (KSI)	WIDTH W (IN.)	THICK-NESS B (IN.)	LOAD P-MAX (KIPS)	GROSS STRESS FG (KSI)	CRACK AREA CA (SQ-IN)	NET STRESS FN (KSI)	CRACK DEPTH AO (IN.)	CRACK LENGTH 2C (IN.)	CRACK SHAPE AO/2C	NORM. DEPTH AO/B	AO/B	FG/FTY	CA/BW	PLANE STRAIN KIC
74-A-1	164.3	174.0	0.997	0.127	21.0	166.0	0.0017	168.3	0.0290	0.0740	0.39	0.016	0.229	1.01	0.01	41.5 *
74-A-2	164.3	174.0	0.994	0.128	18.2	143.6	0.0023	146.2	0.0340	0.0850	0.40	0.018	0.266	0.87	0.02	38.0
74-A-3	164.3	174.0	0.994	0.127	19.9	157.2	0.0017	159.3	0.0290	0.0760	0.38	0.017	0.228	0.96	0.01	39.5
74-A-4	164.3	174.0	0.996	0.125	10.5	84.5	0.0119	93.4	0.0660	0.2290	0.29	0.043	0.528	0.51	0.10	34.2 *
74-A-5	164.3	174.0	0.997	0.127	12.2	96.9	0.0101	105.4	0.0620	0.2080	0.30	0.040	0.490	0.59	0.08	37.8
74-A-6	164.3	174.0	0.996	0.128	13.7	107.7	0.0093	116.2	0.0590	0.2010	0.29	0.039	0.462	0.66	0.07	41.4
74-B-1	165.0	173.7	0.997	0.127	19.7	156.1	0.0019	158.4	0.0320	0.0750	0.43	0.017	0.252	0.95	0.01	39.1
74-B-2	165.0	173.7	0.996	0.122	18.8	153.9	0.0020	156.4	0.0320	0.0780	0.41	0.017	0.261	0.93	0.02	39.2
74-B-3	165.0	173.7	0.995	0.126	19.8	158.2	0.0018	160.5	0.0310	0.0740	0.42	0.016	0.246	0.96	0.01	39.4
74-B-4	165.0	173.7	0.995	0.126	11.3	89.8	0.0105	98.1	0.0630	0.2130	0.30	0.041	0.500	0.54	0.08	35.3
74-B-5	165.0	173.7	0.997	0.126	12.6	100.2	0.0097	108.6	0.0600	0.2050	0.29	0.039	0.476	0.61	0.08	38.7
74-B-6	165.0	173.7	0.996	0.126	11.8	93.6	0.0104	102.1	0.0650	0.2040	0.32	0.040	0.516	0.57	0.08	36.5 *
75-A-1	164.7	176.7	0.996	0.125	20.1	161.5	0.0024	164.7	0.0340	0.0900	0.38	0.020	0.272	0.98	0.02	44.3
75-A-3	164.7	176.7	0.997	0.123	18.7	152.3	0.0025	155.5	0.0370	0.0860	0.43	0.019	0.300	0.92	0.02	40.8
75-A-6	164.7	176.7	0.997	0.125	19.0	153.3	0.0029	157.0	0.0390	0.0950	0.41	0.021	0.313	0.93	0.02	43.1
75-A-2	164.7	176.7	0.997	0.125	11.7	94.0	0.0106	102.7	0.0620	0.2170	0.29	0.041	0.496	0.57	0.08	37.1
75-A-4	164.7	176.7	0.996	0.126	13.4	106.8	0.0106	116.6	0.0600	0.2240	0.27	0.042	0.475	0.65	0.08	42.6
75-A-5	164.7	176.7	0.996	0.125	12.5	100.4	0.0101	109.3	0.0630	0.2050	0.31	0.040	0.502	0.61	0.08	39.1 *
76-A-1	161.3	171.7	0.996	0.126	19.4	154.9	0.0021	157.5	0.0340	0.0790	0.43	0.017	0.270	0.96	0.02	39.9
76-A-3	161.3	171.7	0.993	0.126	20.1	160.6	0.0017	162.8	0.0300	0.0730	0.41	0.016	0.238	1.00	0.01	39.9
76-A-5	161.3	171.7	0.994	0.126	18.4	146.7	0.0026	149.7	0.0370	0.0880	0.42	0.019	0.293	0.91	0.02	39.7
76-A-2	161.3	171.7	0.997	0.125	12.2	97.3	0.0096	105.3	0.0600	0.2030	0.30	0.039	0.478	0.60	0.08	37.5
76-A-4	161.3	171.7	0.998	0.124	11.9	95.8	0.0101	104.3	0.0610	0.2110	0.29	0.040	0.491	0.59	0.08	37.5
76-A-6	161.3	171.7	0.994	0.126	12.1	96.7	0.0099	105.0	0.0620	0.2040	0.30	0.040	0.492	0.60	0.08	37.5

* INDICATES PLANE STRAIN FRACTURE TOUGHNESS VALUES (KSI-IN.1/2) OBTAINED FROM TESTS WHICH EXCEEDED ONE OR MORE OF THE FOLLOWING LIMITS. FG/FTY=1.0, AO/B=0.5, AND/OR CA/BW=0.1

PART-THROUGH-CRACK TENSILE DATA FOR MINUTEMAN 6AL-4V TITANIUM EXTRUDED CYLINDERS

FORGING SPECIMEN NUMBER	YIELD STRESS FTY (KSI)	ULT. STRESS FTU (KSI)	WIDTH W (IN.)	THICK-NESS B (IN.)	LOAD P-MAX (KIPS)	GROSS STRESS FG (KSI)	CRACK AREA CA (SQ.IN)	NET STRESS FN (KSI)	CRACK DEPTH AO (IN.)	CRACK LENGTH 2C (IN.)	CRACK SHAPE AO/2C	NORM. DEPTH AO/B	AO/B	FG/FTY	CA/BW	PLANE STRAIN KIC	
77-A-1	164.0	175.3	0.995	0.125	19.2	154.1	0.0020	156.7	0.0320	0.0810	0.40	0.018	0.256	0.94	0.02	40.0	
77-A-3	164.0	175.3	0.997	0.124	18.9	152.3	0.0022	155.8	0.0340	0.0840	0.40	0.018	0.274	0.93	0.02	40.5	
77-A-5	164.0	175.3	0.995	0.124	18.9	152.9	0.0020	155.4	0.0330	0.0760	0.43	0.017	0.266	0.93	0.02	38.5	
77-A-2	164.0	175.3	0.996	0.126	11.7	93.4	0.0101	101.6	0.0630	0.2040	0.31	0.040	0.501	0.57	0.08	36.2	*
77-A-4	164.0	175.3	0.997	0.125	11.2	89.7	0.0101	97.6	0.0620	0.2080	0.30	0.040	0.497	0.55	0.08	34.9	
77-A-6	164.0	175.3	0.997	0.126	11.9	95.4	0.0103	104.0	0.0640	0.2050	0.31	0.040	0.510	0.58	0.08	37.2	*
77-B-3	163.3	176.0	0.994	0.126	19.2	153.1	0.0020	155.7	0.0330	0.0790	0.42	0.017	0.262	0.94	0.02	39.4	
77-B-4	163.3	176.0	0.997	0.127	18.6	146.7	0.0022	149.3	0.0350	0.0800	0.44	0.017	0.276	0.90	0.02	37.8	
77-B-5	163.3	176.0	0.996	0.122	18.2	150.0	0.0020	152.5	0.0310	0.0840	0.37	0.018	0.254	0.92	0.02	39.4	
77-B-1	163.3	176.0	0.996	0.125	10.7	85.7	0.0125	95.3	0.0650	0.2450	0.27	0.045	0.520	0.53	0.10	35.3	*
77-B-2	163.3	176.0	0.997	0.126	11.2	89.2	0.0110	97.7	0.0600	0.2330	0.26	0.042	0.475	0.55	0.09	35.7	
77-B-6	163.3	176.0	0.995	0.126	11.7	93.7	0.0116	103.3	0.0660	0.2240	0.29	0.043	0.526	0.57	0.09	37.8	*
78-A-3	170.3	178.3	0.996	0.126	18.3	145.9	0.0020	148.3	0.0330	0.0790	0.42	0.017	0.261	0.86	0.02	37.2	
78-A-5	170.3	178.3	0.996	0.125	18.9	152.2	0.0019	154.6	0.0300	0.0800	0.37	0.017	0.240	0.89	0.02	39.0	
78-A-6	170.3	178.3	0.997	0.125	17.6	141.0	0.0023	143.6	0.0340	0.0850	0.40	0.018	0.271	0.83	0.02	37.1	
78-A-1	170.3	178.3	0.994	0.127	8.0	63.4	0.0239	78.2	0.0830	0.3660	0.23	0.061	0.654	0.37	0.19	30.4	*
78-A-2	170.3	178.3	0.997	0.122	10.3	84.7	0.0112	93.3	0.0600	0.2370	0.25	0.042	0.491	0.50	0.09	33.9	
78-A-4	170.3	178.3	0.995	0.124	9.2	74.4	0.0134	83.4	0.0690	0.2470	0.28	0.045	0.555	0.44	0.11	30.9	*
79-A-1	163.7	173.7	0.996	0.127	19.6	155.6	0.0019	158.0	0.0300	0.0820	0.37	0.018	0.237	0.95	0.02	40.5	
79-A-3	163.7	173.7	0.996	0.122	18.3	150.7	0.0020	153.2	0.0300	0.0850	0.35	0.018	0.246	0.92	0.02	39.7	
79-A-5	163.7	173.7	0.995	0.126	19.4	154.5	0.0020	157.0	0.0310	0.0820	0.38	0.018	0.245	0.94	0.02	40.3	
79-A-2	163.7	173.7	0.994	0.123	11.1	91.3	0.0097	99.3	0.0580	0.2140	0.27	0.040	0.473	0.56	0.08	35.4	
79-A-4	163.7	173.7	0.997	0.124	11.9	96.4	0.0104	105.2	0.0600	0.2200	0.27	0.041	0.483	0.59	0.08	38.0	
79-A-6	163.7	173.7	0.994	0.124	11.8	96.1	0.0100	104.6	0.0580	0.2200	0.26	0.040	0.468	0.59	0.08	37.6	

* INDICATES PLANE STRAIN FRACTURE TOUGHNESS VALUES (KSI-IN.1/2) OBTAINED FROM TESTS WHICH EXCEEDED ONE OR MORE OF THE FOLLOWING LIMITS. FG/FTY=1.0, AO/B=0.5, AND/OR CA/BW=0.1

PART-THROUGH-CRACK TENSILE DATA FOR MINUTEMAN 6AL-4V TITANIUM EXTRUDED CYLINDERS

FORGING SPECIMEN NUMBER	YIELD STRESS FTY (KSI)	ULT. STRESS FTU (KSI)	WIDTH W (IN.)	THICK -NESS B (IN.)	LOAD P-MAX (KIPS)	GROSS STRESS FG (KSI)	CRACK AREA CA (SQ.IN)	NET STRESS FN (KSI)	CRACK DEPTH AO (IN.)	CRACK LENGTH 2C (IN.)	CRACK SHAPE AO/2C	NORM. DEPTH AO/B	AO/B	FG/FTY	CA/BW	PLANE STRAIN KIC
79-B-1	160.7	172.0	0.996	0.124	19.5	158.0	0.0018	160.4	0.0260	0.0830	0.34	0.018	0.225	0.98	0.01	41.3
79-B-3	160.7	172.0	0.994	0.123	18.8	153.2	0.0021	155.9	0.0320	0.0840	0.38	0.018	0.259	0.95	0.02	40.5
79-B-5	160.7	172.0	0.995	0.126	18.8	150.7	0.0018	152.9	0.0280	0.0820	0.34	0.018	0.223	0.94	0.01	39.0
79-B-2	160.7	172.0	0.996	0.122	11.1	91.5	0.0096	99.3	0.0600	0.2040	0.29	0.039	0.492	0.57	0.08	35.2
79-B-4	160.7	172.0	0.995	0.125	11.2	90.3	0.0093	97.5	0.0590	0.2000	0.29	0.038	0.472	0.56	0.07	34.4
79-B-6	160.7	172.0	0.995	0.126	11.4	91.2	0.0098	98.9	0.0600	0.2080	0.29	0.039	0.476	0.57	0.08	35.3
80-A-1	163.7	175.0	0.995	0.127	20.8	164.8	0.0018	167.2	0.0290	0.0770	0.38	0.017	0.229	1.01	0.01	42.0 *
80-A-3	163.7	175.0	0.996	0.126	19.6	156.1	0.0021	158.7	0.0320	0.0820	0.39	0.018	0.254	0.95	0.02	40.8
80-A-5	163.7	175.0	0.995	0.127	20.5	162.4	0.0019	164.9	0.0300	0.0810	0.37	0.018	0.236	0.99	0.02	42.3
80-A-2	163.7	175.0	0.995	0.125	13.2	106.2	0.0092	114.7	0.0580	0.2020	0.29	0.039	0.465	0.65	0.07	40.8
80-A-4	163.7	175.0	0.993	0.125	12.5	100.5	0.0093	108.7	0.0590	0.2010	0.29	0.039	0.472	0.61	0.08	38.5
80-A-6	163.7	175.0	0.995	0.126	13.3	106.4	0.0095	115.1	0.0590	0.2040	0.29	0.039	0.469	0.65	0.08	41.1
80-B-1	160.3	173.7	0.996	0.126	19.9	157.8	0.0021	160.5	0.0330	0.0820	0.40	0.018	0.261	0.98	0.02	41.5
80-B-2	160.3	173.7	0.997	0.127	19.9	157.8	0.0020	160.4	0.0320	0.0810	0.40	0.018	0.253	0.98	0.02	41.2
80-B-3	160.3	173.7	0.996	0.127	20.4	161.7	0.0019	164.2	0.0300	0.0820	0.37	0.018	0.236	1.01	0.02	42.4 *
80-B-4	160.3	173.7	0.996	0.127	13.0	102.3	0.0099	110.9	0.0580	0.2170	0.27	0.040	0.456	0.64	0.08	40.1
80-B-5	160.3	173.7	0.996	0.127	13.8	109.1	0.0093	117.8	0.0560	0.2120	0.26	0.040	0.441	0.68	0.07	42.4
80-B-6	160.3	173.7	0.996	0.126	11.8	94.4	0.0112	103.6	0.0620	0.2290	0.27	0.043	0.492	0.59	0.09	37.9
81-A-1	163.7	176.7	0.995	0.126	19.8	157.9	0.0022	160.7	0.0330	0.0830	0.40	0.018	0.262	0.96	0.02	41.7
81-A-2	163.7	176.7	0.996	0.126	20.1	160.1	0.0019	162.5	0.0320	0.0760	0.42	0.017	0.254	0.98	0.02	40.5
81-A-4	163.7	176.7	0.996	0.126	20.1	159.6	0.0021	162.2	0.0340	0.0770	0.44	0.017	0.269	0.97	0.02	40.7
81-A-3	163.7	176.7	0.995	0.126	12.3	97.6	0.0100	106.0	0.0610	0.2080	0.29	0.040	0.483	0.60	0.08	38.0
81-A-5	163.7	176.7	0.994	0.126	12.4	98.9	0.0098	107.4	0.0600	0.2090	0.29	0.040	0.477	0.60	0.08	38.5
81-A-6	163.7	176.7	0.995	0.127	12.4	98.4	0.0094	106.3	0.0590	0.2020	0.29	0.039	0.465	0.60	0.07	37.7

* INDICATES PLANE STRAIN FRACTURE TOUGHNESS VALUES (KSI-IN.1/2) OBTAINED FROM TESTS WHICH EXCEEDED ONE OR MORE OF THE FOLLOWING LIMITS. FG/FTY=1.0, AO/B=0.5, AND/OR CA/BW=0.1

PART-THROUGH-CRACK TENSILE DATA FOR MINUTEMAN 6AL-4V TITANIUM EXTRUDED CYLINDERS

FORGING SPECIMEN NUMBER	YIELD STRESS FTY (KSI)	ULT. STRESS FTU (KSI)	WIDTH W (IN.)	THICK-NESS B (IN.)	LOAD P-MAX (KIPS)	GROSS STRESS FG (KSI)	CRACK AREA CA (SQ.IN)	NET STRESS FN (KSI)	CRACK DEPTH AO (IN.)	CRACK LENGTH 2C (IN.)	CRACK SHAPE AO/2C	NORM. DEPTH AO/B	AO/B	FG/FTY	CA/BW	PLANE STRAIN KIC
82-A-1	161.0	173.7	1.001	0.125	20.2	161.2	0.0021	163.9	0.0330	0.0850	0.36	0.019	0.247	1.00	0.02	43.0 *
82-A-2	161.0	173.7	1.000	0.126	20.7	164.5	0.0021	167.2	0.0300	0.0890	0.34	0.019	0.239	1.02	0.02	44.7 *
82-A-3	161.0	173.7	1.000	0.126	19.9	157.1	0.0023	160.9	0.0340	0.0870	0.39	0.019	0.269	0.98	0.02	42.4
82-A-4	161.0	173.7	1.002	0.124	12.6	101.3	0.0104	110.5	0.0620	0.2140	0.29	0.041	0.500	0.63	0.08	40.0 *
82-A-5	161.0	173.7	1.000	0.126	13.0	103.4	0.0123	114.6	0.0640	0.2440	0.26	0.045	0.508	0.64	0.10	42.8 *
82-A-6	161.0	173.7	0.993	0.122	12.7	104.9	0.0093	113.7	0.0570	0.2080	0.27	0.039	0.467	0.65	0.08	40.5
83-A-1	163.0	173.7	0.996	0.127	20.1	158.0	0.0023	160.8	0.0350	0.0820	0.43	0.018	0.275	0.97	0.02	41.5
83-A-3	163.0	173.7	0.996	0.126	19.7	158.0	0.0021	160.7	0.0340	0.0780	0.44	0.017	0.271	0.97	0.02	40.5
83-A-5	163.0	173.7	0.997	0.126	20.3	161.5	0.0020	164.1	0.0330	0.0760	0.43	0.017	0.262	0.99	0.02	41.0
83-A-2	163.0	173.7	0.997	0.127	14.3	113.1	0.0099	122.7	0.0630	0.2010	0.31	0.040	0.495	0.69	0.08	44.1
83-A-4	163.0	173.7	0.995	0.124	15.2	123.2	0.0090	132.9	0.0580	0.1970	0.29	0.039	0.467	0.76	0.07	47.4
83-A-6	163.0	173.7	0.996	0.123	14.4	117.9	0.0093	127.6	0.0590	0.2010	0.29	0.039	0.482	0.72	0.08	45.6
D84B-1	158.7	167.0	0.996	0.125	20.2	162.2	0.0021	165.0	0.0330	0.0800	0.41	0.018	0.264	1.02	0.02	42.3 *
D84B-3	158.7	167.0	0.993	0.127	20.5	163.1	0.0022	165.9	0.0330	0.0830	0.40	0.019	0.261	1.03	0.02	43.3 *
D84B-4	158.7	167.0	0.997	0.127	20.6	162.2	0.0021	164.9	0.0330	0.0800	0.41	0.018	0.259	1.02	0.02	42.3 *
D84B-2	158.7	167.0	0.995	0.126	17.1	136.9	0.0094	147.9	0.0590	0.2020	0.29	0.041	0.469	0.86	0.07	53.9
D84B-5	158.7	167.0	0.995	0.126	16.9	135.2	0.0099	146.8	0.0620	0.2040	0.30	0.042	0.493	0.85	0.08	53.8
D84B-6	158.7	167.0	0.997	0.125	17.6	140.9	0.0095	152.5	0.0580	0.2080	0.28	0.042	0.463	0.89	0.08	56.1
L84B-3	159.0	167.0	0.764	0.124	14.5	152.7	0.0022	156.3	0.0334	0.0822	0.41	0.018	0.269	0.96	0.02	40.1
L84B-4	159.0	167.0	0.764	0.124	14.2	149.7	0.0024	153.5	0.0358	0.0838	0.43	0.018	0.289	0.94	0.02	39.6
L84B-6	159.0	167.0	0.764	0.124	14.5	153.5	0.0019	156.7	0.0312	0.0796	0.39	0.018	0.252	0.97	0.02	39.6
L84B-1	159.0	167.0	0.763	0.124	10.6	111.7	0.0087	123.0	0.0541	0.2041	0.27	0.038	0.436	0.70	0.09	42.7
L84B-2	159.0	167.0	0.764	0.124	9.8	103.4	0.0093	114.7	0.0572	0.2078	0.28	0.039	0.461	0.65	0.10	40.0
L84B-5	159.0	167.0	0.763	0.125	9.3	98.1	0.0093	108.7	0.0572	0.2067	0.28	0.039	0.459	0.62	0.10	37.7

* INDICATES PLANE STRAIN FRACTURE TOUGHNESS VALUES (KSI-IN.1/2) OBTAINED FROM TESTS WHICH EXCEEDED ONE OR MORE OF THE FOLLOWING LIMITS. FG/FTY=1.0, AO/B=0.5, AND/OR CA/BW=0.1

PART-THROUGH-CRACK TENSILE DATA FOR MINUTEMAN 6AL-4V TITANIUM EXTRUDED CYLINDERS

FORGING SPECIMEN NUMBER	YIELD STRESS FTY (KSI)	ULT. STRESS FTU (KSI)	WIDTH W (IN.)	THICK-NESS B (IN.)	LOAD P-MAX (KIPS)	GROSS STRESS FG (KSI)	CRACK AREA CA (SQ.IN)	NET STRESS FN (KSI)	CRACK DEPTH AO (IN.)	CRACK LENGTH 2C (IN.)	CRACK SHAPE AO/2C	NORM. DEPTH AO/B	AO/B	FG/FTY	CA/BW	PLANE STRAIN KIC
86-A-1	163.0	171.3	0.997	0.128	21.7	170.2	0.0019	172.8	0.0330	0.0740	0.45	0.017	0.258	1.04	0.02	42.8 *
86-A-3	163.0	171.3	0.997	0.125	21.3	170.8	0.0020	173.6	0.0330	0.0770	0.43	0.017	0.264	1.05	0.02	43.9 *
86-A-4	163.0	171.3	0.995	0.125	21.5	172.1	0.0019	174.8	0.0300	0.0820	0.37	0.018	0.239	1.06	0.02	45.4 *
86-A-2	163.0	171.3	0.996	0.127	16.3	129.2	0.0096	139.8	0.0630	0.1940	0.32	0.040	0.498	0.79	0.08	50.2
86-A-5	163.0	171.3	0.995	0.126	17.2	137.2	0.0098	148.8	0.0610	0.2050	0.30	0.041	0.484	0.84	0.08	54.5
86-A-6	163.0	171.3	0.998	0.127	17.1	135.2	0.0095	146.2	0.0590	0.2040	0.29	0.041	0.466	0.83	0.07	53.2
87-A-1	159.7	171.3	1.000	0.126	20.5	163.2	0.0022	166.1	0.0350	0.0800	0.44	0.018	0.278	1.02	0.02	42.6 *
87-A-3	159.7	171.3	1.001	0.126	20.4	162.3	0.0022	165.2	0.0340	0.0820	0.41	0.018	0.270	1.02	0.02	42.9 *
87-A-4	159.7	171.3	1.001	0.125	20.1	160.3	0.0022	163.1	0.0340	0.0830	0.41	0.018	0.272	1.00	0.02	42.5 *
87-A-2	159.7	171.3	1.002	0.127	14.3	113.2	0.0101	123.0	0.0620	0.2070	0.30	0.041	0.490	0.71	0.08	44.6
87-A-5	159.7	171.3	1.001	0.127	15.2	119.8	0.0096	129.6	0.0610	0.2000	0.31	0.040	0.481	0.75	0.08	46.7
87-A-6	159.7	171.3	1.001	0.124	13.0	104.8	0.0133	117.3	0.0690	0.2450	0.28	0.047	0.555	0.66	0.11	44.2 *
87-B-1	162.3	175.0	0.993	0.127	20.8	165.5	0.0019	168.0	0.0320	0.0750	0.43	0.017	0.253	1.02	0.01	41.8 *
87-B-2	162.3	175.0	0.995	0.126	20.7	165.6	0.0020	168.3	0.0310	0.0830	0.37	0.018	0.246	1.02	0.02	43.8 *
87-B-3	162.3	175.0	0.993	0.125	20.0	161.0	0.0019	163.5	0.0310	0.0860	0.39	0.018	0.248	0.99	0.02	41.8
87-B-4	162.3	175.0	0.998	0.126	13.0	103.4	0.0099	112.2	0.0600	0.2100	0.29	0.040	0.475	0.64	0.08	40.4
87-B-5	162.3	175.0	0.999	0.123	14.9	121.3	0.0093	131.2	0.0590	0.2000	0.29	0.040	0.480	0.75	0.08	47.0
87-B-6	162.3	175.0	0.996	0.126	14.0	111.7	0.0092	120.6	0.0580	0.2020	0.29	0.039	0.461	0.69	0.07	43.0
90-A-1	158.3	171.7	1.000	0.125	20.2	162.5	0.0020	165.1	0.0320	0.0790	0.41	0.018	0.257	1.03	0.02	42.1 *
90-A-3	158.3	171.7	1.000	0.125	20.0	160.1	0.0022	163.0	0.0340	0.0810	0.42	0.018	0.272	1.01	0.02	42.0 *
90-A-5	158.3	171.7	1.001	0.127	20.8	164.3	0.0020	167.0	0.0330	0.0790	0.42	0.018	0.261	1.04	0.02	42.7 *
90-A-2	158.3	171.7	1.000	0.126	15.1	119.7	0.0098	129.8	0.0600	0.2090	0.29	0.041	0.475	0.76	0.08	47.2
90-A-4	158.3	171.7	1.000	0.126	14.4	114.6	0.0093	123.7	0.0600	0.1980	0.30	0.039	0.477	0.72	0.07	44.3
90-A-6	158.3	171.7	0.999	0.123	14.0	113.7	0.0093	122.9	0.0590	0.2010	0.29	0.039	0.478	0.72	0.08	44.0

* INDICATES PLANE STRAIN FRACTURE TOUGHNESS VALUES (KSI-IN.1/2) OBTAINED FROM TESTS WHICH EXCEEDED ONE OR MORE OF THE FOLLOWING LIMITS. FG/FTY=1.0, AO/B=0.5, AND/OR CA/BW=0.1

PART-THROUGH-CRACK TENSILE DATA FOR MINUTEMAN 6AL-4V TITANIUM EXTRUDED CYLINDERS

FORGING SPECIMEN NUMBER	YIELD STRESS FTY (KSI)	ULT. STRESS FTU (KSI)	WIDTH W (IN.)	THICK-NESS B (IN.)	LOAD P-MAX (KIPS)	GROSS STRESS FG (KSI)	CRACK AREA CA (SQ.IN)	NET STRESS FN (KSI)	CRACK DEPTH AO (IN.)	CRACK LENGTH 2C (IN.)	CRACK SHAPE AO/2C	NORM. DEPTH AO/B	AO/B	FG/FTY	CA/BW	PLANE STRAIN KIC	
90-B-1	161.0	174.0	0.992	0.125	20.3	163.0	0.0019	165.5	0.0310	0.0770	0.40	0.017	0.247	1.01	0.02	41.7	*
90-B-2	161.0	174.0	0.995	0.124	19.6	159.0	0.0021	161.8	0.0340	0.0800	0.42	0.018	0.275	0.99	0.02	41.3	
90-B-4	161.0	174.0	0.994	0.125	19.8	159.3	0.0020	161.9	0.0330	0.0790	0.42	0.018	0.263	0.99	0.02	41.2	
90-B-3	161.0	174.0	0.996	0.126	13.7	108.8	0.0094	117.6	0.0610	0.1960	0.31	0.039	0.484	0.68	0.07	41.8	
90-B-5	161.0	174.0	0.995	0.123	12.3	100.3	0.0097	108.9	0.0610	0.2020	0.30	0.039	0.494	0.62	0.08	38.8	
90-B-6	161.0	174.0	0.996	0.126	13.3	105.7	0.0093	114.1	0.0600	0.1980	0.30	0.039	0.475	0.66	0.07	40.6	
91-A-1	162.7	175.0	0.996	0.127	21.0	165.6	0.0020	168.3	0.0320	0.0810	0.40	0.018	0.251	1.02	0.02	43.4	*
91-A-3	162.7	175.0	0.996	0.125	19.0	152.4	0.0026	155.6	0.0360	0.0910	0.40	0.020	0.287	0.94	0.02	42.0	
91-A-5	162.7	175.0	0.996	0.126	19.8	157.6	0.0021	160.3	0.0330	0.0820	0.40	0.018	0.262	0.97	0.02	41.4	
91-A-2	162.7	175.0	0.997	0.126	12.6	100.3	0.0108	109.7	0.0640	0.2140	0.30	0.041	0.508	0.62	0.09	39.8	*
91-A-4	162.7	175.0	0.996	0.125	11.5	92.8	0.0098	100.7	0.0610	0.2050	0.30	0.039	0.490	0.57	0.08	35.9	
91-A-6	162.7	175.0	0.995	0.123	12.3	100.1	0.0106	109.6	0.0640	0.2110	0.30	0.041	0.519	0.62	0.09	39.5	*
91-B-3	161.7	172.3	0.904	0.123	18.2	163.8	0.0020	166.8	0.0320	0.0790	0.41	0.018	0.261	1.01	0.02	42.4	*
91-B-6	161.7	172.3	0.915	0.124	17.9	158.2	0.0023	161.4	0.0330	0.0880	0.37	0.019	0.266	0.98	0.02	42.9	
91-B-1	161.7	172.3	0.990	0.124	12.6	102.4	0.0099	111.3	0.0610	0.2060	0.30	0.040	0.491	0.63	0.08	39.9	
91-B-2	161.7	172.3	0.904	0.127	11.5	99.7	0.0109	110.0	0.0630	0.2200	0.29	0.042	0.494	0.62	0.09	39.8	
92-A-1	165.3	175.0	0.996	0.126	20.1	160.6	0.0020	163.3	0.0320	0.0840	0.37	0.018	0.247	0.97	0.02	42.5	
92-A-2	165.3	175.0	0.995	0.126	20.3	162.3	0.0020	165.0	0.0320	0.0810	0.40	0.018	0.254	0.98	0.02	42.4	
92-A-4	165.3	175.0	0.995	0.123	19.7	161.3	0.0020	164.0	0.0330	0.0780	0.42	0.017	0.269	0.98	0.02	41.4	
92-A-3	165.3	175.0	0.995	0.125	14.8	119.0	0.0098	129.2	0.0600	0.2080	0.29	0.041	0.479	0.72	0.08	46.7	
92-A-5	165.3	175.0	0.996	0.127	14.2	112.5	0.0096	121.8	0.0590	0.2080	0.28	0.040	0.465	0.68	0.08	43.9	
92-A-6	165.3	175.0	0.996	0.127	13.5	107.2	0.0098	116.2	0.0610	0.2050	0.30	0.040	0.482	0.65	0.08	41.7	

* INDICATES PLANE STRAIN FRACTURE TOUGHNESS VALUES (KSI-IN.1/2) OBTAINED FROM TESTS WHICH EXCEEDED ONE OR MORE OF THE FOLLOWING LIMITS. FG/FTY=1.0, AO/B=0.5, AND/OR CA/BW=0.1

PART-THROUGH-CRACK TENSILE DATA FOR MINUTEMAN 6AL-4V TITANIUM EXTRUDED CYLINDERS

FORGING SPECIMEN NUMBER	YIELD STRESS FTY (KSI)	ULT. STRESS FTU (KSI)	WIDTH W (IN.)	THICK-NESS B (IN.)	LOAD P-MAX (KIPS)	GROSS STRESS FG (KSI)	CRACK AREA CA (SQ.IN)	NET STRESS FN (KSI)	CRACK DEPTH AO (IN.)	CRACK LENGTH 2C (IN.)	CRACK SHAPE AO/2C	NORM. DEPTH AO/Q	AO/B	FG/FTY	CA/BW	PLANE STRAIN KIC	
93-A-1	162.3	174.0	0.996	0.126	17.5	139.9	0.0027	143.0	0.0370	0.0930	0.40	0.020	0.294	0.86	0.02	38.6	
93-A-3	162.3	174.0	0.996	0.125	19.0	152.4	0.0020	155.0	0.0320	0.0810	0.40	0.018	0.255	0.94	0.02	39.6	
93-A-4	162.3	174.0	0.995	0.126	19.8	158.0	0.0021	160.6	0.0320	0.0820	0.39	0.018	0.254	0.97	0.02	41.4	
93-A-2	162.3	174.0	0.997	0.126	14.6	116.0	0.0097	125.7	0.0800	0.2050	0.29	0.040	0.476	0.71	0.08	45.3	
93-A-5	162.3	174.0	0.997	0.123	12.8	104.2	0.0092	112.6	0.0570	0.2050	0.28	0.039	0.464	0.64	0.07	40.0	
93-A-6	162.3	174.0	0.994	0.124	11.3	91.5	0.0104	99.9	0.0630	0.2100	0.30	0.040	0.506	0.56	0.08	35.8	*
93B-1	161.0	172.3	0.764	0.128	14.7	150.1	0.0020	153.3	0.0300	0.0852	0.35	0.018	0.234	0.93	0.02	39.7	
93B-2	161.0	172.3	0.765	0.127	14.3	147.1	0.0022	150.5	0.0336	0.0840	0.40	0.018	0.265	0.91	0.02	38.8	
93B-6	161.0	172.3	0.764	0.127	15.0	154.3	0.0020	157.5	0.0312	0.0804	0.39	0.018	0.245	0.96	0.02	40.0	
93B-3	161.0	172.3	0.766	0.127	9.0	91.9	0.0098	102.2	0.0600	0.2088	0.29	0.040	0.471	0.57	0.10	35.7	*
93B-4	161.0	172.3	0.765	0.124	9.6	101.0	0.0094	112.1	0.0588	0.2036	0.29	0.039	0.474	0.63	0.10	38.9	
93B-5	161.0	172.3	0.765	0.127	9.2	94.4	0.0096	104.7	0.0600	0.2036	0.29	0.039	0.471	0.59	0.10	36.4	
94B-4	160.0	171.3	0.766	0.124	14.8	156.1	0.0020	159.4	0.0306	0.0816	0.37	0.018	0.247	0.98	0.02	40.8	
94B-5	160.0	171.3	0.764	0.124	13.9	146.6	0.0020	149.8	0.0312	0.0828	0.38	0.018	0.252	0.92	0.02	38.3	
94B-6	160.0	171.3	0.765	0.124	13.8	145.3	0.0022	148.7	0.0336	0.0840	0.40	0.018	0.271	0.91	0.02	38.3	
94B-1	160.0	171.3	0.766	0.124	9.0	94.8	0.0094	105.2	0.0576	0.2088	0.28	0.039	0.465	0.59	0.10	36.5	
94B-2	160.0	171.3	0.765	0.124	8.8	92.7	0.0096	103.1	0.0588	0.2088	0.28	0.039	0.474	0.58	0.10	35.8	*
94B-3	160.0	171.3	0.766	0.123	9.4	98.9	0.0092	109.6	0.0576	0.2036	0.28	0.039	0.466	0.62	0.10	37.9	
96A-1	160.0	171.0	0.763	0.127	14.4	149.6	0.0020	152.8	0.0324	0.0804	0.40	0.018	0.256	0.94	0.02	38.7	
96A-5	160.0	171.0	0.763	0.125	14.5	152.0	0.0021	155.4	0.0324	0.0816	0.40	0.018	0.259	0.95	0.02	39.7	
96A-6	160.0	171.0	0.762	0.125	14.6	153.3	0.0021	156.8	0.0324	0.0840	0.39	0.018	0.259	0.96	0.02	40.6	
96A-2	160.0	171.0	0.762	0.125	8.6	90.3	0.0094	100.3	0.0588	0.2036	0.29	0.039	0.472	0.56	0.10	34.6	
96A-3	160.0	171.0	0.763	0.125	8.7	91.5	0.0092	101.3	0.0576	0.2036	0.28	0.038	0.463	0.57	0.10	34.9	
96A-4	160.0	171.0	0.762	0.127	9.0	93.2	0.0094	103.8	0.0588	0.2036	0.29	0.039	0.465	0.59	0.10	35.9	

* INDICATES PLANE STRAIN FRACTURE TOUGHNESS VALUES (KSI-IN.1/2) OBTAINED FROM TESTS WHICH EXCEEDED ONE OR MORE OF THE FOLLOWING LIMITS. FG/FTY=1.0, AO/B=0.5, AND/OR CA/BW=0.1

PART-THROUGH-CRACK TENSILE DATA FOR MINUTEMAN 6AL-4V TITANIUM EXTRUDED CYLINDERS

FORGING SPECIMEN NUMBER	YIELD STRESS FTY (KSI)	ULT. STRESS FTU (KSI)	WIDTH W (IN.)	THICK-NESS B (IN.)	LOAD P-MAX (KIPS)	GROSS STRESS FG (KSI)	CRACK AREA CA (SQ.IN)	NET STRESS FN (KSI)	CRACK DEPTH AO (IN.)	CRACK LENGTH 2C (IN.)	CRACK SHAPE AO/2C	NORM. DEPTH AO/B	AO/B	FG/FTY	CA/BW	PLANE STRAIN KIC
96B-1	167.0	176.7	0.761	0.125	14.3	150.7	0.0021	154.1	0.0312	0.0840	0.37	0.018	0.250	0.90	0.02	39.6
96B-3	167.0	176.7	0.761	0.126	15.1	157.7	0.0020	161.1	0.0324	0.0792	0.41	0.017	0.257	0.94	0.02	40.6
96B-6	167.0	176.7	0.762	0.123	14.5	154.6	0.0018	157.6	0.0276	0.0816	0.34	0.017	0.224	0.93	0.02	39.2
96B-2	167.0	176.7	0.760	0.122	9.3	100.8	0.0086	111.1	0.0540	0.2036	0.27	0.038	0.443	0.60	0.09	38.1
96B-4	167.0	176.7	0.760	0.125	10.6	111.8	0.0086	123.1	0.0540	0.2036	0.27	0.038	0.434	0.67	0.09	42.5
96B-5	167.0	176.7	0.760	0.123	9.7	102.9	0.0092	114.1	0.0564	0.2088	0.27	0.039	0.457	0.62	0.10	39.6
97A-1	163.0	175.0	0.761	0.125	14.5	152.9	0.0020	156.2	0.0324	0.0804	0.40	0.018	0.259	0.94	0.02	39.6
97A-2	163.0	175.0	0.760	0.125	14.5	152.9	0.0021	156.4	0.0324	0.0816	0.40	0.018	0.259	0.94	0.02	39.9
97A-6	163.0	175.0	0.761	0.127	14.9	154.5	0.0022	158.1	0.0336	0.0840	0.40	0.018	0.265	0.95	0.02	40.9
97A-3	163.0	175.0	0.761	0.126	8.8	92.2	0.0098	102.7	0.0600	0.2088	0.29	0.040	0.476	0.57	0.10	35.7 *
97A-4	163.0	175.0	0.761	0.126	9.1	95.2	0.0090	105.1	0.0564	0.2036	0.28	0.038	0.449	0.58	0.09	38.2
97A-5	163.0	175.0	0.760	0.125	9.2	96.3	0.0094	106.9	0.0576	0.2088	0.28	0.039	0.461	0.59	0.10	37.1
97B-1	164.0	176.3	0.763	0.125	14.3	148.3	0.0019	151.4	0.0300	0.0816	0.37	0.018	0.238	0.90	0.02	38.4
97B-3	164.0	176.3	0.764	0.124	14.1	149.2	0.0121	152.6	0.0324	0.0828	0.39	0.018	0.261	0.91	0.02	39.0
97B-6	164.0	176.3	0.764	0.125	15.2	160.1	0.0018	163.2	0.0288	0.0804	0.36	0.018	0.231	0.98	0.02	41.4
97B-2	164.0	176.3	0.763	0.126	9.7	101.3	0.0092	112.1	0.0564	0.2088	0.27	0.039	0.449	0.62	0.10	39.0
97B-4	164.0	176.3	0.763	0.123	9.7	103.4	0.0092	114.7	0.0564	0.2088	0.27	0.039	0.459	0.63	0.10	39.8
97B-5	164.0	176.3	0.764	0.124	8.5	89.9	0.0091	99.4	0.0552	0.2088	0.26	0.038	0.445	0.55	0.10	34.2
98A-3	161.0	174.3	0.765	0.125	14.8	155.0	0.0020	158.2	0.0312	0.0804	0.39	0.018	0.251	0.96	0.02	40.2
98A-4	161.0	174.3	0.765	0.126	15.0	155.8	0.0018	158.7	0.0288	0.0780	0.37	0.017	0.229	0.97	0.02	39.7
98A-5	161.0	174.3	0.765	0.123	14.6	154.4	0.0019	157.6	0.0300	0.0804	0.37	0.018	0.243	0.96	0.02	39.9
98A-1	161.0	174.3	0.765	0.123	10.3	109.6	0.0090	121.1	0.0576	0.1984	0.29	0.038	0.468	0.68	0.10	41.9
98A-2	161.0	174.3	0.764	0.123	9.2	97.9	0.0096	109.1	0.0588	0.2088	0.28	0.039	0.478	0.61	0.10	38.0 *
98A-6	161.0	174.3	0.765	0.124	9.8	103.1	0.0096	114.7	0.0600	0.2036	0.29	0.039	0.484	0.64	0.10	39.9 *

* INDICATES PLANE STRAIN FRACTURE TOUGHNESS VALUES (KSI-IN.1/2) OBTAINED FROM TESTS WHICH EXCEEDED ONE OR MORE OF THE FOLLOWING LIMITS. FG/FTY=1.0, AO/B=0.5, AND/OR CA/BW=0.1

PART-THROUGH-CRACK TENSILE DATA FOR MINUTEMAN 6AL-4V TITANIUM EXTRUDED CYLINDERS

FORGING SPECIMEN NUMBER	YIELD STRESS FTY (KSI)	ULT. STRESS FTU (KSI)	WIDTH W (IN.)	THICK-NESS B (IN.)	LOAD P-MAX (KIPS)	GROSS STRESS FG (KSI)	CRACK AREA CA (SQ.IN)	NET STRESS FN (KSI)	CRACK DEPTH AO (IN.)	CRACK LENGTH 2C (IN.)	CRACK SHAPE AO/2C	NORM. DEPTH AO/B	AO/B	FG/FTY	CA/BW	PLANE STRAIN KIC	
100A-1	161.0	173.3	0.765	0.125	14.8	154.9	0.0021	158.3	0.0312	0.0840	0.37	0.018	0.250	0.96	0.02	40.9	
100A-4	161.0	173.3	0.766	0.125	14.8	154.6	0.0019	157.8	0.0312	0.0792	0.39	0.017	0.250	0.96	0.02	39.8	
100A-5	161.0	173.3	0.764	0.125	14.8	155.2	0.0019	158.3	0.0300	0.0804	0.37	0.018	0.240	0.96	0.02	40.1	
100A-2	161.0	173.3	0.760	0.125	10.0	105.4	0.0096	116.5	0.0564	0.2036	0.28	0.039	0.453	0.65	0.10	40.4	
100A-3	161.0	173.3	0.765	0.126	10.2	106.7	0.0087	117.3	0.0552	0.2009	0.27	0.038	0.440	0.66	0.09	40.6	
100A-6	161.0	173.3	0.759	0.124	10.2	108.2	0.0084	118.8	0.0540	0.1984	0.27	0.037	0.435	0.67	0.09	40.8	
100B-2	166.0	175.3	0.764	0.127	15.0	155.1	0.0021	158.5	0.0324	0.0816	0.40	0.018	0.256	0.93	0.02	40.4	
100B-5	166.0	175.3	0.763	0.126	15.1	157.2	0.0022	160.8	0.0336	0.0816	0.41	0.018	0.267	0.95	0.02	41.1	
100B-6	166.0	175.3	0.764	0.126	15.2	158.3	0.0020	161.7	0.0312	0.0816	0.38	0.018	0.248	0.95	0.02	41.3	
100B-1	166.0	175.3	0.761	0.127	10.5	108.4	0.0089	119.4	0.0564	0.2009	0.28	0.038	0.444	0.65	0.09	41.4	
100B-3	166.0	175.3	0.763	0.127	9.7	100.2	0.0094	111.0	0.0588	0.2036	0.29	0.039	0.463	0.60	0.10	38.5	
100B-4	166.0	175.3	0.763	0.126	9.9	103.0	0.0094	114.1	0.0588	0.2036	0.29	0.039	0.467	0.62	0.10	39.6	
101A-1	163.0	174.7	0.764	0.125	14.9	155.5	0.0020	158.8	0.0312	0.0816	0.38	0.018	0.250	0.95	0.02	40.5	
101A-2	163.0	174.7	0.764	0.125	14.8	155.4	0.0019	158.6	0.0300	0.0816	0.37	0.018	0.240	0.95	0.02	40.4	
101A-4	163.0	174.7	0.764	0.126	14.9	154.9	0.0019	158.1	0.0312	0.0792	0.39	0.017	0.248	0.95	0.02	39.8	
101A-3	163.0	174.7	0.765	0.125	9.3	96.9	0.0096	107.7	0.0588	0.2088	0.28	0.039	0.470	0.59	0.10	37.5	*
101A-5	163.0	174.7	0.765	0.125	10.1	105.3	0.0092	116.5	0.0576	0.2036	0.28	0.039	0.461	0.65	0.10	40.5	
101A-6	163.0	174.7	0.764	0.125	10.2	106.4	0.0096	118.4	0.0588	0.2088	0.28	0.040	0.470	0.65	0.10	41.4	*
102A-1	159.0	171.3	0.763	0.127	15.3	157.4	0.0019	160.6	0.0300	0.0816	0.37	0.018	0.236	0.99	0.02	41.1	
102A-2	159.0	171.3	0.763	0.127	15.1	156.2	0.0020	159.5	0.0312	0.0804	0.39	0.018	0.246	0.98	0.02	40.6	
102A-4	159.0	171.3	0.763	0.127	15.1	156.3	0.0018	159.3	0.0288	0.0792	0.36	0.017	0.227	0.98	0.02	40.2	
102A-3	159.0	171.3	0.763	0.127	11.1	114.6	0.0096	127.2	0.0600	0.2036	0.29	0.040	0.474	0.72	0.10	44.7	
102A-5	159.0	171.3	0.763	0.127	10.5	107.8	0.0102	120.6	0.0624	0.2088	0.30	0.041	0.491	0.68	0.11	42.5	*
102A-6	159.0	171.3	0.763	0.127	10.5	108.9	0.0096	120.9	0.0600	0.2036	0.29	0.040	0.472	0.69	0.10	42.3	

* INDICATES PLANE STRAIN FRACTURE TOUGHNESS VALUES (KSI-IN.1/2) OBTAINED FROM TESTS WHICH EXCEEDED ONE OR MORE OF THE FOLLOWING LIMITS. FG/FTY=1.0, AO/B=0.5, AND/OR CA/BW=0.1

PART-THROUGH-CRACK TENSILE DATA FOR MINUTEMAN 6AL-4V TITANIUM EXTRUDED CYLINDERS

FORGING SPECIMEN NUMBER	YIELD STRESS FTY (KSI)	ULT. STRESS FTU (KSI)	WIDTH W (IN.)	THICK-NESS B (IN.)	LOAD P-MAX (KIPS)	GROSS STRESS FG (KSI)	CRACK AREA CA (SQ.IN)	NET STRESS FN (KSI)	CRACK DEPTH AO (IN.)	CRACK LENGTH 2C (IN.)	CRACK SHAPE AO/2C	NORM. DEPTH AO/B	AO/B	FG/FTY	CA/BW	PLANE STRAIN KIC	
102B-1	163.0	175.7	0.765	0.124	15.3	161.4	0.0018	164.6	0.0288	0.0804	0.36	0.018	0.232	0.99	0.02	41.8	
102B-3	163.0	175.7	0.764	0.125	14.7	154.3	0.0020	157.6	0.0312	0.0804	0.39	0.018	0.251	0.95	0.02	39.9	
102B-4	163.0	175.7	0.764	0.124	15.4	163.3	0.0019	166.3	0.0300	0.0792	0.38	0.018	0.242	1.00	0.02	42.1	
102B-2	163.0	175.7	0.766	0.124	10.5	111.1	0.0096	123.6	0.0600	0.2036	0.29	0.040	0.484	0.68	0.10	43.1	*
102B-5	163.0	175.7	0.766	0.124	11.0	115.8	0.0096	128.8	0.0600	0.2036	0.29	0.040	0.484	0.71	0.10	45.1	*
102B-6	163.0	175.7	0.765	0.124	11.7	123.0	0.0091	136.0	0.0552	0.2088	0.26	0.040	0.445	0.75	0.10	47.8	
104A-1	162.0	173.0	0.767	0.126	14.8	153.6	0.0021	157.1	0.0336	0.0804	0.42	0.018	0.268	0.95	0.02	39.9	
104A-3	162.0	173.0	0.761	0.124	14.5	153.2	0.0021	156.7	0.0324	0.0828	0.39	0.018	0.261	0.95	0.02	40.3	
104A-4	162.0	173.0	0.761	0.127	14.4	150.1	0.0021	153.5	0.0324	0.0840	0.39	0.018	0.256	0.93	0.02	39.6	
104A-2	162.0	173.0	0.761	0.123	11.0	117.6	0.0088	129.9	0.0552	0.2036	0.27	0.039	0.449	0.73	0.09	45.2	
104A-5	162.0	173.0	0.761	0.124	10.8	114.0	0.0096	126.9	0.0600	0.2036	0.29	0.040	0.484	0.70	0.10	44.4	*
104A-6	162.0	173.0	0.766	0.123	9.6	101.9	0.0094	113.2	0.0588	0.2036	0.29	0.039	0.478	0.63	0.10	39.2	
104B-1	161.0	173.0	0.762	0.125	15.0	157.4	0.0021	160.9	0.0324	0.0828	0.39	0.018	0.259	0.98	0.02	41.5	
104B-3	161.0	173.0	0.763	0.126	15.0	156.0	0.0021	159.5	0.0324	0.0828	0.39	0.018	0.257	0.97	0.02	41.1	
104B-6	161.0	173.0	0.762	0.126	14.8	154.0	0.0023	157.8	0.0348	0.0840	0.41	0.019	0.276	0.96	0.02	40.9	
104B-7	161.0	173.0	0.762	0.126	11.2	106.4	0.0100	118.8	0.0612	0.2088	0.29	0.040	0.486	0.66	0.10	41.7	*
104B-4	161.0	173.0	0.762	0.127	10.3	107.4	0.0097	119.4	0.0624	0.1984	0.31	0.039	0.493	0.67	0.10	41.5	*
104B-5	161.0	173.0	0.763	0.126	9.9	103.7	0.0099	115.6	0.0600	0.2099	0.29	0.040	0.478	0.64	0.10	40.5	*
105A-3	162.0	174.3	0.763	0.125	15.1	158.5	0.0019	161.8	0.0300	0.0816	0.37	0.018	0.241	0.98	0.02	41.4	
105A-4	162.0	174.3	0.764	0.125	14.9	155.7	0.0021	159.2	0.0324	0.0828	0.39	0.018	0.259	0.96	0.02	41.0	
105A-5	162.0	174.3	0.764	0.125	15.0	157.5	0.0021	161.0	0.0312	0.0852	0.37	0.019	0.251	0.97	0.02	41.9	
105A-1	162.0	174.3	0.764	0.124	9.8	103.4	0.0100	115.6	0.0612	0.2088	0.29	0.040	0.494	0.64	0.11	40.5	*
105A-2	162.0	174.3	0.764	0.125	9.8	103.6	0.0098	115.8	0.0600	0.2088	0.29	0.040	0.482	0.64	0.10	40.4	*
105A-6	162.0	174.3	0.765	0.124	10.0	105.7	0.0094	117.4	0.0588	0.2036	0.29	0.039	0.474	0.65	0.10	40.8	

* INDICATES PLANE STRAIN FRACTURE TOUGHNESS VALUES (KSI-IN.1/2) ORTAINED FROM TESTS WHICH EXCEEDED ONE OR MORE OF THE FOLLOWING LIMITS. FG/FTY=1.0, AO/BW=0.5, AND/OR CA/BW=0.1

PART-THROUGH-CRACK TENSILE DATA FOR MINUTEMAN 6AL-4V TITANIUM EXTRUDED CYLINDERS

FORGING SPECIMEN NUMBER	YIELD STRESS FTY (KSI)	ULT. STRESS FTU (KSI)	WIDTH W (IN.)	THICK-NESS B (IN.)	LOAD P-MAX (KIPS)	GROSS STRESS FG (KSI)	CRACK AREA CA (SQ.IN)	NET STRESS FN (KSI)	CRACK DEPTH AO (IN.)	CRACK LENGTH 2C (IN.)	CRACK SHAPE AO/2C	NORM. DEPTH AO/B	AO/B	FG/FTY	CA/BW	PLANE STRAIN KIC
105B-2	161.0	174.0	0.764	0.124	14.5	153.3	0.0021	156.8	0.0336	0.0804	0.42	0.018	0.271	0.95	0.02	39.8
105B-5	161.0	174.0	0.764	0.124	14.8	156.3	0.0021	159.9	0.0336	0.0804	0.42	0.018	0.271	0.97	0.02	40.7
105B-6	161.0	174.0	0.764	0.123	14.8	157.8	0.0022	161.6	0.0336	0.0840	0.40	0.019	0.273	0.98	0.02	42.0
105B-1	161.0	174.0	0.763	0.124	10.6	111.6	0.0096	124.2	0.0600	0.2036	0.29	0.040	0.484	0.69	0.10	43.4 *
105B-3	161.0	174.0	0.764	0.125	10.3	108.4	0.0096	120.5	0.0600	0.2036	0.29	0.040	0.480	0.67	0.10	42.1 *
105B-4	161.0	174.0	0.763	0.124	10.0	105.6	0.0096	117.5	0.0600	0.2036	0.29	0.039	0.484	0.66	0.10	40.9 *
107A-2	159.0	171.0	0.763	0.123	13.7	146.5	0.0019	149.5	0.0300	0.0816	0.37	0.018	0.245	0.92	0.02	37.9
107A-3	159.0	171.0	0.763	0.125	15.1	158.7	0.0018	161.9	0.0300	0.0780	0.38	0.017	0.240	1.00	0.02	40.7
107A-6	159.0	171.0	0.763	0.125	15.3	160.9	0.0018	164.1	0.0288	0.0804	0.36	0.018	0.230	1.01	0.02	41.8 *
107A-1	159.0	171.0	0.762	0.126	10.5	109.3	0.0096	121.5	0.0588	0.2088	0.28	0.040	0.467	0.69	0.10	42.6 *
107A-4	159.0	171.0	0.763	0.127	10.9	113.1	0.0088	124.4	0.0564	0.1984	0.28	0.038	0.446	0.71	0.09	43.2
107A-5	159.0	171.0	0.762	0.126	10.7	111.3	0.0092	123.2	0.0576	0.2036	0.28	0.039	0.457	0.70	0.10	43.0
107B-1	159.0	170.3	0.765	0.126	14.5	150.8	0.0022	154.4	0.0336	0.0840	0.40	0.018	0.268	0.95	0.02	40.0
107B-3	159.0	170.3	0.766	0.125	14.7	153.9	0.0021	157.5	0.0324	0.084	0.39	0.018	0.259	0.97	0.02	40.8
107B-6	159.0	170.3	0.766	0.125	14.9	155.5	0.0019	158.7	0.0300	0.0816	0.37	0.018	0.240	0.98	0.02	40.6
107B-2	159.0	170.3	0.766	0.125	10.5	109.4	0.0092	121.2	0.0576	0.2036	0.28	0.039	0.461	0.69	0.10	42.3
107B-4	159.0	170.3	0.765	0.125	9.8	102.9	0.0094	114.2	0.0588	0.2036	0.29	0.039	0.470	0.65	0.10	39.7
107B-5	159.0	170.3	0.766	0.125	10.6	111.0	0.0094	123.1	0.0588	0.2036	0.29	0.040	0.470	0.70	0.10	43.0
108A-2	163.0	174.3	0.761	0.126	14.2	149.1	0.0022	152.6	0.0336	0.0828	0.41	0.018	0.268	0.91	0.02	39.1
108A-5	163.0	174.3	0.761	0.126	15.0	156.6	0.0021	160.1	0.0324	0.0816	0.40	0.018	0.257	0.96	0.02	40.9
108A-6	163.0	174.3	0.761	0.126	15.2	158.2	0.0024	162.3	0.0360	0.0864	0.42	0.019	0.286	0.97	0.03	42.7
108A-1	163.0	174.3	0.762	0.126	10.8	104.1	0.0094	115.5	0.0576	0.2088	0.28	0.039	0.457	0.64	0.10	40.3
108A-3	163.0	174.3	0.762	0.121	10.7	116.3	0.0092	129.1	0.0588	0.1984	0.30	0.039	0.486	0.71	0.10	44.6
108A-4	163.0	174.3	0.760	0.125	10.0	104.8	0.0094	116.3	0.0588	0.2036	0.29	0.039	0.470	0.64	0.10	40.4

* INDICATES PLANE STRAIN FRACTURE TOUGHNESS VALUES (KSI-IN.1/2) OBTAINED FROM TESTS WHICH EXCEEDED ONE OR MORE OF THE FOLLOWING LIMITS. FG/FTY=1.0, AO/B=0.5, AND/OR CA/BW=0.1

PART-THROUGH-CRACK TENSILE DATA FOR MINUTEMAN 6AL-4V TITANIUM EXTRUDED CYLINDERS

FORGING SPECIMEN NUMBER	YIELD STRESS FTY (KSI)	ULT. STRESS FTU (KSI)	WIDTH W (IN.)	THICK-NESS B (IN.)	LOAD P-MAX (KIPS)	GROSS STRESS FG (KSI)	CRACK AREA CA (SQ.IN)	NET STRESS FN (KSI)	CRACK DEPTH AO (IN.)	CRACK LENGTH 2C (IN.)	CRACK SHAPE AO/2C	NORM. DEPTH AO/B	AO/B	FG/FTY	CA/BW	PLANE STRAIN KIC
1088-2	161.0	173.0	0.765	0.126	15.1	157.0	0.0022	160.7	0.0336	0.0840	0.40	0.019	0.267	0.97	0.02	41.7
1088-5	161.0	173.0	0.764	0.127	14.9	153.9	0.0023	157.6	0.0360	0.0816	0.44	0.018	0.283	0.96	0.02	40.3
1088-6	161.0	173.0	0.764	0.126	14.9	155.6	0.0019	158.7	0.0300	0.0804	0.37	0.018	0.239	0.97	0.02	40.3
1088-1	161.0	173.0	0.766	0.127	9.4	96.3	0.0092	106.4	0.0576	0.2036	0.28	0.039	0.454	0.60	0.09	36.9
1088-3	161.0	173.0	0.765	0.127	9.8	101.1	0.0092	111.7	0.0564	0.2088	0.27	0.039	0.444	0.63	0.10	38.9
1088-4	161.0	173.0	0.765	0.126	9.8	101.9	0.0096	113.2	0.0588	0.2088	0.28	0.048	0.467	0.63	0.10	39.6
1098-2	161.0	172.7	0.764	0.125	14.8	154.7	0.0021	158.1	0.0324	0.0816	0.40	0.018	0.259	0.96	0.02	40.4
1098-4	161.0	172.7	0.763	0.125	14.8	155.9	0.0020	159.3	0.0312	0.0828	0.38	0.018	0.251	0.97	0.02	41.0
1098-6	161.0	172.7	0.761	0.125	14.6	153.3	0.0022	156.9	0.0324	0.0864	0.37	0.019	0.259	0.95	0.02	41.1
1098-1	161.0	172.7	0.764	0.122	9.7	104.1	0.0092	115.6	0.0564	0.2088	0.27	0.039	0.462	0.65	0.10	40.2
1098-3	161.0	172.7	0.763	0.125	9.6	100.8	0.0086	110.9	0.0540	0.2036	0.27	0.038	0.434	0.63	0.09	38.2
1098-5	161.0	172.7	0.762	0.125	9.8	103.2	0.0092	114.3	0.0576	0.2036	0.28	0.039	0.461	0.64	0.10	39.6
1108-2	161.0	172.3	0.761	0.126	15.3	159.6	0.0019	162.8	0.0300	0.0804	0.37	0.018	0.238	0.99	0.02	41.4
1108-5	161.0	172.3	0.761	0.126	15.4	160.9	0.0022	164.6	0.0324	0.0852	0.38	0.019	0.258	1.00	0.02	43.1
1108-6	161.0	172.3	0.760	0.126	15.4	160.7	0.0020	164.2	0.0312	0.0828	0.38	0.018	0.248	1.00	0.02	42.4
1108-1	161.0	172.3	0.759	0.126	11.7	123.0	0.0092	136.2	0.0576	0.2036	0.28	0.048	0.459	0.76	0.10	47.9
1108-3	161.0	172.3	0.761	0.126	11.9	124.6	0.0092	137.9	0.0576	0.2036	0.28	0.048	0.459	0.77	0.10	48.5
1108-4	161.0	172.3	0.761	0.126	11.3	118.3	0.0092	130.9	0.0576	0.2036	0.28	0.048	0.459	0.73	0.10	45.9
1118-2	161.0	170.7	0.764	0.124	14.3	151.4	0.0019	154.5	0.0312	0.0792	0.39	0.017	0.252	0.94	0.02	38.9
1118-4	161.0	170.7	0.765	0.125	14.7	153.9	0.0018	156.9	0.0288	0.0792	0.36	0.017	0.230	0.96	0.02	39.4
1118-6	161.0	170.7	0.764	0.126	14.6	152.0	0.0022	155.5	0.0336	0.0828	0.41	0.018	0.267	0.94	0.02	40.0
1118-1	161.0	170.7	0.765	0.125	11.1	116.9	0.0098	130.2	0.0612	0.2036	0.30	0.048	0.492	0.73	0.10	45.7 *
1118-3	161.0	170.7	0.764	0.125	10.5	109.7	0.0100	122.5	0.0624	0.2036	0.31	0.048	0.499	0.68	0.10	42.9 *
1118-5	161.0	170.7	0.764	0.125	10.5	109.4	0.0096	121.7	0.0588	0.2080	0.28	0.048	0.470	0.68	0.10	42.7 *

* INDICATES PLANE STRAIN FRACTURE TOUGHNESS VALUES (KSI-IN.1/2) OBTAINED FROM TESTS WHICH EXCEEDED ONE OR MORE OF THE FOLLOWING LIMITS. FG/FTY=1.0, AO/B=0.5, AND/OR CA/BW=0.1

PART-THROUGH-CRACK TENSILE DATA FOR MINUTEMAN 6AL-4V TITANIUM EXTRUDED CYLINDERS

FORGING SPECIMEN NUMBER	YIELD STRESS FTY (KSI)	ULT. STRESS FTU (KSI)	WIDTH W (IN.)	THICK-NESS B (IN.)	LOAD P-MAX (KIPS)	GROSS STRESS FG (KSI)	CRACK AREA CA (SQ.IN)	NET STRESS FN (KSI)	CRACK DEPTH AO (IN.)	CRACK LENGTH 2C (IN.)	CRACK SHAPE AO/2C	NORM. DEPTH AO/B	AO/B	FG/FTY	CA/BW	PLANE STRAIN KIC	
112A-2	161.0	173.3	0.766	0.124	14.5	152.3	0.0019	155.5	0.0312	0.0792	0.39	0.017	0.252	0.95	0.02	39.1	
112A-4	161.0	173.3	0.765	0.124	15.0	157.6	0.0016	160.4	0.0264	0.0792	0.33	0.017	0.213	0.98	0.02	40.2	
112A-5	161.0	173.3	0.765	0.129	14.9	151.1	0.0019	154.0	0.0300	0.0804	0.37	0.027	0.233	0.94	0.02	39.0	
112A-1	161.0	173.3	0.765	0.124	10.7	113.1	0.0098	126.2	0.0600	0.2088	0.29	0.041	0.484	0.70	0.10	44.4	*
112A-3	161.0	173.3	0.765	0.123	10.6	112.2	0.0098	125.3	0.0600	0.2088	0.29	0.040	0.486	0.70	0.10	44.0	*
112A-6	161.0	173.3	0.766	0.125	11.1	115.7	0.0091	127.8	0.0552	0.2088	0.26	0.039	0.442	0.72	0.09	44.8	
112B-4	163.0	175.3	0.762	0.127	15.4	158.6	0.0020	161.9	0.0300	0.0840	0.36	0.018	0.236	0.97	0.02	41.9	
112B-5	163.0	175.3	0.762	0.127	15.8	163.3	0.0018	166.3	0.0288	0.0792	0.36	0.017	0.227	1.00	0.02	42.0	*
112B-6	163.0	175.3	0.761	0.126	15.5	161.9	0.0018	164.9	0.0276	0.0816	0.34	0.018	0.219	0.99	0.02	42.0	
112B-1	163.0	175.3	0.763	0.126	11.5	120.3	0.0088	132.5	0.0564	0.1984	0.28	0.039	0.449	0.74	0.09	46.1	
112B-2	163.0	175.3	0.762	0.126	11.6	120.4	0.0090	132.9	0.0564	0.2036	0.28	0.039	0.448	0.74	0.09	46.5	
112B-3	163.0	175.3	0.762	0.126	11.5	120.1	0.0088	132.2	0.0552	0.2036	0.27	0.039	0.438	0.74	0.09	46.2	

ADDENDUM B-2

COMPUTER PROGRAM DETAILS

Appendix B

I. GE-225 COMPUTER SYSTEM

The computer programs used in this study were written by Mr. Robert I. Uecker of the Propulsion R&D Division, Aerojet, Sacramento, for a General Electric 225 Information Processing System. The GE-225 computer is a medium-scale, general-purpose digital system which provides an economical means of processing large volumes of data at high speed. The computer is a solid-state, single-address system which operates under both stored program and operator control. The system is buffered with an input-output priority system which permits simultaneous operations such as reading, printing, and processing. The access time associated with transferring a word into and out of memory is 18 microsec. The memory-core storage is limited to 8,000 locations.

The programing language is card FORTRAN IV, which may be considered a sub-set of the IBM 709/90 FORTRAN language. These computer programs could be accepted by other computer systems with only a minimum amount of programing alterations.

The computer accepts the program input data from punched IBM cards containing alphabetic and numeric data. The output data can be in the form of printed reports, punched IBM cards, or a combination of both methods.

II. PROGRAM FOR COMPUTING K_{Ic}

A. OBJECTIVE

To compute the plane-strain fracture-toughness (K_{Ic}) from FTC tensile data.

B. COMPUTER PROGRAM INPUT

1. Specimen Designation Number
2. Failure Load, PF
3. Fatigue Crack Depth, AO

II, B, Computer Program Input (cont.)

4. Fatigue Crack Length, 2C
5. Specimen Width, W
6. Specimen Thickness, B
7. Tensile Yield Strength, Fty
8. Computer Program Flags

C. PROGRAM EQUATIONS

1. $$\phi = \int_0^{\pi/2} \sqrt{1 - \left[\frac{(2C/2)^2 - AO^2}{(2C/2)^2}\right] SIN^2\,\theta}\; d\theta$$

2. $$FG = PF/WxB$$

3. $$Q = \phi^2 - .212\left(\frac{FG}{FTY}\right)^2$$

4. $$CA = \pi/4 \times AO \times 2C$$

5. $$FN = PF/(WxB - \pi/4 \times AO \times 2C)$$

6. $$K_{Ic}^2 = 1.21\pi \times AO \times FG^2/Q$$

7. $$2RP = \frac{1}{2\pi\sqrt{2}} \left(\frac{K_{Ic}}{FTY}\right)^2$$

8. $$K_{Ic} = \left[1 + 0.12\,(1 - \frac{AO}{C})\right] \frac{F(\pi AO)^{1/2}}{\phi} \left[\frac{2B}{\pi AO} \tan \frac{\pi AO}{2B}\right]^{1/2}$$

D. PROGRAM OUTPUT

1. Specimen Number
2. Failure Load, PF
3. Gross Stress, FG
4. Fatigue Crack Depth, AO
5. Fatigue Crack Length, 2C
6. Ratio of Crack Depth to Length, AO/2C

II, D, Program Output (cont.)

7. Flaw-Shape Parameter, Q
8. Normalized Crack Depth, A/Q
9. Fracture Toughness, K_{Ic}

   a. As computed from Irwin's expression (C,6)
   b. As computed from Paris' expression (C,8)

10. Ratios of Irwin's and Paris' K_{Ic} Values
11. Fatigue Crack Area, CA
12. Net Stress, Fnet
13. Ratioed-Values

   a. Crack Depth to Specimen Thickness, AO/B
   b. Crack Area to the Product of the Specimen Width and Thickness, CA/BW
   c. Net Stress to the Tensile Yield Strength, Fnet/Fty
   d. Gross Stress to the Tensile Yield Strength, FG/FTY
   e. Thickness to Plastic-Zone Size, B/2RP

III. COMPUTER ITERATION PROGRAM

A. OBJECTIVES

1. To calculate the area of the fatigue crack when the net stress (plus or minus 0.1 ksi) is equal to the 0.2% offset yield strength.

2. To calculate the net stress when the area of the crack is 0.010 sq in.

III, Computer Iteration Program (cont.)

B. COMPUTER PROGRAM INPUT

1. Specimen Number
2. Average K_{IC} factor for specimens corresponding to a nominal crack size of:

   a. 0.002 sq in.
   b. 0.010 sq in.

3. Average ratios of the fatigue crack depth to crack length (A0/2C) for specimens corresponding to a nominal crack size of:

   a. 0.002 sq in.
   b. 0.010 sq in.

4. Average product of the specimen thickness and specimen width.
5. Tensile yield strength (0.2% offset) for each ring material.
6. First estimate of the ratio of the gross stress and the tensile yield strength.
7. The required area of the fatigue crack.

C. COMPUTER PROGRAM NOMENCLATURE

SYMBOL	DESCRIPTION
AK_{Ic}	Average K_{Ic} factor for specimens containing a designated size of crack
DTOL	Average ratio of the fatigue crack depth to crack length for specimens containing a designated size of crack
BW	Average product of the specimen thickness and specimen width
Fty	0.2% offset yield strength for each ring material

III, C, Computer Program Nomenclature (cont.)

SYMBOL	DESCRIPTION
FG	Gross stress
Fnet	Net stress
AO	Fatigue-crack depth
2C	Fatigue-crack length
PF	Failure load
Q	Flaw-shape parameter
CA	Area of the fatigue crack
RB	Variable upper limit for the iteration on the ratio of the gross stress to the tensile yield strength
RS	Variable lower limit for the iteration on the ratio of the gross stress to the tensile yield strength
F	Variable estimate of the ratio of the gross stress to the tensile yield strength
A1	Computed fatigue crack depth derived from the input crack area and the iteration scheme on the fracture toughness equation
ϕ	The value of the elliptical integral computed from the input value of the ratio of the fatigue crack depth to crack length
RGUS	First estimate of the ratio of the gross stress and the tensile yield strength.

D. INITIAL CALCULATION

The value of the elliptical integral

$$\phi = \int_0^{\frac{\pi}{2}} \sqrt{1 - \left[1 - (2\text{xDTOL})^2\right] \sin^2\theta} \; d\theta$$

III, Computer Iteration Program (cont.)

E. ITERATION SCHEME

1. Initial Calcuations

$$RB = 2 \times RGUS$$

$$FG = RB \times Fty$$

$$Q = \phi 2 - 0.212 \times FG^2$$

$$AO = \frac{AKIc^2 \times Q}{1.21 \times \pi \times FG^2}$$

$$2C = AO/DTOL$$

$$PF = BW \times FG$$

$$Fnet = PF/\left(BW - \left[\pi/4 \times AO \times 2C\right]\right) \quad \text{*Note}$$

2. First Net-Stress-Value Test Fnet $\leq$ Fty

a. If the net-stress test statement is true, the computed value of net stress is too small. Therefore, RB is also too small and must be increased.

(1) RB = 2 x RB

(2) Return to iteration scheme (step E,1)

b. If the net-stress test statement is not true, the computed value of net stress is too large. Therefore, the current estimate of the ratio of the gross stress to tensile yield strength (F) must be smaller than RB.

*Note:
The remaining portion of the iteration pertains only to the first program objective. The same iteration method is used to achieve the second objective, except the iteration is used to calculate a fatigue crack depth instead of a net stress.

III E, Iteration Scheme (cont.)

(1) RS = o.
(2) F = (RF + RS)/2
(3) FG = F x Fty
(4) Q = $\phi 2 - 0.212 \times F^2$
(5) AO = $AK_{Ic}^2 \times Q/1.21 \pi \times FG^2$
(6) 2C = AO/DTOL
(7) BW = BW x FG
(8) Fnet = PF$\left[BW - (\pi/4 \times AO \times 2C) \right]$

3. Second Net-Stress-Value Test: For absolute value of (Fnet = Fty)$\leq$ 100

a. If the net-stress-value test statement is true, the present value of the net stress meets the requirement listed in the first program objective

(1) Compute the area of the fatigue crack using the present values of the crack parameters (AO) and(2C).

$$CA = \pi/4 \times AO \times 2C$$

(2) Print the entire program output.

b. If the net-stress-value test is not true, test to determine if the present value of the net stress is smaller than, equal to, or greater than the input tensile yield strength.

(1) Fnet < Fty

If this test statement is true, the current estimate of the ratio of the gross stress to the tensile yield strength (F) is too small. Therefore RS = F.

III, E, Iteration Scheme (cont.)

Test to determine if the current upper limit for the iteration and lower limit for the iteration still differ by at least 0.000001.

(a) If the limiting-values test is true, compute a new current estimate of the ratio of the gross stress to the tensile yield strength, by returning to step E,2,b,(2), of the iteration scheme.

(b) If the limiting-values test fails, the first program objective cannot be achieved. Therefore, calculate the area of the fatigue crack using the present values of AO and 2C, and print out the entire program output.

(2) Fnet = Fty

If this test statement is true, the first program objective is satisfied.

(a) Calculate the area of the fatigue crack using the present values of AO and 2C.

(b) Print the entire program output.

(3) Fnet > Fty

(a) If this test statement is true, the current estimate of the ratio of the gross stress to the tensile yield strength (F) is too large. Therefore set RB = F.

III, E, Iteration Scheme (cont.)

(b) Go to the test to determine if the current upper limit for the iteration and lower limit for the iteration still differ by at least 0.000001 (step E,3,b,(1)).

F. COMPUTER PROGRAM OUTPUT FOR THE FIRST OBJECTIVE*

1. Specimen Number
2. Fatigue Crack Depth
3. Fatigue Crack Length
4. Gross Stress
5. Net Stress
6. Ratio of Gross Stress to Tensile Yield Strength, F/Fty
7. Flaw Shape Parameter, Q
8. Area of the Fatigue Crack at Fnet = Fty

*See Paragraph III,A,1, and footnote on page 6 of this appendix.

ADDENDUM B-3

EFFECT OF HEAT TINTING ON PLASTICALLY DEFORMED METAL

Appendix B

TABLE OF CONTENTS

Addendum B-3

		Page
I.	Background	168
II.	Objective	168
III.	Procedure	168
IV.	Discussion of Results	168
V.	Conclusion	170

Appendix B

FIGURE LIST

	Figure
Typical Load-Elongation Curves for Ti-6Al-4V Prestrained, Heated to 800°F for 1 hr, and Reloaded--Ring 26, Specimen 3	1
Typical Load-Elongation Curves for Ti-6Al-4V Prestrained and Reloaded Without 800°F for 1 hr Treatment--Ring 26, Specimen 9	2

Appendix B

I. BACKGROUND

When the PTC tensile specimens are precracked by fatigue cycling, a plastic zone forms at the tip of fatigue crack. It is in this zone that the initial crack extension (pop-in) occurs during tensile testing. In this study, to facilitate the measurement of crack area after testing, all specimens were heat tinted after being fatigue cracked. This staining procedure was required by STL and consisted of heating the specimens in air to 800°F for a period of 1 hr.

III. OBJECTIVE

The objective of the following tests was to determine the effect of the heat staining on the mechanical properties of plastically deformed 6Al-4V titanium.

III. PROCEDURE

Nine 0.250-in.-dia tensile specimens were tested from each of three forgings. Duplicate specimens from each group were heated to 800°F for 1 hr without prestrain, cooled to room temperature, and tensile tested to failure. A third specimen from each group was prestrained, unloaded and then reloaded to failure, without intermediate heating. The remaining six specimens were prestrained, heated to 800°F/1 hr, and then reloaded to failure. The prestraining was 1, 2, and 4% elongation over a 1-in. gage length.

From these tests, the following comparisons were made to determine if the 800°F for 1-hr treatment produced an effect on the mechanical properties of the plastically deformed metal: (1) compare yield strength (0.2% offset) with and without the 800°F for 1-hr treatment; (2) compare the load elongation curves obtained in the prestraining operation with the load elongation curves obtained in reloading; (3) compare the ultimate tensile strength after the 800°F for 1 hr treatment, with and without prestraining; and (4) compare the tensile ductility (percent reduction of area), with and without the 800°F for 1-hr treatment.

IV. DISCUSSION OF RESULTS

A. EFFECT OF 800°F FOR 1-HR TREATMENT ON YIELD STRENGTH

Duplicate specimens from each ring were heated to 800°F for 1 hr and then tested to failure without prestraining. A comparison of the yield strength obtained from these specimens and from specimens tested without the 800°F for 1-hr treatment (viz., data from integral-coupon qualification tests and data from the prestraining operation) is shown below and indicates slightly lower yield strength after heating to 800°F for 1 hr.

IV, A, Effect of 800°F for 1-Hr Treatment on Yield Strength (cont.)

Forging Number	0.2% Offset Yield Strength (ksi) Qualification Test Data	Prestrained Material	800°F-1 hr (Not Prestrained)
26	157-160 Av (3) 159	154.0-164.0 Av (7) 159.4	153.6-154.0 Av (2) 153.8
56A	160-165 Av (3) 163	156.6-168.5 Av (7) 163.4	159.5-164.1 Av (2) 161.8
109B	160-163 Av (3) 161	160.2-164.0 Av (7) 162.3	159.8-161.3 Av (2) 160.5

Note that excellent agreement was obtained between the yield strengths measured in the qualification tests and those measured in the prestraining operation (before the 800°F for 1-hr treatment).

B. EFFECT OF 800°F FOR 1 HR ON PRESTRAINED MATERIAL

Three criteria were used in evaluating the possible effect of the 800°F for 1-hr heat-tinting operation on the mechanical properties of plastically deformed metal at a crack tip: (1) a comparison of the maximum stress used in prestraining and the 0.2% offset yield stress on reloading after heat tinting; (2) a comparison of the ultimate tensile strength after heat tinting, with and without prestraining; and (3) a comparison of ductility (percent reduction of area) with and without heat tinting. The test results (Table 1 of this Appendix) indicated that heat tinting following prestraining had a strengthening effect on plastically deformed metal. The effect appeared to be independent of the amount of strain in the range investigated (1 to 4%). Conversely, reduction of area measurements indicated the 800°F for 1-hr treatment following prestraining had no effect on the material. The following summarizes the test results based on average increases in strength produced by prestraining followed by heating to 800°F for 1 hr:

Ring No.	Increase in Stress on Reloading (psi)	Increase in Tensile Strength (psi)*
26	2600 - 6200 Av (6) 4200	900 - 10800 Av (6) 7400
56A	5100 - 7700 Av (6) 6400	6000 - 13300 Av (6) 10300
109B	5000 - 7600 Av (6) 6400	400 - 7200 Av (6) 4500

*The increase in tensile strength is based on a comparison between heat stained material with and without prestrain; thus, from Table 1, 1% prestrain raised the tensile strength of Ring 26 material from 164.6 to 169.6 ksi, or 5000 psi.

IV, Discussion of Results (cont.)

C. EFFECT OF PRESTRAINING WITHOUT THE 800°F FOR 1-HR TREATMENT

In the absence of strain aging, theoretically the load-elongation curve on reloading should be simply an extension of the initial load-elongation curve. Figure 1 of this appendix presents the load-elongation curves for Ring 26, Specimen 2, which was strained 1.0%, unloaded, heated to 800°F for 1 hr and then reloaded to failure. An increase in load (at 0.2% offset) after the 800°F for 1 hr treatment is clearly seen. Figure 2 of this appendix presents the load-elongation curves for Ring 26, Specimen 9, which was strained 1.0% and then immediately reloaded without the 800°F for 1-hr treatment. No significant increase is seen between the load corresponding to the prestraining value and the 0.2% offset value on reloading. The following table summarizes the effect of 1.0% prestrain with and without the 800°F for 1-hr treatment:

Ring No.	Pre-Strain	800°F for 1 hr	Stress Increase on Reloading (psi)	Increase in Tensile Strength (psi)
26	0.9	No	1800	----
	1.0	Yes	4400	1400*
56A	1.0	No	160	----
	1.0	Yes	6000	4100*
109B	1.0	No	3600	----
	1.0	Yes	7200	600*

V. CONCLUSION

Prestraining alone (without subsequent elevated temperature treatment) caused a small increase in the yield strength; whereas, heat tinting alone (without prestraining) caused a small decrease in the yield and ultimate tensile strengths. Conversely, the combination of prestrain and an 800°F for 1-hr treatment caused a significant increase in the yield strength of all three ring materials investigated. Therefore, it can be concluded that the 800°F for 1-hr heat-tinting operation following fatigue cracking of the PTC specimens may have altered the mechanical properties of the plastically deformed metal along the fatigue-crack front.

*NOTE: The increase in tensile strength is based on a comparison between prestrained material with and without heat staining; thus, in Table 1 800°F for 1 hr raised the tensile strength of 1% prestrained, Ring-26 material from 168.2 to 169.6 ksi, or 1400 psi.

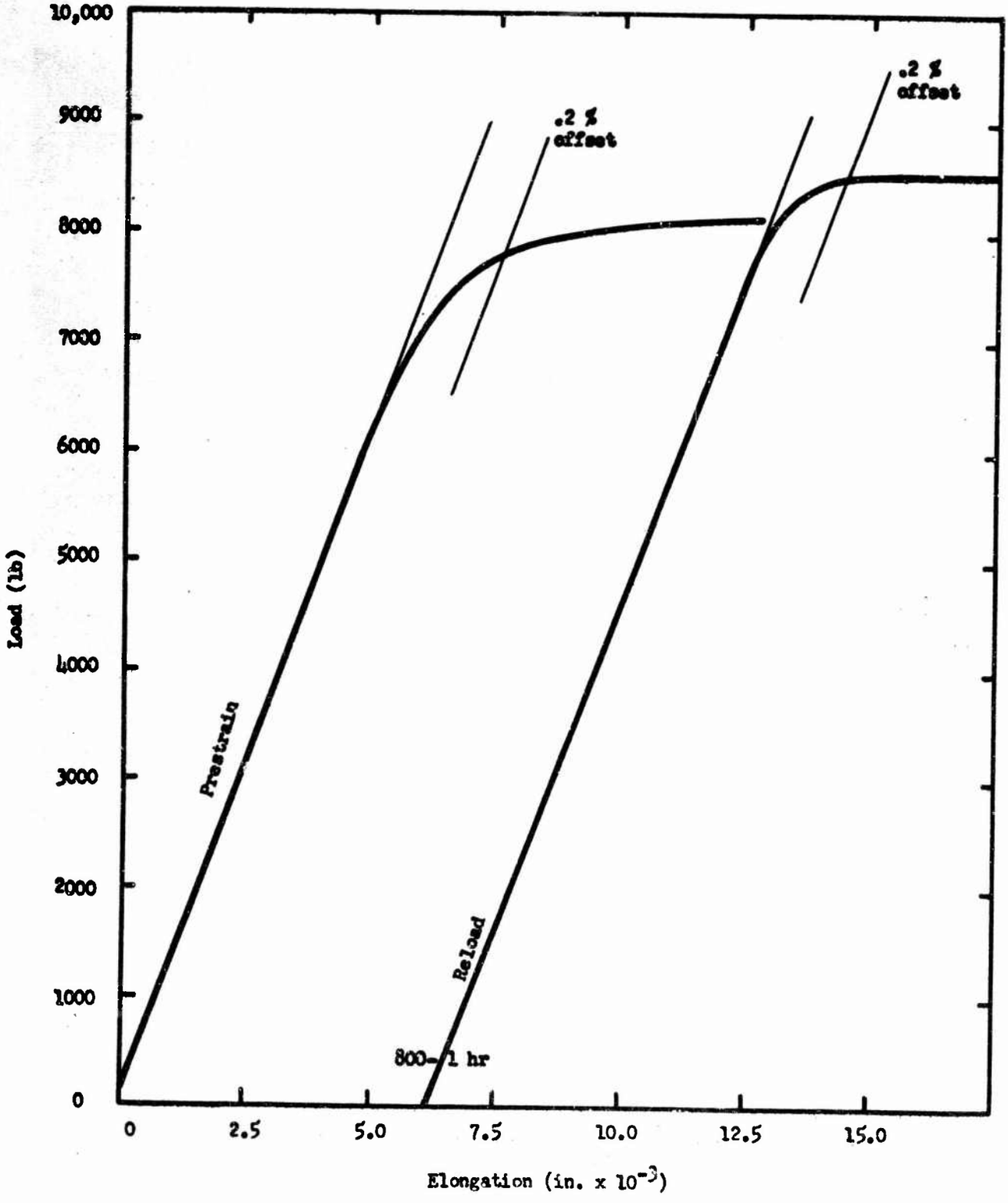


Figure 1. Typical Load-Elongation Curves for Ti-6Al-4V Prestrained, Heated to 800°F for 1 hr, and Reloaded--Ring 26, Specimen 3

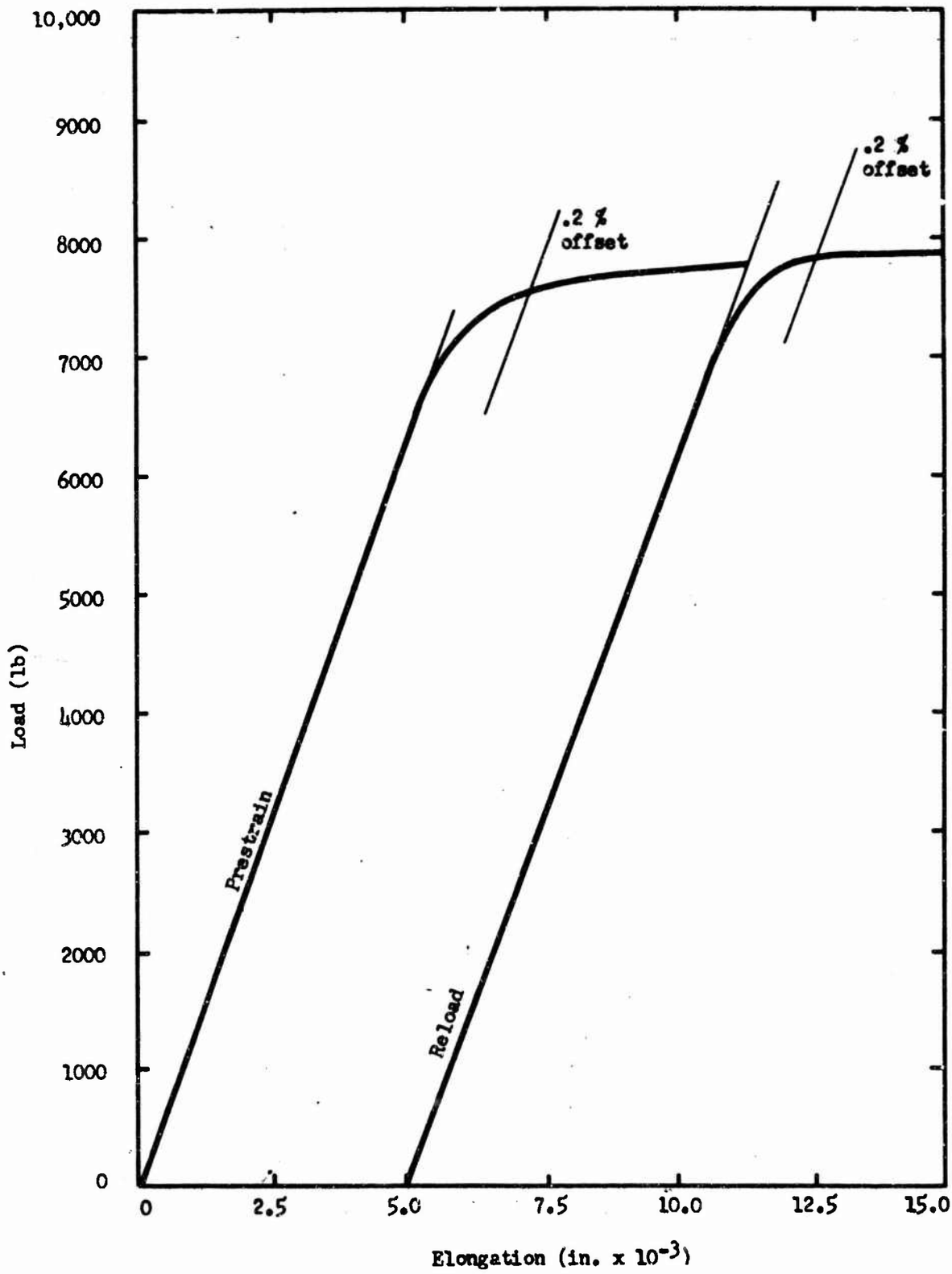


Figure 2. Typical Load-Elongation Curves for Ti-6Al-4V Prestrained and Reloaded Without 800°F for 1 hr Treatment--Ring 26, Specimen 9

TABLE I

EFFECT OF THE 800°F FOR 1-HR HEAT-TINTING TREATMENT ON THE TENSILE PROPERTIES OF 6A1-4V TITANIUM

Remarks	Specimen Number	Pre Strain (%)	0.2% Offset Yield (ksi)	Prestraining Stress at Unloading (ksi)	Reloading 0.2% Offset Stress (ksi)	Reload Stress Increase (ksi)	Ultimate Tensile (ksi)	Reload Increase (ksi)	R.A. (%)
26	Ring Qualification		159(*1)				171(*1)		
	Heat Tint Only								
	1	-	154.0	-	-	-	164.3	-	44.1
	2	-	153.6	-	-	-	164.9	-	42.3
			Av 153.8(*2)				Av 164.6(*2)		
	Prestrain Followed by Heat Tint								
	3	1.0	159.5(*3)	167.5	173.7	6.2	173.7	9.1	41.1
	4	1.0	154.0(*3)	161.0	163.6	2.6	165.5	0.9	46.6
				Av 164.2	Av 168.6	Av 4.4	Av 169.6	Av 5.0 (*5)	
	5	1.9	160.0(*3)	168.0	172.3	4.3	172.4	7.8	47.2
	6	2.0	161.5(*3)	170.8	173.4	4.6	173.4	10.8	44.0
				Av 169.4	Av 173.8	Av 4.4	Av 173.9	Av 9.3 (*6)	
	7	3.8	164.0(*3)	171.0	174.1	3.1	174.9	10.3	44.6
	8	4.0	161.0(*3)	166.0	170.1	4.1	170.4	5.8	38.5
				Av 168.5	Av 172.1	Av 3.6	Av 172.6	Av 8.0 (*6)	
	Prestrain Only								
	9	0.9	196.8(*3) 199.4(*3)	160.0	161.8	1.8(*4)	168.2	1.4(*5)	32.2
96A	Ring Qualification		163(*1)				176(*1)		
	Heat Tint Only								
	1	-	164.1	-	-	-	176.6	-	37.6
	2	-	159.5	-	-	-	164.1	-	35.8
			Av 161.8(*2)				Av 170.3(*2)		
	Prestrain Followed by Heat Tint								
	3	1.0	156.5(*3)	170.8	176.1	5.3	176.3	6.0	39.3
	4	0.9	165.5(*3)	175.0	181.8	6.8	182.9	11.6	42.2
				Av 172.9	Av 178.9	Av 6.0	Av 179.1	Av 8.8 (*6)	
	5	2.0	161.5(*3)	172.8	180.5	7.7	180.6	10.3	38.6
	6	2.1	166.0(*3)	176.0	183.4	7.4	183.6	13.3	39.2
				Av 174.4	Av 181.9	Av 7.5	Av 182.1	Av 11.8 (*6)	
	7	4.0	168.5(*3)	176.1	181.2	5.1	181.4	11.1	36.1
	8	3.9	165.5(*3)	173.5	179.3	5.8	179.4	9.1	35.5
				Av 174.8	Av 180.2	Av 5.4	Av 180.4	Av 10.1 (*6)	
	Prestrain Only								
	9	1.0	160.0(*3) 163.4(*3)	169.8	169.9	0.16(*4)	175.0	4.1(*5)	36.7
109B	Ring Qualification		164.5(*1)				173(*1)		
	Heat Tint Only								
	1	-	161.3	-	-	-	172.5	-	34.5
	2	-	160.8	-	-	-	170.3	-	36.0
			Av 161.1(*2)				Av 171.4(*2)		
	Prestrain Followed by Heat Tint								
	3	1.0	164.0(*3)	165.0	171.8	6.8	171.8	0.4	38.4
	4	1.0	162.0(*3)	168.5	176.1	7.6	176.1	4.7	40.8
				Av 166.8	Av 173.9	Av 7.2	Av 173.9	Av 2.6 (*6)	
	5	1.9	161.5(*3)	169.0	175.8	6.8	176.0	4.6	39.5
	6	2.0	163.0(*3)	172.0	178.6	6.6	178.6	7.2	36.0
				Av 170.5	Av 177.2	Av 6.7	Av 177.3	Av 5.9 (*6)	
	7	3.8	161.5(*3)	169.0	174.0	5.0	174.4	3.0	43.1
	8	3.7	164.0(*3)	172.5	178.4	5.9	178.5	7.1	39.6
				Av 170.8	Av 176.2	Av 5.4	Av 176.4	Av 5.6 (*6)	
	Prestrain Only								
	9	1.0	160.2(*3)	164.8	168.4	3.6(*4)	173.3	0.6(*5)	38.6
			Av 162.3(*3)						

NOTE:

(*1) From integral coupon qualification tests
(*2) After heat tinting at 800°F-1 hr
(*3) 0.2% Offset yield strength in prestraining before heat tinting
(*4) Reloaded without heat tinting
(*5) Comparison of UTS after 1.0% pre-strain with and without heat tinting
(*6) Comparison of UTS after Heat tinting with and without prestrain

APPENDIX C

CENTER-NOTCH TENSILE TESTING FOR K_{Ic} AND K_c DATA

Appendix C

TABLE OF CONTENTS

		Page
A.	Center-Notch-Tensile Test Material	176
B.	CN-Tensile Test Procedures and Calculations	181
C.	Tabulation of Center-Notch-Tensile Data	193
	1. Table I--Room Temperature Data for Parent Metal	194
	2. Table II--Elevated-Temperature Data for Parent Metal	196
	3. Table III-Room Temperature Data for Welds in Chamber SN 673078.	197

LIST OF FIGURES

Figure		
1	Fracture in 44-in.-dia Minuteman Chamber S/N 2191456. Failure originated in the forward girth weld at 457 psig (circles denote weld repairs).	177
2	Center-Notch Tensile Specimen	182
3	Calibration Curve for Converting Crack Opening Displacement to Crack Length of CN-Tensile Specimen (0.200-in. gage length)	183
4	Typical Plots of Stress-Wave Emission Count Rate (SWE/sec) versus Load	184
5	Heat-Tinted CN-Tensile Fracture Surfaces Showing Crack Length at Maximum Load	186
6	K Calibration for the CN-Tensile Test. $K = Y \cdot Pa^{1/2}/BW$.	191

Appendix C

A. CENTER-NOTCH TENSILE TEST MATERIAL

The following is a brief history of the chambers from which the CN-tensile data have been taken.

1. Chamber R26

Chamber R26 failed during proof test at 96 ksi with the fracture origin in the forward cylinder. Examination of the fracture surface revealed a surface crack in the forward cylinder near the heat-affected zone of the weld; the defect was approximately semi-circular, 0.10-in. deep and 0.18-in. long in the ID surface. Allison Division of General Motors Corporation conducted PTC tensile tests of the material near the fracture origin as well as in the aft cylinder. A limited number of precrack Charpy impact (PCI) and slow-bend (PCSB) tests were made on the casualty material at Aerojet-Sacramento. The data suggested the following observations: (1) the PTC data showed little or no difference between the following observations, (2) both PCI and PCSB test data showed the forward cylinder (fracture origin) to have the lower toughness, and (3) there was a marked loss of toughness in slow bend as compared with impact.

2. Chamber 2191456

Chamber 2191456 failed during proof test at a pressure of 457 psig (proof pressure is 627 psig). The failure origin was located in a repair of the forward girth weld. Examination of the fracture surfaces revealed porosity in the weld-repair area with two closely-spaced pores (0.045-in. dia and 0.020-in. dia) at approximately mid-thickness, resulting in an embedded flaw approximately 0.065-in. deep and 0.045-in. long. PCI test data showed the cylinder next to the forward girth weld* (fracture origin) to have the lowest toughness of the three components tested. Figure 1 shows the fractured chamber.

*The forward girth weld of Chamber 2191456 had appreciably lower toughness than any weld tested to date. The following table shows the PCI W/A and associated half-crack sizes for welds in successfully hydrotested chambers for comparison with the premature-burst chamber:

Motor No.	Weld Yield, ksi	PCI W/A (in.-lb/in.^{2})
2191456	155	742
673196	147	1077
673097	144	1366
673122	123	1577

Appendix C

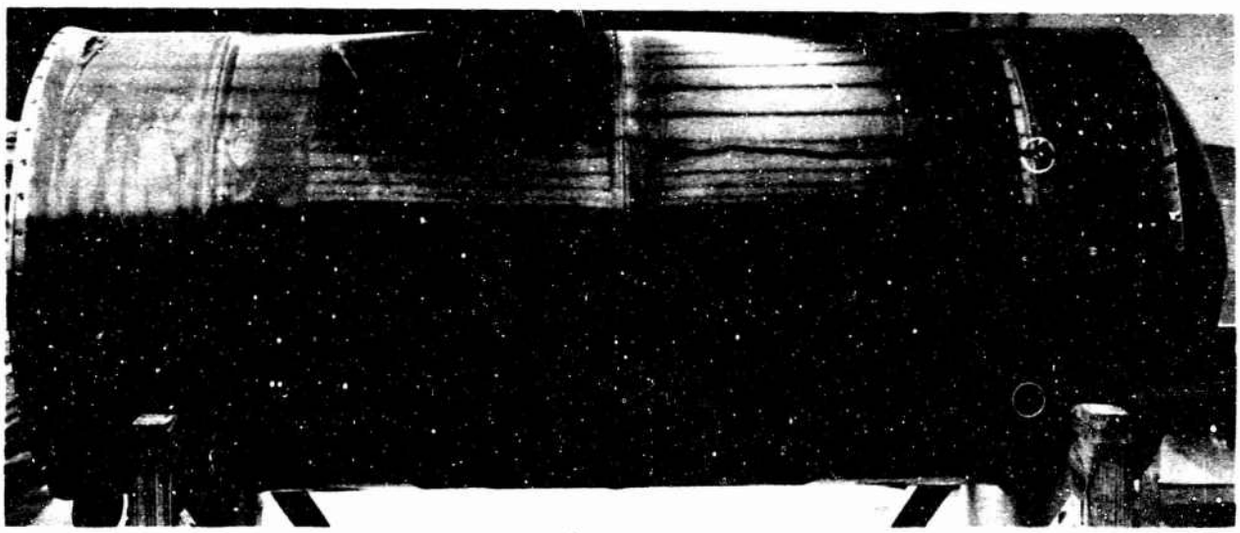


Figure 1. Fracture in 44-in.-dia Minuteman Chamber S/N 2191456. Failure originated in the forward girth weld at 457 psig (circles denote weld repairs).

3. Chamber 673078

Chamber 673078 was a 44-in.-dia motor case from Wing II of the MINUTEMAN program. The proof test procedure at that time was three cycles with 90-second holds at 590 psig.

Chamber S/N 673078 constituted a special case, because it not only contained over-strength components, but also involved a cracking problem. The girth welds consisted of one fusion pass the two filler passes with all welding done from the outside. After three proof-test cycles to 587 psig, cracks were noted on the inside-diameter surface at the root of the weld. Subsequently, the welds were routed out and rewelded with two passes on the inside diameter. After three proof-test cycles to 587 psig, cracks were noted on the inside-diameter surface at the root of the weld. Subsequently, the welds were routed out and rewelded with two passes on the inside diameter. After welding, the chamber was again stress relieved and then subjected to three additional proof-test cycles to 587 psig. The welds were found to be free of cracks. Chamber S/N 673078 was subsequently selected for AFBSD qualification testing because both the forward cylinder and the forward closure were overstrength (183.5 and 182.6 ksi ultimate tensile strength, respectively). As a result of O-ring problems during hydrotest, the chamber was subjected to five additional proof-test cycles, with failure on the fifth cycle:

Cycle Number	Pressure (psig)	Time at Pressure, sec	
		Rise Time	Hold
1	600	548	0
2	530	400	0
3	630	638	96
	720	328	0
4	620	616	120
	670	156	0
5	590	360	Burst

Thus, the chamber was subjected to a total of 11 hydroburst cycles, with failure originating from the inside-diameter surface in the vicinity of the center girth weld. After the burst, X-ray inspection of the welds revealed two transverse cracks in the inside-diameter surface of the weld-reinforced region of the center girth weld, approximately 180 degrees away from the fracture origin. The two cracks, within 2 in. of each other, were approximately 1/8-in. long by 0.060-in. deep, extending from the weld fusion line into the heat-affected base metal.

4. Chamber R369

This 52-in.-dia chamber was a premature proof-test failure. The fracture origin was a semi-elliptical crack in the ID surface of the aft cylinder near the aft girth weld. The flaw was large, penetrating almost through the wall with an a/2c ratio of about 0.17. Failure occurred on rising load to 380 psig. No fracture tests were made on this chamber material prior to the current investigation.

5. Chambers 673095, 673147, and 674514

These 44-in.-dia chambers were a hydroburst test series, performed as part of a qualification program originated by the Air Force Ballistic Systems Division (AFBSD) to evaluate motor cases with high-strength components (in excess of 180 ksi ultimate tensile strength). Specific requirements were assigned to these discrepant chambers to prove the structural integrity of each unit. The first requirement was that the chambers be subjected to a hydrostatic proof-pressure test of one cycle with a 90-sec hold at 640 psig. The second requirement was that the chambers subjected to hydrostatic burst test, where the minimum burst pressure at room temperature would be 772 psig*, obtained as follows:

$$P_b(\text{min}) = \frac{\text{MEOP} \times \text{FS} \times 5\ (\text{max})}{K_{tu}\ (320^\circ\text{F}) \times t\ (\text{min})}$$

$$= \frac{534 \times 1.15 \times 0.101}{0.835 \times 0.096}$$

$$= 772$$

where MEOP = Maximum Expected Operating Pressure

= 534 psig at 320°F

FS = design minimum Factor of Safety

= 1.15

t (max)/(min) = design thickness range

= 0.101/0.096 in.

K_{tu} (320°F) = ultimate strength degradation factor at 320°F

= 0.835

*This is a more severe requirement than usual. Minimum burst pressure at ambient temperature normally does not include the thickness ratio and is, therefore, only 737 psig.

It was specified that to be considered successful, the hydroburst tests would have to demonstrate considerable radial deformation preceding burst and have a factor of safety (FS) of 1.15 or higher, based on the above minimum burst pressure. The factor of safety in hydroburst testing was calculated as follows:

$$FS = FS \text{ (design)} \times \frac{P_b \text{ (test)}}{P_b \text{ (min)}}$$

Chamber S/N 673147, a MINUTEMAN 2nd-stage Wing II motor case, was successfully burst tested on 12 March 1964. The chamber was categorized as "over-strength" in that component sections exceeded the maximum acceptable ultimate strength defined by MINUTEMAN design. This chamber was subjected to a proof test of one cycle at 657 psig for 90 sec prior to burst. No yielding was observed during the proof-pressure test. The chamber was then taken to burst; the burst pressure was 860 psig, 88 psig above the minimum acceptable burst pressure. Maximum radial deformation (RD) computed from strain data was 0.384 in. The factor of safety (FS) was 1.28. There was no evidence that the motor case was degraded by the presence of the over-strength components.

Similar behavior was observed in Chambers S/N 673095 and 674514. The chamber manufacturer's qualification, quality control, integral coupon, tensile data for the over-strength components of each of these motor cases follow:

Component	FTU (min)	FTU (Avg.)
S/N 673147: FS 1.28 RD 0.384		
Fwd Cyl.	181.1	181.9
Aft. Cyl.	180.7	181.7
S/N 673095: FS 1.33, RD 0.335		
Fwd Dome	180.4	181.2
Aft Cyl.	183.5	183.8
S/N 674514: FS 1.34, RD 0.336		
Fwd Dome	183.3	183.7

6. Chambers S/N 673122 and 2192109

Both of these chambers were tested at service temperature. Chamber S/N 673122 was tested at 320°F and burst at 713 psig, with fracture originating near the center of the aft cylinder. The tensile strength of both the forward and aft cylindrical sections were within specifications (173.7 and 174.2 ksi ultimate tensile strength, respectively). Chamber S/N 2192109 was tested at 212°F and burst at 728 psig with fracture originating in the aft cylinder. The tensile strength of both the forward and aft cylindrical sections of Chamber 2192109 were within specifications (173.3 and 174.0 ksi ultimate tensile strength, respectively).

B. CN-TENSILE TEST PROCEDURE AND CALCULATIONS

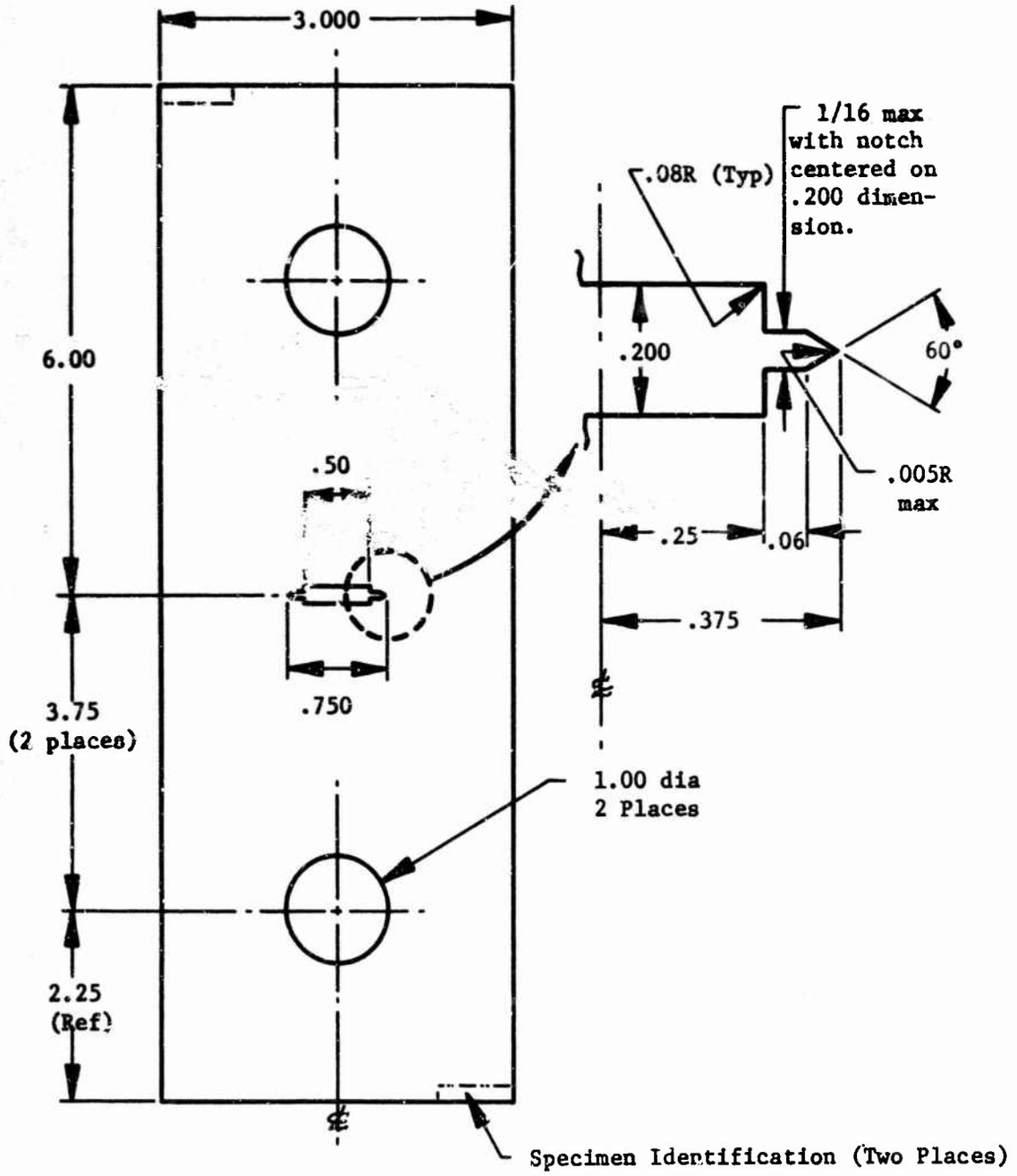
The center-notch fracture-toughness testing was done with 3 x 12-in. panels containing an electric-discharge-machined slot, extended and sharpened by fatigue cycling. The test-specimen design is shown in Figure 2. The load used in fatigue precracking the CN-tensile specimens was typically 5000 lb maximum to 500 lb minimum. The eloxed center notch was lengthened approximately 0.1-in. at each end to make a nominal $2a_o$ crack length of 0.95 in. This would correspond to a stress intensity of 21.6 ksi-in.$^{1/2}$ at 5000 lb load. The number of cycles required to produce a 0.2-in. overall increase in center-notch length ranged from 10,000 to 50,000 cycles (at a cycling rate of 30 cps). The number of cycles required to grow the crack to the desired length varied from forging to forging and sometimes from specimen to specimen.

The CN-tensile specimens were cut from 44- and 52-in.-dia barrel sections with the length of the test specimen in the axial-direction of the chamber. The 52-in.-dia curvature was left in the test pieces. The specimens were tested in a pin-and-clevis loading fixture at 10,000 psi/min loading speed using a Baldwin-Weidermann 60,000 lb tensile machine. The tests were conducted in air at room temperature (70°F). The components from the chambers hydroburst at 212 and 320°F were tested at the respective hydrotest temperature as well as at room temperature.

Each center-notch tensile test was instrumented with two crack-opening-displacement (COD) gages and an accelerometer. The COD gages were calibrated to provide data on the crack length at any given load (Figure 3) and were used to detect plane-strain instability (pip-in). The COD gages were inserted in the ELOX slot, one on each side of the test specimen. The output signal from the COD gage was recorded on a Sanborn strip chart; the other on an X-Y recorder.

The accelerometer was used to detect both the plane-strain instability (pop-in) and the final plane-stress instability. The instrumentation system consisted of a filter set to cut out all noise below 7500 cps, a low-noise charge amplifier, an oscilloscope, and a tape recorder. Details on the Aerojet Stress-Wave Analysis Technique (SWAT) are contained in the literature[1 - 5]* and the reader is referred to these documents for a detailed discussion of the system. The tape-recorded accelerometer data, indexed for load, were subsequently played back at reduced speed on an oscilloscope; this provided data on both pop-in and final crack instability. The final instability was determined by plotting stress-wave count-rate measurements versus load. Figure 4 shows a typical plot. The inflection in the curve was taken to be the onset of plane-stress instability.

*List of references at end of appendix.



Note: Pin holes and center notch both must be located on specimen centerline ± .005.

Figure 2. Center-Notch Tensile Specimen

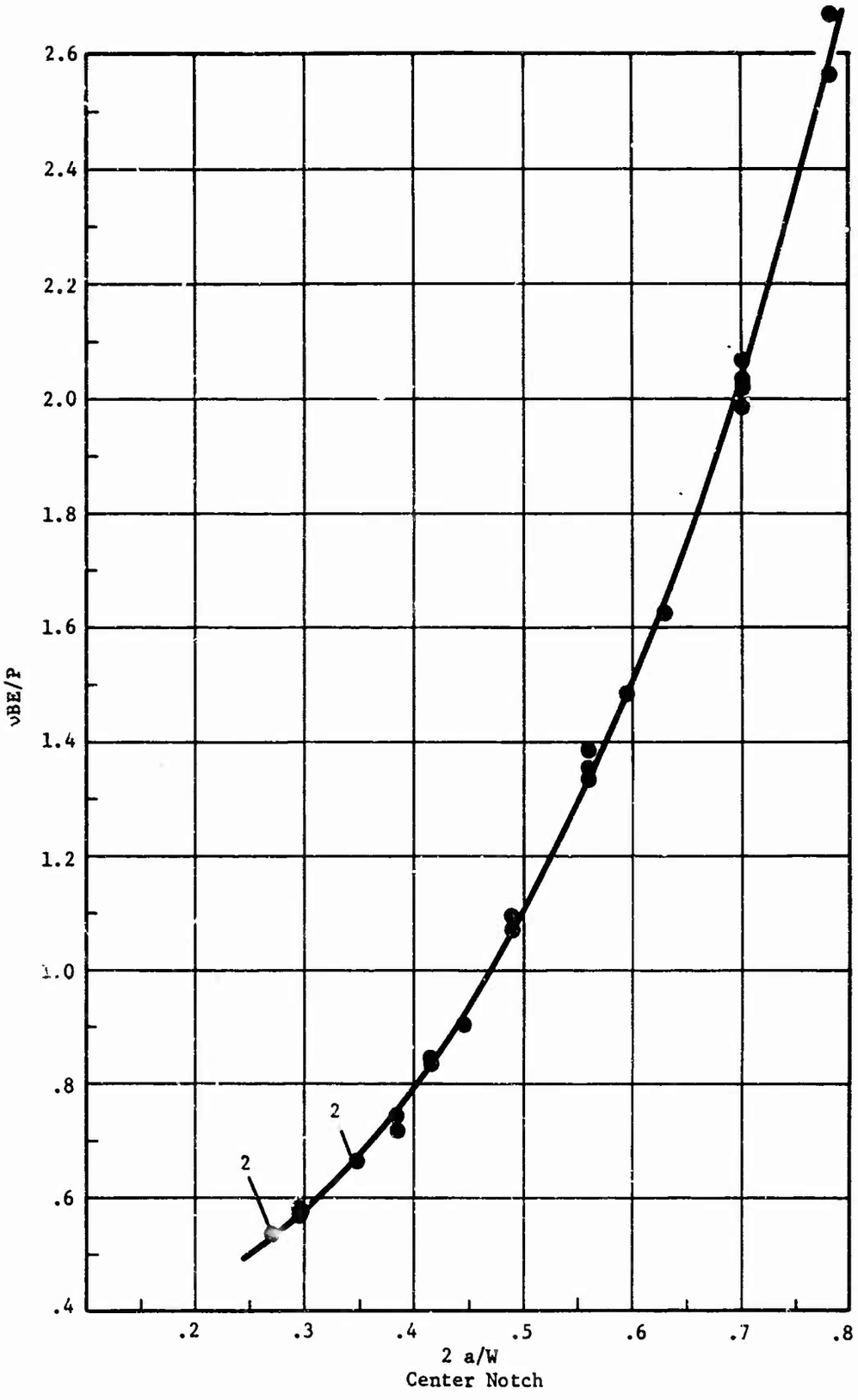


Figure 3. Calibration Curve for Converting Crack Opening Displacement to Crack Length of CN-Tensile Specimen (0.200-in. gage length)

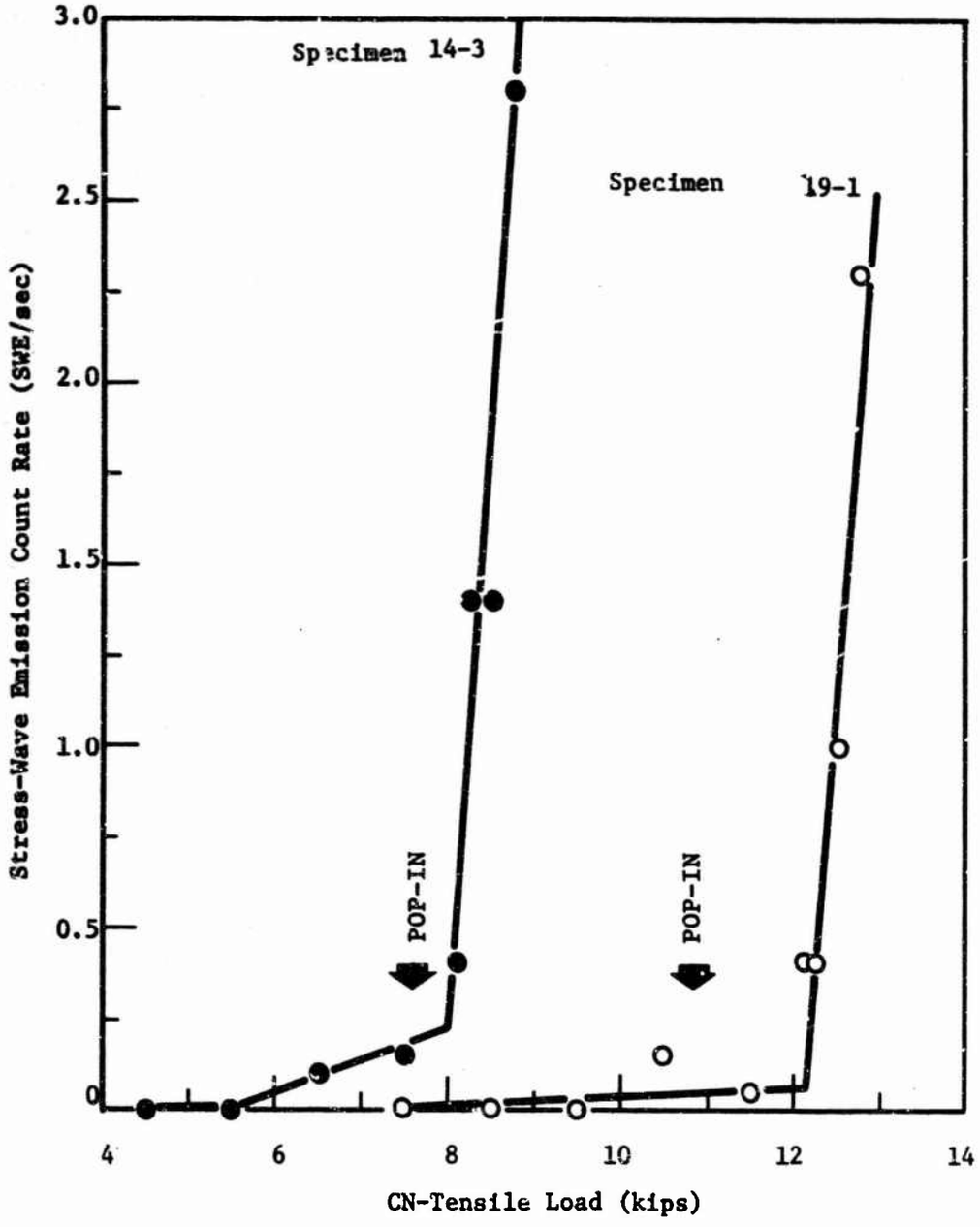


Figure 4. Typical Plots of Stress-Wave Emission Count Rate (SWE/sec) vs Load

Appendix C

Obviously, no consideration in fracture testing is more important than the method of crack-length measurement if meaningful, reproducible values of plane-stress crack toughness are to be obtained. In plane-strain fracture testing, the K_{Ic} value is based on the Initial fatigue-precrack dimensions. In most materials, this is easily measured by direct observation of the fracture surfaces. The crack length used in the plane-stress fracture-toughness calculation, on the other hand, usually involves considerable extension of the initial precrack before final instability. The accurate measurement of crack length at the onset of instability is the most difficult aspect of the fracture-testing procedures. One method for direct measurement of the crack length at instability is to unload the specimen when maximum load is reached, heat-tint the crack and then break the specimen*. At maximum load, the fracture test is complete - all meaningful data have been taken; thus, no measurements had to be taken on reloading to fracture after heat-tinting, other than a direct measurement of crack length as read in the heat-tinited fracture surface. This crack length plus a plastic-zone correction was taken as the effective crack length at maximum load, and was used as a check on the COD-gage crack length. Figure 5 shows the heat-tinted fracture surface for a number of fractured CN-tensile specimens.

The crack-opening displacement (COD) gage used to calculate crack length consisted of a double cantilever beam with a full bridge of electric-resistance strain gages (120 ohm) mounted on the flexural elements which deform elastically as the crack opens. Solution-treated beta-titanium (B120VCA) was used for the flexural elements because of its high yield-strength-to-modulus ratio. The gage is linear within 0.0001-in. over the range of 0.200 to 0.250-in. In testing the CN-tensile specimens, the gage was inserted in the eloxed center-notch slot, which was machined to a width (gage length) of 0.200 in. A Sanborn Model 150 recorder was used to display the crack opening displacement on a strip chart. A calibration curve to relate crack-opening displacement (ν) to crack length (2a) was constructed by using a calibration specimen of the same dimension as the test specimen and (1) cutting a slot of known length, (2) loading the specimen to about 20% of yield, and (3) recording ν from the strip chart and the corresponding load (P) This procedure was repeated several times, increasing the slot length approximately 0.050 in. each time. The calibration curve (Figure 3) is plotted using Young's Modulus (E), the specimen thickness (B), specimen width (W), and the above developed information. From Figure 3, one may convert the COD measurement to 2a/W for any specimen having the same geometric proportions as the calibration specimen[6].

*This simplified procedure obviously can be applied only to those materials which undergo slow crack growth and thereby develop a more or less gradual leveling out at maximum load in the load-versus-heat-movement X-Y plot. The use of heat-tinted crack lengths requires a plastic-zone correction; whereas, the crack-opening displacement gage provides an integration of crack length and plastic-zone size in a single measurement.

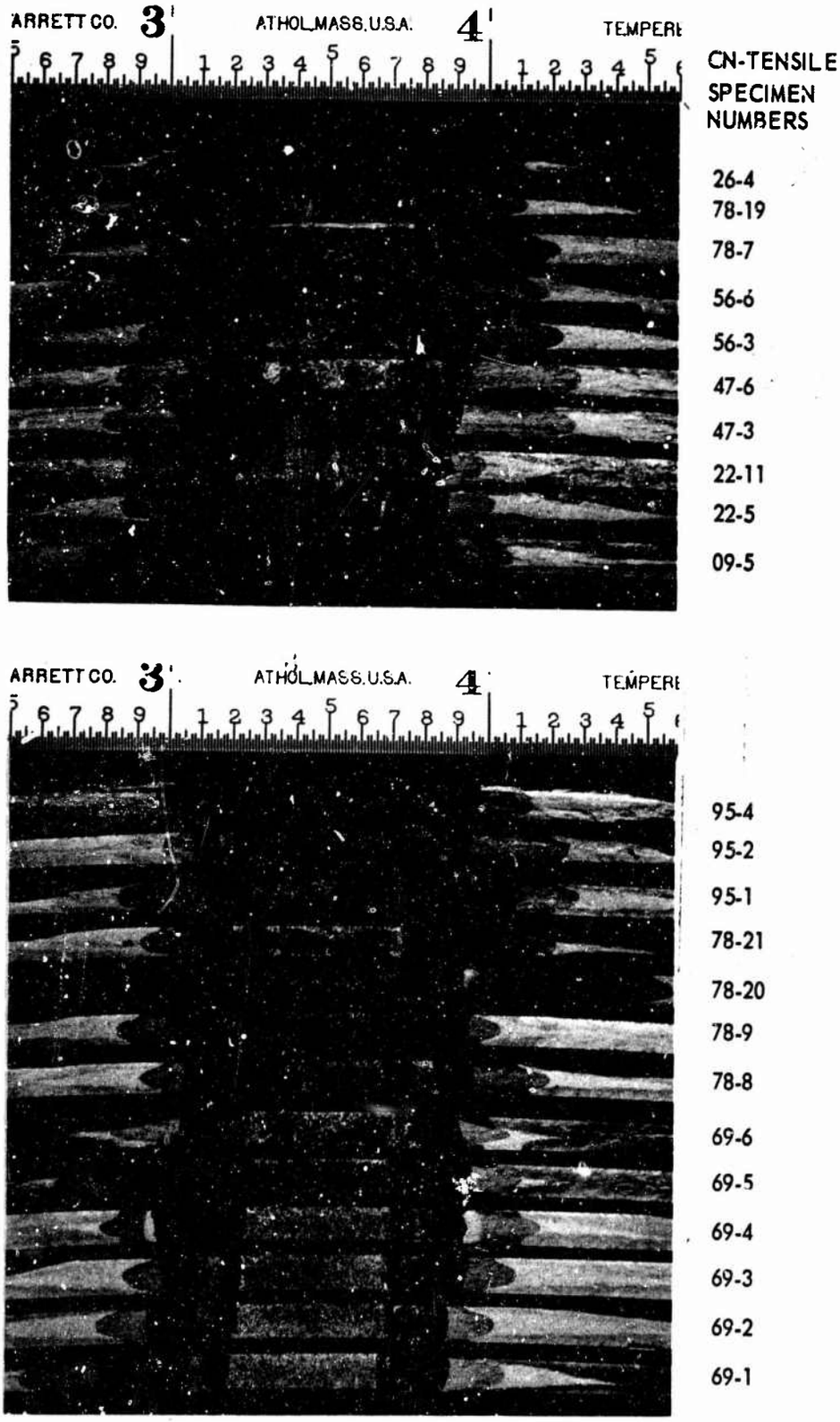


Figure 5a. Heat-Tinted CN-Tensile Fracture Surfaces Showing Crack Length at Maximum Load



Figure 5b. Heat-Tinted CN-Tensile Fracture Surfaces Showing Crack Length at Maximum Load

Appendix C

It is possible to check the COD measurement system with every test by comparing the calculated value of crack length with the measured fatigue crack. The check measurement is made at a low percentage of yield to minimize the plastic-zone contribution to crack-opening displacement. If the crack length as determined from the calibration curve does not agree with the direct measurement, a correction factor is used to change the calculated crack size to agree with that of the measured crack. An additional check was made on the calculated crack size by comparing the crack length at failure with the heat-tinted crack length.

Consider, for example, the crack-length measurements in specimen 22-1:

Fatigue crack length (2AO) = 0.916 in.

2AO/W = 0.305

Heat tinted crack length (2AA) = 1.11 in.

Specimen width (W) = 3.01 in.

Specimen thickness (B) = 0.101 in.

BE = 1.667×10^6

ν_o = crack opening displacement from the calibration curve

ν_m = actual crack opening displacement from the Sanborn for 240/W = 0.305, ν BE/P = 0.583 (from Figure 3)

Check at 3000-lb Load

$$\nu_o = 0.583\ P/1.667 \times 10^6$$

$$= 0.001049 \text{ in.}$$

but

$$\nu_m = 0.001214 \text{ in.}$$

as measured from the Sanborn strip chart; thus, the correction factor is

$$CF = 1049/1214$$

$$= 0.86$$

Check at 4000-lb load

ν_o = 0.001398 in.

ν_m = 0.001634 in.

CF = 1398/1634

= 0.86

Check at maximum load

$\nu_o = \nu_m \cdot CF$

$= 73.2 \times 10^{-4} \times 0.86$

= 0.00630 in.

ν BE/P = $6.30 \times 10^{-3} \times 1.67 \times 10^{6}/13900$

= 0.756

From Figure 3, for

ν BE/P = 0.756

2a/W = 0.388

2a = 1.168 in.

The crack length (heat tinted) at maximum load was 2AA = 1.110 in. The difference between the measured value (1.110 in.) and the calculated value can be attributed to the plastic zone; i.e., the effective overall crack length was

2AE = 2(AA + RY)

From Table I, the plastic-zone correction is 0.0309 in. which, when added to the measured crack length

2AE = 1.110 + 0.0618

= 1.172 in.

as compared to 1.168 in. from the corrected COD measurement.

Appendix C

All calculations were done by computer, programmed to print out in table form the overall test results. The input to the computer was as follows: forging number, thickness and width of test specimen, yield stress; AO, the half length of the fatigue-cracked center notch; AP, the COD-gage crack length, and PP, the load at stress-wave pop-in (pop-in seldom was detected by COD gage); AD, the COD-gage half-crack length, and PD, the load at deviation from linearity in the COD-gage strip chart; AC, the half-crack length, and PC, the load at the inflection on the stress-wave count rate plot; AM, the half-crack length, and PM, the load at the maximum in the COD-versus-load X-Y plot; and AA, the measured half-crack length in the heat-tinted fracture surface.

The computer output contained the corresponding values of fracture toughness. Not all of the calculated values are useful, nor were they intended for use other than as verifying data. For example, K_{Ic} values calculated from AO and PD (deviation from linearity) provided consistently low values - but with little or no physical significance between deviation from linearity consistently preceded the pop-in as seen by stress-wave measurement.

The expressions used for calculating fracture toughness were (1) a third-degree polynomial[7] which is accurate to within 0.5 percent over the range of 2a/W from 0 to 0.7.

$$K_I \, BW/Pa^{1/2} = 1.77 + 0.227(2a/W) - 0.510(2a/W)^2 + 2.7(2a/W)^3$$

and (2) a secant expression[8] which is accurate to within 0.3 percent over the range of 2a/W from 0 to 0.8.

$$K = \left[\pi \, a \, \text{secant} \left(\frac{\pi a}{W}\right) \right]^{1/2} P/BW$$

Both plane-strain (K_{Ic}) and plane-stress (K_c) fracture toughness were calculated from these expressions by use of the appropriate values of crack length and load. The K_c value calculated from the direct measurement of crack length (AA) at maximum load required a plastic-zone correction; whereas, the crack lengths obtained from COD measurements had a self-contained plastic-zone correction. The K_c value based on AE (the plastic-zone-corrected AA) was calculated only from the more compact secant expression.

Figure 6 provides a graphical solution of the third-degree polynomial for CN-tensile tests for 2a/W ratios up to 0.6. The computer solution of equations (1) and (2) for the various combinations of crack length and load are tabulated as computer printout in Tables I, II, and III.

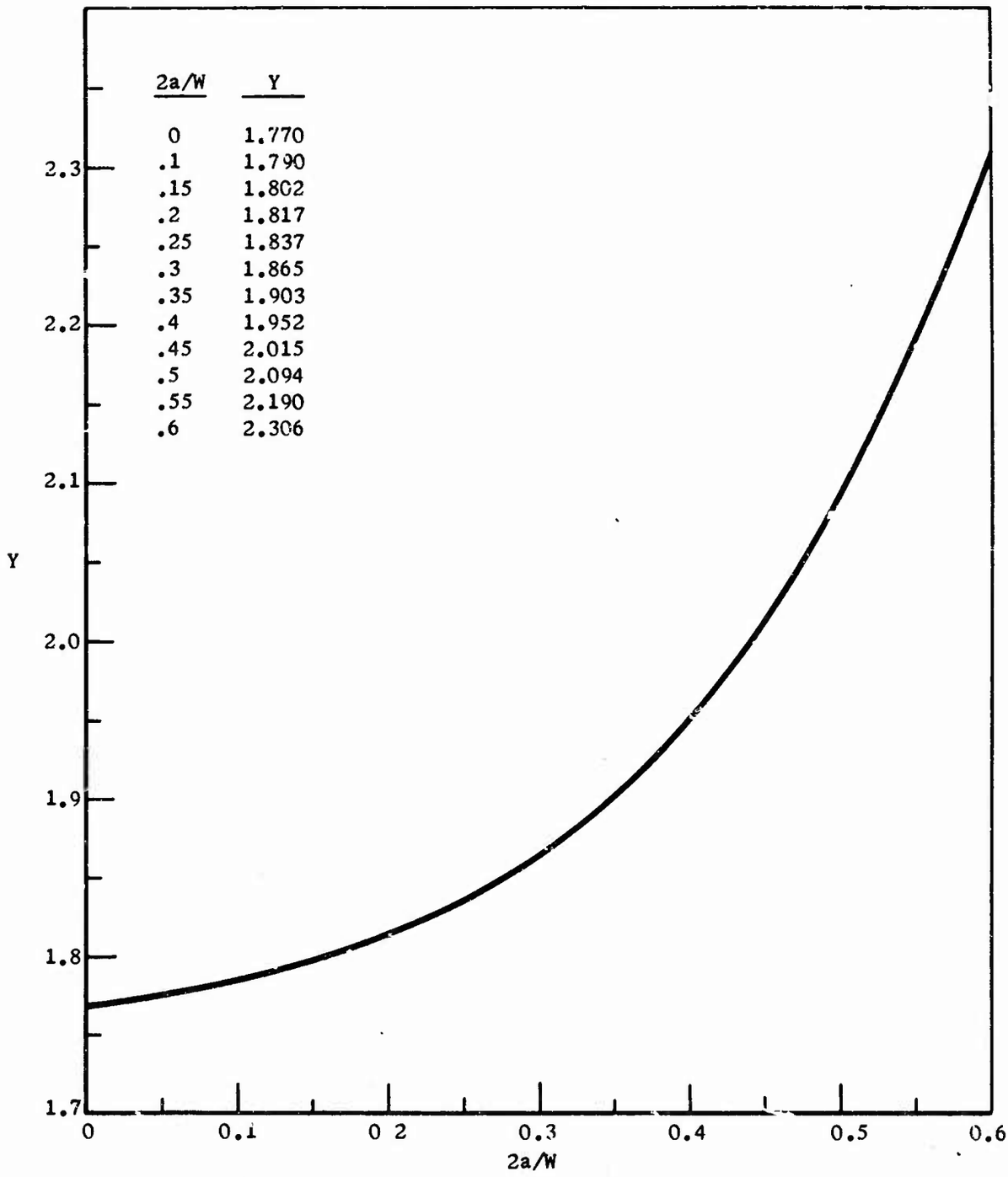


Figure 6. K Calibration for the CN-Tensile Test.
$K = Y \cdot Pa^{1/2}/BW$.

REFERENCES

1. C. E. Hartbower, W. W. Gerberich and P. P. Crimmins, Characterization of Fatigue-Crack Growth by Stress-Wave Emission, Final Report CR-66303 of June 1966, available from the NASA Scientific and Technical Information Facility, P.O. Box 5700, Bethesday, Maryland, 20014.

2. C. E. Hartbower, W. W. Gerberich and P. P. Crimmins, Mechanisms of Slow Crack Growth in High-Strength Steels, AFML-TR-67-26, Vol. 1, February 1967, also THE WELDING JOURNAL, Vol. 47(1) p.1-s (Jan 1968); also PROCEEDINGS Conference on Fundamental Aspects of Stress Corrosion Cracking, Ohio State University, Sept. 1967.

3. G. S. Baker, Acoustic Emission and Prefracture Processes in High-Strength Steels, Final Report AFML-TR-67-266, November 1967, Contract AF 33(615)-5027.

4. H. L. Dunegan, D. O. Harris and C. A. Tatro, "Fracture Analysis by Use of Acoustic Emission," presented at the National Symposium on Fracture Mechanics, Lehigh University, Bethlehem, Pa., June 19-21, 1967. To be published in the Journal of Engineering Fracture Mechanics, April 1968.

5. C. E. Hartbower, W. W. Gerberich and Harold Liebowitz, "Investigation of Crack-Growth Stress-Wave Relationships," presented at the National Symposium on Fracture Mechanics, Lehigh University, Bethlehem, Pa., June 19-21, 1967. To be published in the Journal of Engineering Fracture Mechanics.

6. W. F. Brown and J. E. Strawley, "Fracture Testing and Its Applications," ASTM STP-381, pp. 173-188.

7. W. F. Brown, Jr. and J. E. Srawley, "Plane-Strain Crack Toughness Testing of High-Strength Metallic Materials," ASTM-STP-410, Dec. 1967.

8. C. E. Fedderson, Ibid, p. 77.

Appendix C

COMPUTER PRINTOUT TABULATION

OF CN-TENSILE DATA

TABLE I

ROOM TEMPERATURE DATA FOR PARENT METAL

TABLE 1A - CENTER-NOTCH-TENSILE FRACTURE TOUGHNESS OF 9AL-4V TITANIUM TESTED AT 70 DEG. F INPUT TO COMPUTER PROGRAM

FORGING SPECIMEN NUMBER	THICKNESS B (IN.)	WIDTH W (IN.)	YIELD STRESS FTY (KSI)	FATIGUE AO (IN.)	CRACK LENGTHS: POP-IN AP (IN.)	DEV. FROM LINEARITY AO (IN.)	ONSET OF RAPID SWE AC (IN.)	AT MAX. LOAD AM (IN.)	MEASURED AT PMAX. AA (IN.)
					LOADS: POP-IN PP (KIPS)	DEV. FROM LINEARITY PO (KIPS)	ONSET OF RAPID SWE PC (KIPS)	MAXIMUM LOAD PM (KIPS)	
09-1	0.109	3.002	163.	0.572	0.847 10.8	0.599 7.1	0.672 12.1	0.715 12.9	0.938
09-2	0.108	3.005	163.	0.339	0.909 9.8	0.576 9.2	0.636 10.9	0.997 11.9	0.922
06-5	0.109	3.006	163.	0.495	0.618 12.0	0.519 7.0	0.626 12.4	0.978 13.3	0.630
09-7	0.109	3.005	163.	0.340	0.822 9.2	0.570 9.7	0.613 9.8	0.679 9.9	0.835
09-9	0.107	3.005	193.	0.475	0.323 8.7	0.498 6.7	0.619 11.0	0.950 11.1	0.383
14-1	0.102	3.002	199.	0.515	0.559 8.3	0.340 3.5	0.623 9.2	0.702 8.2	0.680
14-5	0.101	3.001	198.	0.565	0.626 7.6	0.602 6.7	0.644 8.0	0.719 9.0	0.673
14-9	0.100	3.000	164.	0.499	0.539 7.5	0.304 6.4	0.570 7.7	0.928 9.1	0.912
14-6	0.100	3.005	164.	0.536	0.000 0.0	0.506 6.2	0.364 7.1	0.934 8.1	0.895
22-1	0.101	3.006	133.	0.659	0.506 12.2	0.461 7.2	0.332 13.4	0.594 13.9	0.553
22-2	0.102	3.002	135.	0.642	0.536 13.7	0.446 6.8	0.382 15.4	0.599 15.7	0.593
22-5	0.102	3.003	135.	0.445	0.508 12.5	0.352 6.6	0.330 13.1	0.564 13.3	0.349
22-7	0.099	3.005	191.	0.459	0.530 10.6	0.510 9.7	0.568 12.0	0.628 12.9	0.562
22-9	0.098	3.005	191.	0.440	0.523 11.9	0.430 6.0	0.560 13.1	0.574 13.5	0.523
22-11	0.068	3.004	161.	0.632	0.494 11.6	0.444 10.0	0.335 12.6	0.360 13.3	0.532
29-1	0.101	3.011	195.	0.440	0.332 12.5	0.496 7.9	0.570 13.2	0.624 13.9	0.430
26-2	0.102	2.999	193.	0.479	0.322 10.1	0.472 6.5	0.609 12.0	0.934 12.4	0.610
29-4	0.100	3.006	145.	0.638	0.332 16.3	0.444 10.3	0.390 20.7	0.900 21.7	0.340
26-5	0.101	3.008	165.	0.639	0.523 17.5	0.452 9.3	0.374 20.0	0.584 20.9	0.948
29-6	0.102	3.010	195.	0.442	0.522 17.3	0.492 12.7	0.000 0.0	0.900 20.1	0.560
47-1	0.100	3.002	199.	0.329	0.566 10.3	0.334 8.4	0.592 10.9	0.652 11.3	0.950
47-2	0.100	3.002	199.	0.432	0.000 0.0	0.458 9.7	0.352 14.0	0.399 14.9	0.000
47-3	0.066	3.003	198.	0.432	0.425 8.3	0.423 9.6	0.388 11.6	0.928 12.3	0.702
47-4	0.066	3.002	169.	0.445	0.472 8.8	0.448 7.6	0.539 11.2	0.578 11.5	0.618
47-5	0.066	3.003	168.	0.430	0.000 0.0	0.414 8.1	0.000 0.0	0.539 11.4	0.930

ZERO VALUES INDICATE NO DATA.

TABLE 1A - CENTER-NOTCH-TENSILE FRACTURE TOUGHNESS OF 6AL-4V TITANIUM TESTED AT 70 DEG. F COMPUTER PROGRAM OUTPUT

FORGING SPECIMEN NUMBER	PLANE STRAIN TOUGHNESS KSI-IN 1/2 EQUATION (1)* KIC FOR AO - PO	KIC FOR AO - PO	KIC FOR AO - PP	KIC FOR AP - PP	PLANE STRESS TOUGHNESS KSI-IN 1/2 EQUATION (1)* KC FOR AC - PC	KC FOR AM - PM	KC FOR AE - PP	GROSS STRESS AT MAX. LOAD FG (KSI)	STRESS RATIO FG/FTY
	PLANE STRAIN TOUGHNESS KSI-IN 1/2 EQUATION (2)* KIC FOR AO - PO	KIC FOR AO - PO	KIC FOR AO - PP	KIC FOR AP - PP	PLANE STRESS TOUGHNESS KSI-IN 1/2 EQUATION (2)* KC FOR AC - PC	KC FOR AM - PM	KC FOR AE - PP	EFFECTIVE CRACK AE (IN.)	1/2 PLASTIC ZONE SIZE RY (IN.)
06-1	32.1 32.3	33.1 33.4	49.9 46.2	53.4 53.8	91.9 62.0	68.6 69.5	67.1	39.7 0.695	0.2637 0.0270
09-2	33.3 33.9	37.3 37.6	42.3 42.6	46.3 46.7	52.5 53.0	91.9 62.3	58.3	39.3 0.692	0.2232 0.0204
06-5	28.2 29.4	26.3 26.5	49.2 49.5	56.2 57.3	39.0 56.5	67.4 69.0	69.2	40.9 0.726	0.2461 0.0262
09-7	26.7 29.6	30.9 31.0	40.6 40.6	44.8 45.2	43.4 43.7	92.1 92.5	30.7	31.3 0.930	0.1622 0.0159
09-9	16.2 19.5	16.0 16.6	27.2 27.4	28.6 29.2	32.6 59.5	33.9 36.1	32.9	34.6 0.601	0.2123 0.0167
14-1	23.9 23.8	24.5 24.7	28.3 29.5	26.9 30.1	41.9 42.2	91.8 92.0	91.5	30.1 0.993	0.1906 0.0132
14-5	31.1 32.4	33.9 33.6	36.3 36.6	36.1 36.4	42.1 42.4	31.5 31.8	90.3	29.9 0.686	0.1790 0.0145
14-9	27.4 27.6	28.7 29.9	32.0 32.2	33.8 36.1	37.4 37.7	42.7 43.0	42.7	27.2 0.622	0.1697 0.0107
14-6	26.0 26.2	30.1 30.3	0.0 0.0	0.0 0.0	33.4 35.7	43.5 43.8	43.9	26.6 0.707	0.1638 0.0126
22-1	30.1 30.3	30.3 30.4	50.5 51.1	54.0 54.4	61.3 51.9	97.6 68.5	99.7	45.9 0.985	0.2939 0.0306
22-2	30.9 36.1	36.1 36.3	53.5 55.5	52.7 63.2	74.6 79.0	76.6 77.9	79.1	54.5 0.565	0.8307 0.0405
22-5	33.6 36.1	36.3 36.5	50.2 50.5	54.9 54.9	59.5 39.9	93.8 84.4	65.6	44.1 0.576	0.2931 0.0290
22-7	37.4 37.8	40.0 40.2	46.7 47.2	51.5 51.9	96.3 59.7	67.1 67.7	64.4	42.9 0.587	0.2636 0.0255
22-9	25.3 23.6	23.9 26.0	46.9 50.0	35.4 55.6	64.1 64.6	97.3 97.6	65.9	49.6 0.569	0.2867 0.0264
22-11	41.6 41.9	42.5 42.5	48.4 48.7	52.6 53.3	61.0 61.3	89.5 64.0	66.0	45.4 0.558	0.2619 0.0266
29-1	32.6 35.1	32.7 32.9	52.3 52.6	58.9 58.3	93.3 63.6	70.8 71.4	74.9	45.9 0.662	0.2758 0.0327
26-2	27.4 27.9	27.2 27.4	43.6 43.9	48.1 46.4	60.6 61.1	64.6 65.4	65.6	41.0 0.655	0.2605 0.0251
29-4	42.5 42.7	42.9 45.0	80.1 80.5	62.7 63.5	102.9 103.6	109.3 110.2	112.1	72.2 0.613	0.4388 0.0734
26-5	35.7 35.6	33.4 33.6	72.3 72.8	78.7 79.3	96.5 97.2	103.6 101.4	105.0	67.9 0.612	0.4109 0.0645
29-6	31.2 31.5	32.6 32.9	70.0 70.4	77.7 78.2	0.0 0.0	99.1 99.6	102.5	65.5 0.621	0.3971 0.0614
47-1	39.9 40.2	39.2 39.5	47.9 48.2	50.1 50.5	53.2 53.7	59.9 60.1	63.0	37.6 0.672	0.2253 0.0275
47-2	36.8 40.0	41.2 41.5	0.0 0.0	0.0 0.0	66.5 67.0	79.4 76.0	0.0	49.9 0.080	0.2966 0.0000
47-3	33.4 33.6	33.1 33.9	35.1 35.2	36.7 36.9	57.0 57.5	84.9 65.6	14.2	31.6 0.752	0.2465 0.0340
47-4	32.1 32.2	32.2 32.4	37.4 37.9	39.9 39.0	92.8 53.2	57.4 57.9	62.3	55.6 0.636	0.2811 0.0217
47-5	33.4 33.5	32.6 32.9	0.0 0.0	0.0 0.0	0.0 0.0	34.1 33.5	33.2	38.6 0.567	0.2295 0.0171

ZERO VALUES INDICATE NO DATA.
* EQUATION (1) IS 3RD DEGREE POLYNOMIAL & EQUATION (2) IS SECANT.

TABLE I (cont.)

TABLE 1A - CENTER-NOTCH-TENSILE FRACTURE TOUGHNESS OF 6AL-4V TITANIUM
TESTED AT 70 DEG. F
INPUT TO COMPUTER PROGRAM

FORGING SPECIMEN NUMBER	THICKNESS B (IN.)	WIDTH W (IN.)	YIELD STRESS FTY (KSI)	FATIGUE AO (IN.)	CRACK LENGTHS: POP-IN AP (IN.)	DEV. FROM LINEARITY AO (IN.)	ONSET OF RAPID SWE AC (IN.)	AT MAX. LOAD AF (IN.)	MEASURED AT PMAX. AA (IN.)
					LOADS: POP-IN PP (KIPS)	DEV. FROM LINEARITY PO (KIPS)	ONSET OF RAPID SWE PC (KIPS)	MAXIMUM LOAD PM (KIPS)	
47-6	0.099	3.001	168.	0.440	0.461 11.5	0.414 9.9	0.477 11.9	0.608 12.1	0.685
56-1	0.100	2.969	159.	0.435	0.509 9.5	0.423 7.0	0.526 10.0	0.604 10.8	0.590
56-2	0.099	3.010	159.	0.482	0.548 9.7	0.488 8.1	0.584 10.2	0.673 11.0	0.675
56-3	0.100	3.010	159.	0.440	0.477 10.0	0.420 7.1	0.540 11.4	0.600 11.5	0.612
56-4	0.102	9.005	182.	0.440	0.575 10.0	0.462 9.0	0.585 10.1	0.650 10.9	0.600
56-5	0.100	3.010	162.	0.448	0.000 0.0	0.462 10.6	0.592 17.5	0.617 18.1	0.585
56-6	0.100	2.997	162.	0.458	0.488 13.5	0.446 9.1	0.562 16.8	0.642 18.6	0.630
69-1	0.110	3.002	181.	0.538	0.680 11.6	0.576 6.8	0.670 11.2	0.758 11.9	0.722
69-2	0.108	3.003	161.	0.465	0.555 11.5	0.478 7.6	0.580 12.4	0.622 9.1	0.585
69-3	0.110	3.009	161.	0.472	0.484 6.6	0.492 8.0	0.607 12.2	0.703 12.9	0.575
69-4	0.106	3.005	166.	0.515	0.612 13.9	0.951 8.4	0.644 19.1	0.720 19.8	0.650
69-5	0.106	3.003	166.	0.558	0.694 12.5	0.560 8.3	0.695 14.9	0.734 15.4	0.675
69-6	0.106	3.003	166.	0.432	0.530 15.9	0.442 7.8	0.625 19.1	0.644 19.8	0.578
78-7	0.099	9.005	169.	0.478	0.524 10.8	0.490 8.1	0.576 15.2	0.656 16.1	0.609
78-8	0.100	3.005	169.	0.450	0.512 13.1	0.434 8.7	0.541 16.1	0.586 15.0	0.595
78-9	0.100	3.007	169.	0.460	0.475 9.3	0.448 8.2	0.532 12.5	0.572 13.3	0.565
78-19	0.098	3.008	164.	0.438	0.486 9.7	0.468 8.4	0.620 15.1	0.658 15.5	0.585
78-20	0.098	3.004	164.	0.895	0.934 6.5	0.925 6.0	0.998 8.1	1.046 8.5	1.000
78-21	0.098	9.004	164.	0.508	0.000 0.0	0.523 6.3	0.602 12.9	0.656 15.8	0.605
95-1	0.100	3.005	161.	0.500	0.544 10.5	0.496 7.9	0.638 11.8	0.654 12.0	0.680
95-2	0.100	3.002	161.	0.430	0.507 11.9	0.446 9.8	0.602 13.3	0.608 13.4	0.608
95-3	0.101	3.006	161.	0.428	0.502 11.5	0.426 7.2	0.575 14.1	0.695 14.1	0.000
95-4	0.100	3.005	172.	0.496	0.442 7.5	0.443 7.4	0.508 9.5	0.504 9.5	0.542
95-5	0.098	3.005	172.	0.430	0.490 7.3	0.462 7.7	0.520 9.4	0.534 9.7	0.000

TABLE 1A - CENTER-NOTCH-TENSILE FRACTURE TOUGHNESS OF 6AL-4V TITANIUM
TESTED AT 70 DEG. F
COMPUTER PROGRAM OUTPUT

FORGING SPECIMEN NUMBER	PLANE STRAIN TOUGHNESS KSI-IN 1/2 EQUATION (1): KIC FOR AO - PO	KIC FOR AO - PO	KIC FOR AO - PP	KIC FOR AP - PP	PLANE STRESS TOUGHNESS KSI-IN 1/2 EQUATION (1): KC FOR AC - PC	KC FOR AM - PM	GROSS STRESS AT MAX. LOAD FG (KSI)	GTHES RATIO FG/FT
	PLANE STRAIN TOUGHNESS KSI-IN 1/2 EQUATION (2): KIC FOR AO - PD	KIC FOR AO - PD	KIC FOR AO - PP	KIC FOR AP - PP	KC FOR AC - PC	KC FOR AM - PM	KC FOR AE - PP	EFFECTIVE CRACK AE (IN.)	1/2 PLASTI ZONE SIZE RY (IN.)
47-6	24.5 24.7	23.7 29.8	47.8 48.0	49.2 49.4	52.2 52.5	62.3 62.8	71.2	40.7 0.713	0.2419 0.0284
56-1	29.0 29.2	28.6 28.8	39.4 39.6	43.4 43.7	46.6 46.9	55.9 56.3	56.8	36.6 0.610	0.2301 0.0292
56-2	27.0 27.2	27.3 27.4	42.7 43.0	46.4 46.8	50.7 51.2	61.1 61.5	63.6	36.9 0.700	0.2521 0.0253
56-3	29.5 29.8	21.9 28.8	41.0 41.2	43.1 43.3	53.4 53.8	59.8 60.3	69.0	39.5 0.636	0.2480 0.0249
56-4	36.2 36.4	36.3 96.5	72.4 72.8	86.5 87.2	87.6 88.5	99.0 99.8	101.3	41.6 0.662	0.5805 0.0423
56-5	44.2 44.6	45.0 45.3	0.0 0.0	0.0 0.0	87.1 97.8	92.8 93.6	96.4	60.1 0.441	0.5711 0.0964
56-6	37.6 97.8	38.0 38.2	34.8 55.5	58.5 58.5	81.0 81.6	101.7 102.5	107.2	62.3 0.699	0.3847 0.0697
69-1	29.2 29.6	30.6 30.9	49.2 49.6	58.5 58.9	55.8 56.2	64.0 64.4	65.6	56.0 0.748	0.2292 0.0262
69-2	30.0 30.2	30.5 30.7	49.5 49.6	50.8 51.2	96.4 96.9	65.1 65.6	62.6	40.6 0.608	0.2513 0.0239
69-3	31.2 71.4	92.0 32.2	29.0 29.2	29.4 29.6	56.6 57.0	59.5 59.8	59.3	39.0 0.556	0.2415 0.0214
69-4	36.2 36.5	57.9 58.2	59.4 59.9	67.0 67.5	73.6 76.2	87.0 87.6	84.5	49.7 0.690	0.2984 0.0449
69-5	37.8 98.1	37.9 38.2	58.2 58.7	65.4 65.9	79.4 80.0	86.4 87.0	85.1	48.5 0.716	0.2915 0.0415
69-6	29.9 30.0	30.5 30.5	61.2 61.5	69.5 70.1	95.6 96.5	99.5 100.1	99.0	6..2 0.654	0.3755 0.0561
78-7	35.5 35.7	36.1 36.3	47.4 47.7	50.2 50.6	65.4 65.9	75.3 75.9	75.7	47.6 0.654	0.2813 0.0318
78-8	36.2 36.4	35.4 35.6	54.8 55.1	59.5 59.9	85.0 46.5	74.5 75.1	79.2	50.0 0.625	0.2955 0.0348
78-9	28.5 28.7	26.1 28.2	59.2 59.5	60.0 60.5	57.8 58.5	65.0 65.5	66.9	44.4 0.585	0.2624 0.0248
78-19	35.1 35.5	36.6 36.8	40.5 40.7	45.2 45.4	79.5 80.0	85.5 86.1	82.8	52.6 0.625	0.3209 0.0403
78-20	44.6 44.7	44.4 46.5	46.5 47.0	49.3 49.4	68.8 69.1	76.9 77.6	76.3	29.0 1.034	0.1764 0.0345
78-21	25.3 29.5	29.8 30.1	0.0 0.0	0.0 0.0	66.4 67.0	75.5 76.5	74.8	46.8 0.657	0.2851 0.0325
95-1	55.2 55.6	55.0 59.5	47.1 47.4	51.0 51.4	62.2 82.7	64.8 65.5	69.5	49.1 0.705	0.2990 0.0299
95-2	40.0 40.2	42.0 42.5	48.8 48.8	93.8 94.1	67.2 67.7	68.6 69.0	71.6	44.8 0.859	0.2777 0.0314
95-3	28.9 29.1	28.9 29.0	47.7 47.9	52.8 53.0	68.0 68.5	75.3 75.5	0.0	48.7 0.000	0.2857 0.0000
95-4	31.5 31.5	30.7 30.9	31.8 31.9	31.1 31.2	44.5 44.8	44.5 44.7	47.6	33.0 0.554	0.1920 0.0122
95-5	32.0 32.2	33.6 33.6	30.5 30.6	31.3 31.5	45.7 46.1	46.2 46.6	0.0	33. 0.000	0.1926 0.0000

ZERO[illegible]S INDI[illegible]DATA. [illegible] VALUES[illegible]TE NO D[illegible] DEGR[illegible]OMIAL [illegible]ION (2[illegible]ANT.

TABLE II

ELEVATED-TEMPERATURE DATA FOR PARENT METAL

TABLE 1A - CENTER-NOTCH-TENSILE FRACTURE TOUGHNESS OF 8AL-4V TITANIUM
TESTED AT 212 DEG. F
INPUT TO COMPUTER PROGRAM

FORGING SPECIMEN NUMBER	THICKNESS B (IN.)	WIDTH W (IN.)	YIELD STRESS FTY (KSI)	CRACK LENGTHS: FATIGUE AO (IN.)	POP-IN AP (IN.)	DEV. FROM LINEARITY AO (IN.)	ONSET OF RAPID SWE AC (IN.)	AT MAX. LOAD AM (IN.)	MEASURED AT PMAX. AA (IN.)
					LOADS: POP-IN PP (KIPS)	DEV. FROM LINEARITY PO (KIPS)	ONSET OF RAPID SWE PC (KIPS)	MAXIMUM LOAD PM (KIPS)	
09-5	0.108	5.009	158.	0.500	0.000 0.0	0.512 5.8	0.000 0.0	0.840 20.4	0.795
09-6	0.109	5.004	158.	0.540	0.A00 12.A	0.5A0 7.0	0.71A 19.8	0.73A 20.2	0.A90
09-11	0.100	5.005	158.	0.420	0.642 9.8	0.642 9.8	0.AA6 25.7	0.798 24.5	0.688
09-12	0.108	5.000	158.	0.445	0.5R0 1A.5	0.456 A.5	0.842 21.8	0.72A 22.5	0.705

TABLE 1A - CENTER-NOTCH-TENSILE FRACTURE TOUGHNESS OF 8AL-4V TITANIUM
TESTED AT 212 DEG. F
COMPUTER PROGRAM OUTPUT

FORGING SPECIMEN NUMBER	PLANE STRAIN TOUGHNESS KSI-IN 1/2 EQUATION (1)* KIC FOR AO - PO	KIC FOR AO - PO	KIC FUR AO - PP	KIC FUR AP - PP	PLANE STRESS TOUGHNESS KSI-IN 1/2 EQUATION (1)* KC FOR AC - PC	KC FUR AP - PM	GROSS STRESS AT MAX. LOAD FG (KSI)	STRESS RATIO FG/FTY
	PLANE STRAIN TOUGHNESS KSI-IN 1/2 EQUATION (2)* KIC FOR AO - PO	KIC FOR AO - PO	KIC FOR AO - PP	KIC FOR AP - PP	PLANE STRESS TOUGHNESS KSI-IN 1/2 EQUATION (2)* KC FOR AC - PC	KC FUR AM - PM	KC FOR AE - PM	EFFECTIVE CRACK AE (IN.)	1/2 PLASTIC ZONE SIZE RY (IN.)
09-5	25.2 25.4	25.A 25.8	0.0 0.0	0.0 0.0	0.0 0.0	12T.5 127.9	157.4	62.P 1.000	0.A341 0.2050
08-6	50.0 30.2	50.T 51.0	5A.1 54.5	58.2 58.7	104.9 105.A	110.1 110.8	115.A	61.8 0.79A	0.A455 0.1048
09-11	38.5 58.7	5T.6 57.8	36.5 36.7	5T.A 57.8	118.A 120.5	145.2 145.8	175.4	T5.4 0.858	0.9442 0.2488
08-12	24.5 24.A	24.8 25.0	A5.3 65.7	T5.2 T5.8	10T.1 108.0	121.4 122.2	148.8	68.8 0.888	0.4868 0.1852

TABLE 1A - CENTER-NOTCH-TENSILE FRACTURE TOUGHNESS OF 6AL-4V TITANIUM
TESTED AT 520 DEG. F
INPUT TO COMPUTER PROGRAM

FORGING SPECIMEN NUMBER	THICKNESS B (IN.)	WIDTH W (IN.)	YIELD STRESS FTY (KSI)	CRACK LENGTHS: FATIGUE AO (IN.)	POP-IN AP (IN.)	DEV. FROM LINEARITY AO (IN.)	ONSET OF RAPID SWE AC (IN.)	AT MAX. LOAD AM (IN.)	MEASURED AT PMAX. AA (IN.)
					LOADS: POP-IN PP (KIPS)	DEV. FROM LINEARITY PO (KIPS)	ONSET OF RAPID SWE PC (KIPS)	MAXIMUM LOAD PM (KIPS)	
22-5	0.102	5.005	128.	0.440	0.55A 18.8	0.446 10.5	0.000 0.0	0.721 28.8	0.555
22-4	0.102	5.004	12A.	0.440	0.4A6 19.2	0.45R 7.0	0.A10 25.4	0.789 2A.4	0.578
22-12	0.098	5.001	130.	0.435	0.56T 22.4	0.446 T.8	0.A94 25.5	0.755 25.9	0.585
22-10	0.098	5.002	130.	0.455	0.585 22.1	0.482 12.1	0.A88 25.9	0.78A 24.4	0.A22
22-9	0.098	5.005	130.	0.435	0.A0G 24.0	0.496 8.9	0.T45 25.T	0.85A 2A.8	0.5A5
22-6	0.102	5.005	12A.	0.488	0.555 19.5	0.452 8.0	0.000 0.0	0.844 25.A	0.A25

TABLE 1A - CENTER-NOTCH-TENSILE FRACTURE TOUGHNESS OF 6AL-4
TESTED AT 520 DEG. F
COMPUTER PROGRAM OUTPUT

FORGING SPECIMEN NUMBER	PLANE STRAIN TOUGHNESS KSI-IN 1/2 EQUATION (1)* KIC FOR AO - PO	KIC FOR AO - PO	KIC FUR AO - PP	KIC FUR AP - PP	PLANE STRESS TOUGHNESS EQUATION (1)* KC FUR AC - PC	KC FUR AP - PP	FTY
	PLANE STRAIN TOUGHNESS KSI-IN 1/2 EQUATION (2)* KIC FOR AO - PO	KIC FUR AO - PO	KIC FUR AO - PP	KIC FOR AP - PP	PLANE STRESS TOUGHNESS KSI-IN 1/2 EQUATION (2)* KC FUR AC - PC	KC FUR AM - PM	KC FUR AE - PM	EFFECTIVE CRACK AE (IN.)	PLASTIC ZONE SIZE RY (IN.)
22-5	42.5 42.5	42.7 42.9	78.8 80.2	87.1 87.7	0.0 0.0	155.5 156.5	185.7	•T.5 0.90A	0.A8U1 0.3710
22-4	28.4 28.A	28.5 28.5	77.8 78.0	80.2 80.8	12A.8 128.0	1A4.1 1A4.8	18T.5	8A.2 0.952	0.A7W8 0.5544
22-12	52.5 52.7	55.0 55.2	93.4 95.9	110.7 111.A	147.0 148.0	160.8 1A1.T	19A.4	88.5 0.95A	0.A747 0.5510
22-10	52.1 52.A	54.0 54.5	94.8 95.3	112.8 113.7	138.4 137.4	157.2 158.0	190.4	84.8 0.958	0.8855 0.3548
22-9	57.4 5T.8	40.5 40.8	100.1 100.5	125.4 124.4	157.7 158.7	187.5 187.8	19A.A	90.5 0.924	0.A91T 0.5592
22-6	35.8 54.0	55.1 55.5	81.2 81.T	90.4 91.1	0.0 0.0	1T0.5 1T0.7	184.5	85.5 0.8Av	0.A98A 0.3558

ZERO VALUES INDICATE NO DATA.

ZERO VALUES INDICATE NO DATA.
* EQUATION (1) IS 3RD DEGREE POLYNOMIAL & EQUATION (2) IS SECANT.

TABLE III

ROOM TEMPERATURE DATA FOR WELDS IN CHAMBER SN 673078

TABLE 16 - CENTER-NOTCH-TENSILE FRACTURE TOUGHNESS OF 6AL-4V TITANIUM 6I6TH WELDS OF CHAMBER 673078 TESTED AT 70 DEG. F INPUT TO COMPUTER PROGRAM

FORGING SPECIMEN NUMBER	THICKNESS B (IN.)	WIDTH W (IN.)	YIELD STRESS FTY (KSI)	CRACK LENGTHS: FATIGUE AO (IN.)	POP-IN AP (IN.)	DEV. FROM LINEARITY AD (IN.)	ONSET OF RAPID SWE AC (IN.)	AT MAX. LOAD AM (IN.)	MEASURED AT PMAX. AA (IN.)
					LOADS: POP-IN PP (KIPS)	DEV. FROM LINEARITY PD (KIPS)	ONSET OF RAPID SWE PC (KIPS)	MAXIMUM LOAD PM (KIPS)	
FORWARD 6I8TH WELD									
78-2	0.186	3.000	132.	0.810	0.000 0.0	0.792 12.2	0.000 0.0	0.896 25.2	0.840
78-3	0.186	2.998	132.	0.660	0.000 0.0	0.665 10.6	0.000 0.0	0.868 30.8	0.735
78-4	0.184	3.010	132.	0.782	0.000 0.0	0.822 12.5	0.000 0.0	1.000 23.7	0.830
78-5	0.180	3.000	132.	0.782	0.000 0.0	0.812 10.0	0.000 0.0	0.960 24.4	0.830
78-6	0.183	3.002	132.	0.515	0.000 0.0	0.358 13.0	0.000 0.0	0.391 27.5	0.320
CENTER 6I8TH WELD									
78-13	0.183	2.993	140.	0.815	0.000 0.0	0.806 11.4	0.000 0.0	0.854 28.7	0.865
78-14	0.178	3.001	140.	0.768	0.000 0.0	0.752 15.3	0.000 0.0	0.885 23.8	0.785
78-16	0.190	2.998	140.	0.782	0.000 0.0	0.760 11.5	0.005 0.0	1.017 28.5	0.863
78-17	0.188	3.006	140.	0.565	0.000 0.0	0.572 8.7	0.000 0.0	0.800 12.3	0.565
AFT 6I8TH WELD									
78-22	0.180	3.000	130.	0.640	0.000 0.0	0.633 14.0	0.000 0.0	0.762 28.0	0.675
78-24	0.187	3.000	130.	0.755	0.000 0.0	0.507 10.0	0.000 0.0	1.054 30.6	0.000
78-25	0.182	3.001	130.	0.520	0.000 0.0	0.335 11.7	0.000 0.0	0.594 27.8	0.535
78-26	0.187	2.998	130.	0.630	0.000 0.0	0.822 11.0	0.000 0.6	1.078 28.2	0.800
78-27	0.183	2.996	130.	0.790	0.000 0.0	0.788 12.6	0.000 0.0	1.058 27.0	0.900

ZERO VALUES INDICATE NO DATA.

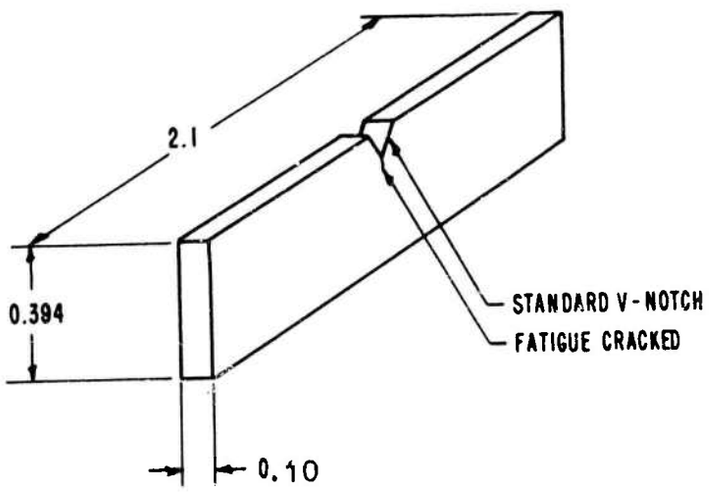
TABLE 16 - CENTER-NOTCH-TENSILE FRACTURE TOUGHNESS OF 6AL-4V TITANIUM 6I8TH WELDS OF CHAMBER 673078 TESTED AT 70 DEG. F COMPUTER PROGRAM OUTPUT

FORGING SPECIMEN NUMBER	PLANE STRAIN TOUGHNESS KSI-IN 1/2 EQUATION (1)* KIC FOR AO - PD	KIC FOR AO - PD	KIC FOR AO - PP	KIC FOR AP - PP	PLANE STRESS TOUGHNESS KSI-IN 1/2 EQUATION (1)* KC FOR AC - PC	KC FOR AM - PM		GROSS STRESS AT MAX. LOAD PG (KSI)	STRESS RATIO PG/FT
	PLANE STRAIN TOUGHNESS KSI-IN 1/2 EQUATION (2)* KIC FOR AO - PD	KIC FOR AO - PD	KIC FOR AO - PP	KIC FOR AP - PP	PLANE STRESS TOUGHNESS KSI-IN 1/2 EQUATION (2)* KC FOR AC - PC	KC FOR AM - PM	KC FOR AE - PM	EFFECTIVE CRACK AE (IN.)	1/2 PLASTIC ZONE SIZE RY (IN.)
FORWARD 6I8TH WELD									
78-2	42.8 43.1	41.7 41.6	0.0 0.0	0.0 0.0	0.0 0.0	98.5 98.7	104.4	43.2 0.850	0.3428 0.0997
78-5	30.6 30.8	30.7 30.8	0.0 0.0	0.0 0.0	0.0 0.0	114.7 ** 113.0 **	112.3 **	34.5 0.850	0.4134 0.1138
78-4	42.5 42.7	44.6 44.8	0.0 0.0	0.0 0.0	0.0 0.0	106.3 106.8	121.0	42.7 1.083	0.3241 0.1338
78-5	34.6 35.1	36.2 38.4	0.0 0.0	0.0 0.0	0.0 0.0	107.2 ** 107.4 **	108.3 **	43.2 0.853	0.3430 0.1056
78-6	32.2 32.4	33.1 33.4	0.0 0.0	0.0 0.0	0.0 0.0	80.6 ** 81.2 **	60.0 **	35.8 0.578	0.4078 0.0585
CENTER 6I8TH WELD									
78-13	40.8 41.0	40.4 40.6	0.0 0.0	0.0 0.0	0.0 0.0	115.1 113.5	127.2	40.8 1.028	0.3486 0.1714
78-14	46.8 47.1	45.6 46.2	0.0 0.0	0.0 0.0	0.0 0.0	103.6 104.1	103.6	48.5 0.862	0.3436 0.0872
78-16	38.1 38.3	37.1 37.3	0.0 0.0	0.0 0.0	0.0 0.0	129.8 130.5	126.5	50.7 0.993	0.3626 0.1301
78-17	22.2 22.3	22.3 22.3	0.0 0.0	0.0 0.0	0.0 0.0	32.7 ** 33.0 **	32.0 **	21.8 0.373	0.1946 0.0063
AFT 6I8TH WELD									
78-22	41.1 41.3	40.8 41.1	0.0 0.0	0.0 0.0	0.0 0.0	99.3 98.0	80.0	51.6 0.781	0.3888 0.0869
78-24	32.3 32.7	34.7 34.8	0.0 0.0	0.0 0.0	0.0 0.0	143.3 147.8	0.0	34.3 0.000	0.4199 0.0000
78-25	28.5 28.8	30.8 30.6	0.0 0.0	0.0 0.0	0.0 0.0	76.8 ** 77.3 **	78.8 **	31.8 0.390	0.3923 0.0937
78-26	38.3 38.4	38.8 38.0	0.0 0.0	0.0 0.0	0.0 0.0	140.0 141.8	149.5	30.3 1.110	0.3678 0.2163
78-27	43.7 43.8	43.6 43.8	0.0 0.0	0.0 0.0	0.0 0.0	126.3 ** 130.5 **	140.3 **	46.2 1.083	0.3791 0.1838

ZERO VALUES INDICATE NO DATA.
* EQUATION (1) IS 3RD DEGREE POLYNOMIAL & EQUATION (2) IS SECANT.
** FAILED THROUGH DOUBLED SPOT WELD. THEREFORE KC CALCULATED FROM PM IS A MINIMUM VALUE.

APPENDIX D

PRECRACK CHARPY TESTING FOR FRACTURE TOUGHNESS



Appendix D

TABLE OF CONTENTS

	Page
INTRODUCTION	203
PRECRACKING AND TESTING TECHNIQUES	205
MERITS AND LIMITATIONS OF THE PRECRACK CHARPY TEST	207
METALLURGICAL COMPLICATIONS TO FRACTURE-TESTING CORRELATIONS	218
EFFECT OF THICKNESS IN CHARPY TESTING	223
EFFECT OF LOADING RATE IN CHARPY TESTING	228
PRECRACK CHARPY TESTING IN THE MINUTEMAN PROGRAM	233
Tests of MINUTEMAN Qualification Trim Stock	233
Effect of Solution Treatment Temperature	237
Effect of Aging Temperature	238
Effect of Heat Treatment on ELI 6Al-4V Sheet Material	238
Effect of Shear Spinning	243
TABULATED DATA FOR MIL-HDBK-5	250
Table XII - Precrack Charpy Impact Data for 6Al-4V Titanium	251
Table XIII - Precrack Charpy Slow Bend Data for 6Al-4V Titanium	258

Appendix D

LIST OF TABLES

Table		Page
I	Prediction of Fracture Stress and Strain Energy Release Rate (G_c) Based on Precrack Charpy Impact Tests.	219
II	Metallurgical Size-Effects in Testing for Plane-Stress Fracture Toughness, K_c.	220
III	Variation in Crack Toughness as a Function of Coupon Size in Heat Treatment.	221
IV	Correlation Between Precrack Charpy Impact and CN-Tensile Tests in D6aC Low-Alloy Steel.	222
V	Precrack Charpy Slow-Bend and Impact Data for Three Materials.	232
VI	Fracture Toughness Measured in MINUTEMAN 6Al-4V Titanium Qualification Rings. Precrack Charpy Specimens 0.10-in. Thick as Tested.	234
VII	Fracture Toughness Measured in MINUTEMAN 6Al-4V Tensile Coupons. Precrack Charpy Impact Specimens 0.10-in., as Tested.	236
VIII	Effect of Solution Treatment on Fracture Toughness as Measured by PTC-Tensile Tests and Calculated from Precrack Charpy Tests. MINUTEMAN Forging S/N XEOB-2M, Heat Treated 0.55-in. Thick and Tested 0.10-in. Thick.	241
IX	Effect of Aging Temperature on Fracture Toughness as Measured by PTC-Tensile Tests and Calculated from Precrack Charpy Tests. MINUTEMAN Forging S/N XEOB-2M, Heat Treated 0.55-in. Thick and Tested 0.10-in. Thick.	242
X	Precrack Charpy Fracture Toughness of 6Al-4V Titanium Sheet. Heat M4790 was Tested 0.10-in. Thick.	244
XI	Precrack Charpy Impact W/A Values for Shear-Spun 6Al-4V Titanium MINUTEMAN Forging S/N 108.	248
XII	Precrack Charpy Impact W/A Values from MINUTEMAN Forgings Used in Mil-Hdbk-5 Data Collection.	251
XIII	Precrack Charpy Slow-Bend W/A Values from MINUTEMAN Forging Used in Mil-Hdbk-5 Data Collection.	258

Appendix D

ILLUSTRATIONS

Figure		Page
1	Comparison Between Standard V-Notch and Precrack Charpy Impact Tests.	204
2	Impact-Testing and Fatigue-Precracking Machines for the Precrack Charpy Test.	206
3	Fatigue-Precracked V-Notch Charpy Impact Transition Curves for Two AMS 6434 Steel Melting Practices. Numbers at the Data Points are Percent Slant Fracture.	209
4	Precrack Charpy Impact and K_{c3} Data for 0.054-in. Mill-Annealed 6Al-4V Titanium. CN-Tensile was 1.5-in. Wide.	210
5	Precrack Charpy Impact and K_c Data for 6Al-4V Titanium. CN-Tensile was 9-in. Wide.	211
6	Effect of Fatigue-Precrack Depth on Charpy W/A Impact Values.	213
7	Prediction of Fracture Stress in Aluminum 6-in. Wide Center-Notch Tensiles Based on Precrack Charpy Slow Bend (Figure 7a) and Impact (Figure 7b) W/A Values.	214
8	Measured and Predicted Fracture Stress in 0.050-in. Thick, 8-in. Wide CN-Tensile Tests. Prediction is based on Precrack Charpy Impact W/A Values.	217
9	Method Used to Obtain Charpy Coupons for Effect-of-Thickness Testing.	224
10	Effect of Thickness on Precrack Charpy Impact Transition Curves for 4340 Steel Tempered at 450 and 800°F.	225
11	Variation in Precrack Charpy Impact W/A Value as a Function of Thickness for 4340 Steel Tempered at 800°F (Figure 11a) and Tempered at 450°F (Figure 11b).	226
12	Comparison of Crack Toughness in Two Heats of D6aC Steel at Two Thicknesses. D6aC Austenitized at 1550 (1/4 hr), Air Cooled and Tempered at 1000°F (4 hr).	229

Appendix D

ILLUSTRATIONS (cont.)

Figure		Page
13	Effect of Loading Rate on Various Aluminum Sheet Alloys.	231
14	Microstructure of MINUTEMAN 6Al-4V Titanium Forging 4A. Specimen Etched with 1% Hf, 2% HNO_3. Magnification 250X.	235
15	Effect of Solution Treatment on Precrack Charpy and PTC-Tensile Test Results When Aged at 950°F (Figure 15a) and When Aged at 1100°F (Figure 15b). Material was a 6Al-4V MINUTEMAN Forging S/N XEOB-2M of 0.55-in. Wall Thickness. Specimens were 0.10-in. Thick.	239
16	Precrack Charpy Impact and Slow-Bend W/A Values for ELI 6Al-4V Titanium Sheet as a Function of Solution Treatment Temperature (Figure 16a) and Aging Temperature (Figure 16b). Material was 0.10-in. Thick, as Tested.	245

Appendix D

INTRODUCTION

Although many fracture tests have been devised since the turn of the 20th Century for evaluating the notch sensitivity of structural materials, the Charpy impact test continues to be used more than all other fracture tests combined. Probably the greatest single impetus to general acceptance of th V-notch Charpy test is the United States was the statistical evaluation of casualty ship plate conducted at the National Bureau of Standards during and after World War II. Casualty plate was placed in categories according to whether it corresponded to "fracture source, fracture through, or fracture end". V-notch Charpy impact tests showed that "fracture-source" plates were more notch sensitive than plates which did not contain a fracture source. The average energy absorptions were 7 ft-lb for source plates, 10 ft-lb for through plates, and 16 ft-lb for end plates. On the basis of these test results, a 15 ft-lb criterion is in general use for rimmed and semi-killed steels of the type used in ship-hull construction. It is important to note that the correlation between 15 ft-lb and service is reliable only for the particular type of steel used in ship construction.

In recent years, Orner and Hartbower[1,2,3,4,5,6]* demonstrated that by precracking the V-notch test piece to simulate an actual defect, the Charpy test became a semi-quantitative measure of fracture toughness in the various steel, titanium, and aluminum alloys investigated, one in some materials and/or material conditions, the precrack Charpy was a quantitative measure of fracture toughness. An important advantage in precracking over the relatively blunt machined V-notch used in the casualty-ship-plate investigations is the elimination of certain energy losses which tend to make measurements with uncracked V-notched specimens fictitiously high in brittle materials.[4] This effect is shown in Figure 1, which indicates that a ductile-to-brittle transition occurs in the precracked Charpy energy-temperature curve which coincides in temperature with the transition indicated by fracture appearance. With the conventional (uncracked) V-notch Charpy test, the transition is obscured by elastic energy losses in the low-temperature range. Additional evidence of elastic-energy loss is found in the fracture behavior of the specimens. Without precracking, the specimens tested in the low-temperature range are ejected from the anvils with considerable velocity in a direction opposite to the movement of the pendulum. Thus, the elastic energy stored in the specimen and adjacent parts of the machine, over and above that required to propagate fracture, is converted into kinetic energy. Note from Figure 1, that precracking reduces the energy-to fracture value by approximately 80% in the brittle range, but by less than 30% in the ductile range.

*References at the end of the Appendix.

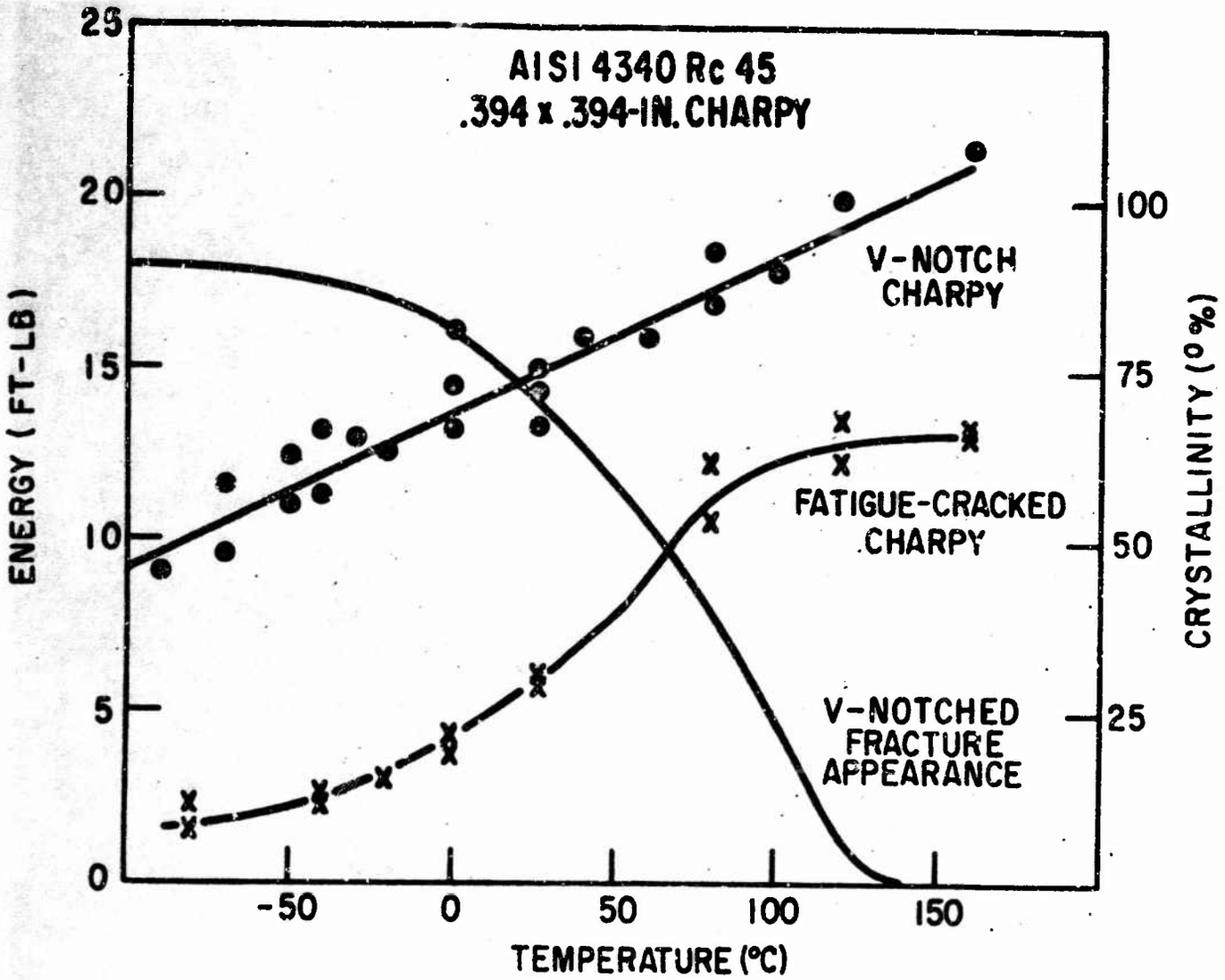


Figure 1. Comparison Between Standard V-Notch and Precrack Charpy Impact Tests

Appendix D

It is the purpose of this appendix to describe (1) the technique used in precrack Charpy testing, (2) the merits and limitations of the test, particularly with regard to its use for measuring fracture toughness, (3) the effect of thickness, temperature, and loading rate (slow-bend versus impact) on the crack-toughness measurement, and (4) precrack Charpy data obtained in the MINUTEMAN program prior to the present contract for MIL-HDBK-5 data collection. The latter include precrack Charpy impact and slow-bend tests of trim stock cut from production-lot motor cases, and studies of the effect of heat treatment and shear spinning on the precrack Charpy W/A value. Attached to this appendix are the tabulated precrack Charpy impact (Table XII) and slow-bend (Table XIII) data collected in the MIL-HDBK-5 test program.

PRECRACKING AND TESTING TECHNIQUES

The precrack Charpy test is similar to the standard V-notch Charpy impact test, except that (1) the machined notch in the specimen is sharpened by fatigue cracking, (2) the width of the specimen is generally the material thickness (the width may be as small as 0.03-in. in testing high-strength sheet and as large as 0.8-in., limit imposed by impact-testing-machine design), (3) the specimen is tested at two widely different loading rates, and (4) the result is expressed in terms of energy absorbed per unit of fracture area (W/A). If fracture toughness is defined as the resistance of a material to the propagation of a crack, expressed in terms of energy absorbed (work done) in producing each unit of new crack area, then it follows that the precracked Charpy test measures fracture toughness directly. In notched tensile testing, on the other hand, the specimen is stressed in the presence of a crack until a condition of instability is established where the elastic-energy release rate (G_c) is calculated using modified Griffith-type equations.

The precracking of Charpy specimens is best accomplished by fatigue cycling. The time to produce a crack at the base of the standard Charpy V-notch is normally about 2-3 minutes per specimen. A special machine, designed by Orner at MANLABS, Inc., is used for precracking Charpy specimens. Crack depths are normally held to approximqtely 0.025-in. deep, but may vary considerably without significantly affecting the results. Since the results are expressed in terms of work divided by fracture area (W/A in.-lb/in.^{2}), the lower energy values resulting from the more deeply cracked specimens are compensated for by the decrease in fracture area. Thus, the measurement of W/A is largely insensitive to precrack depth within practical limits.

Impact testing precracked specimens is conducted using standard Charpy techniques; however, owing to the low-energy values often encountered in precracked high-strength materials, a sub-size impact-testing machine is used which reads in very small energy increments. This machine, together with the precracking machine, are shown in Figure 2.

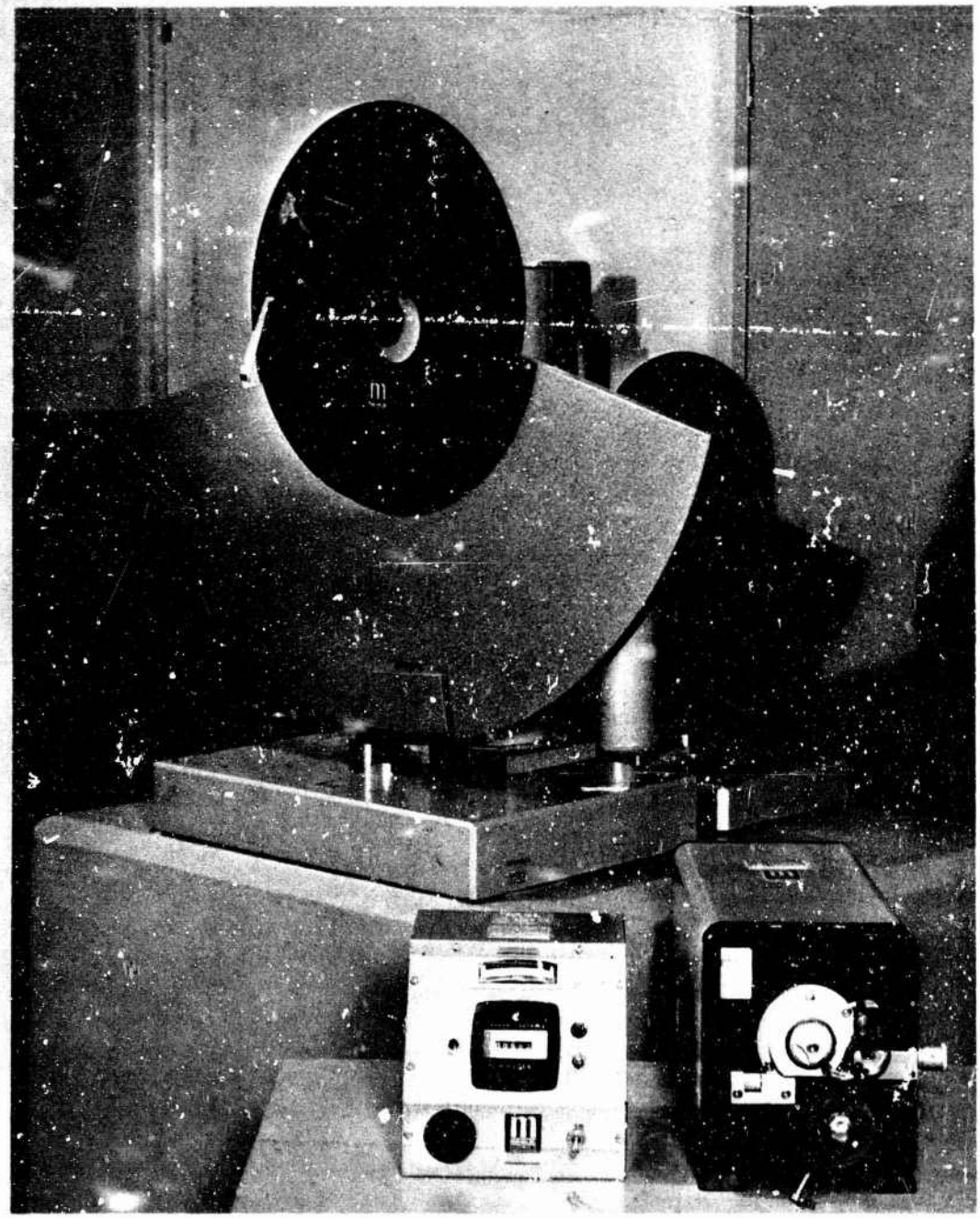


Figure 2. Impact-Testing and Fatigue-Precracking Machines for the Precrack Charpy Test

Appendix D

It has been shown that high-strength-sheet materials generally exhibit lower fracture toughness at low rates of strain than in impact[4,6] and, since nearly all structures are called upon to withstand static as well as occasional dynamic loads, both slow-bend and impact testing of precracked Charpy specimens is desirable, since the comparison of slow-bend and impact test results provides information on the strain-rate sensitivity of a material. Slow-bend testing can be carried out on standard tensile equipment using special fixtures; however, apparatus designed by Orner at MANLABS, Inc. is commercially available for fracturing precrack Charpy specimens at low strain rates while providing direct read-out of maximum load, energy-to-fracture and load-deflection curve.

In the MIL-HDBK-5 data collection described in the body of this report, the following precracking and testing procedures were used. Precracking was accomplished in approximately three minutes (at 1725 cpm) using a MANLABS Fatigue Precracking machine and load-ring number one. Loading was in tension-zero-tension, and the outer fiber stress was nominally 45 ksi.

The precrack Charpy specimens were tested on a MANLABS Impact Tester Model CIM-24. Impact testing at room and elevated temperature was conducted using standard Charpy techniques. The elevated temperature was obtained in a bath of silicone-base oil and the desired temperature maintained within $\pm 2°F$. The test pieces were soaked for a minimum of 30 minutes at temperature, and the maximum time for testing each specimen was 3 seconds.

MERITS AND LIMITATIONS OF THE PRECRACK CHARPY TEST

The ASTM Special Committee on Fracture Testing has suggested that in selecting a screening test for fracture toughness 1) the test should permit rapid evaluation of a large number of alloys, metallurgical variables and testing conditions with a minimum expenditure of time, money and materials; 2) the sensitivity should be sufficient to reveal changes in specimen brittleness as influenced by composition and heat treatment; and 3) the test should be easily conducted, even by those with minimum training in stress analysis or metallurgy."[7]

The precrack Charpy test is believed to fulfill all these requirements and has been shown to correlate with other more widely used fracture toughness tests. The Charpy test has been shown to be highly sensitive to variations in toughness as influenced by composition and heat treatment, as well as to heat-to-heat and even sheet-to-sheet variations[4,6]. The economy of the test is obvious from the fact that approximately 1 sq in. of material is required as compared with 36 sq in. (3 x 12 in.) and sometimes much larger tensile tests. Moreover, the test is easily and inexpensively conducted over a wide range of temperatures and at widely different rates of loading.

Appendix D

Impact tests of fatigue precracked sheet Charpy specimens have been conducted at temperatures up to approximately 1800°F and commonly down to -320°F (liquid nitrogen). For low temperatures, the specimen is immersed in a suitable bath using liquid helium, nitrogen or dry ice. Above room temperature, the specimens are heated in air, silicon oil, or other suitable medium. Comparisons between the relative positions of the resulting toughness-temperature transition curves provide a sensitive and practical criteria for rating materials, or for assessing the effect of metal processing or chemistry in a given material. For example, in Figure 3, two heats of AMS 6434 steel are compared, where one was consutrode melted and the other air melted. Note the markedly superior performance of the consutrode-melted heat, and the effect of thickness on the air-melted heat.

In common with other fracture toughness test specimens, the precracked Charpy suffers from limitations due to the small size of the specimen. However, the capacity of this specimen to measure high values of fracture toughness is much greater than its small size would indicate. This is because yielding of the net section, which occurs in tough materials, has relatively little effect on the total energy absorbed in fracturing a Charpy specimen. The energy absorbed in yielding the net section merely represents a normal part of the energy required to propagate the crack. In fracture toughness tests requiring Griffith-type elastic-energy analysis, net-section yielding precludes meaningful calculations because with extensive plastic deformation the analysis, which assumes elastic conditions, is no longer valid. Furthermore, additional load increase after the onset of net-section yielding is limited and the stress necessary to establish the critical energy balance may not be attainable. Thus, the use of maximum load for critical load is not justifiable if net-section yield has occurred. The data in Figure 4 illustrates this point. Note that 1-1/2-in. wide fatigue-cracked center-notched tensile specimens from mill-annealed 6Al-4V titanium sheet indicate decreasing K_c values with increasing temperature at temperatures above that at which the net fracture stress equals the yield stress. The Charpy, on the other hand, indicates increasing fracture toughness with increasing temperature. For valid K_c or G_c values, the notched tensile specimen should have been much wider.

A comparison of center-notch tensile K_c data from the SST program[8] also illustrates this point. The data shown in Figure 5 were obtained with 9-in. wide, center-notch panels of various thicknesses of 6Al-4V titanium heat-treated to 165 ksi ultimate tensile strength. The critical crack length at final instability was measured by motion-picture photography. Note that the panels indicated decreasing K_c values with increasing temperature; the data points marked with an arrow involved excessive net-fracture-stress. The fatigue precrack Charpy impact tests, on the other hand, indicated continuously increasing fracture toughness with increasing test temperature.

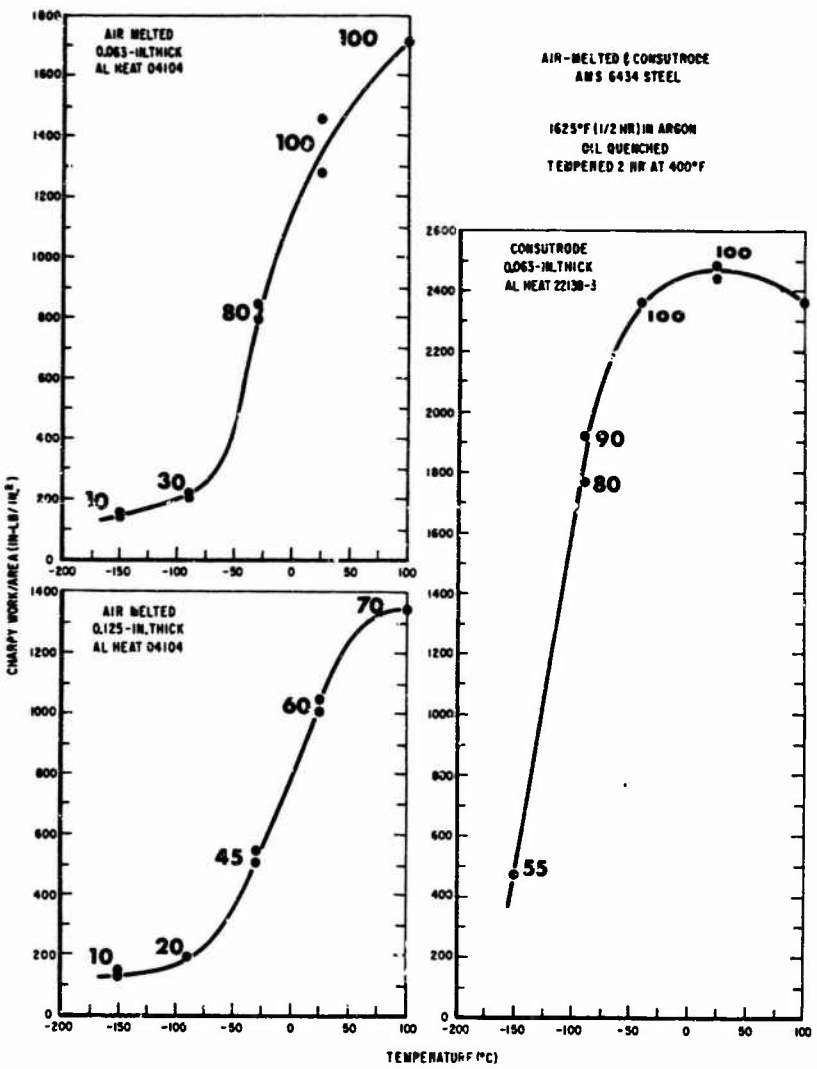


Figure 3. Fatigue-Precracked V-Notch Charpy Impact Transition Curves for Two AMS 6434 Steel Melting Practices. Numbers at the Data Points are Percent Slant Fracture

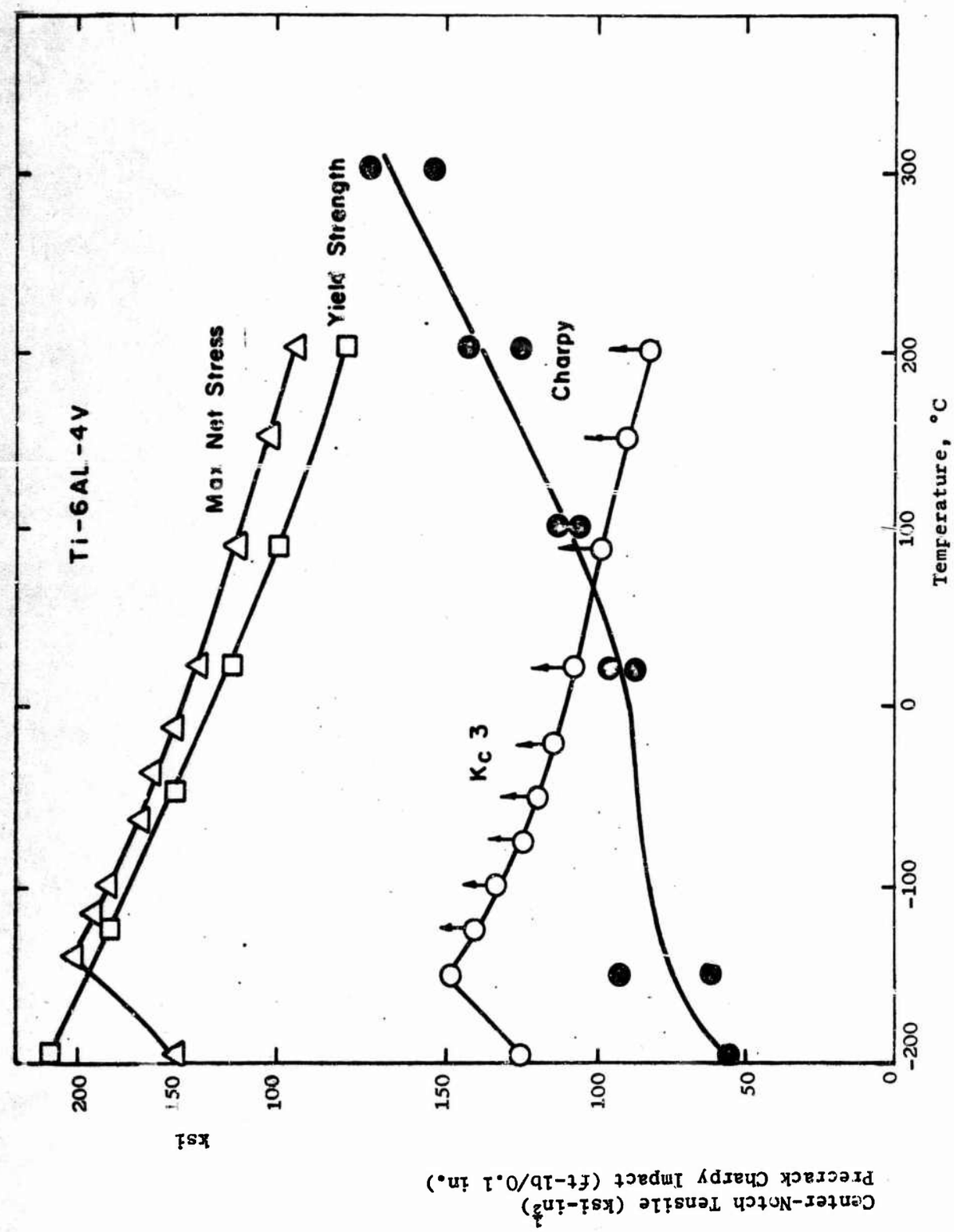


Figure 4. Precrack Charpy Impact and K_{c3} Data for 0.054-in. Mill-Annealed 6Al-4V Titanium. CN-Tensile was 1.5-in. Wide

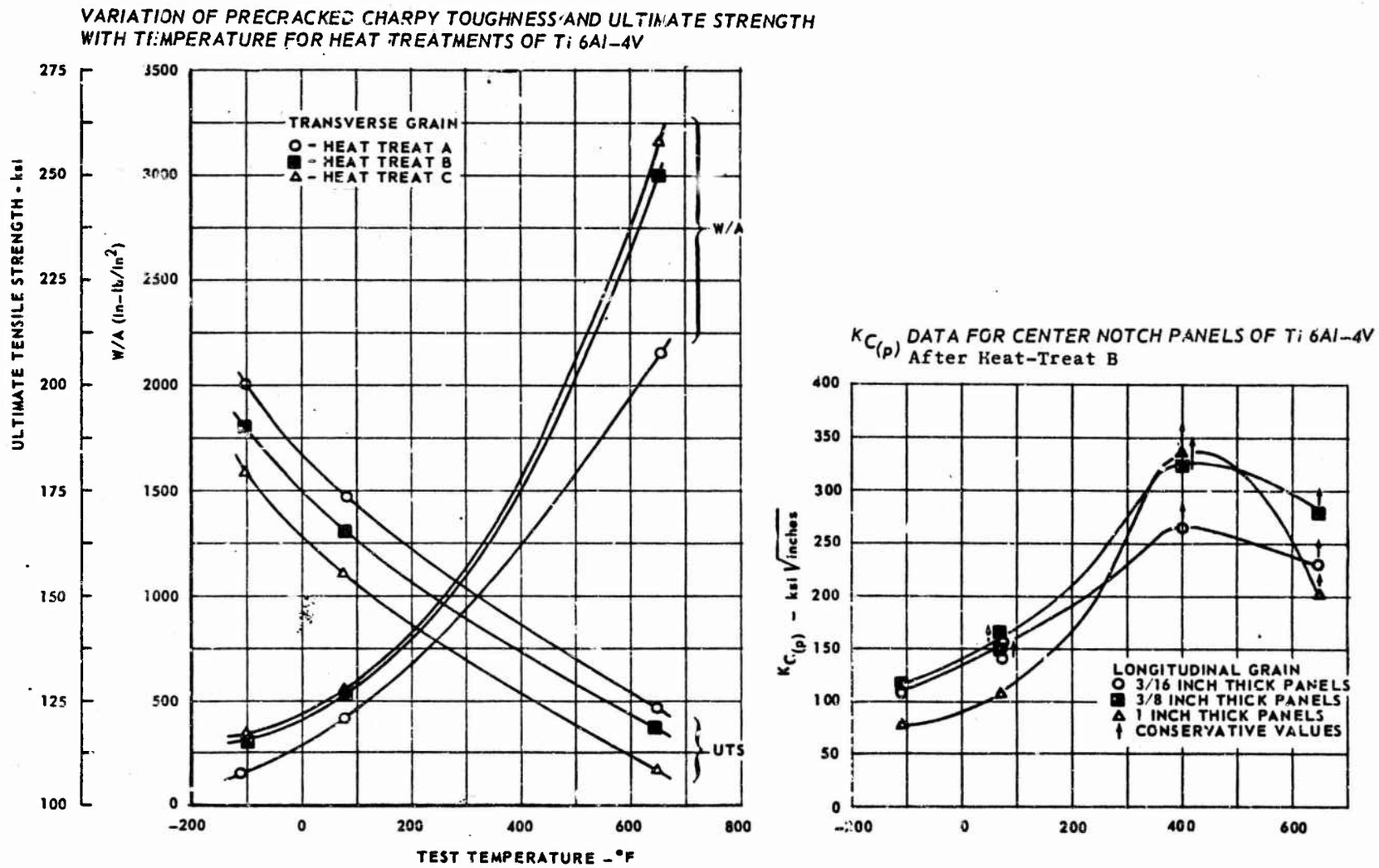


Figure 5. Precrack Charpy Impact and K_c Data for 6Al-4V Titanium. CN-Tensile was 9-in. Wide

Appendix D

In materials sufficiently tough to develop shear lips at the free surfaces of the test piece, the initial stage of crack propagation is associated with a relatively low-energy square (flat) fracture with slant (shear) fracture at the sides of the test piece as the crack propagates through the specimen. It is this behavior that is responsible, also, for the decrease in W/A values that occurs with increasing fatigue crack depth in relatively tough materials. As the fatigue crack deepens, the remaining depth of specimen is reduced, allowing less and less distance for the shear lips to develop. The percentage of flat fracture in the fracture surface is, therefore, increased, lowering the observed W/A values. The effect is illustrated by the data in Figure 6. Sheet Charpy specimens in 4340 tempered at 410°F were tested in impact with fatigue-crack depths ranging from about 0.005 to 0.20 in. Note that at the high-energy level (i.e., room temperature tests) the W/A values decreased with increasing crack depth, while at the low energy level (-40° tests), the W/A values were essentially independent of crack depth. It should be noted, however, that with fatigue crack depth in the range usually employed (approximately 0.02 to 0.04 in.), the change in W/A is almost insignificant.

The ultimate goal in fracture testing is the development of a simple laboratory test which will predict the maximum stress that a structure will withstand in the presence of a flaw of known dimensions. It has been demonstrated that the precrack Charpy test can be used in some materials and/or material conditions to predict the approximate stress at which a center-notched tensile specimen will fail.[6] Consider the Griffith equation as it applies to a wide center-notch panel

$$K_c^2 = \pi a F^2$$

where a is the half-crack length and F is the gross stress. Substituting EG_c for K_c^2 and solving for a

$$a = EG_c/\pi F^2$$

Assuming the precrack Charpy W/A value can be used as an approximation of the strain energy release rate, G_c, substitute W/A for G_c

$$a = E(W/A)/\pi F^2$$

It has been shown that fracture stress can be determined in aluminum alloys by using precrack Charpy slow-bend values for W/A and <u>initial</u> crack length ($2a_o$) in the above expression. For example, Figure 7a shows the slow-bend W/A prediction obtained for 2024-T81, 2024-T86, 2014-T6, and 7075-T6 aluminum alloys tested as 6-in.-wide, 80-mil thick, center-notch tensile specimens. When the prediction is based on the precrack Charpy impact W/A value and the <u>critical</u> crack length ($2a_c$), except for 7075-T6, an equally good prediction obtains as seen in Figure 7b.

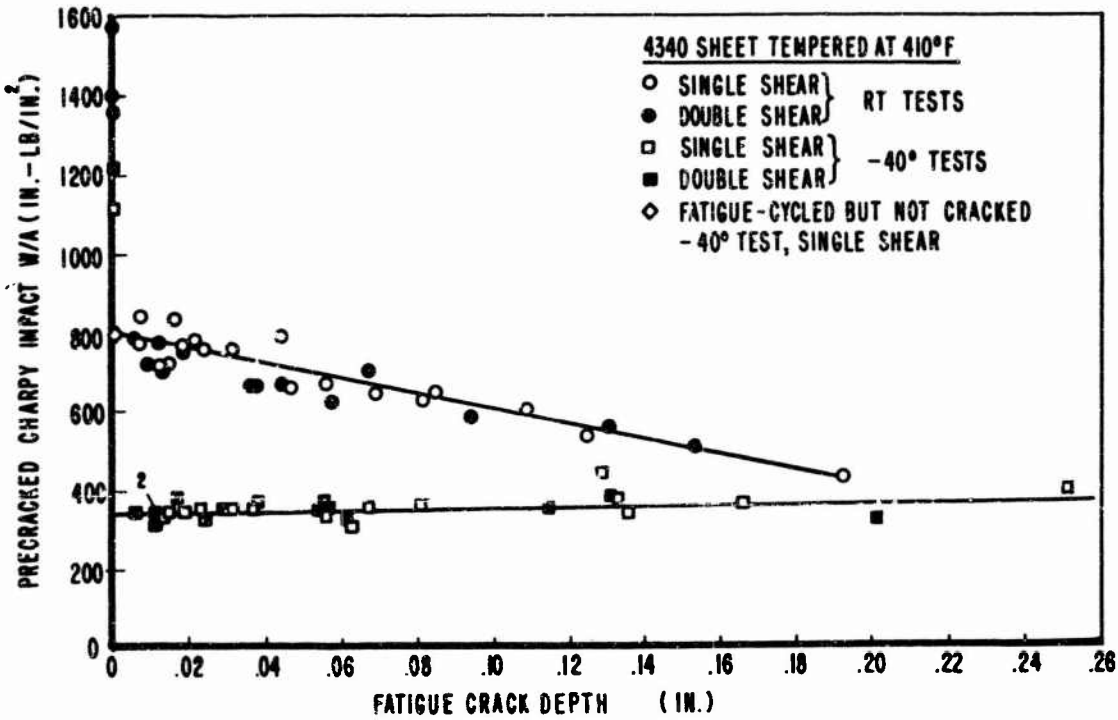


Figure 6. Effect of Fatigue-Precrack Depth on Charpy W/A Impact Values

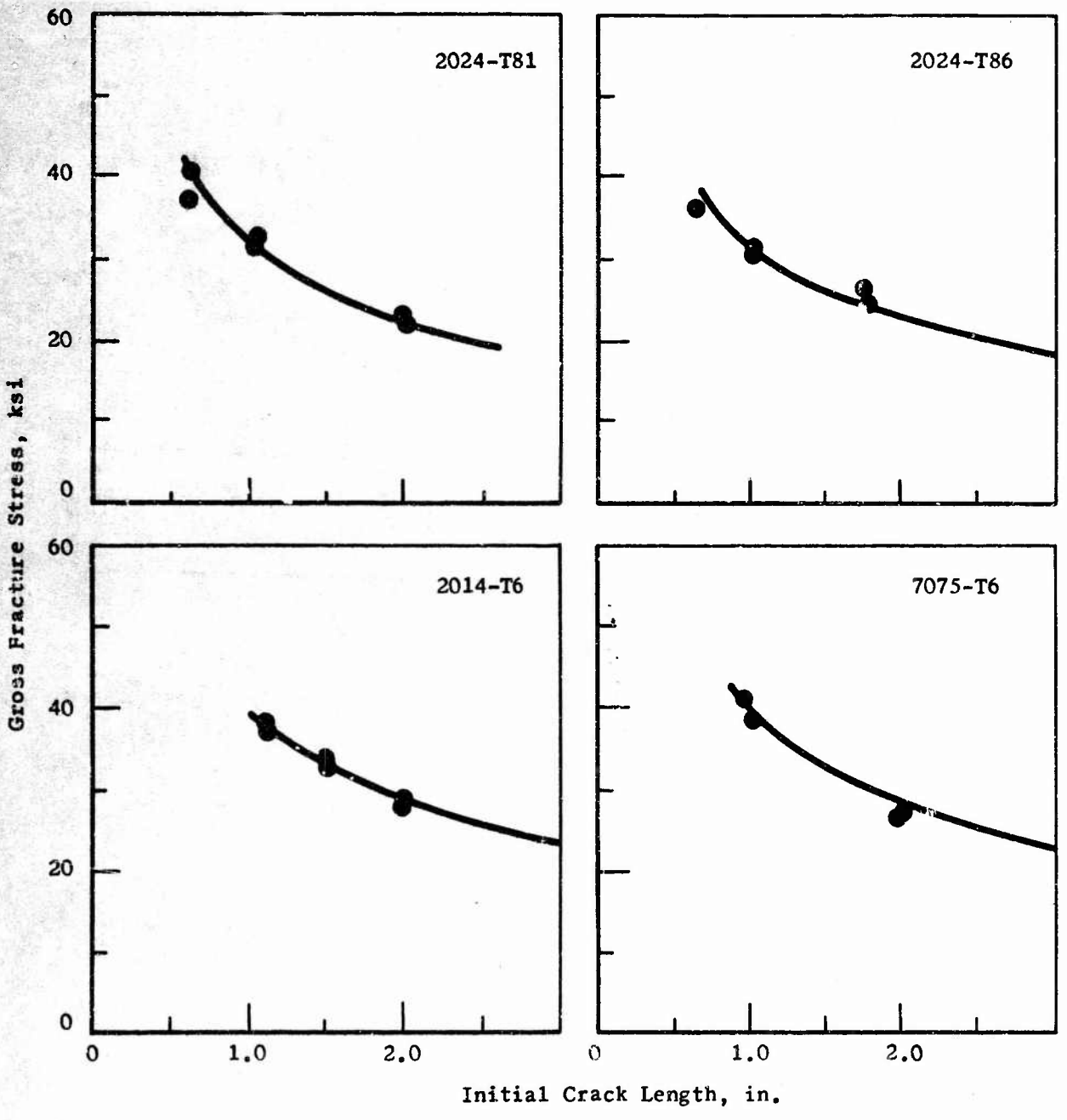


Figure 7a. Prediction of Fracture Stress in Aluminum 6-in. Wide Center-Notch Tensiles Based on Precrack Charpy Slow Bend (Figure 7a) and Impact (Figure 7b) W/A Values

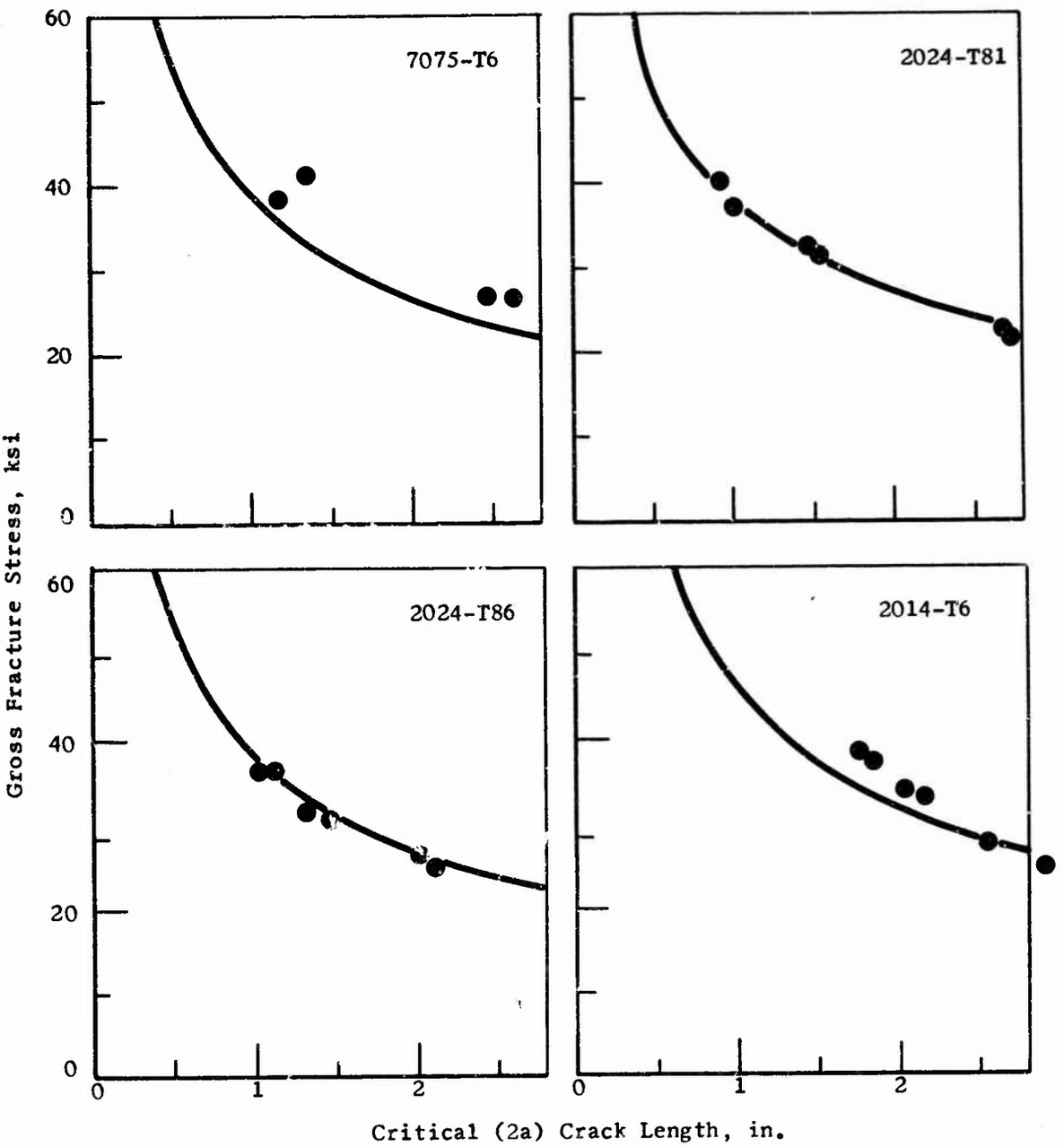


Figure 7b. Prediction of Fracture Stress in Aluminum 6-in. Wide Center-Notch Tensiles Based on Precrack Charpy Slow Bend (Figure 7a) and Impact (Figure 7b) W/A Values

Appendix D

Most attempts at predicting fracture stress based on precrack Charpy testing have utilized slow-bend test results and the initial ($2a_o$) crack length on the assumption that slow bend more nearly duplicated crack speed in the tensile tests. However, there is some question as to whether the crack speed in notched tensile testing is more nearly duplicated by slow bend or impact. In the tensile test, the load and crack length corresponding to the onset of unstable crack growth are used in calculating fracture toughness (G_c). At the onset of instability, the crack front is moving at a speed which is dependent upon the resistance of the material to crack propagation and the tensile-machine rate of loading. The fact that ink staining has been used in the past as a convenient technique for determining the length of crack at the onset of "fast" fracture in tensile testing, attests to a considerable crack velocity (it has been shown that when the crack is growing at a speed of approximately 10 in./sec, the ink is no longer capable of following the crack). Thus, in most materials, the onset of instability is attended by a running crack.

At high crack speed, the plastic zone in front of the advancing crack is adiabatic because there is insufficient time for the heat to be dissipated before the crack extends through the plastic zone. Moreover, when the crack front is moving rapidly there is insufficient time for such time-dependent phenomena as the diffusion of interstitial elements, strain aging, and stress-induced transformations--all of which tend to produce an apparent loss of toughness under slow bend or static load. Thus, in materials where these phenomena are involved, one would not expect a correlation between precracked Charpy slow-bend W/A values and notched tensile G_c values which involve running (unstable) cracks. However, the replot of Figure 7a, based on impact W/A values and the 2a (critical) crack length gives about equally good agreement (Figure 7b). In this case, the increase in the predicted gross stress resulting from the use of higher (i.e., impact) W/A values is largely offset by the increase in crack lengths (2a as compared with $2a_o$). For materials which exhibit low slow-bend values, recent work at Aerojet-General has indicated that precrack Charpy impact values give better predictions of fracture strength than slow-bend.

The data presented in Figure 8 and Table I were obtained from a variety of sheet materials. The 8-in. wide, center-notch tensile tests were conducted by Douglas Aircraft Company.[9] The broken CN-tensile specimens were supplied to MANLABS, Inc., as the source of material for precrack Charpy testing. The initial crack length in the center-notch tensiles were approximately 2 in.; the crack direction was oriented parallel to the rolling direction. In fatigue precracking the panels, a maximum gross stress of 40 ksi was used for Rene' 41, 35 ksi for the stainless steels, and 25 ksi for the titanium alloys. As described by Lement[10] precrack Charpy impact and slow bend specimens were machined from broken CN-tensile panels at locations adjacent to the panel fractures and in an orientation such that the tensile and Charpy fractures were parallel.

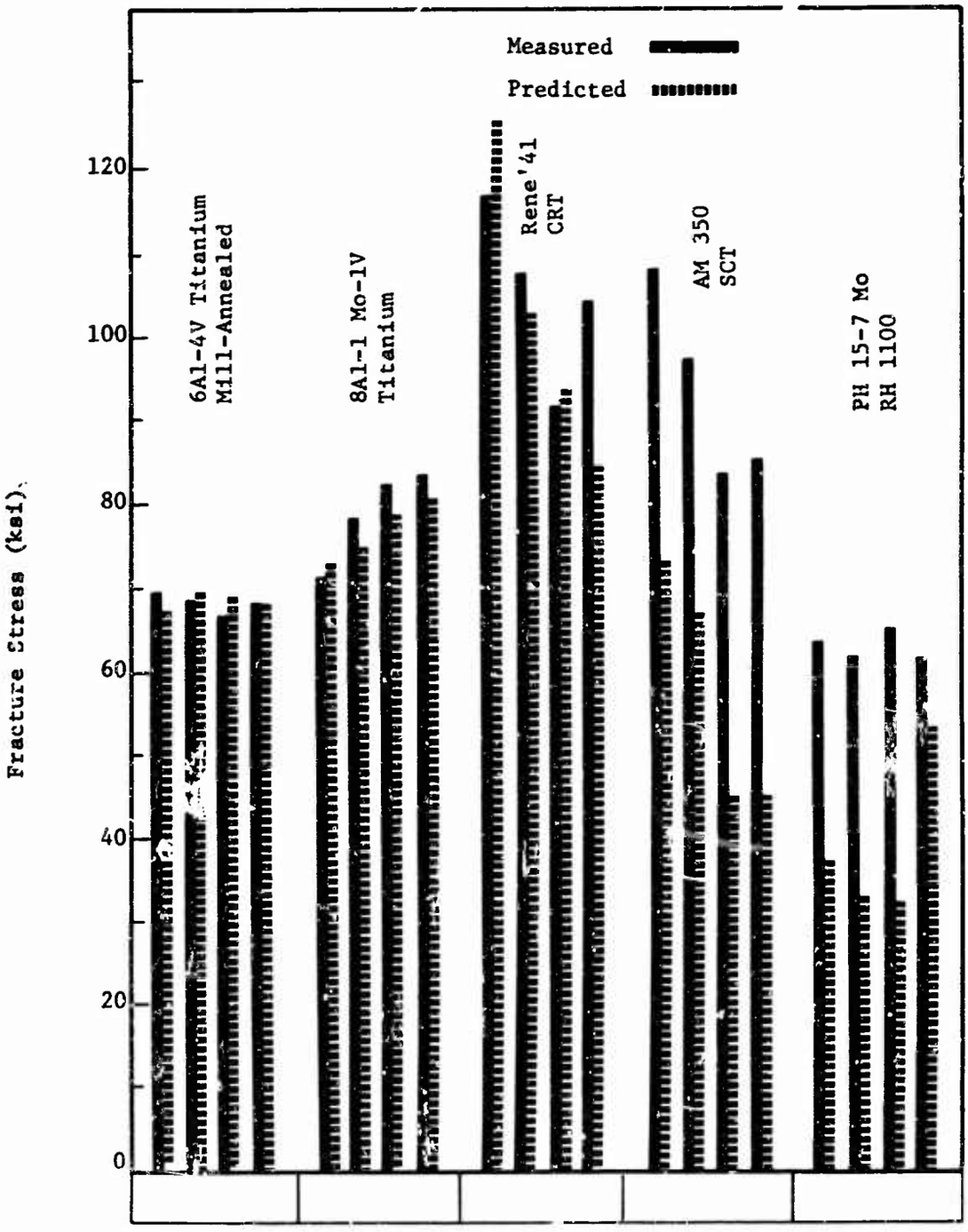


Figure 8. Measured and Predicted Fracture Stress in 0.050-in. Thick, 8-in. Wide CN-Tensile Tests. Prediction is based on Precrack Charpy Impact W/A Values

Appendix D

The prediction of fracture stress based on precrack Charpy impact and critical (2a) crack length, as shown in Figure 8, was excellent for the two titanium alloys (two heats of each alloy) and good for the two heats of Rene '41. However, in stainless steel AM350 (SCT) and PH 15-7 Mo (RH1100), the prediction was only qualitative and seriously unconservative. It is significant to note, in this connection, that the stainless steels developed higher W/A values when tested in slow-bend than in impact. Thus, in the case of the stainless steels, the W/A values as measured in slow-bend were closer to the CN-tensile G_c values than the impact W/A values. From the last column in Table I (ratio of precrack Charpy slow-bend to CN-tensile G_c values) note that the reverse was true in the case of 6Al-4V titanium.

METALLURGICAL COMPLICATIONS TO FRACTURE-TESTING CORRELATIONS

In the comparisons described above, the precrack Charpy specimens were cut from the CN-tensile specimens, with the Charpy specimens so oriented that the crack propagation direction was the same as in the tensile tests. When comparisons are attempted between specimens invclving different thicknesses, different notch orientations, different heats, different sheets of the same heat, or even different locations within a given sheet, there can be metallurgical complications which preclude correlation. Consider, for example, an attempt to correlate CN-tensile and precrack Charpy test results as a function of heat treatment in D6aC low-alloy steel.

D6aC low-alloy steel has widely variable response to heat-treatment procedure. Consider, for example, two austenitizing treatments, one of which is effective in solutionizing vanadium carbide (1750°F for 1/2 hr) and the other is ineffective as a solutionizing treatment (1550°F for 1/4 hr). The latter followed by a 400°F temper results in 155 ksi 0.2% offset yield strength, whereas the 1750°F treatment followed by a 1100°F temper results in over 200 ksi yield strength.

In an attempt to establish correlation between fatigue-cracked center-notch panels and precrack Charpy impact tests, 1/2 x 2-in. blanks were cut from 1/8-in.-thick sheet of D6aC together with 3 x 12-in. and 8 x 24-in. CN-tensile specimens. All specimens were austenitized in salt, with the Charpy blanks wired in a triangular array to assure free flow of salt around the blanks and to assure uniform air cooling on removal from the salt pot. The Charpy blanks were heat-treated in the salt pot with the 3 x 12-in. tensile specimens.

Comparisons between the crack-toughness measurements as obtained from the two sizes of CN tensile and the precrack Charpy impact specimens indicated poor correlations between the two sizes of CN-tensile specimen and between the precrack Charpy and the CN-tensile test. These data are presented in Table II.

TABLE I

PREDICTION OF FRACTURE STRESS AND STRAIN ENERGY RELEASE RATE (G_c) BASED ON PRECRACK CHARPY IMPACT TESTS

		8-in.-Wide CN-Tensile Test[a]			Precrack Charpy Impact Test[b]				
Alloy	Heat and Panel No.	Crack 2a(in.)	Gross Stress	G_c (in-lb/in^2)	W/A(in-lb/in^2)	Fracture St-ess(ksi)	σ Calc. / σ Obs.	PCI/ G_c	PCSB/ G_c
6A1-4V	D2963-248	2.040	69.8	1180	890	67.5	0.96	0.76	0.67
Mill-	-250	2.010	68.2	1100	930	69.5	1.02	0.84	0.69
Annealed	D2382-283	2.030	66.4	1045	910	68.4	1.03	0.88	0.74
	-285	2.040	68.4	1130	915	68.4	1.00	0.81	0.72
8A1-1Mo-1V	D1237-11T1	1.995	71.7	1280	910	73.3	1.02	0.71	0.64
	-11T2	2.005	78.3	1550	950	74.7	0.96	0.61	0.52
	D3369-12T3	2.012	82.3	1610	1070	79.2	0.96	0.66	0.57
	-12T4	2.010	83.6	1675	1130	81.4	0.97	0.68	0.53
Rene' 41	V2185-150	2.020	117.0	1880	1660	126.0	1.08	0.88	1.00
CRT	-152	2.020	107.9	1630	1070	103.0	0.96	0.66	0.66
	V2178-189	2.020	91.8	1020	880	93.6	1.02	0.86	0.62
	-191	2.000	103.9	1340	710	84.5	0.82	0.53	0.57
AM350	55306-1T1	1.910	108.0	1430	550	72.9	0.68	0.38	0.42
SCT	-1T2	2.018	97.4	1330	485	66.6	0.68	0.36	0.61
	69766-14T1	2.006	83.7	915	210	44.0	0.52	0.23	0.74
	-14T2	2.060	84.8	970	225	45.0	0.53	0.23	0.71
PH 15-7 Mo	810112-52	2.040	63.0	490	150	36.8	0.58	0.31	0.68
RH1100	-54	2.040	61.6	470	120	33.0	0.54	0.26	0.75
	800709-88	2.090	64.2	525	115	31.9	0.50	0.22	0.65
	-90	2.080	61.6	480	320	53.3	0.86	0.67	0.75

(a) Crack length and gross stress at maximum load.
(b) Fracture stress calculated from $\sigma^2 = E(W/A)/\pi a$.

Appendix D

TABLE II

METALLURGICAL SIZE EFFECTS IN K_c TESTING

Heat Treatment	Charpy Impact Heat Treated as 1/2 x 2-in. Blanks W/A (in.-lb/in.^{2})	Charpy Impact Heat Treated as 1/2 x 2-in. Blanks K_c (ksi-in.$^{1/2}$)	K_c (ksi-in.$^{1/2}$) 3 x 12-in. CN-Tensile	K_c (ksi-in.$^{1/2}$) 8 x 24-in. CN-Tensile
1550°F/1/4 hr 400°F/2 hr F_{ty} 155 ksi	148 - 154 Avg(2) 151	66	105	80
1750°F/1/2 hr 1100°F/2 hr F_{ty} 203 ksi	1078 - 1110 Avg(2) 1094	101	156	234

When R_c hardness measurements were taken on the Charpy blanks and on the two sizes of CN tensile, different values were obtained, indicating a metallurgical variable, probably due to differences in cooling rate. Therefore, Charpy blanks were cut from the broken CN-tensile specimens. The results of the precrack Charpy impact specimens separately heat-treated as 1/2 x 2-in. blanks, and cut from the broken CN tensiles, are presented in Table III.

Note that the material heat treated in the form of 3 x 12-in. and 8 x 24-in. sheets had markedly different toughness from one panel size to the other (as measured by precrack Charpy impact test) and that the material heat treated in the form of Charpy blanks had markedly different toughness from that in the panels. Time-temperature data for the air cooling of each specimen configuration, together with knowledge of the continuous-cooling transformation products produced in each specimen configuration for each austenitizing treatment are required to interpret the differences in toughness indicated in this table. In other words, the fact that the material in the form of 1/2 x 2-in. blanks produced the lowest toughness when austenitized from 1550°F (alloy-depleted matrix) and the material in the form of 1/2 x 2-in. blanks produced the highest toughness when austenitized from 1750°F (alloy-rich matrix) simply suggests a difference in transformation product when air cooled in the different specimen configurations, depending upon the austenitizing treatment.

When the precrack Charpy specimens were cut from the panels and the impact test results compared with the K_c values as determined from the CN-tensile tests, the precrack Charpy impact test gave a close approximation of the CN-tensile K_c value in the brittle-material condition, but only a qualitative correlation in the tough condition (Table IV). It should be noted in this connection that at high toughness (high fracture stress) there is as much or more reason to question the validity of the K_c value as measured in the CN-tensile as the precrack Charpy impact test result. Obviously, based on the

TABLE III

VARIATION IN CRACK TOUGHNESS AS A FUNCTION OF COUPON SIZE IN HEAT TREATMENT

D6aC Low-Alloy Steel

Heat Treatment	Precrack Charpy Impact Specimens*		
	Heat Treated as 1/2 x 2-in. Blanks	Cut from Panels 3 x 12-in.	Cut from Panels 8 x 24-in.
1550°F/1/4 hr 400°F/2 hr 155 ksi F_{ty}	148 - 154 Avg(2) 151	258 - 315 Avg(3) 287	166 - 175 Avg(2) 170
1750°F/1/2 hr 1100°F/2 hr 203 ksi F_{ty}	1078 - 1110 Avg(2) 1094	403 - 483 Avg(3) 441	564 - 662 Avg(3) 602

*All specimens 1/8-in. thick

Appendix D

TABLE IV

CORRELATION BETWEEN PRECRACKED CHARPY IMPACT AND CN-TENSILE TESTS
D6aC Low-Alloy Steel*

Heat Treatment	3 x 12-in. Panels		8 x 24-in. Panels	
	Charpy Test $\sqrt{(E \cdot W/A)}$	CN Tensile K_c	Charpy Test $\sqrt{(E \cdot W/A)}$	CN Tensile K_c
	($ksi\text{-}in.^{1/2}$)		($ksi\text{-}in.^{1/2}$)	
1550°F/1/4 hr 400°F/2 hr 155 ksi F_{ty}	91	105	70	80
1750°F/1/2 hr 1100°F/2 hr 302 ksi F_{ty}	113	156	132	234

*All specimens 1/8-in. thick; Charpys cut from fractured panels

test results presented in Table III, one cannot evaluate the geometrical effects of panel size on the K_c values because of metallurgical complications that could only be avoided by heat-treating at the larger panel size and then cutting 8 x 24-in. blanks into 3 x 12-in. test specimens for valid comparison with 8 x 24-in. test panels.

EFFECT OF THICKNESS IN CHARPY TESTING

The effect of thickness on the K_c values as measured in a CN-tensile test is well known. The precrack Charpy test shows a similar effect; consequently, the specimen thickness in which the measurements are made must always be given in reporting K_c and W/A values. Consider a series of precrack Charpy impact tests made with specimens ranging in thickness from 0.032 to 0.394-in. The material used for this study (see Ref 6) was cold-rolled 4340 bar stock (1/2-in. thick x 6-in. wide). Preparatory to machining, 2-in.-wide blocks were cut from bar stock, normalized at 1675°F and tempered at 1200°F for 2 hr. The blocks were then ground to a thickness of 0.394 in. and V-notched in the 6-in. direction; i.e., transverse to the rolling direction (Figure 9). Specimens of various widths were then sliced off with a milling saw, allowing approximately 0.010 in. on each side for grinding to final thickness after heat treatment. The finish-machined specimens were austenitized at 1525°F for 30 minutes, quenched in oil at room temperature, and tempered for 4 hr at 450 and 800°F. The specimens were wired together side by side in bundles of approximately uniform thickness with dummy specimens at either end to eliminate the variations in cooling rate that would otherwise have occurred during quenching as a result of the thickness variation. Full transition curves were determined for each of the following specimens sizes: 0.032, 0.046, 0.062, 0.098, 0.197, and 0.394 in. Prior to testing, all specimens were fatigue precracked to a depth of approximately 0.032 in.

The fracture toughness transition curves obtained for the specimens in the various thicknesses tested are presented in Figure 10. Note that in some cases, considerable scatter is evident at the high-energy levels. Much of the scatter is due to variations in the mode of fracture. In Charpy testing, two types of oblique shear fracture are observed; it was found that when specimens fracture completely or nearly completely in shear, the energy absorbed is generally higher when the shear is of orthogonal rather than single-shear type.

The variation in fracture toughness with sheet thickness at each of four temperature levels is shown in Figure 11. For the 800°F temper (Figure 11a), the fracture toughness as measured at +100°C increases to a maximum value at a thickness between 0.1 and 0.2 in. This initial increase in fracture toughness is believed to reflect an increase in the volume of plastically deformed metal that is associated with the occurrence of lateral contraction preceding the tip of the advancing crack.

With increase in thickness beyond that corresponding to the toughness maximum, the observed decrease in fracture toughness is believed to reflect the occurrence of increasing amounts of flat fracture in the center portion of the specimens. At a test temperature of -120°C, however, fracture toughness

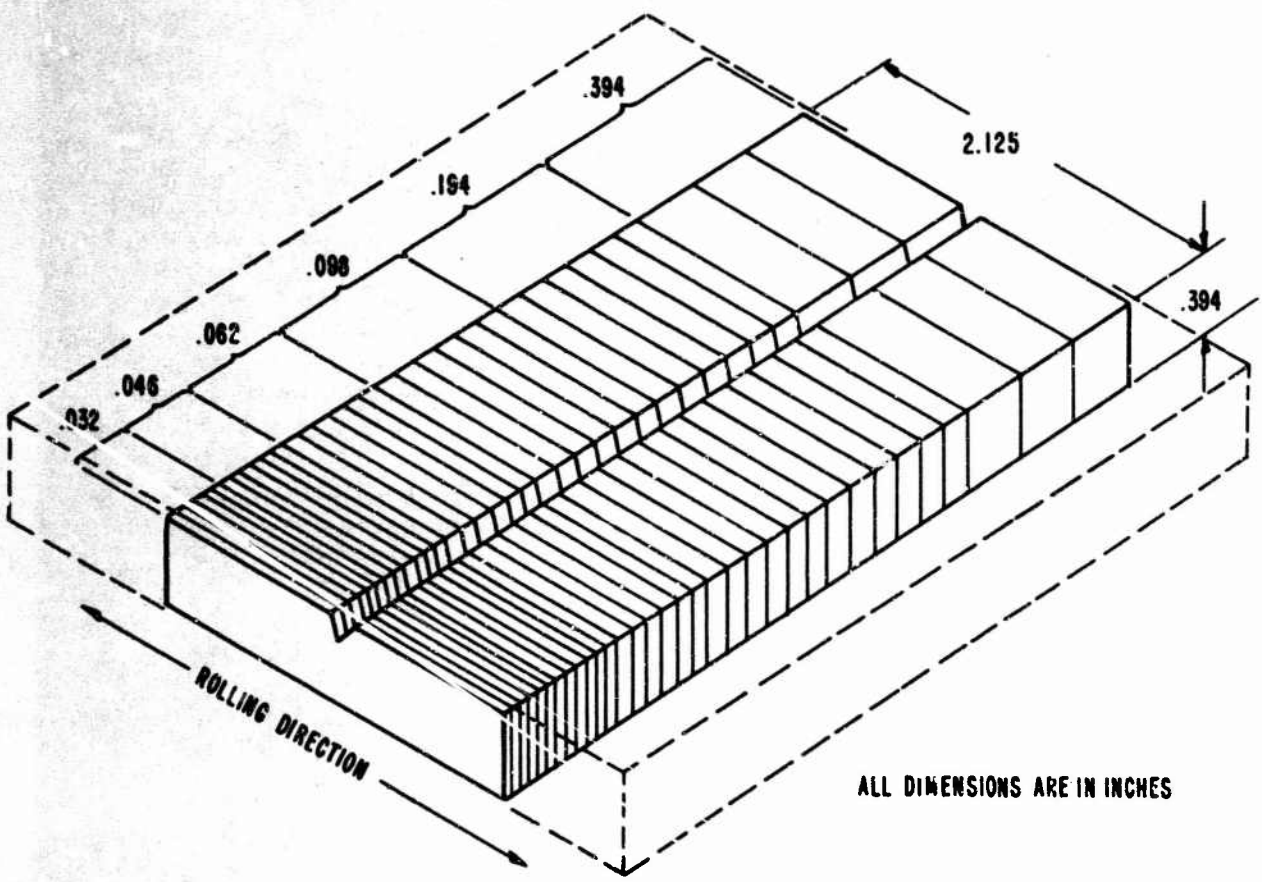


Figure 9. Method Used to Obtain Charpy Coupons for Effect-of-Thickness Testing

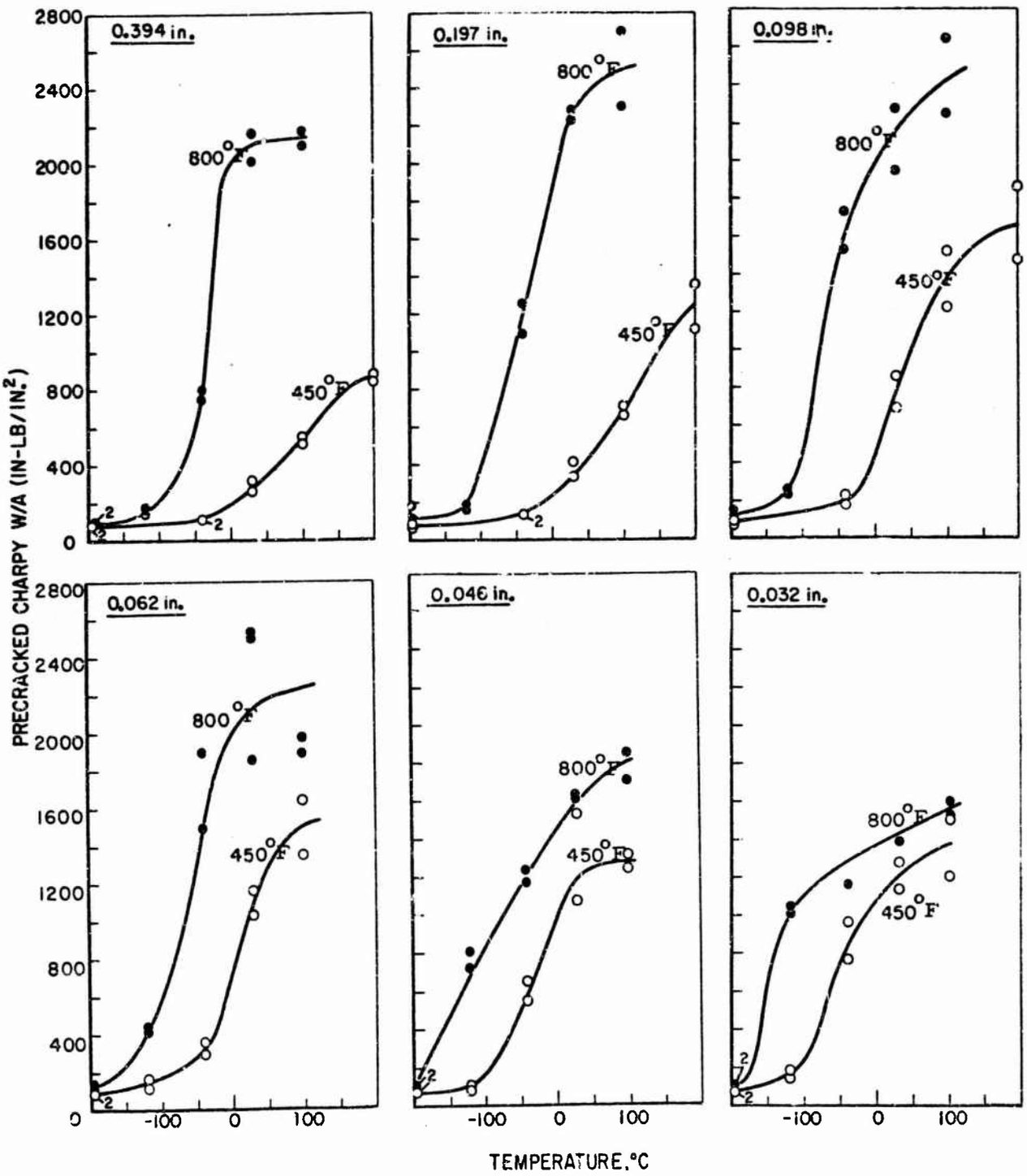


Figure 10. Effect of Thickness on Precrack Charpy Impact Transition Curves for 4340 Steel Tempered at 450 and 800°F

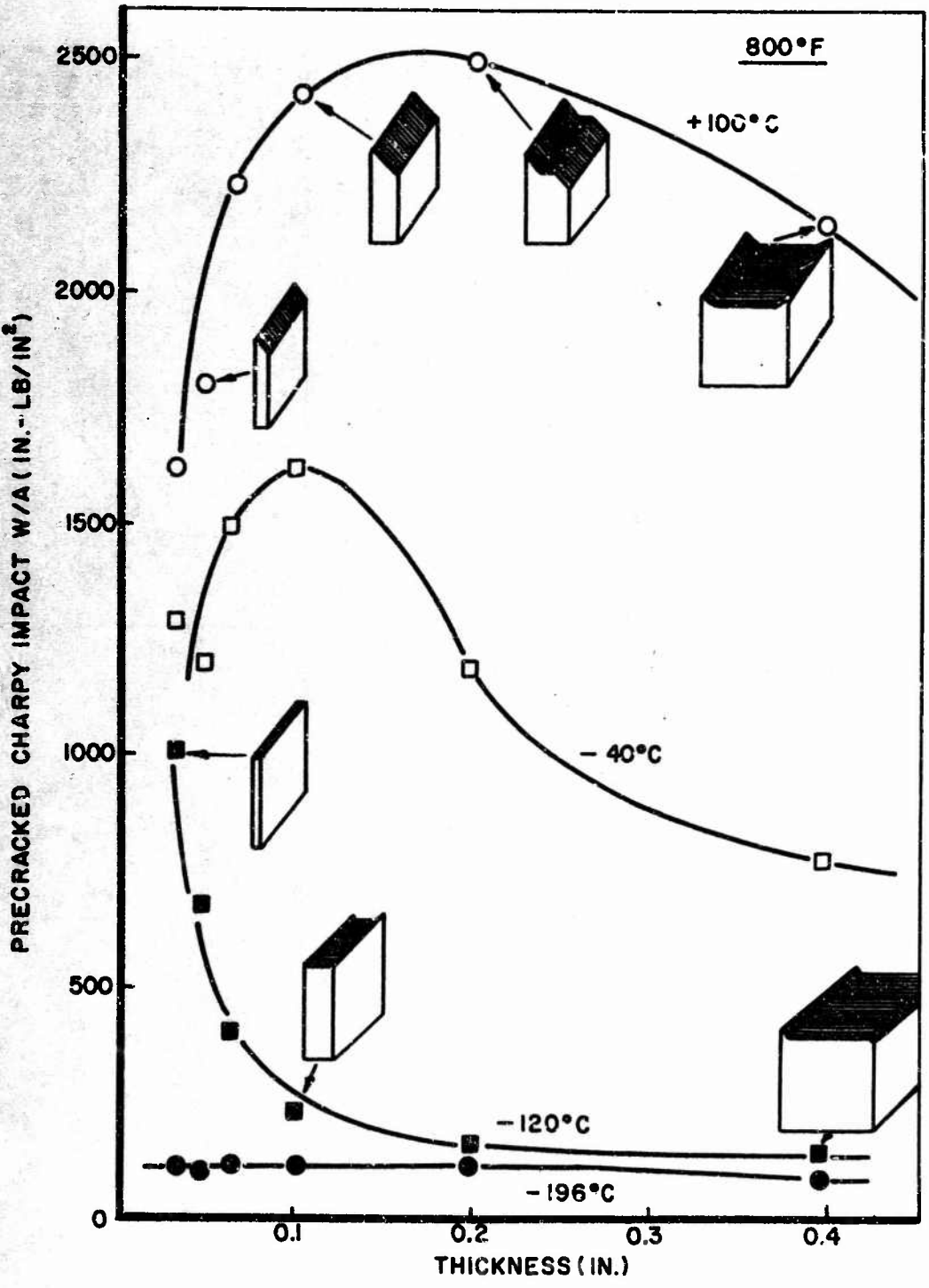


Figure 11a. Variation in Precrack Charpy Impact W/A Value as a Function of Thickness for 4340 Steel Tempered at 800°F (Figure 11a) and Tempered at 450°F (Figure 11b)

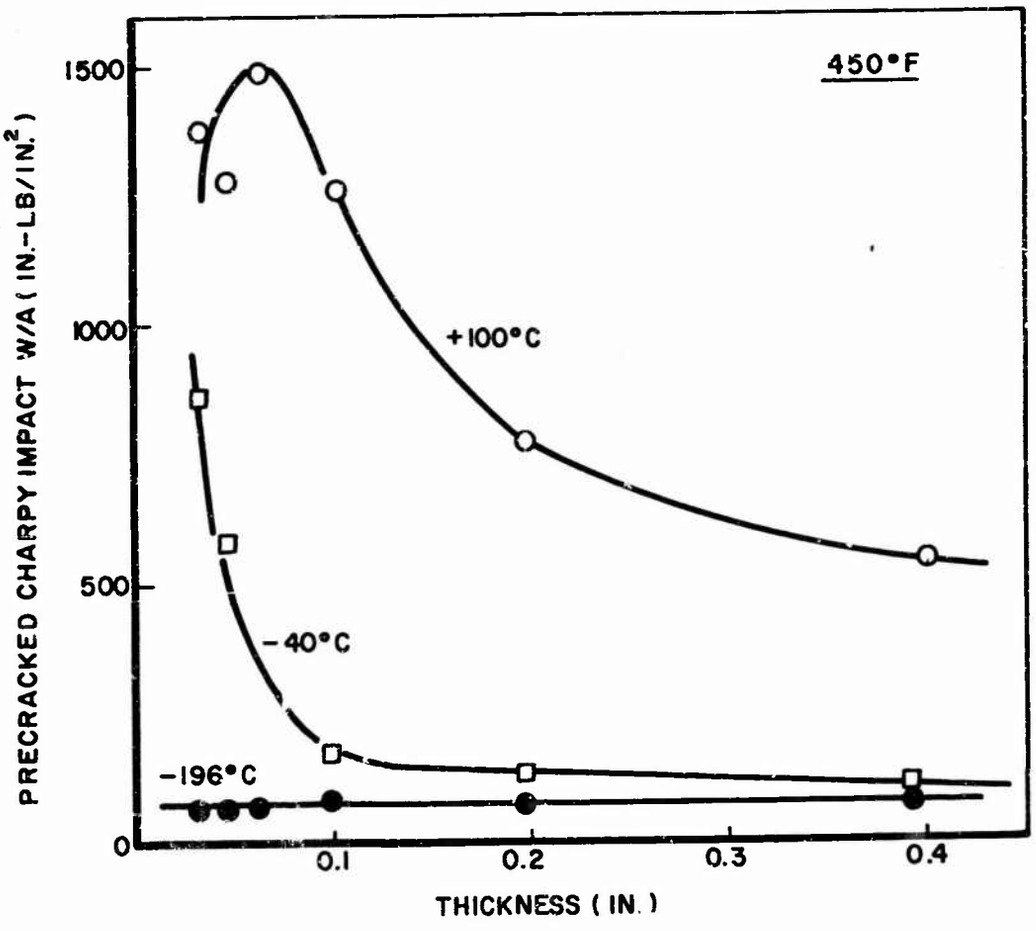


Figure 11b. Variation in Precrack Charpy Impact W/A Value as a Function of Thickness for 4340 Steel Tempered at 800°F (Figure 11a) and Tempered at 450°F (Figure 11b)

decreases markedly with increasing sheet thickness. This apparently reflects the increasing amount of flat (brittle) fracture that occurs even in the thinnest specimen tested. At -196°C, the fracture is virtually completely brittle with little evidence of shear at the free surfaces.

Figure 11b shows similar trends for a 450°F temper. However, due to the more brittle nature of the material tempered at 450°F, the curves are displaced toward higher test temperatures. Note that the -40°C curve for the 450°F tempered material is essentially the same as the -120°C curve for the 800°F tempered material.

In Figure 12, precrack Charpy impact data are plotted versus test temperature for two heats of D6aC steel of similar manufacturing history. The two heats were rolled to different thicknesses. For valid comparison between the heats, it was necessary to grind the thicker sheet down to 0.069 in. Note that the apparent difference between the heats was shown to be real. The difference between the heats can be ascribed to differences in chemistry and/or the metallurgical effect of rolling to different thicknesses. Although the effect of thickness proved to be small in this case, a valid comparison between the heats was not possible until they were machined to a common thickness.

EFFECT OF LOADING RATE IN CHARPY TESTING

In mild steel, with increased rate of loading, there is a loss of toughness. This is well known and consistent with the traditional concept that impact is the most severe test of a metal. Unfortunately, the time-worn concept does not hold for all metals - in fact for many metals the opposite is true; that is to say, slow bending is a more severe test than impact for many of the metals used today.

Crack velocity effects have been discussed by Kraft and Irwin in ASTM STP 381, p. 114. They point out that the phenomenon of adiabatic heating is involved; i.e., at the crack-tip, plastic-zone formation is attended by a temperature rise. If the rate of loading is sufficiently slow, the heat will be dissipated by conduction into the surrounding metal. Thus, the crack-initiation process in K_{Ic} fracture testing, with its inherently small plastic zone, is isothermal; whereas, the crack-propagation process in K_c fracture testing (which focuses on a running crack) with its inherently large plastic zone is adiabatic. Thus, as pointed out by Kraft and Irwin in their paper, it would be expected that the initiation of crack propagation would be easier for static than for dynamic loading.

Slow bend versus impact rates of loading in Charpy testing involve five orders-of-magnitude difference in loading speed. Thus, slow-bend testing can be considered isothermal and impact testing can be considered to involve adiabatic heating in the crack-tip plastic zone.

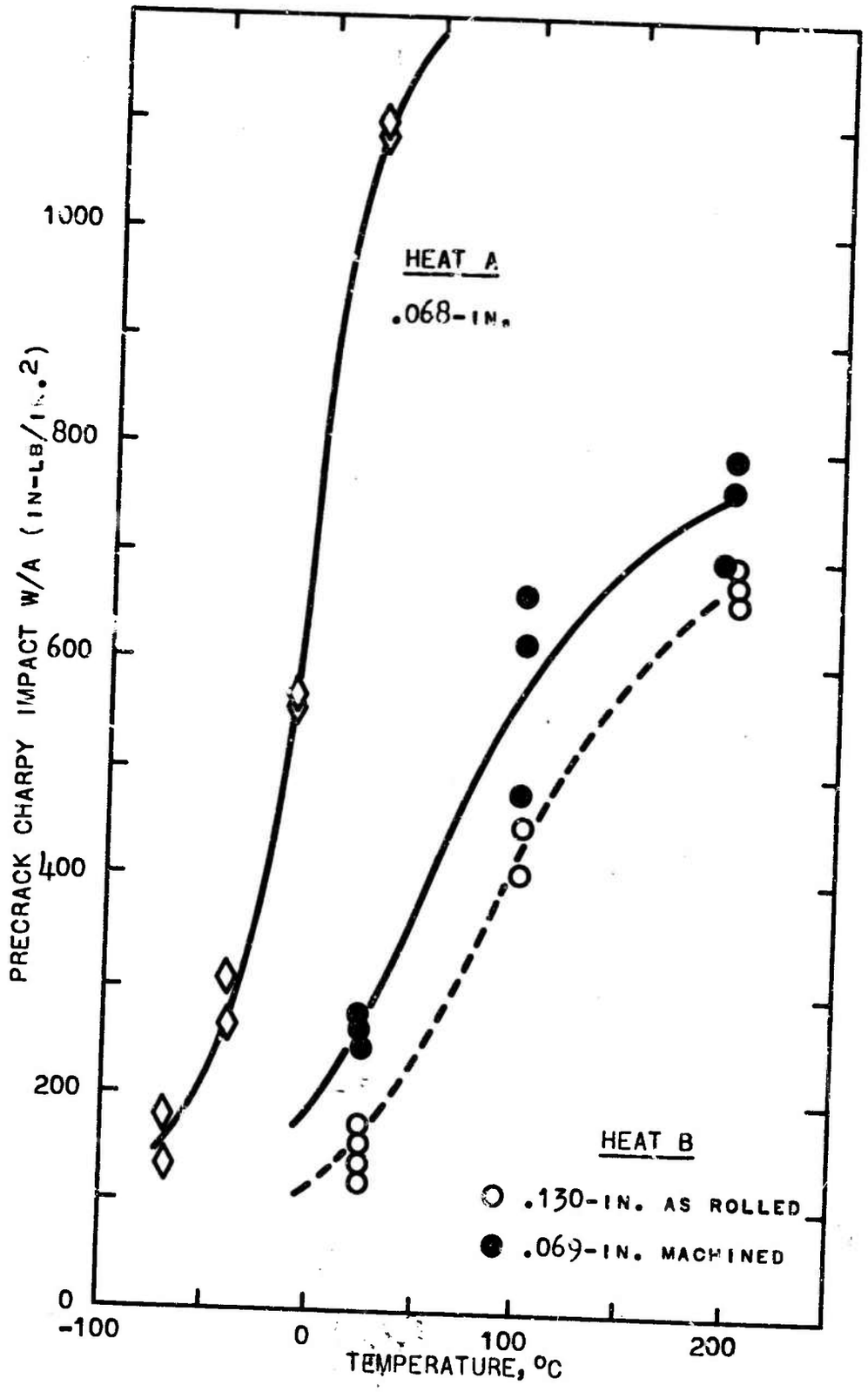


Figure 12. Comparison of Crack Toughness in Two Heats of D6aC Steel at two Thicknesses. D6aC Austenitized at 1550 (1/4 hr), Air Cooled and Tempered at 1000°F (4 hr)

Appendix D

A comparison made with MINUTEMAN 6Al-4V titanium by Kraft and Irwin between precrack Charpy slow-bend and impact tests and their SEN-tensile tests conducted over a similar range of loading speeds showed lower crack toughness at slow rates than at high rates of loading. The precrack Charpy slow-bend test result gave somewhat higher values than the slow SEN tensile tests because the Charpy W/A values include some surface shear lip energy which is not included in the plane-strain determination of the SEN tensile test.

The phenomenon of increasing fracture toughness with increasing rate of loading has been observed by Hartbower and Orner in many metals using the precrack Charpy test (see Figures 16 and 17 in the Welding Journal, Vol. 40(9), Sept. 1961, p. 405-s,[4] and Table 4 in Air Force Technical Documentary Report No. ASD-TDR-62-868, October 1962.[6] Morison, et al,[11] in an investigation of the crack-propagation resistance of high-strength alloys and heat-resistant alloys found strain aging to occur spontaneously in 4130 steel and in a molybdenum alloy (0.5 Ti- 0.08 Zr) when tensile tested under certain conditions of strain rate and test temperature. At high strain rate (between 2×10^3 and 2×10^5 lb/sec) the phenomenon disappeared. Steigerwald and Hanna[12] in an investigation of spontaneous strain aging in high-strength steels found significant strain aging effects in low-alloy martensitic 300M and 4340 steel, in precipitation hardening AM355 and in maraging 18% nickel steel (at temperatures above 400°F).

Hartbower and Orner[4,6] have observed a loss of toughness in precrack Charpy slow-bend testing several materials, including aluminum. Figure 13 shows the precrack Charpy impact and slow-bend test results for a variety of aluminum alloys supplied by Alcoa Research Laboratories. Note that the higher strength alloys showed the least velocity effect. Note, also, that the loss of energy was verified by a measurement of lateral expansion (the Poisson effect) in the plane of the notch. The data of Table V compare the W/A values as obtained from slow bend and impact tests of 6Al-6V-2Sn titanium, A286 superalloy and 4340 steel. Note that the difference between slow bend and impact, in the case of A286 alloy, was most pronounced at 400°F. Tests of cold-drawn and aged 18% nickel maraging steel also showed a loss of toughness in slow bend at 400°F (the slow-bend W/A value was 540 as compared with 800 in.-lb/in.^{2} in impact); however, there was little or no difference between slow bend and impact at either room temperature or at -320°F. The loss of toughness in slow bending at elevated temperature is consistent with embrittling mechanisms involving the diffusion of interstitial elements.

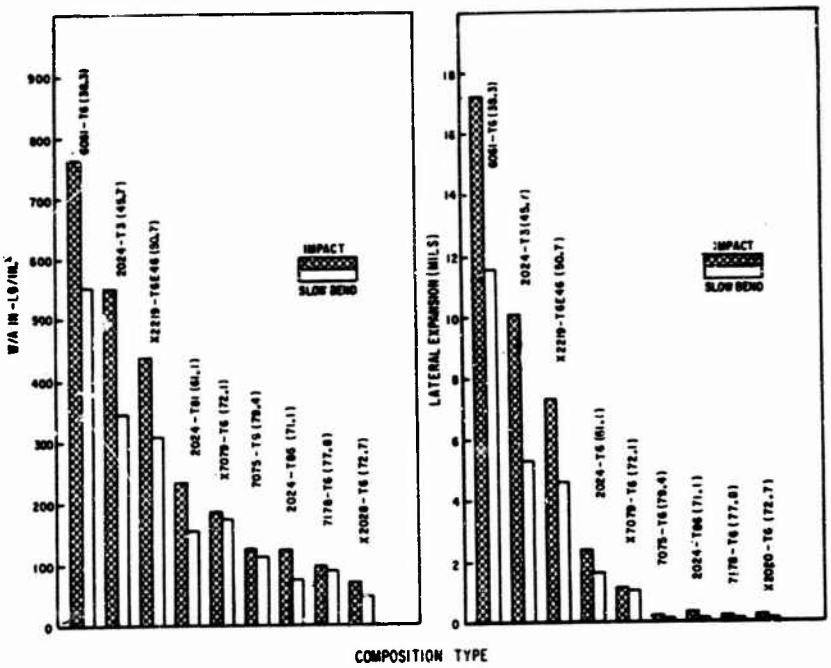


Figure 13. Effect of Loading Rate on Various Aluminum Sheet Alloys

Appendix D

TABLE V

PRECRACK CHARPY SLOW-BEND AND IMPACT DATA FOR THREE MATERIALS

A286 SUPER ALLOY*

Test Temp (°F-hr)	Strength, ksi	Precracked Charpy (in-lb/in^2) Slow-Bend	Impact
-320	243	813 - 1022 Avg(2) 918	607 - 609 Avg(2) 608
RT	211	450 - 533 Avg(2) 491	800 - 909 Avg(2) 854
400	194	377 - 416 Avg(2) 396	920 - 1002 Avg(2) 961

* Material supplied in the form of 1/2-in. dia cold-drawn rounds in the aged condition. Charpy specimens were 0.3 x 0.3 x 2.0 in.

AISI 4340 STEEL*

Tempering Temp (°F-hr)	Yield Strength, ksi	Precrack Charpy Test Slow-Bend in-lb/in^2	% Shear	Impact Test in-lb/in^2	% Shear
410-1	230	261 - 277	40	618 - 636	70
410-4	230	288 - 313	45	652 - 672	75
600-4	225	641 - 728	100	913 - 935	100
800-4	200	1257 - 1573	100	1560 - 1806	100

* Material was normalized at 1650°F, austenitized at 1525°F (1/2 hr) and oil quenched. Specimens were 0.394 x 0.394 x 2.1-in., tested at room temperature.

6AL-6V-2SN TITANIUM*

Aging Temp (°F-hr)	Yield Strength, ksi	Precrack Charpy (in-lb/in^2) Slow-Bend	Impact
950-4	200	17	128
1050-4	190	58	232
1150-4	180	145	448

* 0.1-in. sheet material tested at room temperature.

Appendix D

PRECRACK CHARPY TESTING Ti-6AL-4V FORGINGS IN THE MINUTEMAN PROGRAM

Precrack Charpy Tests of MINUTEMAN Qualification Trim Stock

Prior to initiation of the current MIL-HDBK-5 data collection, a number of MINUTEMAN forgings were tested using the precrack Charpy specimen.

Trim stock (segments approximately 0.6-in. thick by 3/4-in. wide) cut from heat-treated parts in the aged-buy-off condition were obtained from Aerojet-Downey and machined into Charpy specimens. Because of the limited amount of material available, the specimens were machined two-high; i.e., two 0.10-in. thick specimens were machined from each 2-inches of ring material, one from the OD side and one from the ID side of the ring centerline (within 0.045-in. of ring mid-thickness). Control of specimen location with respect to ring thickness was considered necessary because of possible metallurgical variation from surface to center due to the limited hardenability of 6Al-4V. The specimens were fatigue precracked and then tested in duplicate at both impact and slow-bend (5×10^{-2} in./min) rates of loading.

Table VI presents the data obtained from the 14 qualification rings, tabulated in the order of increasing yield strength. Note that there is considerable variation in toughness from forging-to-forging. Note, also, that with one exception (Ring 4A), the precrack Charpy slow-bend test result was appreciably lower than the impact test result. The slow-bend W/A value for ring 4A was the highest of the 14 rings, and the highest room-temperature slow-bend value ever measured at Aerojet on MINUTEMAN material. The oxygen content in this forging (0.12 wt%) was lower than any other forging investigated; however, the nitrogen content (0.022 wt%) was higher than in most forgings. The microstructure of ring 4A is shown in Figure 14.

In addition to the precrack Charpy specimens cut from trim stock, a number of tensile coupons in the form of rough-machined cylindrical bars, cut originally from qualification trim stock, were machined into 0.10-in.-thick precrack Charpy specimens. The tensile coupons were wired to the respective chambers during the final stress-relief aging treatment. Table VII presents the data obtained from the tensile-coupon material, tabulated in the order of increasing yield strength. The precrack Charpy impact tests were conducted at two temperatures, room temperature and at +320°F. Note that the effect of testing temperature was widely variable, with some forgings developing only slightly increased toughness at 320°F. The first dome forging, for example, showed little or no increase in toughness over the temperature range tested; whereas, the toughness of the second dome listed was almost doubled at +320°F. Thus, there was considerable variation from forging to forging (heat-to-heat) in the degree of increased toughness associated with elevated temperature. Although the heat-to-heat variability precludes any conclusion with regard to the variability in K_{Ic} produced by forging practice with this small a test sample, the following summary (from Table VII)

Appendix D

TABLE VI

FRACTURE TOUGHNESS MEASURED IN MINUTEMAN 6Al-4V TITANIUM QUALIFICATION RINGS. PRECRACK CHARPY SPECIMENS 0.10-in. THICK AS TESTED

		Age Buy-Off Properties		Precrack Charpy(a) Fracture Toughness (in.-in./lb^2)			
Ring	Forging	Yield, ksi	Ultimate, ksi	Impact	(W/A) Avg	Slow Bend	(W/A) Avg
R4A	-	152	167	361-507	434	740-480	610
R108-1	Cyl.	155	167	690-700	695	233-250	241
R216	Dome	160	171	421-428	425	139-164	151
k201	Dome	162	176	583-412	498	(b)73-157	157
R217	Flange	162	175	456-546	501	160-148	154
R149-1	Cyl.	162	174	608-558	583	170-109(b)	170
R229	Flange	163	173	284-278	281	147-170	158
R223	Dome	164	176	469-424	446	179-188	184
R72	Flange	168	179	338-317	328	124-102(b)	124
R237	Dome	168	175	1190-917	1054	206-190	198
R208	Dome	170	181	373-357	365	149-103	126
R63	Dome	170	180	508-382	445	141-92(b)	141
R71	Dome	173	182	293-350	322	121-86(b)	121
R206	Dome	173	180	307-492	400	98-99	98

(a) Specimens cut from within 3/64" of midthickness - specimens on OD and ID side of centerline (with respect to thickness).
(b) Fatigue precracked too deep.

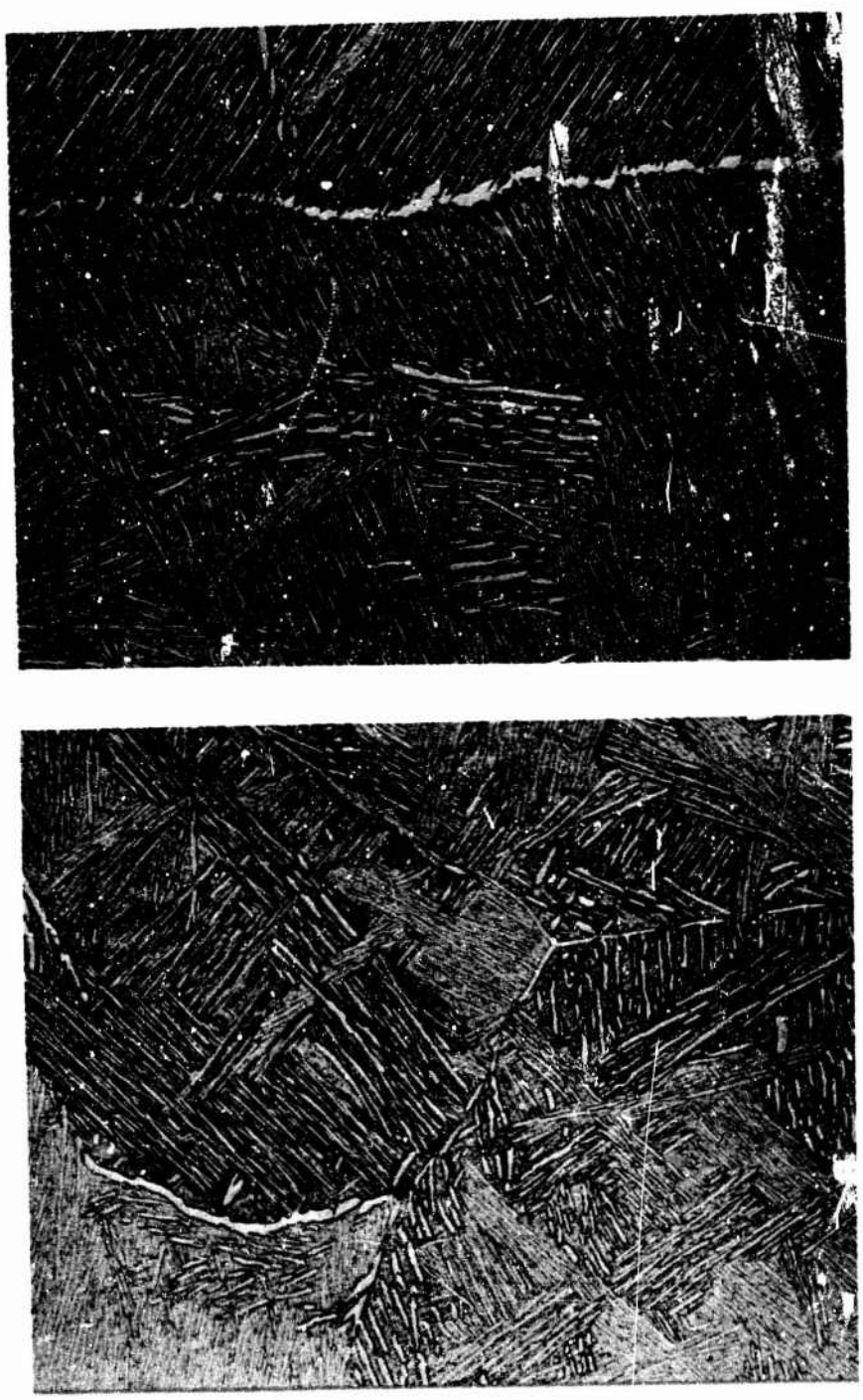


Figure 14. Microstructure of MINUTEMAN 6Al-4V Titanium Forging 4A Specimen Etched with 1% Hf, 2% HNO_3. Magnification 250X

TABLE VII

TENSILE STRENGTH AND FRACTURE TOUGHNESS FROM VENDOR TENSILE COUPONS
(PCI Specimens 0.10-in. Thick)

Forging	Chamber S/N	Tensile Strength, ksi		Precrack Charpy Impact, in.-lb/in.^{2})			
		Yield	Ultimate	Room Temp.	Avg.	+320°F	Avg.
Dome	673085	161.3	177.4	641-713	677	596-616-845	686
	673093	168.6	180.5	570-645	607	1105-1135	1120
	673102	168.7	179.7	813-832	822	1010-1206	1108
	673096	171.4	181.3	563-617	590	748-988	868
Cyl.	673085	158.0	173.2	565-615	590	733-748	740
	673085	---	175.4	567-582	574	901-987	944
	673093	165.2	176.9	422-447	434	707-818	762
	673093	166.4	179.1	425-428	426	734-810	772
	673096	167.9	179.9	408-504	456	700-717	708
	673096	169.3	180.2	441-539	490	763-791	777
	673102	170.6	181.8	403-492	447	826-876	851
	673102	171.5	185.4	388-504	446	675-775	725
Adapter	673085	160.4	178.1	363-815	589	638-1104	871
	673096	166.7	178.1	523-615	569	902-920	911
	673093	170.0	182.3	482-485	483	740-778	859
	673102	172.5	185.4	313-337	325	492-539	515
Closure	621062	---	177.5	427-542	484	913-958	935
	673096	173.4	190.1	422-435	428	728	728
	673102	175.8	191.0	378-401	389	678-793	735
	673093	177.1	190.0	373-384	378	590-608	599

Type of Forging	Precrack Charpy Impact Room Temp.	at 320°F
Dome and Closure	373 - 832 Avg(16) 548	590 - 1206 Avg(16) 845
Cylinder	388 - 615 Avg(16) 483	675 - 987 Avg(16) 785
Adapter	313 - 815 Avg(8) 492	492 - 1104 Avg(8) 764

suggests that there may be no significant difference between the ring-rolled and extruded parts (the cylinder components going into the S/N 675---chambers may not have been forged by Cameron; i.e., they may have been ring rolled).

Effect of 6Al-4V Solution-Treatment Temperature

A study was conducted at Allison Division of General Motors Corp.[15] to determine the effect of varying the solution temperature from 35°F above the beta transus to 300°F below in MINUTEMAN titanium. The evaluation was based on uniaxial tensile tests and part-through-crack tensile fracture-toughness tests. The forging was an extruded cylinder forged by Wyman Gordon Co., with the following chemistry:

0.016C 6.13Al 4.02V 0.18Fe 0.180$_2$ 0.013N_2 0.0024H_2

The beta transus was 1845°F. The material was solution treated two hours, water quenched, and aged for 8 hr.

Precrack Charpy specimens were cut from the broken PTC-tensile specimens at Aerojet-Sacramento; both the PTC tensiles and the precrack Charpys were tested in the 0.10-in. thickness.

Lowering the solution temperatures from 35°F to 200°F below the beta transus had no appreciable effect on uniaxial tensile properties when employing a 950°F age. However, lowering the solution temperature in this same range while employing an 1100°F aging treatment was accompanied by a decrease in tensile strength of approximately 10,000 psi. Raising the solution temperatures from 35°F below to 35°F above the beta transus reduced the tensile strength about 5000 psi.

The PTC tensile test generally showed little change in toughness with the variation in solution-treatment temperatures investigated. The precrack Charpy slow-bend and impact tests, on the other hand, showed marked changes in toughness with variation in solution-treatment temperature. Figures 15a and 15b are plots of the PTC-tensile and the precrack Charpy data. Note that if

one were seeking correlation between the PTC-tensile K_{Ic} value and the PCSB test result, the latter becomes markedly higher than the K_{Ic} (in.-lb/in.^{2}) value with decreasing solution-treatment temperature. At the solution-treatment temperature used in the MINUTEMAN program (approximately 60°F below the beta transus) the correlation is good. The data plotted in Figures 15a and 15b are presented in Table VIII.

Effect of 6Al-4V Aging Temperature

Aging temperatures from 900 to 1200°F also were investigated by Allison Division of General Motors.[13]. The forging was a ring-rolled cylinder forged by Ladish Co., with the following chemistry:

0.035C 6.44Al 3.90V 0.15Fe 0.180_2 $0.021N_2$ $0.0028H_2$

The beta transus was 1860°F. The thermal processing consisted of solution treating at 60°F below the beta transus for two hours, water quenching, and aging for 8 hr.

Varying the aging temperature in the 900 to 1050°F range had no appreciable effect on the uniaxial strength. Aging at temperatures of 1100°F and above was accompanied by a reduction in strength to the extent that aging at 1200°F produced strengths approximately 12 to 15 ksi lower than those achieved by aging in the 900 to 1050°F range.

PTC-tensile tests also were made as a function of aging temperature. The K_{Ic} values increased from approximately 100 ksi-in.$^{1/2}$ for a 900°F age to approximately 125 ksi-in.$^{1/2}$ for a 1200°F age.

The precrack Charpy slow-bend specimens cut from the broken PTC-tensile specimens showed the same trend, but with higher toughness values indicated at the higher aging temperatures. The correlation between the two tests was good for the low aging temperatures investigated, but the PCSB test result was increasingly unconservative as an estimate of K_{Ic} as the material was toughened by increasing aging temperature. The precrack Charpy impact test, on the other hand, was relatively unaffected by the variation in aging temperature in this material. The test results are presented in Table IX.

Effect of Heat Treatment on ELI 6Al-4V Sheet Material

Precrack Charpy slow-bend data from 6Al-4V titanium sheet with low oxygen content indicated excellent toughness. The chemistry of the 0.125-in.-thick sheet was as follows:

0.020C 6.0Al 4.0V 0.10Fe 0.107_2 $0.018N_2$ $0.004H_2$

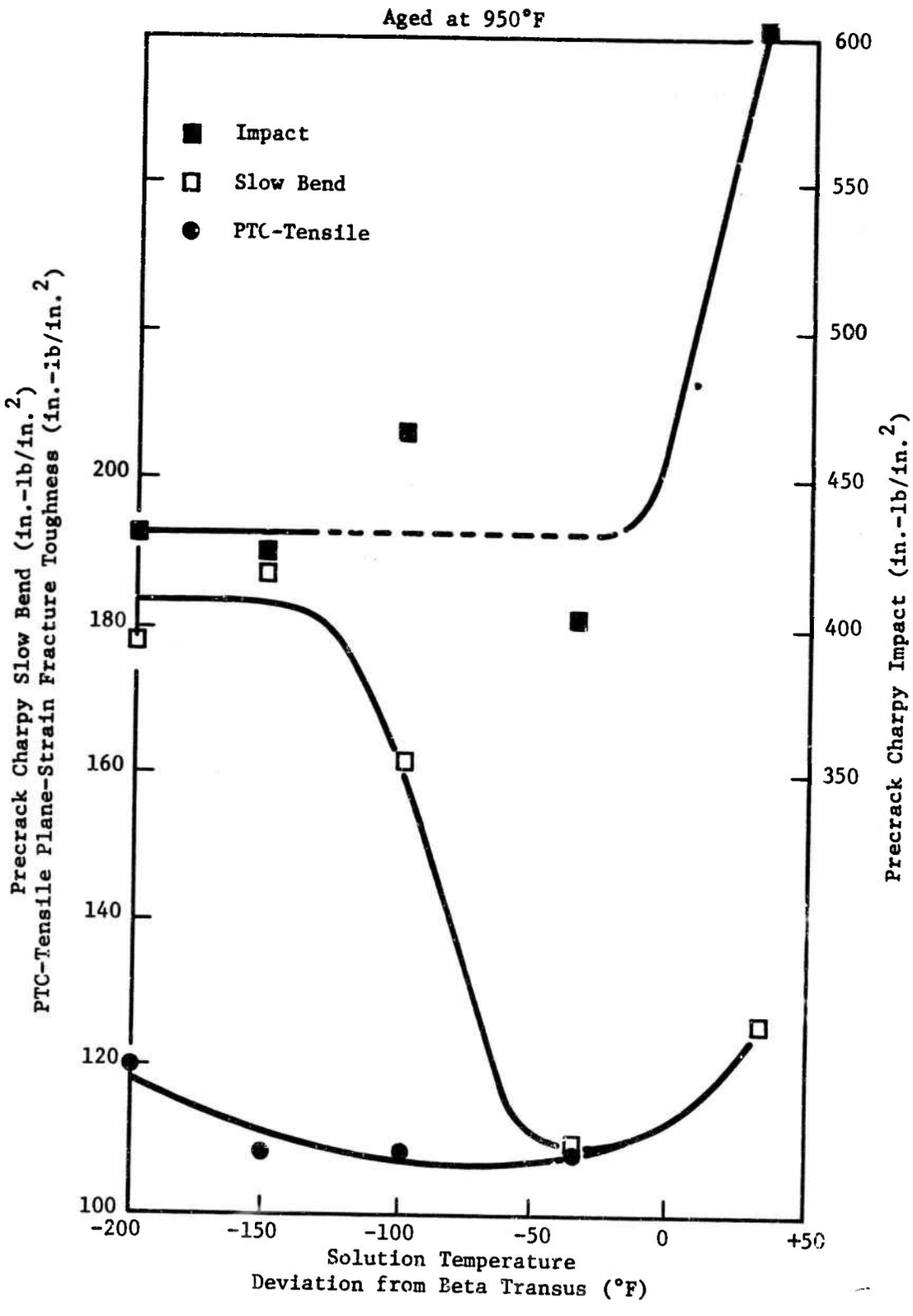


Figure 15a. Effect of Solution Treatment on Precrack Charpy and PTC-Tensile Test Results When Aged at 950°F (Figure 15a) and When Aged at 1100°F (Figure 15b). Material was a 6Al-4V MINUTEMAN Forging S/N XEOB-2M of 0.55-in. Wall Thickness. Specimens were 0.10-in. Thick.

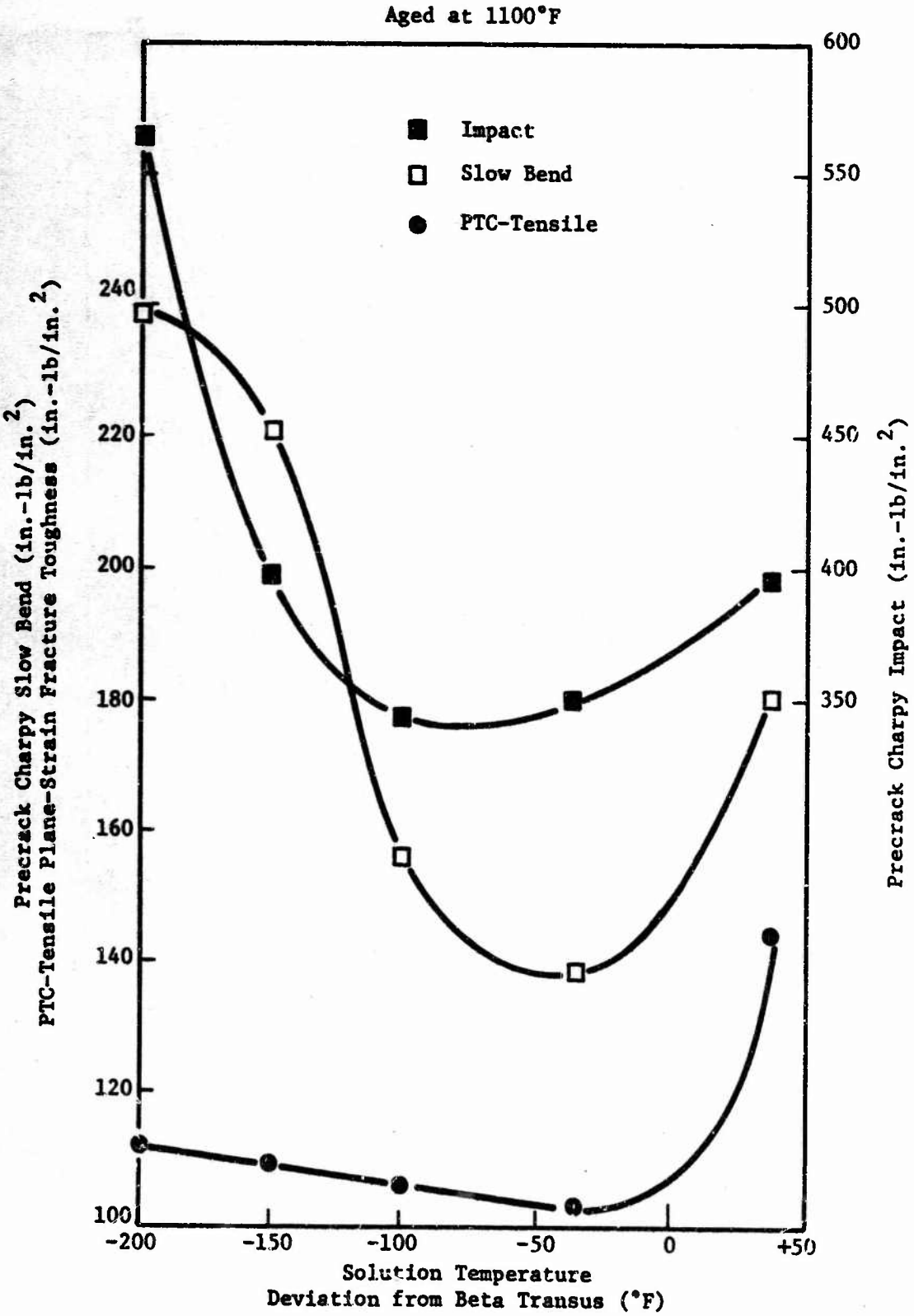


Figure 15b. Effect of Solution Treatment on Precrack Charpy and PTC-Tensile Test Results When Aged at 950°F (Figure 15a) and When Aged at 1100°F (Figure 15b). Material was a 6Al-4V MINUTEMAN Forging S/N XEOB-2M of 0.55-in. Wall Thickness. Specimens were 0.10-in. Thick.

TABLE VIII

COMPARISON OF FRACTURE TOUGHNESS CALCULATED FROM PART-THROUGH-CRACK TENSILE TESTS AND PRECRACK CHARPY TESTS

(Forging XEOB-2M, 0.55-in. wall, Tested 0.10-in. Thick)

Solution °F Above (+) or Below Transus	Aging Temp/Time (°F/hr)	0.2% Yield Strength, ksi	Ultimate Strength, ksi	Part-through-Crack Tensile K_{Ic} (b) (ksi $\sqrt{in.}$)	Part-through-Crack Tensile G_{Ic} (c) (in.-lb/in.^{2})	Precrack Charpy (W/A, in.-lb/in.^{2}) Slow Bend	Precrack Charpy (W/A, in.-lb/in.^{2}) Impact
+35(a)	950/8		---	---	---	126	606
-35		160.5	172.0	44724	108	109	402
-100		162.2	172.6	44882	108	162	465
-150		157.6	169.4	44753	108	187	426
-200		157.8	168.7	47273	120	178	431
+35	1100/8	156.9	166.0	50712	143	180	445
-35		161.8	170.2	44003	104	139	400
-100		158.3	165.6	44267	106	156	392
-150		154.3	161.8	44920	109	221	448
-200		152.6	159.9	45576	112	238	614

(a) 35°F above the beta transus (1845°F)
(b) Average stress intensity factor (K_{Ic}) value (gross stress to yield strength ratio < 1.0)
(c) Average energy release rate (G_{Ic}) calculated from the relationship $(1-\nu^2)\ K_{Ic}^2 = EG_{Ic}$.

TABLE IX

COMPARISON OF FRACTURE TOUGHNESS CALCULATED FROM PART-THROUGH-CRACK TENSILE TESTS AND PRECRACK CHARPY TESTS
(Forging MTC-202, Solution Treated 1800°F, Tested 0.10-in. Thick)

Aging Temp., °F	0.2% Yield Strength, ksi	Ultimate Strength, ksi	Part-thru-Crack Tensile K_{Ic}[a] (psi $\sqrt{in.}$)	Part-thru-Crack Tensile G_{Ic}[b] (in.-lb/in.^{2})	Precrack Charpy Test (W/A), in.-lb/in.^{2} Slow Bend	Precrack Charpy Test (W/A), in.-lb/in.^{2} Impact W/A
900	167.6	179.6	43020	102	112	446
950	165.0	177.1	43761	103	125	361
1000	167.9	178.8	42779	98	125	416
1050	167.1	173.7	43250	101	161	360
1100	164.0	174.2	45706	113	-	423
1150	155.6	164.5	44204	105	205	390
1200	151.6	165.1	48066	124	-	413

(a) Average stress intensity factor (K_{Ic}) value (gross stress to yield strength ratio < 1.0).
(b) Average energy release rate (G_{Ic}) calculated from the relationship $(1-\nu^2)\, K_{Ic}^2 = EG_{Ic}$.

The sheet material was solution treated and aged at various temperatures, as indicated in Table X. After heat treatment, 0.010 to 0.015-in. was removed from each surface to remove the contaminated surface layer; the final test-specimen thickness was 0.10 in. Precrack Charpy slow-bend and impact tests were made as a function of solution treatment temperature and aging temperature. The test results are plotted in Figures 16a and 16b. Note that the fracture toughness increased with decreasing solution-treating temperature and with increasing aging temperature.

Most noteworthy is the difference between the precrack Charpy slow-bend values as determined in the ELI sheet material and in the 6Al-4V forged material used in the MINUTEMAN. The precrack Charpy results, as reported in Tables VI and VII, gave the following range and arithmetical averages for MINUTEMAN forgings:

Slow-Bend	Impact
98 - 241*	284 - 1190
Avg(21) 159	Avg(70) 485

whereas, the ELI sheet material for a comparable solution treatment and age (1750/1100°F) gave

Slow-Bend	Impact
274 - 372	514 - 628
Avg(4) 312	Avg(2) 571

In considering the above comparisons, it should be noted that the ELI sheet had lower oxygen than the MINUTEMAN forgings (typically 0.18 wt%); whereas, the nitrogen and hydrogen contents were comparable to that of the MINUTEMAN forgings.

The lower oxygen content of the ELI sheet does not necessarily mean a serious loss of strength potential. A companion heat (M4789) from the DOD titanium alloy sheet rolling program, with even lower interstitial content (0.092% O_2, 0.004% H_2, 0.012% N_2) was solution treated at 1750°F-1/4 hr, water quenched (0.125-in.-thick) and aged at 900°F-24 hr. With this treatment, the alloy developed 163 ksi yield strength (0.2% offset) and 172 ksi ultimate strength (see Ref 3).

Effect of Shear Spinning

A 6Al-4V titanium preform was solution treated at 1550°F, aged at 1000°F for 10 hr and spun at 1200°F. The cylinder was reduced to 60, 70, and 80% of its original wall thickness.

* The exceptionally high PCSB values measured in R4A were omitted from the average.

Appendix D

TABLE X

PRECRACK CHARPY FRACTURE TOUGHNESS OF 6A1-4V TITANIUM SHEET
(Heat M4790, 0.10-in. Thick)

Material Condition	Impact (in.-lb/in.^{2}) Room Temp	Slow Bend Data (in.-lb/in.^{2}) Instron(b) Room Temp	Manlabs Machine Room Temp	Manlabs Machine +320°F
1750/1100(a)	514 - 628 Avg(2) 571	274 - 280 Avg(2) 277	321 - 372 Avg(2) 347	786 - 802 Avg(2) 794
1650/1100	1415- 1844 Avg(3)1575	891 - 1035 Avg(2) 963	932 - 1090 Avg(2) 1011	2000 - 2095 Avg(2) 2048
1550/1100	1658 - 2035 Avg(2) 1846	908 - 1300 Avg(2) 1104	1175 - 1495 Avg(2) 1335	2110 - 2320 Avg(2) 2215
1650/900	885 - 1005 Avg(2) 945	474 - 484 Avg(2) 479	460 - 468 Avg(2) 464	1460 - 1520 Avg(2) 1490
1650/1000	1441 - 1505 Avg(2) 1473	696 - 710 Avg(2) 703	775 - 980 Avg(2) 878	1680 - 1792 Avg(2) 1736
1650/1100	1415 - 1844 Avg(3) 1575	891 - 1035 Avg(2) 963	932 - 1090 Avg(2) 1011	2000 - 2095 Avg(2) 2048
1650/1200	1935 - 1950 Avg(2) 1942	918 - 1210 Avg(2) 1064	1210 - 1260 Avg(2) 1235	1870 - 2420 Avg(2) 2145

(a) Solution treated at 1750°F for 1 hr, quenched in vigorously agitated water 6-8 sec after removal from furnace (i.e., delayed quench 6-sec min, 8-sec max) and aged at 1100°F for 8 hr.
(b) Instron head speed 0.05 in./min; Manlabs slow-bend machine 0.10 in./min.

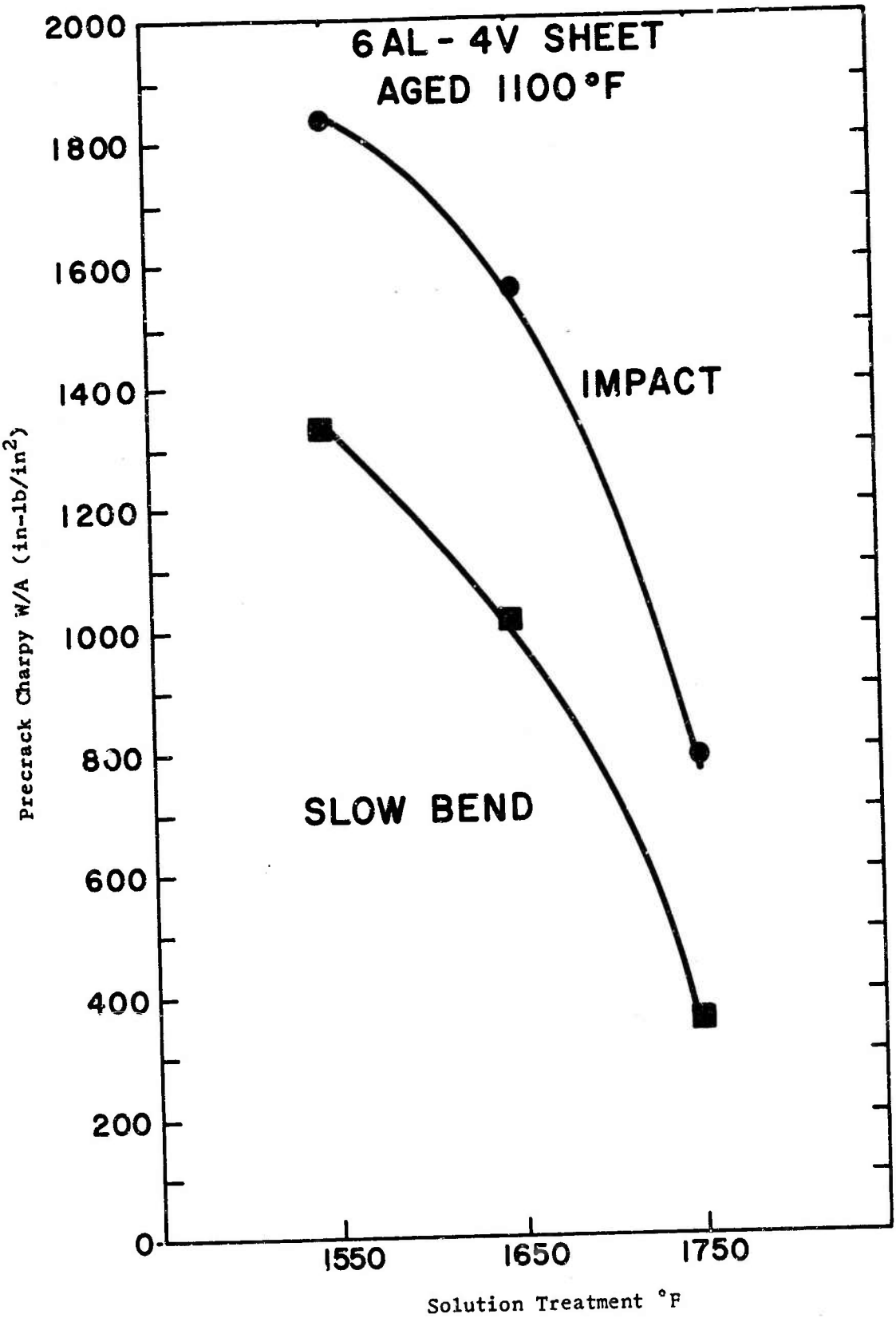


Figure 16a. Precrack Charpy Impact and Slow-Bend W/A Values for ELI 6Al-4V Titanium Sheet as a Function of Solution Treatment Temperature (Figure 16a) and Aging Temperature (Figure 16b) Material was 0.10-in. Thick, as Tested

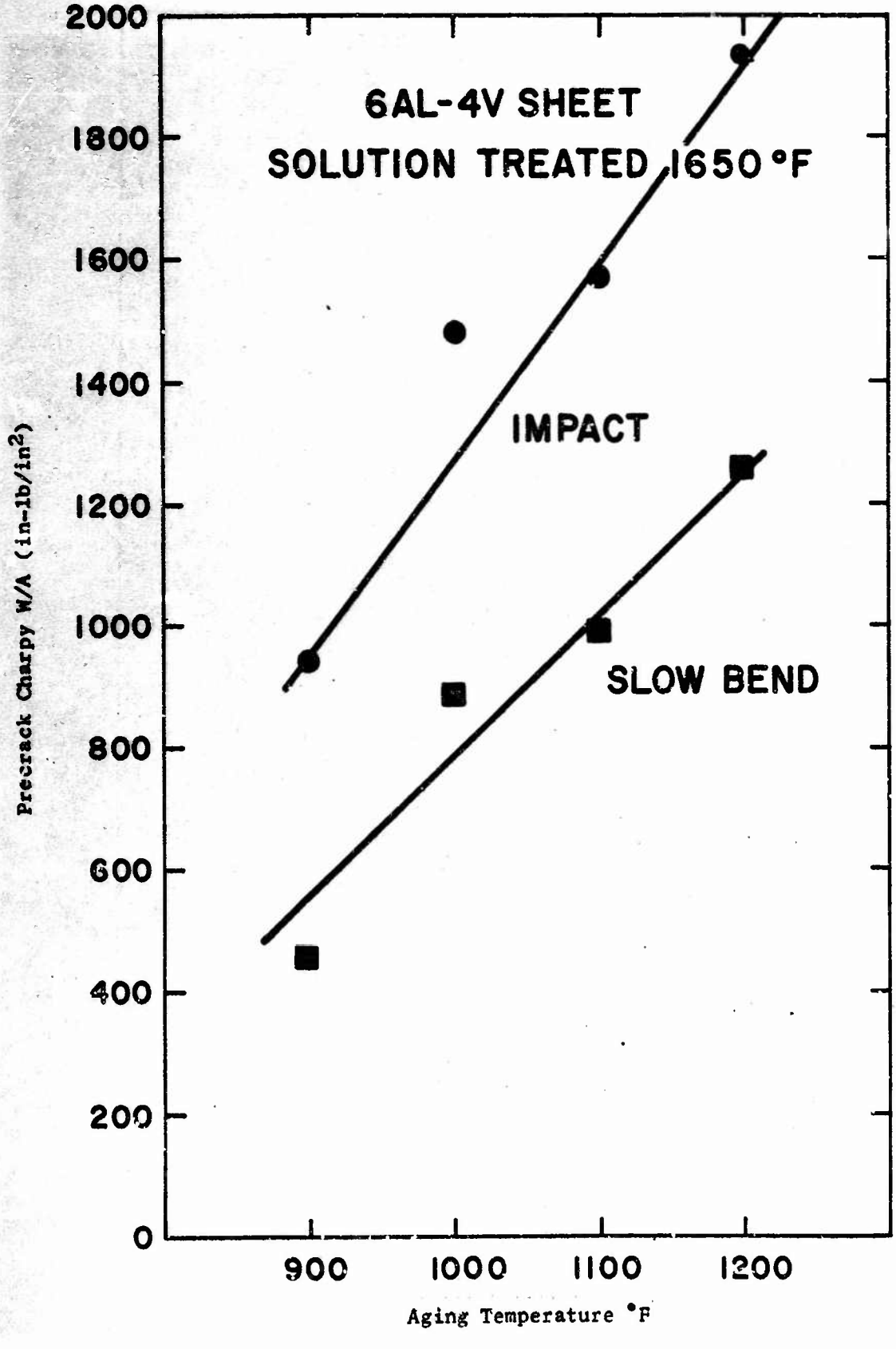


Figure 16b. Precrack Charpy Impact and Slow-Bend W/A Values for ELI 6Al-4V Titanium Sheet as a Function of Solution Treatment Temperature (Figure 16a) and Aging Temperature (Figure 16b) Material was 0.10-in. Thick, as Tested

Appendix D

Tensile specimens were cut from the cylinder wall, perpendicular to the spinning marks. The specimens were milled on both surfaces to remove the spinning feed lines. The test results were as follows:

Percent Reduction	0.2% Offset Yield Strength, ksi	Ultimate Strength, ksi
60	158.3 - 162.3 Avg(6) 161.0	162.8 - 172.4 Avg(6) 165.8
70	160.4 - 167.7 Avg(6) 163.4	167.0 - 174.8 Avg(6) 169.3
80	167.8 - 176.3 Avg(6) 173.5	178.9 - 189.4 Avg(6) 185.2

Precrack Charpy impact specimens were cut from the cylinder and tested both in the as-spun wall thickness and after machining to a common thickness (0.090 in.). The Charpy data are presented in Table XI. Note that with increasing strength there was a loss of toughness; the W/A value was approximately halved by increasing the spinning reduction from 60 to 80%. Note, also, that the marked increase in toughness at 320°F appeared to compensate for the loss of toughness produced by increasing the reduction from 60 to 70%; however, after 80% reduction, the increase in test temperature produced relatively little increase in toughness.

Appendix D

TABLE XI

TOUGHNESS OF 6Al-4V TITANIUM MATERIAL FROM SHEAR-SPUN CHAMBER S/N 108

Reduction, %	Spun-Wall Thickness	0.2% Offset Yield Strength, ksi	Precrack Charpy Impact (in.-lb/in.^{2}) Tested in As-Spun Thickness			Machined to 0.090-in. Thickness		
			RT	200	320°F	RT	200	320°F
60	0.210	161	506	785	1260	540	630	1060
			615	900	1570	855	768	1095
			561	843	1315	698	699	1078
70	0.165	163	455	550	1560	563	700	1050
			510	727	1575	623	743	1580
			483	639	1568	593	722	1315
80	0.100	173	308	312	472	305	308	533
			310	356	505	315	405	624
			309	334	489	310	357	579

Appendix D

REFERENCES

1. Hartbower, C. E., "Crack Initiation and Propagation in V-Notch Charpy Impact," ASTM Proceedings, 1956, Vol. 56, p.521; also WELDING JOURNAL, Nov. 1957, Vol. 36 (11), p.494-s.

2. Orner, G. M. and Hartbower, C. E., "The Low-Blow Transition Temperature," ASTM Proceedings 1958, Vol. 58, p.623.

3. Orner, G. M. and Hartbower, C. E., An Engineering Evaluation of Notch Sensitivity in High-Strength Sheet Materials, Technical Report AMC-TR-60-7-662, March 1960 on Air Force Contract MIPR-30(600)-8-None-114; also WELDING JOURNAL, Vol. 39(4), p.147-s, April 1960.

4. Orner, G. M. and Hartbower, C. E., "Sheet Fracture Toughness Evaluated by Charpy Impact and Slow Bend," WELDING JOURNAL, Vol. 40(9), p.405-s, Sept. 1961.

5. Orner, G. M. and Hartbower, C. E., "Transition-Temperature Correlations in Constructional Alloy Steels," WELDING JOURNAL, Oct. 1961, Vol. 40(10), p.459-s.

6. Hartbower, C. E. and Orner, G. M., Metallurgical Variables Affecting Fracture Toughness in High-Strength Sheet Alloys, Air Force Contract AF 33(606)-8155 Technical Documentary Report No. ASD-TDR-62-868, Oct. 1962.

7. ASTM Committee on Fracture Testing of High-Strength Metallic Materials "Fracture Testing of High-Strength Sheet Materials," ASTM Bulletin, Jan. (Part I) and Feb. (Part II) 1960.

8. Thick Section Fracture Toughness, Technical Documentary Report ML-TDR-64-236 on Contract AF 33(657)-11461, a Boeing-North American joint venture, Oct. 1964.

9. Bentley, C. W., Notch Resistance and Fracture Toughness Characteristics of High-Strength Metals, ASD-TDR-63-494, Sept. 1963.

10. Lement, B. S., Kreder, K., and Tushman, H., Investigation of Fracture Toughness in High-Strength Alloys, ASD-TDR-62-868, Part II, Jan. 1964.

11. Morrison, J. D., Jenkins, P. C. and Kattus, J. R. An Investigation of the Crack-Propagation Resistance of High-Strength Alloys and Heat-Resistant Alloys, Summary Technical Report prepared under Navy BuWeps Contract NOw 61-0392-d, 21 Nov. 1962.

12. Steigerwald, E. A. and Hanna, G. L., "Spontaneous Strain Aging in High-Strength Steels," ASM TRANS. QUARTERLY, Vol. 56(3), P.656, Sept. 1963.

13. Hellmann, V. L., Allison Engineering Dept., Report No. 3590, 15 Oct 1963.

Appendix D

TABLES XII AND XIII

PRECRACK CHARPY SLOW-BEND AND IMPACT DATA FROM MINUTEMAN ROCKET MOTOR CASES

R26

2191456

673078

673095

673147

674514

673122

2192109

R369

Appendix D

TABLE XII

PRECRACK CHARPY IMPACT DATA FOR 6Al-4V TITANIUM

Chamber	Cylinder	Spec. No.	Notch Direct.	Width, in.	DBN-cd, in.	C.D., in.	Area, sq. in.	W/A, $in.-lb/in.^2$
R26	Fwd	A4	Hoop	0.101	0.2751	0.0396	0.0278	471.2
		5		0.101	0.2674	0.0485	0.0270	533.0
		6		0.101	0.2766	0.0390	0.0279	554.1
		7	Axial	0.1005	0.2791	0.0391	0.0280	810.0
		8		0.1005	0.2759	0.0425	0.0277	862.1
		9		0.101	0.2814	0.0375	0.0284	1009.9
		A13	Hoop	0.1025	0.2652	0.0505	0.0272	581.6
		14		0.1025	0.2652	0.0504	0.0272	520.2
		15		0.103	0.2633	0.0523	0.0271	570.5
		16	Axial	0.102	0.2771	0.0401	0.0283	826.9
		17		0.1015	0.2734	0.0426	0.0278	859.0
R26	Aft	B1	Hoop	0.100	0.2620	0.0548	0.0262	792.0
		2		0.100	0.2883	0.0288	0.0288	863.0
		3		0.100	0.2858	0.0305	0.0286	981.0
		7	Axial	0.100	0.2860	0.0327	0.0286	814.0
		8		0.100	0.2882	0.0318	0.0288	900.0
		B13	Hoop	0.102	0.2830	0.0329	0.0289	884.4
		14		0.1015	0.2726	0.0440	0.0277	862.1
		15		0.101	0.2859	0.0308	0.0289	903.1
		16	Axial	0.101	0.2834	0.0364	0.0286	937.8
		17		0.1005	0.2811	0.0376	0.0283	922.3
		18		0.100	0.2827	0.0341	0.0283	873.5
		19	Hoop	0.100	0.2802	0.0348	0.0280	103.3
		20		0.100	0.2800	0.0351	0.0279	920.0
		21		0.100	0.2753	0.0380	0.0275	975.0
		22		0.100	0.2697	0.0447	0.0268	837.0
		23		0.100	0.2747	0.0380	0.0275	934.0
		24		0.100	0.2787	0.0364	0.0277	884.0
2191456	Fwd	C4	Hoop	0.0995	0.2704	0.0442	0.0269	450.2
		5		0.0995	0.2667	0.0490	0.0265	444.2
		6		0.0995	0.2731	0.0441	0.0272	386.0
		7	Axial	0.100	0.2813	0.0386	0.0281	478.6
		8		0.100	0.2757	0.0413	0.0276	500.0
		9		0.100	0.2820	0.0380	0.0282	506.0

TABLE XII (cont.)

Chamber	Cylinder	Spec. No.	Notch Direct.	Width, in.	DBN-cd, in.	C.D., in.	Area, sq. in.	W/A, in.-lb/in.^{2}
2191456	Fwd	C13	Hoop	0.099	0.2613	0.0549	0.0259	425.9
		14		0.0985	0.2695	0.0493	0.0265	498.5
		15		0.099	0.2774	0.0407	0.0275	452.4
		16	Axial	0.099	0.2764	0.0431	0.0274	503.6
		17		0.099	0.2790	0.0374	0.0276	454.7
2191456	Aft	D4	Hoop	0.1025	0.2831	0.0334	0.0290	1032.4
		5		0.1025	0.2790	0.0355	0.0286	971.3
		6		0.1025	0.2804	0.0344	0.0287	967.9
		7	Axial	0.102	0.2843	0.0360	0.0290	777.9
		8		0.102	0.2887	0.0330	0.0294	771.4
		9		0.102	0.2847	0.0381	0.0290	701.4
		D13	Hoop	0.101	0.2810	0.0331	0.0284	919.0
		14		0.1015	0.2819	0.0323	0.0286	948.3
		15		0.1025	0.2788	0.0367	0.0286	868.5
		16	Axial	0.1025	0.2950	0.0260	0.0302	673.5
		17		0.1025	0.2828	0.0364	0.0290	767.6
		18		0.1025	0.2815	0.0372	0.0289	813.8
673078	Fwd	E4	Hoop	0.098	0.2753	0.0448	0.0270	648.9
		5		0.099	0.2820	0.0330	0.0279	575.6
		6		0.0995	0.2809	0.0368	0.0279	649.5
		7	Axial	0.100	0.2836	0.0366	0.0284	482.0
		8		0.100	0.2778	0.0410	0.0278	525.9
		9		0.100	0.2734	0.0442	0.0273	531.1
		E13	Hoop	0.099	0.2758	0.0377	0.0273	672.5
		14		0.099	0.2636	0.0543	0.0261	569.3
		15		0.0985	0.2770	0.0391	0.0273	650.5
		16	Axial	0.100	0.2729	0.0466	0.0273	505.5
		17		0.1005	0.2817	0.0375	0.0283	500.0
		18		0.100	0.2871	0.0322	0.0287	623.0
673078	Aft	H4	Hoop	0.098	0.2756	0.0394	0.0270	702.2
		5		0.0985	0.2721	0.0469	0.0268	662.7
		6		0.0985	0.2668	0.0496	0.0263	610.6
		7	Axial	0.098	0.2828	0.0375	0.0277	584.1
		8		0.099	0.2809	0.0354	0.0278	577.7
		9		0.0985	0.2840	0.0351	0.0280	607.9

TABLE XII (cont.)

Chamber	Cylinder	Spec. No.	Notch Direct.	Width, in.	DBN-cd, in.	C.D., in.	Area, sq. in.	W/A, $in.-lb/in.^2$
673078	Aft	H13	Hoop	0.097	0.2801	0.0361	0.0272	683.8
		14		0.097	0.2731	0.0418	0.0265	619.6
		15		0.097	0.2845	0.0326	0.0276	634.8
		16	Axial	0.0975	0.2728	0.0429	0.0266	527.8
		17		0.0975	0.2752	0.0428	0.0268	519.4
		18		0.0975	0.2806	0.0391	0.0274	594.9
673095	Fwd	J4	Hoop	0.100	0.2840	0.0338	0.0284	621.1
		5		0.1005	0.2804	0.0367	0.0282	642.6
		6		0.1005	0.2806	0.0356	0.0282	659.6
		7	Axial	0.101	0.2723	0.0406	0.0275	628.4
		8		0.101	0.2757	0.0387	0.0278	695.0
		9		0.101	0.2748	0.0389	0.0278	746.8
		J13	Hoop	0.101	0.2760	0.0418	0.0279	632.3
		14		0.101	0.2753	0.0427	0.0278	712.2
		15		0.101	0.2829	0.0350	0.0286	629.4
		16	Axial	0.101	0.2712	0.0419	0.0274	748.9
		17		0.101	0.2781	0.0357	0.0281	704.6
		18		0.101	0.2657	0.0483	0.0268	779.1
673095	Aft	K4	Hoop	0.100	0.2580	0.0575	0.0258	345.7
		5		0.1005	0.2795	0.0362	0.0281	323.8
		6		0.101	0.1766	0.1185	0.0178	330.3
		7	Axial	0.1015	0.2905	0.0266	0.0295	451.9
		8		0.099	0.2826	0.0374	0.0280	522.1
		9		0.100	0.2865	0.0339	0.0287	405.9
		K13	Hoop	0.0985	0.2737	0.0417	0.0270	344.1
		14		0.0985	0.2651	0.0506	0.0261	337.5
		15		0.099	0.2325	0.0815	0.0230	303.0
		16		0.099	0.2694	0.0502	0.0267	377.9
		17		0.1005	0.2818	0.0365	0.0283	415.9
		18		0.0985	0.2708	0.0471	0.0267	355.8
673147	Fwd	L4	Hoop	0.0995	0.2682	0.0498	0.0267	508.2
		5		0.0995	0.2577	0.0604	0.0256	525.4
		6		0.0995	0.2659	0.0504	0.0265	520.8
		7	Axial	0.100	0.2682	0.0460	0.0268	545.5
		8		0.100	0.2696	0.0466	0.0270	550.4
		9		0.101	0.2760	0.0382	0.0276	568.8

TABLE XII (cont.)

Chamber	Cylinder	Spec. No.	Notch Direct.	Width, in.	DBN-cd, in.	C.D., in.	Area, sq. in.	W/A, in.-lb/in.^{2}
673147	Fwd	L13	Hoop	0.099	0.2527	0.0659	0.0250	475.2
		14		0.099	0.2602	0.0561	0.0258	490.7
		15		0.099	0.2654	0.0506	0.0263	533.8
		16	Axial	0.101	0.2725	0.0425	0.0275	557.8
		17		0.099	0.2758	0.0391	0.0273	588.3
		18		0.0995	0.2693	0.0454	0.0268	653.7
673147	Aft	[illegible]	Hoop	0.099	0.2727	0.0422	0.0270	481.5
		5		0.0988	0.2403	0.0761	0.0237	443.0
		6		0.0988	0.2749	0.0377	0.0272	473.5
		7	Axial	0.0987	0.2814	0.0327	0.0278	543.2
		8		0.099	0.2777	0.0363	0.0275	497.8
		9		0.0991	0.2795	0.0342	0.0277	662.8
		M13	Hoop	0.0987	0.2716	0.0450	0.0268	407.5
		14		0.0988	0.2804	0.0366	0.0277	433.2
		15		0.0987	0.2841	0.0279	0.0280	509.6
		16	Axial	0.0988	0.2714	0.0434	0.0268	545.5
		17		0.0992	0.2811	0.0332	0.0279	528.7
		18		0.0990	0.2780	0.0364	0.0275	501.8
674514	Fwd	O-4	Hoop	0.0995	0.2473	0.0664	0.0246	358.1
		5		0.1005	0.2233	0.0931	0.0224	339.7
		6		0.100	0.2645	0.0523	0.0265	396.2
		7	Axial	0.0985	0.2947	0.0212	0.0290	440.3
		8		0.0995	0.2645	0.0508	0.0263	399.2
		9		0.100	0.2770	0.0363	0.0277	371.8
		O-13	Hoop	0.101	0.2482	0.0684	0.0251	402.0
		14		0.101	0.2674	0.0470	0.0270	396.3
		15		0.1005	0.2677	0.0459	0.0269	382.9
		16	Axial	0.101	0.2687	0.0474	0.0271	399.1
		17		0.100	0.2886	0.0300	0.0289	407.3
		18		0.0995	0.2624	0.0531	0.0261	364.0
674514	Aft	R4	Hoop	0.100	0.2797	0.0367	0.0280	274.3
		5		0.100	0.2807	0.0363	0.0281	317.4
		6		0.100	0.2746	0.0407	0.0275	317.1
		7	Axial	0.0995	0.2783	0.0374	0.0277	346.6
		8		0.0995	0.2728	0.0414	0.0271	387.5
		9		0.100	0.2659	0.0479	0.0266	364.7

Appendix D

TABLE XII (cont.)

Chamber	Cylinder	Spec. No.	Notch Direct.	Width, in.	DBN-cd, in.	C.D., in.	Area, sq. in.	W/A, $in.-lb/in.^2$
674514	Aft	R13	Hoop	0.0995	0.2472	0.0702	0.0246	301.6
		14		0.0995	0.2711	0.0456	0.0270	330.4
		15		0.0991	0.2692	0.0453	0.0267	307.1
		16	Axial	0.0992	0.2368	0.0733	0.0235	359.6
		17		0.100	0.2769	0.0384	0.0277	343.0
		18		0.1003	0.2798	0.0332	0.0281	395.7
673122	Fwd	S4	Hoop	0.1016	0.2859	0.0312	0.0290	653.8
		5		0.1015	0.2770	0.0392	0.0281	580.1
		6		0.1021	0.2781	0.0390	0.0284	582.4
		7	Axial	0.1021	0.2939	0.0166	0.0300	660.0
		8		0.1022	0.2881	0.0290	0.0294	608.2
		9		0.1024	0.2825	0.0320	0.0289	668.5
		S13	Hoop	0.1017	0.2610	0.0569	0.0265	547.2
		14		0.1018	0.2779	0.0393	0.0283	631.8
		15		0.1018	0.2809	0.0343	0.0286	557.3
		16	Axial	0.1018	0.2879	0.0262	0.0293	712.6
		17		0.1020	0.2862	0.0276	0.0292	772.6
		18		0.1020	0.2911	0.0255	0.0297	731.3
TESTED At 320°F		S23	Hoop	0.1013	0.2815	0.0274	0.0285	1187.4
		24		0.1014	0.2760	0.0325	0.0280	1137.9
		25		0.1015	0.2816	0.0316	0.0286	1107.7
		29		0.1023	0.2776	0.0278	0.0284	1033.1
		30		0.1021	0.2819	0.0318	0.0288	1018.8
		31		0.1022	0.2759	0.0378	0.0282	996.0
673122	Aft	T4	Hoop	0.0983	0.2908	0.0258	0.0286	759.4
		5		0.0985	0.2669	0.0484	0.0263	647.1
		6		0.0982	0.2886	0.0275	0.0283	623.3
		7	Axial	0.0987	0.2868	0.0277	0.0283	597.2
		8		0.0991	0.2821	0.0316	0.0280	467.9
		9		0.0998	0.2880	0.0250	0.0287	551.2
		T13	Hoop	0.0983	0.2817	0.0348	0.0277	797.1
		14		0.0981	0.2774	0.0384	0.0272	657.4
		15		0.0979	0.2681	0.0450	0.0262	603.8
		16	Axial	0.0982	0.2802	0.0358	0.0275	672.0
		17		0.0985	0.2771	0.0382	0.0273	544.3
		18		0.0982	0.2851	0.0320	0.0280	594.3

TABLE XII (cont.)

Chamber	Cylinder	Spec. No.	Notch Direct.	Width, in.	DBN-cd, in.	C.D., in.	Area, sq. in.	W/A, in.-lb/in.^{2}
TESTED At 320°F		T23	Hoop	0.0992	0.2812	0.0311	0.0279	1107.5
		24		0.0987	0.2805	0.0309	0.0277	979.1
		25		0.0989	0.2627	0.0465	0.0260	1003.8
		29		0.0993	0.2773	0.0321	0.0275	1088.7
		30		0.0986	0.2819	0.0281	0.0278	1135.3
		31		0.0989	0.2801	0.0297	0.0277	1189.2
2192109	Fwd	U4	Hoop	0.1094	0.2643	0.0509	0.0289	518.3
		5		0.1087	0.2762	0.0408	0.0300	460.0
		6		0.1090	0.2530	0.0626	0.0276	458.7
		7	Axial	0.1079	0.2613	0.0544	0.0282	448.9
		8		0.1080	0.2870	0.0281	0.0310	398.1
		9		0.1073	0.2902	0.0250	0.0311	403.5
		U13	Hoop	0.1082	0.2750	0.0418	0.0298	495.0
		14		0.1087	0.2736	0.0449	0.0297	512.5
		15		0.1082	0.2697	0.0466	0.0292	488.7
		16	Axial	0.1082	0.2787	0.0369	0.0302	453.6
		17		0.1076	0.2753	0.0407	0.0296	439.2
		18		0.1075	0.2917	0.0257	0.0314	450.6
TESTED At 212°F		U23	Hoop	0.1078	0.2633	0.0444	0.0284	680.2
		24		0.1077	0.2591	0.0490	0.0279	692.4
		25		0.1081	0.2652	0.0440	0.0287	677.4
		29		0.1081	0.2664	0.0414	0.0288	675.0
		30		0.1075	0.2764	0.0330	0.0297	694.9
		31		0.1074	0.2744	0.0316	0.0295	654.9
2192109	Aft	X4	Hoop	0.1066	0.2849	0.0332	0.0304	524.3
		5		0.1074	0.2764	0.0442	0.0297	504.4
		6		0.1068	0.2701	0.0458	0.0288	528.5
		7	Axial	0.1076	0.2756	0.0383	0.0297	422.6
		8		0.1075	0.2638	0.0515	0.0284	366.2
		9		0.1074	0.2646	0.0509	0.0284	391.5
		X13	Hoop	0.1076	0.2816	0.0375	0.0303	478.5
		14		0.1072	0.2751	0.0236	0.0295	483.7
		15		0.1064	0.2816	0.0332	0.0300	471.7
		16	Axial	0.1063	0.2773	0.0362	0.0295	410.5
		17		0.1058	0.2703	0.0442	0.0286	339.2
		18		0.1065	0.2646	0.0492	0.0282	357.8

TABLE XII (cont.)

Chamber	Cylinder	Spec. No.	Notch Direct.	Width, in.	DBN-cd, in.	C.D., in.	Area, sq. in.	W/A ^{2} in.-lb/in.
TESTED At 212°F		X23	Hoop	0.1060	0.2715	0.0345	0.0288	683.3
		24		0.1061	0.2752	0.0334	0.0292	665.8
		25		0.1077	0.2691	0.0394	0.0290	686.9
		29		0.1072	0.2658	0.0404	0.0285	635.8
		30		0.1060	0.2705	0.0361	0.0287	631.4
		31		0.1082	0.2786	0.0284	0.0301	661.8
R369	Fwd	Y4	Hoop	0.1100	0.2779	0.0412	0.0306	399.6
		5		0.1097	0.2857	0.0337	0.0313	422.0
		6		0.1098	0.2777	0.0358	0.0305	400.9
		7	Axial	0.1100	0.2300	0.0814	0.0253	337.5
		8		0.1105	0.2562	0.0571	0.0283	374.5
		9		0.1100	0.2779	0.0353	0.0306	403.2
		Y13	Hoop	0.1091	0.2800	0.0375	0.0305	397.0
		14		0.1097	0.2797	0.0379	0.0307	379.4
		15		0.1097	0.2803	0.0365	0.0307	398.3
		16	Axial	0.1090	0.2703	0.0428	0.0295	308.4
		17		0.1094	0.2759	0.0380	0.0302	347.6
		18		0.1092	0.2759	0.0394	0.0301	302.3
R369	Aft	Z4	Hoop	0.1062	0.2833	0.0325	0.0301	665.7
		5		0.1063	0.2821	0.0332	0.0300	676.0
		6		0.1062	0.2827	0.0328	0.0300	696.0
		7	Axial	0.1064	0.2860	0.0310	0.0304	469.4
		8		0.1063	0.2726	0.0408	0.0290	467.9
		9		0.1056	0.2712	0.0435	0.0286	527.9
		Z13	Hoop	0.1058	0.2828	0.0346	0.0299	674.2
		14		0.1058	0.2734	0.0427	0.0289	701.7
		15		0.1057	0.2818	0.0352	0.0298	696.6
		16	Axial	0.1058	0.2746	0.0414	0.0291	482.4
		17		0.1063	0.2671	0.0485	0.0284	482.0
		18		0.1057	0.2634	0.0503	0.0278	492.4

Appendix D

TABLE XIII

PRECRACK CHARPY SLOW BEND DATA FOR 6Al-4V-TITANIUM

Chamber	Cylinder	Spec. No.	Notch Direct.	Width, in.	DBN-cd, in.	C.D., in.	Area, sq. in.	W/A, $in.^2$-lb/in.
R26	Fwd	A1	Hoop	0.1005	0.2758	0.0408	0.0276	180.9
		2		0.1005	0.2683	0.0480	0.0268	238.2
		3		0.1005	0.2745	0.0403	0.0275	203.3
		A10	Axial	0.1015	0.2730	0.0453	0.0278	192.5
		11		0.1015	0.2640	0.0522	0.0269	173.1
		12		0.1015	0.2765	0.0395	0.0282	178.3
R26	Aft	B4	Hoop	0.100	0.2773	0.0400	0.0277	410.7
		5		0.100	0.2690	0.0485	0.0269	343.9
		6		0.100	0.2767	0.0392	0.0277	358.7
		B10	Axial	0.102	0.2836	0.0334	0.0289	436.0
		11		0.102	0.2648	0.0539	0.0270	365.3
		12		0.102	0.2768	0.0401	0.0282	349.4
2191456	Fwd	C1	Hoop	0.100	0.2698	0.0448	0.0270	132.4
		2		0.100	0.2695	0.0463	0.0270	121.3
		3		0.0995	0.2698	0.0464	0.0270	123.1
		C10	Axial	0.099	0.2726	0.0436	0.0270	118.7
		11		0.099	0.2686	0.0485	0.0266	120.5
		12		0.099	0.2681	0.0499	0.0265	120.0
2191456	Aft	D1	Hoop	0.1025	0.2821	0.0336	0.0288	280.8
		2		0.1025	0.2814	0.0335	0.0287	300.2
		3		0.1025	0.2714	0.0423	0.0277	310.6
		D10	Axial	0.1005	0.2801	0.0321	0.0280	267.4
		11		0.1005	0.2703	0.0446	0.0270	278.2
		12		0.1005	0.2767	0.0343	0.0277	276.4
673078	Fwd	E1	Hoop	0.0985	0.2840	0.0332	0.0278	208.5
		2		0.0985	0.2651	0.0513	0.0260	247.4
		3		0.098	0.2839	0.0325	0.0278	216.3
		E10	Axial	0.0995	0.2817	0.0346	0.0282	192.8
		11		0.099	0.2661	0.0506	0.0263	176.6
		12		0.099	0.2769	0.0397	0.0274	215.0
673078	Aft	H1	Hoop	0.098	0.2797	0.0360	0.0274	164.2
		2		0.098	0.2418	0.0741	0.0237	163.0
		3		0.098	0.2791	0.0364	0.0274	215.9
		H10	Axial	0.0975	0.2799	0.0364	0.0274	182.6
		11		0.0975	0.2768	0.0396	0.0271	186.0
		12		0.0975	0.2765	0.0394	0.0271	190.4
673095	Fwd	J1	Hoop	0.101	0.2796	0.0365	0.0282	182.1
		2		0.101	0.2883	0.0285	0.0291	173.2
		3		0.1005	0.2727	0.0453	0.0273	186.8
		J10	Axial	0.101	0.2735	0.0422	0.0276	193.9
		11		0.101	0.2568	0.0583	0.0259	165.4
		12		0.1005	0.2783	0.0385	0.0279	148.9

TABLE XIII (cont.)

Chamber	Cylinder	Spec. No.	Notch Direct.	Width, in.	DBN-cd, in.	C.D., in.	Area, sq. in.	W/A, $in.-lb/in.^2$
673095	Aft	K1	Hoop	0.099	0.2426	0.0735	0.0240	92.0
		2		0.099	0.2480	0.0673	0.0246	98.0
		3		0.099	0.2748	0.0409	0.0272	104.1
		K10	Axial	0.098	0.2601	0.0558	0.0255	86.1
		11		0.0985	0.2378	0.0792	0.0233	64.9
		12		0.0985	0.1861	0.1297	0.0182	126.6
673147	Fwd	L1	Hoop	0.100	0.2763	0.0400	0.0276	161.3
		2		0.1005	0.2823	0.0352	0.0282	150.2
		3		0.100	0.2814	0.0345	0.0281	154.2
		L10	Axial	0.099	0.2775	0.0398	0.0275	138.8
		11		0.099	0.2815	0.0356	0.0279	135.5
		12		0.099	0.2742	0.0428	0.0271	148.3
673147	Aft	M1	Hoop	0.099	0.2791	0.0365	0.0276	117.0
		2		0.099	0.2767	0.0375	0.0274	112.6
		3		0.099	0.2853	0.0302	0.0282	128.5
		M10	Axial	0.0985	0.2824	0.0322	0.0277	128.2
		11		0.0986	0.2621	0.0533	0.0259	136.7
		12		0.0987	0.2799	0.0357	0.0274	134.5
674514	Fwd	0-1	Hoop	0.100	0.2642	0.0513	0.0264	135.9
		2		0.100	0.2664	0.0484	0.0266	124.1
		3		0.1005	0.2734	0.0408	0.0273	121.3
		0-10	Axial	0.101	0.2511	0.0626	0.0254	128.5
		11		0.101	0.2615	0.0536	0.0264	112.7
		12		0.101	0.2681	0.0458	0.0271	116.0
674514	Aft	R1	Hoop	0.100	0.2768	0.0392	0.0277	95.7
		2		0.0995	0.2798	0.0378	0.0280	93.0
		3		0.0995	0.2768	0.0393	0.0277	88.4
		R10	Axial	0.0995	0.2748	0.0422	0.0275	88.6
		11		0.0995	0.2515	0.0653	0.0252	86.7
		12		0.100	0.2688	0.0484	0.0269	92.3
673122	Fwd	S1	Hoop	0.1015	0.2782	0.0390	0.0284	163.1
		2		0.1014	0.2632	0.0540	0.0266	144.8
		3		0.1010	0.2894	0.0277	0.0292	188.6
		S10	Axial	0.1020	0.2736	0.0430	0.0279	175.5
		11		0.1016	0.2718	0.0445	0.0277	168.1
		12		0.1018	0.2744	0.0430	0.0280	191.1

TABLE XIII (cont.)

Chamber	Cylinder	Spec. No.	Notch Direct.	Width in.	DBN-cd, in.	C.D., in.	Area sq. in.	W/A in.-lb/in.^{2}
Tested at 320°F		S20	Hoop	0.1016	0.2736	0.0318	0.0279	1289.9
		21		0.1014	0.2701	0.0424	0.0273	1071.2
		22		0.1014	0.2692	0.0413	0.0272	1157.2
		26		0.1021	0.2846	0.0286	0.0290	1355.2
		27		0.1019	0.2734	0.0366	0.0279	1053.8
		28		0.1022	0.2822	0.0346	0.0288	1299.2
673122	Aft	T1	Hoop	0.0988	0.2882	0.0278	0.0285	368.4
		2		0.0982	0.2806	0.0356	0.0275	277.5
		3		0.0988	0.2856	0.0300	0.0283	275.2
		T10	Axial	0.099	0.2748	0.0401	0.0272	231.6
		11		0.0985	0.2825	0.0335	0.0277	193.6
		12		0.0985	0.2802	0.0358	0.0275	218.2
673122	Aft							
Tested at 320°F		T20	Hoop	0.0987	0.2754	0.0384	0.0273	1166.6
		21		0.0987	0.2835	0.0302	0.0281	1411.4
		22		0.0988	0.2762	0.0373	0.0273	1250.5
		26		0.0984	0.2782	0.0318	0.0273	1481.8
		27		0.0989	0.2782	0.0359	0.0275	1212.7
		28		0.0992	0.2772	0.0376	0.0274	1229.3
2192109	Fwd	U1	Hoop	0.1088	0.2908	0.0262	0.0317	149.9
		2		0.1086	0.2813	0.0354	0.0307	138.4
		3		0.1086	0.2838	0.0331	0.0309	129.3
		U10	Axial	0.1085	0.2700	0.0465	0.0292	134.8
		11		0.1091	0.2798	0.0357	0.0305	124.3
		12		0.1087	0.2707	0.0447	0.0295	135.1
Tested at 212°F		U20	Hoop	0.1073	0.2817	0.0283	0.0301	651.0
		21		0.1075	0.2617	0.0483	0.0283	639.9
		22		0.1082	0.2755	0.0357	0.0298	608.1
		26		0.1074	0.2771	0.0321	0.0296	609.3
		27		0.1078	0.2860	0.0296	0.0309	593.0
		28		0.1082	0.2610	0.0487	0.0282	569.8
2192109	Aft	X1	Hoop	0.1076	0.2830	0.0338	0.0306	135.7
		2		0.1071	0.2751	0.0426	0.0294	142.9
		3		0.1047	0.2717	0.0452	0.0285	120.0
		X10	Axial	0.1077	0.2797	0.0355	0.0302	119.2
		11		0.1078	0.2721	0.0457	0.0294	139.2
		12		0.1075	0.2784	0.0374	0.0301	119.2

TABLE XIII (cont.)

Chamber	Cylinder	Spec. No.	Notch Direct.	Width in.	DBN-cd, in.	C.D., in.	Area sq. in.	W/A $in.-lb/in.^2$
Tested at 212°F		X20	Hoop	0.1074	0.2714	0.0441	0.0290	562.8
		21		0.1070	0.2621	0.0463	0.0280	525.9
		22		0.1069	0.2739	0.0354	No Test	
		26		0.1065	0.2723	0.0352	0.0289	548.1
		27		0.1050	0.2661	0.0431	0.0279	526.5
		28		0.1065	0.2726	0.0375	0.0289	539.8
R369	Fwd	Y1	Hoop	0.1098	0.2771	0.0397	0.0305	141.6
		2		0.1099	0.2797	0.0384	0.0308	139.1
		3		0.110	0.2761	0.0415	0.0304	142.5
		Y10	Axial	0.1079	0.2810	0.0324	0.0303	140.2
		11		0.1078	0.2809	0.0358	0.0303	135.4
		12		0.1088	0.2687	0.0490	0.0293	129.0
R369	Aft	Z1	Hoop	0.1060	0.2829	0.0337	0.0300	245.6
		2		0.1061	0.2826	0.0332	0.0300	232.4
		3		0.1062	0.2783	0.0387	0.0295	229.0
		Z10	Axial	0.1059	0.2724	0.0431	0.0289	238.3
		11		0.1057	0.2834	0.0369	0.0300	256.4
		12		0.1058	0.2720	0.0398	0.0288	237.1

APPENDIX E

STATISTICAL ANALYSIS OF SOLUTION-TREATED AND AGED Ti-6Al-4V

APPENDIX E

TABLE OF CONTENTS

		Page
A.	Introduction	271
B.	Evaluation of Room Temperature Uniaxial Tensile Data	284
	1. Ultimate Tensile Strength	284
	2. Yield Strength at 0.2% Offset	286
	3. Percent Elongation (4D)	288
C.	Elevated Temperature Tensile Data	290
	1. Ultimate Tensile Data	290
	2. Yield Strength at 0.2% Offset	291
	3. Percent Elongation (4D)	291
D.	Part-Through-Crack Tensile Data	292
	1. Crack Intensity (a/Q) Approximately 0.02	292
	a. Tested at Aerojet-Sacramento	292
	b. Tested at Aerojet-Downey	295
	c. Tested at Lycoming	297
	d. Comparison of Data Collected at Each Laboratory	298
	2. Crack Intensity (a/Q) Approximately 0.04	303
	a. Tested at Aerojet-Sacramento	303
	b. Tested at Aerojet-Downey	305
	c. Tested at Lycoming	306
	3. Difference in K_{Ic} That Can be Detected for the Different Curve Areas	308

Appendix E

TABLE LIST

Table		Page
I	Room Temperature Tensile Results, Ultimate Tensile Strength	321
II	Bartlett's Test, Room Temperature, Tensile Strength	325
III	ANOVA Test, Room Temperature, Tensile Strength	326
IV	Multi- and Single Forging Heats, Tensile Strength	328
V	Room Temperature Tensile Results, Yield Strength	330
VI	Bartlett's Test, Room Temperature, Yield Strength	334
VII	ANOVA Test, Room Temperature, Yield Strength	335
VIII	Multi- and Single Forging Heats, Yield Strength	337
IX	Room Temperature Tensile Results, Percent Elongation	339
X	Bartlett's Test, Room Temperature, Percent Elongation	343
XI	ANOVA Test, Room Temperature, Percent Elongation	344
XII	Multi- and Single Forging Heats, Percent Elongation	346
XIII	Room Temperature K_{Ic} (Aerojet-Sacramento a/Q $\sim$ 0.02)	348
XIV	Bartlett's Test for Multi-Forging Heats (Aerojet-Sacramento a/Q $\sim$ 0.02)	350
XV	ANOVA Test for Multi-Forging Heats (Aerojet-Sacramento a/Q $\sim$ 0.02)	351
XVI	Comparison of Means for Multi-Forging Heats vs Single Forging Heats (Aerojet-Sacramento a/Q $\sim$ 0.02)	352
XVII	Room Temperature K_{Ic} Results (Aerojet-Downey a/Q $\sim$ 0.02)	353
XVIII	Bartlett's Test for Multi-Forging Heats (Aerojet-Downey a/Q $\sim$ 0.02)	355
XIX	ANOVA Test for Multi-Forging Heats (Aerojet-Downey a/Q $\sim$ 0.02)	356
XX	Comparison of Means for Multi-Forging Heats vs Single Forging Heats (Aerojet-Downey a/Q $\sim$ 0.02)	357
XXI	Room Temperature K_{Ic} Results (Lycoming a/Q $\sim$ 0.02)	358
XXII	Bartlett's Test for Multi-Forging Heats (Lycoming a/Q 0.02)	360
XXIII	ANOVA Test for Multi-Forging Heats (Lycoming a/Q $\sim$ 0.02)	361
XXIV	Comparison of Means for Multi-Forging Heats vs Single Forging Heats (Lycoming a/Q $\sim$ 0.02)	362
XXV	Common Forgings Tested at all Three Laboratories (a/Q $\sim$ 0.02)	363

TABLE LIST (cont.)

Table		Page
XXVI	Room Temperature K_{Ic} Results (Aerojet-Sacramento a/Q ∿ 0.04)	361
XXVII	Bartlett's Test for Multi-Forging Heats (Aerojet-Sacramento a/Q ∿ 0.04)	369
XXVIII	ANOVA Test for Multi-Forging Heats (Aerojet-Sacramento a/Q ∿ 0.04)	370
XXIX	Room Temperature K_{Ic} Results (Aerojet-Downey a/Q ∿ 0.04)	371
XXX	Bartlett's Test for Multi-Forging Heats (Aerojet-Downey a/Q ∿ 0.04)	373
XXXI	ANOVA Test for Multi-Forging Heats (Aerojet-Downey a/Q ∿ 0.04)	374
XXXII	Room Temperature K_{Ic} Results (Lycoming a/Q ∿ 0.04)	375
XXXIII	Bartlett's Test for Multi-Forging Heats (Lycoming a/Q ∿ 0.04)	377
XXXIV	ANOVA Test for Multi-Forging Heats (Lycoming a/Q ∿ 0.04)	378

Appendix E

ILLUSTRATIONS

Figure		Page
1	Frequency of Ultimate Tensile Strength Data at 250°F	311
2	Cumulative Frequency of Ultimate Tensile Strength Data at 250°F	312
3	Ultimate Tensile Strength at 250°F versus Probability	313
4	Determination of Working Curve (Ultimate Tensile Strength)	314
5	K_{Ic} or F_G/F_{ty} versus Probability for Aerojet-Sacramento ($a/Q \sim 0.04$)	315
6	K_{Ic} or F_G/F_{ty} versus Probability for Aerojet-Downey ($a/Q \sim 0.04$)	316
7	K_{Ic} or F_G/F_{ty} versus Probability for Lycoming ($a/Q \sim 0.04$)	317
8	K_{Ic} or F_G/F_{ty} versus Probability for $a/Q \sim C.04$	318
9	K_{Ic} versus Crack Area to Cross-Sectional Area Ratio (Ca/BW)	319
10	K_{Ic} versus Crack Depth to Thickness Ratio (a/B)	320

Appendix E

NOMENCLATURE

α - The percentage of the time of rejecting the hypothesis when it is true.

β - The percentage of the time of accepting the hypothesis when it is false.

X - Value of an individual measurement.

ΣX - Sum of individual measurements.

ΣX^2 - Sum of squared individual measurements.

$(\Sigma X)^2$ - Square of the sum of individual measurements.

$\overline{X}_F$ - Mean value of a forging, $\overline{X}_F = \frac{\sum_{i=1}^{n_i} Xi,}{n_i}$ i = refers to a forging.

$\overline{X}_H$ - Mean value of a heat, $\overline{X}_H = \frac{\sum_{f=1}^{n_f} \overline{X}_F}{n_f}$ f refers to number of forgings in a heat

$\overline{X}_{MF}$ - Mean value of multi-forging heats, $\overline{X}_{MF} = \frac{\sum_{h=1}^{n_h} \overline{X}_H (MF)}{n_h (MF)}$

h refers to number of multi-forging heats

$\overline{X}_{SF}$ - Mean value of single-forging heats, $\overline{X}_{SF} = \frac{\sum_{h=1}^{n_h} \overline{X}_H (SF)}{n_h (SF)}$

h refers to number of single-forging heats

Appendix E

NOMENCLATURE (cont.)

$\bar{X}_T$ - Mean value of heats, $\bar{X}_T = \frac{\sum_{H=1}^{n_H} \bar{X}_H}{n_H}$ H refers to number of heats

$\bar{X}_L$ - Best estimate of population mean from one laboratory, $\bar{X}_L = \frac{\Sigma X_j}{n_j}$ j refers to a laboratory.

$\bar{X}_{LM}$ - Mean value of laboratory means, $\bar{X}_{LM} = \frac{\sum_{l=1}^{n=l} \bar{X}_L}{n_l}$ l refers to number of laboratories.

$\bar{X}_P$ - Best estimate of population mean from more than one laboratory, $\bar{X}_P = \frac{\Sigma Xi}{n_i}$, i refers to i^{th} observation from all laboratories.

n - Number of samples

n_i - Number of samples in i^{th} group

k - Number of groups.

n_f - Number of forgings in a single heat

n_F - Number of total forgings

$n_{H(MF)}$ - Number of multi-forging heats

$n_{H(SF)}$ - Number of single-forging heats

n_H - Number of total heats

n_e - Number of laboratories

S - Standard Deviation

SS - Sum of squares, $SS = \Sigma (X-\bar{X})^2$

NOMENCLATURE (cont.)

S^2 - Sample variance

S_e^2 - Test or error variance, $S_e^2 = \dfrac{\sum_{i=1}^{m} \sum_{j=1}^{n} (X - \bar{X}_F)^2}{df_i}$

j refers to number of observations for each forging

i refers to number of forgings

S_F^2 - Forging-to-forging variation, $S_F^2 = \dfrac{\sum_{h=1}^{m} \sum_{f=1}^{n}}{df_f} (\bar{X}_F - \bar{X}_H)^2$

f refers to number of forgings per heat

h refers to number of multi-forging heats

S_H^2 - Heat-to-heat variation, $S_H^2 = \dfrac{\sum_{H=1}^{n} (\bar{X}_H - \bar{X}_T)^2}{df_H}$

H refers to number of heats

S_L^2 - Best estimate of population variance from one laboratory, S_L^2 determined from probability curve by subtracting $\bar{X}_L$ from value at 84 percent, and then squaring the value.

S_{LM}^2 - Laboratory-to-laboratory variation, $S_{LM}^2 = \dfrac{\sum (X_L - X_{LM})^2}{df_l}$

S_o^2 - Best estimate of population variance from more than one laboratory, S_L^2 determined from probability curve by subtracting $\bar{X}_P$ from value at 84 percent, and then squaring the value.

df - Degree of freedom

df_i - Degree of freedom in the ith group

df_F - Degree of freedom for forgings, $df_F = n_F - 1$

NOMENCLATURE (cont.)

df_H	-	Degree of freedom for heats, $df_H = n_H - 1$
df_f	-	Degree of freedom for a heat, df_f equal number of forgings in a heat minus one.
k_A	-	One sided tolerance limit where at least 99 percent of the population of values is expected to fall with a confidence of 95 percent.
k_B	-	One sided tolerance limit where at least 90 percent of the population of values is expected to fall with a confidence of 95 percent.
>	-	Greater than
<	-	Less than
∞	-	Infinity
f_1 or f_2	-	Degrees of freedom

Appendix E

A. INTRODUCTION

The purpose of this analysis was to supply room temperature and elevated temperature uniaxial tensile results and K_{Ic} results from part-through-crack (PTC) tensile specimens for input to Mil-Hdbk-5. The material tested was 6Al-4V titanium supplied by one of three vendors for extrusion by Cameron Iron Works, Inc., Houston, Texas.

Three sets of data were analyzed, of which the room temperature tensile results were collected at several laboratories, the elevated temperature tensile results were collected at one laboratory, and the K_{Ic} results were collected at three laboratories. In all instances, the data analyzed were obtained from solution-treated (1750°F-1 hour) and aged (1000°F-8 hours) Ti-6Al-4V. The information needed to fulfill Mil-Hdbk-5 requirements was the best estimate of the population mean ($\bar{X}_P$) and the standard deviation (S_o). Required additional information is as follows:

1. The test variation (S_e^2), that error attributed to test procedure, mechanical variation, and/or forging heterogeniety.

2. The forging-to-forging variation (S_F^2), that variation attributed to the variability of forgings for the same heat.

3. The heat-to-heat variation (S_H^2), that variation attributed to the variability of heats.

4. The laboratory-to-laboratory variation (S_{LM}^2), that variation attributed to differences in test procedure, mechanical variation, personnel, etc., between laboratories.

Because of past experience at Aerojet-General Corporation in relating the classical statistical approach and the graphical approach for

evaluating statistical parameters, classical statistics were used to supply the desired information, but were augmented by the use of probability paper.

The construction of a probability curve is presented below. The following table was constructed using ultimate tensile strength data, at 250°F (see Table I, Appendix A).

ULTIMATE TENSILE STRENGTH FOR Ti-6Al-4V
TESTED AT 250°F

Class				Cumulative		
Column 1 Interval, ksi	Column 2 Midpoint, ksi	Col. 3 Frequency	Column 4 Proportions	Column 5 Proportions	Col. 6 Frequency	Column 7 Frequency ÷ Total Freq. +one
143.0-143.9	143.5	1	0.0063	0.0063	1	0.63
144.0-144.9	144.5	3	0.0190	0.0253	4	2.52
145.0-145.9	145.5	2	0.0127	0.0380	6	3.77
146.0-146.9	146.5	1	0.0063	0.0443	7	4.40
147.0-147.9	147.5	2	0.0127	0.0570	9	5.66
148.0-148.9	148.5	7	0.0443	0.1013	16	10.1
149.0-149.9	149.5	10	0.0633	0.1643	26	16.4
150.0-150.9	150.5	7	0.0443	0.2089	33	20.8
151.0-151.9	151.5	14	0.0886	0.2975	47	29.6
152.0-152.9	152.5	13	0.0823	0.3798	60	37.7
153.0-153.9	153.5	16	0.1012	0.4810	76	47.8
154.0-154.9	154.5	21	0.1329	0.6139	97	61.0
155.0-155.9	155.5	12	0.0760	0.6899	109	68.5
156.0-156.9	156.5	14	0.0886	0.7785	123	77.4
157.0-157.9	157.5	9	0.0569	0.8354	132	83.0
158.0-158.9	158.5	7	0.0443	0.8797	139	87.4
159.0-159.9	159.5	6	0.0380	0.9177	145	91.2
160.0-160.9	160.5	2	0.0127	0.9304	147	92.5
161.0-161.9	161.5	2	0.0127	0.9431	149	93.7
162.0-162.9	162.5	4	0.0253	0.9684	153	96.2
163.0-163.9	163.5	1	0.0063	0.9747	154	96.9
164.0-164.9	164.5	2	0.0127	0.9874	156	98.1
165.0-165.9	165.5	1	0.0063	0.9937	157	98.8
166.0-166.9	166.5	1	0.0063	1.0000	158	99.3
			1.0000			

Appendix E

Column 1 is any convenient interval, the normal method of obtaining the interval is to divide the range of data points into 8 to 25 equal intervals. Column 3 lists the number of occurrences where data points fall in a particular interval. Figure 1, made up from Columns 2 and 3, illustrates the relative frequency with which all test values occurred. Figure 1 has a slight negative skew as may be seen by the shift of the mean from the mode. For a completely normal distribution, the plot would be a bell-shaped curve symmetrical about the mean extending to both the left and right. Figure 2, made up from Columns 1, 5, and 6, illustrates the probability of a random observation being less than or equal to any point on the curve. For example, point A on the curve means that 75 percent of the time a random observation will be less than or equal to 156.65 ksi. Figure 3, made up from Columns 2 and 7, is another illustration of the distribution of data. The data exhibit a normal distribution if the points fall on a straight line. The points of Figure 3 do not all lie on a straight line, but for sample size on the order of 100 only those points between 10 and 90 percent need be considered[1]. Data will exhibit either a normal or a nonnormal distribution. If the data exhibits a normal distribution, then it may be used to make decisions such as A- and B-Basis values, which are put in Mil-HDBD-5 for design purposes. For a normal distribution, as illustrated in Figure 3, the mean ($\bar{X}$) is that value at 50 percent and the standard deviation (S) is the difference between 84 and 50 percent. Utilizing the information in Figure 3, the A-Basis value would be calculated as follows:

$\bar{X} - k_A S$, where $\bar{X}$ = 153.7 ksi, S = 4.0 ksi, and $k_A^{(1)}$ = 2.60 for N = 158

(1) D. P. Moon and W. S. Hyler, Mil-HDBK-5, Guidelines for the Presentation of Data, Air Force Materials Laboratory Tech. Rpt., AFML-TR-66-386, Feb. 1967.

153.7 - 2.6(4.0) = 143.3 ksi

If the data does not exhibit a normal distribution; i.e., not a straight line on probability paper, there are problems associated in making decisions. For a non-normal distribution, 296 observations are required to make a decision regarding the A-Basis. If the required data points are not available, there are three alternatives and they are as follows:

(1) Draw a best line through the data points and assume a best normal.

(2) Plot the data as two or more normal plots; there is an explanation for each population but this often requires considerable investigation to identify.

(3) Plot the data on log normal paper to see if the points are on a straight line.

As our objective is to submit A- and B-Basis values to Mil-HDBK-5, it is not pertinent what type of distribution the data exhibits as long as it is possible to make a decision regarding the A- and B-Basis.

Probability paper allows the engineer to determine the following:

1. Readily detect all statistical information.
2. Non-normal data may be meaningfully presented from a probability standpoint.

3. Engineers are more able to interpret graphical solutions more meaningfully when related to engineering factors. An example would be the necessity of an engineering explanation of a discontinuity in a probability plot.

4. Data may be easily presented for suggested input to Mil-Hdbk-5. A step-by-step process of the techniques used in the analysis of the data is presented as follows:

1. Determine if the data have a near-normal distribution, this was done by using probability paper.

2. Determine forging means ($\bar{X}_F$) using the observations for each forging.

$$\bar{X}_F = \frac{\sum_{i=1}^{n} X_i}{N_i}$$ where i refers to the number of observations per forging.

3. Determine the test variation (S_e^2) utilizing the forging means and observations. The test variation is found by calculating the total sum of squares (SS) divided by the total degrees of freedom.

$$S_e^2 = \sum_{j=1}^{k} \sum_{i=1}^{n} (X_{ij} - \bar{X}_F)^2 / df_F$$ where $df_F = \sum_{j=1}^{k} (n_j - 1)$ and k is the total number of forgings.

4. Determine the heat means ($\bar{X}_H$) using the forging means. The best estimate of the forging was the forging mean, which was used regardless of the number of specimens for each forging. To determine if the forging means are equal, in order to combine forgings to obtain heat values, it is necessary that the standard deviations are homogeneous.

Appendix E

a. To test the significance of the variance, the (F) test for comparing two variances or Bartlett's test for comparing three or more variances are utilized.

(F) Test - Test of S_1 versus S_2, σ unknown

Compute $F_{calc} = S_1^2/S_2^2$ where $S_1 > S_2$

and compare to $F_{tab} = F_{.05}(f_1, f_2)$, where $f_1 = n_1 - 1$ and $f_2 = n_2 - 1$ and n is the number of observations per each forging. F_{tab} is found by using the (F) tables and f_1 and f_2 degrees of freedom at the 0.05 level of significance. If $F_{calc} > F_{tab}$, the standard deviations are considered to be statistically significant from each other.

Bartlett's Test - Test of S_1 versus S_2 versus S_k, σ unknown

Again F_{calc} is compared to F_{tab} using the following procedure:

$$S_P^2 = \frac{\sum_{j=1}^{k} \sum_{i=1}^{n} (X - \bar{X}_F)^2}{\sum_{i=1}^{n} df_i}$$, where j is the number of forgings per heat.

$$m = \left(\sum_{i=1}^{n} df_i\right) \log_e S_P^2 - \sum_{j=1}^{k} df_i \log_e S_i^2$$

$$f_1 = k-1, \quad a = \frac{1}{3(f_1)} \left[\sum_{j=1}^{k} \frac{1}{df_1} - \frac{1}{\sum_{j=1}^{k} df_1}\right], \quad f_2 = \frac{k+1}{a^2}$$

$$b = \frac{f_2}{1+2/f_2 - a}$$

Appendix E

$F_{calc} = \frac{f_2 m}{f_1(b-m)}$, $F_{tab} = F_{.05}(f_1, f_2)$ where f_1 and f_2 are respective degrees of freedom defined above.

Using the (F) tables and f_1 and f_2 degrees of freedom at the 0.05 level of significance, if $F_{calc} > F_{tab}$, the standard deviations are considered to be statistically significant from each other.

An example of the Bartlett test is illustrated below for the ultimate tensile strength of Heat No. 2993.

Forging No.	$\sum_{i=1}^{n} (X-X_i)^2$	df_i	S_i^2	$\log_e S_i^2$	$df \log_e S_i^2$	$1/df_i$
61A	20.66	2	10.33	2.335	4.670	0.5
61B	2.67	2	1.33	0.285	0.570	0.5
62A	21.46	2	10.73	2.375	4.750	0.5
62B	2.67	2	1.33	0.285	0.570	0.5
	47.46	8			10.560	2.0

$$S_P^2 = \frac{47.46}{8} = 5.92 \qquad m = (8)(1.778) - 10.560 = 3.664$$

$$f_1 = 4 - 1 = 3, \quad a = \frac{1}{(3)(3)}\left(2.0 - \frac{1}{8}\right) = 0.208$$

$$f_2 = \frac{4+1}{(.208)^2} = 116.3, \quad b = \frac{116.3}{1.2/116.3 - 0.208} = 143.8$$

$$F_{calc} = \frac{(116.3)(3.7)}{3(143.8 - 3.7)} = 1.02, \quad F_{tab} = F_{.05}(3,16) = 3.23$$

Since $F_{calc} < F_{tab}$ there is no reason to assume that the standard deviations are not from the same population.

b. To determine whether or not the averages differ significantly, use the (t) test for comparing two means or analysis of variance test (ANOVA) for comparing three or more means.

(t) Test, $\bar{X}_1$ vs $\bar{X}_2$, σ unknown but equal

$$\text{Compute } t_{calc} = \frac{u}{S_P\sqrt{\frac{n_1+n_2}{n_1 n_2}}}$$

$$\text{where } u = \bar{X}_1 - \bar{X}_2, \text{ and } S_P = \sqrt{\frac{(n_1-1)S_1^2 + (n_2-1)S_2^2}{n_1+n_2-2}}$$

and compare to $(t)_{tab} = t_{.05}$ for df = $(n_1+n_2 - 2)$ degrees of freedom. $(t)_{tab}$ is found by using the (t) tables and (df) degree of freedom at the 0.05 level of significance. If $t_{calc} > t_{tab}$, the means are considered to be statistically different.

Analysis of Variance (ANOVA) Test, $\bar{X}_1$ vs $\bar{X}_2$ vs ... $\bar{X}_k$, σ unknown but equal. Again F_{calc} is compared to F_{tab} using the following procedure,

F_{calc} = Between Mean Square ÷ Inherent Error Mean Square

The Between mean square = Between error sum of squares ÷ Between df

Inherent error mean square = Inherent error SS ÷ Inherent error df.

The total error SS equals the inherent error SS (within error) plus the between error SS. It is normal to determine the inherent error, the total error and then subtract the inherent error from the total error to find the between error.

Appendix E

$F_{tab} = F_{.05}$ (Between error df, inherent error df)

Using the (F) tables and the appropriate degrees of freedom at the 0.05 level of significance if $F_{calc} > F_{tab}$, the means are considered to be statistically different. This test is best described by an example of the ultimate tensile strength for Heat No. 2993.

Item No. (n)	Forging #61A		Forging #61B		Forging #62A		Forging #62B		
	X	X^2	X	X^2	X	X^2	X	X^2	
1	172	29584	172	29584	176	30976	172	29584	
2	178	31684	172	29584	172	29584	170	28900	
3	176	30976	174	30276	179	32041	171	29241	
									Total
n	3		3		3		3		12
df=n-1	2		2		2		2		8

Calculations for the inherent error are as follows:

$\sum X$	526	518	527	513	2084
$(\sum X)^2$	276676	268324	277729	263169	
$\sum X^2$	92244	89444	92601	87725	362014
$(\sum X)^2/n$	92225.3	89441.3	92576.3	87723	
$SS = \sum X^2 - (\sum X)^2/n$					
SS	18.7	2.7	24.7	2.0	48.1

The inherent error SS = 48.1 and the inherent error df = 8.

Calculations for the total error are as follows:

$$N = \sum_{i=1}^{k} n = 12 \qquad \sum X^2 = 362,014$$

$$CF = (\sum X)^2/N = \frac{4,343,056}{12} = 361,921.3$$

$$\sum X = 2084$$

$$(\sum X)^2 = (2084)^2 = 4,343,056 \qquad \text{Total SS} = \sum X^2 - CF = 82.7$$

Calculations for the between error are as follows:

The between forging error SS = total SS - inherent error SS = 34.6

The between forging df = 4 - 1 = 3

The between forging mean square = $\frac{34.6}{3}$ = 11.5

The inherent error mean square = $\frac{48.1}{8}$ = 6.0

$F_{calc} = \frac{11.5}{6} = 1.9, \quad F_{tab} = F_{.05}(3, 8) = 5.4$

Since $F_{calc} < F_{tab}$ at the 0.05 level of significance, there is no reason to assume that the means are not equal.

If it is acceptable to combine forgings to obtain heat values, then determining the heat mean ($\bar{X}_H$) using the forging means

$$\bar{X}_H = \frac{\sum_{i=1}^{k} \bar{X}_F}{n_k}$$ where n_k equals the number of forgings for a particular heat.

5. Determine the forging-to-forging variation (S_F^2) utilizing the heat and forging means.

$$S_F^2 = \frac{\sum_{j=1}^{k} \sum_{i=1}^{n} (X_F - \bar{X}_H)^2}{df}$$ where $df = \sum_{j=1}^{k} (n-1)$, and k is the total number of heats.

6. Determine the heat-to-heat variation (S_H^2) utilizing the heat means. The heats are listed in two columns, one for multi-forging heats and the other for single-forging heats. In order to add the multi-forging heats, it must first be proven that the standard deviations are homogeneous and the means are equal.

a. To determine whether the variances differ significantly, use the Bartlett test as described in Step No. 4(a).

b. To determine whether the averages differ significantly, use the analysis of variance test as described in Step No. 4(b).

If the above tests indicate homogeneity of means and variances, determine $\bar{X}_{MF}$ and S^2_{MF} for the multi-forging heats. Since there were a number of heats containing single forgings, determine if the single forging heats may be added without biasing the results. This is done by comparing the means of the single and multiple forging heats. The single forging heats are averaged and $\bar{X}_{SF}$ and S^2_{SF} calculated. Using the (F) test and the (t) test, as described in Step No. 4, determine if $S^2_{MF} = S^2_{SF}$ and $\bar{X}_{MF} = \bar{X}_{SF}$. If these values are not equal, the data are segregated into homogeneous lots.

The means from the acceptable heats are averaged to obtain $\bar{X}_T$. The best estimate of the heat was the heat mean which was used regardless of the number of forgings for each heat. The heat-to-heat variation (S^2_H) is found by using heat means and $\bar{X}_T$.

$$S^2_H = \frac{\sum_{i=1}^{n_H} (X_H - \bar{X}_T)^2}{df_H} \quad \text{where } df_H = n_H - 1$$

7. Determine the best estimate of the population mean from one laboratory ($\bar{X}_L$) utilizing all acceptable observations. Plot all the data on probability paper and $\bar{X}_L$ is that value at 50 percent.

8. The standard deviation (S_L) for one laboratory (S^2_o) is determined from the probability plot by taking that value at 84 percent and subtracting $\bar{X}_L$.

9. If the test results are from different laboratories, the data would be analyzed separately for each laboratory to this point. If the results are from two laboratories, use the (F) test and (t) test to test equality. If the results are from three or more laboratories, use Bartlett's test and ANOVA to test equality.

If the tests indicate equality, combine the laboratory means to find $\bar{X}_{LM}$ where $\bar{X}_{LM} = \frac{\sum_{i=1}^{n} \bar{X}_L}{n_L}$ and n_L is the number of laboratories.

10. Determine the laboratory-to-laboratory variation (S^2_{LM}) utilizing $\bar{X}_{LM}$ and the laboratory means $\bar{X}_L$.

$$S^2_{LM} = \frac{\sum_{i=1}^{n} (\bar{X}_{LM} - \bar{X}_L)^2}{n_L - 1}$$

11. Determine the best estimate of the population mean ($\bar{X}_P$) for more than one laboratory by using all data from all laboratories. Plot all the data on probability paper and $\bar{X}_P$ is that value at 50 percent.

12. Determine the overall standard deviation (S_o) from the probability plot by taking the value at 84 percent and subtracting $\bar{X}_P$.

13. Make a decision regarding the value of either (A) or (B) basis to be submitted for suggested input to Mil-Hdbk-5.

Appendix E

For normal distribution, the (A) and (B) bases are calculated as follows:

a. (A) Basis use $\bar{X}-k_A S$, where $k_A = k_{.99,.95,n}$ and $S = S_o$

b. (B) Basis use $\bar{X}-k_B S$, where $k_B = k_{.90,.95,n}$ and $S = S_o$

For a non-normal distribution, list all of the test observations in sequence starting with the smallest value as number 1. Use a table entitled "Ranks, r, of Observations for an Unknown Distribution Having the Probability and Confidence of A and B Values,"[3] to determine the rank corresponding to A and B bases.

(3) D. P. Moon and W. S. Hyler, Mil-Hdbk-5, Guidelines for the Presentation of Data, Air Force Materials Laboratory Tech. Rpt., AFML-TR-66-386, February 1967.

B. EVALUATION OF ROOM TEMPERATURE UNIAXIAL TENSILE DATA

The room temperature tensile results were obtained from 1/4-in. round tensile specimens tested at several laboratories.

1. Ultimate Tensile Strength

Table I lists forging averages, whether or not one may add forgings to obtain heat values for multi-forging heats, heat averages, and the sum of the square for each heat. Only the forging averages are reported in Table I, as it is felt that by reporting the sum of the squares and the degrees of freedom, it would be possible to estimate the individual observations. In almost all instances, there are three specimens per forging. From Table I, the test variation (S_e^2) and the forging-to-forging variation (S_F^2) are found as follows:

$$S_e^2 = \frac{\Sigma\Sigma (X-\bar{X}_F)^2}{\Sigma df_i} = \frac{600.48}{192} = 3.13 \text{ ksi}^2$$

$$S_F^2 = \frac{\Sigma\Sigma (\bar{X}_F-\bar{X}_H)^2}{\Sigma df_f} = \frac{127.60}{46} = 2.77 \text{ ksi}^2$$

Before adding multi-forging heats to obtain an estimate of the population mean, use Bartlett's test and ANOVA test to determine if the heats are from the same population. The Bartlett's test and ANOVA test are found in Tables II and III, respectively, but the results are summarized below:

Bartlett's Test

$$F_{calc} = 0.83, \quad F_{tab} = F_{.05}(23, 426) = 1.66$$

Appendix E

ANOVA Test

$$F_{calc} = 1.09, \quad F_{tab} = F_{.05}(23,46) = 2.00$$

Because $F_{calc} < F_{tab}$, there is no reason to assume that the multi-forging heats are not from the same population. In order to determine if the single forging heats may be added to the multi-forging heats, without biasing the results, compare $\bar{X}_{MF}$ with $\bar{X}_{SF}$ and S^2_{MF} and S^2_{SF}, see Table IV. The results from Table IV are summarized below:

(F) Test

$$F_{calc} = 2.89, \quad F_{tab} = F_{.05}(26,23) = 2.28$$

Since $F_{calc} > F_{tab}$, there is a significant difference at the 0.05 level of significance. But the standard error is unusually small as indicated by the fact that 50 percent of the multi-forging heats is less than one; therefore, from an engineering viewpoint, the statistical significance is not practically meaningful, and the variance will be considered equal.

(t) Test

$$t_{calc} = 0.82, \quad t_{tab} = t_{.05}(49) = 2.01$$

Because $t_{calc} < t_{tab}$, the two subpopulations represented by the multi-forging heats and the single forging heats are equal. The average of the heat means is determined from Table IV as follows:

$$\bar{X}_T = \frac{\Sigma \bar{X}_H}{n_H} = \frac{8853.3}{51} = 173.6 \text{ ksi}$$

The heat-to-heat variation (S^2_H) is determined by:

$$S^2_H = \frac{347.99}{51-1} = 6.96 \text{ (ksi)}^2$$

Appendix E

The best estimate of the population mean ($\bar{X}_p$) and the standard deviation (S_o) are determined by plotting all of the observations. From Figure 4 of the text, $\bar{X}_p$ = 173.8 ksi and S_o = 2.7 ksi.

2. Yield Strength at 0.2% Offset

Table V lists forging averages, whether or not one may add forgings to obtain heat values for multi-forging heats, heat averages, and the sum of the squares for each heat. From Table V, the test variation (S_e^2) and the forging-to-forging variation (S_F^2) are found as follows:

$$S_e^2 = \frac{792.58}{192} = 4.13 \text{ ksi}^2$$

$$S_F^2 = \frac{155.09}{42} = 3.59 \text{ ksi}^2$$

Before adding multi-forging heats to obtain an estimate of the population mean, use Bartlett's test and ANOVA test to determine if the heats are from the same population. The Bartlett's test and ANOVA test are found in Tables VI and VII, respectively.

Bartlett's Test

$$F_{calc} = 0.86, \quad F_{tab} = F_{.05}\ (21, 400) = 1.69$$

ANOVA Test

$$F_{calc} = 1.36, \quad F_{tab} = F_{.05}\ (21, 42) = 2.05$$

Since $F_{calc} < F_{tab}$, there is no reason to assume that the multi-forging heats are not from the same population. In order to determine if the single-forging heats may be added to the multi-forging heats, without biasing the results,

one must compare $\bar{X}_{MF}$ with $\bar{X}_{SF}$ and S^2_{MF} with S^2_{SF}, see Table VIII. The results of Table VIII are summarized below:

(F) Test

$$F_{calc} = \frac{12.00}{4.99} = 2.41, \quad F_{tab} = F_{.05}(31, 21) = 2.30$$

Since $F_{calc} > F_{tab}$, there is a significant difference at the 0.05 level of significance. But the standard error is unusually small as indicated by the fact that 40 percent of the multi-forging heats are less than one; therefore, from an engineering standpoint, the statistical significance is not practically meaningful, and the variance with be considered equal.

(t) Test

$$t_{calc} = 0.48, \quad t_{tab} = t_{.05}(52) = 2.00$$

Because $t_{calc} < t_{tab}$, the two subpopulations represented by the multi-forging heats and the single forging heats are equal. The average of the heat means is determined from Table VIII as follows:

$$\bar{X}_T = \frac{\Sigma \bar{X}_H}{n_H} = \frac{8802.5}{54} = 163.0 \text{ ksi}$$

The heat-to-heat variation (S^2_H) is determined by

$$S^2_H = \frac{470.30}{54-1} = 8.87 \text{ ksi}^2$$

The best estimate of the population mean $\bar{X}_P$ and standard deviation (S_o) are determined by plotting all of the observations on probability paper. As may be observed in Figure 4 of the text, the data does not exhibit a normal distribution. It is apparent from Figure 4 that the data exhibits two populations, but the reason is unknown. The data was plotted on log-normal paper but there still existed two populations. A best line was drawn through the data points and it was assumed that the data was normal, $\bar{X}_P = 162.4$ ksi and $S_o = 3.4$ ksi.

3. Percent Elongation (4D)

Table IX lists forging averages, whether or not one may add forgings to obtain heat values for multi-forging heats, heat averages, and the sum of the squares for each heat. From Table IX the test variation (S_e^2) and the forging-to-forging variation (S_F^2) are found as follows:

$$S_e^2 = \frac{123.50}{191} = 0.65$$

$$S_F^2 = \frac{22.42}{47} = 0.48$$

Before adding multi-forging heats to obtain an estimate of the population mean, use Bartlett's test and ANOVA test to determine if the heats are from the same population. The bartlett's test and ANOVA test are found in Table X and XI, respectively, but the results are summarized below:

Bartlett's Test

$$F_{calc} = 1.07, \quad F_{tab} = F_{.05}(23, 572) = 1.66$$

ANOVA Test

$$F_{calc} = 1.08, \quad F_{tab} = F_{.05}(23, 47) = 1.97$$

Because $F_{calc} < F_{tab}$, there is no reason to assume that the multi-forging heats are not from the same population. In order to determine if the single forging heats may be added to the multi-forging heats, without biasing the results, one must compare $\bar{X}_{MF}$ with $\bar{X}_{SF}$ and S_{MF}^2 with S_{SF}^2, see Table XII. The results of Table XII are summarized below:

Appendix E

(F) Test

$$F_{calc} = 5.29, \quad F_{tab} = F_{.05}\ (24, 23) = 3.02$$

Since $F_{calc} > F_{tab}$, some of the single forging heats will be segregated into homogeneous lots until $F_{calc} < F_{tab}$.

Segregating heats 1968, 2169, 2204, and 2479 from the balance of the heats.

(F) Test

$$F_{calc} = 2.21, \quad F_{tab} = F_{.05}\ (20, 22) = 2.39$$

(t) Test

$$t_{calc} = 1.33, \quad t_{tab} = t_{.05}\ (43) = 2.02$$

Because $t_{calc} < t_{tab}$, the two subpopulations represented by the multi-forging heats and the single forging heats are equal. The average of the heat means is determined from Table XII.

$$\bar{X}_t = \sum \bar{X}_H / n_H = \frac{600.1}{45} = 13.3\% \text{ elongation}$$

The heat-to-heat variance is determined by

$$S_H^2 = \frac{25.66}{45-1} = 0.58\ (\% \text{ elongation})^2$$

The best estimate of the population mean $\bar{X}_p$ and standard deviation (S_o) are determined by plotting all of the observations on probability paper. From Figure 4, of the text, $\bar{X}_p = 13.2\%$ El. and $S_o = 1.1\%$ El.

C. ELEVATED TEMPERATURE TENSILE DATA

The elevated temperature tensile results were obtained from 1/4-in. round tensile specimens tested at one laboratory. The data for each temperature is plotted on probability paper and the mean and range are transferred to stress-versus-temperature plots. The object of the stress-versus-temperature plots is to obtain working curves and then develop the percentage curve for input to Mil-Hdbk-5.

The specimens were tested at 150°F, 200°F, 250°F, 280°F, and 330°F and the results are listed in Appendix A, Table I.

1. Ultimate Tensile Strength

Probability curves were plotted utilizing the data from Appendix A, Table I (see Figure 5 of the text). The minimum value and the mean for each temperature were taken from Appendix A, Table I, and from Figure 5 of the text, respectively, and plotted on Figure 4A. A working curve is then constructed in Figure 4A "in such a manner that, except at room temperature, it lies not higher than a best smooth curve drawn through the averages at each temperature nor higher than 5 percent above a smooth curve drawn through the minimum boundary of individually plotted points."(4) The value to be used at room temperature is always the mean. To develop the percentage curve from Figure 4A, one converts the values on Figure 4A to percentages of the room temperature mean, see Figure 8 of the text. Figure 8 is the plot to be submitted for input to Mil-Hdbk-5.

(4) D. P. Moon and W. S. Hyler, Mil-Hdbk-5, Guidelines for the Presentation of Data, Air Force Material Laboratory Technical Report, AFML-TR-66-386, February 1967.

2. Yield Strength

Probability curves were plotted utilizing the data from Appendix A, Table I (see Figure 6 of the text). The minimum value and the mean for each temperature were taken from Appendix A, Table I, and Figure 6 of the text, respectively, and plotted on Figure 4B. The working curve in Figure 4B is constructed in the same manner as for the ultimate tensile strength in Figure 4A. To develop the percentage curve from Figure 4B, one converts the values in Figure 4B to percentages of the room temperature mean, see Figure 9 of the text. Figure 9 of the text is the plot to be submitted for input to Mil-Hdbk-5.

3. Percent Elongation

Probability curves were plotted utilizing the data from Appendix A, Table I (see Figure 7 of the text). The mean was recorded from each temperature tested, from Figure 7, and the best smooth curve drawn through the means is located in Figure 10 of the text. Percent elongation values are not converted to percentages of the room-temperature value; therefore, Figure 10 of the text is the curve to be submitted for input to Mil-Hdbk-5.

D. PART-THROUGH-CRACK TENSILE DATA

Evaluation of K_{Ic} Data

The K_{Ic} test data was obtained from PTC specimens tested at three laboratories. Each laboratory was analyzed separately and the results compared to each other. Because of the non-uniformity of data for crack intensities of $a/Q \sim 0.02$ and $a/Q \sim 0.04$, the data was analyzed on the basis of $a/Q \sim 0.02$ or $a/Q \sim 0.04$ for each laboratory.

1. Crack Intensity (a/Q) Approximately 0.02

a. Tested at Aerojet-Sacramento

Table XIII lists forging averages, whether or not one may add forgings to obtain heat values for multi-forging heats, heat averages, and the sum of the square for each heat. Only the forging averages are reported in Table XIII, as it is felt that by reporting the sum of the squares and the degrees of freedom, it would be possible to estimate the individual observations. Originally, there were three specimens per forging, but some observations were discarded when $F_G/F_{ty} > 1.0$, $ao/B > 0.5$ or $Ca/BW > 0.10$. From Table XIII, the test variation (S_e^2) and the forging-to-forging variation (S_F^2) are found as follows:

$$S_e^2 = \frac{\Sigma\Sigma(X-\bar{X}_F)^2}{\Sigma df_i} = \frac{137.97}{84} = 1.64 \text{ (ksi}\sqrt{\text{in.}})^2$$

$$S_F^2 = \frac{\Sigma\Sigma(\bar{X}_F-\bar{X}_H)^2}{\Sigma df} = \frac{9.71}{16} = 0.61 \text{ (ksi}\sqrt{\text{in.}})^2$$

Before adding multi-forging heats to obtain an estimate of the population mean, use Bartlett's test and ANOVA test to

determine if the heats are from the same population. The Bartlett's test and ANOVA test are found in Table XIV and XV, respectively, but the results are summarized below:

Bartlett's Test

$$F_{calc} = 1.12, \quad F_{tab} = F_{.05}(11, 135) = 2.10$$

ANOVA Test

$$F_{calc} = 3.16, \quad F_{tab} = F_{.05}(11, 16) = 2.94$$

Since $F_{calc} > F_{tab}$, there is a significant difference at the 0.05 level of significance. But the inherent error is unusually small that from an engineering standpoint, the statistical significance is not practically meaningful and the means will be considered equal. In order to determine if the single forging heats may be added to the multi-forging heats without biasing the results, one must compare $\bar{X}_{MF}$ with $\bar{X}_{SF}$ and S^2_{MF} with S^2_{SF}, see Table XVI. The results of Table XVI are summarized below:

(F) Test

$$F_{calc} = 2.01, \quad F_{tab} = F_{.05}(13, 11) = 3.40$$

(t) Test

$$t_{calc} = 1.67, \quad t_{tab} = t_{.05}(14 + 12-2) = 2.06$$

Because $t_{calc} < t_{tab}$, there is no reason to conclude that the subpopulation represented by single forging heats and multi-forging heats do not belong to the same population. The average of the heat means is determined from Table XVI as follows:

$$\bar{X}_T = \frac{\sum \bar{X}_H}{n_H} = \frac{1014.4}{26} = 39.0 \text{ ksi}\sqrt{\text{in.}}$$

The heat-to-heat variation is determined by

$$S_H^2 = \frac{\Sigma(\bar{X}_H - \bar{X}_T)}{\Sigma df_H} = \frac{38.58}{26-1} = 1.54 \ (\text{ksi}\sqrt{\text{in.}})^2$$

The best estimate of the population mean (X_L) and standard deviation (S_L) for one laboratory, are determined by plotting all of the observations on probability paper. From Figure 11 of the text.

$$\bar{X}_L = 38.3 \text{ ksi}\sqrt{\text{in.}} \text{ and } S_L^2 = 2.89 \text{ ksi in.}$$

b. Tested at Aerojet-Downey

Table XVII lists forging averages, whether or not one may add forgings to obtain heat values for multi-forging heats, heat averages, and the sum of the squares for each heat. From Table XVII, the test variation (S_e^2) and the forging-to-forging variation (S_F^2) are found as follows:

$$S_e^2 = \frac{\Sigma\Sigma(X - \bar{X}_F)^2}{\Sigma df_i} = \frac{37.23}{41} = 0.91$$

$$S_F^2 = \frac{\Sigma\Sigma(\bar{X}_F - \bar{X}_H)^2}{\Sigma df} = \frac{13.00}{15} = 0.87$$

Before adding multi-forging heats to obtain an estimate of the population mean, use Bartlett's test and ANOVA to determine if the heats are from the same population. The Bartlett test and ANOVA test

are found in Table XVIII and XIX respectively, but the results are summarized below:

Bartlett's Test

$$F_{calc} = 0.56, \quad F_{tab} = 2.41$$

ANOVA Test

$$F_{calc} = 5.46, \quad F_{tab} = 3.41$$

Since $F_{calc} > F_{tab}$, there is a significant difference at the 0.05 level of significance. But the inherent error is unusually small that from an engineering standpoint, the statistical significance is not practically meaningful, and the means will be considered equal. If the heats had SS comparable to the average, than $F_{calc} < F_{tab}$; therefore, it is assumed that the heats are from the same population.

In order to determine if the single forging heats may be added to the multi-forging heats without biasing the results, one must compare $\bar{X}_{MF}$ with $\bar{X}_{SF}$ and S^2_{MF} with S^2_{SF}, see Table XX. The results of Table XX are summarized below.

(F) Test

$$F_{calc} = 2.21, \quad F_{tab} = F_{.05}(4, 6) = 6.23$$

(t) Test

$$t_{calc} = 0.34, \quad t_{tab} = t_{.05}(7 + 5 - 2) = 2.23$$

There is no reason to assume that the subpopulations represented by single forging heats and multi-forging heats do not belong to the same population. The mean of the heat means is determined from Table XX as follows:

$$\bar{X}_T = \frac{\sum \bar{X}_H}{n_H} = \frac{492.4}{12} = 40.6 \text{ ksi}\sqrt{\text{in.}}$$

The heat-to-heat variance is determined by

$$S_H^2 = \frac{\Sigma(\bar{X}_H - \bar{X}_T)}{\Sigma df_n} = \frac{23.90}{12-1} \quad 2.17 \text{ ksi}^2\text{-in.}$$

The best estimate of the population mean ($\bar{X}_L$) and standard deviation (S_L), from one laboratory, are determined by plotting all of the observations on probability paper. From Figure 11 of the text, $\bar{X}_L$ = 40.1 ksi$\sqrt{\text{in.}}$ and S_L^2 = 2.25 ksi^2-in.

c. Tested at Lycoming

Table XXI lists forging averages, whether or not one may add forging to obtain heat values for multi-forging heats, heat averages, and the sum of the squares for each heat. From Table XXI the test variation (S_e^2) and the forging-to-forging variation (S_F^2) are found as follows:

$$S_e^2 = \frac{\Sigma\Sigma(X - \bar{X}_F)^2}{\Sigma df_i} = \frac{47.87}{59} = 0.81$$

$$S_F^2 = \frac{\Sigma\Sigma(\bar{X}_F - \bar{X}_H)^2}{\Sigma df} = \frac{12.00}{19} = 0.63$$

Before adding multi-forging heats to obtain an estimate of the population mean, use Bartlett's test and ANOVA test to determine if the heats are from the same population. The Bartlett test and ANOVA test are found in Tables XXII and XXIII, respectively, but the results are summarized below.

Appendix E

Bartlett's Test

$$F_{calc} = 1.56, \qquad F_{tab} = 2.29$$

ANOVA Test

$$F_{calc} = 1.57, \qquad F_{tab} = 3.05$$

There is no reason to assume that the multi-forging heats are not from the same population. To determine if the single forging heats may be added to the multi-forging heats without biasing the results, one must compare $\bar{X}_{MF}$ and $\bar{X}_{MF}$ with S^2_{MF} and S^2_{SF}, see Table XXIV. The results of Table XXIV are summarized below:

(F) Test

$$F_{calc} = 3.80, \qquad F_{tab} = 39.4$$

(t) Test

$$t_{calc} = 1.58, \qquad t_{tab} = 2.26$$

There is no reason to assume that the subpopulation represented by single forging heats and multi-forging heats do not belong to the same population. The average of the heat means is determined from Table XXIV as follows:

$$\bar{X}_T = \frac{\sum \bar{X}_H}{n_H} = \frac{439.5}{11} = 40.0 \text{ ksi } \sqrt{\text{in.}}$$

The heat-to-heat variation is determined by

$$S^2_H = \frac{\Sigma(\bar{X}_H - \bar{X}_T)}{\Sigma df_i} = \frac{3.81}{11-1} = 0.38 \text{ ksi}^2\text{-in.}$$

Appendix E

The best estimate of the population mean ($\bar{X}_L$) and standard deviation (S_L), from one laboratory, are determined by plotting all of the observations from acceptable heats on probability paper. From Figure 11 of the text, $\bar{X}_L$ = 39.9 ksi $\sqrt{in.}$ and S_L = 1.2 ksi $\sqrt{in.}$

d. Comparison of the Data Collected at Each Laboratory

In order to determine if the means of each laboratory are equal, it must first be proven that the standard deviations are homogeneous by using Bartlett's test. The information used in this test came from Figure 11 of the text.

Laboratory	$(\bar{X}-\bar{\bar{X}})^2$	df_i	S_L^2	$\ln S_L^2$	$df_i \ln S_L^2$	$1/df_i$
Sacramento	364.14	126	2.89	1.061	133.686	0.00793
Downey	150.75	67	2.25	0.811	54.337	0.01494
Lycoming	126.72	88	1.44	0.365	32.120	0.01137
	641.61	281			220.143	0.03424

$$S_p^2 = \frac{641.61}{281} = 2.28 \quad M = 281\,(0.824) - 220.143 = 11.40$$

$$\nu_1 = 2,\ a = \frac{1}{(3)(2)}\left(0.03424 - \frac{1}{281}\right) = 0.000511,\ \nu_2 = \frac{4}{(5.11 \times 10^{-2})} = 1.53 \times 10^5$$

$$b = \frac{1.53 \times 10^5}{1 + 2/1.66 \times 10^5 - 0.00491} = 1.54 \times 10^5$$

$$F_{calc} = \frac{1.53 \times 10^5\,(11.4)}{2(1.54 \times 10^5 - 11.4)} = \frac{17.44 \times 10^5}{3.08 \times 10^5} = 5.66$$

$$F_{tab} = F_{p\,5}\ (2,\ 00) = 3.69$$

Appendix E

Statistically, there is a significant difference at the 0.5 level of significance. But the standard error is unusually small, for Lycoming, that from an engineering standpoint, the statistical significance is not practically meaningful, and the variance will be considered equal. Assuming the standard deviations are homogeneous, test the laboratory means by ANOVA to determine if they are from the same population.

ANCVA Test

Sacramento		Downey		Lycoming		
$\bar{X}_H$	X^2	$\bar{X}_H$	X^2	$\bar{X}_H$	X^2	
36.4	1325.0	40.5	1640.2	39.4	1552.4	
39.2	1536.6	39.7	1576.1	39.3	1554.5	
38.4	1474.6	41.9	1755.6	39.9	1592.0	
38.8	1505.4	39.5	1560.2	39.8	1584.0	
39.6	1568.2	39.4	1552.4	40.7	1656.5	
39.3	1544.5	42.2	1780.3	40.5	1640.2	
38.4	1474.6	42.6	1814.8	40.8	1664.6	
40.2	1616.0	37.6	1413.8	40.7	1656.5	
38.6	1490.0	41.0	1681.0	39.4	1552.4	
37.8	1428.8	42.7	1823.3	39.2	1536.6	
38.2	1459.2	41.0	1681.0	39.8	1584.0	
38.0	1444.0	39.9	1592.0			
38.8	1505.4					
41.6	1730.6					
38.4	1474.6					
40.2	1616.0					
40.8	1664.6					
39.1	1528.8					
40.4	1632.2					
40.6	1648.4					
40.5	1640.2					
38.7	1497.7					
36.9	1361.6					
39.1	1528.8					
37.0	1369.0					
39.4	1552.4					
						Total
n 26		12		11		49
df(n-1) 25		11		10		46

Appendix E

Calculations for the inherent error are as follows:

ΣX	1014.4	488.0	439.5	1941.9
$(\Sigma X)^2$	1029007.4	238144.0	193160.2	
$(\Sigma X^2$	39617.2	19871.2	17563.7	77052.1
$(\Sigma X)^2/n$	39577.2	19845.3	17560.0	
$SS = \Sigma X^2 - (\Sigma X)^2/n$				
SS	40.0	25.9	3.7	69.6

The inherent error SS = 69.6 and the inherent error df = 46

Calculations for the total error are as follows:

$$N = \frac{\sum_{i=1}^{K} n}{} = 49 \qquad \Sigma X^2 = 77052.1$$

$$\Sigma X = 1941.9 \qquad CF = (\Sigma X)^2/N = \frac{3,770,975.6}{49} = 76958.7$$

$$(\Sigma X)^2 = 3770975.6 \qquad \text{Total SS} = \Sigma X^2 - CF = 93.4$$

Calculations for the between error are as follows:

The between laboratory error SS = 93.4 - 69.6 = 23.8

The between laboratory df = 3-1 = 2

The between laboratory mean square = $\frac{23.8}{2} = 11.9$

The inherent error means square = $\frac{69.6}{46} = 1.51$

$$F_{calc} = \frac{11.9}{1.51} = 7.88, \qquad F_{tab} = F_{.05}(2, 46) = 4.01$$

Since $F_{calc} > F_{tab}$, there is a significant difference between the laboratories at the 0.05 level of significance. Because of the apparent differences between the laboratories an attempt was made to determine the reason; the test results for each laboratory, from Figure 11 of the text, are listed below.

Appendix E

	$\bar{X}$ ksi $\sqrt{\text{in.}}$	S_L^2 $(\text{ksi}\sqrt{\text{in.}})^2$	
Sacramento	38.3	2.89	126
Downey	40.1	2.25	68
Lycoming	39.9	1.44	89

Comparing results from Sacramento and Downey

(t) Test

$$U = 40.1 - 38.3 = 1.8$$

$$S_p = \sqrt{\frac{126\,(2.89) + 67\,(2.28)}{126 + 68}} = 1.64$$

$$\sqrt{\frac{n_1 + n_2}{n_1 + n_2}} = \sqrt{\frac{196}{8763}} = 0.15$$

$$t_{calc} = \frac{8}{1.64\,(0.15)} = 7.32, \quad t_{tab} = t_{.05}\,(194) = 1.96$$

Since $t_{calc} > t_{tab}$, there is a significant difference between the two means.

Comparing results from Downey and Lycoming

$$U = 40.1 - 39.9 = 0.2$$

$$S_p = \sqrt{\frac{67\,(2.25 + 88\,(1.44)}{68 + 89 - 2}} = \sqrt{\frac{277.47}{155}} = 1.34$$

$$\sqrt{\frac{n_1 + n_2}{n_1 + n_2}} = \sqrt{\frac{157}{6052}} = 161$$

$$t_{calc} = \frac{0.2}{(1.34)(0.16)} = 0.93, \quad t_{tab} = t_{.05}(155) = 1.96$$

Because $t_{calc} < t_{tab}$, there is no reason to assume that the subpopulation represented by Downey and Lycoming are not from the same population.

The subpopulation represented by Sacramento did not appear to belong to the same population as did Downey and Lycoming. But the reason may be that Sacramento tested more forgings and twice as many heats as Downey or Lycoming. There were several forgings that were tested by all three laboratories, and will be used as further evidence of the applicability of using Sacramento data, see Table XXV. The results of Table XXV are summarized below:

Sacramento vs Downey

Forging	F_{calc}	F_{tab}	t_{calc}	t_{tab}
69B	5.27	39.00	0.49	2.78
70A	1.29	799.50	4.39	3.18
70B	2.04	39.00	1.06	2.78
71A	1.22	39.00	3.89(1)	2.78

(1) The standard deviations are quite small, being 0.44 and 0.36.

Sacramento vs Lycoming

63A	5.06	39.00	2.29	2.78
63B	3.98	39.00	0.99	2.78
69A	14.58	39.00	2.00	2.78

Appendix E

Of the seven sets of forgings tested at more than one laboratory, only for forging 70A does the $t_{calc} > t_{tab}$. With this in mind, it was decided to pool all of the observations from all of the laboratories in order to obtain the best estimate of the population mean ($\bar{X}_p$). The pooled data was plotted on probability paper, see Figure 11 in text, and the best estimate of the population mean and the standard deviation are $\bar{X}_p$ = 39.1 ksi $\sqrt{in.}$ and S_o = 1.6 ksi $\sqrt{in.}$, respectively.

The laboratory-to laboratory variation (S_T^2) is determined as follows:

Test Laboratory	$\bar{X}_L$	$(\bar{X}_L - \bar{X}_{LM})^2$
Sacramento	38.3	1.21
Downey	40.1	0.49
Lycoming	39.9	0.25
	118.3	1.95

$$\bar{X}_{LM} = 39.4 \text{ ksi } \sqrt{in.} \quad S_{LM}^2 = \frac{1.95}{2} = 1.0 (\text{ksi } \sqrt{in})^2$$

$\bar{X}_{LM}$ is unweighted since the value of each laboratory mean ($\bar{X}_L$) is the best estimate for that laboratory.

2. Crack Intensity (a/Q) Approximately 0.04

a. Tested at Aerojet-Sacramento

The data was plotted on probability paper, and as seen in Figure 12 of the text, there appears to be two populations. Even though the data appeared to be made up of two populations, an attempt was made to treat the data as being from a single population.

Appendix E

Table XXVI, Appendix D, lists forging averages, whether or not one may add forgings to obtain heat values for multi-forging heats, heat averages, and the sum of the squares for each heat. From Table XXVI the test variation (S_e^2) and the forging-to-forging variation (S_F^2) are found as follows:

$$S_e^2 = \frac{\Sigma\Sigma (X-\bar{X}_F)^2}{\Sigma df_i} = 6.37 \text{ ksi}^2\text{-in.}$$

$$S_F^2 = \frac{\Sigma\Sigma (\bar{X}_F-\bar{X}_H)^2}{\Sigma df} = 1.98 \text{ ksi}^2\text{-in.}$$

Before adding multi-forging heats to obtain an estimate of the population mean, use Bartlett's test and ANOVA test to determine if the heats are from the same population. The Bartlett test and ANOVA test are found in Tables XXVII and XXVIII, Appendix D, respectively, but the results are summarized below:

Bartlett's Test

$F_{calc} = 1.17, \quad F_{tab} = 2.26$

ANOVA Test

$F_{calc} = 10.0, \quad F_{tab} = 3.44$

Statistically, there is a significant difference and it would require segregating half of the heats in order to get $F_{calc} < F_{tab}$. Therefore, the analysis of this data will not be continued.

b. Tested at Aerojet-Downey

The data was plotted on probability paper and, as seen in Figure 12 of the text, there appears to be two populations. It is interesting to note that the plot is very similar to that for Sacramento. Even though the data appeared to consist of two populations, an attempt was made to treat the data as being from a single population.

Table XXIX lists forging averages, whether or not one may add forgings to obtain heat values for multi-forging heats, heat averages, and the sum of the squares for each heat. From Table XXIX, the test variation (S_e^2) and the forging-to-forging variation (S_F^2) are found as follows:

$$S_e^2 = \frac{\Sigma\Sigma (X-\bar{X}_F)^2}{\Sigma df_i} = 3.24 \text{ ksi}^2\text{-in.}$$

$$S_F^2 = \frac{\Sigma\Sigma (\bar{X}_F-\bar{X}_H)^2}{\Sigma df} = 2.77 \text{ ksi}^2\text{-in.}$$

Before adding multi-forging heats to obtain an estimate of the population mean, one must use Bartlett's test and ANOVA test to determine if the heats are from the same population. The Bartlett test and ANOVA test are found in Tables XXX and XXXI, respectively, but the results are summarized below:

Bartlett's Test

$F_{calc} = 1.52, \qquad F_{tab} = 2.41$

ANOVA Test

$F_{calc} = 12.16, \qquad F_{tab} = 3.41$

Statistically, there is a significant difference and it would require segregating almost half of the heats in order to get $F_{calc} < F_{tab}$. Therefore, the analysis of this data is discontinued.

c. Tested at Lycoming

The data was plotted on probability paper and, as seen in Figure 12 of the text, the data exhibits a near normal distribution.

Table XXXII lists forging averages, whether or not one may add forgings to obtain heat values for multi-forging heats, heat averages, and the sum of the square for each heat. From Table XXXII the test variation (S_e^2) and the forging-to-forging variation (S_F^2) are found as follows:

$$S_e^2 = \frac{\Sigma\Sigma (X-\bar{X}_F)^2}{\Sigma df_i} = 2.79 \text{ ksi}^2\text{-in.}$$

$$S_F^2 = \frac{\Sigma\Sigma (\bar{X}_F-\bar{X}_H)^2}{xdf} = 2.09 \text{ ksi}^2\text{-in.}$$

Before adding multi-forging heats to obtain an estimate of the population mean, one must use Bartlett's test and ANOVA test to determine if the heats are from the same population. The Bartlett's test and ANOVA tests are found in Tables XXXIII and XXXIV, respectively, but the results are summarized below:

Bartlett's Test

$F_{calc} = 0.93, \qquad F_{tab} = 2.11$

ANOVA Test

$F_{calc} = 15.0, \qquad F_{tab} = 2.98$

Statistically, there is a significant difference; therefore, the analysis of this data is discontinued.

Since the normality plot and ANOVA results indicated there were two or more populations, there must be a metallurgical or mechanical reason for it. An attempt was made to correlate K_{Ic}, for each laboratory, with crack area to cross-sectional area (Ca/BW), crack depth to thickness ratio (a/B), or gross stress to yield stress ratio (F_G/F_{ty}). The data for Ca/BW, a/B, and F_G/F_{ty}, from each test, were plotted on probability paper and there was no apparent relationship between K_{Ic} and Ca/BW or a/B. In Figures 5, 6 and 7 both the K_{Ic} data and the F_G/F_{ty} data are plotted on probability paper and there is an obvious relationship. That there is a relationship is evidenced by the similarity of the inflection points and the corresponding straight lines have a similar change in slope. The data for each figure was divided into subpopulations and the dividing point was the inflection point. For the Lycoming data, the inflection point was almost indistinguishable, but it may be determined by observing the dashed lines in Figure 7. The subpopulations were plotted on probability paper, see Figures 5, 6, and 7 and the results are summarized below:

Test Laboratory	Inflection Point (F_G/F_{ty})	K_{Ic} Ksi- in.	K_{Ic} Ksi- in.
Sacramento	0.58	34.5	40.9
Downey	0.60	36.1	42.1
Lycoming	0.58	34.6	41.1
Pooled Data	0.58	34.6	40.1

In all three instances, the data falling to the left of the inflection point plotted a near normal distribution. The data to the right of the inflection point exhibited a near-normal distribution for Figure 7 and two or more populations for Figures 5 and 6.

The data were pooled for all three laboratories, see Figure 8, and the inflection point is reported in the above table. As observed in Figure 8, there exists one population for $F_G/F_{ty} \leq 0.58$ and two or more populations for $F_G/F_{ty} > 0.58$. The significance of the above observation, at this point, is uncertain.

3. Differences in K_{Ic} That Can be Detected for the Different Crack Areas

To try and obtain a better understanding of what was causing the difficulty in the analysis, all of the data was pooled and analyzed according to $a/Q \sim 0.02$ and $a/Q \sim 0.04$.

Figure 9(a) and (b) are plots of Ca/BW versus K_{Ic} for $a/Q \sim 0.02$ and $a/Q \sim 0.04$, respectively. Observing each figure individually, there appears to be no dependence of K_{Ic} on Ca/BW for a constant a/Q if the small n values are omitted. Comparing the two figures, it is evident that K_{Ic} is not dependent on Ca/BW, even for a changing a/Q, since Figures 6(a) and 6(b) have nearly the same "average" value. It is interesting to note that for $a/Q \sim 0.04$, the data has much more scatter than for $a/Q \sim 0.02$. The increased scatter in K_{Ic} may be a function of Ca/BW, especially since Ca/BW is near the recommended limit of 0.1, or it may be a metallurgical phenomenon due to the crack depth (a).

Figures 10(a) and (b) are plots of K_{Ic} versus a/B for $a/Q \sim 0.02$ and $a/Q \sim 0.04$, respectively. Observing each figure individually, there appears to be no dependence of K_{Ic} on a/B for a constant a/Q. Comparing the two figures, it is evident that K_{Ic} is not dependent on Ca/BW, even for a changing a/Q, since Figures 8(a) and (b) have nearly the same "average" value. It is interesting to note that for $a/Q \sim 0.04$, the data has much more

scatter than for $a/Q \sim 0.02$. The increased scatter in K_{Ic} may be a function of a/B, especially since a/B is near the recommended maximum limit of 0.5, or it may be a metallurgical phenomenon due to the crack depth (a).

Figures 13 and 14 of the text are plots of F_G/F_{ty} versus K_{Ic} for $a/Q \sim 0.02$ and $a/Q \sim 0.04$, respectively. Observing each figure individually, there appears to be considerable dependence of K_{Ic} on F_G/F_{ty} for a constant a/Q. Figure 14 has considerable scatter about K_{Ic} = 40 ksi$\sqrt{in.}$ but there is little scatter about the band of data whose slope equal 0.63 ksi$\sqrt{in.}$ Figure 13 has little scatter about K_{Ic} = 40 ksi $\sqrt{in.}$, but there is more scatter about the band of data whose slope equal 0.34 ksi $\sqrt{in.}$

As observed in Figures 13 and 14, K_{Ic} is clearly a function of F_G/F_{ty} and this dependence increases as F_G/F_{ty} approaches the recommended maximum limit of 1.0.

It is interesting to note that even though it was statistically incorrect to analyze the $a/Q \sim 0.04$ data, that $\bar{X}_p$ is very similar to that of $a/Q \sim 0.02$. Assuming a normal distribution for $a/Q \sim 0.04$, the results are listed as follows:

	ksi $\sqrt{in.}$			
a/Q	X_p	S_o	A_{Basis}	B_{Basis}
0.02	39.1	1.6	34.7	36.3
0.04	38.8	4.8	25.4	30.3

	For a Non-Normal Distribution
	B_{Basis}
0.02	-
0.04	34.9

Even though $\bar{X}_p$ values were similar, the standard deviation was considerably larger for $a/Q \sim 0.04$ than for $a/Q \sim 0.02$. As may be seen in the above table, the large S_o for $a/Q \sim 0.04$ has a tremendous effect on A-Basis and B-Basis. The B-Basis value for $a/Q \sim 0.04$, based on a non-normal distribution, is also listed in the above table. As expected, for the B-Basis the assumed normal distribution yield a very conservative value as compared to the non-normal value. But the non-normal distribution value for $a/Q \sim 0.04$ is very conservative when compared to the normal distribution value for $a/Q \sim 0.02$.

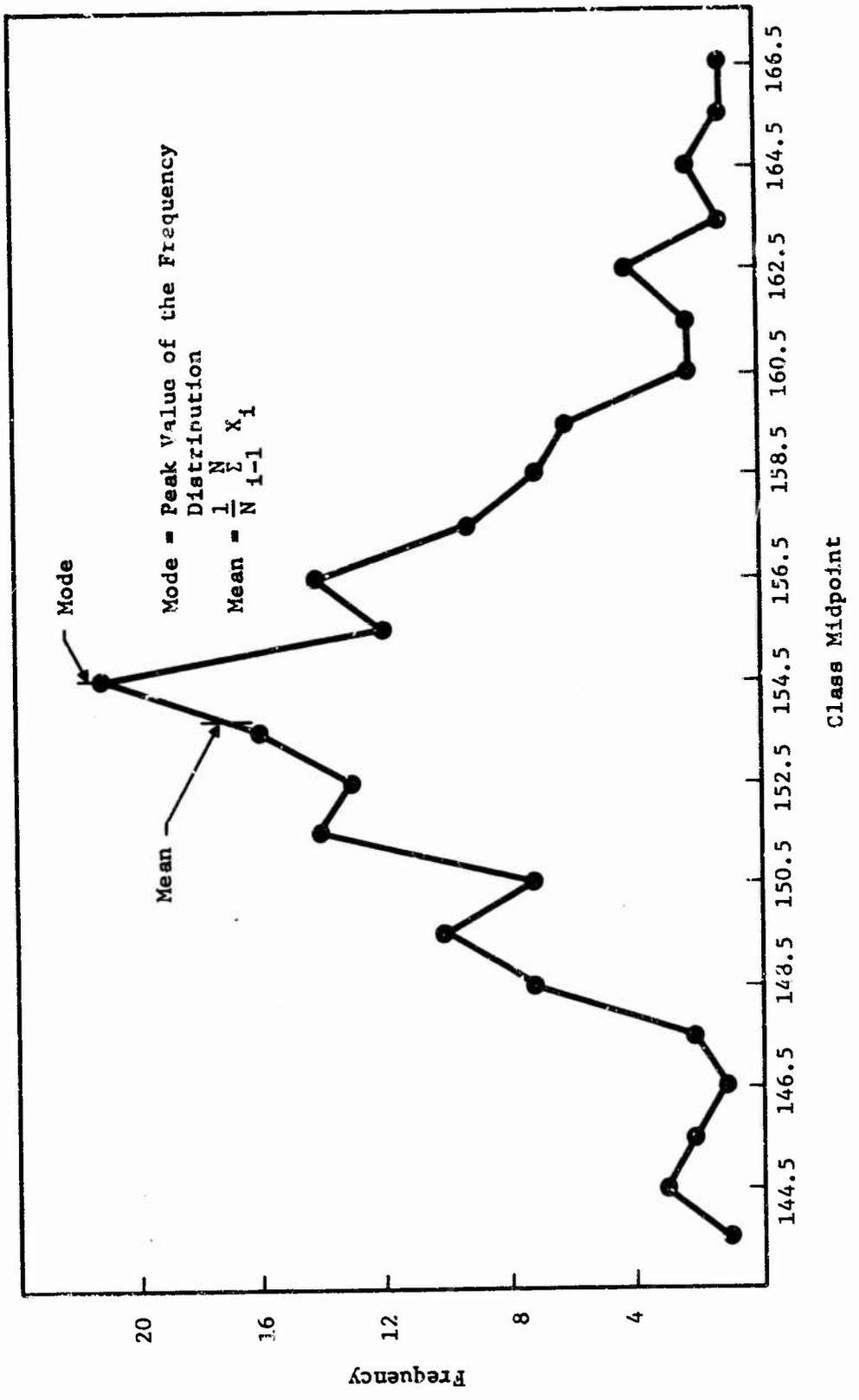


Figure 1. Frequency of Ultimate Tensile Strength Data at 250°F

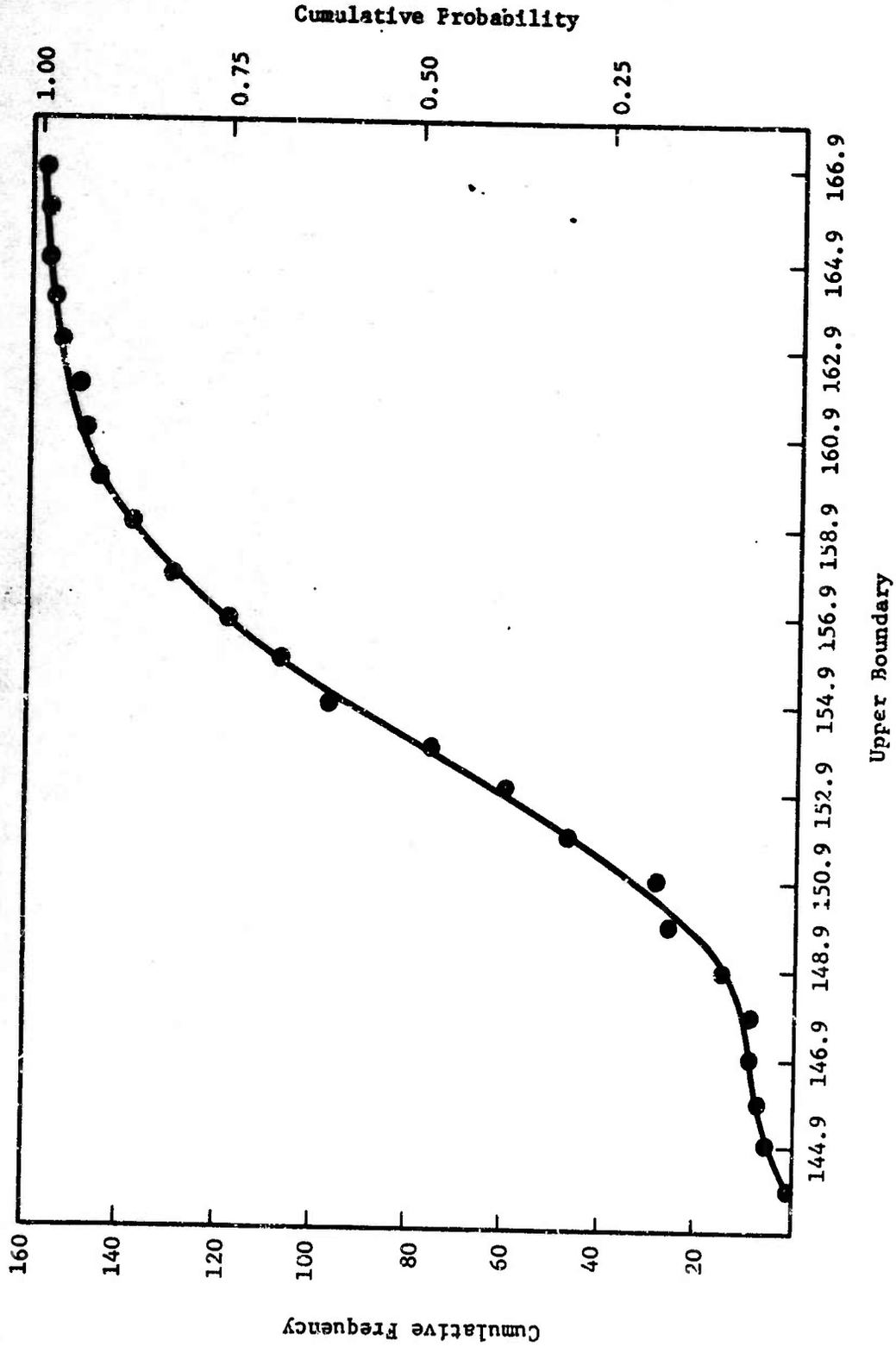


Figure 2. Cumulative Frequency of Ultimate Tensile Strength Data at 250°F

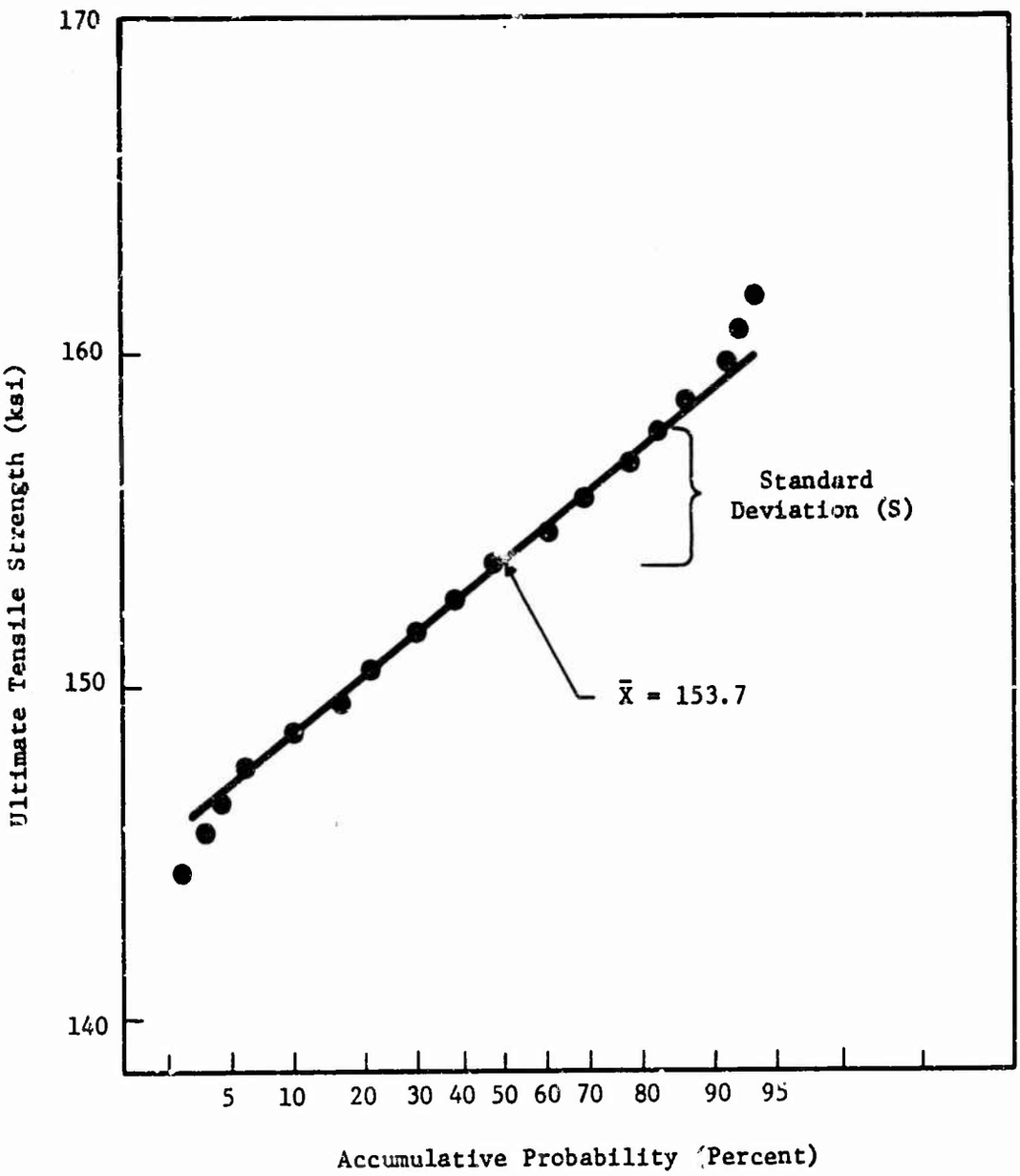


Figure 3. Ultimate Tensile Strength at 250°F vs Probability

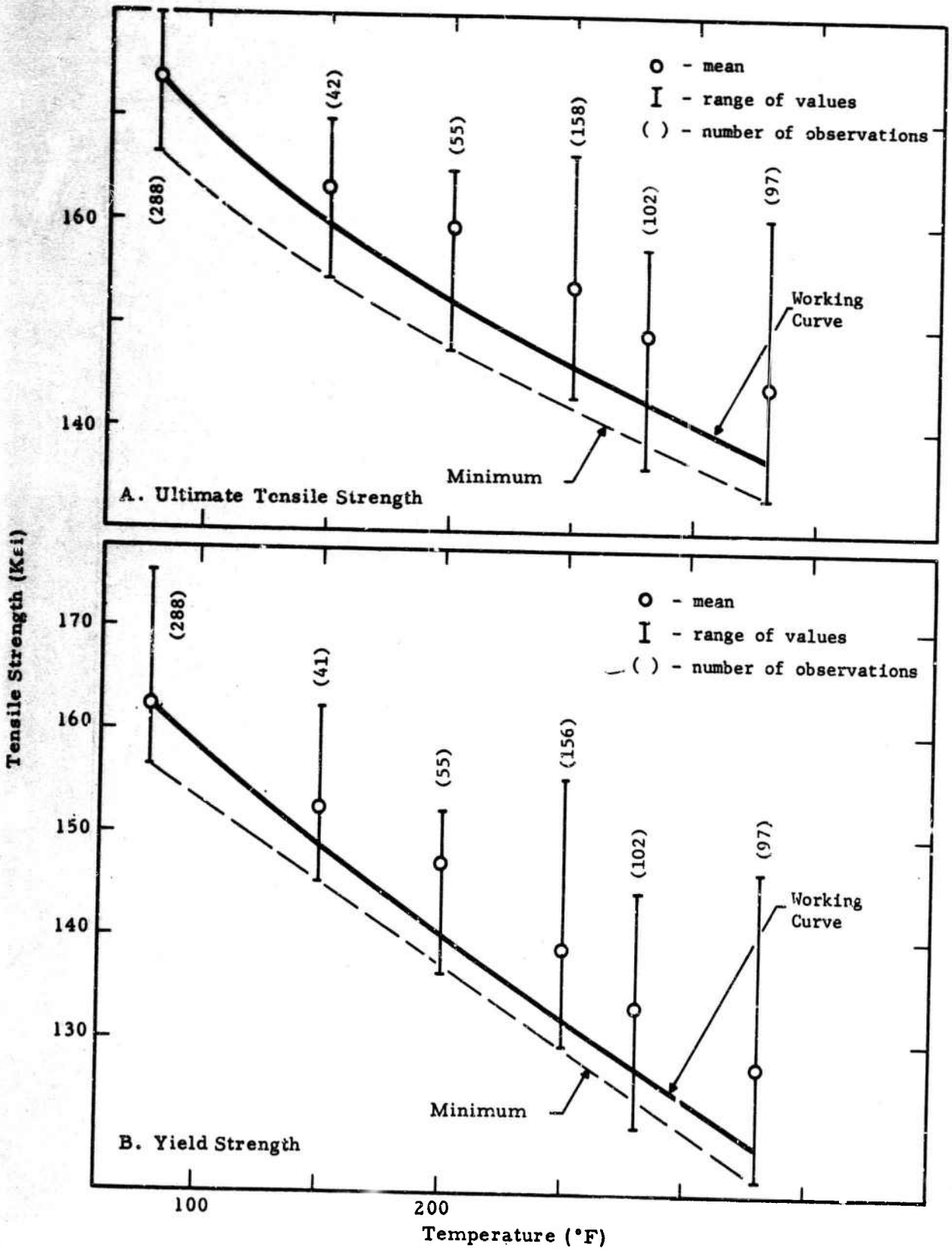


Figure 4. Determination of Working Curve (Ultimate Tensile Strength)

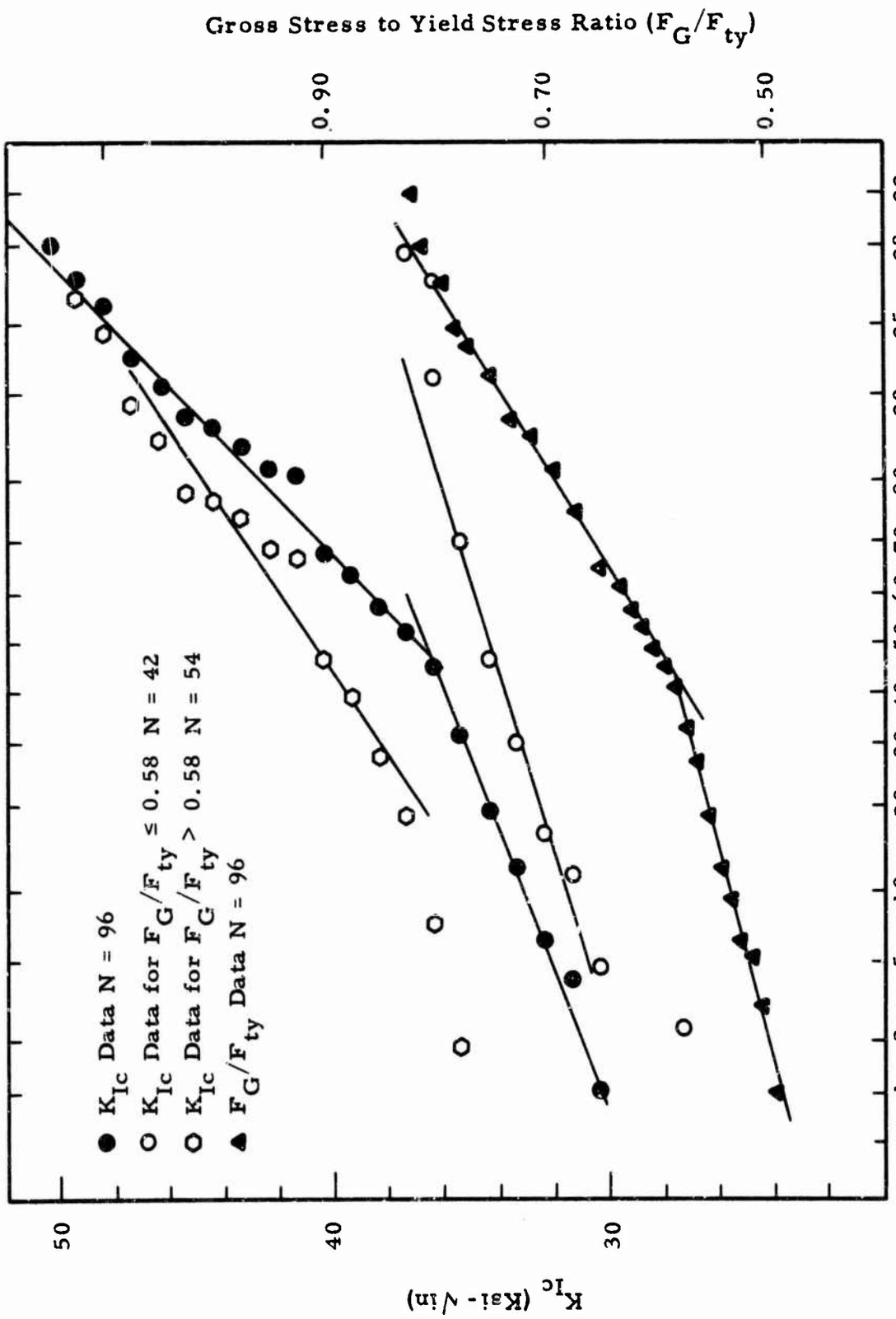


Figure 5. K_{Ic} or F_G/F_{ty} vs Probability for Aerojet-Sacramento (a/Q ~ 0.04)

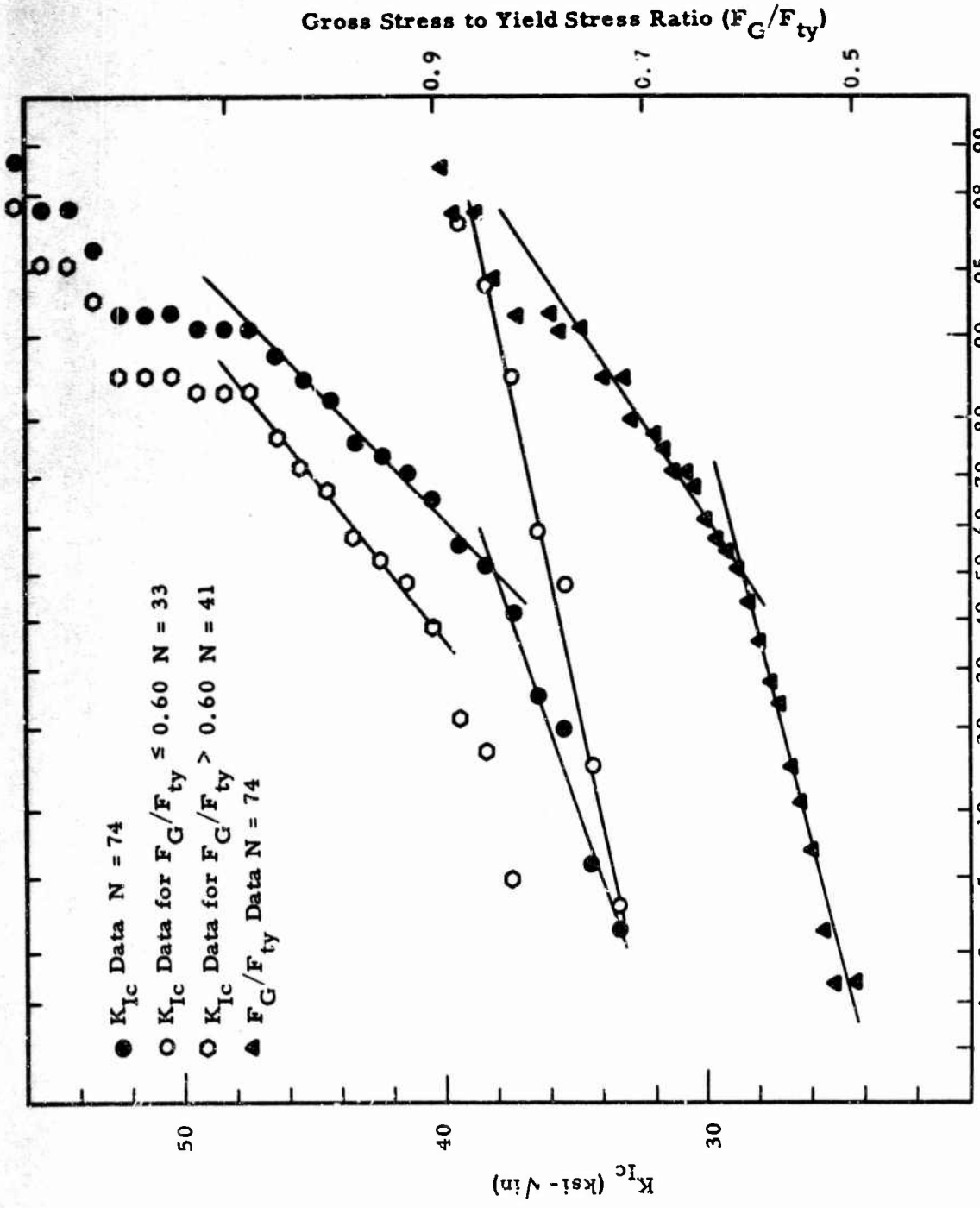


Figure 6. K_{Ic} or F_G/F_{ty} vs Probability for Aerojet-Downey (a/Q ~ 0.04)

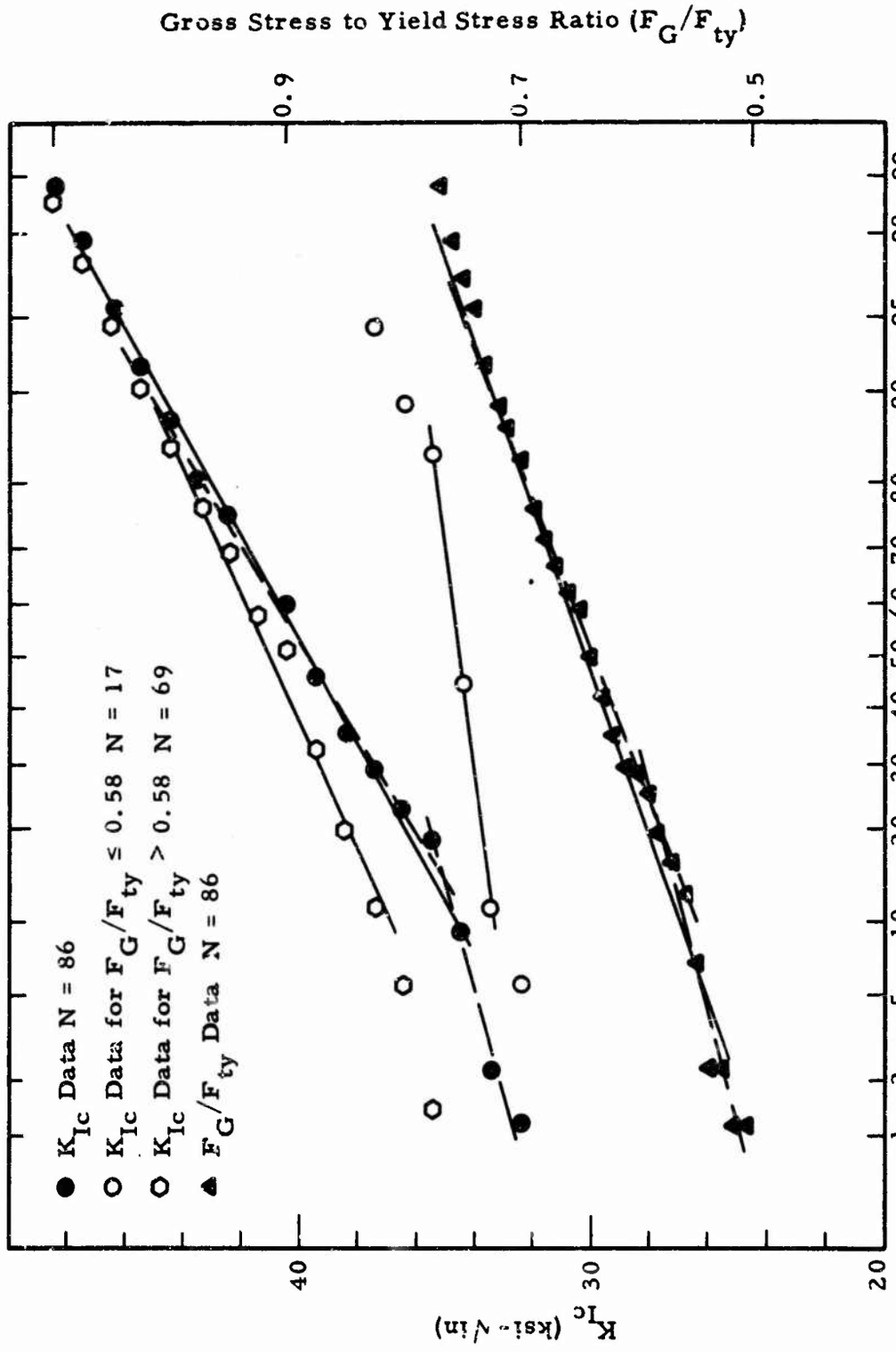


Figure 7. K_{Ic} or F_G/F_{ty} vs Probability for Lycoming (a/Q ∿ 0.04)

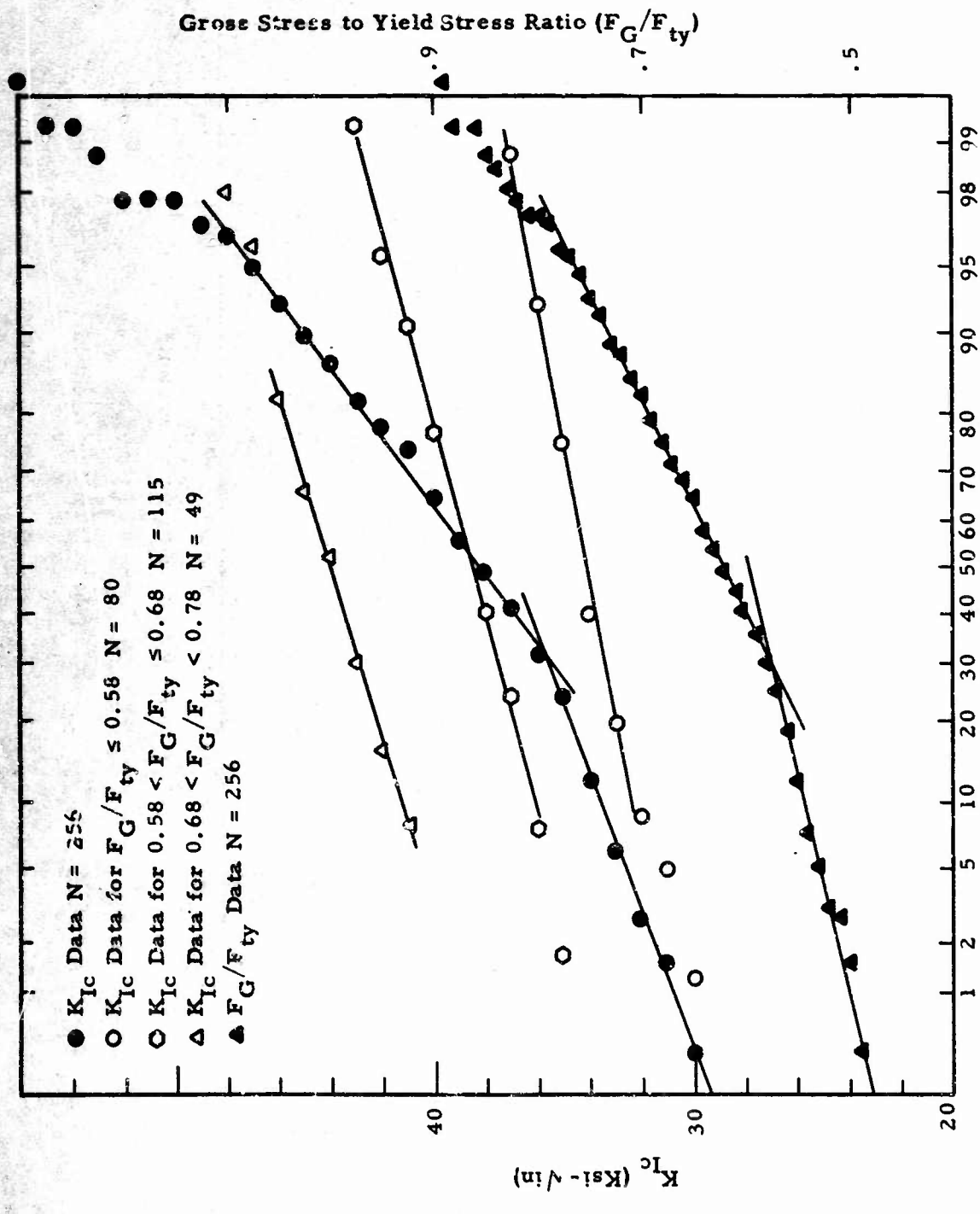


Figure 8. K_{Ic} or F_G/F_{ty} vs Probability for a/Q ~ 0.04

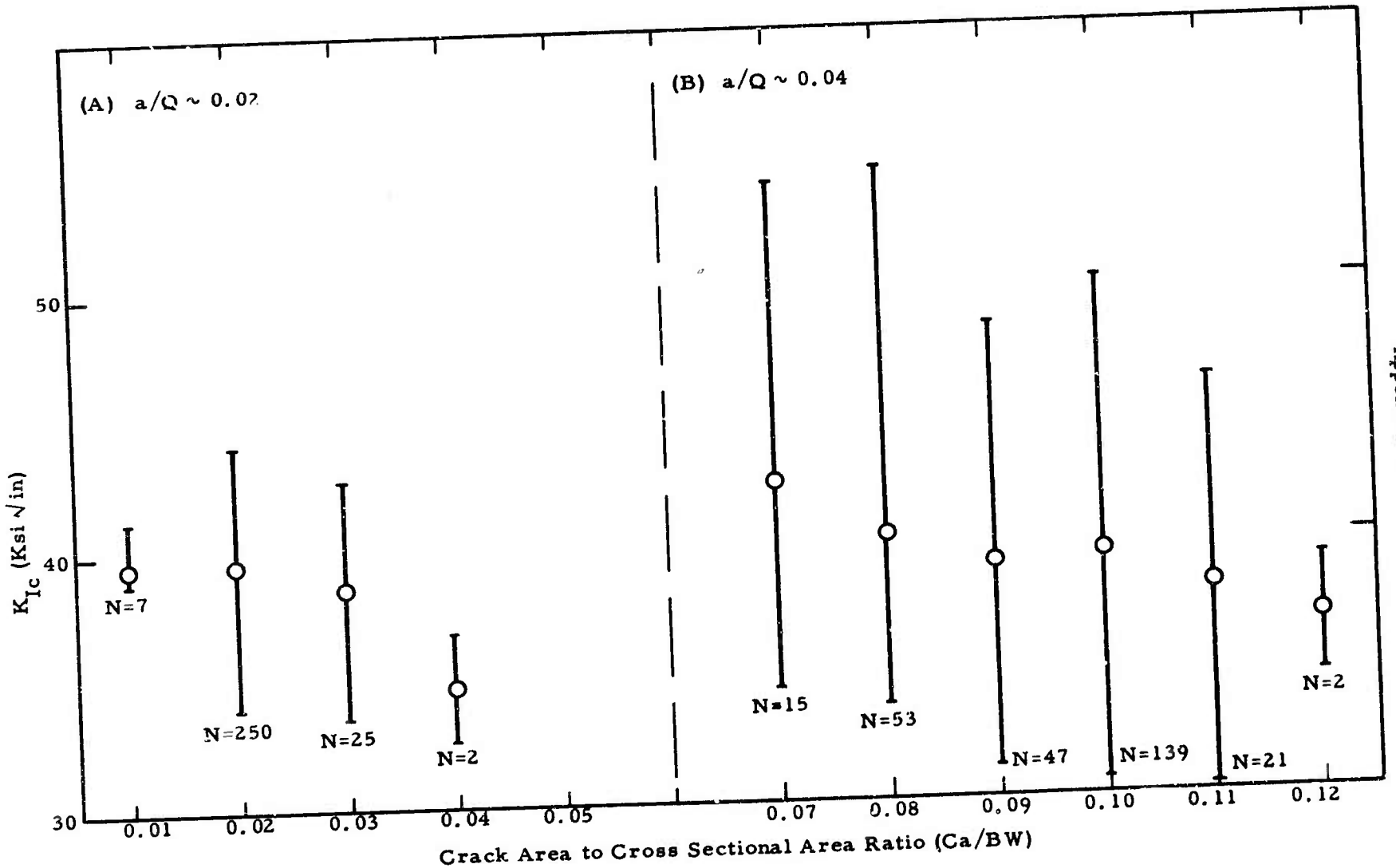


Figure 9. K_{Ic} vs Crack Area to cross-Sectional Area Ratio (Ca/BW)

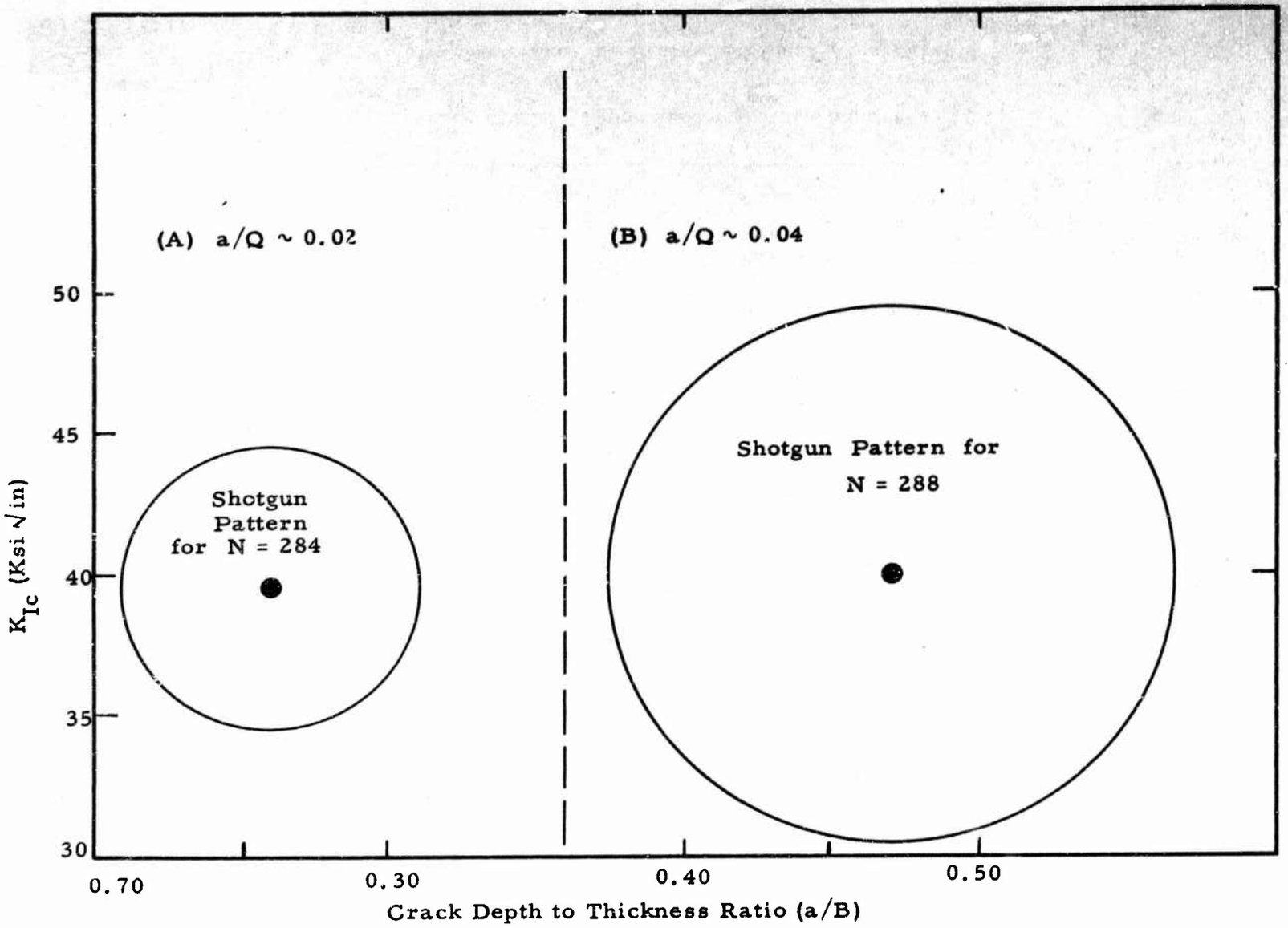


Figure 10. K_{Ic} vs Crack Depth to Thickness Ratio (a/B)

TABLE I

ROOM TEMPERATURE TENSILE RESULTS, ULTIMATE TENSILE STRENGTH

Heat No.	Forging No.	$\bar{X}_F$ ksi	$\Sigma(\bar{X}-X)^2$ ksi^2	df_i	(F) or Bartlett's Test	$F_{.05}$ (f_1,f_2)	(t)or ANOVA Test	$t_{.05}$ (n_1+n_2-2)	$\bar{X}_H$ ksi	$(\bar{X}_F-\bar{X}_H)^2$ ksi^2
1643	9	168.3	0.39	2						
1644	5	169.3	18.67	2						
1968	13	171.3	0.67	2						
2018	17	177.0	8.00	2						
2047	23	173.7	4.67	2						
2073	26	171.0	2.00	2						
2074	27	176.7	16.66	2						
2100	29	174.3	4.67	2						
2102	30	175.3	2.67	2						
2148	31A	176.7	12.67	2						
	31B	176.7	2.67	2	4.76	39.00	0	2.78	176.7	0
2150	33A	168.3	8.67	2						
	33B	168.3	4.67	2	1.86	39.00	0	2.78	168.3	0
2169	43A	177.3	42.68	2						3.24
	43B	173.7	0.67	2	64.8(1)	39.00	1.33	2.78		3.24
									175.5	6.48
2201	45A	172.3	0.67	2						
2202	36A	177.7	4.67	2						1.44
	36B	175.3	4.67	2	1.00	39.00	1.93	2.78		1.44
									176.5	2.88
2203	37B	169.3	2.67	2						
2204	44B	171.0	6.00	2						
205	39A	171.7	8.67	2						
274	42B	176.3	2.67	2						
	42C	172.0	2.00	2	1.33	39.00	4.83	2.78		
2395	50B	173.0	6.00	2						
2398	53B	177.3	0.67	2						1.96
	54A	173.7	4.67	2						4.84
	54B	176.7	12.67	2	2.21	3.77	3.82	7.26		0.64
									175.9	7.44
2479	56B	176.0	8.00	2						1.44
	60B	173.7	68.59	2	8.60	39.00	0.64	2.78		1.21
									174.8	2.65

TABLE I (cont.)

Heat No.	Forging No.	$\bar{X}_F$ ksi	$\Sigma(\bar{X}-X)^2$ ksi^2	df_i	(F) or Bartlett's Test	$F_{.05}$ (f_1,f_2)	(t)or ANOVA Test	$t_{.05}$ (n_1+n_2-2)	$\bar{X}_{II}$ ksi	$(\bar{X}_F-\bar{X}_{II})^2$ ksi^2
2480	57B	170.3	12.67	2						
	58B	178.0	2.00	2	6.33	39.00	4.90	2.78		
2481	59A	178.0	2.00	2						
2528	61A	175.3	18.66	2						
	61B	172.7	2.67	2						2.56
	62A	175.7	24.67	2						1.00
	62B	171.0	2.00	2	1.19	3.23	1.93	5.42		4.00
									173.7	7.29
										14.85
2529	63A	172.3	12.67	2						
	63B	171.3	2.67	2	4.76	39.00	0.62	2.78		0.25
										0.25
									171.8	0.50
2531	65A	172.7	10.67	2						
2532	66B	177.0	14.00	2						
2554	69A	174.7	0.67	2						
	69B	175.3	0.67	2	1.00	39.00	1.25	2.78		0.09
										0.09
									175.0	0.18
2555	70A	172.0	0	2						
	70B	172.7	8.67	2						1.69
	71A	175.3	2.67	2	0.25	3.77	5.00	7.26		0.36
										4.00
									173.3	6.05
2576	73A	173.7	0.67	2						
	73B	176.7	16.67	2						0.64
	74A	174.0	0	2						4.84
	74B	173.7	0.67	2	1.92	3.23	2.80	5.42		0.25
										0.64
									174.5	6.37
2577	75A	176.7	0.67	2						
	80A	175.0	2.00	2						2.56
	80B.	173.7	0.67	2	0.34	3.77	12.2	7.26		0.01
										1.96
									175.1	4.53

TABLE I (cont.)

Heat No.	Forging No.	$\bar{X}_F$ ksi	$\Sigma(\bar{X}-X)^2$ ksi^2	df_i	(F) or Bartlett's Test	$F_{.05}$ (f_1,f_2)	(t)or ANOVA Test	$t_{.05}$ (n_1+n_2-2)	$\bar{X}_H$ ksi	$(\bar{X}_F-\bar{X}_H)^2$ ksi^2
2578	76A	171.7	4.67	2						6.76
	77A	175.3	2.67	2						1.00
	77B	176.0	8.00	2	0.25	3.77	6.40	7.26		2.89
									174.3	10.65
2579	78A	178.3	16.65	2						
2579	79A	173.7	.67	2						0.81
	79B	172.0	0	2	∞ (1)	39.00	3.87(1)	2.78		0.64
									172.8	1.45
2634	81A	176.7	4.67	2						
2635	82A	173.7	2.67	2						
2636	83A	173.7	2.67	2						
	84B	167.0	6.00	2	2.3	39.00	5.56	2.78		
2696	86A	176.7	2.67	2						5.76
	87A	171.3	0.67	2						9.00
	87B	175.0	14.00	2	1.72	3.77	7.72(1)	7.26		0.49
									174.3	15.25
2697	90A	174.0	0	2						3.61
	90B	175.0	2.00	2						0.16
	91A	172.3	0.67	2						1.96
	91B	175.0	14.00	2						1.69
	92A	174.0	8.00	2	0.95	2.88	1.88	4.47		1.96
									173.6	9.38
2700	93A	174.0	8.00	2						0.64
	93B	172.3	0.67	2	11.94	39.00	1.41	2.78		0.81
									173.2	1.45
2701	94B	171.3	2.67	2						
2714	96A	171.0	6.00	2						9.00
	96B	176.7	16.66	2						7.29
	98A	174.3	4.67	2	0.40	3.77	5.30	7.26		0.09
									174.0	16.38

TABLE I (cont.)

Heat No.	Forging No.	$\bar{X}_F$ ksi	$\Sigma(\bar{X}-X)^2$ ksi^2	df_i	(F) or Bartlett's Test	$F_{.05}$ (f_1,f_2)	(t)or ANOVA Test	$t_{.05}$ (n_1+n_2-2)	$\bar{X}_H$ ksi	$(\bar{X}_F-\bar{X}_H)^2$ ksi^2
2715	97A	175.0	2.00	2						
	97B	176.3	8.67	2	4.33	39.00	0.97	2.78		0.36
										0.49
									175.6	0.85
2779	100A	173.3	0.67	2						
	100B	175.3	20.66	2						0.64
	101A	174.7	2.67	2						1.44
	102A	171.3	2.67	2						0.36
	102B	175.7	4.67	2	1.29	2.88	3.00	4.47		7.84
										2.56
									174.1	12.84
2803	104A	173.0	2.00	2						
	104B	173.0	2.00	2						0.36
	105A	174.3	4.67	2						0.36
	105B	174.0	2.00	2	0.16	3.24	1.06	5.42		0.49
										0.09
									173.6	1.30
2803	107A	171.0	2.00	2						
	107B	170.3	0.67	2	4.00	39.00	1.04	2.78		0.16
										0.09
									170.6	0.25
2846	108A	174.3	0.67	2						
	108B	173.0	6.00	2						2.89
	109B	172.7	2.67	2						0.16
	110B	172.3	0.67	2						0.01
	111B	170.7	0.67	2	0.66	2.88	4.88(1)	4.47		0.09
										3.61
									172.6	3.87
2847	112A	173.3	2.67	2						
	112B	175.3	0.67	2	4.00	39.00	1.89	2.78		1.00
										1.00
									174.3	2.00
			600.48	192						127.60

$$S_e^2 = \frac{600.48}{192} = 3.13 \text{ ksi}^2$$

$$S_F^2 = \frac{127.60}{46} = 2.77 \text{ ksi}^2$$

(1) Statistically a significant difference, but from a practical standpoint, the denominator is much smaller than normal; therefore, the results will be added.

Appendix E

TABLE II

BARTLETT'S TEST, ROOM TEMPERATURE, TENSILE STRENGTH

Heat No.	$\sum (X-\bar{X})^2$	df_i	S_i^2	$\ln S_i^2$	$df \ln S_i^2$	$1/df_i$
2148	0	1	0	5.395-10	5.395-10	1.00
2150	0	1	0	5.395-10	5.395-10	1.00
2169	6.48	1	6.48	1.869	1.869	1.00
2202	2.88	1	2.88	1.058	1.058	1.00
2398	7.44	2	3.72	1.314	2.628	0.50
2479	2.65	1	2.65	0.975	0.975	1.00
2528	14.85	3	4.95	1.599	4.797	0.33
2529	0.50	1	0.050	9.307-10	9.307-10	1.00
2554	0.18	1	0.18	8.285-10	8.285-10	1.00
2555	6.05	2	3.02	1.105	2.210	0.50
2576	6.37	3	2.12	0.715	2.145	0.33
2577	4.53	2	2.26	0.815	1.630	0.50
2578	10.65	2	5.32	1.671	3.342	0.50
2579	1.45	1	1.45	0.372	0.372	1.00
2696	15.25	2	7.62	2.031	4.062	0.50
2697	9.38	4	2.34	0.850	3.400	0.25
2700	1.45	1	1.45	0.372	0.372	1.00
2714	16.38	2	8.19	2.103	4.206	0.50
2715	0.85	1	0.85	9.837-10	9.837-10	1.00
2779	12.84	4	3.21	1.166	4.664	0.25
2803	1.30	3	0.43	9.156-10	27.468-30	0.33
2803	0.25	1	0.25	8.614-10	8.614-10	1.00
2846	3.87	4	0.97	9.970-10	39.880-40	0.25
2847	2.00	1	2.00	0.693	0.693	1.00
	127.60	46			153.000-130	16.74

$$S_p^2 = \frac{127.60}{46} = 2.77 \qquad m = 46(1.019) - 23.00 = 23.874$$

$$f_1 = 24-1 = 23, \qquad a = \frac{1}{(3)(23)}\left[16.74 - \frac{1}{46}\right] = 0.242$$

$$f_2 = \frac{25}{(0.242)^2} = 426 \qquad b = \frac{426}{1+2/426 - 0.242} = 558$$

$$F_{calc} = \frac{426\ (23.9)}{23(558-23.9)} = 0.83, \qquad F_{tab} = F_{.05}\ (23,426) = 1.66$$

Appendix E

TABLE III

ANOVA TEST, ROOM TEMPERATURE, TENSILE STRENGTH

	$\bar{X}$	$\bar{X}^2$	$\bar{X}$	$\bar{X}^2$	$\bar{X}$	$\bar{X}^2$	$\bar{X}$	$\bar{X}^2$	$\bar{X}$	$\bar{X}^2$
Heat:	2148		2150		2169		2202		2398	
	176.7	31222.9	168.3	28324.9	177.3	31435.3	177.7	31577.3	177.3	31435.3
	176.7	31222.9	168.3	28324.9	173.7	30171.7	175.3	30730.1	173.7	30171.7
									176.7	31222.9
	353.4	62445.8	336.6	56649.8	351.0	61607.0	353.0	62307.4	527.7	92829.9
Heat:	2479		2528		2529		2554		2555	
	176.0	30976.0	175.3	30730.1	172.3	29687.3	174.7	30520.1	172.0	29584.0
	173.7	30171.7	172.7	29825.3	171.3	29343.7	175.3	30730.1	172.7	29825.3
			175.7	30870.5					175.3	30730.1
			171.0	29241.0						
	349.7	61147.7	694.7	120666.9	343.6	59031.0	350.0	61250.2	520.0	90139.4
Heat:	2576		2577		2578		2579		2696	
	173.7	30171.7	176.7	31222.9	171.7	29480.9	173.7	30171.7	176.7	31222.9
	176.7	31222.9	175.0	30625.0	175.3	30730.1	172.0	29584.0	171.3	29343.7
	174.0	30276.0	173.7	30171.7	176.0	30976.0			175.0	30625.0
	173.7	30171.7								
	698.1	121841.3	525.4	92019.6	523.0	91187.0	345.7	59755.7	523.0	91191.6
Heat:	2697		2700		2714		2715		2779	
	174.0	30276.0	174.0	30276.0	171.0	29241.0	175.0	30625.0	173.3	30032.9
	175.0	30625.0	172.3	29687.3	176.7	31222.9	176.3	31081.7	175.3	30730.1
	172.3	29687.3			174.3	30380.5			174.7	30520.1
	175.0	30625.0							171.3	29343.7
	174.0	30276.0							175.7	30870.5
	870.3	151489.3	346.3	59963.3	522.0	90844.4	351.3	61706.7	870.3	151497.3
Heat:	2803		2803		2846		2847			
	173.0	29929.0	171.0	29241.0	174.3	30380.5	173.3	30032.9		
	173.0	29929.0	170.3	29002.1	173.0	29929.0	175.3	30730.1		
	174.3	30380.5			172.7	29825.3				
	174.0	30276.0			172.3	29687.3				
					170.7	29138.5				
	694.3	120514.5	341.3	58243.1	863.0	148900.6	348.6	60763.0		

$\Sigma X = 12002.3$ $\quad (\Sigma X)^2 = 144055205.3$ $\quad \Sigma X^2 = 2088053.5$

$N = \Sigma n = 69$ $\quad CF = \frac{144055205.3}{69} = 2087756.6$

Total SS = 2088053.5 - 2087756.6 = 296.9

Appendix E

TABLE III (cont.)

Heat No.	SS	df	Heat No.	SS	df	Heat No.	SS	df
2148	0	1	2554	0.18	1	2700	1.45	1
2150	0	1	2555	6.05	2	2714	16.38	2
2169	6.48	1	2576	6.37	3	2715	0.85	1
2202	2.88	1	2577	4.53	2	2779	12.84	4
2398	7.44	2	2578	10.65	2	2803	1.30	3
2479	2.65	1	2579	1.45	1	2803	0.25	1
2528	14.85	3	2696	15.25	2	2846	3.87	4
2529	0.50	1	2697	9.38	4	2847	2.00	1
							127.60	46

Inherent error SS = 127.60, inherent error df = 46

Between heat SS = 296.9 - 127.6 = 69.3, between heat df = 24-1 = 23

Between heat mean square = $\frac{69.3}{23}$ = 3.01, inherent error mean square = $\frac{127.60}{46}$ = 2.77

$F_{calc} = \frac{3.01}{2.77} = 1.09$, $F_{tab} = F_{.05}(23,46) = 2.00$

Appendix E

TABLE IV

MULTI- AND SINGLE-FORGING HEATS, TENSILE STRENGTH

Multi-Forging Heats			Single-Forging Heats		
Heat No.	$\bar{X}_H$ ksi	$(\bar{X}_H-\bar{X}_T)^2$ $(ksi)^2$	Heat No.	$\bar{X}_H$ ksi	$(\bar{X}_H-\bar{X}_T)^2$ $(ksi)^2$
2148	176.7	9.61	1643	168.3	28.09
2150	168.3	28.09	1644	169.3	18.49
2169	175.5	3.61	1968	171.3	5.29
2202	176.5	8.41	2018	177.0	11.56
2398	175.9	5.29	2047	173.7	0.01
2479	174.8	1.44	2073	171.0	6.76
2528	173.7	0.01	2074	176.7	9.61
2529	171.8	3.24	2100	174.3	0.49
2554	175.0	1.96	2102	175.3	2.89
2555	173.3	0.09	2201	172.3	1.69
2576	174.5	0.81	2203	169.3	18.49
2577	175.1	2.25	2204	171.0	6.76
2578	174.3	0.49	2205	171.7	3.61
2579	172.8	0.64	2274	176.3	7.29
2696	174.3	0.49	2274	172.0	2.56
2697	173.6	0.00	2395	173.0	0.36
2700	173.2	0.16	2480	170.3	10.89
2714	174.0	0.16	2480	178.0	19.36
2715	175.6	4.00	2481	178.0	19.36
2779	174.1	0.25	2531	172.7	0.81
2803	173.6	0.00	2532	177.0	11.56
2803	170.6	9.00	2579	178.3	22.09
2846	172.6	1.00	2634	176.7	9.61
2847	174.3	0.49	2635	173.7	0.01
	4174.1		2636	173.7	0.01
			2636	167.0	43.56
			2701	171.3	5.29
				4679.2	

$\bar{X}_{MF} = 173.9$ ksi

$s^2_{MF} = \frac{79.03}{24-1} - 3.43\ ksi^2$ $\qquad \bar{X}_{SF} = 173.3$ ksi, $\quad s^2_{SF} = \frac{258.13}{27-1} = 9.93\ ksi^2$

(F) Test

$F_{calc} = 3.43 = 2.89, \quad F_{tab} = F_{.05}\ (26, 23) = 2.28$

TABLE IV (cont.)

(t) Test

$$U = 173.9-173.3 = 0.6$$

$$Sp = \sqrt{\frac{79.30+258.13}{24+27-2}} = 2.62 \qquad \sqrt{\frac{n_1+n_2}{n_1 n_2}} = \sqrt{\frac{51}{648}} = 0.28$$

$$t_{calc} = \frac{0.6}{(2.62)(0.28)} = 0.82, \quad t_{tab} = t_{.05}\ (49) = 2.01$$

Since $t_{calc} < t_{tab}$, the two subpopulations represented by the multi-forging heats and the single forging heats are equal.

$$\bar{X}_T = \frac{4174.1 + 4679.2}{51} = 173.6 \text{ ksi}$$

$$S_H^2 = \frac{374.99}{51-1} = 6.96 \text{ ksi}^2$$

TABLE V

ROOM TEMPERATURE TENSILE RESULTS, YIELD STRENGTH

Heat No.	Forging No.	$\bar{X}_F$ ksi	$\Sigma(\bar{X}-X)^2$ ksi^2	df_i	(F) or Bartlett's Test	$F_{.05}$ (f_1,f_2)	(t)or ANOVA Test	$t_{.05}$ (n_i+n_{2-2})	$\bar{X}_H$ ksi	$(\bar{X}_F-\bar{X}_H)^2$ ksi^2
1643	9	157.7	8.67	2						
1644	5	160.7	42.67	2						
1968	13	161.3	2.67	2						
2018	17	166.3	4.67	2						
2047	23	162.7	10.67	2						
2073	26	159.0	6.00	2						
2074	27	166.3	12.67	2						
2100	29	164.7	4.67	2						
2102	30	164.3	4.67	2						
2148	31A	167.3	8.67	2						0.04
	31B	167.7	28.68	2	3.31	39.00	0.16	2.78		0.04
									167.5	0.08
2150	33A	158.3	8.67	2						
	33B	158.3	0.54	2	16.0	39.00	0	2.78		
									158.3	0
2169	43A	170.7	68.59	2						
	43B	164.7	0.67	2	102.4	39.00				
2201	45A	161.0	2.00	2						
2202	36A	167.7	4.67	2						1.00
	36B	165.7	2.67	2	1.75	39.00	1.80	2.78		1.00
									166.7	2.00
2203	37B	160.3	4.67	2						
2204	44B	159.3	2.67	2						
2205	39A	161.3	10.67	2						
2274	42B	167.7	0.67	2						
	42C	160.0	0	2	∞ (1)	39.00	22.9	2.78		
2395	50B	163.0	14.00	2						
2398	53B	161.3	0.67	2						3.24
	54A	162.7	18.66	2						0.16
	54B	165.3	12.67	2	1.72	3.77	1.06	7.26		4.84
									163.1	8.24
2479	56A	163.0	14.00	2						2.56
	60B	166.3	80.66	2	5.76	39.00	0.83	2.78		2.89
									164.6	5.45

TABLE V (cont.)

Heat No.	Forging No.	$\bar{X}_F$ ksi	$\Sigma(\bar{X}-X)^2$ ksi^2	df_i	(F) or Bartlett's Test	$F_{.05}(f_1,f_2)$	(t)or ANOVA Test	$t_{.05}(n_1+n_2-2)$	$\bar{X}_H$ ksi	$(\bar{X}_F-\bar{X}_H)^2$ ksi^2
2480	57B	160.3	24.65	2						9.00
	58B	166.3	24.65	2	1.00	39.00	2.09	2.78		9.00
									163.3	18.00
2481	59A	166.0	8.00	2						
2528	61A	164.7	20.66	2						0.16
	61B	160.7	2.67	2						12.96
	62A	167.7	21.46	2						11.56
	62B	154.3	2.67	2	1.02	3.23	3.99	5.42		0
									164.3	24.68
2529	63A	166.0	6.00	2						
	63B	160.7	4.67	2	1.29	39.00	3.95	2.78		
2531	65A	162.3	7.47	2						
2532	66B	167.7	28.68	2						
2554	69A	163.3	2.67	2						0.09
	69B	162.7	2.67	2	1.00	39.00	0.64	2.78		0.09
									163.0	0.18
2555	70A	159.0	0	2						6.25
	70B	163.3	4.67	2						3.24
	71A	162.3	8.67	2	4.16(1)	3.77	6.97	7.26		0.64
									161.5	10.13
2576	73A	158.7	2.67	2						
2576	73B	168.3	12.67	2						5.76
	74A	164.3	4.67	2						2.56
	74B	165.0	2.00	2	0.55	3.77	4.29	7.26		0.81
									165.9	9.13
2577	75A	164.7	2.67	2						3.24
	80A	163.7	0.67	2						0.64
	80B	160.3	0.67	2	0.61	3.77	23.1(1)	7.26		6.76
									162.9	10.64
2578	76A	161.3	2.67	2						2.56
	77A	164.0	6.00	2						1.21
	77B	163.3	8.67	2	0.28	3.77	2.01	7.26		0.16
									162.9	3.93

TABLE V (cont.)

Heat No.	Forging No.	$\bar{X}_F$ ksi	$\Sigma(\bar{X}-X)^2$ ksi^2	df_i	(F) or Bartlett's Test	$F_{.05}$ (f_1,f_2)	(t)or ANOVA Test	$t_{.05}$ (n_1+n_2-2)	$\bar{X}_H$ ksi	$(\bar{X}_F-\bar{X}_H)^2$ ksi^2
2579	78A	170.3	12.67	2						
2579	79A	163.7	0.67	2						2.25
	79B	160.7	0.67	2	1.00	39.00	6.31(1)	2.78		2.25
									162.2	4.50
2634	81A	163.7	4.67	2						
2635	82A	164.0	6.00	2						
2636	83A	163.7	0	2						
	84B	158.7	0.67	2	∞ (1)	39.00	12.66	2.78		
2696	86A	163.0	6.00	2						1,69
	87A	159.7	0.67	2						4.00
	87B	162.3	4.67	2	0.90	3.77	4.97	7,26		0.36
									161.7	6.05
2697	90A	158.3	0.67	2						6.76
	90B	161.0	0	2						0.01
	91A	162.7	0.67	2						3.24
	91B	161.7	4.67	2	0.25	3.24	13.25(1)	5.42		0.64
									160.9	10.65
2697	92A	165.3	8.67	2						
2700	93A	162.3	8.67	2						0.25
	93B	161.3	4.67	2	1.86	39.00	0.67	2.78		0.25
									161.8	0.50
2701	94B	159.7	8.67	2						
2714	96B	167.0	14.00	2						
2714	96A	159.7	8.67	2						0.64
	98B	161.3	10.67	2	1.23	39.00	0.89	2.78		0.64
									160.5	1.28
2715	97A	163.0	2.00	2						0.16
	97B	163.7	4.67	2	2.33	39.00	0.66	2.78		0.09
									163.4	0.25

TABLE V (cont.)

Heat No.	Forging No.	$\bar{X}_F$ ksi	$\Sigma(\bar{X}-X)^2$ ksi^2	df_i	(F) or Bartlett's Test	$F_{.05}$ (f_1,f_2)	(t)or ANOVA Test	$t_{.05}$ (n_1+n_2-2)	$\bar{X}_H$ ksi	$(\bar{X}_F-\bar{X}_H)^2$ ksi^2
2779	100A	160.7	0.67	2						2.56
	100B	166.3	34.67	2						16.00
	101A	162.7	2.67	2						0.16
	102A	159.3	0.67	2						9.00
	102B	162.7	0.67	2	3.07(1)	2.88	5.32(1)	4.47		0.16
									162.3	27.88
2803	104A	161.7	0.67	2						0.81
	104B	161.3	0.67	2						0.25
	105A	162.0	8.00	2						1.44
	105B	161.3	2.67	2						0.25
	107A	159.3	2.67	2						2.25
	107B	159.3	4.67	2	0.75	2.65	2.61	3.89		2.25
									160.8	7.25
2846	108A	162.3	0.67	2						1.44
	108B	161.3	2.67	2						0.04
	109B	161.0	6.00	2						0.01
	110B	160.7	2.67	2						0.16
	111B	160.3	0.67	2	0.72	2.88	1.38	4.47		0.64
									161.1	3.29
2847	112A	161.3	2.67	2						0.49
	112B	162.7	0.67	2	4.00	39.00	1.87	2.78		0.49
									162.0	0.98
			792.58	192						155.09

$$S_e^2 = \frac{792.58}{192} = 4.13 \text{ ksi}^2$$

$$S_F^2 = \frac{155.09}{42} = 3.59 \text{ ksi}^2$$

(1) Statistically, a significant difference, but from a practical standpoint, the sum of the square is much smaller than usual; therefore, the results will be added.

Appendix E

TABLE VI

BARTLETT'S TEST, ROOM TEMPERATURE, YIELD STRENGTH

Heat No.	$\sum (X-\bar{X})^2$	df_i	S_i^2	$\ln S_i^2$	$df \ln S_i^2$	$1/df_i$
2148	0.08	1	0.08	7.474-10	7.474-10	1.00
2150	0	1	0	5.395-10	5.395-10	1.00
2202	2.00	1	2.00	0.693	0.693	1.00
2398	8.24	2	4.12	1.416	2.832	0.50
2479	5.45	1	5.45	1.696	1.696	1.00
2480	18.00	1	18.00	2.890	2.890	1.00
2528	24.68	3	8.29	2.115	6.345	0.33
2554	0.18	1	0.18	8.285-10	8.285-10	1.00
2555	10.13	2	5.06	1.621	3.242	0.50
2576	9.13	2	4.56	1.515	3.030	0.50
2577	10.64	2	5.32	1.671	3.342	0.50
2578	3.93	2	1.96	0.673	1.346	0.50
2579	4.50	1	4.50	1.504	1.504	1.00
2696	6.05	2	3.02	1.105	2.210	0.50
2697	10.65	3	3.55	1.267	3.801	0.33
2700	0.50	1	0.50	9.307-10	9.307-10	1.00
2714	1.28	1	1.28	0.247	0.247	1.00
2715	0.25	1	0.25	8.614-10	8.614-10	1.00
2779	27.88	4	6.97	1.942	7.768	0.25
2803	7.25	5	1.45	0.372	1.860	0.20
2846	3.29	4	0.82	9.802-10	39.208-40	0.25
2847	0.98	1	0.98	9.980-10	9.980-10	1.00
	155.09	42			131.069-100	15.36

$$S_p^2 = \frac{155.09}{42} = 3.59 \qquad m = 42(1.278) - 31.069 = 22.6$$

$$f_1 = 22-1 = 21, \quad a = \frac{1}{(3)(21)}\left[15.36 - \frac{1}{42}\right] = 0.24, \quad f_2 = \frac{22+1}{(0.24)^2} = 400$$

$$b = \frac{400}{1+2/400-0.24} = 526$$

$$F_{calc} = \frac{400\ (22.6)}{21(526-22.6)} = \frac{9040}{10563} = 0.86, \quad F_{tab} = F_{.05}\ (21,400) = 1.69$$

Appendix E

TABLE VII

ANOVA TEST, ROOM TEMPERATURE, YIELD STRENGTH

	$\bar{X}$	$\bar{X}^2$	$\bar{X}$	$\bar{X}^2$	$\bar{X}$	$\bar{X}^2$	$\bar{X}$	$\bar{X}^2$	$\bar{X}$	$\bar{X}^2$
Heat:	2148		2150		2202		2398		2479	
	167.3	27989.3	158.3	25058.9	167.7	28123.3	161.3	26017.7	163.0	26569.0
	167.7	28123.3	158.3	25058.9	165.7	27456.5	162.7	26471.3	166.3	27655.7
							165.3	27324.1		
	335.0	56112.6	316.6	50117.8	333.4	55579.8	489.3	79813.1	329.3	54224.7
Heat:	2480		2528		2554		2555		2576	
	160.3	25696.1	164.7	27126.1	163.3	26666.9	159.0	25281.0	168.3	28324.9
	166.3	27655.7	160.7	25824.5	162.7	26471.3	163.3	26666.9	164.3	26994.5
			167.7	28123.3			162.3	26341.3	165.0	27225.0
			164.3	26994.5						
	326.6	53351.8	657.4	108068.4	326.0	53138.2	484.6	78289.2	497.6	82544.4
Heat:	2577		2578		2579		2696		2697	
	164.7	27126.1	161.3	26017.7	163.7	26797.7	163.0	26569.0	158.3	25058.9
	163.7	26797.7	164.0	26896.0	160.7	25824.5	159.7	25504.1	161.0	25921.0
	160.3	25696.1	163.3	26666.9			162.3	26341.3	162.7	26471.3
									161.7	26017.7
	488.7	79619.9	488.6	79580.6	324.4	52622.2	485.0	78414.4	643.7	103468.9
Heat:	2700		2714		2715		2779		2803	
	162.3	26341.3	159.7	25504.1	163.0	26569.0	160.7	25824.5	161.7	26146.9
	161.3	26017.7	161.3	26017.7	163.7	26797.7	166.3	27655.7	161.3	26017.7
							162.7	26471.3	162.0	26244.0
							159.3	25376.5	161.3	26017.7
							162.7	26471.3	159.3	25376.5
									159.3	25376.5
	323.6	52359.0	321.0	51521.8	326.7	53366.7	811.7	131799.3	964.9	155179.3
Heat:	2846		2847							
	162.3	26341.3	161.3	26017.7						
	161.3	26017.7	162.7	26471.3						
	161.0	25921.0								
	160.7	25824.5								
	160.3	25696.1								
	805.6	129800.6	324.0	52489.0						

$\sum X = 10403.7 \quad (\sum X)^2 = 108236973.7$

$(\sum X^2) = 1691461.7 \qquad N = 64$

$CF = \frac{108236973.7}{64} = 1691202.7$

Total SS = 1691461.7-1691202.7 = 259.0 ksi^2

TABLE VII (cont.)

Heat No.	SS ksi^2	df	Heat No.	SS ksi^2	df	Heat No.	SS ksi^2	df
2148	0.08	1	2555	10.03	2	2714	1.28	1
2150	0.00	1	2576	9.13	2	2715	0.25	1
2202	2.00	1	2577	10.64	2	2779	27.88	4
2398	8.24	2	2578	3.93	2	2803	7.25	5
2479	5.45	1	2579	4.50	1	2846	3.29	4
2480	18.00	1	2696	6.05	2	2847	0.98	1
2528	24.68	3	2697	10.65	3		155.09	42
2554	0.18	1	2700	0.50	1			

Inherent error SS = 155.09 ksi^2, inherent error df = 42

Between heat SS = 259.0-155.1 = 103.9 ksi^2, between heat df = 22-1 = 21

Between heat mean Sq = $\frac{103.9}{21}$ = 4.90 ksi^2, inherent error mean Sq = $\frac{155.1}{42}$ = 3.59 ksi^2

$F_{calc} = \frac{4.90}{3.59} = 1.36$, $F_{tab} = F_{.05}(21,42) = 2.05$

Appendix E

TABLE VIII

MULTI- AND SINGLE-FORGING HEATS, YIELD STRENGTH

Multi-Forging Heats			Single-Forging Heats		
Heat No.	$\bar{X}_H$ ksi	$(\bar{X}_H-\bar{X}_T)^2$ $(ksi)^2$	Heat No.	$\bar{X}_H$ ksi	$(\bar{X}_H-\bar{X}_T)^2$ $(ksi)^2$
2148	167.5	20.25	1643	157.7	28.09
2150	158.3	22.09	1644	160.7	5.29
2302	166.7	13.69	1968	161.3	2.89
2398	163.1	0.01	2018	166.3	10.89
2479	164.6	2.56	2047	162.7	0.09
2480	163.3	0.09	2073	159.0	16.00
2528	164.3	1.69	2074	166.3	10.89
2554	163.0	0.00	2100	164.7	2.89
2555	161.5	2.25	2102	164.3	1.69
2576	165.9	8.41	2169	170.7	60.84
2577	162.9	0.01	2169	164.7	2.89
2578	162.9	0.01	2201	161.0	4.00
2579	162.2	0.64	2203	160.3	7.29
2696	161.7	1.69	2204	159.3	13.69
2697	160.9	4.41	2205	161.3	2.89
2700	161.8	1.44	2274	167.7	22.09
2714	160.5	6.25	2274	160.0	9.00
2715	163.4	0.16	2395	163.0	0.00
2779	162.3	0.49	2481	166.0	9.00
2803	160.8	4.84	2529	166.0	9.00
2846	161.1	3.61	2529	160.7	5.29
2847	162.0	1.00	2531	162.3	0.49
	3580.7		2532	167.7	22.09
			2576	158.7	18.49
			2579	170.3	53.29
			2634	163.7	0.49
			2635	161.0	4.00
			2636	163.7	0.49
			2636	158.7	18.49
			2697	165.3	5.29
			2701	159.7	10.89
			2714	167.0	16.00
				5221.8	470.30

$\bar{X}_{MF}$ = 162.8 ksi

$S^2_{MF} = \frac{104.75}{22-1} = 4.99\ ksi^2$

$\bar{X}_{SF} = \frac{5221.8}{32} = 163.2\ ksi$ $\qquad S^2_{SF} = \frac{372.12}{32-1} = 12.00\ ksi^2$

$\bar{X}_T = \frac{3580.7 + 5221.8}{22 + 32} = 163.0\ ksi$ $\qquad S^2_H = \frac{470.30}{54-1} = 8.87\ ksi^2$

TABLE VIII (cont.)

(F) Test

$$F_{calc} = \frac{12.00}{4.99} = 2.41, \quad F_{tab} = F_{.05}\,(31,21) = 2.30$$

(t) Test

$$U = 163.2 - 162.8 = 0.4 \text{ ksi}$$

$$Sp = \sqrt{\frac{104.75 + 372.12}{22 + 32 - 2}} = 3.02$$

$$\sqrt{\frac{n_1+n_2}{n_1 n_2}} = \sqrt{\frac{22 + 32}{(22)\ 32}} = 0.28$$

$$t_{calc} = \frac{0.4 \text{ ksi}}{(3.02)(0.28)} = 0.48, \quad t_{tab} = t_{.05}\,(52) = 2.00$$

TABLE IX

ROOM TEMPERATURE TENSILE RESULTS, PERCENT ELONGATION

Heat No.	Forging No.	$\bar{X}_F$ % El.	$\Sigma(\bar{X}-X)^2$ (% El)^2	df_i	(F) or Bartlett's Test	$F_{.05}$ (f_1,f_2)	(t) or ANOVA Test	$t_{.05}$ (n_1+n_2-2)	$\bar{X}_H$ % El.	$(\bar{X}_F-\bar{X}_H)^2$ (% El)^2
1643	9	14.0	0	2						
1644	5	14.7	2.67	2						
1968	13	16.0	0	2						
2018	17	13.0	0	2						
2047	23	14.7	2.67	2						
2073	26	13.7	0.67	2						
2074	27	13.7	0.67	2						
2100	29	12.3	2.67	2						
2102	30	13.0	0	2						
2148	31A	12.3	2.67	2						0.25
	31B	13.3	0.67	2	4.00	39.00	1.35	2.78		0.25
									12.8	0.50
2150	33A	13.0	0	2						0.25
	33B	12.0	14.00	2	∞ (1)	39.00	0.67	2.78		0.25
									12.5	0.50
2169	43A	14.3	0.67	2						
	43B	17.0	2.00	2	3.00	39.00	4.39	2.78		
2201	45A	14.0	0	2						
2202	36A	12.3	2.67	2						0.25
	36B	13.3	0.67	2	4.00	39.00	1.33	2.78		0.25
									12.8	0.50
2203	37B	13.0	0	2						
2204	44B	18.0	0	2						
2205	39A	13.0	0	2						
2274	42B	15.0	0	2						0.25
	42C	14.0	0	2	1.00	39.00	∞ (1)	2.78		0.25
									14.5	0.50
2395	50B	12.3	2.67	2						
2398	53B	13.7	0.67	2						0.25
	54A	13.0	0	2						0.04
	54B	13.0	0	2	3.21	3.77	4.5	4.26		0.04
									13.2	0.33

TABLE IX (cont.)

Heat No.	Forging No.	$\bar{X}_F$ % El.	$\Sigma(\bar{X}-X)^2$ (% El)^2	df_i	(F) or Bartlett's Test	$F_{.05}$ (f_1, f_2)	(t)or ANOVA Test	$t_{.05}$ (n_1+n_2-2)	$\bar{X}_H$ % El.	$(\bar{X}_F-\bar{X}_H)^2$ (% El)^2
2479	56A	13.0	0	2						
	60B	16.0	0	2	1.00	39.00	∞	2.78		
2480	57B	13.7	0.67	2						
	58B	13.7	0.67	2	1.00	39.00	0	2.78		
									13.7	0
2481	59A	13.0	0	2						
2528	61A	14.3	0.67	2						0.25
	61B	12.3	2.67	2						2.25
	62A	14.0	6.00	2						0.04
	62B	14.7	2.67	2	0.58	3.24	2.15	5.42		0.81
									13.8	3.35
2529	63A	16.3	2.67	2						2.89
	63B	13.0	0	1	∞ (1)	799.5	3.84(1)	3.18		2.56
									14.6	5.45
2531	65A	13.3	0.67	2						
2532	66B	15.0	0	2						
2554	69A	13.0	0	2						
	69B	12.3	2.67	2	∞ (1)	39.00	1.10	2.78		0.16
									12.6	0.09
										0.25
2555	70A	13.7	0.67	2						
	70B	12.7	0.17	2						
	71A	13.0	0	2	1.98	3.77	0.54	7.26		0.16
									13.1	0.01
										0.53
2576	73A	13.3	0.67	2						
	73B	13.3	0.67	2						0.01
	74A	13.0	0	2						0.01
	74B	14.0	0	2	2.50	3.24	3.12	5.42		0.16
									13.4	0.36
										0.54
2577	75A	13.7	0.67	2						
	80A	11.7	10.67	2						1.69
	80B	11.7	2.67	2	1.41	3.77	1.72	7.26		0.49
									12.4	0.49
										2.67

TABLE IX (cont.)

Heat No.	Forging No.	$\bar{X}_F$ % El.	$\Sigma(\bar{X}-X)^2$ (% El)^2	df_i	(F) or Bartlett's Test	$F_{.05}$ (f_1,f_2)	(t)or ANOVA Test	$t_{.05}$ (n_1+n_2-2)	$\bar{X}_H$ % El.	$(\bar{X}_F-\bar{X}_H)^2$ (% El)^2
2578	77A	15.0	0	2						
2578	76A	13.0	0	2						0.16
	77B	12.3	2.67	2	∞ (1)	39.00	1.04	2.78		0.09
									12.6	0.25
2579	78A	12.7	0.67	2						
	79A	12.3	2.67	2						0.16
	79B	13.0	0	2	3.21	3.77	0.62	7.26		0.09
									12.7	0.25
2634	81A	13.3	0.67	2						
2635	82A	12.3	2.67	2						
2636	83A	14.0	0	2						0.04
	84B	14.3	0.67	2	∞ (1)	39.00	0.89	2.78		0.01
									14.2	0.05
2696	86A	13.0	6.00	2						0.04
	87A	13.7	0.67	2						0.25
	87B	13.0	0	2	4.40(1)	3.77	0.41	7.26		0.04
									13.2	0.33
2697	90A	13.7	0.67	2						0.04
	90B	13.3	0.67	2						0.04
	91A	13.3	0.67	2						0.04
	91B	13.3	0.67	2						0.04
	92A	14.0	2.00	2	0.27	2.88	0.53	4.47		0.25
									13.5	0.41
2700	93A	12.3	2.67	2						0.49
	93B	13.7	0.67	2	4.00	39.00	1.95	2.78		0.49
									13.0	0.98
2701	94B	13.7	0.67	2						
2714	96A	13.3	0.67	2						0.25
	96B	12.8	0.17	2						0
	98A	12.3	2.67	2	1.85	3.77	1.28	7.26		0.25
									12.8	0.50

TABLE IX (cont.)

Heat No.	Forging No.	$\bar{X}_F$ (% El)	$\Sigma(\bar{X}-X)^2$ / (% El)^2	df_i	(F) or Bartlett's Test	$F_{.05}$ (f_1, f_2)	(t)or ANOVA Test	$t_{.05}$ (n_1+n_2-2)	$\bar{X}_H$ % El.	$(\bar{X}_F-\bar{X}_H)^2$ / (% El)^2
2715	97A	11.7	2.67	2						
	97B	12.3	2.67	2	1.00	39.00	0.64	2.78		0.09
										0.09
									12.0	0.18
2779	100A	13.0	0	2						
	100B	13.7	2.67	2						0.49
	101A	13.0	0	2						0
	102A	13.0	0	2						0
	102B	12.3	2.67	2	4.56(1)	2.88	1.27	4.47		0.49
									13.0	0.98
2803	104A	11.7	2.67	2						1.96
	104B	13.3	0.67	2						0.04
	105A	13.3	0.67	2						0.04
	105B	13.7	0.67	2						0.36
	107A	13.7	0.67	2						0.36
	107B	13.0	0	2	1.32	2.65	3.77	3.89		0.01
									13.1	2.77
2846	108A	13.0	0	2						0.01
	108B	12.7	4.67	2						0.16
	109B	13.0	0	2						0.01
	110B	13.7	0.67	2						0.36
	111B	13.0	0	2	5.00(1)	2.88	0.76	4.47		0.01
									13.1	0.55
2847	112A	13.0	0	2						0.04
	112B	13.3	0.67	2	∞ (1)	39.00	0.34	2.78		0.01
									13.2	0.05
			134.19	191						22.42

$S_e^2 = \frac{123.50}{191} = 0.65$

$S_F^2 = \frac{22.42}{47} = 0.48$

(1) Statistically, a significant difference, but from a practical standpoint, the sum of the squares is much smaller then usual; therefore, the results will be added.

Appendix E

TABLE X

BARTLETT'S TEST, ROOM TEMPERATURE, PERCENT ELONGATION

Heat No.	$\sum (X-\bar{X})^2$	df_i	S_i^2	$\ln S_i^2$	$df \ln S_i^2$	$1/df_i$
2148	0.50	1	0.50	9.307-10	9.307-10	1.00
2150	0.50	1	0.50	9.307-10	9.307-10	1.00
2202	0.50	1	0.50	9.307-10	9.307-10	1.00
2274	0.50	1	0.50	9.307-10	9.307-10	1.00
2398	0.33	2	0.16	7.187-10	14.374-20	0.50
2480	0	1	0	5.395-10	5.395-10	1.00
2528	3.35	3	1.12	0.113	0.339	0.33
2529	5.45	1	5.45	1.696	1.696	1.00
2554	0.25	1	0.25	8.614-10	8.614-10	1.00
2555	0.53	2	0.26	8.653-10	17.306-20	0.50
2576	0.54	3	0.18	8.285-10	24.855-30	0.33
2577	2.67	2	1.33	0.285	0.570	0.50
2578	0.25	1	0.25	8.614-10	8.614-10	1.00
2579	0.25	2	0.12	7.880-10	15.760-20	0.50
2636	0.05	1	0.05	7.004-10	7.004-10	1.00
2696	0.33	2	0.16	8.167-10	16.334-20	0.50
2697	0.41	4	0.10	7.697-10	30.788-40	0.25
2700	0.98	1	0.98	9.980-10	9.980-10	1.00
2714	0.50	2	0.25	8.614-10	17.228-20	0.50
2715	0.18	1	0.18	8.285-10	8.285-10	1.00
2779	0.98	4	0.24	8.573-10	34.292-40	0.25
2803	2.77	5	0.55	9.402-10	47.010-50	0.20
2846	0.55	4	0.14	8.034-10	32.136-40	0.25
2847	0.05	1	0.05	7.004-10	7.004-10	1.00
	22.42	47			344.812-410	16.61

$S_p^2 = \frac{22.42}{47} = 0.48$ $\quad m = 47(9.266-10) - (-66.884) = 30.69$

$f_1 = 24-1 = 23, \quad a = \frac{1}{(3)(23)}\left[16.61 - \frac{1}{47}\right] = 0.24, \quad f_2 = \frac{24+1}{(0.24)^2} = 434$

$b = \frac{434}{1+2/434-0.24} = 572$

$F_{calc} = \frac{434\ (30.7)}{23(572-30.7)} = 1.07, \quad F_{tab} = F_{.05}\ (23,572) = 1.66$

Appendix E

TABLE XI

ANOVA TEST, ROOM TEMPERATURE, PERCENT ELONGATION

	$\bar{X}$	$\bar{X}^2$	$\bar{X}$	$\bar{X}^2$	$\bar{X}$	$\bar{X}^2$	$\bar{X}$	$\bar{X}^2$	$\bar{X}$	$\bar{X}^2$
Heat:	2148		2150		2202		2274		2398	
	12.3	151.3	13.0	169.0	12.3	151.3	15.0	225.0	13.7	187.7
	13.3	176.9	12.0	144.0	13.3	176.9	14.0	196.0	13.0	169.0
									13.0	169.0
	25.6	328.2	25.0	313.0	25.6	328.2	29.0	421.0	39.7	525.7
Heat:	2480		2528		2529		2554		2555	
	13.7	187.7	14.3	204.5	16.3	265.7	13.0	169.0	13.7	187.7
	13.7	187.7	12.3	151.3	13.0	169.0	12.3	151.3	12.7	161.3
			14.0	196.0					13.0	169.0
			14.7	206.1						
	27.4	375.4	55.3	757.9	29.3	434.7	25.3	320.3	39.4	518.0
Heat:	2576		2577		2578		2579		2636	
	13.3	176.9	13.7	187.7	13.0	169.0	12.7	161.3	14.0	196.0
	13.3	176.9	11.7	136.9	12.3	151.3	12.3	151.3	14.3	204.5
	13.0	169.0	11.7	136.9			13.0	169.0		
	14.0	196.0								
	53.6	718.8	37.1	461.5	25.3	320.3	38.0	481.3	28.3	400.5
Heat:	2696		2697		2700		2714		2715	
	13.0	169.0	13.7	187.7	12.3	151.3	13.3	176.9	11.7	136.9
	13.7	187.7	13.3	176.9	13.7	187.7	12.8	163.8	12.3	151.3
	13.0	169.0	13.3	176.9			12.3	151.3		
			13.3	176.9						
			14.0	196.0						
	39.7	525.7	67.6	914.4	26.0	339.0	38.4	492.0	24.0	288.2
Heat:	2779		2803		2846		2847			
	13.0	169.0	11.7	136.9	13.0	169.0	13.0	169.0		
	13.7	187.7	13.3	176.9	12.7	161.3	13.3	176.9		
	13.0	169.0	13.3	176.9	13.0	169.0				
	13.0	169.0	13.7	187.7	13.7	187.7				
	12.3	151.3	13.7	187.7	13.0	169.0				
			13.0	169.0						
	65.0	846.0	78.7	1035.1	65.4	856.0	26.3	345.9		

$\Sigma X = 935.0$ $(\Sigma X)^2 = 874225.0$ $\Sigma X^2 = 12347.4$ $N = 71$

$CF = \frac{874225.0}{71} = 12313.0$ Total SS=12347.4 - 12313.0 = 34.4

Appendix E

TABLE XI (cont.)

Heat No.	SS	df	Heat No.	SS	df	Heat No.	SS	df
2148	0.50	1	2555	0.53	2	2700	0.98	1
2150	0.50	1	2576	0.54	3	2714	0.50	2
2202	0.50	1	2577	2.67	2	2715	0.18	1
2274	0.50	1	2578	0.25	1	2779	0.98	4
2398	0.33	2	2579	0.25	2	2803	2.77	5
2480	0.00	1	2636	0.05	1	2846	0.55	4
2528	3.35	3	2696	0.33	2	2847	0.05	1
2529	5.45	1	2697	0.41	4		22.42	47
2554	0.25	1						

Inherent error SS = 22.42, inherent error df = 47

Between heat SS = 34.4 - 22.4 = 12.0, between heat df = 24-1 = 23

Between heat mean square / $= \frac{12.0}{23} = 0.52$, inherent error mean square / $= \frac{22.4}{47} = 0.48$

$$F_{calc} = \frac{0.52}{0.48} = 1.08, \quad F_{tab} = F_{.05}\,(23,47) = 1.97$$

Appendix E

TABLE XII

MULTI- AND SINGLE-FORGING HEATS, PERCENT ELONGATION

Multi-Forging Heats			Single-Forging Heats		
Heat No.	$\bar{X}_H$ (% El)	$(\bar{X}_H-\bar{X}_T)^2$ (% El)^2	Heat No.	$\bar{X}_H$ (% El)	$(\bar{X}_H-\bar{X}_T)^2$ (% El)^2
2148	12.8	0.25	1643	14.0	0.49
2150	12.5	0.64	1644	14.7	1.96
2202	12.8	0.25	1968	16.0	omit
2274	14.5	1.44	2018	13.0	0.09
2398	13.2	0.01	2047	14.7	1.96
2480	13.7	0.16	2073	13.7	0.16
2528	13.8	0.25	2074	13.7	0.16
2529	14.6	1.69	2100	12.3	1.00
2554	12.6	0.49	2102	13.0	0.09
2555	13.1	0.04	2169	14.3	1.00
2576	13.4	0.01	2169	17.0	omit
2577	12.4	0.81	2201	14.0	0.49
2578	12.6	0.49	2203	13.0	0.09
2579	12.7	0.36	2204	18.0	omit
2636	14.2	0.81	2205	13.0	0.09
2696	13.2	0.01	2395	12.3	1.00
2697	13.5	0.04	2479	13.0	0.09
2700	13.0	0.09	2479	16.0	omit
2714	12.8	0.25	2481	13.0	0.09
2715	12.0	1.69	2531	13.3	0.00
2779	13.0	0.09	2532	15.0	2.89
2803	13.1	0.04	2578	15.0	2.89
2846	13.1	0.04	2634	13.3	0.00
2847	13.2	0.01	2635	12.3	1.00
	315.8		2701	13.7	0.16
				351.3	25.66

$$\bar{X}_{MF} = \frac{315.8}{24} = 13.2 \text{ \% El}$$

$$S^2_{MF} = \frac{9.52}{24-1} = 0.41 \text{ (\% El)}^2$$

$$\bar{X}_{SF} = \frac{350.0}{25} = 14.1 \text{ \% El} \qquad S^2_{SF} = \frac{51.98}{25-1} = 2.17 \text{ (\% El)}^2$$

$$\bar{X}_T = \frac{315.8 + 284.3}{24 + 21} = 13.3 \text{ (\% El)}$$

$$S^2_H = \frac{25.66}{45-1} = 0.58 \text{ (\% El)}^2$$

Appendix E

TABLE XII (cont.)

(F) Test

$$F_{calc} = \frac{2.17}{0.41} = 5.29, \quad F_{tab} = F_{.05}\,(24,23) = 3.02$$

Since $F_{calc} > F_{tab}$, some of the single forging heats will have to be segregated until $F_{calc} < F_{tab}$.

Discard Heats 1968, 2169, 2704, and 2479

$$\bar{X}_{SF} = \frac{284.3}{21} = 13.5 \qquad S^2_{SF} = \frac{14.54}{21-1} = 0.73$$

(F) Test

$$F_{calc} = \frac{0.73}{0.33} = 2.21, \quad F_{tab} = F_{.05}\,(20,22) = 2.39$$

(t) Test

$$U = 13.5-13.2 = 0.3$$

$$Sp = \sqrt{\frac{9.52+14.54}{21-24-2}} = 0.75 \qquad \sqrt{\frac{n_1+n_2}{n_1 n_2}} = \sqrt{\frac{45}{504}} = 0.30$$

$$t_{calc} = \frac{0.3}{(0.75)(0.30} = 1.33, \quad t_{tab} = t_{.05}\,(43) = 2.02$$

TABLE XIII

ROOM TEMPERATURE K_{Ic} (AEROJET-SACRAMENTO a/Q ~ 0.02)

Heat No.	Forging No.	$\bar{X}_F$ ksi $\sqrt{in.}$	$\sum(X-\bar{X})^2$ $(ksi\ \sqrt{in.})^2$	df_i	(F) or Bartlett's Test	$F_{.05}$ (f_1,f_2)	(t)or ANOVA Test	$t_{.05}$ (n_1+n_2-2)	$\bar{X}_H$ ksi $\sqrt{in.}$	$(\bar{X}_F-\bar{X}_H)^2$ $(ksi\ \sqrt{in.})^2$
1644	5	38.8	0	1						
1968	13	41.6	1.81	1						
2018	17	38.4	0.78	2						
2047	23	40.2	0.89	2						
2074	27	40.8	0.19	2						
2100	29	39.1	1.28	1						
2102	30	40.4	3.12	2						
2148	31A	36.7	0.29	2						
	31B	36.1	8.82	2	30.4	39.0	0.49	2.78		0.09
									36.4	0.09
										0.18
2150	33A	38.7	0.24	2						
	33B	39.7	2.06	2	8.58	39.0	1.61	2.78		0.25
									39.2	0.25
										0.50
2169	43A	38.6	0.08	2						
	43B	38.2	1.45	2	18.14	39.0	0.78	2.78		0.04
									38.4	0.04
										0.08
2201	45A	40.6	1.33	2						
2202	36A	38.7	1.68	2						
	36B	38.8	0.99	2	1.70	39.0	0.15	2.78		0.01
									38.8	0.00
										0.01
2203	37B	40.5	4.03	2						
2204	44B	38.7	0.65	2						
2205	39A	36.9	10.21	2						
2274	42B	40.0	2.24	2						
	42C	39.2	3.49	3	1.03	39.2	0.98	2.57		0.16
									39.6	0.16
										0.32
2395	50A	39.1	1.15	2						
2398	53B	38.5	0.45	2						
	54A	40.5	4.69	2						0.64
	54B	39.0	0.61	2	1.4	3.09	3.5	7.26		1.44
										0.09
									39.3	2.17

TABLE XIII (cont.)

Heat No.	Forging No.	$\bar{X}_F$ ksi $\sqrt{in.}$	$\sum (X-\bar{X})^2$ $(ksi\sqrt{in.})^2$	df_i	(F) or Bartlett's Test	$F_{.05}$ (f_1,f_2)	(t)or ANOVA Test	$t_{.05}$ (n_1+n_2-2)	$\bar{X}_H$ ksi $\sqrt{in.}$	$(\bar{X}_F-\bar{X}_H)^2$ $(ksi\sqrt{in.})^2$
2479	56B	38.6	4.49	2						0.04
	60B	38.3	19.34	2	4.31	39.0	0.15	2.78		0.01
									38.4	0.05
2480	57B	40.1	5.54	2						0.01
	58B	40.2	3.13	2	1.77	39.0	0	2.78		0
									40.2	0.01
2481	59A	37.0	0.51	2						
2528	61A	39.4	2.48	2						0.64
	61B	40.0	0.99	2						1.96
	62A	37.7	3.12	2						0.81
	62B	37.2	2.21	2	0.13	3.21	4.88	5.42		1.96
									38.6	5.37
2529	63A	37.8	3.44	2						0
	63B	37.8	2.42	2	1.42	39.0	0	2.78		0
									37.8	0
2531	65A	39.4	6.02	2						
2532	66B	33.5	1.45	2						
2554	69A	38.0	2.04	2						0.04
	69B	38.5	16.99	2	8.34	39.0	0.28	2.78		0.09
									38.2	0.13
2555	70A	37.6	2.83	2						0.16
	70B	37.7	8.01	2						0.09
	71A	38.8	0.73	2	1.05	3.89	0.77	7.26		0.64
									38.0	0.89
										9.71
			137.97	84						

$$S_e^2 = \frac{137.97}{84} = 1.64$$

$$S_F^2 = \frac{9.71}{16} = 0.61$$

Appendix E

TABLE XIV

BARTLETT'S TEST FOR MULTI-FORGING HEATS (AEROJET-SACRAMENTO a/Q ~ 0.02)

Heat No.	$\sum (X-\bar{X})^2$	df_i	S_i^2	$\ln S_i^2$	$df \ln S_i^2$	$1/df_i$
2148	0.18	1	0.18	8.285-10	8.285-10	1.00
2150	0.50	1	0.50	9.307-10	9.307-10	1.00
2169	0.08	1	0.08	7.474-10	7.474-10	1.00
2202	0.01	1	0.01	5.395-10	5.395-10	1.00
2274	0.32	1	0.32	8.861-10	8.861-10	1.00
2398	2.17	2	1.08	0.077	0.154	0.50
2479	0.05	1	0.05	7.004-10	7.004-10	1.00
2480	0.01	1	0.01	5.395-10	5.395-10	1.00
2528	5.37	3	1.79	0.582	1.746	0.33
2529	0.00	1	0.00	5.395-10	5.395-10	1.00
2554	0.13	1	0.13	7.960-10	7.960-10	1.00
2555	0.89	2	0.44	9.179-10	18.358-20	0.50
	9.71				85.334-110	10.33

$S_p^2 = \frac{9.71}{16} = 0.61$ $\quad m = 16(9.506-10) - (-24.666) = 16.762$

$f_1 = 12 - 1 = 11$, $\quad a = (10.33-\frac{1}{16}) = 0.31$, $\quad f_2 = \frac{12+1}{(0.31)^2} = 135.3$

$b = \frac{135.3}{1+2/135.3-0.31} = 193.3$

$F_{calc} = \frac{135.3(16.8)}{(11)(193.3-16.8)} = \frac{2173.0}{1941.5} = 1.12$

$F_{tab} = F_{.05}\,(11,135.3) = 2.10$

Since $F_{calc} < F_{tab}$, there is no reason to believe that the variances are not homogeneous.

---

* To determine if variances are homogeneous.

Appendix E

TABLE XV

ANOVA TEST FOR MULTI-FORGING HEATS (AEROJET-SACRAMENTO a/Q ~ 0.02)

	$\bar{X}$	$\bar{X}^2$	$\bar{X}$	$\bar{X}^2$	$\bar{X}$	$\bar{X}^2$	$\bar{X}$	$\bar{X}^2$	$\bar{X}$	$\bar{X}^2$
Heat:	2148		2150		2169		2202		2274	
	36.7	1346.9	38.7	1497.7	38.6	1490.0	38.7	1497.7	40.0	1600.0
	36.1	1303.2	39.7	1576.1	38.2	1459.2	38.8	1505.4	39.2	1536.6
	72.8	2650.1	78.4	3073.8	76.8	2949.2	77.5	3003.1	79.2	3136.6
Heat:	2398		2479		2480		2528		2529	
	38.5	1482.2	38.6	1490.0	40.1	1608.0	39.4	1552.4	37.8	1428.8
	40.5	1640.2	38.3	1466.9	40.2	1616.0	40.0	1600.0	37.8	1428.8
	39.0	1521.0					37.7	1421.3		
							37.2	1383.8		
	118.0	4643.4	76.9	2956.9	80.3	3224.0	154.3	5957.5	75.6	2857.6
Heat:	2554		2555							
	38.0	1444.0	37.6	1413.8						
	38.5	1482.2	37.7	1421.3						
			38.8	1505.4						
	76.5	2926.2	114.1	4340.5						

$\Sigma X = 1080.4$, $(\Sigma X)^2 = 1,167,264.2$

$\Sigma X^2 = 41718.9$ $\quad N = \Sigma n2 = 28$

$CF = \frac{1167264.2}{28} = 41688.0$

Total SS = 41718.9 - 41688.0 = 30.9

Heat No.	SS	df
2148	0.18	1
2150	0.50	1
2169	0.08	1
2202	0.01	1
2274	0.32	1
2398	2.17	2
2479	0.05	1
2480	0.01	1
2528	5.37	3
2529	0.00	1
2554	0.13	1
2555	0.89	2
	9.71	16

error
Inherent/SS = 9.71, inherent error df = 16

Between forging SS = 30.9 - 9.7 = 21.2, Between forging df = 12 - 1 = 11

Between forging mean square = $\frac{21.2}{11}$ = 1.93, Inherent error mean square = $\frac{9.71}{16}$ = 0.61

$F_{calc} = \frac{1.93}{0.61} = 3.16$ $\qquad F_{tab} = F_{.05}\ (11,16) = 2.94$

Since $F_{calc} > F_{tab}$ statistically there is a significant difference, but practically since the inherent error mean square is so small, the data will be added.

Appendix E

TABLE XVI

COMPARISON OF MEANS FOR MULTI-FORGING HEATS vs SINGLE-FORGING HEATS (AEROJET-SACRAMENTO a/Q ~ 0.02)

Multi-forging Heats		Single-forging Heats		
Heat No.	$\bar{X}_H$ (ksi)	Heat No.	$\bar{X}_H$ (ksi)	
2148	36.4	1644	38.8	
2150	39.2	1968	41.6	
2169	38.4	2018	38.4	
2202	38.8	2047	40.2	
2274	39.6	2074	40.8	
2398	39.3	2100	39.1	
2479	38.4	2102	40.4	
2480	40.2	2201	40.6	
2528	38.6	2203	40.5	
2529	37.8	2204	38.7	
2554	38.2	2205	36.9	
2555	38.0	2395	39.1	
	462.9	2481	37.0	
		2531	39.4	
		2532	33.5	omitted
			585.0	

$$\bar{X}_{MF} = \frac{462.9}{12} = 38.6 \text{ ksi} \qquad \bar{X}_{SF} = \frac{585.0}{15} = 39.0 \text{ ksi}$$

$$S^2_{MF} = \frac{10.53}{12-1} = 0.96 \qquad S^2_{SF} = 4.11$$

(F) Test

$$F_{calc} = \frac{4.11}{0.96} = 4.28, \qquad F_{tab} = F_{.05}\,(14,11) = 3.36$$

Omit Heat No. 2532 $\bar{X}_{SF} = 39.4$, $S^2_{SF} = 1.93$

$$F_{calc} = \frac{1.93}{0.96} = 2.01 \qquad F_{tab} = F_{.05}\,(13,11) = 3.40$$

(t) Test

$$U = 39.4-38.6 = 0.8, \qquad S_p = \sqrt{\frac{10.53+25.09}{14+12-2}} = 1.22$$

$$\sqrt{\frac{n_1+n_2}{n_1 n_2}} = \sqrt{\frac{14+12}{(14)12}} = 0.39$$

$$t_{calc} = \frac{0.8}{(0.39)(1.22)} = 1.67, \qquad t_{tab} = t_{.05}\,(14+12-2) = 2.06$$

Since $t_{calc} < t_{tab}$, there is no reason to believe that the heats, except for 2532, are not from the same population.

TABLE XVII

ROOM TEMPERATURE K_{Ic} RESULTS (AEROJET-DOWNEY a/Q ~ 0.02)

Heat No.	Forging No.	$\bar{X}_F$ ksi √in.	$\sum (X-\bar{X})^2$ (ksi √in.)^2	df_i	(F) or Bartlett's Test	$F_{.05}$ (f_1,f_2)	(t)or ANOVA Test	$t_{.05}$ (n_1+n_2-2)	$\bar{X}_H$ ksi √in.	$(\bar{X}_F-\bar{X}_H)^2$ (ksi √in.)^2
2554	69B	37.6	3.21	2						1.96
2555	70A	41.9	0.98	1						1.69
	70B	39.2	3.93	2						0.04
	71A	40.3	0.89	2	0.42	4.00	3.66	8.43	40.5	3.69
2576	73A	40.6	3.09	2						0.81
	73B	40.1	0.69	2						0.16
	74A	38.8	1.13	1						0.81
	74B	39.2	0.05	2	1.84	3.27	2.57	5.89	39.7	0.25
										2.03
2577	75A	42.7	6.33	2						0.64
	80A	41.6	1.13	1						0.09
	80B	41.4	0.05	1	1.12	4.22	0.72	10.65	41.9	0.25
										0.98
2578	76A	39.8	0.03	2						0.09
	77A	39.7	2.17	2						0.04
	77B	38.9	1.71	2	2.2	3.85	1.15	7.26	39.5	0.36
										0.49
2579	78A	37.8	2.29	2						2.56
	79A	40.2	0.35	2						0.64
	79B	40.3	2.73	2	0.78	3.85	6.61	7.26	39.4	0.81
										4.01
2634	81A	41.0	0.83	2						
2635	82A	42.7	0.18	1						
2636	83A	41.0	0.50	2						
2696	87A	42.5	-	0						0.09
	87B	41.8	-	0	Is excepted because values are so close.				42.2	0.16
										0.25

TABLE XVII (cont.)

Heat No.	Forging No.	$\bar{X}_F$ ksi in.	$\sum (X-\bar{X})^2$ $(\text{ksi in.})^2$	df_i	(F) or Bartlett's Test	$F_{.05}$ (f_1, f_2)	(t) or ANOVA Test	$t_{.05}$ (n_1+n_2-2)	$\bar{X}_H$ ksi in.	$(\bar{X}_F-\bar{X}_H)^2$ $(\text{ksi in.})^2$
2697	90B	41.2	0.01	1						0.64
	91A	41.7	0.18	1						0.09
	91B	42.9	-	0						0.81
	92A	42.1	0.74	2	0.88	4.22	3.04	9.98		0.01
									42.0	1.55
2700	93A	39.9	4.03	2						
			37.23	41						13.00

$$S_e^2 = \frac{37.23}{41} = 0.91$$

$$S_F^2 = \frac{13.00}{15} = 0.87$$

Appendix E

TABLE XVIII

BARTLETT'S TEST FOR MULTI-FORGING HEATS (AEROJET-DOWNEY a/Q ~ 0.02)

Heat No.	$\Sigma (X-\bar{X})^2$	df_i	S_i^2	$\ln S_i^2$	$df \ln S_i^2$	$1/df_i$
2555	3.69	2	1.84	0.610	1.220	0.5
2576	2.03	3	0.68	9.614-10	28.842-30	0.33
2578	0.49	2	0.24	8.573-10	17.146-20	0.50
2579	4.01	2	2.00	0.693	1.386	0.50
2577	0.98	2	0.49	9.287-10	18.574-20	0.50
2696	0.25	1	0.25	8.614-10	8.614-10	1.00
2697	1.55	3	0.52	9.346-10	28.038-30	0.33
	13.00	15			103.820-110	3.67

$$S_p^2 = \frac{13.00}{15} = 0.87 \qquad m = 15(9.861\text{-}10) - (-6.180) = 4.10$$

$$f_1 = 7\text{-}1 = 6, \qquad a = \frac{1}{(31)(6)}\left(3.67 - \frac{1}{15}\right) = 0.20, \qquad f_2 = \frac{7+1}{(.2)^2} = 200$$

$$b = \frac{200}{1+2/200-0.20} = 247$$

$$F_{calc} = \frac{200(4.1)}{(6)(247-4.1)} = 0.56, \qquad F_{tab} = F_{.05}(6,247) = 2.41$$

*To determine if variances are homogeneous.

Appendix E

TABLE XIX

ANOVA TEST FOR MULTI-FORGING HEATS (AEROJET-DOWNEY a/Q ∿ 0.02)

	$\bar{X}$	$\bar{X}^2$	$\bar{X}$	$\bar{X}^2$	$\bar{X}$	$\bar{X}^2$	$\bar{X}$	$\bar{X}^2$	$\bar{X}$	$\bar{X}^2$
Heat:	2555		2576		2577		2578		2579	
	41.9	1755.6	40.6	1648.4	42.7	1823.3	39.8	1584.0	37.8	1428.8
	39.2	1536.6	40.1	1608.0	41.6	1730.6	39.7	1576.1	40.2	1616.0
	40.3	1624.1	38.2	1505.4	41.4	1714.0	38.9	1513.2	40.3	1624.1
			39.2	1536.6						
	121.4	4916.3	158.7	6298.4	125.7	5267.9	118.4	4673.3	118.3	4668.9
Heat:	2696		2697							
	42.5	1806.2	41.2	1697.4						
	41.8	1747.2	41.7	1738.9						
			42.9	1840.4						
			42.1	1772.4						
	84.3	3553.4	167.9	7049.1						

$\Sigma X^2 = 894.7$

$(\Sigma X)^2 = 800,488.1$

$\Sigma X^2 = 36427.3$

$N = \Sigma n = 22$

$CF = \frac{800,488.1}{22} = 36385.8$ Total SS = 36427.3 - 36385.8 = 41.5

Heat No.	SS	df
2555	3.69	2
2576	2.03	3
2577	0.98	2
2578	0.49	2
2579	4.01	2
2696	0.25	1
2697	1.55	3
	13.00	15

Inherent error SS = 13.00, inherent error df = 15

Between heat df = 7-1 = 6, Between heat SS = 41.5 - 13.0 = 28.5

Between heat mean square = $\frac{28.5}{6}$ = 4.75, Inherent error mean square = $\frac{13.00}{15}$ = 0.87

$F_{calc} = \frac{4.75}{0.87} = 5.46$, $F_{tab} = F_{.05}(6,15) = 3.41$

Appendix E

TABLE XX

COMPARISON OF MEANS FOR MULTI-FORGING HEATS vs SINGLE-FORGING HEATS
(AEROJET-DOWNEY a/Q ≈ 0.02)

Multi-forging Heats	
Heat No.	$\bar{X}_H$ (ksi)
2555	40.5
2576	39.7
2577	41.9
2578	39.5
2579	39.4
2696	42.2
2697	42.6
	285.2

Single-forging Heats	
Heat No.	$\bar{X}_H$ (ksi)
2554	37.6
2634	41.0
2635	42.7
2636	41.0
2700	39.9
	202.2

$\bar{X}_{MF} = 40.7$ ksi $\qquad \bar{X}_{SF} = 40.4$ ksi

$S^2_{MF} = 1.59$ $\qquad S^2_{SF} = 3.52$

(F) Test

$$F_{calc} = \frac{3.52}{1.59} = 2.21, \qquad F_{tab} = F_{.05}\,(4,6) = 6.23$$

(t) Test

$$U = 40.7-40.4 = 0.3, \qquad S_p = \sqrt{\frac{9.55+14.10}{7+5-2}} = 1.54$$

$$\sqrt{\frac{n_1+n_2}{n_1\ n_2}} = 0.58$$

$$t_{calc} = \frac{0.3}{1.54(0.58)} = 0.34, \qquad t_{tab} = t_{.05}\,(7+5-2) = 2.23$$

TABLE XXI

ROOM TEMPERATURE K_{Ic} RESULTS (LYCOMING a/Q ~ 0.02)

Heat No.	Forging No.	$\bar{X}_F$ ksi $\sqrt{in.}$	$\sum (X-\bar{X})^2$ $(ksi\sqrt{in.})^2$	df_i	(F) or Bartlett's Test	$F_{.05}$ (f_1,f_2)	(t)or ANOVA Test	$t_{.05}$ (n_1+n_2-2)	$\bar{X}_H$ ksi $\sqrt{in.}$	$(\bar{X}_F-\bar{X}_H)^2$ $(ksi\sqrt{in.})^2$
2529	63A	39.7	0.69	2						0.09
	63B	39.2	9.63	2	13.95	39.0	0.38	2.78		0.04
									39.4	0.13
2532	66B	39.4	0.62	2						
2554	69A	39.2	0.14	2						
2636	84B	39.8	0.17	2						
2700	93B	39.5	0.78	2						0.04
	94B	39.1	4.17	2	5.35	39.0	0.44	2.78		0.04
									39.3	0.08
2714	96A	39.7	1.81	2						0.04
	96B	40.0	0.56	2						0.01
	98A	39.9	0.13	2	0.98	3.88	0.24	7.26		-
									39.9	0.05
2715	97A	40.1	0.93	2						0.09
	97B	39.6	5.04	2	5.42	39.0	0.50	2.78		0.04
									39.8	0.13
2779	100A	40.3	0.65	2						0.16
	100B	40.9	0.45	2						0.04
	101A	40.2	0.29	2						0.25
	102A	40.6	0.41	2						0.01
	102B	41.3	2.85	2	0.83	2.79	1.26	4.47		0.36
									40.7	0.82
2803	104A	39.9	0.25	2						0.36
	104B	41.2	0.22	2						0.49
	105A	41.4	0.41	2						0.81
	105B	40.8	2.45	2						0.09
	107A	39.3	3.92	1						1.44
	107B	40.5	0.35	2	1.50	2.60	2.79	4.04		0
									40.5	3.19

TABLE XXI (cont.)

Heat No.	Forging No.	$\bar{X}_F$ ksi $\sqrt{in.}$	$\Sigma (X-\bar{X})^2$ $(ksi\ \sqrt{in.})^2$	df_i	(F) or Bartlett's Test	$F_{.05}$ (f_1,f_2)	(t) or ANOVA Test	$t_{.05}$ (n_1+n_2-2)	$\bar{X}_H$ ksi $\sqrt{in.}$	$(\bar{X}_F-\bar{X}_H)^2$ $(ksi\ \sqrt{in.})^2$
2846	108A	40.9	6.48	2						0.01
	108B	40.8	1.31	2						0
	109B	40.8	0.29	2						0
	110B	42.3	1.46	2						2.25
	111B	39.4	0.61	2	1.17	2.79	3.04	4.47		1.96
									40.8	4.22
2847	112A	39.4	0.89	2						1.69
	112B	42.0	0.01	2	89(1)	39.0	4.90	2.78		1.69
									40.7	3.38
			47.87	59						12.00

$$S_e^2 = \frac{47.87}{59} = 0.81 \qquad S_F^2 = \frac{12.00}{19} = 0.63$$

(1) Statistically, there is a significant difference, but practically the denominator is much smaller than normal; therefore, the values will be added.

Appendix E

TABLE XXII

BARTLETT'S TEST FOR MULTI-FORGING HEATS (LYCOMING a/Q ~ 0.02)

Heat No.	$\Sigma (X-\bar{X})^2$	df_i	S_i^2	$\ln S_i^2$	$df \ln S_i^2$	$1/df_i$
2529	0.13	1	0.13	7.960-10	7.960-10	1.0
2700	0.08	1	0.08	7.474-10	7.474-10	1.0
2714	0.05	2	0.02	6.088-10	12.176-20	0.5
2715	0.13	1	0.13	7.960-10	7.960-10	1.0
2779	0.82	4	0.20	8.391-10	33.564-40	0.25
2803	3.19	5	0.64	9.554-10	47.770-50	0.20
2846	4.22	4	1.06	0.058	0.232	0.25
2847	3.38	1	3.38	1.118	1.118	1.0
	12.00	19			118.254-140	5.20

$$S_p^2 = \frac{12.00}{19} = 0.63 \qquad m = 19(9.538-10) - (-21.746) = 12.968$$

$$f_1 = 8-1 = 7, \quad a = \frac{1}{(3)(7)}\left(5.20-\frac{1}{19}\right) = 0.25, \quad f_2 = \frac{8+1}{(0.25)^2} = 144.0$$

$$b = \frac{144}{1+2/144-0.23} = 185$$

$$F_{calc} = \frac{144.0(13.0)}{7(185.0-13.0)} = 1.56, \quad F_{tab} = F_{.05}(7,144) = 2.29$$

---

* To determine if variances are homogeneous.

Appendix E

TABLE XXIII

ANOVA TEST FOR MULTI-FORGING HEATS (Lycoming a/Q ∿ 0.02)

	$\bar{X}$	$\bar{X}^2$	$\bar{X}$	$\bar{X}^2$	$\bar{X}$	$\bar{X}^2$	$\bar{X}$	$\bar{X}^2$	$\bar{X}$	$\bar{X}^2$
Heat:	2529		2700		2714		2715		2779	
	39.7	1576.1	39.5	1560.2	39.7	1576.1	40.1	1608.0	40.3	1624.1
	39.2	1536.6	39.1	1528.8	40.0	1600.0	39.6	1568.2	40.9	1672.8
					39.9	1592.0			40.2	1616.0
									40.6	1648.4
									41.3	1705.7
	78.9	3112.7	78.6	3089.0	119.6	4768.1	79.7	3176.2	203.3	8267.0
Heat:	2803		2846		2847					
	39.9	1592.0	40.9	1672.8	39.4	1552.4				
	41.2	1697.4	40.8	1664.6	42.0	1764.0				
	41.4	1714.0	40.8	1664.6						
	40.8	1664.6	42.3	1789.3						
	39.3	1544.5	39.4	1552.4						
	40.5	1640.2								
	243.1	9852.7	204.2	8343.7	81.4	3316.4				

$\Sigma X = 1{,}088.8$

$(\Sigma X)^2 = 1{,}185{,}485.4$

$\Sigma X^2 = 43925.8$

$N = 27$

$CF = \frac{1185485.4}{27} = 43906.9$ Total SS = 43925.8 - 43906.9 = 18.9

Heat No.	SS	df
2529	0.13	1
2700	0.08	1
2714	0.05	2
2715	0.13	1
2779	0.82	4
2803	3.19	5
2846	4.22	4
2847	3.38	1
	12.00	19

Inherent error SS = 12.00, inherent error df = 19

Between forging SS = 18.9 - 12.0 = 6.9, between forging df = 8-1 = 7

Between heat mean square $= \frac{6.9}{7} = 0.99$, inherent error mean square $= \frac{12.00}{19} = 0.63$

$F_{calc} = \frac{0.99}{0.63} = 1.57$, $F_{tab} = F_{.05}(7,19) = 3.05$

Appendix E

TABLE XXIV

COMPARISON OF MEANS FOR MULTI-FORGING HEATS vs SINGLE-FORGING HEATS
(LYCOMING a/Q ∿ 0.02)

Multi-forging Heats		Single-forging Heats	
Heat No.	$\bar{X}_H$ (ksi)	Heat No.	$\bar{X}_H$ (ksi)
2529	39.4	2532	39.4
2700	39.3	2554	39.2
2714	39.9	2636	39.8
2715	39.8		118.4
2779	40.7		
2803	40.5		
2846	40.8		
2847	40.7		
	321.1		

$\bar{X}_{MF} = 40.1$ ksi $\qquad \bar{X}_{SF} = 39.5$ ksi

$S^2_{MF} = 0.38$ $\qquad S^2_{SF} = 0.10$

(F) Test

$$F_{calc} = \frac{0.38}{0.10} = 3.80, \qquad F_{tab} = F_{.05}(7,2) = 39.4$$

(t) Test

$$U = 40.1-39.5 = 0.6 \qquad S_p = \sqrt{\frac{2.63+0.19}{9}} = 0.56$$

$$\sqrt{\frac{n_1+n_2}{n_1 n_2}} = \sqrt{\frac{8+3}{8(3)}} = 0.68$$

$$t_{calc} = \frac{0.6}{(0.56)(0.68)} = 1.58, \qquad t_{tab} = t_{.05}(8+3-2) = 2.26$$

Appendix E

TABLE XXV

COMMON FORGINGS TESTED AT ALL THREE LABORATORIES (a/Q ~ 0.02)

Laboratory	Forging	$\bar{X}$ (ksi)	SS	df
Sacramento	63A	37.8	3.44	2
	63B	37.8	2.42	2
	66B	33.5	1.45	2
	69A	38.0	2.04	2
	69B	38.5	16.99	2
	70A	37.6	2.53	2
	70B	37.7	8.01	2
	71A	38.8	0.73	2
Downey	69B	37.6	3.21	2
	70A	41.9	0.98	1
	70B	39.2	3.93	2
	71A	40.3	0.89	2
Lycoming	63A	39.7	0.69	2
	63B	39.2	9.63	2
	66B	39.4	0.62	2
	69A	39.2	0.14	2

SACRAMENTO AND DOWNEY

Forging 69B

(F) Test

$$F_{calc} = \frac{8.44}{1.60} = 5.27 \qquad F_{tab} = F_{.05}(2,2) = 39.00$$

(t) Test

$$U = 38.5 - 37.6 = 0.9 \qquad S_p = \sqrt{\frac{16.99+3.21}{3+3-2}} = 2.24$$

$$t_{calc} = \frac{0.9}{(2.24)(0.82)} = 0.49 \qquad t_{tab} = t_{.05}(3+3-2) = 2.78$$

Forging 70A **TABLE XXV (cont.)**

(F) Test

$$F_{calc} = \frac{1.26}{0.98} = 1.29 \qquad F_{tab} = F_{.05}\,(2,1) = 799.50$$

(t) Test

$$U = 41.9-37.6 = 4.3 \qquad S_p = \sqrt{\frac{2.53+10.98}{3+2-2}} = 1.08$$

$$\sqrt{\frac{n_1+n_2}{n_1 n_2}} = \sqrt{\frac{3+2}{(3)(2)}} = 0.91$$

$$t_{calc} = \frac{4.3}{(0.91)(1.08)} = 4.39 \qquad t_{tab} = t_{.05}\,(3+2-2) = 3.18$$

Forging 70B

(F) Test

$$F_{calc} = \frac{4.00}{1.96} = 2.04 \qquad F_{tab} = 39.00$$

(t) Test

$$U = 39.2-37.7 = 1.5 \qquad S_p = \sqrt{\frac{8.01+3.93}{3+3-2}} = 1.72$$

$$\sqrt{\frac{n_1+n_2}{n_1 n_2}} = 0.82$$

$$t_{calc} = \frac{1.5}{(0.82)1.72} = 1.06 \qquad t_{tab} = t_{.05}\,(3+3-2) = 2.78$$

Forging 71A

(F) Test

$$F_{calc} = \frac{0.44}{0.36} = 1.22 \qquad F_{tab} = F_{.05}\,(2,2) = 39.00$$

(t) Test

$$U = 40.3-38.8 = 1.5 \qquad S_p = \sqrt{\frac{0.73+0.89}{3+3-2}} = 0.63$$

$$\sqrt{\frac{n_1+n_2}{n_1 n_2}} = 0.82$$

TABLE XXV (cont.)

$$t_{calc} = \frac{1.5}{(0.82)(0.63)} = 2.89^{*} \qquad t_{tab} = t_{.05}\ (3+3-2) = 2.78$$

SACRAMENTO-LYCOMING

Forging 63A

(F) Test

$$F_{calc} = \frac{1.72}{0.34} = 5.06 \qquad F_{tab} = F_{.05}\ (2,2) = 39.00$$

(t) Test

$$U = 39.7-37.8 = 1.9 \qquad S_p = \sqrt{\frac{3.44+0.69}{6-2}} = 1.01$$

$$\sqrt{\frac{n_1+n_2}{n_1 n_2}} = 0.82$$

$$t_{calc} = \frac{1.9}{(1.01)(0.82)} = 2.29 \qquad t_{tab} = t_{.05}\ (3+3-2) = 2.78$$

Forging 63B

(F) Test

$$F_{calc} = \frac{4.82}{1.21} = 3.98 \qquad F_{tab} = F_{.05}\ (2,2) = 39.00$$

(t) Test

$$U = 39.2-37.8 = 1.4 \qquad S_p = \sqrt{\frac{9.63+2.42}{3+3-2}} = 1.73$$

$$\sqrt{\frac{n_1+n_2}{n_1 n_2}} = 0.82$$

$$t_{calc} = \frac{1.4}{(0.82)(1.73)} = 0.99 \qquad t_{tab} = t_{.05}\ (3+3-2) = 2.78$$

Forging 66B

(Sacramento 66B was considered invalid for Sacramento Analysis).

Forging 69A

(F) Test

$$F_{calc} = \frac{1.02}{0.07} = 14.58 \qquad F_{tab} = F_{.05}\ (2,2) = 39.00$$

(t) Test

$$U = 39.2-38.0 = 1.2 \qquad S_p = \sqrt{\frac{2.04+0.14}{3+3-2}} = 0.73$$

*Both variances will be considered equal.

TABLE XXV (cont.)

$$\sqrt{\frac{n_1+n_2}{n_1 n_2}} = 0.82$$

$$t_{calc} = \frac{1.2}{(0.82)(0.73)} = 2.00, \qquad t_{tab} = t_{.05}\ (3+3-2) = 2.78$$

TABLE XXVI

ROOM TEMPERATURE K_{Ic} RESULTS (AEROJET-SACRAMENTO a/Q ~ 0.04)

Heat No.	Forging No.	$\bar{X}_F$ ksi √in.	$\sum(X-\bar{X})^2$ $(\text{ksi}\sqrt{\text{in.}})^2$	df_i	(F) or Bartlett's Test	$F_{.05}$ (f_1,f_2)	(t) or ANOVA Test	$t_{.05}$ (n_1+n_2-2)	$\bar{X}_H$ ksi √in.	$(\bar{X}_F-\bar{X}_H)^2$ $(\text{ksi}\sqrt{\text{in.}})^2$
1643	9	47.9	7.21	2						
1644	5	48.6	-	0						
1968	13	47.2	0.61	1						
2018	17	36.1	5.18	2						
2047	23	43.7	-	0						
2073	26	48.3	-	0						
2074	27	38.6	34.34	2						
2100	29	35.2	6.32	2						
2102	30	48.2	4.81	1						
2148	31A	31.0	18.13	2						0.16
	31B	31.8	0.72	1	12.6	799.5	0.35	3.18		0.16
									31.4	0.32
2150	33A	40.9	3.55	2						4.00
	33B	44.9	19.41	2	5.48	39.00	2.07	2.78		4.00
									42.9	8.00
2169	43A	35.4	6.74	2						1.76
	43B	38.3	9.50	2	1.41	39.00	1.82	2.78		2.25
									36.8	4.21
2201	45A	40.1	5.13	2						
2202	36A	35.8	4.21	1						0.16
	36B	35.1	2.73	2	3.10	38.51	0.51	3.18		0.09
									35.4	0.25
2203	37B	41.6	0.13	1						
2205	39A	40.0	40.67	2						
2274	42B	36.6	1.33	2						3.61
	42C	40.4	-	0	-		4.05	4.30		3.61
									38.5	7.22
2395	50A	36.9	3.38	1						
2398	53B	38.3	18.60	1						0
	54A	38.6	1.45	1						0.09
	54B	38.1	14.12	2	0.5	4.22	0.01	10.65		0.04
									38.3	0.13

TABLE XXVI (cont.)

Heat No.	Forging No.	$\bar{X}_F$ ksi √in.	$\sum (X-\bar{X})^2$ $(\text{ksi}\sqrt{\text{in.}})^2$	df_i	(F) or Bartlett's Test	$F_{.05}$ (f_1,f_2)	(t)or ANOVA Test	$t_{.05}$ (n_1+n_2-2)	$\bar{X}_H$ ksi √in.	$(\bar{X}_F-\bar{X}_H)^2$ $(\text{ksi}\sqrt{\text{in.}})^2$
2479	56B	34.4	9.26	1						0.16
	60B	33.7	0.85	1	10.9	647.79	0.31	4.3		0.09
									34.0	0.25
2480	57B	39.8	14.92	2						0.49
	58B	38.4	13.48	2	1.10	39.0	0.64	2.78		0.49
									39.1	0.98
2481	59A	34.0	10.46	2						
2528	61B	35.9	3.65	2						1.44
	62A	37.9	42.34	2						0.64
	62B	37.5	32.02	2	1.03	3.88	0.30	7.26		0.16
									37.1	2.24
2529	63A	35.6	-	0						0.09
	63B	35.0	-	0	-		-			0.09
									35.3	0.18
2531	65A	39.8	-	0						
2554	69A	38.2	0.50	1						
2555	70A	30.6	-	0						
	71A	40.4	1.63	2			9.46	4.30		
			337.38	53						23.78

$$S_e^2 = \frac{337.38}{53} = 6.37$$

$$S_H^2 = \frac{23.78}{12} = 1.98$$

Appendix E

TABLE XXVII

BARTLETT'S TEST FOR MULTI-FORGING HEATS (AEROJET-SACRAMENTO a/Q ~ 0.04)

Heat No.	$\Sigma (X-\bar{X})^2$	df_i	S_i^2	$\ln S_i^2$	$df \ln S_i^2$	$1/df_i$
2148	0.32	1	0.32	8.861-10	8.861-10	1.00
2150	8.00	1	8.00	2.079	2.079	1.00
2169	4.21	1	4.21	1.437	1.437	1.00
2202	0.25	1	0.25	8.614-10	8.614-10	1.00
2274	7.22	1	7.22	1.977	1.977	1.00
2398	0.13	2	0.06	7.187-10	14.374-20	0.50
2479	0.25	1	0.25	8.614-10	8.614-10	1.00
2480	0.98	1	0.98	9.980-10	9.980-10	1.00
2528	2.24	2	1.12	0.113	0.226	0.50
2529	0.18	1	0.18	8.285-10	8.285-10	1.00
	23.78	12			64.447-70	9.00

$S_p^2 = \frac{23.78}{12} = 1.98$ $\quad m = 12(0.683)-(-5.553) = 13.749$

$f_1 = 10-1 = 9, \quad a = \frac{1}{(3)(9)}\left[9-\frac{1}{12}\right] = 0.324, \quad f_2 = \frac{10+1}{(0.32)^2} = 107.3$

$b = \frac{107.3}{1+2/107.3-0.32} = 153.2$

$F_{calc} = \frac{107.3\ (13.7)}{9(153.2-13.7)} = \frac{1470.0}{1255.5} = 1.17$

$F_{tab} = F_{.05}\ (9,107) = 2.26$

---

* To determine if variances are homogeneous.

Appendix E

TABLE XXVIII

ANOVA TEST FOR MULTI-FORGING HEATS (AEROJET-SACRAMENTO a/Q ∿ 0.04)

	$\bar{X}$	$\bar{X}^2$	$\bar{X}$	$\bar{X}^2$	$\bar{X}$	$\bar{X}^2$	$\bar{X}$	$\bar{X}^2$	$\bar{X}$	$\bar{X}^2$
eat:	2148		2150		2169		2202		2274	
	31.0	961.0	40.9	1672.8	35.4	1253.2	35.8	1281.6	36.6	1339.6
	31.8	1011.2	44.9	2016.0	38.3	1466.9	35.1	1232.0	40.4	1632.2
	62.8	1972.2	85.8	3688.8	73.7	2720.1	70.9	2513.6	77.0	2971.8
Heat:	2398		2479		2480		2528		2529	
	38.3	1466.9	34.4	1183.4	39.8	1584.0	35.9	1288.8	35.6	1267.4
	38.6	1490.0	33.7	1135.7	38.4	1474.6	37.9	1436.4	35.0	1225.0
	38.1	1451.6					37.5	1406.2		
	115.0	4408.5	68.1	2319.1	78.2	3058.6	111.3	4131.4	70.6	2492.4

$\leq X = 813.4$, $(\leq X)^2 = 661619.6$, $\leq X^2 = 30276.5$, $N = \leq n = 22$

$CF = \frac{661619.6}{22} = 30073.6$, Total SS = 30276.5 - 30073.6 = 202.9

Heat No.	SS	df
2148	0.32	1
2150	8.00	1
2169	4.21	1
2202	0.25	1
2274	7.22	1
2398	0.13	2
2479	0.25	1
2480	0.98	1
2528	2.24	2
2529	0.18	1
	23.78	12

Inherent error SS = 23.78, inherent error df = 12

Between heat df = 10-1 = 9, between heat SS = 202.9 - 23.8 = 179.1

Between heat mean square = $\frac{179.1}{9} = 19.9$, inherent error mean square = $\frac{23.78}{12} = 1.98$

$F_{calc} = \frac{19.9}{1.98} = 10.0$, $F_{tab} = F_{.05}(9,12) = 3.44$

TABLE XXIX

ROOM TEMPERATURE K_{Ic} RESULTS (AEROJET-DOWNEY a/Q ~ 0.04)

Heat No.	Forging No.	$\bar{X}_F$ ksi $\sqrt{in.}$	$(X-\bar{X})^2$ $(ksi\ \sqrt{in.})^2$	df_i	(F) or Bartlett's Test	$F_{.05}$ (f_1, f_2)	(t) or ANOVA Test	$t_{.05}$ (n_1+n_2-2)	$\bar{X}_H$ ksi $\sqrt{in.}$	$(\bar{X}_F-\bar{X}_H)^2$ $(ksi\ \sqrt{in.})^2$
2554	69B	35.0	2.91	2						
2555	70A	35.9	0.03	2						0.81
	70B	37.9	4.02	2						1.21
	71A	36.6	0.05	1	5.20(1)	4.00	3.78	8.43		0.04
									36.8	2.06
2576	73A	36.6	7.09	2						0.49
	73B	36.1	1.61	2						1.44
	74A	39.6	6.48	1						5.29
	74B	37.0	5.78	1	0.37	3.40	1.58	6.60		0.09
									37.3	7.31
2577	75A	39.9	15.13	1						0.01
	80A	40.1	4.05	2						0.01
	80B	40.1	10.13	2	0.58	4.02	0	8.43		0.01
									40.0	0.03
2578	76A	37.5	0	2						2.25
	77A	34.9	0	0						1.21
	77B	35.7	0	0			∞(1)	39.0		0.09
									36.0	3.55
2579	78A	33.9	0	0						1.96
	79A	37.0	3.92	2						2.89
	79B	35.0	0.49	2	8.00	39.0	4.54	10.65		0.09
									35.3	4.94
2634	81A	38.1	0.33	2						
2635	82A	40.2	0.13	1						
2636	83A	45.7	5.46	2						
	84B	54.6	3.35	2	1.63	39.0	7.35	2.78		
2696	86A	52.6	9.73	2						
2696	87A	45.6	2.21	1						1.21
	87B	43.5	22.12	2	10.0	799.50	0.81	3.18		1.00
									44.5	2.21

TABLE XXIX (cont.)

Heat No.	Forging No.	$\bar{X}_F$ ksi $\sqrt{in.}$	$(X-\bar{X})^2$ $(ksi\sqrt{in.})^2$	df_i	(F) or Bartlett's Test	$F_{.05}$ (f_1,f_2)	(t)or ANOVA Test	$t_{.05}$ (n_1+n_2-2)	$\bar{X}_H$ ksi $\sqrt{in.}$	$(\bar{X}_F-\bar{X}_H)^2$ $(ksi\sqrt{in.})^2$
2697	90A	45.2	6.25	2						7.84
	90B	40.4	4.56	2						4.00
	91A	35.9		0		Cannot add 91A				
	91B	39.8	0.01	1						
	92A	44.1	12.56	2	1.47	3.29	5.60	5.89		6.76
										2.89
									42.4	21.49
2700	93A	42.6	14.05	1						
			142.45	44						41.59

$$S_e^2 = \frac{142.45}{44} = 3.24$$

$$S_F^2 = \frac{41.59}{15} = 2.77$$

(1) Statistically significant, but from a practical standpoint, one or more of the variances is much smaller than has been normally noticed; therefore, the results will be added.

Appendix E

TABLE XXX

BARTLETT'S TEST FOR MULTI-FORGING HEATS (AEROJET-DOWNEY a/Q ∿ 0.04)

Heat No.	$\Sigma (X-\bar{X})^2$	df_i	S_i^2	$\ln S_i^2$	$df \ln S_i^2$	$1/df_i$
2555	2.06	2	1.03	0.030	0.060	0.5
2576	7.31	3	2.44	0.892	2.576	0.33
2577	0.03	2	0.02	6.088-10	12.176-20	0.5
2578	3.55	2	1.78	0.577	1.154	0.5
2579	4.94	2	2.47	0.904	1.808	0.5
2696	2.21	1	2.21	0.793	0.793	1.0
2697	21.49	3	7.16	1.969	5.907	0.33
	41.59	15			24.474-20	3.67

$S_p^2 = \frac{41.59}{15} = 2.77$ $\quad m = 15(1.019) - 4.474 = 10.811, \quad f_1 = 7-1 = 6$

$a = \frac{1}{(3)(6)}\left(3.67-\frac{1}{15}\right) = 0.20, \quad f_2 = \frac{7+1}{(0.2)^2} = 200, \quad b = \frac{200}{1+2/200-0.2} = 247$

$F_{calc} = \frac{200(10.8)}{6(247-10.8)} = \frac{2160.0}{1417.2} = 1.52, \quad F_{tab} = F_{.05}(6,200) = 2.41$

---

* To determine if variances are homogeneous.

Appendix E

TABLE XXXI

ANOVA TEST FOR MULTI-FORGING HEATS (AEROJET-DOWNEY a/Q ∿ 0.04)

	$\bar{X}$	$\bar{X}^2$	$\bar{X}$	$\bar{X}^2$	$\bar{X}$	$\bar{X}^2$	$\bar{X}$	$\bar{X}^2$	$\bar{X}$	$\bar{X}^2$
Heat:	2555		2576		2577		2578		2579	
	35.9	1288.8	36.6	1339.6	39.9	1592.0	37.5	1406.2	33.9	1149.2
	37.9	1436.4	36.1	1303.2	40.1	1608.0	34.9	1218.0	37.0	1369.0
	36.6	1339.6	39.6	1568.2	40.1	1608.0	35.7	1274.5	35.0	1225.0
			37.0	1369.0						
	110.4	4064.8	149.3	5580.0	120.1	4808.0	108.1	3898.7	105.9	3743.2
Heat:	2696		2697							
	45.6	2079.4	45.2	2043.0						
	43.5	1892.2	40.4	1632.2						
			39.8	1584.0						
			44.1	1944.8						
	89.1	3971.6	169.5	7204.0						

$\Sigma X^2 = 852.4$, $(\Sigma X)^2 = 726585.8$

$\Sigma X^2 = 33270.3$

$N = \Sigma n = 22$

$CF = \frac{726585.8}{22} = 33026.6$ Total SS = 33270.3 - 33026.6 = 243.7

Heat No.	SS	df
2555	2.06	2
2576	7.31	3
2577	0.03	2
2578	3.55	2
2579	4.94	2
2696	2.21	1
2697	21.49	3
	41.59	15

*Inherent error df = 15

Inherent error SS = 41.59

Between forging df = 7-1 = 6, between forging SS = 243.7 - 41.6 = 202.1

Between forging mean square = $\frac{202.1}{6}$ = 33.7, inherent error mean square = $\frac{41.59}{15}$ = 2.77

$F_{calc} = \frac{33.7}{2.77} = 12.16$, $F_{tab} = F_{.05}(6,15) = 3.41$

TABLE XXXII

ROOM TEMPERATURE K_{Ic} RESULTS (LYCOMING a/Q ~ 0.04)

Heat No.	Forging No.	$\bar{X}_F$ ksi $\sqrt{in.}$	$(X-\bar{X})^2$ $(ksi\sqrt{in.})^2$	df_i	(F) or Bartlett's Test	$F_{.05}$ (f_1,f_2)	(t)or ANOVA Test	$t_{.05}$ (n_1+n_2-2)	$\bar{X}_H$ ksi $\sqrt{in.}$	$(\bar{X}_F-\bar{X}_H)^2$ $(ksi\sqrt{in.})^2$
2529	63A	35.0	0.53	2						0.16
	63B	34.1	-	0	-		1.53	4.30		0.25
									34.6	0.41
2532	66B	33.9	5.66	2						
2554	69A	35.5	4.16	2						
2636	84B	40.1	12.53	2						
2700	93B	37.0	5.66	2						0.04
	94B	36.7	2.29	2	2.47	39.00	0.26	2.78		0.01
									36.8	0.05
2714	96A	35.1	0.93	2						10.89
	96B	40.1	10.01	2						2.89
	98A	39.9	7.61	2	0.95	3.88	7.61(1)	7.26		2.25
									38.4	16.03
2715	97A	36.3	1.01	2						0.49
	97B	37.7	18.36	2	18.17	39.00	0.78	2.78		0.49
									37.0	0.98
2779	100A	40.6	0.08	2						0.25
	100B	39.8	4.29	2						0.09
	101A	39.8	8.34	2			0.29	7.26		0.09
									40.1	0.43
2779	102A	43.5	2.88	1						0.8
	102B	45.4	11.14	2	1.5	2.93	0.97	3.18		1.00
									44.4	1.81
2803	104A	42.9	21.23	2						1.00
	104B	41.2	0.83	2						0.49
	105A	40.6	0.08	1						1.69
	105B	42.1	3.13	2						0.04
	107A	42.9	0.19	2						1.00
	107B	41.7	6.05	2	2.1	2.60	0.78	4.04		0.04
									41.9	4.26

TABLE XXXII (cont.)

Heat No.	Forging No.	$\bar{X}_F$ ksi $\sqrt{in.}$	$\Sigma(X-\bar{X})^2$ $(ksi\ \sqrt{in.})^2$	df_i	(F) or Bartlett's Test	$F_{.05}$ (f_1,f_2)	(t)or ANOVA Test	$t_{.05}$ (n_1+n_2-2)	$\bar{X}_H$ ksi $\sqrt{in.}$	$(\bar{X}_F-\bar{X}_H)^2$ $(ksi\ \sqrt{in.})^2$
2846	108A	41.8	13.21	2						3.61
	108B	38.5	3.93	2						1.96
	109B	39.3	2.11	2			2.86	7.26		0.36
									39.9	5.93
2846	110B	47.4	3.71	2						3.24
	111B	43.8	5.63	2	0.41	2.79	2.88	2.78		3.24
									45.6	6.48
2847	112A	44.4	0.32	2						1.00
	112B	46.3	0.09	2	3.56	39.00	7.3(1)	2.78		0.81
									45.4	1.81
			155.99	56						35.50

$$S_e^2 = \frac{155.99}{56} = 2.79$$

$$S_{\bar{X}}^2 = \frac{35.50}{17} = 2.09$$

(1) Statistically significant but from a practical standpoint, one or more of the variances is much smaller than has been normally noticed; therefore, the results will be added.

Appendix E

TABLE XXXIII

BARTLETT'S TEST FOR MULTI-FORGING HEATS (LYCOMING a/Q ∿ 0.04)

Heat No.	$\Sigma(X-\bar{X})^2$	df_i	S_i^2	$\ln S_i^2$	$df \ln S_i^2$	$1/df_i$
2529	0.41	1	0.41	9.108-10	9.108-10	1.0
2700	0.05	1	0.05	7.004-10	7.004-10	1.0
2714	16.03	2	8.02	2.082	4.164	0.5
2715	0.98	1	0.98	9.980-10	9.980-10	1.0
2779	0.43	2	0.22	8.486-10	16.972-20	0.5
2779(a)	1.81	1	1.81	0.593	0.593	1.0
2803	4.26	5	0.85	9.837-10	49.185-50	0.2
2846	5.93	2	2.96	1.085	2.170	0.5
2846(a)	6.48	1	6.48	1.869	1.869	1.0
2847	1.81	1	1.81	0.593	0.593	1.0
	35.50	17			101.638-100	7.7

$S_p^2 = \frac{35.50}{17} = 2.09$ $\quad m = 17(0.737)-1.638 = 10.154,\ f_1 = 10-1 = 9$

$a = \frac{1}{(3)(9)}\left(7.7-\frac{1}{17}\right) = 0.206,\quad f_2 = \frac{10+1}{(0.206)^2} = 259,$

$b = \frac{259}{1+2/259-0.206} = 324$

$F_{calc} = \frac{259(10.2)}{9(324-10.2)} = \frac{2641.8}{2834.2} = 0.93,\quad F_{tab} = F_{.05}(9,259) = 2.11$

---

* To determine if variances are homogeneous

Appendix E

TABLE XXXIV

ANOVA TEST FOR MULTI-FORGING HEATS (Lycoming a/Q ∿ 0.04)

	$\bar{X}$	$\bar{X}^2$	$\bar{X}$	$\bar{X}^2$	$\bar{X}$	$\bar{X}^2$	$\bar{X}$	$\bar{X}^2$	$\bar{X}$	$\bar{X}^2$
Heat:	2529		2700		2714		2715		2779	
	35.0	1225.0	37.0	1369.0	35.1	1232.0	36.3	1317.7	40.6	1648.4
	34.1	1162.8	36.7	1346.9	40.1	1608.0	37.7	1421.3	39.8	1584.0
					39.9	1592.0			39.8	1584.0
	69.1	2387.8	73.7	2715.9	115.1	4432.0	74.0	2739.0	120.2	4816.4
Heat:	2779(a)		2803		2846		2846(a)		2847	
	43.5	1892.2	42.9	1840.4	41.8	1747.2	47.4	2246.8	44.4	1971.4
	45.4	2061.2	41.2	1697.4	38.5	1482.2	43.8	1918.4	46.3	2143.7
			40.6	1648.4	39.3	1544.5				
			42.1	1772.4						
			42.9	1840.4						
			41.7	1738.9						
	88.9	3953.4	251.4	10537.9	119.6	4773.9	91.2	4165.2	90.7	4115.1

$\Sigma X = 1093.9$, $(\Sigma X)^2 = 1{,}196{,}617.2$, $\Sigma X^2 = 44636.6$ $\quad N = \Sigma n = 27$

$CF = \frac{1196617.2}{27} = 44319.2$ $\quad$ Total SS = 44636.6 - 44319.2 = 317.4

Heat inherent error SS = 35.5, inherent error df = 17

Between forging df = 10-1=9, between forging SS = 317.4-35.5 = 281.9

Between forging mean square $= \frac{281.9}{9} = 31.3$, inherent error mean square $= \frac{35.5}{17} = 2.09$

$F_{calc} = \frac{31.3}{2.09} = 15.0$ $\quad F_{tab} = F_{.05}\ (9,17) = 2.98$

Eliminate
2779(a), 2846(a), 2847 $\quad \Sigma X = 823.1$, $(\Sigma X)^2 = 677493.6$, $\Sigma X^2 = 32402.9$, N=21

CF = 32261.6 $\quad$ Total SS = 32402.9 - 32261.6 = 141.3

Inherent error SS = 24.1, inherent error df = 14

Between forging df = 7-1 = 6, between forging SS = 141.3-24.1 = 117.2

Between forging mean square $= \frac{117.2}{6} = 19.5$, inherent error mean square $= \frac{24.1}{14} = 1.71$

$F_{calc} = \frac{19.5}{1.71} = 11.4$, $\quad F_{tab} = F_{.05}\ (6,14) = 3.50$

Unclassified
Security Classification

DOCUMENT CONTROL DATA - R&D
(Security classification of title, body of abstract and indexing annotation must be entered when the overall report is classified)

1 ORIGINATING ACTIVITY (Corporate author)
Aerojet-General Corporation
Sacramento, California 95813

2a REPORT SECURITY CLASSIFICATION
Unclassified

2b GROUP
N/A

3 REPORT TITLE
Tensile Properties and Fracture Toughness of 6Al-4V Titanium

4 DESCRIPTIVE NOTES (Type of report and inclusive dates)
February 1967 to April 1968

5 AUTHOR(S) (Last name, first name, initial)
Hartbower, C. E., Reuter, W. G., and Crimmins, P. P.

6 REPORT DATE	7a TOTAL NO. OF PAGES	7b NO. OF REFS
September 1968	378	44

8a CONTRACT OR GRANT NO.	9a ORIGINATOR'S REPORT NUMBER(S)
USAF Contract F33615-67-C-1358	N/A
b PROJECT NO. 7381	9b OTHER REPORT NO(S) (Any other numbers that may be assigned this report)
c Task 738106	AFML-TR-68-163 - Vol - I

10 AVAILABILITY/LIMITATION NOTICES This document is subject to special export controls and each transmittal to foreign governments or foreign nationals may be made only with prior approval of the Air Force Materials Laboratory

11 SUPPLEMENTARY NOTES	12 SPONSORING MILITARY ACTIVITY
	Air Force Materials Laboratory Wright-Patterson AFB, Ohio

13 ABSTRACT

See Attached

DD FORM 1 JAN 64 1473

Unclassified
Security Classification

Unclassified

Security Classification

14. KEY WORDS	LINK A		LINK B		LINK C	
	ROLE	WT	ROLE	WT	ROLE	WT
6Al-4V-Titanium						
Mil-Hdbk-5 Data						
Fracture Toughness						
Tensile Properties						
Fracture Testing						

INSTRUCTIONS

1. **ORIGINATING ACTIVITY:** Enter the name and address of the contractor, subcontractor, grantee, Department of Defense activity or other organization *(corporate author)* issuing the report.

2a. **REPORT SECURITY CLASSIFICATION:** Enter the overall security classification of the report. Indicate whether "Restricted Data" is included. Marking is to be in accordance with appropriate security regulations.

2b. **GROUP:** Automatic downgrading is specified in DoD Directive 5200.10 and Armed Forces Industrial Manual. Enter the group number. Also, when applicable, show that optional markings have been used for Group 3 and Group 4 as authorized.

3. **REPORT TITLE:** Enter the complete report title in all capital letters. Titles in all cases should be unclassified. If a meaningful title cannot be selected without classification, show title classification in all capitals in parenthesis immediately following the title.

4. **DESCRIPTIVE NOTES:** If appropriate, enter the type of report, e.g., interim, progress, summary, annual, or final. Give the inclusive dates when a specific reporting period is covered.

5. **AUTHOR(S):** Enter the name(s) of author(s) as shown on or in the report. Enter last name, first name, middle initial. If military, show rank and branch of service. The name of the principal author is an absolute minimum requirement.

6. **REPORT DATE:** Enter the date of the report as day, month, year, or month, year. If more than one date appears on the report, use date of publication.

7a. **TOTAL NUMBER OF PAGES:** The total page count should follow normal pagination procedures, i.e., enter the number of pages containing information.

7b. **NUMBER OF REFERENCES:** Enter the total number of references cited in the report.

8a. **CONTRACT OR GRANT NUMBER:** If appropriate, enter the applicable number of the contract or grant under which the report was written.

8b, 8c, & 8d. **PROJECT NUMBER:** Enter the appropriate military department identification, such as project number, subproject number, system numbers, task number, etc.

9a. **ORIGINATOR'S REPORT NUMBER(S):** Enter the official report number by which the document will be identified and controlled by the originating activity. This number must be unique to this report.

9b. **OTHER REPORT NUMBER(S):** If the report has been assigned any other report numbers *(either by the originator or by the sponsor)*, also enter this number(s).

10. **AVAILABILITY/LIMITATION NOTICES:** Enter any limitations on further dissemination of the report, other than those imposed by security classification, using standard statements such as:

(1) "Qualified requesters may obtain copies of this report from DDC."

(2) "Foreign announcement and dissemination of this report by DDC is not authorized."

(3) "U. S. Government agencies may obtain copies of this report directly from DDC. Other qualified DDC users shall request through _____."

(4) "U. S. military agencies may obtain copies of this report directly from DDC. Other qualified users shall request through _____."

(5) "All distribution of this report is controlled. Qualified DDC users shall request through _____."

If the report has been furnished to the Office of Technical Services, Department of Commerce, for sale to the public, indicate this fact and enter the price, if known.

11. **SUPPLEMENTARY NOTES:** Use for additional explanatory notes.

12. **SPONSORING MILITARY ACTIVITY:** Enter the name of the departmental project office or laboratory sponsoring *(paying for)* the research and development. Include address.

13. **ABSTRACT:** Enter an abstract giving a brief and factual summary of the document indicative of the report, even though it may also appear elsewhere in the body of the technical report. If additional space is required, a continuation sheet shall be attached.

It is highly desirable that the abstract of classified reports be unclassified. Each paragraph of the abstract shall end with an indication of the military security classification of the information in the paragraph, represented as *(TS)*, *(S)*, *(C)*, or *(U)*.

There is no limitation on the length of the abstract. However, the suggested length is from 150 to 225 words.

14. **KEY WORDS:** Key words are technically meaningful terms or short phrases that characterize a report and may be used as index entries for cataloging the report. Key words must be selected so that no security classification is required. Identifiers, such as equipment model designation, trade name, military project code name, geographic location, may be used as key words but will be followed by an indication of technical context. The assignment of links, rules, and weights is optional.

Unclassified

Security Classification

ABSTRACT

Phase I of a MIL-HDBK data collection has been completed to provide room- and elevated-temperature-tensile and fracture-toughness data on 6Al-4V titanium at a 0.2% offset yield strength of approximately 160 ksi. The material was from second-stage Minuteman rocket-motor cases. The elevated-temperature tensile data were for temperatures up to 330°F. The fracture-toughness data include plane-strain K_{Ic} from part-through-crack (PTC) tensile tests of 109 forgings, plane-stress K_c from fatigue-precracked center-notch (CN) tensile tests of 18 forgings, and precrack Charpy slow-bend and impact tests of specimens cut from the fractured CN-tensile specimens. The latter 18 forgings were from nine hydroburst chambers, four of which were premature proof-test failures and five were deliberately hydroburst in the Minuteman development program.

The uniaxial tensile-data means were determined for each temperature and plots of percent-of-room temperature tensile-properties versus temperature were constructed for input to MIL-HDBK-5. For room-temperature, the A-basis values of ultimate strength, yield strength, and percent elongation were 166.3 ksi, 153.0 ksi, and 10.2%, respectively; the B-basis values were 168.8 ksi and 156.4 ksi, respectively. The PTC-tensile K_{Ic} data were examined for the variation in fracture toughness attributable to between-forging, between-heat, and between-test-laboratory variability, first on the basis of engineering plots of data from individual laboratories, forgings, billets, and heats, and then by statistical-analysis techniques. Based on the engineering plots, tests of multiple forgings from a single heat of titanium and multiple forgings from a single billet of titanium revealed differences in K_{Ic} from forging to forging when the surface precrack was deep (approximately 50% of specimen thickness) but little or no difference in K_{Ic} with a shallow crack (approximately 25% of specimen thickness). Comparisons between laboratories revealed differences between test results in some forgings but not all. Based on statistical analysis, a significant difference was indicated between K_{Ic} values at the two crack depths investigated. However, statistically, there was not a significant difference between forgings or between heats with shallow cracks, whereas, with deeper cracks there was a significant difference between heats but not a significant difference between forgings. When the data from the shallow cracks were pooled and plotted on probability paper, the population mean was 39.1 ksi-in.$^{\frac{1}{2}}$ with a standard deviation of 1.6 ksi-in.$^{\frac{1}{2}}$. Based on all of the 540 tests, treated as a non-normal distribution, the A-basis value was 30.6 and the B-basis value was 35.2 ksi-in.$^{\frac{1}{2}}$.

The CN-tensile K_{Ic} values ranged from 31.2 to 74.6 ksi-in.$^{\frac{1}{2}}$; thus, the K_{Ic} values in some forgings were appreciably higher than any values measured in the PTC-tensile tests of 109 forgings tested with a different crack orientation. Precrack Charpy slow-bend W/A values were found to provide a good estimate of the CN-tensile K_{Ic} values through the relationship $K_{Ic} = 0.17(W/A)_{PCSB} + 16.2$ ksi-in.$^{\frac{1}{2}}$ where $(W/A)_{PCSB}$ is the precrack Charpy slow-bend value in in.-lb/in.^{2}. The CN-tensile K_c data based on the onset of crack instability as determined by an acoustical technique ranged from 71 to 137 ksi-in.$^{\frac{1}{2}}$ for the 18 forgings tested. Precrack Charpy impact W/A values were found to provide a good estimate of the CN-tensile K_c values through the relationship $K_c = 0.10(W/A)_{PCI} + 6.7$ ksi-in.$^{\frac{1}{2}}$.

THIS ABSTRACT IS SUBJECT TO SPECIAL EXPORT CONTROLS AND EACH TRANSMITTAL TO FOREIGN GOVERNMENTS OR FOREIGN NATIONALS MAY BE MADE ONLY WITH PRIOR APPROVAL OF THE AIR FORCE MATERIALS LABORATORY (MAAE), WRIGHT-PATTERSON AIR FORCE BASE, OHIO 45433.